Annual reports on
NMR Spectroscopy

Volume 63

Annual Reports on

NMR SPECTROSCOPY

VOLUME **63**

This page intentionally left blank

Annual Reports on
NMR SPECTROSCOPY

VOLUME **63**

Edited by

GRAHAM A. WEBB
Royal Society of Chemistry
Burlington House
Piccadilly, London, UK

ELSEVIER

Amsterdam • Boston • Heidelberg • London • New York • Oxford
Paris • San Diego • San Francisco • Singapore • Sydney • Tokyo
Academic Press is an imprint of Elsevier

ACADEMIC
PRESS

Academic Press is an imprint of Elsevier
84 Theobald's Road, London WC1X 8RR, UK
Radarweg 29, PO Box 211, 1000 AE Amsterdam, The Netherlands
Linacre House, Jordan Hill, Oxford OX2 8DP, UK
30 Corporate Drive, Suite 400, Burlington, MA 01803, USA
525 B Street, Suite 1900, San Diego, CA 92101-4495, USA

First edition 2008

ISBN: 978-0-12-374294-0
ISSN: 0066-4103

Printed and bound in USA

08 09 10 11 12 10 9 8 7 6 5 4 3 2 1

CONTENTS

CONTRIBUTORS

Michèle Auger
Département de Chimie, CERSIM, CREFSIP, Université Laval, Québec, Québec, Canada, G1 K 7P4

Alex D. Bain
Department of Chemistry, McMaster University, 1280 Main St. West, Hamilton, Ontario, Canada L8S 4M1

Laurence Carlton
Molecular Sciences Institute, School of Chemistry, University of the Witwatersrand, Johannesburg, South Africa

Jonathan A. Iggo
Department of Chemistry, University of Liverpool, Donnan and Robert Robinson Laboratories, Oxford Street, Liverpool L69 7ZD, UK

Jianke Liu
Department of Chemistry, University of Liverpool, Donnan and Robert Robinson Laboratories, Oxford Street, Liverpool L69 7ZD, UK

Marise Ouellet
Département de Chimie, CERSIM, CREFSIP, Université Laval, Québec, Québec, Canada, G1 K 7P4

Gillian Overend
Department of Chemistry, University of Liverpool, Donnan and Robert Robinson Laboratories, Oxford Street, Liverpool L69 7ZD, UK

This page intentionally left blank

PREFACE

The catholic nature of NMR is clearly demonstrated by the wide selection of topics covered in this volume of Annual Reports on NMR. In common with previous members of this series, Volume 63 features accounts of progress in six diverse areas of NMR spectroscopy.

The volume commences with a review on 'Structure and Membrane Interactions of Antimicrobial Peptides as Viewed by Solid-State NMR Spectroscopy' by M. Ouellet and M. Auger; the topic of 'Chemical Exchange' is covered by A.D. Bain; L. Carlton reports on 'Rhodium-103 NMR'; J.A. Iggo, J. Liu and G. Overend review 'The Indirect Detection of Metal Nuclei by Correlation Spectroscopy (HSQC and HMQC)'.

It gives me great pleasure to thank all of these reporters for their very interesting contributions on recent research developments in their chosen areas of activity. My thanks are also due to the production staff at Elsevier for their assistance in the production of regular volumes of Annual Reports on NMR.

G.A. Webb
Royal Society of Chemistry
Burlington House
Piccadilly
London, UK

This page intentionally left blank

CHAPTER 1

Structure and Membrane Interactions of Antimicrobial Peptides as Viewed by Solid-State NMR Spectroscopy

Marise Ouellet and **Michèle Auger**

Contents

Abstract

Solid-state NMR spectroscopy is a well-suited technique to study the membrane interactions of antimicrobial peptides by taking advantage of the orientational dependence of nuclear spin interactions. This paper discusses several solid-state NMR experiments to extract information on the peptide structure and dynamics as well as on the effect of antimicrobial peptides on model membranes. More specifically, studies of peptide dynamics by ^{13}C and ^{15}N CP MAS and static experiments are reported. Also, the peptide orientation and location in membranes can be extracted from ^{15}N 1D NMR spectra and spin diffusion NMR, whereas PISEMA experiments that correlate ^{15}N chemical shifts and ^{15}N–^{1}H dipolar couplings allow the complete determination of membrane topology by specifying the peptide orientation and tilt angle. In addition, examples of peptide structure determination by isotropic chemical shifts, internuclear distance and torsion angle

Département de Chimie, CERSIM, CREFSIP, Université Laval, Québec, Québec, Canada, G1K 7P4

Annual Reports on NMR Spectroscopy, Volume 63
ISSN 0066-4103, DOI 10.1016/S0066-4103(07)63001-4

measurements are described. Finally, ^{31}P NMR and ^{2}H NMR experiments are commonly used to obtain information on both the polar region and the hydrophobic core of phospholipid bilayers. ^{31}P NMR spectra reflect the nature of lipid phases and the conformation of the phospholipid polar headgroup, whereas ^{2}H NMR spectra are indicative of acyl chain orientational order.

1. INTRODUCTION

The need to discover and develop novel antimicrobial compounds defeating the known mechanisms of bacterial resistance by the use of novel modes of action is becoming increasingly important due to the dramatic increase in bacterial resistance to numerous conventional antibiotics.[1] In recent years, there has therefore been an increased popularity in the investigation of antimicrobial peptides that are found in several organisms and for which the structural and functional characteristics make them very promising therapeutic agents.[2–7] Even though the exact mechanisms of action by which these antimicrobial peptides kill bacteria are still not completely understood, several studies have demonstrated that the interactions between antimicrobial peptides and the lipid membrane, leading to an increase in membrane permeability, play a major role in antimicrobial activity. In addition, because of these interactions, the antimicrobial peptides adopt a three-dimensional structure resulting in an amphipathic character.[8–10] One of the most important factors that affects the activity of antimicrobial peptides appears to be the amphipathic character that is essential for the affinity of these peptidic units for the lipid bilayer.[11–13] Several general mechanisms have been proposed in the literature in light of these studies to explain the membrane permeability caused by membrane-active peptides, and more specifically antimicrobial peptides. These general mechanisms, namely the ''barrel-stave'', ''carpet-like'' and ''toroidal'' models, [14,15] are illustrated in Figure 1.

One of the best suited techniques to investigate the structure and dynamics of peptides in interaction with anisotropic lipid membranes is solid-state nuclear magnetic resonance (NMR) spectroscopy.[16–18] Several approaches have been developed to study these systems in which the restricted molecular motions leading to anisotropic nuclear spin interactions result in broad NMR spectra. An overview of the use of solid-state NMR spectroscopy to investigate both the structure and dynamics of antimicrobial peptides in interaction with membranes as well as the effects of antimicrobial peptides on membrane integrity are presented in this manuscript. Numerous techniques to investigate the structure, topology and dynamics of antimicrobial peptides in membranes will be presented in the first section while the second part will be devoted to the use of ^{31}P and ^{2}H solid-state NMR spectroscopy to study the effect of antimicrobial peptides on the hydrophilic and hydrophobic regions of lipid bilayers. Both sections will be supported by recent examples.

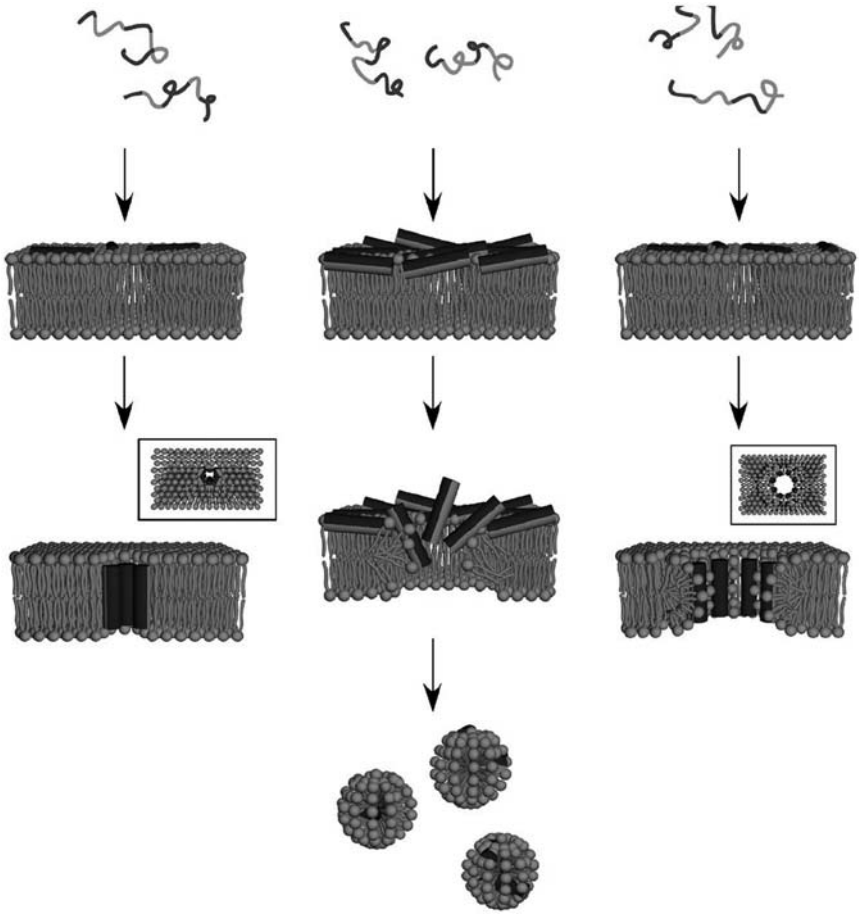

Figure 1 Cartoon illustrating membrane permeabilization mechanisms of antimicrobial peptides, namely the barrel-stave (*left row*), the carpet-like (*middle row*) and the toroidal (*right row*) models. The hydrophilic and hydrophobic faces of the peptide are coloured in black and grey, respectively. Top views are displayed for barrel and toroidal pores. Adapted from ref. 102 and reproduced with permissions.

2. STUDY OF ANTIMICROBIAL PEPTIDES IN MEMBRANES

The structure and dynamics of peptides that are immobilized on the relevant NMR time scale[17,19–21] can be investigated using solid-state NMR spectroscopy. Orientation-dependent shifts and splittings of the peptide resonances occur due to the anisotropic interactions that dominate solid-state NMR spectra. The study of NMR parameters such as the ^{15}N and ^{13}C chemical shifts and chemical shift anisotropy (CSA), and the dipolar couplings between ^{1}H, ^{13}C and ^{15}N is therefore of great interest. This section will demonstrate how these parameters can be

exploited to obtain information on the structure and dynamics of antimicrobial peptides in interaction with lipids.

2.1 Dynamics of antimicrobial peptides

The analysis of the spinning sideband intensity in magic-angle spinning (MAS) ^{13}C or ^{15}N spectra or of the CSA in static spectra can provide information about the dynamics of antimicrobial peptides incorporated into lipid membranes. The dynamics of the 18-residue antimicrobial peptide protegrin (PG-1) has been investigated by Buffy et al.[22] using MAS spectra and this study has demonstrated that the dynamics differs depending on the lipid membrane composition. As shown in Figure 2, the intensity of the spinning sidebands in ^{13}C NMR MAS

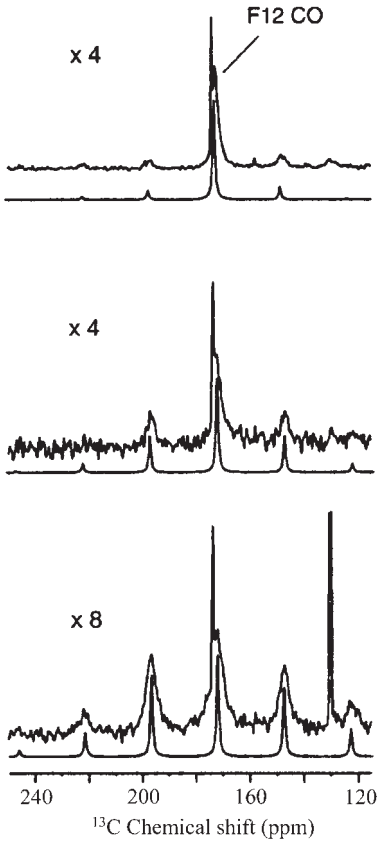

Figure 2 ^{13}C CP-MAS spectra of the F12 ^{13}CO- and L5 $^{13}C_{\alpha}$-labelled Protegrin-1 peptide in DLPC (T=295 K) (*top row*), DMPC (T=313 K) (*middle row*) and POPC (T=295 K) (*bottom row*) bilayers with 2.5 kHz spinning. Best fits for the carbonyl spinning sideband patterns are shown below each experimental spectrum. Adapted from ref. 22 and reproduced with permissions.

spectra of the ^{13}C labelled peptide is less important in dilauroylphosphatidylcholine (DLPC) bilayers compared to dimyristoylphosphatidylcholine (DMPC) and palmitoyloleoylphosphatidylcholine (POPC) bilayers, indicating a more rigid peptide in thicker lipid bilayers. The analysis of the $^{13}C_\alpha$–H_α dipolar couplings for the Leu5 residue, which are 11.9 kHz in POPC and 2.0 kHz in DLPC, yielded similar results. The dynamics of PG-1 in DLPC bilayers was also investigated by Yamaguchi et al.[23] using static ^{15}N NMR spectroscopy. The decrease of the ^{15}N CSA observed for PG-1 in lipid bilayers indicates increased motion compared to the static peptide. Buffy et al.[24] have also performed similar studies with the cyclic antimicrobial peptide RTD-1 and the analysis of the spinning sidebands in ^{15}N and ^{13}C MAS spectra for the solid peptide and the peptide incorporated into DLPC bilayers demonstrated that the peptide is immobilized in bilayers.

2.2 Membrane orientation and topology of antimicrobial peptides

The membrane orientation of antimicrobial peptides can be determined using samples oriented with their normal parallel to the external magnetic field B_0. These samples can be obtained by the mechanical alignment of the lipids between glass plates[25] and the use of lanthanide-doped bicelles[26] and these experiments are performed with peptides either selectively or uniformly labelled with ^{15}N and/or ^{13}C.

2.2.1 Membrane orientation from 1D spectra

The chemical shift obtained in samples oriented in the magnetic field B_0 can be used to determine the membrane orientation of helicoidal antimicrobial peptides selectively ^{15}N labelled at one position in the amino acid sequence. In particular, the σ_{33} element of the ^{15}N CSA tensor is aligned along the NH bond for a α-helical peptide, and the NH bond vector is almost parallel to the helix axis. The peptide orientation can therefore be estimated by the analysis of the ^{15}N chemical shift[27] as illustrated in Figure 3. For peptides in β-sheet conformation, the situation is however more complex since the membrane orientation has to be determined from both the ^{13}C and ^{15}N chemical shifts of the carbonyl and amide groups, respectively. Since the majority of antimicrobial peptides present a helicoidal structure, these will be discussed in the present review. For more information about β-sheet peptides, the reader is referred to Buffy et al.[24] and Yamaguchi et al.[23]

Yamaguchi et al.[28] have investigated the 18-residue antimicrobial peptide ovispirin, which presents a large spectrum of activity. They have demonstrated, by selectively ^{15}N labelling the peptide at residues Leu3, Ile6, Ile11 and Gly18, that ovispirin adopts a surface orientation in bilayers of POPC and palmitoyloleoylphosphatidylglycerol (POPG) (3 : 1), except for a small portion of the C-terminal region of the helix which appears to deviate from the surface of the bilayer. In addition, the analysis of the ^{15}N CSA of the peptide incorporated into a non-oriented POPC/POPG system indicates that ovispirin undergoes uniaxial rotational diffusion around the bilayer normal. This is reflected in the ^{15}N spectra by a decrease of the CSA compared to that of a powder spectrum, namely a decrease from 150 ppm to 75 ppm. The membrane orientation of the peptide

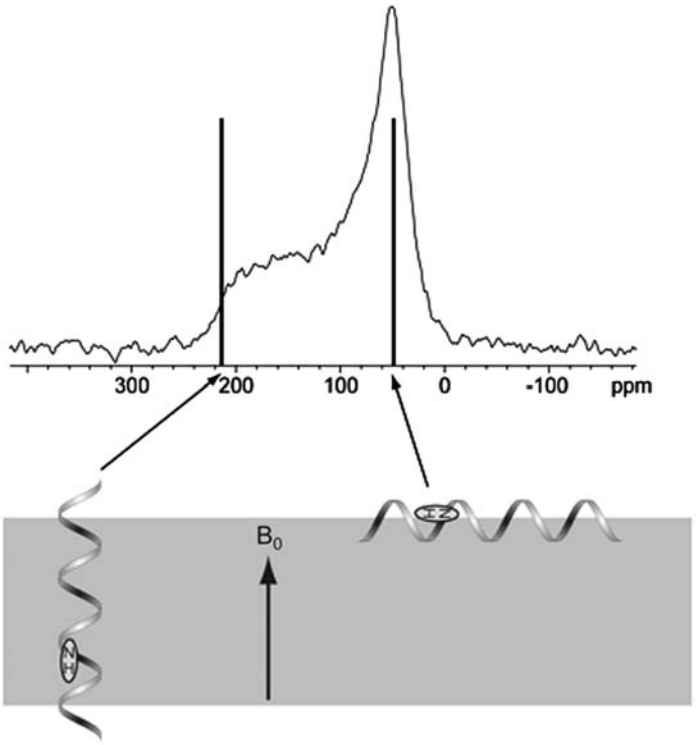

Figure 3 Membrane topology of a ^{15}N labelled α-helical peptide in a lipid bilayer. The helical peptide in a transmembrane orientation gives chemical shift close to 200 ppm which corresponds to the downfield edge of the ^{15}N powder pattern. A peptide flat on the bilayer surface gives a chemical shift close to 50 ppm which corresponds to the upfield edge of the ^{15}N powder pattern. Adapted from ref. 27 and reproduced with permissions.

cecropin A incorporated into DMPC/dimyristoylphosphatidylglycerol (DMPG) (4:1) membranes has also been determined by Marassi et al.[29] using a similar approach. The oriented and non-oriented ^{15}N NMR spectra of cecropin A selectively labelled at residues Val11 and Ala27 indicate that the peptide is oriented perpendicular to the membrane normal and is immobile relative to the NMR time scale. The membrane orientation of a series of magainin analogues, namely MSI-78, MSI-594 and MSI-843, has also been investigated by 1D ^{15}N NMR spectroscopy to determine the type of membrane perturbation induced by these peptides.[30] Results obtained by Thennarasu et al. on oriented bilayers of different lipidic composition such as POPC, POPG, POPC/POPG (3:1) and *E. coli* membranes revealed that the peptides induce membrane curvature strains leading to the membrane permeabilization. They also studied the membrane behaviour of the cyclic antimicrobial peptide subtilosin A at different concentrations in POPC, POPG and DMPC bilayers.[31] Their results suggest that the subtilosin A peptide does not permeabilize membranes by forming pores like

other cyclic antimicrobial peptides, but it seems to induce local defects which may lead to membrane permeabilization.

Bechinger et al.[32] have investigated the membrane orientation of the 21-residue antimicrobial peptide PGLa from ^{15}N NMR spectra of the peptide incorporated into bilayers oriented between glass plates. More specifically, they have synthesized several peptides selectively ^{15}N labelled at residues Ala3, Ala10, Ala14, Val16 and Ala20 and incorporated these peptides into palmitoyloleoylphosphatidylethanolamine (POPE) and POPG (3 : 1) bilayers. The determination of both the orientation and dynamics of these residues along the peptide backbone via the chemical shift values was possible because of this multiple labelling scheme. Their results demonstrate a surface orientation for residues Ala10 to Ala20, while residue Ala3 has an isotropic chemical shift characteristic of a higher degree of liberty in the N-terminal region. The ^{15}N NMR spectra of non-oriented samples in which an increase of the CSA is observed from the N-terminal to the C-terminal regions also confirm the conclusion regarding the dynamics of several residues.

Finally, the last example presented in this section is related to the determination of the membrane orientation of the β-sheet antimicrobial peptide tachyplesin I without macroscopic sample alignment by using powder samples and the rotational diffusion approach.[33] Hong and Doherty showed that motionally averaged ^{13}C and ^{15}N NMR powder spectra have their 0° frequency, corresponding to the downfield edge of the powder spectra, at the same frequency of the 0° peak in oriented samples. This approach has been useful to determine the surface orientation of the peptide tachyplesin I in DLPC membranes. Also, this technique has a great potential in the determination of membrane orientation of peptides that cannot be reconstituted in bilayers stacked between glass plates due to their size and/or lipid alignment defects induced by the peptide binding.

Even though the membrane orientation of antimicrobial peptides can be estimated from one-dimensional ^{15}N NMR spectra, this approach does not allow the determination of the peptide tilt angle with great precision for peptides singly labelled at one amino acid residue. However, as discussed in the next section, this type of analysis can be carried out using peptides ^{15}N labelled at multiple sites on a single peptide.

2.2.2 The PISEMA approach

The PISEMA (polarization inversion spin-exchange at the magic-angle) technique combines the measurement of both the ^{15}N CSA and the dipolar coupling between the ^{15}N and ^{1}H nuclei of the amide group.[34] Figure 4 illustrates 2D PISEMA spectra of fully ^{15}N labelled peptides assuming helicoidal, β-strand-I and β-strand-II conformations. Regular patterns called PISA (polar index slant angle) wheels are formed by the resonances and it is possible from these patterns to extract both the tilt and rotation angle of the peptide.[34–37] The use of oriented samples in the magnetic field is also required with this approach.

Magainin, a 23-residue peptide of amphibian origin, is one of the antimicrobial peptides most studied using the PISEMA approach. Magainin had

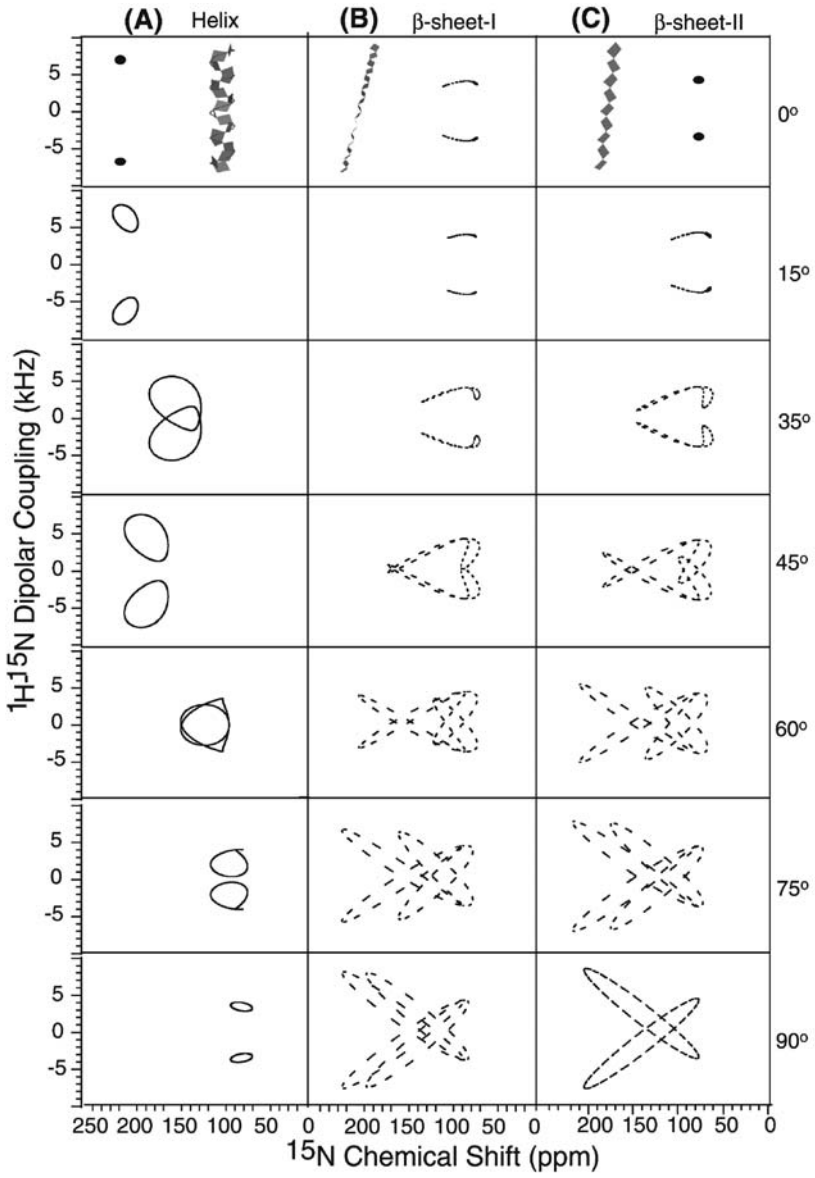

Figure 4 Two-dimensional simulated PISEMA spectra calculated for a 300-residue polyalanine peptide in (A) α-helical, (B) β-strand-I and (C) β-strand-II conformations at different tilt angles from 0° to 90°. The principal values and molecular orientation of the ^{15}N chemical shift tensor (δ_{33}=64 ppm; δ_{22}=77 ppm; δ_{11}=217 ppm; δ_{33} $\angle$NH=17°), and the NH bond distance (1.07 Å) were used in the simulation. Adapted from ref. 34 and reproduced with permissions.

been shown to adopt a surface orientation in lipid bilayers[38] but the rotation angle could not be determined from 1D ^{15}N NMR spectra. However, Marassi et al. have confirmed using the PISEMA approach that magainin is oriented perpendicular to the membrane normal. In addition, they have determined the polarity of the α-helix, namely a helix oriented in such a way that residues Phe5, Phe12 and Phe16 are at the apolar/polar interface, with charged residues such as lysines exposed to the hydrophilic side of the bilayer.[39] The observation of well-resolved single resonances from individual backbone amide sites in the PISEMA spectrum also indicates that magainin binds tightly to the membrane surface with a unique orientation. The study of a peptide from a fragment of the C-terminal region of colicin B, a channel bacterial toxin,[40] is also another very interesting example demonstrating the potential of the PISEMA approach in the structural study of peptides. More specifically, the mode of insertion of colicin B in POPC/POPG (4 : 1) bilayers has been determined by Lambotte et al.[40] using the PISEMA approach. The detailed analysis of the PISEMA spectra indicates regions characteristic of both transmembrane and in-plane helices. These results suggest that colicin B preferentially adopts an ''umbrella'' type conformation in lipid bilayers. Another peptide from the same family as colicin B, namely colicin E1, has also been studied by the PISEMA approach.[41]

2.2.3 ^{1}H spin diffusion

Another approach that has been used to investigate the approximate location of peptides or proteins in lipid bilayers is the ^{1}H spin diffusion 2D NMR technique under MAS.[42] ^{1}H magnetization is transferred from mobile lipids to the rigid peptide via distance-dependent ^{1}H–^{1}H dipolar couplings (see Figure 5(A)). The 2D peak intensities as a function of the spin-diffusion mixing time yield a magnetization transfer curve that reflects the proximity of the lipid protons to the peptide protons since the rate of spin diffusion is greater in rigid media such as peptides compared to that in mobile media such as lipids. Huster et al.[43] have investigated the membrane topology of the bacterial peptide colicin Ia in interaction with POPC/POPG (3 : 1) bilayers using ^{1}H spin diffusion by selectively labelling the peptide with ^{13}C on the α-carbon of the Ala13 residue. Previous studies had revealed that colicin Ia is incorporated in the bilayer, without any information however on its degree of insertion. As illustrated on the spin-diffusion curves in Figure 5(B), these authors have observed a fast magnetization transfer between C_{α}Ala13 and the lipid terminal CH_3 groups, estimating from simulation a distance of 2–4 Å between these two moieties. Magnetization transfers have also been observed between C_{α}Ala13 and other regions of the lipid, namely the acyl chain CH_2 groups and the lipid polar headgroup. This model of interaction is in agreement with the ''umbrella'' model, which can explain the contact of the peptide with both the lipid polar headgroup and acyl chains.

Buffy et al.[44] have also investigated the membrane topology of another antimicrobial peptide, PG-1, by ^{1}H spin diffusion. They have determined that PG-1, like colicin Ia, is in contact with both the lipid polar headgroup and the acyl chains when incorporated into POPC bilayers. However, the proposed mode of

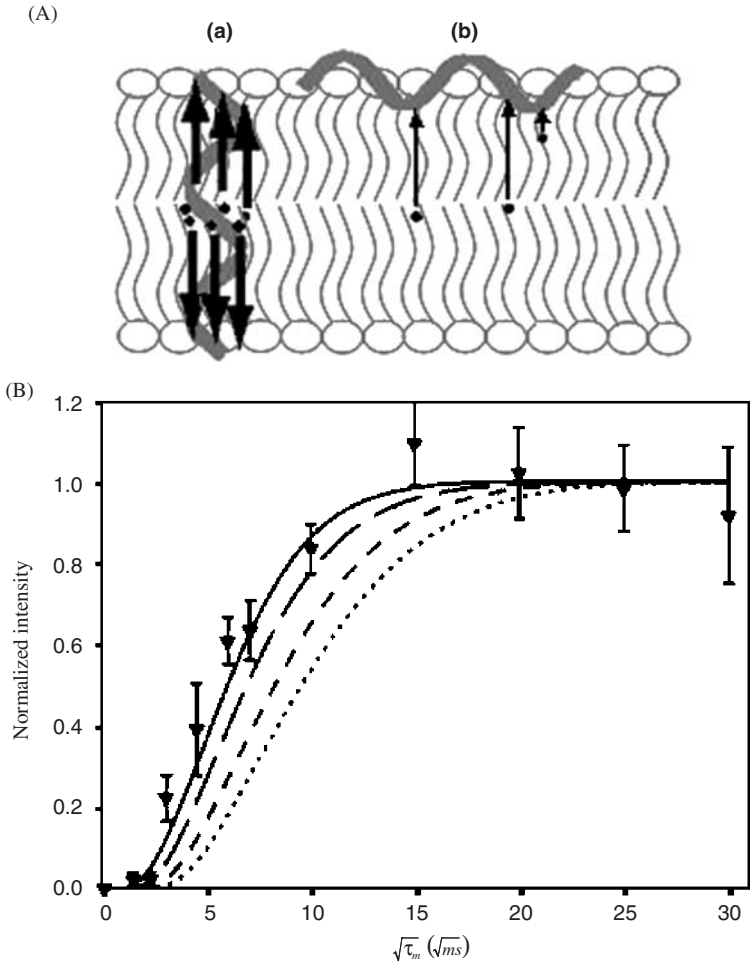

Figure 5 (A) Illustration of a (a) transmembrane and (b) interface-bound α-helical peptide in a lipid bilayer. Thick arrows represent the fast spin diffusion between the lipid chain terminus and the transmembrane peptide. The thin arrows illustrate the slow spin diffusion through the lipid chain terminus and the interface-bound peptide. (B) Experimental data points and simulated spin-diffusion curves from lipid methyl protons to the colicin peptide for methyl/peptide distances of 2 Å (solid line), 4 Å (long dashed line), 6 Å (short dashed line) and 8 Å (dotted line). The 2 Å curve best fits the experimental data. Adapted from ref. 43 and reproduced with permissions.

interaction is different, being more similar to the toroidal model where the PG-1 aggregates only need to span one monolayer to create the pore. The same research group has also determined the degree of penetration of PG-1 in DLPC bilayers using the paramagnetic ion Mn^{2+}.[44] A comparison of the T_2 relaxation enhancement of PG-1 carbons to that of the lipid carbons reveals that the relative

depth of PG-1 with respect to the lipid moieties can be determined. These results demonstrate that PG-1 is completely inserted in the bilayer and tilted from the bilayer normal, with Val16 as the most deeply embedded residue and Gly2 as the closest to the membrane surface phosphate group. The proposed mode of interaction is the ''snorkel'' model, where the peptide hydrophobic residues are incorporated into the bilayer while the polar residues remain in contact with the aqueous phase.

2.3 Secondary structure of antimicrobial peptides

Several studies have demonstrated that most antimicrobial peptides adopt a random conformation in solution and defined secondary structures, such as α-helices and β-sheets, only upon interaction with the membrane. The study of the secondary structure of antimicrobial peptides incorporated into membranes is therefore very interesting. Several experiments designed to provide information on the conformation of antimicrobial peptides will be presented in the next section.

2.3.1 ^{13}C isotropic chemical shifts

The secondary structure of a specifically ^{13}C labelled residue in an antimicrobial peptide can be determined by measuring its isotropic chemical shift in MAS spectra. In this simple approach, the values of the carbonyl and C_α chemical shifts for several amino acids are dependent on the peptide secondary structure.[45] The structure of melittin, a peptide that possesses both haemolytic and antimicrobial activities, in interaction with DMPC membranes has been investigated by Naito et al.[46] Isotropic chemical shifts of 173.2 ppm and 15.8 ppm have been obtained for melittin labelled at residues [1-^{13}C]Gly3 and [3-^{13}C]Ala15, confirming the α-helicoidal structure for this peptide. The helicoidal structure of the human peptide LL-37 has also been determined from the isotropic chemical shifts of 175.8 ppm and 53.5 ppm for the [^{13}C=O]Leu31 and [$^{13}C_\alpha$]Ala13 residues, respectively.[47]

2.3.2 Internuclear distances

The rotational echo double resonance (REDOR) and rotational resonance (RR) are most often used for the measurement of homo- and heteronuclear distances in solid-state MAS NMR spectra of antimicrobial peptides.[48–52] The dephasing of the magnetization of the observed nucleus (typically ^{13}C) due to the coupling with a second nuclear spin (typically ^{15}N) is the basis of the REDOR technique. The difference in the intensity of the spectra obtained with and without the ^{15}N pulses depends solely on the ^{13}C–^{15}N dipolar coupling, and this coupling is related to the heteronuclear distance between the nuclei. A dephasing curve is obtained as a function of mixing time from the dephased ^{13}C{^{15}N} NMR spectra, from which the distance can be extracted. As shown in the examples discussed below, the REDOR technique can also be used to remove the natural abundance contribution of the lipid carbons in ^{13}C NMR spectra.

Porcelli et al.[53] have investigated the structure of the 33-residue antimicrobial peptide pardaxin. A bend-helix-bend-helix conformation had first been

determined in sodium dodecylphosphocholine (DPC) micelles by ^{1}H solution NMR and the REDOR technique was then used to confirm the helicoidal structure in the C-terminal region of this peptide selectively ^{13}C and ^{15}N labelled at residues Leu18 and Leu19 and incorporated into DMPC, POPC and POPE/POPG (3:1) multilamellar vesicles.[53] More specifically, the $^{13}C\{^{15}N\}$ REDOR dephased spectra of pardaxin consist of a single peak with a frequency value of approximately 176 ppm, consistent with the helical conformation of this C-terminal segment. Another example of structural studies of antimicrobial peptides by REDOR is related to the synthetic peptide K3, a 21-residue analogue of the natural peptide magainin, in interaction with dipalmitoylphosphatidylcholine/dipalmitoylphosphatidylglycerol (DPPC/DPPG) (1:1) bilayers.[54] The authors have determined the structure of the magainin analogue bound to lipid membranes by analysing ^{13}C chemical shifts and by using the REDOR technique in this case as a spectral editing tool to minimize the ^{13}C lipid background signal. The REDOR spectra are displayed in Figure 6. More specifically, by analysing the isotropic chemical shifts in the REDOR spectra of residues [1-^{13}C]Ala17 and [3-^{13}C]Ala3 dephased by residues [^{15}N]Gly18 and [^{15}N]Gly4, they have concluded that the isotropic chemical shifts of 177 ppm and 16 ppm are only consistent with a single α-helical structure for the K3 peptide.

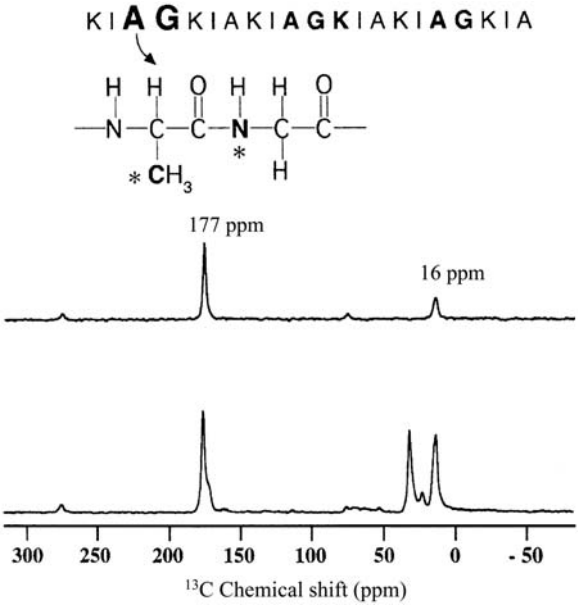

Figure 6 Solid-state $^{13}C\{^{15}N\}$ REDOR spectra of [3-^{13}C]Ala3-[^{15}N]Gly4-[1-^{13}C]Ala10-[2-^{13}C]Gly11-[6-^{15}N]Lys12-[1-^{13}C]Ala17-[^{15}N]Gly18-(KIAGKIA)$_3$-NH_2 incorporated into multilamellar vesicles of DPPC/DPPG (1:1) at a lipid/peptide molar ratio of 10:1, after 48 rotor cycles of dipolar evolution with MAS at 5,000 Hz. The difference (ΔS) and full-echo (S_0) spectra are shown on top and bottom rows. Adapted from ref. 54 and reproduced with permissions.

The fast magnetization exchange between two spins when the sample spinning speed (ν_r) is equal to the frequency separation ($\Delta\nu$) of the two resonances for the two spins, i.e., when $\Delta\nu = n\nu_r$, where n=1, 2, 3, etc. is the basis of the RR method. The reintroduction of the dipolar coupling gives rise to magnetization exchange between the two spins, and a magnetization exchange curve as a function of mixing time is obtained and fitted to a specific homonuclear distance between these two spins.

An interesting example of the RR technique is the structural study of gramicidin S, a bacterial antimicrobial peptide.[55] In this case, homonuclear distances between two ^{19}F nuclei have been measured from static spectra using a modified CPMG (Carr–Purcell–Meiboom–Gill) sequence.[56] The conformation of gramicidin S had previously been determined as a cyclic antiparallel β-sheet peptide by ^{1}H solution NMR and X-ray crystallography and by studying gramicidin S in which the Leu3 and Leu8 residues have been replaced by the non-natural amino acid 4F-phenylglycine (4F-Phg). Lam et al.[57] have also illustrated the potential of the RR technique for the structural study of the antimicrobial peptide melittin in interaction with ditetradecylphosphatidylcholine (DTPC) membranes. Several peptides ^{13}C labelled at different positions along the amino acid sequence have been synthesized and for example, a distance of (2.5 ± 0.2) Å has been obtained between residues [^{13}C=O]Gly3 and [$^{13}C_\alpha$]Ala4. This homonuclear distance is consistent with the expected α-helical structure.

2.3.3 Torsion angles

The measurement of internuclear distances in the structural study of antimicrobial peptides can be complemented by a variety of experiments that have recently been developed to determine the torsion angles (ϕ and ψ) between peptide planes in peptides and proteins. These techniques have been mostly applied so far to peptides with only a few amino acid residues. However, the application of these techniques to antimicrobial peptides is growing, and the results obtained are really promising. The basic principle in the measurement of torsion angles lies in the correlation between the orientation of two anisotropic tensors, such as two dipolar tensors, two CSA tensors, or one CSA and one dipolar tensors. Since most experiments require the use of MAS, the interactions averaged out by MAS are reintroduced via specific pulse sequences, as is the case for the internuclear distance measurement techniques described above.

The mono- and tripeptides *N*-acetyl-D, L-valine (NAV) and *N*-formyl-[U-^{13}C, ^{15}N]Met-Leu-Phe (MLF) have been used by several research groups as model peptides for the development of torsion angle measurement experiments since the crystalline structure of these peptides has been determined by X-ray crystallography. For example, the torsion angle ψ for the tripeptide MLF has been determined by Ladizhansky et al.[58] with a HCCN dipolar correlation MAS experiment that measures ψ in the angular range of -20° to -70°, characteristic of α-helices. The monopeptide NAV was used by Hong et al.[59] to determine the torsion angle ϕ via the correlation of the ^{15}N chemical shift and C_α–H_α dipolar coupling tensor orientations under MAS. Their results indicate that the technique exhibits the highest sensitivity to ϕ angles typical of β-sheet conformations

($\phi \approx -140^\circ$). This angle has also been determined by the measurement of the relative orientation of the N–H_N and C_α–H_α bonds, which is manifested in the rotational sideband spectrum of the sum and difference of the two corresponding dipolar couplings, and they obtained a ϕ angle of –135°.[60] Both techniques applied on the monopeptide NAV are in good agreement with the angle of –136.5° determined by X-ray diffraction. Recently, Doherty et al.[61] have determined torsion angles (ϕ,ψ) for the antimicrobial peptide tachyplesin I bound to DMPC bilayers. The HNCH technique allowed the accurate determination of the ϕ angle by correlating dipolar coupling between $^1H^N$–^{15}N and $^{13}C_\alpha$–$^1H_\alpha$ of residue Val6. On the other hand, the NCCN technique allowed the measurement of the ψ angle by correlating the dipolar coupling between $^{15}N_i$–$^{13}C_{\alpha i}$ and $^{13}CO_i$–$^{15}N_{i+1}$. As displayed in Figure 7, by the use of spectral simulations, they have extracted $|\phi|$ and $|\psi|$ values of $167 \pm 10^\circ$ and $142 \pm 2^\circ$,

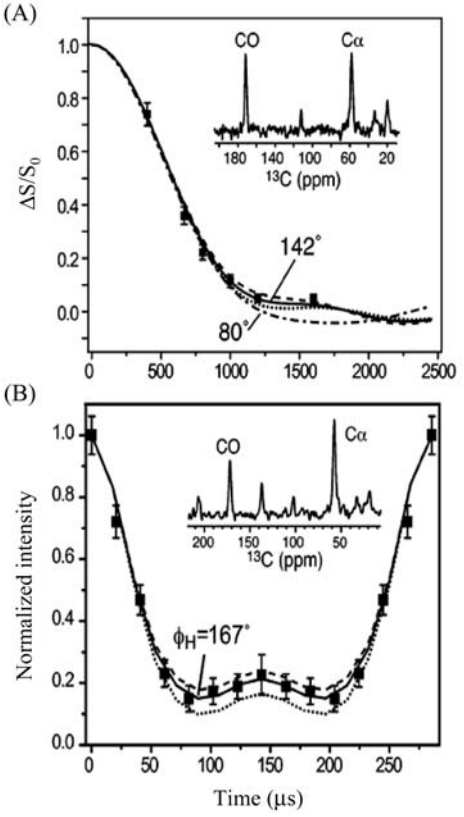

Figure 7 Determination of ϕ and ψ torsion angles of Val6 of antimicrobial peptide tachyplesin I in DMPC bilayers at 233 K. (A) NCCN experimental data for the ψ angle determination with corresponding simulated curves. The best fit is obtained with ψ angle of $\pm 142°$. (B) HNCH experimental data for the ϕ angle determination with corresponding simulated curves. The best fit is obtained with a ϕ_H angle of $\pm 167°$. Adapted from ref. 61 and reproduced with permissions.

which correspond to an antiparallel β-sheet conformation. The pairs of torsion angles (ϕ,ψ) can also be determined simultaneously by 2D spin diffusion solid-state NMR experiments under off MAS[62–64] or using the Double Quantum Spectroscopy (DOQSY) approach.[65,66]

The validity of a new technique to measure torsion angles in larger peptides has been demonstrated by Gabrys et al.[67] using melittin. This method relies on 2D slow-spinning, rotor-synchronized MAS exchange spectroscopy (SSRS-MASE), in which the relative CSA tensor orientation is extracted from the intensity of the off-diagonal cross-peaks on the 2D spectrum, since these intensities are related to the magnetization transfer between the two coupled sites. The (ϕ,ψ) torsion angles can be extracted after simulation of the experimental spectrum and the results once again confirm that melittin adopts a helicoidal structure when incorporated into lipid bilayers.

3. EFFECTS OF ANTIMICROBIAL PEPTIDES ON MODEL LIPID MEMBRANES

3.1 ^{31}P NMR spectroscopy[68,69]

Phosphorus-31 NMR spectroscopy is a very sensitive and useful technique to investigate the structure and dynamics of the polar headgroup of phospholipids, which are the main constituent of biological membranes.[70] Several approaches can be taken, in particular the measurement of static ^{31}P NMR spectra which are dominated by the CSA, the use of the MAS technique which averages the CSA to its isotropic values,[71] and finally the use of samples macroscopically oriented in the magnetic field.

The nature of the lipid phase is one of the main information that can be obtained from static ^{31}P NMR spectra. More specifically, the interactions between lipids and antimicrobial peptides can lead to the formation of non-lamellar phases, such as isotropic, cubic and hexagonal phases. This has been observed with several antimicrobial peptides of amphibian origin such as caerin 1.1, maculatin 1.1 and caerin 4.1 for which the ^{31}P NMR spectra have revealed the formation of isotropic or cubic structures within the lipid system,[72] as well as for bacterial antimicrobial peptides such as gramicidin S, A and D which are known to induce a hexagonal phase in model membranes.[73–75]

The study of the dynamics and orientation of the lipid polar headgroup is another interesting application of ^{31}P NMR spectroscopy. In fact, several natural and synthetic membrane-active peptides have demonstrated a strong interaction with the polar headgroup and this is reflected in the ^{31}P NMR spectra by a change of the CSA.[76,77] This change of CSA can be expressed in a quantitative way by calculating an order parameter S_2 which is governed by the lipid dynamics and/or orientation and which compares the CSA of two systems.[78] S_2 can vary from 1 for a lipid system in which the dynamics is the same as that in the reference system, namely the pure lipid system without the peptide, to 0 if the peptide-containing system is totally isotropic. Also, the ^{31}P NMR spectra line

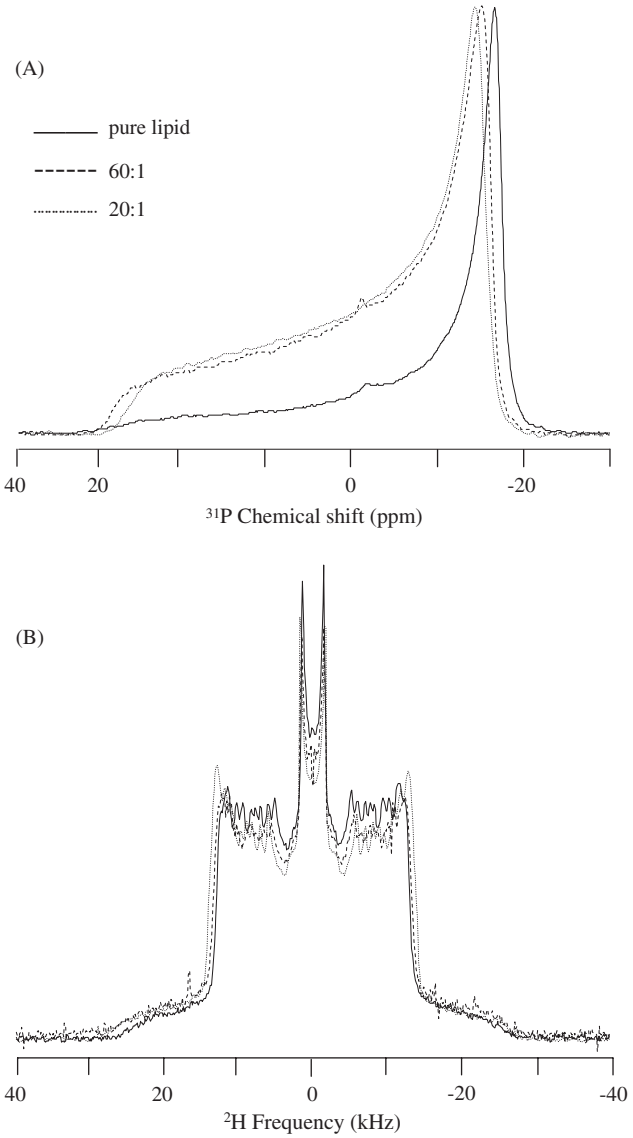

Figure 8 (A) ^{31}P and (B) ^{2}H NMR spectra of DMPC multilamellar vesicles at 37°C in the absence and presence of the 14-mer peptide at lipid/peptide molar ratios of 60:1 and 20:1. Adapted from ref. 77 and reproduced with permissions.

shape is sensitive to the macroscopic orientational degree of model membranes in the magnetic field, and the orientational degree is function of the bilayer composition and fluidity.[79,80]

An example is illustrated in Figure 8(A) for a membrane-active synthetic 14-mer peptide incorporated in DMPC multilamellar vesicles.[77] This synthetic 14-mer peptide, which is composed of leucines and phenylalanines modified by

the addition of crown ethers, has been synthesized to study the membrane interactions involved in the haemolytic activity of antimicrobial peptides.[81,82] An order parameter, denoted S_1, can also be calculated from ^{31}P NMR spectra to quantitatively measure the degree of macroscopic orientation of model membranes in the magnetic field, and it takes the form

$$S_1 = \frac{M_1 - \delta_{iso}}{(-2\delta_{\perp} - \delta_{iso})} = \frac{M_1 - \delta_{iso}}{\delta} \quad (1)$$

where M_1 is the first spectral moment, δ_{iso} the isotropic chemical shift, and δ the CSA calculated from the perpendicular chemical shift $\delta_{\perp}$ and δ_{iso}.[78,83] S_1 order parameter values close to 1 indicate that all molecules are oriented with their main axis parallel to the magnetic field, whereas S_1 values close to -0.5 indicate that the molecule main axes are nearly perpendicular to the magnetic field. As shown in Figure 8(A), the S_1 order parameter of the 14-mer peptide-containing vesicles are -0.02 and -0.01 for lipid/peptide molar ratios of 60 : 1 and 20 : 1 compared to the S_1 order parameter of -0.17 for the pure lipid system. These results indicate that the peptide-containing vesicles are more spherical than the lipid ellipsoidal vesicles without the 14-mer peptide. Also, S_2 order parameter values of 0.91 and 0.86 for lipid/peptide molar ratios of 60 : 1 and 20 : 1 indicate that the 14-mer peptide perturbs the dynamics and/or orientation of DMPC lipid polar headgroups.

The dynamics and orientation of the lipid polar headgroup can also be studied in mechanically aligned bilayers stacked between glass plates, with the bilayer normal parallel to the magnetic field direction. This technique is used to determine the alignment quality of oriented samples to be used for the determination of the membrane orientation of peptides, as discussed previously in this manuscript. These experiments also give information on the lipid phase and constraints induced by membrane-active peptides to the oriented bilayers. Dynamics and/or orientation perturbation induced at the lipid polar headgroup by a great variety of antimicrobial peptides, namely PG-1, subtilosin A, alamethicin, MSI-78, MSI-843 and MSI-594 magainin analogues, have been investigated in oriented bilayers stacked between glass plates.[30,31,84–87]

In addition, 2D ^{31}P exchange experiments may be used to investigate bilayer structure and dynamics upon membrane-active peptide binding.[88,89] These experiments can be performed on both unoriented and oriented bilayers, and are based on the lateral diffusion of lipid molecules within the lipidic system. Using 2D ^{31}P exchange experiments, Picard et al.[90] determined that the lateral diffusion D_L of DPPC lipids in radius-controlled supported vesicles is significantly reduced by the interaction with melittin, suggesting that the peptide strongly affects bilayer motions by hindering lipid lateral diffusion. Buffy et al. performed 2D ^{31}P exchange NMR experiments at different mixing times to determine the size of lipid structures formed in oriented bilayers of POPC/POPG upon RTD-1 peptide binding. The results suggest that the RTD-1 peptide induces the formation of lipid cylinders with diameter on the order of microns. This has been reflected in 2D ^{31}P NMR spectra by the presence of off-diagonal intensities between 0° and 90° components at a mixing time of 400 ms.[24] Finally, Mani et al.[91]

used the same approach to determine whether the isotropic phase observed on ^{31}P spectra of oriented POPC/POPG bilayers was separated from or part of lamellar bilayers. The presence of only weak cross-peaks for a mixing time range of 5–400 ms suggests that the isotropic component is not part of the oriented bilayers and resides somewhere in a separate region.

Binary lipid mixtures can be studied using the MAS technique in ^{31}P NMR spectroscopy since different lipids can be discriminated on the basis of their non-equivalent isotropic chemical shifts. For example, the interactions between the antimicrobial peptide nisin with equimolar mixtures of DMPC and DMPG has been investigated by Bonev et al.[92] and the ^{31}P MAS NMR spectra have demonstrated a preferential interaction of the peptide with the anionic lipid (DMPG). The use of samples macroscopically oriented with their normal parallel to the magnetic field B_0 is another way to investigate the effect of antimicrobial peptides on the orientational order and conformation of lipid polar headgroups. The ^{31}P NMR spectra of antimicrobial peptides studied with this approach, such as LL-37,[47] protegrin,[23] RTD-1[24] and pardaxin,[93] have demonstrated a shift of the lipid resonances towards lower frequencies, a line broadening and/or the presence of non-oriented lipid structures, depending on the peptide concentration and on the nature of the lipid investigated.

3.2 ^{2}H NMR spectroscopy

^{2}H NMR spectroscopy is a very powerful technique to study the membrane hydrophobic core by replacing the acyl chain protons by deuterons. This technique is complementary to ^{31}P NMR spectroscopy which, as demonstrated above, is used to investigate the hydrophilic region of lipid bilayers. Deuterium is a spin-1 nucleus with a quadrupole moment that interacts with the electric field gradient at the nucleus, giving rise to the quadrupolar interaction. Two spin transitions are possible and a doublet of resonances is observed on a ^{2}H NMR spectrum, separated by the quadrupolar splitting $\Delta\nu_Q$. For a system with axially symmetric motions, the quadrupolar splitting is given by

$$\Delta\nu_Q = \frac{3}{4}\left(\frac{e^2qQ}{h}\right)\left(3\cos^2\theta - 1\right)S_{CD} \tag{2}$$

where (e^2qQ/h) is the quadrupole coupling constant ($\sim$170 kHz for aliphatic C–D),[94] θ is the angle between the bilayer normal and the external magnetic field B_0 and S_{CD} is the order parameter of a deuterium bond vector. As described extensively, this order parameter is the product of several contributions, including intramolecular motions such as *trans*-gauche isomerizations, and anisotropic reorientation of the whole phospholipid molecules. Hence, it is possible to determine variations in lipid chain order by monitoring changes in $\Delta\nu_Q$ values.[95]

Examples of ^{2}H NMR spectra obtained for the 14-mer peptide incorporated in DMPC vesicles at lipid/peptide molar ratio of 60 : 1 and 20 : 1 are illustrated in Figure 8(B).[77] As revealed by the change in the quadrupolar splitting $\Delta\nu_Q$ for a lipid/peptide ratio of 20 : 1, the lipid acyl chains are slightly ordered upon the

14-mer peptide addition. This is reflected by an S_{CD} order parameter of 0.21 compared to the S_{CD} order parameter of 0.20 for the DMPC pure lipid system. On the other hand, the ^{2}H NMR spectra of phospholipids in the presence of amphibian antimicrobial peptides such as aurein 1.1, citropin 1.1 and maculatin 1.1,[76] as well as the peptides nisin produced by *Lactococcus lactis*[92] and LL-37 found in humans,[96] indicate that these peptides induce disorder in the lipid acyl chains.

Deuterated lipid polar headgroups can also be investigated by ^{2}H NMR spectroscopy. In particular, DMPC deuterated on the choline headgroup at positions α and β is known to act as a ''molecular voltmeter'', sensing the accumulation of charges at the surface of the bilayer.[97,98] This phenomenon has been observed with the antibacterial peptide PGLa in interaction with DMPC-d_4 membranes, for which a decrease (increase) of the quadrupolar splitting for the α (β) deuterons reflects a change of conformation of the choline headgroup known as a tilt of the $^-$P–N$^+$ dipole induced by the presence of positive charges.[99] Wieprecht et al.[99] have concluded from the analysis of these ^{2}H NMR spectra that the peptide PGLa is located at the surface of the bilayer and is intercalated between the polar headgroups, resulting in a change of conformation of these headgroups.

4. CONCLUSIONS

Little is known so far about the detailed mechanisms of action of antimicrobial peptides but new methods are continually being developed to better understand these mechanisms and to develop novel peptides having the desired selectivity towards bacterial cells.[100] An overview of different solid-state NMR methods that have been developed to investigate the structure and interactions of antimicrobial peptides in membranes has been presented in this manuscript and these methods have been illustrated with several examples on most commonly studied antimicrobial peptides. This review therefore clearly demonstrates that solid-state NMR is a very powerful technique to investigate the conformation adopted by antimicrobial peptides upon binding to lipid bilayers as well as the mutual interactions between these components. The readers are referred to recent papers by Huster,[101] and Strandberg and Ulrich[27] for more exhaustive reviews.

REFERENCES

1. F. R. Schmidt, *Appl. Microbiol. Biotechnol.*, 2004, **63**, 335.
2. R. E. W. Hancock, *Drugs*, 1999, **57**, 469.
3. R. E. W. Hancock and D. S. Chapple, *Antimicrob. Agents Chemother.*, 1999, **43**, 1317.
4. R. E. W. Hancock and R. Lehrer, *Trends Biotechnol.*, 1998, **16**, 82.
5. H. Jenssen, P. Hamill and R. E. W. Hancock, *Clin. Microbiol. Rev.*, 2006, **19**, 491.
6. A. K. Marr, W. J. Gooderham and R. E. W. Hancock, *Curr. Opin. Pharmacol.*, 2006, **6**, 468.
7. K. V. R. Reddy, R. D. Yedery and C. Aranha, *Int. J. Antimicrob. Agents*, 2004, **24**, 536.
8. N. Sitaram and R. Nagaraj, *Biochim. Biophys. Acta*, 1999, **1462**, 29.
9. H. W. Huang, *Biochim. Biophys. Acta*, 2006, **1758**, 1292.

10. K. A. Brogden, *Nature*, 2005, **3**, 238.
11. M. Dathe, J. Meyer, M. Beyermann, B. Maul, C. Hoischen and M. Bienert, *Biochim. Biophys. Acta*, 2002, **1558**, 171.
12. M. Dathe and T. Wieprecht, *Biochim. Biophys. Acta*, 1999, **1462**, 71.
13. R. M. Epand, Y. Shai, J. P. Segrest and G. M. Anantharamaiah, *Biopolymers*, 1995, **37**, 319.
14. B. Bechinger, *Biochim. Biophys. Acta*, 1999, **1462**, 157.
15. O. Toke, L. Cegelski and J. Schaefer, *Biochim. Biophys. Acta*, 2006, **1758**, 1314.
16. J. H. Davis and M. Auger, *Prog. NMR Spectrosc.*, 1999, **35**, 1.
17. R. Fu and T. A. Cross, *Ann. Rev. Biophys. Biomol. Struct.*, 1999, **28**, 235.
18. D. D. Laws, H.-M. L. Bitter and A. Jerschow, *Angew. Chem. Int. Ed.*, 2002, **41**, 3096.
19. B. Bechinger, R. Kinder, M. Helmle, T. C. B. Vogt, U. Harzer and S. Schinzel, *Biopolymers*, 1999, **51**, 174.
20. B. Bechinger and C. Sizun, *Concepts Magn. Reson.*, 2003, **18A**, 130.
21. T. A. Cross and J. R. Quine, *Concepts Magn. Reson.*, 2000, **12**, 55.
22. J. J. Buffy, A. J. Waring, R. I. Lehrer and M. Hong, *Biochemistry*, 2003, **42**, 13725.
23. S. Yamaguchi, T. Hong, A. Waring, R. I. Lehrer and M. Hong, *Biochemistry*, 2002, **41**, 9852.
24. J. J. Buffy, M. J. McCormick, S. Wi, A. Waring, R. I. Lehrer and M. Hong, *Biochemistry*, 2004, **43**, 9800.
25. K. J. Hallock, K. Henzler Wildman, D.-K. Lee and A. Ramamoorthy, *Biophys. J.*, 2002, **82**, 2499.
26. R. S. Prosser, S. A. Hunt, J. A. DiNatale and R. R. Vold, *J. Am. Chem. Soc.*, 1996, **118**, 269.
27. E. Strandberg and A. S. Ulrich, *Concepts Magn. Reson.*, 2004, **23A**, 89.
28. S. Yamaguchi, D. Huster, A. Waring, R. I. Lehrer, W. Kearney, B. F. Tack and M. Hong, *Biophys. J.*, 2001, **81**, 2203.
29. F. M. Marassi, S. J. Opella, P. Juvvadi and R. B. Merrifield, *Biophys. J.*, 1999, **77**, 3152.
30. S. Thennarasu, D.-K. Lee, A. Tan, P. Kari and A. Ramamoorthy, *Biochim. Biophys. Acta*, 2005, **1711**, 49.
31. S. Thennarasu, D.-K. Lee, A. Poon, K. E. Kawulka, J. C. Vederas and A. Ramamoorthy, *Chem. Phys. Lipids*, 2005, **137**, 38.
32. B. Bechinger, M. Zasloff and S. J. Opella, *Biophys. J.*, 1998, **74**, 981.
33. M. Hong and T. Doherty, *Chem. Phys. Lett.*, 2006, **432**, 296.
34. A. Ramamoorthy, *Annu. Rep. NMR Spectrosc.*, 2004, **52**, 1.
35. F. M. Marassi, *Biophys. J.*, 2001, **80**, 994.
36. F. M. Marassi, *Concepts Magn. Reson.*, 2002, **14**, 212.
37. S. J. Opella and F. M. Marassi, *Chem. Rev.*, 2004, **104**, 3587.
38. B. Bechinger, M. Zasloff and S. J. Opella, *Protein Sci.*, 1993, **2**, 2077.
39. F. M. Marassi, C. Ma, J. J. Gesell and S. J. Opella, *J. Magn. Reson.*, 2000, **144**, 156.
40. S. Lambotte, P. Jasperse and B. Bechinger, *Biochemistry*, 1998, **37**, 16.
41. Y. Kim, K. Valentine, S. J. Opella, S. L. Schendel and W. A. Cramer, *Protein Sci.*, 1998, **7**, 342.
42. K. K. Kumashiro, K. Schmidt-Rohr, O. J. Murphy III, K. L. Ouellette, W. A. Cramer and L. K. Thompson, *J. Am. Chem. Soc.*, 1998, **120**, 5043.
43. D. Huster, X. Yao and M. Hong, *J. Am. Chem. Soc.*, 2002, **124**, 874.
44. J. J. Buffy, T. Hong, S. Yamaguchi, A. J. Waring, R. I. Lehrer and M. Hong, *Biophys. J.*, 2003, **85**, 2363.
45. H. Saito, *Magn. Reson. Chem.*, 1986, **24**, 835.
46. A. Naito, T. Nagao, K. Norisada, T. Mizuno, S. Tuzi and H. Saitô, *Biophys. J.*, 2000, **78**, 2405.
47. K. A. Henzler Wildman, D.-K. Lee and A. Ramamoorthy, *Biochemistry*, 2003, **42**, 6545.
48. S. L. Grage and A. Watts, *Annu. Rep. NMR Spectrosc.*, 2007, **60**, 191.
49. F. A. Kovacs, D. J. Fowler, G. J. Gallagher and L. K. Thompson, *Concepts Magn. Reson.*, 2007, **30A**, 21.
50. M. Auger, *J. Chim. Phys.*, 1995, **92**, 1751.
51. T. Gullion, *Concepts Magn. Reson.*, 1998, **10**, 277.
52. D. P. Raleigh, M. H. Levitt and R. G. Griffin, *Chem. Phys. Lett.*, 1988, **146**, 71.
53. F. Porcelli, B. Buck, D.-K. Lee, K. J. Hallock, A. Ramamoorthy and G. Veglia, *J. Biol. Chem.*, 2004, **279**, 45815.
54. O. Toke, W. L. Maloy, S. J. Kim, J. Blazyk and J. Schaefer, *Biophys. J.*, 2004, **87**, 662.
55. J. Salgado, S. L. Grage, L. H. Kondejewski, R. S. Hodges, R. N. McElhaney and A. S. Ulrich, *J. Biomol. NMR*, 2001, **21**, 191.

56. S. Meiboom and D. Gill, *Rev. Sci. Instrum.*, 1958, **29**, 688.
57. Y.-H. Lam, S. R. Wassall, C. J. Morton, R. Smith and F. Separovic, *Biophys. J.*, 2001, **81**, 2752.
58. V. Ladizhansky, M. Veshtort and R. G. Griffin, *J. Magn. Reson.*, 2002, **154**, 317.
59. M. Hong, J. D. Gross, W. Hu and R. G. Griffin, *J. Magn. Reson.*, 1998, **135**, 169.
60. M. Hong, J. D. Gross and R. G. Griffin, *J. Phys. Chem. B*, 1997, **101**, 5869.
61. T. Doherty, A. J. Waring and M. Hong, *Biochemistry*, 2006, **45**, 13323.
62. J. Ashida, K. Ohgo and T. Asakura, *J. Phys. Chem. B*, 2002, **106**, 9434.
63. J. Ashida, K. Ohgo, K. Komatsu, A. Kubota and T. Asakura, *J. Biomol. NMR*, 2003, **25**, 91.
64. Y. Nakazawa, M. Bamba, S. Nishio and T. Asakura, *Protein Sci.*, 2003, **12**, 666.
65. K. Schmidt-Rohr, *Macromolecules*, 1996, **29**, 3975.
66. J. D. van Beek, L. Beaulieu, H. Schäfer, M. Demura, T. Asakura and B. H. Meier, *Nature*, 2000, **405**, 1077.
67. C. M. Gabrys, J. Yang and D. P. Weliky, *J. Biomol. NMR*, 2003, **26**, 49.
68. A. Iuga, C. Ader, C. Gröger and E. Brunner, *Annu. Rep. NMR Spectrosc.*, 2007, **60**, 145.
69. I. C. P. Smith and I. H. Ekiel, *Phosphorus-31 NMR: Principles and Applications*, Academic Press, London, 1984, p. 447.
70. J. Seelig, *Biochim. Biophys. Acta*, 1978, **515**, 105.
71. S. O. Smith, K. Aschheim and M. Groesbeek, *Q. Rev. Biophys.*, 1996, **29**, 395.
72. C. S. B. Chia, J. Torres, M. A. Cooper, I. T. Arkin and J. H. Bowie, *FEBS Lett.*, 2002, **512**, 47.
73. M. Bouchard, C. Le Guernevé and M. Auger, *Biochim. Biophys. Acta*, 1998, **1415**, 181.
74. A. J. M. Driessen, H. W. van den Hooven, W. Kuiper, M. van de Kamp, H.-G. Sahl, R. N. H. Konings and W. N. Konings, *Biochemistry*, 1995, **34**, 1606.
75. E. J. Prenner, R. N. A. H. Lewis, K. C. Neuman, S. M. Gruner, L. H. Kondejewski, R. S. Hodges and R. N. McElhaney, *Biochemistry*, 1997, **36**, 7906.
76. M. S. Balla, J. H. Bowie and F. Separovic, *Eur. Biophys. J.*, 2004, **33**, 109.
77. M. Ouellet, G. Bernard, N. Voyer and M. Auger, *Biophys. J.*, 2006, **90**, 4071.
78. F. Picard, M. Pézolet, P. E. Bougis and M. Auger, *Can. J. Anal. Sci. Spectrosc.*, 2000, **45**, 72.
79. X. Qiu, P. A. Mirau and C. Pidgeon, *Biochim. Biophys. Acta*, 1993, **1147**, 59.
80. J. Seelig, F. Borle and T. A. Cross, *Biochim. Biophys. Acta*, 1985, **814**, 195.
81. M. Ouellet, J.-D. Doucet, N. Voyer and M. Auger, *Biochemistry*, 2007, **46**, 6597.
82. Y. R. Vandenburg, B. D. Smith, E. Biron and N. Voyer, *Chem. Commun.*, 2002, **16**, 1694.
83. F. Picard, M.-J. Paquet, J. Lévesque, A. Bélanger and M. Auger, *Biophys. J.*, 1999, **77**, 888.
84. P. C. Dave, E. Billington, Y.-L. Pan and S. K. Straus, *Biophys. J.*, 2005, **89**, 2434.
85. R. Mani, A. J. Waring, R. I. Lehrer and M. Hong, *Biochim. Biophys. Acta*, 2005, **1716**, 11.
86. A. Mecke, D.-K. Lee, A. Ramamoorthy, B. G. Orr and M. M. Banaszak Holl, *Biophys. J.*, 2005, **89**, 4043.
87. A. Ramamoorthy, S. Thennarasu, D.-K. Lee, A. Tan and L. Maloy, *Biophys. J.*, 2006, **91**, 206.
88. D. B. Fenske and H. C. Jarrell, *Biophys. J.*, 1991, **59**, 55.
89. J. Jeener, B. H. Meier, P. Bachmann and R. R. Ernst, *J. Chem. Phys.*, 1979, **71**, 4546.
90. F. Picard, M.-J. Paquet, E. J. Dufourc and M. Auger, *Biophys. J.*, 1998, **74**, 857.
91. R. Mani, J. J. Buffy, A. Waring, R. I. Lehrer and M. Hong, *Biochemistry*, 2004, **43**, 13839.
92. B. B. Bonev, W. C. Chan, B. W. Bycroft, G. C. K. Roberts and A. Watts, *Biochemistry*, 2000, **39**, 11425.
93. K. J. Hallock, D.-K. Lee, J. Omnaas, H. I. Mosberg and A. Ramamoorthy, *Biophys. J.*, 2002, **83**, 1004.
94. J. H. Davis, *Biochim. Biophys. Acta*, 1983, **737**, 117.
95. J. Seelig and A. Seelig, *Q. Rev. Biophys.*, 1980, **13**, 19.
96. K. A. Henzler Wildman, G. V. Martinez, M. F. Brown and A. Ramamoorthy, *Biochemistry*, 2004, **43**, 8459.
97. P. M. Macdonald, *Acc. Chem. Res.*, 1997, **30**, 196.
98. F. M. Marassi and P. M. Macdonald, *Biochemistry*, 1992, **31**, 10031.
99. T. Wieprecht, O. Apostolov, M. Beyermann and J. Seelig, *Biochemistry*, 2000, **39**, 442.
100. G. Saberwal and R. Nagaraj, *Biochim. Biophys. Acta*, 1994, **1197**, 109.
101. D. Huster, *Prog. Nucl. Magn. Reson. Spectrosc.*, 2005, **46**, 79.
102. O. Toke, *Biopolymers*, 2005, **80**, 717.

This page intentionally left blank

CHAPTER 2

Chemical Exchange

Alex D. Bain

Contents

Abstract

A general overview of chemical exchange and dynamic NMR is presented. This includes a brief overview of the theory, some comments on new techniques and methodology and some personal comments from the author on trends and opinions. Following that are some recent examples of applications (2005 and later). These are mainly within the chemical field (including solid-state NMR), but there are some references to studies of exchange in biological macromolecules. The list of applications is by no means complete, but it is hoped that most of the major fields have been mentioned, and that the selection is representative. The conclusion is that dynamic effects are very widespread in the NMR of many molecules, and that there is a wide range of experiments that are becoming accessible to almost all NMR spectroscopists.

1. INTRODUCTION

In NMR, chemical exchange turns up in many places. The anecdotal evidence is that everyone has encountered its effects is some spectrum somewhere. The aim of this review is to cover as many of those "somewheres" as possible, and to give a broad overview of the effects of chemical dynamics on a range of NMR spectra.

Department of Chemistry, McMaster University, 1280 Main St. West, Hamilton, Ontario, Canada L8S 4M1

Annual Reports on NMR Spectroscopy, Volume 63
ISSN 0066-4103, DOI 10.1016/S0066-4103(07)63002-6

Any attempt at being truly comprehensive is futile, but it is hoped that enough literature is touched on to give a doorway into a number of different fields and applications.

The terms ''chemical exchange'', ''dynamic NMR'', ''fluxionality'', ''stereochemical non-rigidity'' are not exactly synonymous, but all reflect the same basic phenomenon. During the timescale of the experiment, the magnetic properties of the nuclear environment change, leading to an observable change in the NMR experiment. The timescale, the magnetic properties and the experiment are deliberately left vague at the moment, but given this broad definition, it is easy to see why dynamics has such a wide application. There is a further subdivision into slow, intermediate and fast exchange, depending on the timescale. This definition of chemical exchange clearly overlaps with spin relaxation, with good reason. There are strong similarities in the basic physical mechanisms and the theory, and many of the experiments used to probe relaxation can also be applied to chemical exchange. Although a rigid definition of chemical exchange is not possible, this review should provide enough examples to illustrate its relevance to a wide range of systems.

The review will begin with an overview, including some comments on trends and some personal opinions. It is hoped that any particularly idiosyncratic personal opinions of the author's will be labeled as such, but the reader should be aware. This will be followed by a review of the theory. Much of this is already well-covered in the literature, so this section will be brief and non-specific. However, there are some new developments that deserve comment. The next section will discuss methodology. For measurements in the slow, intermediate and fast exchange regimes, the techniques are quite different. Again, the basic ideas are well-established, but there are some elegant and useful extensions that will be discussed. The final section will cover applications.

Applications could fill several books and still be incomplete. There are the classic organic examples of ring conformations and restricted rotations around partial double bonds. Recently, there have been many investigations of sterically crowded systems undergoing chemical exchange. Another rich source of chemical exchange phenomena is organometallic chemistry. Ligands can undergo both intermolecular and intramolecular exchange, since the bonds can be quite weak. Two-dimensional methods, such as EXSY, are excellent in revealing this fluxionality where it would not have been noticed in a one-dimensional spectrum. The NMR of biological molecules is now an independent field of NMR, and has developed its own dialects and variations on the basic experiments. In this case, chemical exchange often includes unstable or partially folded states of a protein. Fast-exchange methods, often neglected in classic chemical applications, have turned out to be very useful and sensitive to minor conformations of biological macromolecules. Finally, the rapid development of solid-state NMR has revealed a good deal of dynamics within what is nominally a rigid crystal lattice or glass. These are just some of the many examples.

The literature review in this paper is mainly concentrated in the years 2005 through to the present (mid-2007), although some earlier papers will be quoted. A concerted effort was made to make the search at least representative, if not

exhaustive. However, since exchange phenomena are now a routine part of NMR, it is clear that even the modern literature-searching tools will miss many important and relevant papers. The author apologizes to any researchers whose work has been overlooked.

2. OVERVIEW, TRENDS AND OPINIONS

Chemical exchange has been a part of NMR spectroscopy[1,2] for more than 50 years now. The subject is discussed in many of the excellent recent texts,[3–5] and there are several specialized books[6–10] and standard reviews.[11–20] In particular, the book edited by Jackman and Cotton is an essentially complete review of the field until the early 1970s and covers the fundamentals. It predates most of the pulse NMR methods, but it does an excellent job of covering essentially all the basic chemical processes that cause exchange. Sandstrom's book is a very readable practical introduction, but it again is somewhat dated in parts. There is also a worked-through undergraduate lab experiment published,[21] for training the next generation. More recently, there is a general review[22] (mainly concentrating on the principles and the theory) and a book chapter[23] by the author, a review of tautomerism,[24] a review of large rings,[25] reviews on motions in solids,[26–28] novel applications in organic chemistry,[29] reviews of ligand and solvent exchange[30,31] and an excellent overview of chiral organometallic complexes.[32] This review will not duplicate these efforts, but will pick up some of the literature that has been published since their appearance.

Some trends deserve comment – these are personal opinions, but it is hoped that the reader will agree. One is that for reasonable sized molecules, it is now feasible for many researchers to do good-quality *ab initio* molecular electronic structure calculations. Computers are cheap and fast, and good software is available to make the calculations accessible to non-specialists. A substantial number of the papers reviewed in the applications section have taken advantage of this,[33–39] and soon this will become a necessary part of these investigations. Calculations can help validate the structures of the various conformations, but also can aid in elucidating the nature of the transition state. This latter task is considerably more difficult than the former, but it should be attempted whenever it is reasonable.

In the regime of slow exchange, it is the author's opinion that the two-dimensional EXSY experiment[16,40–43] is an excellent qualitative tool, but not a good quantitative one. As an experiment for probing for chemical exchange, EXSY and its related experiments is unrivaled. Its widespread use is fully justified. In many cases, a routine NOESY or ROESY characterization has revealed peaks due to chemical exchange that have led on to productive further investigations. For simple, two-site kinetics EXSY is quite reliable. However, for more complicated kinetic schemes, the choice of mixing times becomes important. For instance, consider the case of three sites, *A*, *B* and *C*, in which both *A* and *B* exchange with *C*, but the barrier between *A* and *B* is too high to allow direct exchange. A spurious cross peak between *A* and *B* may appear if the

mixing time is too long, due to a two-step exchange for *A* to *C*, then from *C* to *B*. All cross peaks in an EXSY must be critically evaluated.

Furthermore, when quantitative data is needed to measure rates and barriers, it is the author's opinion that one-dimensional experiments give better data faster. These 1D experiments are a variation on selective inversion-recovery T_1 experiments,[44–51] and go by a number of different names and variations, such as the *zz* experiment,[52] the Forsen–Hoffman experiment[44] or 1D EXSY.[53,54] In the time required for one EXSY (and a number of these experiments are needed, as a function of the mixing time), 15 or 20 points on a recovery curve can be collected as one-dimensional spectra. One-dimensional spectra have better digitization and can be integrated more reliably. These data can be analyzed using the full kinetic scheme,[46,51] so that situations like the three-site case are treated correctly. Finally, the design of the selective inversion gives a measure of control over what parameters we measure.[55] For instance, in the three-site case, selective inversion of the *A* and *B* sites, without perturbing *C*, emphasizes the *A*-to-*C* and *B*-to-*C* processes, but suppresses the contribution from the *A*-to-*B* process. Different parts of the kinetic scheme can be enhanced or suppressed by clever design of the initial conditions. The experiments are, admittedly, more difficult to set up and analyze than a quantitative EXSY, but they give better data. This use of one-dimensional experiments has some support in the literature,[53,54,56–59] and it is hoped that it will grow.

In intermediate exchange, there are a number of papers that still refer to coalescence temperatures. The author sees this as an obsolete concept, only appropriate for fiddling with the temperature controller on an HA100 until the top of the lineshape was appropriately flat. The raw data are accessible on modern spectrometers and a number of programs are available to do complete bandshape analysis, this also should soon be standard.

A trend that is clearly growing is the observation and measurement of chemical exchange and other dynamics in the solid state, as shown by recent reviews.[26–28] Lineshape and coalescence phenomena are well-known in ^{13}C CP/MAS spectra,[60] but the many new timescales in modern solid-state NMR experiments allow new probes for chemical exchange. The naive picture of a rigid molecule in a rigid crystal lattice in a solid is clearly unsatisfactory in many cases. Some recent examples will be given in the applications section.

Finally, there has been a rapid development of the use of fast-exchange methods to probe minor components in a chemical exchange system, particularly in biological molecules. Conventional wisdom had it that by the time a system was in fast exchange, there was little that could be done. However, led by the groups of Palmer[61–66] and Kay,[67–70] it has been found that minor components (of the order of 1% or even less) could be detected with relaxation dispersion methods.[71] This is well-established within the biological NMR community but this potential has not seemed to be exploited much outside that realm.

This review will attempt a fairly broad (and somewhat superficial) overview of dynamic phenomena in NMR, focusing mainly on the recent applications and examples. The basic theory behind these phenomena was covered in a previous

review,[22] so the theory section will be brief, highlighting some recent work. Following that will be a selected group of examples.

3. THEORY

Chemical exchange is usually divided into three regimes: slow, medium and fast. These terms are relative ones, indicating the relationship between the rate of exchange and the frequency associated with the NMR interaction. In most cases, this is a chemical shift difference (in Hertz), but it can be a scalar coupling constant, quadrupole coupling, MAS frequency, mixing time, etc. Figure 1 shows the familiar case of two equally populated uncoupled sites. Each regime has its own set of experiments and its own theoretical tools for analyzing the results.[22] However, in the broad view, the theory is quite straightforward and much the same for all of the regimes.

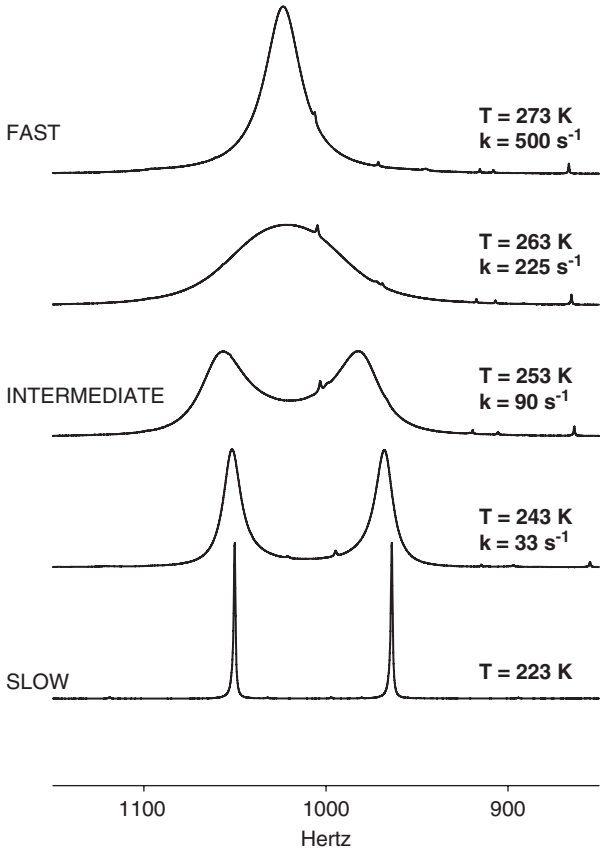

Figure 1 An example of chemical exchange lineshapes of a two-site, equally populated spin system. The data represent the exchange of the methyl signals in an *N,N*-dimethyl group attached to an aromatic ring.[193]

The theory of chemical exchange effects in NMR is best formulated using the density matrix expressed in Liouville space.[72–75] The density matrix, ρ, contains all possible information about the spin system. Normally this is displayed as a matrix (hence the name), but in Liouville space it is written as a vector. For a single spin-1/2, the four density matrix elements are written as a 2×2 matrix (since there are two basis states for a spin-1/2) in Hilbert space, but in the related Liouville space, they are written as a four-element vector. The behavior of this vector is governed by the Liouvillian matrix, **L**. This is closely related to (and can be derived from) the Hamiltonian, but it can also be calculated directly. In standard quantum treatments of spin systems, the first step is to calculate the Hamiltonian; similarly, Liouville-space calculations begin with the calculation of the Liouvillian. The details of the calculation can be complicated, but they are not needed for the present discussion. The importance of the Liouvillian is that it determines the time dependence of the density matrix, via the Liouville–von Neumann equation, Equation (1)

$$\frac{\partial}{\partial t}\rho(t) = -i\mathbf{L}\rho(t) \tag{1}$$

In most cases, the experiment starts at equilibrium, where the density matrix is easy to calculate (in the high temperature approximation, it is proportional to the Hamiltonian). Describing an NMR experiment is then a matter of integrating this differential equation. Formally, since this is a first-order differential equation, this can be done as in Equation (2), in which exp means the exponential of a matrix

$$\rho(t) = \exp(-i\mathbf{L}t)\rho(0) \tag{2}$$

In practice, this means generating a description for a pulse and for a free evolution, since those are the building blocks of a pulse sequence. In a free evolution, the exponential of an imaginary number leads to oscillations, corresponding to the precession of the magnetizations around the magnetic field. It is easy to show that the precession frequencies of density matrix elements are the eigenvalues of the Liouvillian. Thus the frequencies of the lines in the spectrum can be obtained directly, without having to know the energy levels – hence the name "direct method",[73] which was the first use of Liouville-space methods in NMR. This has turned out to be not a particularly good way to calculate a spectrum, but it provides an excellent framework for discussing relaxation and exchange.

Equations (1) and (2) neglect relaxation and exchange. They can be incorporated by including a relaxation matrix, **R**, and a kinetic matrix, **K**, as in Equations (3) and (4)

$$\frac{\partial}{\partial t}\rho(t) = -(i\mathbf{L} + \mathbf{R} + \mathbf{K})\rho(t) \tag{3}$$

$$\rho(t) = \exp(-i\mathbf{L} - \mathbf{R} - \mathbf{K})t\ \rho(0) \tag{4}$$

These matrices contain the relaxation rates and the exchange rates. Note that they are real numbers, rather than the imaginary elements of **L**. The real numbers

in the relaxation and exchange matrices lead to decaying terms in the exponential.

These are formal solutions, so more details are needed to treat each regime of exchange. If there is no rf present, the density matrix elements and the blocks of the Liouvillian matrix can be separated according to coherence order – the number of quanta associated with the coherence. For instance, a system of two spins-1/2 has four energy levels and sixteen density matrix elements. There are four that correspond to the z magnetizations (zero coherence), and then the zero-quantum, single-quantum and double-quantum coherences each have positive- and negative-going parts. In the two-spin system, there is one double-quantum coherence, four single-quantum coherences (the four lines in the spectrum) and one zero-quantum coherence; each of these has two parts, to give twelve density matrix elements. The four z magnetizations bring the total up to sixteen. This means that the Liouvillian matrix forms blocks, as in Equation (5). In this equation, the numbers indicate the coherence order (+0 and −0 indicate the zero-quantum coherence with non-zero frequency), and the large dots in the matrix indicate non-zero elements of the Liouvillian

$$\frac{\partial}{\partial t}\begin{pmatrix} +2\\ +1\\ +1\\ +1\\ +1\\ +0\\ 0\\ 0\\ 0\\ 0\\ -0\\ -1\\ -1\\ -1\\ -1\\ -2 \end{pmatrix} = \begin{pmatrix} \bullet & & & & & & & & & & & & & & & \\ & \bullet & \bullet & \bullet & \bullet & & & & & & & & & & & \\ & \bullet & \bullet & \bullet & \bullet & & & & & & & & & & & \\ & \bullet & \bullet & \bullet & \bullet & & & & & & & & & & & \\ & \bullet & \bullet & \bullet & \bullet & & & & & & & & & & & \\ & & & & & \bullet & & & & & & & & & & \\ & & & & & & \bullet & \bullet & \bullet & \bullet & & & & & & \\ & & & & & & \bullet & \bullet & \bullet & \bullet & & & & & & \\ & & & & & & \bullet & \bullet & \bullet & \bullet & & & & & & \\ & & & & & & \bullet & \bullet & \bullet & \bullet & & & & & & \\ & & & & & & & & & & \bullet & & & & & \\ & & & & & & & & & & & \bullet & \bullet & \bullet & \bullet & \\ & & & & & & & & & & & \bullet & \bullet & \bullet & \bullet & \\ & & & & & & & & & & & \bullet & \bullet & \bullet & \bullet & \\ & & & & & & & & & & & \bullet & \bullet & \bullet & \bullet & \\ & & & & & & & & & & & & & & & \bullet \end{pmatrix} \begin{pmatrix} +2\\ +1\\ +1\\ +1\\ +1\\ +0\\ 0\\ 0\\ 0\\ 0\\ -0\\ -1\\ -1\\ -1\\ -1\\ -2 \end{pmatrix} \tag{5}$$

For different exchange regimes, different parts of this matrix are needed. For the study of slow exchange, the exchange rate is comparable to (and will be measured against) the spin-lattice relaxation times. If there are two equally populated sites, A and B, the exchange couples the relaxation of the two sites, as in Equation (6). There are two sets of z magnetizations, labeled by site, blank

spots imply a zero element and k is the rate of exchange

$$\frac{\partial}{\partial t}\begin{pmatrix} 0A \\ 0A \\ 0A \\ 0A \\ 0B \\ 0B \\ 0B \\ 0B \end{pmatrix} = \begin{pmatrix} \bullet-k & \bullet & \bullet & \bullet & k & & & \\ \bullet & \bullet-k & \bullet & \bullet & & k & & \\ \bullet & \bullet & \bullet-k & \bullet & & & k & \\ \bullet & \bullet & \bullet & \bullet-k & & & & k \\ k & & & & \bullet-k & \bullet & \bullet & \bullet \\ & k & & & \bullet & \bullet-k & \bullet & \bullet \\ & & k & & \bullet & \bullet & \bullet-k & \bullet \\ & & & k & \bullet & \bullet & \bullet & \bullet-k \end{pmatrix} \begin{pmatrix} 0A \\ 0A \\ 0A \\ 0A \\ 0B \\ 0B \\ 0B \\ 0B \end{pmatrix} \tag{6}$$

Since these are z magnetizations, they do not oscillate (they are eigenvectors of **L** with zero eigenvalue), all the matrix elements in Equation (6) are real. The matrix can be easily diagonalized and its exponential calculated[76,77] to give Equation (7):

$$\rho(t) = \exp(-\mathbf{R} - \mathbf{K})t\ \rho(0) \tag{7}$$

The decays are multi-exponential, but they can be fitted to experimental data using standard methods.[46,51] Note that $\rho(0)$ is part of the solution, and is somewhat under experimental control. Different values of the z magnetizations (created by different selective pulses) at the start of relaxation will create different solutions to Equation (7). Multiple experiments can be used to probe multiple parts of the **R** and **K** matrices. This ability to design the experiment is one of the reasons that the author likes these techniques.

Intermediate exchange, where the exchange rate is comparable to the chemical shift differences (in hertz) can be treated in much the same way. In this case, it is the single-quantum block of the Liouvillian for the two sites that is needed, as in Equation (8)

$$\frac{\partial}{\partial t}\begin{pmatrix} +1A \\ +1A \\ +1A \\ +1A \\ +1B \\ +1B \\ +1B \\ +1B \end{pmatrix} = \begin{pmatrix} \bullet-k & \bullet & \bullet & \bullet & k & & & \\ \bullet & \bullet-k & \bullet & \bullet & & k & & \\ \bullet & \bullet & \bullet-k & \bullet & & & k & \\ \bullet & \bullet & \bullet & \bullet-k & & & & k \\ k & & & & \bullet-k & \bullet & \bullet & \bullet \\ & k & & & \bullet & \bullet-k & \bullet & \bullet \\ & & k & & \bullet & \bullet & \bullet-k & \bullet \\ & & & k & \bullet & \bullet & \bullet & \bullet-k \end{pmatrix} \begin{pmatrix} +1A \\ +1A \\ +1A \\ +1A \\ +1B \\ +1B \\ +1B \\ +1B \end{pmatrix} \tag{8}$$

However, the dots are hiding a complication. The elements of the Liouvillian now have imaginary parts as well, and so the matrix in Equation (8) is no longer Hermitian. It can still be diagonalized (with a bit more difficulty), but now both the eigenvalues and the eigenvectors may have real and imaginary

parts. In Equation (2), describing slow exchange using inversion-recovery methods, the eigenvalues were pure imaginary, and the eigenvectors can be made to be pure real.

These complex eigenvalues and eigenvectors are a numerical complication, but it reflects the physics quite well. If relaxation is ignored, then each eigenvalue (a pure imaginary number) of the Liouvillian represents the line position, and its intensity (as a real number) can be calculated from the eigenvector. In the intermediate exchange case, this argument is just extended. The eigenvalue has an imaginary part (which gives the position of the line) and a real part (which gives its width). Similarly, the real and imaginary parts of the eigenvector give rise to an intensity and a phase of the line. Reeves and Shaw[78] showed that the Bloch equations exchange lineshape can always be decomposed into two Lorentzian-type single lines. The lines are strongly distorted in phase, intensity, position and width by the exchange, but if there were n lines in the static spectrum, the strange lineshapes that occur in intermediate exchange still consist of n lines. This is the basis of the author's approach to simulating intermediate exchange spectra.[79]

In fast exchange, the rate dominates the difference in frequencies and the spectrum is effectively now a single Lorentzian line. However, there is a contribution to the spin–spin relaxation time, T_2, due to exchange, which depends on both the exchange rate and the frequency difference between the two sites. For two equally populated sites, if δ is half the frequency difference in radians s^{-1} (i.e., the two non-exchanging signals are at $+/-\delta$) then the exchange contribution to $1/T_2$ is $\delta^2/2k$[22] – the formula for unequally populated sites is more complex, but analogous. The problem is, that without a knowledge of δ, the values of the exchange rate k, can not be extracted. Some other timescale must be imposed on the experiment.

This timescale can be derived from the CPMG experiment for measuring T_2. In this experiment a series of equally spaced π pulses are applied after excitation. These refocus any chemical shift evolution, but any incoherent relaxation and dephasing will continue. This experiment deals with the single-quantum coherences, so Equation (8) is a starting point for the theory. After excitation, the spin system will evolve according to the exponential of the matrix in Equation (8), multiplied by the pulse spacing, τ. A perfect π pulse will take all the +1 coherence into the −1 coherence pathway and vice-versa – in physical terms, the direction of precession is reversed. The theory still deals only with single-quantum coherence. The crux of the experiment is the relative size of the pulse spacing and the timescale of the exchange: is $k\tau$ much less than 1, or much greater? If the pulse spacing is small, and $k\tau \ll 1$, the term in the matrix exponential is close to 1 and the exchange has little effect on the decay during the pulse sequence. However, longer delays allow significant exchange and decay during each delay, and the resulting apparent T_2 will be significantly shorter. A full analysis shows exactly how the decay rate changes with pulse spacing.[71,80–85] There are variations and extensions of the classic CPMG experiment (see Section 4), but this is the basic theoretical idea.

More recently, fast chemical exchange methods have revealed excited or metastable states with quite small equilibrium populations.[86] If a minor component is only 1% of the main peak, its T_2 relaxation will be 100 times faster than the major site, due to the principle of detailed balance. This is a wildly oversimplified argument, but it suggests why a very small population can have a significant effect on the T_2.

Finally, it is usually assumed that the system is in macroscopic equilibrium during the experiment – the sample remains the same and it is only the nuclei themselves that sense the dynamics going on. Recently, this has been extended[87,88] to the case where macroscopic reactions are also occurring, caused, for instance, photochemically.

This has been a very superficial overview of how chemical exchange affects NMR spectra. The fundamental Liouville–von Neumann equation, Equation (5), formulated in Liouville space, can readily be extended and applied to all types of chemical exchange. The actual algebraic and numerical implementation may be tricky, but the basic idea is quite simple.

4. METHODOLOGY

The usual precautions about running NMR spectra apply, of course. Furthermore, temperatures that are both accurate and precise are essential. Modern spectrometers usually have much better temperature control than previous generations, but good calibrations are still necessary. Beyond that, there are a number of experiment-specific techniques that deserve comment. Also, not all techniques are feasible in all situations. For instance, the short T_2's associated with intermediate exchange often prevent using complex pulse sequences and multi-dimensional spectrometers. Particularly in biological NMR, fast and slow exchange methods predominate, since they can be included in indirectly detected and isotope filtered experiments.

In the EXSY experiment, care must be taken in choosing the mixing time.[40–42,89] Erring towards shorter, rather than longer mixing times can minimize the spurious cross peaks due to double exchanges in complex systems.[39] If the contributors to a cross peak are scalar-coupled to each other, then there is the possibility of correlation via zero-quantum coherence. Many pulse programs include a small random variation of the mixing time which helps to suppress this, but it may not always be successful. If the digital resolution is good enough, the zero-quantum correlations are in antiphase, whereas the genuine EXSY peaks are in phase. Finally, exchange processes usually involve a number of spins, so a consistent picture should arise.

There are guidelines for selective-inversion experiments as well.[48,49] In principle, the selective pulse need not be an exact π pulse, and accidental perturbation of other peaks need not nullify the experiment – the state of the spin system at the start of the relaxation is often one of the fitting parameters. However, if the preparation is clean, then the negative transient in the unperturbed peak, seen in Figure 2 is a reliable and useful indication of the

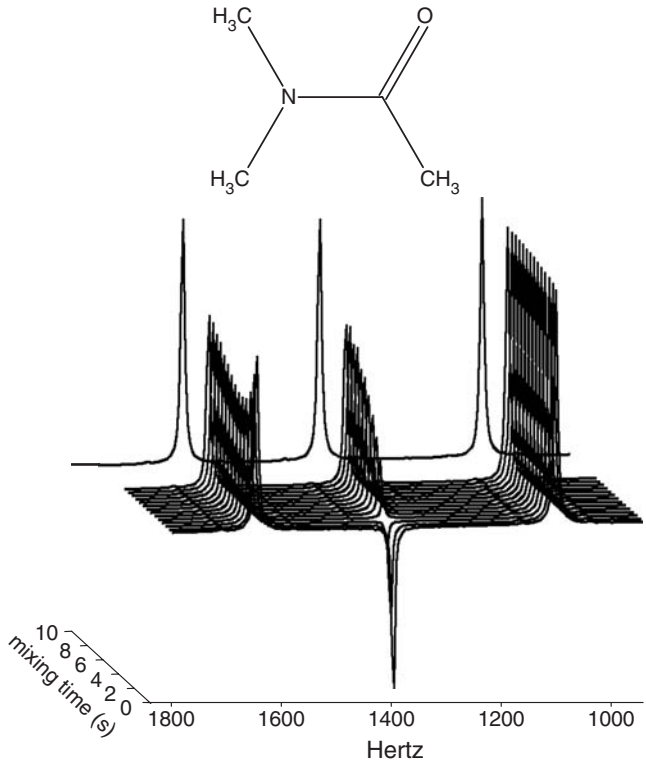

Figure 2 Selective inversion-recovery experiment on the proton spectrum of dimethylacetamide. One of the *N*-methyl signals was inverted at the start of the experiment, and it recovers as a function of mixing time. Its exchange partner (to high frequency in the spectrum) shows a characteristic negative transient.

exchange. If estimates of the rates and the spin-lattice relaxation times are available, then optimal choices of the variable delay times can be made.[49] Because few assumptions go into the analysis (all the parameters are more or less directly observable), this experiment can give excellent rate data.

For ultra-slow exchange, Bodenhausen's group[90] has adapted the very slow relaxation of singlet states.[91] This is not applicable to all systems, but has added at least an order of magnitude to the range of accessible rates.

In the intermediate exchange regime, the assumption of a "natural" linewidth can bedevil the extraction of rates. In many cases, the broadening due to exchange is much greater than the assumed linewidth in the absence of exchange, so the analysis is reliable. However, for cases where it is important, Vassiliev and the late Dimitrov[53] have applied the techniques of reference deconvolution[92] to exchange lineshapes. This removes the contribution of the magnetic field inhomogeneity, and so will produce a better version of the lineshape due to exchange.

The study of fast chemical exchange is based on measurements of the spin–spin relaxation time, T_2. There are two common ways for measuring T_2, each with its timescale. For the CPMG experiment it is the timing of the refocusing π pulses,

and for the $T_{1\rho}$ experiment it is the rate of precession around the spin-locking field. If T_2 is measured at timescales that are slower than the exchange, and faster than the exchange, different apparent T_2 values[71,80–85] will be obtained. A slow timescale will give values corresponding to the observed linewidth, including exchange. A fast timescale will give values reflecting the T_2's of the individual sites, with little influence of exchange. The dispersion in T_2 gives us an absolute estimate of the rate without the necessity for the frequency separation. This is not a panacea, since there are severe limits to how fast you can apply pulses, but it does give a useful extension of the range of rates that are measurable.

An extension of these methods is the constant-time CPMG, in which the time between excitation and acquisition is fixed, but the spacing of the pulses is varied by including more or fewer pulses in that fixed time.[66,69] These experiments are often applied to the amide N–H systems of proteins, in which the scalar coupling provides another degree of control. This allows studies of relaxation dispersion in zero-quantum and double-quantum coherences as well.[68]

The CPMG experiment is quite sensitive to experimental parameters.[93,94] Ideally, the refocusing pulses should be short, and the signals being measured should be close to resonance, so that the magnetization stays close to the rf field supplying the refocusing. In this way, it is close to being spin locked. However, particularly on a high-field instrument with a cryogenic probe, it is not feasible to achieve this for all the signals in a complex sample. However, there have been some recent modifications[95,96] to the basic experiment that provide more reliable data. Furthermore, these efficient probes, combined with samples in 95% H_2O, usually lead to radiation damping,[97] which can be affected by chemical exchange.[98] The CPMG experiment is usually applied to lines that are close to resonance, but off-resonance methods can also be used.[99] This gives an additional measure of experimental control.

The contribution to $1/T_2$ due to fast exchange is $\delta^2/2k$ for two equally populated sites. The two sites are at relative frequencies (in radians s^{-1}) of $+/-\delta$. Since this separation is usually due to chemical shift differences, δ will be proportional to the static magnetic field. If the sample temperatures can be exactly matched, then measuring T_2 at different fields can help extract absolute rates in the fast-exchange regime.[100]

In very fast intermolecular exchange, association constants can be derived by monitoring the chemical shift as the proportion of the two reagents is varied. This is a reliable method if the exchange is fast, but recently, it has been pointed out[101] that errors may occur if the assumptions are not valid.

Magic-angle spinning of solid samples offers new possibilities for exchange methods. The ODESSA,[102,103] PATROS,[104] CAESURA[105] and CODEX[106–109] experiments exploit the spinning sidebands of these spectra. Vold and his group[110] have explored the use of off-angle MAS to tune the timescale of the experiment to the rates of molecular motion.

Each of these techniques is useful, but if the sample and the spectrometer will permit, multiple methods are recommended. This cancels some of the biases in an individual method, and extends the range of rates, so that good activation data can be derived.[111,112]

5. APPLICATIONS

The following are a brief overview of a number of different applications. The numbers indicate that this is by no means a complete list of papers which use or refer to chemical exchange. The author is not an expert in any of these fields, so it is hoped that the reader can pick up some of the papers and follow them into a more detailed examination. For specific fields of chemistry, there are a number of reviews cited above in the overview section[20,24,26–32] and there are many more. In particular, the author's unfamiliarity with the vast biological NMR literature precludes going beyond some recent reviews.[113,114] The papers are grouped under a number of headings: organic systems, inorganic and organometallic systems and solids.

5.1 Organic applications

The work presented here is roughly divided into a number of categories: flexible rings, rotation about partial double bonds, hindered systems and atropisomers.

Since the discovery of the chair–chair interconversion of cyclohexane, large, flexible rings have attracted a great deal of interest. The systems have got larger, such as eight- and nine-membered ring cycloalkenes,[25] cyclodecane,[115,116] which interconverts a boat-chair-boat conformation and cycloundecane,[117] which is roughly 60 : 40 equilibrium of two conformations. In the larger rings the barriers are low, so these investigations require extremely low temperatures (−180°C). Other systems include calixphyrins: analog to porphyrins, except that the small pyrrole rings are joined by sp^3, not sp^2 carbons (Figure 3).[35] The macrocycle is no longer planar, so it can flex in a number of different ways. Derivatives of the seven-membered 1,4-benzodiazpines have been frequently studied because of

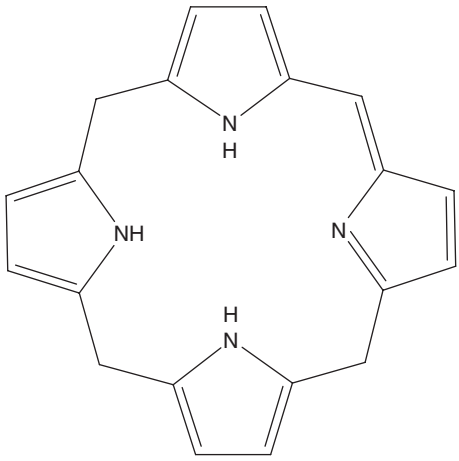

Figure 3 The structure of calyxphyrin.[35] Because of the sp^3 carbons joining the pyrroles, the macrocycle can flex and show exchange effects.

their importance in medicinal chemistry. Recent experimental and theoretical work[36] (Figure 4A) has shown that the ring can adopt a minor and a major conformation in almost equal proportions, and the barrier to interconversion is approximately 70 kJ mol^{-1}. Derivatives of the 1,5-benzodiazapines (Figure 4B) also show similar behavior.[118] Similarly, sesquiterpene lactones called guaianolides containing a seven-membered ring (Figure 5A) show interconversion.[119] One derivative has two almost equally populated chair and twisted chair conformations of the cycloheptane ring, and the other had a ratio of approximately 2 : 1, depending on solvent. The barriers are approximately 53 and 63 kJ mol^{-1}. Resorcinarenes relax into a kite-like cyclochiral conformation stabilized by hydrogen bonds. The two enantiomers interconvert[120] (as shown by EXSY)

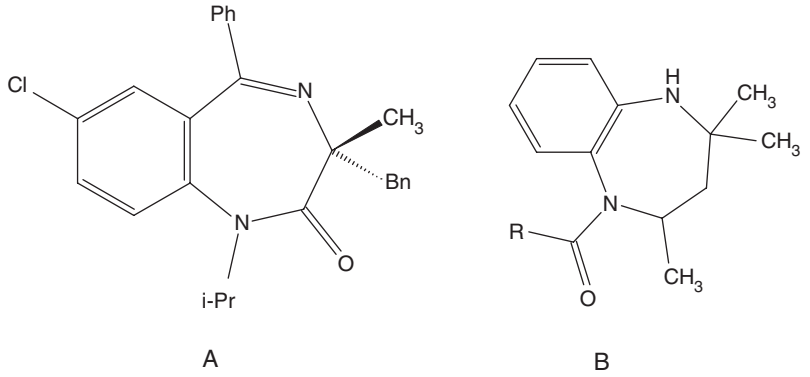

Figure 4 (A) A 1,4-benzodiazepin-2-one, in which the seven-membered ring flexes on the NMR timescale.[36] (B) A similar case with a 1,5-benzodiazepine.[118]

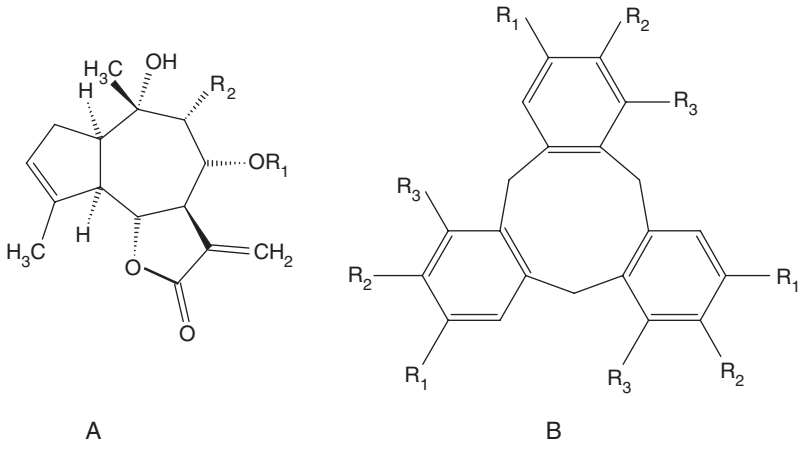

Figure 5 (A) Structure of a guaianolide-type sesquiterpene lactone which shows chemical exchange effects due to flexing of the large ring.[119] (B) Structure of cyclotriveratrylene. Normally this assumes a crown-type conformation, but it has been successfully trapped as a saddle structure.[121]

with a barrier of approximately 70 kJ mol^{-1}. The final example of large rings involves self-assembled rectangles and triangles of Pt(bipyridyl) complexes.[59] In this case, there is restricted rotation about the Pt–N(bipyridyl) bond, with a barrier of approximately 50 kJ mol^{-1}. Rapidly quenching a hot solution allowed the isolation of an unstable saddle form of cyclotriveratrylene (Figure 5B),[121] and its conversion to the crown form was followed by standard kinetic methods. Attempts to quantify the chemical exchange in the saddle form due to pseudorotation were unsuccessful, but did give an upper limit to the barrier.

The restricted rotation about a partial double bond in amides was the first well-characterized example of chemical exchange in NMR, and it still is an active field.[122] One recent example[123] in which the barrier is approximately 62 kJ mol^{-1} has the amide as part of a piperidin ring (Figure 6). Both lineshape and EXSY experiments were used to determine this. In recent work by the author and collaborators,[124] the dynamics in a twisted amide on a glycoluril framework (Figure 7) was determined by both electronic and steric effects. The thiocarbonyl and the carbonyl compete for the nitrogen lone pair, and if the *R* group is *t*-butyl, there is substantial steric crowding, which leads to an asymmetric twisted state (Figure 7). A second example is tertiary aromatic amides bearing an ortho substitutent[125] (Figure 8A) in which the ring and the amide plane are almost perpendicular. Depending on whether the substituent is chiral or not, the exchange connects enantiomers or diastereomers. A number of substituents were studied, and patterns and trends were identified. Similarly, a proprionate sidechain on bonellin (a chlorin – a porphyrin-like structure with three pyrroles and one reduced pyrrole) shows restricted rotation.[126] At sufficiently low temperature, formic acid showed two different conformations.[127] These corresponded to *E* and *Z* conformations about the C–O single bond, and they differed by approximately 4 kJ mol^{-1}. Lineshape analysis of spectra obtained at −143°C gave a barrier of 26 kJ mol^{-1}. Weil's group used the exchange in 2,2′-dimethyl-1-picrylhydrazine[128] (Figure 8B) as a probe of seven different solvents. Very careful experiments yielded high-quality values of the activation parameters.

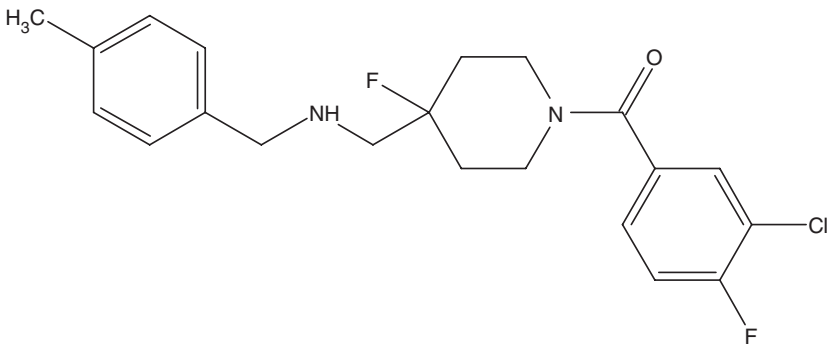

Figure 6 Structure of {1[1-(3-chloro-4-fluorobenzoyl)-4-fluoropiperidin-4yl]methyl} [(5-methylpyridin-2-yl)methyl]amine, which, as its fumaric acid salt, is an interesting compound in medicinal chemistry.[123] NMR shows restricted rotation about the amide bond.

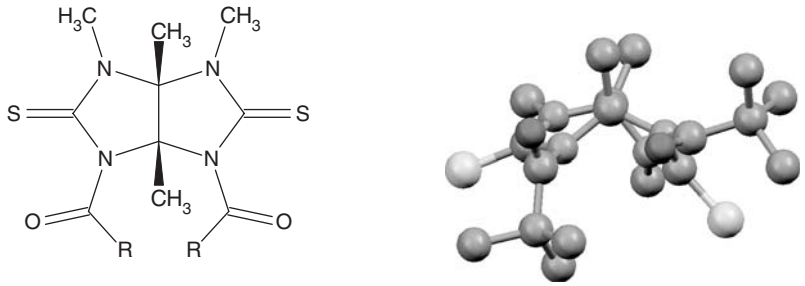

Figure 7 Structure of the dipivaloyl derivative of 3,4,7,8-tetramethyl-2,5-dithioglycoluril.[124] In the three-dimensional structure, the hydrogens have been hidden. The structure can invert via a concerted rotation about the tow amide bonds.

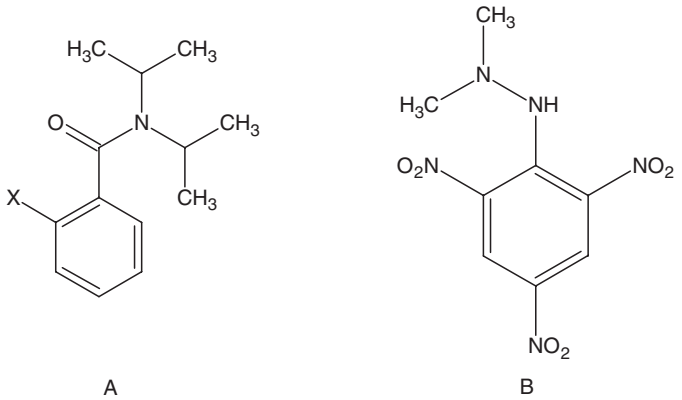

Figure 8 (A) If the X substituent in the aromatic amide is chiral, then rotation about the amide bond creates diastereomers.[125] A number of these have been studied and classified. (B) Exchange in 2,2′-dimethyl-1-picrylhydrazine was studied a number of solvents to probe solution effects.[128]

Sterically hindered systems have long been an interest of Lunazzi's group, such that he recently published[129] paper 100 in a series entitled "Conformational studies by dynamic NMR". Since then, his group has recently looked at ortho-substituted diaryl ethylene and diarylketone,[130] bis (*o*-cumyl) sulfide, sulfoxide and sulfone,[131] hindered terphenyl hydrocarbons,[132,133] tetra (*o*-tolyl)benzene,[134] sterically hindered salophen ligands,[135] hindered aryl carbinols,[136,137] biphenyls,[138,139] benzyl ethers[140] and derivatives of thianthrene oxides.[141] Restricted rotation has also been observed about Rh–carbene bonds,[142] and B–N bonds.[143] Molecular propellers[144,145] such as 1,3,5-tris(pentaphenylphenyl)benzene can show two similar dynamic processes, corresponding to a concerted 60 or 180° rotation about the benzene–phenyl bond. Phosphorus-based propellers[38] with indoles as blades show Mislow's intriguing phenomenon of residual stereoisomerism,[144] which creates enantiomers even when there is no rigid stereogenic center. Finally, the small aromatic ring in a cyclophane

can rotate within the cyclophane ring.[146] If, alternatively, the aromatic ring is considered fixed, this can be described as a ''jump-rope'' motion,[147] like skipping.

Much of this work has been done using proton NMR in homogeneous solution, but there are other methods. For instance, Lesot's group has used liquid crystalline media and the quadrupole coupling of deuterium to study rotational isomerism.[148,149] Additives such as poly-γ-benzyl-l-glutamate have been used to induce weak orientation in a solvent to study residual dipolar couplings, particularly in biological macromolecules. In the present case, the solvent gives a tunable quadrupolar splitting to the deuterium spectrum. If deuterium labels are strategically placed, then deuterium NMR will give clean spectra that undergo coalescence phenomena, which is easy to simulate.

Tautomerism is also widely studied by NMR,[24] and recent work has looked at this phenomenon on the imidazole ring of [1]benzopyrano[3,4-d]imidazol-4(3H)-ones[37] (Figure 9). This group has measured the tautomeric equilibria and then compared them to DFT calculations at various levels of theory and with solvent models. Many of these tautomeric reactions are proton transfer reactions. One group that has studied proton transfer in both breadth and detail is the group of Limbach. Recent studies from this lab include tunneling in solids,[150] non-Arrhenius behavior[151] and the question of intra- vs. intermolecular proton transfer in 1,3-bis(4-fluorophenyl)triazine[152] (Figure 10).

A more complicated tautomerism has been observed in a tungsten silyl alkylidyne complex, which can convert to a bis alkylidene complex.[34] Charged species can often undergo degenerate rearrangements: examples of this with the 9,10-dimethyl-9-vinyl-phenanthrenium ion[153] (Figure 11A) and the 1-(1-methyl-prop-1-en-1-yl)-1,2-dimethylacenaphthylenonium ion[154] (Figure 11B) have recently been presented.

Dynamic NMR can also be used to probe intermolecular interactions. Large polycyclic aromatic systems are known to stack. Derivatives of perylene bisimides self-assemble in this way, and the process was followed by NMR as well as a number of other methods.[155] At ambient temperature in DMSO, the signals are broad, indicating that the stacked molecules are moving slowly around axis of the stack. Raising the temperature produced sharp peaks

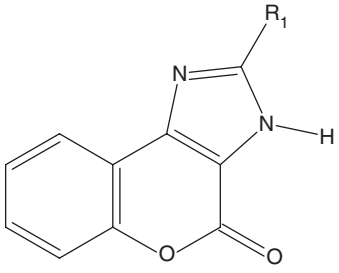

Figure 9 The tautomeric equilibria of a number of [1]benzopyrano[3,4-d]imidazol-4(3H)-ones have been studied.[37]

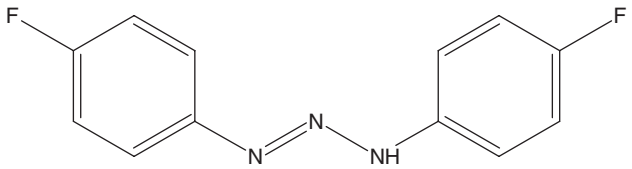

Figure 10 In 1,3-bis(4-fluorophenyl)triazine, there is a question of whether the tautomeric proton transfer is intra- or intermolecular.[152]

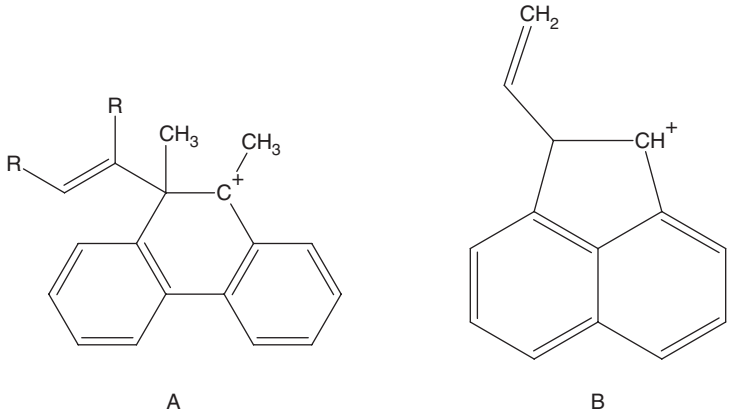

Figure 11 In these ions, there are a number of re-arrangements possible.[153,154]

characteristic of the isolated perylene bisimide. Bis(pentafluorophenyl)borinic acid can exist as a monomer or a trimer, but the equilibrium depends critically on the hydrogen bonding properties of the solvent.[156] Aluminum ions will bind to phosphatidylcholine lipid bilayers. Macdonald's group has done some careful EXSY and selective inversion experiments on the phosphorus spectrum to characterize this process.[56] Perhaps one could argue whether the dynamics in rotaxanes[157–159] is inter- or intramolecular, but in any case, dynamic NMR has been an essential tool for their characterization.

These are just some of the many observations and applications of chemical exchange in organic systems. Organometallic chemistry offers an equally rich harvest of applications.

5.2 Organometallic applications

For much more detailed and complete coverage of this field, the reader is referred to Peter Heard's recent critical review on chiral systems.[32] In this section, we pick a few recent applications.

These include phenyl rotation in bispentafluorophenyl palladium complexes with scorpion-type ligands[33] (Figure 12). Wrackmeyer's group has studied a tetrahedrane complex,[160] with iron tricarbonyl groups at two vertices and a sulfur and an NH filling out the tetrahedron. At room temperature, the carbonyls show

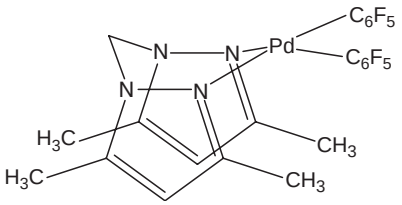

Figure 12 In this palladium complex with scorpion-type ligands,[33] the rotation of the fluorophenyl groups is restricted, and shows chemical exchange effects.

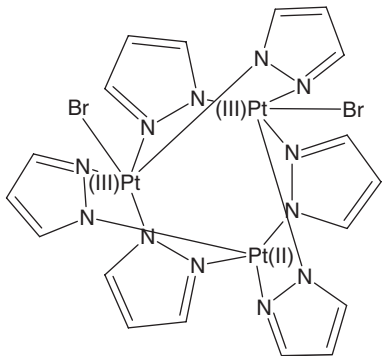

Figure 13 In this platinum complex, the presence of bromide ions helps determine the oxidation number of the platinum, and there are a number of dynamic processes.[162] The authors suggest this is a unique example of valence trapping–detrapping.

only one,^{13}C signal, indicating that they are scrambling. Variable-temperature measurements gave the barrier as approximately 44 kJ mol^{-1} supported by DFT calculations. Furthermore, the paper included a direct observation of the ^{57}Fe spectrum of the complex. Ligand exchange was also found to play a crucial role in copper-mediated and copper-catalyzed allylic substitution with Grignard reagents.[161] In a Pt(II) trimer complex with pyrazolate bridging ligands, addition of bromide gave a mixed valence Pt(II,III,III) complex[162] (Figure 13). The authors claim a unique valence detrapping process underlies the observed chemical exchange. In studies of some cyclopalladated acetate bridged dimers, it was found that the open-book type core observed in the solid state still persists in solution.[163] This restricts motion of the ligands, resulting in broad lines due to chemical exchange. The vanadium trimer species $[V_3O_3(\mu\text{-}O)_3(dmpp)_3(H_2O)](H_2O)_2$ (Hdmpp=3-hydroxy-1,2-dimethyl-4-pyridinone) in methanol/water solutions was found to be in equilibrium with the analogous dimer, a monomer and a number of other species. EXSY was very useful in establishing the assignments of these species. EXSY was also use to look at complexes of nickel, copper and zinc with tripodal scorpionate ligands[39] (Figure 14A). In the case of Zn^{2+}, both octahedral and tetrahedral species were found. Exchange measurements and DFT calculations established the structures and mapped the mechanism of interconversion.

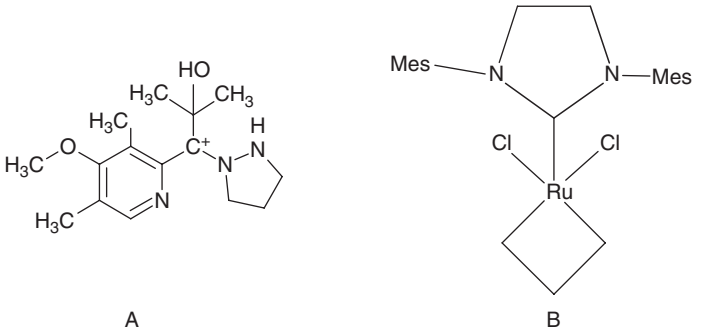

Figure 14 (A) This *N*,*N*′,O-donor heteroscorpionate ligand will bind to Ni^{2+}, Cu^{2+} and Zn^{2+}. In particular, there are a number of octahedral and tetrahedral species with Zn^{2+} that undergo chemical exchange.[39] (B) This 14-electron ruthenacyclobutane undergoes degenerate exchange with free ethylene.

Warren Piers' group has been studying 14-electron ruthenacyclobutanes[164] (Figure 14B) and has found both intermolecular and intramolecular exchange with ethylene. Polynuclear ruthenium hydrido clusters showed broad lines in the hydride region, indicating exchange.[165] The mechanism was mapped out and the barrier was in the range of 40–50 kJ mol^{-1}. The question of whether H_2 coordination is dihydrogen or dihydride still interests us. An osmium complex showed dynamic behavior in the hydride region, which could be frozen out.[166] At low temperature, the protons coupled to two phosphorus ligands to form an AA′XX′ system, in which the protons were chemically, but not magnetically, equivalent. Raymond's group has recently studied tris-catecholate complexes of Ti(IV),[167] and found their isomerization more facile than related Ga(III) and Ge(IV) complexes. In some cases, there is more than one process going on. The mechanism of the reaction was elucidated and supported with DFT calculations. Fluorinated analogs of methionine will form complexes with Pt(II) species, but the stereochemistry at the sulfur will invert only slowly, as recently reported.[168] Finally, one of many main group inorganic applications is included. Boraaminidate ligands will bond with heavy group 15 elements (As, Sb, Bi), to form a number of dynamic species, depending on the metal.[169]

5.3 Applications in solid-state NMR

In the limit of fast spinning, ^{13}C CP/MAS spectra can be treated like liquid-state spectra and any exchange phenomena can be treated in the same way. The classic examples are plastic crystals, such as dimethylsulfone, in which a roughly spherical molecule can rotate freely on it lattice site, and there are other types of dynamics that can be observed as well. A recent example is the observed motion in a molecular gyroscope,[170] in which there are spinning groups on the end of a molecular axle. In the dimeric complex $[(\eta^5\text{-}C_5H_5)Fe(\mu\text{-}CO)(CO)]_2$, the two Cp

rings can be either *cis* (or gauche) or *trans* when observed along the molecular axis. The conversion has been studied in solution, but it has recently also been observed in the solid state.[171]

Deuterium NMR lineshapes are also a standard way of investigating motion in the solid state. It has been used to look at the dynamics of 1,6-dibromohexane in urea inclusion compounds,[172] pyridine adsorbed on a silica surface[173] and the dynamics of dioxane, which forms bridges in an interpenetrating framework of a bimetallic cyano complex, $Cd(C_4H_8O_2)Cu(CN)_3$.[174]

Other nuclei have also been employed. In the study of lithium battery materials and ion conductors, both ^{6}Li and ^{7}Li NMR have become useful tools.[175–178] ^{17}O has been used to probe the dynamics in zirconium tungstenate,[57,179] and Wimperis' group observed dynamic effects (on the microsecond timescale) in the ^{27}Al MQMAS and STMAS of ALPO-14.[180] Taulelle and his group did some elegant work following crystal growth of $GaPO_4$ and the exchange between the solid and solution.[181]

Perhaps it is not clear whether Xe NMR[182,183] is solid-state or gas phase. In any case, it is well-established that the NMR signal from xenon is very sensitive to the size and shape of the cavity containing it. Because of this, it has been a powerful tool for probing porous materials.[184,185] Furthermore, the technology for obtaining hyperpolarized xenon is well advanced, so tremendous increases in signal/noise are now available.[186,187]

Inclusion complexes[188,189] often show dynamic behavior, depending on the details of the guest–host interactions. Recently, there have been a number of these investigations.[190–192]

All these applications illustrate many of the important features of chemical exchange in NMR. Perhaps the most impressive point is the wide range of dynamic processes that molecules undergo. At some timescale, almost any molecule shows dynamic behavior, which can provide important clues to the structure and reactivity of the molecule. For this, and many other reasons, chemical exchange investigations should become part of many NMR characterizations.

6. CONCLUSIONS AND ACKNOWLEDGMENTS

It is hoped that the breadth of the effects of chemical exchange on NMR spectroscopy has been communicated. Dynamic effects on some timescale are present in almost every chemical system, so the curious investigator can usually find an NMR experiment with a matching timescale, be it slow, intermediate or fast exchange. The inclusion of dynamics into the theory and computation of spin dynamics is quite straightforward, especially in the Liouville space formulation, so understanding these experiments is not a big extension. Finally, one of the goals of the study of chemical exchange is the understanding of both the ground states and the transition state. Access to high-quality electronic structure calculations is now good, so these will form a useful basis for the chemical understanding that results.

The author would like to thank the Natural Sciences and Engineering Research Council of Canada for financial support.

REFERENCES

1. H. S. Gutowsky and C. H. Holm, *J. Chem. Phys*., 1956, **25**, 1228.
2. H. M. McConnell, *J. Chem. Phys*., 1958, **28**, 430.
3. J. Keeler, *Understanding NMR Spectroscopy*, Wiley, New York, 2005.
4. J. B. Lambert and E. P. Mazzola, *Nuclear Magnetic Resonance Spectroscopy: An Introduction to Principles, Applications, and Experimental Methods*, Prentice Hall, Upper Saddle River, NJ, 2003.
5. M. H. Levitt, *Spin Dynamics*, Wiley, Chichester, 2001.
6. L. M. Jackman and F. A. Cotton, *Dynamic Nuclear Magnetic Resonance Spectroscopy*, Academic Press, New York, 1975.
7. J. Sandstrom, *Dynamic NMR Spectroscopy*, Academic Press, London, 1982.
8. J. I. Kaplan and G. Fraenkel, *NMR of Chemically Exchanging Systems*, Academic Press, New York, 1980.
9. J. J. Delpeuch, *Dynamics of Solutions and Fluid Mixtures by NMR*, Wiley, Chichester, 1995.
10. R. Tycko, *Nuclear Magnetic Resonance Probes of Molecular Dynamics*, Kluwer Academic Publishers, Boston, MA, 1994.
11. C. S. Johnson, *Adv. Magn. Reson*., 1965, **1**, 33.
12. R. M. Lynden-Bell, *Prog. Nucl. Magn. Reson. Spectrosc*., 1967, **2**, 163.
13. L. W. Reeves, *Adv. Phys. Org. Chem*., 1965, **3**, 187.
14. G. Binsch and H. Kessler, *Angew. Chem. Int. Ed. Engl*., 1980, **19**, 411.
15. K. G. Orrell and V. Sik, *Annu. Rep. NMR Spectrosc*., 1987, **19**, 79.
16. K. G. Orrell, V. Sik and D. Stephenson, *Prog. Nucl. Magn. Reson. Spectrosc*., 1990, **22**, 141.
17. K. G. Orrell and V. Sik, *Annu. Rep. NMR Spectrosc*., 1993, **27**, 103.
18. K. G. Orrell, *The Encyclopedia of NMR*, Wiley, Chichester, 1996, p. 4850.
19. K. G. Orrell, *Annu. Rep. NMR Spectrosc*., 1999, **37**, 1.
20. M. Pons and O. Millet, *Prog. Nucl. Magn. Reson. Spectrosc*., 2001, **38**, 267.
21. Y. Ba, S. Han, L. Ni, T. Su and A. Garcia, *J. Chem. Ed*., 2006, **83**, 296.
22. A. D. Bain, *Prog. Nucl. Magn. Reson. Spectrosc*., 2003, **43**, 63.
23. A. D. Bain, in: *Modern Magnetic Resonance*, Springer, Berlin, 2006.
24. R. M. Claramunt, C. Lopez, M. D. Santa Maria, D. Sanz and J. Elguero, *Prog. Nucl. Magn. Reson. Spectrosc*., 2006, **49**, 169.
25. R. Glaser, I. Ergaz, G. Levi-Ruso, D. Shiftan, A. Novoselesky and S. Geresh, *Annu. Rep. NMR Spectrosc*., 2005, **56**, 141.
26. D. Reichert, *Annu. Rep. NMR Spectrosc*., 2005, **55**, 159.
27. E. R. deAzevedo, T. J. Bonagamba and D. Reichert, *Prog. Nucl. Magn. Reson. Spectrosc*., 2005, **47**, 137.
28. M. J. Duer, *Annu. Rep. NMR Spectrosc*., 2006, **59**, 41.
29. E. Kolehmainen, *Annu. Rep. NMR Spectrosc*., 2003, **49**, 1.
30. A. E. Merbach, F. A. Dunand and L. Helm, *Adv. Inorg. Chem*., 2003, **54**, 1.
31. J. Burgess and C. D. Hubbard, *Adv. Inorg. Chem*., 2003, **54**, 71.
32. P. J. Heard, *Chem. Soc. Rev*., 2007, **36**, 551.
33. M. C. Carrion, F. A. Jalon, I. Lopez-Solera, B. R. Manzano, F. Sepulveda, L. Santos, A. M. Rodriguez, M. Moreno and M. Martinez-Ripoli, *Can. J. Chem*., 2005, **83**, 2106.
34. T. Chen, X. H. Zhang, C. Wang, S. Chen, Z. Wu, L. Li, K. R. Sorasaenee, J. B. Diminnie, H. Pan, I. A. Guzei, A. L. Rheingold, Y. D. Wu and Z. L. Xue, *Organometallics*, 2005, **24**, 1214.
35. M. Bernatkova, H. Dvorakova, B. Andrioletti, V. Kral and P. Bour, *J. Phys. Chem*., 2005, **109A**, 5518.
36. P. C. H. Lam and P. R. Carlier, *J. Org. Chem*., 2005, **70**, 1530.
37. A. Contini, D. Nava and P. Trimarco, *J. Org. Chem*., 2006, **71**, 159.
38. T. Benincori, G. Celentano, T. Pilati, A. Ponti, S. Rizzo and F. Sannicolo, *Angew. Chem. Int. Ed. Engl*., 2006, **45**, 6193.

39. M. Gennari, M. Tegoni, M. Lanfranchi, M. A. Pellinghelli and L. Marchio, *Inorg. Chem.*, 2007, **46**, 3367.
40. J. Jeener, B. H. Meier, P. Bachmann and R. R. Ernst, *J. Chem. Phys.*, 1979, **71**, 4546.
41. C. L. Perrin and T. Dwyer, *Chem. Rev.*, 1990, **90**, 935.
42. C. L. Perrin, *J. Magn. Reson.*, 1989, **82**, 619.
43. E. W. Abel, T. P. J. Coston, K. G. Orrell, V. Sik and D. Stephenson, *J. Magn. Reson.*, 1986, **70**, 34.
44. B. E. Mann, *J. Magn. Reson.*, 1976, **21**, 17.
45. M. Grassi, B. E. Mann, B. T. Pickup and C. M. Spencer, *J. Magn. Reson.*, 1986, **69**, 92.
46. D. R. Muhandiram and R. E. D. McClung, *J. Magn. Reson.*, 1987, **71**, 187.
47. R. E. D. McClung and G. H. M. Aarts, *J. Magn. Reson.*, 1995, **115A**, 145.
48. A. D. Bain and J. A. Cramer, *J. Magn. Reson.*, 1993, **103A**, 217.
49. A. D. Bain and J. A. Cramer, *J. Phys. Chem.*, 1993, **97**, 2884.
50. A. D. Bain and J. A. Cramer, *J. Magn. Reson.*, 1996, **118A**, 21.
51. A. D. Bain and D. A. Fletcher, *Mol. Phys.*, 1998, **95**, 1091.
52. J. Cavanagh, W. J. Fairbrother, A. G. Palmer and N. J. Skelton, *Protein NMR Spectroscopy. Principles and Practice*, Academic Press, San Diego, CA, 1996.
53. N. G. Vassilev and V. S. Dimitrov, *Magn. Reson. Chem.*, 2001, **39**, 607.
54. J. Zhou and P. C. van Zijl, *Prog. Nucl. Magn. Reson. Spectrosc.*, 2006, **48**, 109.
55. A. D. Bain, R. A. Bell, D. A. Fletcher, P. Hazendonk, R. B. Maharajh, S. Rigby and J. F. Valliant, *J. Chem. Soc. Perkin Trans.*, 1999, **2**, 1447.
56. N. MacKinnon, J. Ridgway, K. J. Crowell and P. M. Macdonald, *Chem. Phys. Lipids*, 2006, **139**, 85.
57. P. Hodgkinson and M. R. Hampson, *Solid State Nucl. Magn. Reson.*, 2006, **30**, 98.
58. N. R. Krishna and V. Jayalakshmi, *Prog. Nucl. Magn. Reson. Spectrosc.*, 2006, **49**, 1.
59. G. Tarkanyi, H. Jude, G. Palinkas and P. J. Stang, *Org. Lett.*, 2005, **7**, 4971.
60. J. R. Lyerla, C. S. Yannoni and C. A. Fyfe, *Acc. Chem. Res.*, 1982, **15**, 208.
61. D. Abergel and A. G. Palmer, *J. Phys. Chem.*, 2005, **109B**, 4837.
62. D. Abergel and A. G. Palmer, *Concepts Magn. Reson.*, 2003, **19A**, 134.
63. M. Akke and A. G. Palmer, *J. Am. Chem. Soc.*, 1996, **118**, 911.
64. M. J. Grey, C. Wang and A. G. Palmer, *J. Am. Chem. Soc.*, 2003, **125**, 14324.
65. A. G. Palmer, M. J. Grey and C. Wang, *Methods Enzymol.*, 2005, **394**, 430.
66. J. P. Loria, M. Rance and A. G. Palmer, *J. Am. Chem. Soc.*, 1999, **121**, 2331.
67. P. Nuedecker, A. Zarrine-Afsar, W. Y. Choy, D. R. Muhandiram, A. R. Davidson and L. E. Kay, *J. Mol. Biol.*, 2006, **363**, 958.
68. D. M. Korzhnev, P. Neudecker, A. Mittermaier, V. Y. Orekhov and L. E. Kay, *J. Am. Chem. Soc.*, 2005, **127**, 15602.
69. M. Tollinger, N. R. Skrynnikov, F. A. A. Mulder, J. D. Forman-Kay and L. E. Kay, *J. Am. Chem. Soc.*, 2001, **123**, 11341.
70. D. M. Korzhnev, V. Y. Orekhov, F. W. Dahlquist and L. E. Kay, *J. Biomol. NMR*, 2003, **26**, 39.
71. J. P. Carver and R. E. Richards, *J. Magn. Reson.*, 1972, **6**, 89.
72. U. Fano, in: *Lectures on the Many Body Problem*, Vol. 2, Academic Press, New York, 1964, p. 217.
73. C. N. Banwell and H. Primas, *Mol. Phys.*, 1963, **6**, 225.
74. G. Binsch, *J. Am. Chem. Soc.*, 1969, **91**, 1304.
75. A. D. Bain, *Prog. Nucl. Magn. Reson. Spectrosc.*, 1988, **20**, 295.
76. W. H. Press, B. P. Flannery, S. A. Teukolsky and W. T. Vetterling, *Numerical Recipes in C. The Art of Scientific Computing*, Cambridge University Press, Cambridge, 1988.
77. C. Moler and C. F. van Loan, *SIAM Rev.*, 1978, **20**, 801.
78. L. W. Reeves and K. N. Shaw, *Can. J. Chem.*, 1970, **48**, 3641.
79. A. D. Bain and G. J. Duns, *Can. J. Chem.*, 1996, **74**, 819.
80. A. Allerhand and H. S. Gutowsky, *J. Chem. Phys.*, 1964, **41**, 2115.
81. A. Allerhand and H. S. Gutowsky, *J. Chem. Phys.*, 1965, **42**, 1587.
82. A. Allerhand and H. S. Gutowsky, *J. Chem. Phys.*, 1965, **42**, 4203.
83. C. Deverell, R. E. Morgan and J. H. Strange, *Mol. Phys.*, 1970, **18**, 553.
84. P. Laszlo, *Prog. Nucl. Magn. Reson. Spectrosc.*, 1980, **13**, 257.
85. M. A. K. Williams and T. K. Halstead, *Mol. Phys.*, 1998, **93**, 609.

86. M. Tollinger, K. Kloiber, B. Agoston, C. Dorigoni, R. Lichtenecker, W. Schmid and R. Konrat, *Biochemistry*, 2006, **45**, 8885.
87. S. P. Babailov and D. A. Mainichev, *J. Struct. Chem*., 2006, **47**, 442.
88. S. P. Babailov, D. A. Mainichev and P. A. Purtov, *Concepts Magn. Reson*., 2007, **30A**, 140.
89. P. S. Denkova and V. S. Dimitrov, *Magn. Reson. Chem*., 1999, **37**, 637.
90. R. Sarkar, P. R. Vasos and G. Bodenhausen, *J. Am. Chem. Soc*., 2007, **129**, 328.
91. M. Carravetta and M. H. Levitt, *J. Am. Chem. Soc*., 2004, **126**, 6226.
92. A. Gibbs and G. A. Morris, *J. Magn. Reson*., 1991, **91**, 77.
93. R. L. Vold, R. R. Vold and H. E. Simon, *J. Magn. Reson*., 1973, **11**, 283.
94. N. H. Pawley, M. D. Clark and R. Michalczyk, *J. Magn. Reson*., 2006, **178**, 77.
95. G. N. B. Yip and E. R. P. Zuiderweg, *J. Magn. Reson*., 2004, **171**, 25.
96. G. N. B. Yip and E. R. P. Zuiderweg, *J. Magn. Reson*., 2005, **176**, 171.
97. M. P. Augustine, *Prog. Nucl. Magn. Reson. Spectrosc*., 2002, **40**, 111.
98. J. C. Rodrigues, P. A. Jennings and G. Melacini, *J. Am. Chem. Soc*., 2002, **124**, 6240.
99. J. Milojevic, V. Esposito, R. Das and G. Melacini, *J. Phys. Chem*., 2005, **110B**, 20661.
100. O. Millet, J. P. Loria, C. D. Kroenke, M. Pons and A. G. Palmer, *J. Am. Chem. Soc*., 2000, **122**, 2867.
101. P. Bernatowicz, M. Nowakowski, H. Dodziuk and A. Ejchart, *J. Magn. Reson*., 2006, **181**, 304.
102. V. Gerardy-Montouillout, C. Malveau, P. Tekely, Z. Olender and Z. Luz, *J. Magn. Reson*., 1996, **123A**, 7.
103. D. Reichert, H. Zimmermann, P. Tekely, R. Poupko and Z. Luz, *J. Magn. Reson*., 1997, **125**, 245.
104. D. Reichert, G. Hempel, Z. Luz, P. Tekely and H. Schneider, *J. Magn. Reson*., 2000, **146**, 311.
105. L. Shao and J. J. Titman, *J. Chem. Phys*., 2006, **125**, 064507.
106. E. R. deAzevedo, W. G. Hu, T. J. Bonagamba and K. Schmidt-Rohr, *J. Am. Chem. Soc*., 1999, **121**, 8411.
107. E. R. deAzevedo, W. G. Hu, T. J. Bonagamba and K. Schmidt-Rohr, *J. Chem. Phys*., 2000, **112**, 8898.
108. D. Reichert, T. J. Bonagamba and K. Schmidt-Rohr, *J. Magn. Reson*., 2001, **151**, 129.
109. T. Miyoshi, O. Pascui and D. Reichert, *Macromolecules*, 2002, **35**, 7178.
110. Y. Huang, R. L. Vold and G. L. Hoatson, *J. Chem. Phys*., 2006, **124**, 104504.
111. A. D. Bain, G. J. Duns, F. Rathgeb and J. Vanderkloet, *J. Phys. Chem*., 1995, **99**, 17338.
112. F. J. Monlien, L. Helm, A. Abou-Hamdan and A. E. Merbach, *Inorg. Chem*., 2002, **41**, 1717.
113. D. D. Boehr, H. J. Dyson and P. E. Wright, *Chem. Rev*., 2006, **106**, 3055.
114. T. Stangler, R. Hartmann, D. Willbold and B. W. Koenig, *Z. Physik. Chem. Neue Folge*, 2006, **220**, 567.
115. D. M. Pawar, S. V. Smith, H. L. Mark, R. M. Odom and E. A. Noe, *J. Am. Chem. Soc*., 1998, **120**, 10715.
116. D. M. Pawar, D. Cain, G. Gill, A. D. Bain, R. H. Sullivan and E. A. Noe, *J. Org. Chem*., 2007, **72**, 25.
117. D. M. Pawar, J. Brown, K. H. Chen, N. L. Allinger and E. A. Noe, *J. Org. Chem*., 2006, **71**, 6512.
118. S. Ponnuswamy, R. Murugadoss, R. Jeyaraman, A. Thiruvalluvar and V. Parthasarathy, *Indian J. Chem*., 2006, **45B**, 2059.
119. S. Milosavljevic, I. Juranic, V. Bulatovic, S. Macura, N. Juranic, H. H. Limbach, K. Weisz, V. Vajs and N. Todorovic, *Struct. Chem*., 2004, **15**, 237.
120. A. Szumna, *Org. Biomol. Chem*., 2007, **5**, 1358.
121. H. Zimmermann, P. Tolstoy, H. H. Limbach, R. Poupko and Z. Luz, *J. Phys. Chem*., 2004, **108B**, 18772.
122. A. Greenberg, C. M. Breneman and J. F. Liebman, *The Amide Linkage*, Wiley, Hoboken, NJ, 2003.
123. J. P. Ribet, R. Pena, J. L. Maurel, C. Belin, M. Tillard, B. Vacher, B. Bonnaud and F. Colpaert, *Spectrochim. Acta*, 2005, **62 A**, 353.
124. A. D. Bain, H. Chen and P. H. M. Harrison, *Can. J. Chem*., 2006, **84**, 421.
125. M. S. Betson, J. Clayden, M. Helliwell, P. Johnson, L. W. Lai, J. H. Pink, C. C. Stimson, N. Vassiliou, N. Westlund, S. A. Yasin and L. H. Youssef, *Org. Biomol. Chem*., 2006, **4**, 424.
126. P. H. Hynninen, J. Helaja, F. P. Montforts and C. M. Muller, *J. Porphyrins Phthalocyanines*, 2004, **8**, 1376.
127. D. M. Pawar, D. Cain-Davis and E. A. Noe, *J. Org. Chem*., 2007, **72**, 2003.
128. K. C. Brown, M. El-Bermani, Y. Upadrashta and J. A. Weil, *Can. J. Chem*., 2006, **84**, 1648.

129. D. Casarini, C. Coluccini, L. Lunazzi, A. Mazzanti and R. Rompietti, *J. Org. Chem.*, 2004, **69**, 5746.
130. L. Lunazzi, A. Mazzanti and M. Minzoni, *J. Org. Chem.*, 2005, **70**, 456.
131. L. Lunazzi, A. Mazzanti and M. Minzoni, *Tetrahedron*, 2005, **61**, 6782.
132. L. Lunazzi, A. Mazzanti, M. Minzoni and J. E. Anderson, *Org. Lett.*, 2005, **7**, 1291.
133. L. Lunazzi, A. Mazzanti and M. Minzoni, *J. Org. Chem.*, 2007, **72**, 2501.
134. L. Lunazzi, A. Mazzanti and M. Minzoni, *J. Org. Chem.*, 2005, **70**, 10062.
135. A. Dalla Cort, F. Gasparrini, L. Lunazzi, L. Mandolini, A. Mazzanti, C. Pasquini, M. Pierini, R. Rompietti and L. Schiaffino, *J. Org. Chem.*, 2005, **70**, 8877.
136. D. Casarini, C. Coluccini, L. Lunazzi and A. Mazzanti, *J. Org. Chem.*, 2005, **70**, 5098.
137. D. Casarini, L. Lunazzi, M. Mancinelli and A. Mazzanti, *J. Org. Chem.*, 2007, **72**, 998.
138. A. Mazzanti, L. Lunazzi, M. Minzoni and J. E. Anderson, *J. Org. Chem.*, 2006, **71**, 5474.
139. L. Lunazzi, A. Mazzanti and M. Minzoni, *J. Org. Chem.*, 2006, **71**, 9297.
140. D. Casarini, C. Coluccini, L. Lunazzi and A. Mazzanti, *J. Org. Chem.*, 2006, **71**, 4490.
141. D. Casarini, C. Coluccini, L. Lunazzi and A. Mazzanti, *J. Org. Chem.*, 2006, **71**, 6248.
142. S. Burling, S. Douglas, M. F. Mahon, D. Nama, P. S. Pregosin and M. K. Whittlesay, *Organometallics*, 2006, **25**, 2642.
143. F. Focante, R. Leardini, A. Mazzanti, P. Mercandelli and D. Nanni, *Organometallics*, 2006, **25**, 2166.
144. K. Mislow, *Acc. Chem. Res.*, 1976, **9**, 26.
145. H. Komber, K. Stumpe and B. Voit, *Tetrahedron Lett.*, 2007, **48**, 2655.
146. I. Alfonso, M. I. Burguete and S. V. Luis, *J. Org. Chem.*, 2006, **71**, 2242.
147. N. Kanomata and Y. Ochiaia, *Tetrahedron Lett.*, 2001, **42**, 1045.
148. P. Lesot, O. Lafon, H. B. Kagan and C. A. Fan, *J. Chem. Soc. Chem. Commun.*, 2006, 389.
149. O. Lafon, P. Lesot, C. A. Fan and H. B. Kagan, *Chem. Eur. J.*, 2007, **13**, 3772.
150. G. Buntkowsky and H. H. Limbach, *J. Low Temperature Phys.*, 2006, **141**, 55.
151. H. H. Limbach, J. M. Lopez and A. Kohen, *Phil. Trans. Roy. Soc.*, 2006, **361B**, 1399.
152. H. H. Limbach, F. Mannle, C. Detering and G. S. Denisov, *Chem. Phys.*, 2005, **319**, 69.
153. V. A. Bushmelev, A. M. Genaev and V. G. Shubin, *Russ. J. Org. Chem.*, 2006, **42**, 220.
154. V. A. Bushmelev, A. M. Genaev and V. G. Shubin, *Russ. J. Org. Chem.*, 2006, **42**, 100.
155. Y. Li, Y. Li, J. Li, C. Li, X. Liu, M. Yuan, H. Liu and S. Wang, *Chem. Eur. J.*, 2006, **12**, 8378.
156. T. Beringhelli, G. D'Alfonso, D. Donghi, D. Maggioni, P. Mercandelli and A. Sironi, *Organometallics*, 2007, **26**, 2088.
157. Y. Liu, S. J. Vignon, X. Zhang, P. A. Bonvallet, S. I. Khan, K. N. Houk and J. F. Stoddart, *J. Org. Chem.*, 2005, **70**, 9334.
158. S. Nygaard, K. C. F. Leung, I. Aprahamian, T. Ikeda, S. Saha, B. W. Laursen, S. Y. Kim, S. W. Hansen, P. C. Stein, A. H. Flood, J. F. Stoddart and J. O. Jeppesen, *J. Am. Chem. Soc.*, 2007, **129**, 960.
159. S. J. Vignon and J. F. Stoddart, *Coll. Czech. Chem. Commun.*, 2005, **70**, 1493.
160. B. Wrackmeyer and M. Heberhold, *Struct. Chem.*, 2006, **17**, 79.
161. P. Demel, M. Keller and B. Breit, *Chem. Eur. J.*, 2006, **12**, 6669.
162. K. Umakoshi, T. Kojima, Y. H. Kim, M. Onishi, Y. Nakao and S. Sakaki, *Chem. Eur. J.*, 2006, **12**, 6521.
163. P. G. Evans, N. A. Brown, G. J. Clarkson, C. P. Newman and J. P. Rourke, *J. Organomet. Chem.*, 2006, **691**, 1251.
164. P. E. Romero and W. E. Piers, *J. Am. Chem. Soc.*, 2007, **129**, 1698.
165. M. Ohashi, K. Matsubara and H. Suzuki, *Organometallics*, 2007, **26**, 2330.
166. J. D. Egbert, R. M. Bullock and D. M. Heinekey, *Organometallics*, 2007, **26**, 2291.
167. A. V. Davis, T. K. Firman, B. P. Hay and K. N. Raymond, *J. Am. Chem. Soc.*, 2006, **128**, 9484.
168. M. D. Vaughan, V. J. Robertson and J. F. Honek, *J. Fluorine Chem.*, 2007, **128**, 65.
169. J. Konu, M. S. Balakrishna, T. Chivers and T. W. Swaddle, *Inorg. Chem.*, 2007, **46**, 2627.
170. S. D. Karlen and M. A. Garcia-Garibay, *J. Chem. Soc. Chem. Commun.*, 2005, 189.
171. D. Braga, M. R. Chierotti, N. Garino, R. Gobetto, F. Grepioni, M. Polito and A. Viale, *Organometallics*, 2007, **26**, 2266.
172. X. Yang and K. Muller, *J. Mol. Struct.*, 2007, **831**, 75.
173. J. A. DiVerdi, T. Kobayashi and G. E. Maciel, *J. Phys. Chem.*, 2007, **111C**, 5982.
174. N. Sato and S. Nishikiori, *J. Chem. Soc. Dalton Trans.*, 2007, 1115.

175. R. Bohmer, K. R. Jeffrey and M. Vogel, *Prog. Nucl. Magn. Reson. Spectrosc.*, 2007, **50**, 87.
176. J. Cabana, N. Dupre, G. Rousse, C. P. Grey and M. R. Palacin, *Solid State Ionics*, 2005, **176**, 2205.
177. L. S. Cahill, R. P. Chapman, J. F. Britten and G. R. Goward, *J. Phys. Chem.*, 2006, **110B**, 7171.
178. A. R. Czardybon and G. R. Goward, *Solid State Ionics*, 2006, **177**, 1405.
179. M. R. Hampson, J. S. O. Evans and P. Hodgkinson, *J. Am. Chem. Soc.*, 2005, **127**, 15175.
180. S. Antonijevic, S. E. Ashbrook, S. Biedasek, R. I. Walton, S. Wimperis and H. Yang, *J. Am. Chem. Soc.*, 2006, **128**, 8054.
181. M. Haouas, F. Taulelle, N. Prudhomme and O. Cambon, *J. Cryst. Growth*, 2006, **296**, 197.
182. D. Raftery, *Annu. Rep. NMR Spectrosc.*, 2006, **57**, 205.
183. D. H. Brouwer, S. Alavi and J. A. Ripmeester, *Phys. Chem. Chem. Phys.*, 2007, **9**, 1093.
184. P. Tallavaara and J. Jokisaari, *Phys. Chem. Chem. Phys.*, 2006, **8**, 4902.
185. K. V. Romanenko, P. A. Simonov, O. G. Abrosimov, O. B. Lapina, A. Fonseca, J. B. Nagy, J. B. d'Espinose and J. Fraissard, *React. Kinet. Catal. Lett.*, 2007, **90**, 355.
186. S. Pawsey, I. L. Moudrakovski, J. A. Ripmeester, L.-Q. Wang, G. J. Exharos, J. L. C. Rowsell and O. M. Yaghi, *J. Phys. Chem.*, 2007, **111C**, 6060.
187. R. Simonutti, S. Bracco, A. Comotti, M. Mauri and P. Sozzani, *Chem. Mat.*, 2006, **18**, 4651.
188. M. D. Pluth and K. N. Raymond, *Chem. Soc. Rev.*, 2007, **36**, 161.
189. S. Alavi, J. A. Ripmeester and D. D. Klug, *J. Chem. Phys.*, 2007, **126**, 124708.
190. A. V. Davis, D. Fiedler, G. Seeber, A. Zahl, R. van Eldik and K. N. Raymond, *J. Am. Chem. Soc.*, 2006, **128**, 1324.
191. B. Kesanli, J. E. Halsig, P. Zavalij, J. C. Fettinger, Y. F. Lam and B. W. Eichhorn, *J. Am. Chem. Soc.*, 2007, **129**, 4567.
192. G. S. Ananchenko, K. A. Udachin, A. Dubes, J. A. Ripmeester, T. Perrier and A. W. Coleman, *Angew. Chem. Int. Ed. Engl.*, 2006, **45**, 1585.
193. T. Fauconnier, A. D. Bain, P. Hazendonk, R. A. Bell and C. J. L. Lock, *Can. J. Chem.*, 1998, **76**, 426.

CHAPTER 3

Rhodium-103 NMR

Laurence Carlton

Contents

Molecular Sciences Institute, School of Chemistry, University of the Witwatersrand, Johannesburg, South Africa

Annual Reports on NMR Spectroscopy, Volume 63
ISSN 0066-4103, DOI 10.1016/S0066-4103(07)63003-8

Abstract

Developments in ^{103}Rh NMR from the first directly observed high-resolution spectrum to the use of indirect detection methods, *para*hydrogen-induced polarisation (PHIP)-enhanced measurements and the first solid-state CP-MAS ^{103}Rh spectrum are described together with influences on the chemical shift arising from ligand properties, temperature, solvent, intramolecular rearrangements, diastereomerism and secondary isotope effects. Correlations between $\delta(^{103}Rh)$ and stability and rate constants, structural and steric parameters, Hammett σ and infrared data are discussed as is the use of ^{103}Rh NMR in other aspects of rhodium chemistry relevant to catalysis, namely high-pressure studies and metal clusters. Methods of calculating chemical shifts and of determining the signs of coupling constants are noted. Rhodium-103 chemical shifts are given for more than a thousand complexes and clusters together with coupling constants for complexes showing spin coupling of ^{103}Rh to ^{1}H, ^{13}C, ^{15}N, ^{19}F, ^{29}Si, ^{31}P, ^{77}Se, ^{119}Sn, ^{125}Te and to ^{103}Rh and other metals.

1. INTRODUCTION

Advances in technology and the use of indirect detection methods have greatly facilitated access to ^{103}Rh data in recent years. The chemist working with rhodium can now (in principle at least) obtain a ^{103}Rh spectrum in much less time than would normally be required for ^{13}C, and the inclusion of ^{103}Rh data in published accounts of new work with rhodium reflects a growing, but not yet widespread, interest in ^{103}Rh NMR. This interest is tempered by the recognition that ^{103}Rh data are not as readily amenable to interpretation as, for example, those obtained from ^{13}C or ^{15}N. While the high sensitivity of the ^{103}Rh nucleus to its chemical environment is an obvious advantage, the substantial overlap of chemical shift ranges for complexes of different oxidation states and with different combinations of ligands greatly obscures the picture, putting out of reach the possibility of a rhodium chemical shift chart of the type commonly used for the p-block elements. Such limitations, however, are a feature of transition metal NMR and do not constitute a serious obstacle to its application in studies of structure and reactivity.

In this context one aim of this review is to highlight areas of rhodium chemistry in which ^{103}Rh NMR has made, or can potentially make, a major impact.

Rhodium is widely regarded as being the most versatile catalytic element. Its use in a variety of catalytic processes from alkene hydroformylation and acetic acid production to the stereoselective synthesis of fine chemicals and pharmaceuticals is favoured by the mild conditions under which many rhodium-catalysed reactions proceed. The development of new rhodium-based catalytic materials can be greatly assisted by ^{103}Rh NMR. This has been shown by the work of von Philipsborn with rhodium, among other metals, demonstrating the predictive value of transition metal NMR in catalysis and related chemistry.[1,2]

Rhodium-103 NMR has been the subject of several reviews, some dealing more broadly with transition metal NMR,[1–16] others focusing specifically on rhodium.[17–19] The present review attempts to give a broad picture of the range and variety of work that has made use of ^{103}Rh NMR while at the same time including specific detailed reference material. In order to make this information more accessible it has been extensively tabulated (see Appendix), and a simplified account of factors underlying the chemical shift has been included even though, in various shapes and forms, this subject has been dealt with elsewhere.

2. ACQUISITION OF DATA

Rhodium is one of only five elements that exist as a single isotope with nuclear spin quantum number $I = 1/2$ (the others are ^{19}F, ^{31}P, ^{89}Y and ^{169}Tm). This advantage is greatly offset by the low value of the gyromagnetic ratio $\gamma(^{103}\mathrm{Rh})$ which, via the relation $(\gamma\mathrm{Rh}/\gamma\mathrm{H})^3$, is responsible for the very low sensitivity of the ^{103}Rh nucleus relative to the proton, amounting to no more than a factor of 3.1×10^{-5}. A further problem is the long relaxation time (T_1) of ^{103}Rh in many rhodium compounds. While these factors have historically delayed the development of ^{103}Rh NMR spectroscopy they have now, for many purposes and applications, been successfully overcome.

Prior to the report by Gansow and co-workers[20] in 1979 of directly observed ^{103}Rh the measurement of rhodium chemical shifts was by double resonance methods (which required a continuous wave spectrometer) involving irradiation at the ^{103}Rh frequency during the recording of a ^{1}H, ^{19}F or ^{31}P signal from samples exhibiting Rh-H, Rh-F or Rh-P spin coupling. The spectra recorded by Gansow's group required solutions of 10 ml volume, 2 M concentration and $Cr(acac)_3$ as relaxation agent in tubes of 20 mm diameter, and showed good signal-to-noise ratio ($\sim$20 : 1) after 10 h. The problems of relaxation time can be diminished by the use of relaxation agents or circumvented by means of pulse programs such as insensitive nuclei enhanced by polarisation transfer (INEPT),[21] distortionless enhancement by polarisation transfer (DEPT)[22] or the steady-state method of von Philipsborn.[23] The INEPT method, used by Brevard and co-workers,[24,25] offers signal enhancements up to a maximum of $\gamma_H/\gamma_{Rh} = 32$ with polarisation transfer from protons and $\gamma_P/\gamma_{Rh} = 13$, from phosphorus, and the need to allow only for ^{1}H or ^{31}P relaxation. These methods are discussed by Benn and Rufińska[6] and by Mann.[18] Although

direct observation has been largely superseded by the method of indirect detection a potentially wide range of compounds exists for which neither indirect detection nor simpler polarisation transfer methods such as INEPT are applicable.

The method of indirect detection requires that the ^{103}Rh nucleus be spin coupled to a spin 1/2 nucleus of high γ and high natural abundance (as for DEPT and INEPT). The only candidates are ^{1}H, ^{19}F, ^{31}P and ^{205}Tl and, in practice, only ^{1}H and ^{31}P have any significant value in this regard. Having said this it should be pointed out that other isotopes can be used; for example, ^{13}C has been used for the indirect detection of ^{103}Rh,[26,27] but this requires the use of enriched samples and, in all but a few cases (such as ^{13}CO), the cost of isotopic enrichment will be prohibitive. In outline the indirect detection (heteronuclear multiple quantum coherence, HMQC, or heteronuclear single quantum coherence, HSQC) method involves the encoding in the magnetisation of the sensitive, high-γ nucleus (^{1}H, ^{31}P) the resonance frequency of the low-γ nucleus (here ^{103}Rh) in such a way as to allow the result to be displayed in a two-dimensional spectrum (Figure 1). Indirect detection has two very considerable advantages; one, in common with INEPT and DEPT, is the need to allow only for ^{1}H or ^{31}P relaxation during data acquisition; the other is a very significant enhancement in signal intensity by a factor of as much as $(\gamma_S/\gamma_I)^{5/2}$ (S, sensitive; I, insensitive nucleus). For phosphorus-detected ^{103}Rh the maximum possible enhancement is by a factor of 580, and for proton-detection a factor of 5,600. Data acquisition from a 0.01 M solution requires no more than 15 min. In reality the time taken is longer because it is usually necessary first to establish that the signal has not been folded from outside the observed range and second to narrow the observed range so as to improve the accuracy of the measurement.

Phosphorus detection of ^{103}Rh which, because of the very wide range of rhodium complexes of P-donor ligands, has a greater applicability than proton detection, requires a triple resonance probe with a dedicated ^{31}P channel permitting the application of ^{31}P and ^{103}Rh pulses with simultaneous ^{1}H decoupling. A pulse sequence which has proved to be particularly valuable is that of Bax et al.,[29] shown here adapted for ^{31}P-detected ^{103}Rh.

$$\frac{\pi}{2}(^{31}\mathrm{P}) - 1/[2J(^{103}\mathrm{Rh},^{31}\mathrm{P})] - \frac{\pi}{2}(^{103}\mathrm{Rh}) - \tau - \pi(^{31}\mathrm{P}) - \tau$$
$$- \frac{\pi}{2}(^{103}\mathrm{Rh}) - 1/[2J(^{103}\mathrm{Rh},^{31}\mathrm{P})] - \mathrm{Acq}(^{31}\mathrm{P})$$

Inverse detection methods are discussed in greater detail elsewhere.[15,30–32]

Many rhodium complexes contain neither phosphorus nor ligands that permit measurable spin coupling of ^{103}Rh to protons. For these, at present, there is no alternative to the use of relaxation agents and the accumulation of large numbers of scans.

3. CALIBRATION OF SPECTRA

With few exceptions ^{103}Rh spectra are now referenced to an absolute frequency related to the resonance frequency of the protons of tetramethylsilane.

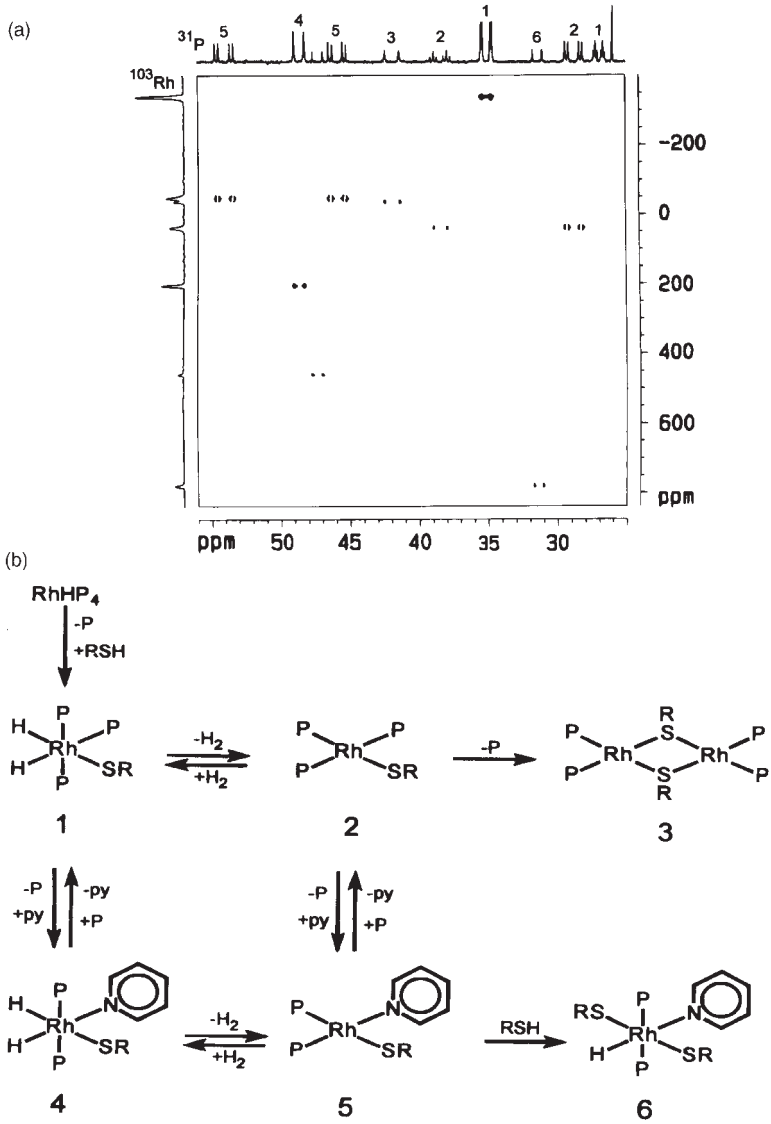

Figure 1 $^{31}P\{^{103}Rh\}$ HMQC spectrum obtained from a mixture of $[Rh(H)(PPh_3)_4]$, CySH and PPh_3 in 10% pyridine/toluene at 248 K. Products are identified in the Scheme. (Reproduced from ref. 28, Copyright (1997) Wiley.)

This method has the great advantages of removing the need for rhodium-containing reference materials, with their associated problems of temperature sensitivity and long relaxation times, and avoiding the situation that exists in ^{15}N or ^{183}W NMR where there is more than one accepted reference material and the conversion of chemical shifts from one scale to another can become an irksome necessity. A few authors still adhere to the use of reference materials but are likely to reduce the impact of their ^{103}Rh work by doing so.

The currently accepted method of referencing ^{103}Rh spectra, introduced in 1978 by Kidd and Goodfellow,[3] makes use of a ^{103}Rh frequency of 3.16 MHz in a field in which the protons of TMS resonate at exactly 100 MHz. This reference frequency is represented as Ξ (^{103}Rh) = 3.16 MHz. Because of the wide range of rhodium chemical shifts (~12,000 ppm) differences between alternative reference points also tend to be large and it is, therefore, not sufficient simply to substitute one reference chemical shift for another. For example, the chemical shift of a signal referenced to rhodium metal, in a field in which the protons of TMS resonate at exactly 100 MHz, is measured in parts per million of 3.155671 MHz (in reality the relevant number is given by the transmitter frequency, but the difference is likely to be negligible), i.e., 1 ppm = 3.155671 Hz, and a signal measured relative to 3.16 MHz has 1 ppm = 3.160000 Hz. If a chemical shift is re-referenced by simple addition or subtraction of a number representing the difference in chemical shift between the two reference points, this mismatch emerges as an error in the calculated value of δ which can amount to several ppm. Chemical shifts are therefore re-referenced using the following equation:[3]

$$\delta = \delta' \frac{\Xi \text{ ref}'}{\Xi \text{ ref}} + \frac{\Xi \text{ ref}' - \Xi \text{ ref}}{\Xi \text{ ref}} \times 10^6 \quad (1)$$

where δ is the corrected chemical shift, δ' the chemical shift with respect to the reported reference, Ξ ref the frequency of the required reference, i.e., Ξ (^{103}Rh) = 3.16 MHz, and Ξ ref′ the frequency of the reported reference. The reported value of Ξ ref′ should ideally be adjusted to correspond to a field in which the protons of TMS resonate at exactly 3.16 MHz or be accompanied by information which permits this number to be calculated.

For a spectrometer in which the protons of TMS resonate at, e.g., 400.13001 MHz the ^{103}Rh frequency of the point defined as zero on the ^{103}Rh scale (giving Ξ(^{103}Rh) = 3.16 MHz) will be 3.16 × 400.13001/100 =12.6444108 MHz. Variations in $\delta(^1\text{H})_{\text{TMS}}$ arising from changes in solvent and temperature are small, translating into insignificant differences on the ^{103}Rh scale, thus eliminating any need for re-referencing (i.e., recalculating the frequency given as 12.644108 MHz). It should be noted that values of Ξ ref′ reported for reference materials, e.g., [Rh(acac)$_3$],[6] will vary with temperature. The re-referencing of a reported chemical shift that is referenced to a chemical standard but is unaccompanied by a value of Ξ ref′ can only be approximate.

4. FACTORS UNDERLYING THE CHEMICAL SHIFT

The following is a much simplified account. For a more rigorous treatment see refs. 33–36. The chemical shift reflects contributions from diamagnetic and paramagnetic shielding effects (σ_D and σ_P, respectively), the former opposing and the latter augmenting the field applied to the sample. For a transition metal the influences on σ_D and σ_P have been shown to be largely separable, the core electrons giving rise to σ_D and the d electrons to σ_P.[36] The value of σ_D for a given metal is regarded as being, to a good approximation, constant. The

paramagnetism referred to by the term σ_P is orbital paramagnetism, created by the mixing (to a small extent) of a singlet excited electronic state with the ground state. Three factors govern the magnitude of this influence: the energy difference (ΔE) between the ground state and a low lying excited state, the degree of imbalance of the electrons in the valence orbitals that is induced by bonding and the average radius of a d orbital. The radius is inversely related to the force of repulsion between the d electrons. The size of an orbital or, more significantly the average distance, $<r>$, of an electron from the nucleus, has a strong influence on the electron's (potential) ability to interact magnetically with the nucleus. To the extent that an electron occupies a singlet excited state, creating orbital (but not spin) paramagnetism, it will generate a field at the nucleus that is proportional to $<r^{-3}>$. The changes in chemical shift of a transition metal nucleus that accompany changes in the coordination sphere are therefore enhanced by effects which favour shrinkage of the valence orbitals and a closing of the energy gap between ground and excited states.

A value for ΔE can be obtained from electronic spectra, as can a quantity that represents the extent to which the average distance from the nucleus of electrons in d orbitals increases as a result of covalent bonding. This quantity is the *nephelauxetic* (Greek: cloud expanding) *ratio*, β, generally defined as the ratio of the Racah parameters B for the complex and for the free ion, B_c/B_f[37–39]. The Racah parameter B is a measure of d–d electronic interactions in the metal and is found to have a smaller value for a complex than for the corresponding free ion, i.e., $\beta = B_c/B_f < 1$. From this it follows that the forces of repulsion between the d electrons are smaller in the complex than in the free ion, with the implication that the average distance between the d electrons is larger in the complex than in the free ion. The orbital expansion involved in this effect is attributed to two simultaneous causes: the reduction of the effective charge on the metal as a result of electron donation via chemical bonding and a covalency effect due to the participation of the metal atomic orbitals in molecular orbitals with the ligands.[37,40] The nephelauxetic ratio therefore provides an experimentally determinable measure of the extent of changes in the distribution of electrons in the valence shell (nominally d electrons) induced by the formation of covalent bonds.

An ordering of ligands according to their influence on β is known as the *nephelauxetic series*[7,37,38] shown (in part) in order of increasing ability to expand the d orbitals (i.e., β decreasing), as follows: $F^- < H_2O < NH_3 < NCS^- < CN^- \cong Cl^- < Br^- < I^-$. For a given metal ion the nephelauxetic effect of the ligand donor atom tends to decrease across a row of the periodic table and tends to increase down a group (e.g., N < P < As < Sb). The influence on the chemical shift of the metal of changing ligands from a lower to a higher nephelauxetic value (β decreasing) is shown on going from $[Rh(Cl)_6]^{3-}$ $\{\delta(^{103}Rh) = 8{,}000\}$ to $[Rh(Br)_6]^{3-}$ $\{\delta(^{103}Rh) = 7{,}000\}$.[41,42] This result, while indicative of processes described above, cannot be viewed in isolation from the effects of changes in ΔE, the energy required for transition to an excited state.

The ability of a ligand to influence ΔE is related to its σ donor/π acceptor properties. In a complex of σ donor (or $\sigma+\pi$ donor) non-π acceptor ligands the buildup of electron density on the metal increases the force of repulsion between

the valence orbitals, with the result that their energy rises and ΔE decreases. In a complex of strong π acceptor ligands much of the electron density brought to the metal by σ donation is transferred back to the ligand with the result that ΔE is large. The relative influence of a ligand upon ΔE is given by the well-known *spectrochemical series*[43] in which ligands are ordered according to their ability to increase ΔE. The series is shown (in part) by $I^- < Br^- < Cl^- < F^- < OH^- < H_2O < NH_3 < NR_3 < PR_3 < CN^-$, $CO \sim PF_3$. The influence on the chemical shift of the metal of a large change in ΔE can be seen for $[Rh(CN)_6]^{3-}$ $\{\delta(^{103}Rh) = 340\}$ which has a chemical shift of over 7,000 ppm lower than that of the chloro complex $[Rh(Cl)_6]^{3-}$ (see above). It should be noted that while, from the spectrochemical series, the sequence $I^- < Br^- < Cl^-$ corresponds (on going from I^- to Cl^-) to a decrease in δ_{metal} (ΔE is increasing), in the nephelauxetic series the same sequence corresponds to an increase in δ_{metal} (the orbitals shrink and the interelectronic forces of repulsion increase). Since the observed change is to higher δ_{metal} on going from Br^- to Cl^- as ligand the nephelauxetic effect clearly predominates, but this is true only for halide ligands[18] and cannot be generalised further (see below).

Some general remarks can be made relating ligand properties to metal chemical shift. According to the spectrochemical series strong σ donors and poor π acceptors ('weak' ligands) will give rise (via low ΔE) to a high δ_{metal} and strong π acceptors to a low δ_{metal}. From the nephelauxetic series ligands of low polarisability will favour a high δ_{metal} (via low r) and ligands of high polarisability will favour a low δ_{metal}. Ligands that are good σ donors, poor π acceptors and only weakly polarisable (e.g., H_2O) will be associated with the highest metal chemical shifts, ligands that are polarisable strong π acceptors (e.g., CN^-) will be associated with low metal chemical shifts, while ligands that are polarisable weakly or non-π accepting σ donors (e.g., SR_2, I^-) or weakly polarisable π acceptors (e.g., $NCBPh_3^-$) will give complexes having metal chemical shifts that may be difficult to predict. For ligands that create a low ΔE polarisability (nephelauxetic) effects will largely determine the value of δ_{metal}, as with the halide ions (noted above).

Modifications of the Ramsey equation,[44] which more than 40 years ago was superseded as a means of calculating nuclear shielding (see Section 13), provide a means by which the influences on the chemical shift can be formulated entirely in terms of observable molecular electronic properties. However, the results obtained in this way can be regarded, at best, as approximate. The paramagnetic shielding, σ_P in Ramseys's equation, contains terms relating to electron distribution that are difficult to quantify. Work in the 1980s[45–47] led to the inclusion of the nephelauxetic ratio β (an experimentally determinable quantity) in the expression for σ_P, shown in the form proposed by Juranić[36] in Equation (2) and confirmed by the correlation of experimental data (^{99}Ru[48] and ^{103}Rh[47] chemical shifts) with $\beta/\Delta E$.

$$\sigma_P = -8\frac{\mu_0\mu_B^2}{\pi} \langle r_d^{-3}\rangle_F \frac{\beta}{\Delta E} \tag{2}$$

The terms μ_0 and μ_B refer to the permittivity of vacuum and the Bohr magneton, respectively, and $<r_d^{-3}>_F$ refers to the d orbital radius of the free ion. For a given oxidation state $<r_d^{-3}>_F$ is constant and a simplified formula for

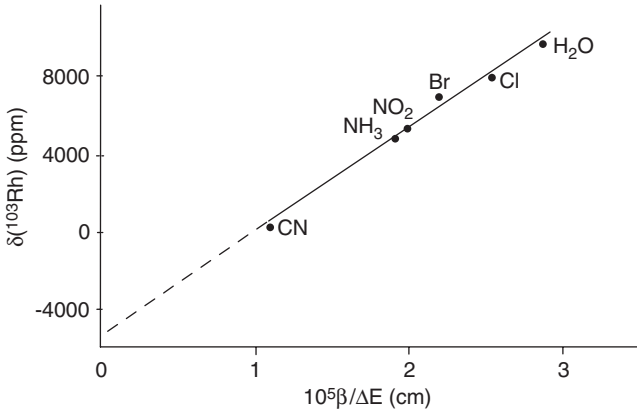

Figure 2 Plot of $\delta(^{103}\text{Rh})$ against $\beta/\Delta E$ for $[\text{Rh(III)X}_6]$ (X = CN^-, NH_3, NO_2^-, Br^-, Cl^-, H_2O). (Data from ref. 49.)

the chemical shift is then

$$\delta_{\text{metal}} = \delta_{\text{D}} + K(\beta/\Delta E) \tag{3}$$

where δ_{D} is the diamagnetic chemical shift (effectively constant for a given metal) and K is a positive constant. A plot of $\delta(^{103}\text{Rh})$ against $\beta/\Delta E$, with values of β and ΔE obtained from the electronic spectra of a series of octahedral Rh(III) complexes of widely differing β and ΔE, is shown in Figure 2.[49] To a good approximation the points define a straight line with intercept $-5{,}000$ ($\pm 1{,}000$) ppm (see also refs. 42,47). This is a measure of δ_{D}, the chemical shift arising from diamagnetic shielding alone.

The effect on δ_{metal} of varying ΔE, for a series of complexes of similar coordination geometry, is shown in plots of δ_{metal} vs. λ, the wavelength of the d–d transition. Data for the complexes $[\text{Rh}(\text{acac}^{\text{F}})(\text{alkene})_2]$ (alkene = ethylene, *cis*- and *trans*-butene),[50] which have $\delta(^{103}\text{Rh})$ in the range 1,296–1,763 ppm, show a linear relationship between $\delta(^{103}\text{Rh})$ and λ, implying that factors represented in Equation (2) by β do not vary much. Similarly, for two series of cobalt complexes,[51,52] the first having ligands with second row donor atoms (C, N, O) and the second series with third row donor atoms (P, S), the relationship between $\delta(^{59}\text{Co})$ and λ within each series is linear. There is, however, a significant difference between the gradients for the two series, indicating limits beyond which the influence of β-related factors cannot be ignored.

5. INFLUENCE OF TEMPERATURE ON THE CHEMICAL SHIFT

The chemical shift of a transition metal (in a complex) is sensitive to temperature, with changes in δ_{metal} of the order of 0.5–1.5 ppm/K being commonly encountered. These changes occur independently of intermolecular effects and have their origin in the vibration of metal–ligand bonds. The d–d transition energy, represented by

the term ΔE in the expression for paramagnetic shielding, is influenced by changes in the population of vibrational excited states, diminishing as the population of these states increases. Thus, an increase in metal chemical shift is observed to accompany an increase in temperature. This effect, known as vibrational shielding, is well documented[53–55] and theoretically accounted for.[56,57]

Superimposed on the effects of vibrational shielding may be a variety of possible interactions with the solvent[34,58,59] and these might also be expected to show some temperature dependence. Therefore, although the response of δ_{metal} to vibrational shielding in the absence of such effects is approximately linear, it cannot be assumed that this fact can be generalised to all situations involving changes in temperature. In particular the temperature response of coordinatively unsaturated complexes, such as those of Rh(I), is likely to include solvent effects (see below).

A recent study[60] of the influence of temperature and solvent effects on the ^{103}Rh chemical shifts of complexes $[Rh(X)(PPh_3)_3]$ (X = Cl, N_3, NCO, NCS, $N(CN)_2$, $NCBPh_3$, $CNBPh_3$, CN) showed solvent-dependent temperature effects in the range 195–300 K. In dichloromethane the temperature response of $\delta(^{103}Rh)$ is approximately linear for all but three of the complexes and all but one show linearity in the range 230–300 K, with gradients that differ slightly (Figure 3), all having $\delta(^{103}Rh)$ decreasing with temperature. While these findings are in broad agreement with predicted vibrational shielding effects the data obtained from solutions in chloroform and toluene, most notably for $[Rh(Cl)(PPh_3)_3]$ and $[Rh(CN)(PPh_3)_3]$, are not. For these complexes an interaction occurs with the solvent that is enhanced as the temperature is lowered, resulting in a shift to *higher* δ. This shift, which is in excess of 1 ppm/K for the CN complex below 250 K, is superimposed on the vibrational shielding gradient (to lower δ as the temperature is reduced) which thus masks a much larger positive shift in $\delta(^{103}Rh)$. These solvent-dependent effects are discussed in the next section.

6. INFLUENCE OF SOLVENT ON THE CHEMICAL SHIFT

The chemical shift of a metal in a dissolved metal complex can be influenced by non-bonded interactions with the solvent arising from bulk susceptibility, magnetic anisotropy, electric field effects and van der Waals interactions,[34,58,59] and by more specific interactions such as hydrogen bonding. Hydrogen bonding effects are likely to be highly solvent-dependent and may involve a direct interaction with the metal or an interaction with a ligand. The complexes $[Rh(X)(PPh_3)_3]$, noted in the previous section, have ^{103}Rh chemical shifts that show both solvent and temperature dependence, which varies with ligand X. These separate influences (ligand, solvent, temperature) are, therefore, not best studied in isolation. A broader picture of the response of $\delta(^{103}Rh)$ to the environment of the metal atom emerges when the ligand X in complexes $[Rh(X)(PPh_3)_3]$ is varied so as to include both good σ (or $\sigma+\pi$) donors (Cl^-, N_3^-), strong π acceptors (CN^-, $CNBPh_3^-$) and both polarisable (CN^-, Cl^-) and more weakly polarisable ($NCBPh_3^-$, $N(CN)_2^-$) ligands and the solvent

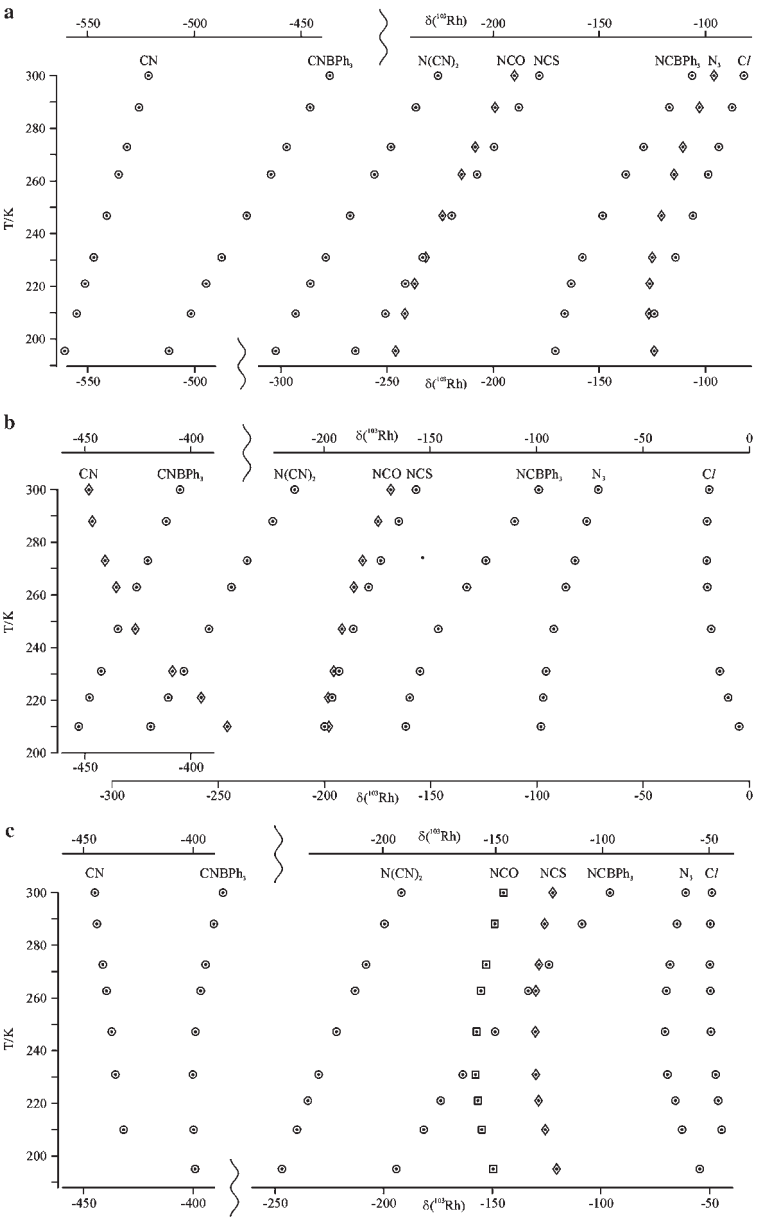

Figure 3 Plot of $\delta(^{103}\text{Rh})$ against temperature for complexes $[Rh(X)(PPh_3)_3]$ (X = Cl, N_3, NCO, NCS, $N(CN)_2$, $NCBPh_3$, $CNBPh_3$, CN) dissolved in (a) dichloromethane, (b) chloroform and (c) toluene (concentrations ~0.01 M). The contraction of the plot, which is intended to eliminate regions without data, causes, in (b), the overlap of data for X = CN (δ −385 to −449 ppm) and for X = $N(CN)_2$ (δ −214 to −280 ppm). (Reproduced from ref. 60, Copyright (2004) Wiley.)

(dichloromethane, chloroform, toluene) and temperature (in the range 195–300 K) are also varied independently.[60] The results of this study are shown in Figure 3.

In Figure 3 the response of $\delta(^{103}Rh)$ of $[Rh(X)(PPh_3)_3]$ to a decrease in temperature follows the expected trend for vibrational shielding (δ decreasing with temperature) in dichloromethane solution, but in chloroform and toluene there are significant departures from the trend. These deviations arise with the more polarisable ligands (CN^-, Cl^-), while the greatest conformity to the expected trend is found for ligands of lower polarisability ($NCBPh_3^-$, $N(CN)_2^-$). The most anomalous response is found for $X = CN^-$ in chloroform solution. These results have been interpreted in terms of a hydrogen-bonded interaction with the solvent, where the δ^+ hydrogen of the polar CH bond of chloroform is attracted to the electron-rich metal. Ligand X (CN^-, Cl^-) acts as a reservoir of electron density that can assist in the process. The bond is viewed as being weak and kinetically labile, becoming increasingly stabilised as the temperature is reduced.

If it is the polarisability of ligand X that underlies the readiness of the metal to interact with the solvent then a complex having a ligand of minimal polarisability might be expected to show a temperature profile that is relatively free of such contributions. This is found to be the case for the complex $[Rh(O_2CCF_3)(PPh_3)_3]$. In Figure 4 the ^{103}Rh chemical shifts at various temperatures are shown for $[Rh(Cl)(PPh_3)_3]$ and for $[Rh(O_2CCF_3)(PPh_3)_3]$ in each of the three solvents dichloromethane, chloroform and toluene.[60] For $X = Cl^-$ the chemical shift

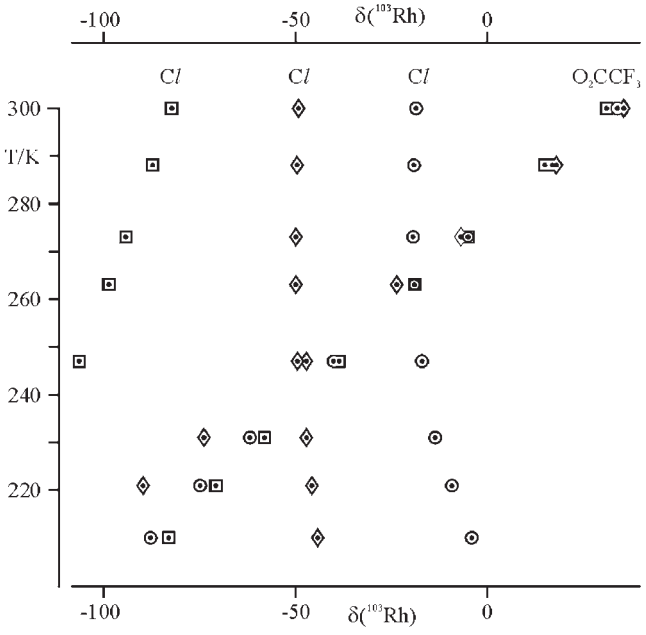

Figure 4 Plot of $\delta(^{103}Rh)$ against temperature for complexes $[Rh(X)(PPh_3)_3]$ (X = Cl, O_2CCF_3) (concentrations ~0.01 M) dissolved in chloroform (⊙), dichloromethane (⊡) and toluene (◈). (Reproduced from ref. 60, Copyright (2004) Wiley.)

differences in the three solvents are large (63 ppm on going from dichloromethane to chloroform at 300 K and more than 100 ppm at 230 K or below) and the gradients differ significantly. For $X = O_2CCF_3^-$ the chemical shift differences are small: 3 ppm on going from dichloromethane to chloroform at 300 K, 4 ppm at 230 K and 5 ppm (300 K) and 16 ppm (230 K) on going from dichloromethane to toluene, giving gradients that are remarkably similar. It would, therefore, appear that with trifluoroacetate as ligand X in the complex $[Rh(X)(PPh_3)_3]$ interaction of the metal with the solvent is effectively discouraged, and the temperature response that is observed arises almost entirely from vibrational shielding.

In a study of alkene-exchange reactions Öhrström and co-workers[61] measured ^{103}Rh chemical shifts of $[Rh(acac)(C_2H_4)_2]$ in a variety of solvents ($CH_2Cl_2|H_2O$, CH_2Cl_2, $CDCl_3$, THF, *n*-pentane, Et_2O, acetone, acetonitrile and methanol) and found only a small variation in the range 1,180–1,167 ppm, showing no correlation with the donor properties of the solvent. The authors comment that these small shifts are unlikely to be caused by coordination of the solvent and might arise from electric field effects or solvent magnetic anisotropy.

7. OTHER INFLUENCES ON THE CHEMICAL SHIFT

7.1 Change in coordination geometry

The changes in coordination geometry that occur when a four-coordinate Rh(I) complex ion in solution combines reversibly with a counterion, such as Cl^-, or where a substituent group attached to a ligand in a neutral complex binds to the metal, are accompanied by large ($\sim$400–900 ppm) changes in $\delta(^{103}Rh)$. These changes in chemical shift are attributed to a reduction in ΔE that is brought about by a transformation from a square planar to a square pyramidal or trigonal bipyramidal geometry.

Elsevier and co-workers[62] have reported ^{103}Rh chemical shifts for $[Rh\{(C_6F_5)_2P(CH_2)_2P(C_6F_5)_2\}_2]^+X^-$ (X = Cl, PF_6) that differ by 834 ppm, increasing from −671 (X = PF_6) to 163 (X = Cl) on exchanging the counterion. For the two complexes $[Rh\{(4\text{-}CF_3C_6H_4)_2P(CH_2)_2P(4\text{-}CF_3C_6H_4)_2\}_2]^+X^-$ (X = Cl, PF_6), however, the difference in $\delta(^{103}Rh)$ is only 36 ppm. This implies that the less electron-rich complex, with C_6F_5 substituents on phosphorus, much more readily combines with chloride than the more electron-rich complex having $C_6H_4CF_3$ substituents, to become five-coordinate ((a)–(c)). A simple exchange of counterion causes only a small change in $\delta(^{103}Rh)$.

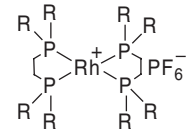

R = C_6F_5 (−671)
R = $C_6F_4CF_3$ (−1215)

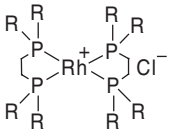

R = $C_6H_4CF_3$ (−1179)

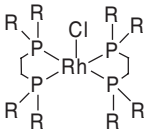

R = C_6F_5 (163)

(a) - (c) $\delta(^{103}Rh)$ in parentheses. Data from ref 62.

The complex [Rh{(*R*,*R*)-$Ph_2PCH_2(CHOH)_2CH_2PPh_2$}(cod)]$^+$ BF_4^-, examined by Bühl et al.,[63] shows temperature-dependence of its ^{103}Rh chemical shift consistent with the existence of two isomeric forms ((d) and (e)) having different coordination geometries. At room temperature a single signal is seen in the ^{103}Rh–^{31}P spectrum. At 185 K this is resolved into two signals in the ^{103}Rh dimension, separated by 474 ppm, one of which (δ −449 ppm) is associated with one signal in the ^{31}P dimension and the other (δ 25 ppm) associated with two ^{31}P signals, indicating a lower symmetry. Density functional theory (DFT) calculations using the model compounds [Rh(*R*,*R*-$H_2PCH_2(CHOH)_2CH_2PH_2$)(diene)]$^+$ (diene = cod, nbd) in gas-phase conditions showed four possible conformations for each complex, one conformer (e) having an Rh–O interaction. The structural parameters obtained by DFT for this conformer (with nbd as diene) to a good approximation match the X-ray crystallographic data for the complex [Rh{*R*,*R*-$Ph_2PCH_2(CHOH)_2CH_2PPh_2$}(nbd)]$^+$ BF_4^-.[64] The cod-containing complex of lower symmetry (phosphines non-equivalent) is considered to have a similar geometry, consistent with its higher rhodium chemical shift than that of the symmetrical (four coordinate) isomer.

(d) δ(^{103}Rh) −449 **(e)** δ(^{103}Rh) 25

Data from ref 63

Lindner and co-workers[65] have shown that the complex [Rh(Cl)($Cy_2PCH_2CH_2OCH_3$)$_2$] can bind sulphur dioxide to give either a five-coordinate (f) or a four-coordinate product (g) depending upon the solvent. In acetone solution the complex behaves as a Lewis base, donating an electron pair to sulphur, whereas in hexane it behaves as a Lewis acid, accepting an electron pair from sulphur. The two isomeric forms can readily be interconverted by a change of solvent. In dichloromethane, a solvent of intermediate polarity, the interconversion is temperature-dependent. At room temperature a mixture of the two isomers is observed becoming converted, at 233 K, entirely into the four-coordinate form. The ^{103}Rh chemical shift changes by 695 ppm on going from the five-coordinate to the four-coordinate form in dichloromethane at 295 K.

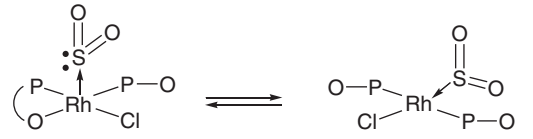

(f) δ(^{103}Rh) 1650 **(g)** δ(^{103}Rh) 955

P⌒O = $Cy_2PCH_2CH_2OCH_3$. Data from ref 65.

Venanzi and co-workers[66,67] have used ^{103}Rh chemical shifts to distinguish between the k^3 and k^2 modes of binding of the tris(pyrazolyl) borate (Tp) ligand (and substituted derivatives such as Tp*) to rhodium in a series of [Rh(Tp)(diene)]

(diene = cod, nbd) complexes. A comparison of $\delta(^{103}Rh)$ for the tris(pyrazolyl)borate complexes and for bis(pyrazolyl)borate complexes (e.g., [Rh(Ph_2Bpz_2)(diene)] and [Rh(BBN(3-Mepz)$_2$)(diene)] (BBN = borabicyclononane)) shows that for the latter (restricted to a k^2 mode of binding) $\delta(^{103}Rh)$ lies in the range 947–1,205 ppm (cod complexes) or in the range 1,034–1,374 (nbd complexes), while for the tris (pyrazolyl)borate complexes $\delta(^{103}Rh)$ lies either in the same range or at a significantly higher value. Thus, the complex [Rh(HB(3-^{i}Pr-4-Brpz)$_3$(nbd)] ($\delta(^{103}Rh)$ = 1,274, 1,293; two isomers) is taken to have a k^2 mode of pyrazolylborate binding and the complexes [Rh(HB(3-Mepz)$_3$)(nbd)] ($\delta(^{103}Rh)$ = 1,619 ppm) and [Rh(Tp*)(nbd)] ($\delta(^{103}Rh)$ = 1,777 ppm) are taken to have, in solution, a significant component of k^3 binding. An X-ray crystal structure[67] of [Rh(MeB(3-Mepz)$_3$)(nbd)] shows the Tp^{Me} ligand to be k^3-bonded.

7.2 Diastereomeric dispersion

Chiral phosphine ligands are extensively used in stereoselective hydrogenation. The presence of two or more chiral centres in a complex gives rise to diastereomers, which exhibit differences in metal chemical shift that range, in the case of rhodium, from a few ppm to more than 200 ppm. In work seeking to elucidate factors governing rhodium-catalysed asymmetric hydrogenation of prochiral enamide substrates von Philipsborn and co-workers[68] examined two series of enamide complexes [Rh{methyl(*Z*)-α-*N*-acetamidocinnamate}(*S,S*-CHIRAPHOS)]$^+$ (**h**) and (**i**) and related compounds and their *S,S*-DIPAMP analogues. The ^{103}Rh signals from the major (sterically favoured) diastereomer (**i**) were found to occur at chemical shifts between 33 and 290 ppm lower than those of the minor diastereomer (**h**) (Figure 5).

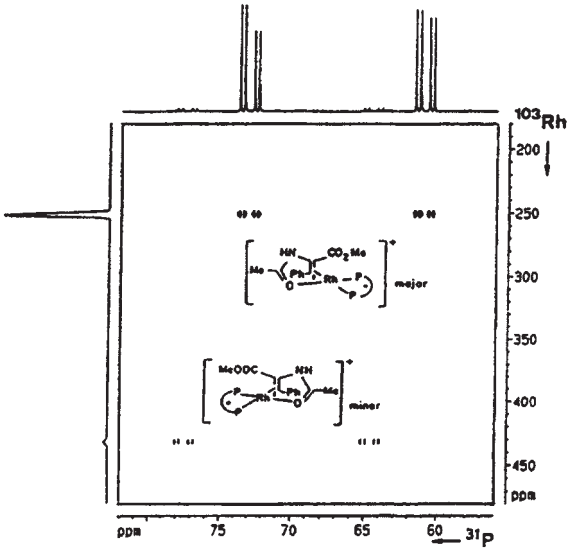

Figure 5 $^{31}P\{^{103}Rh\}$ HMQC spectrum of [methyl(*Z*)-α-*N*-acetamidocinnamate)Rh(*S,S*-CHIRAPHOS)]$^+$ ClO_4^- in CD_3OD at 300 K showing major and minor diastereomers. (Reproduced from ref. 68, Copyright (1993) American Chemical Society.)

The authors comment on the fact that hydrogen is well known to react more quickly with the thermodynamically disfavoured (minor) diastereomer than with the favoured (major) one, and in light of the differences in $\delta(^{103}Rh)$ of the diastereomers of the enamide CHIRAPHOS and DIPAMP complexes, which demonstrate an electronic difference at rhodium, suggest that the H_2-addition step in the catalysed reaction may be electronically controlled. The increased shielding of the metal in the major diastereomers appears to indicate stronger bonding of the substrate, which in turn inhibits the binding of another ligand. The catalysed hydrogenation has been reviewed.[69]

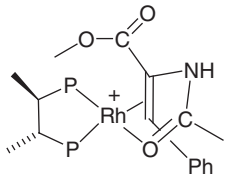

(h) $\delta(^{103}Rh)$ 428 ppm

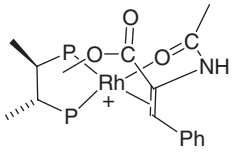

(i) $\delta(^{103}Rh)$ 250ppm

Phenyl groups omitted for clarity. Data from ref. 68.

Other examples of diastereomeric dispersion of the ^{103}Rh signal include: (a) menthyl- and neomenthyl-functionalised indenyl rhodium cyclooctadiene complexes[70] (**j**) and (**k**); (b) methoxytrifluoromethylphenylacetate (MTPA) complexes $[Rh_2(MTPA)_4]$ on interaction with the chiral phosphine $PMePh(NEt_2)$[71] ($\delta(^{103}Rh)$ 6,963, 6,949 ppm); (c) phosphino(sulphinylmethyl)triarylphosphonium ylid rhodium cyclooctadiene complexes[72] ($\delta(^{103}Rh)$ 261, 170 ppm); (d) [Rh(Cl)(cod)(^{Z}AlaSerPhos)] ($\delta(^{103}Rh)$ 372, 365 ppm) and [Rh(cod)(k^2-^{Z}AlaSerPhos)][73] ($\delta(^{103}Rh)$ 426, 413 ppm). In examples (a), (c) and (d) complexes were characterised by X-ray crystallography, which identified (for (a) and (c)) the more sterically hindered diastereomer as having the higher rhodium chemical shift.

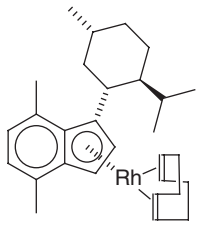

(j) *p*S $\delta(^{103}Rh)$ – 129 ppm

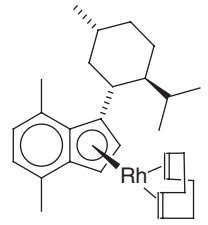

(k) *p*R $\delta(^{103}Rh)$ – 151 ppm

Data from ref. 70

7.3 Secondary isotope effects

In transition metal NMR the most noteworthy secondary isotope effect is that which involves the exchange of hydrogen for deuterium. The replacement

of ^{1}H by ^{2}H in complexes of transition metals having M–H bonds is to increase the shielding of the metal nucleus by an amount in the range 5–13 ppm (e.g., −6 ppm for ^{93}Nb in $[Nb(Cp)(H)(CO)_3]^-$ (ref. 74) and −10 ppm for ^{183}W in $[W(Cp)(H)(CO)_3]^-$ (ref. 75)). The effect is strongly influenced by the co-ligands in a complex (−12.3 and −8.7 ppm for ^{195}Pt in *trans*-$[Pt(X)(H)(PEt_3)_2]$, X = Cl and CN, respectively[76]). For the complex $[Rh(Cp^*)(^1H)_2(^2H)(SiEt_3)]$ {$\delta(^{103}Rh)$ = −1,625 ppm} a shift of −9 ppm relative to that of $[Rh(Cp^*)(^1H)_3(SiEt_3)]$ has been reported.[77] The change in chemical shift that accompanies isotopic exchange can be understood in terms of the changed vibrational properties of the metal–ligand (here hydride) bond. Substitution with a heavy isotope reduces the amplitude of vibrational motion, consequently decreasing the accessibility of electronic excited states (see Section 5) leading to a shielding of the metal nucleus.[34,35,78,79]

The isotope effect does not require that hydrogen be directly bonded to the metal. The exchange of ^{1}H for ^{2}H in $[Co(en)_3]Cl_3$,[80] which occurs spontaneously on dissolving the complex in D_2O, leads to an isotope shift of the ^{59}Co signal of −4.7 ppm per deuterium, or −56 ppm on complete exchange. For $[Co(NH_3)_6]Cl_3$ the shift amounts to −94 ppm. The effect has been attributed to the fact that RN^2H_2 is a stronger base than RN^1H_2, capable of inducing a larger ΔE in its complexes with transition metals and hence a lower contribution to the paramagnetic shift.[80]

The ^{2}H enrichment of the complex $[Rh(Tp^*)(H)_2(H_2)]$ has been examined by von Philipsborn and co-workers[81] who used partial deuteriation in order to obtain data simultaneously (by ^{103}Rh-^{1}H HMQC) from all four ^{1}H-containing isotopomers: $^1H_4$, $^1H_3{}^2H$, $^1H_2{}^2H_2$ and $^1H^2H_3$. Because of rapid exchange processes (even at 160 K) there is only one ^{1}H signal per isotopomer allowing, with an appropriate $^1H/^2H$ ratio, the identification of all four isotopomers and their characterisation by ^{1}H, ^{2}H and ^{103}Rh NMR. The result of a successive increase in the number of ^{2}H nuclei in $[Rh(Tp^*)(H)_2(H_2)]$ is progressively to decrease $\delta(^{103}Rh)$ from 809 ppm ($^1H_4$) to 796 ($^1H_3{}^2H$), 785 ($^1H_2{}^2H_2$) and 775 ($^1H{}^2H_3$) ppm.

The ^{15}N isotope shift of $\delta(^{103}Rh)$ for $[Rh(NCBPh_3)(PPh_3)_3]$ (solvent CD_2Cl_2/CH_2Cl_2, concentration 0.01 M, temperature 300 K) has been found to lie in the range −0.3 to −0.4 ppm.[82]

8. CORRELATION OF $\delta(^{103}Rh)$ WITH CHEMICAL AND STRUCTURAL PARAMETERS

8.1 Correlation of $\delta(^{103}Rh)$ with stability constants

The following account briefly describes work by Preetz and co-workers,[83] by Sandström and co-workers,[42,49] who have shown the value of ^{103}Rh chemical shift data in estimating the stability constants of complexes for which no stability data are available, and by Öhrström and co-workers.[50,84]

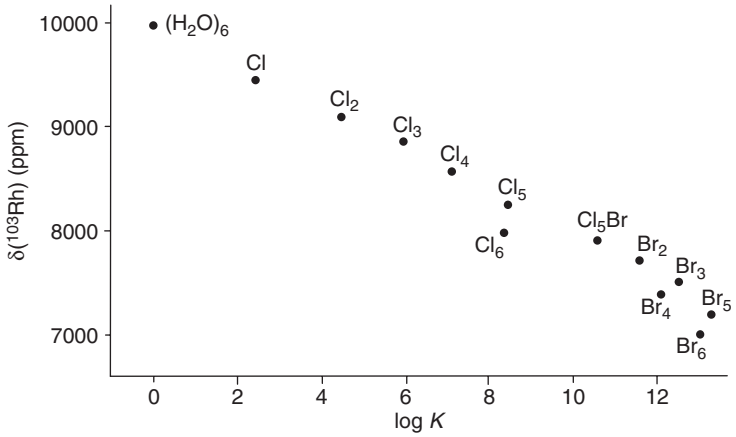

Figure 6 Plot of $\delta(^{103}\text{Rh})$ against log K (K = equilibrium constant) for complexes $[\text{Rh(III)}(\text{Cl})_n(\text{H}_2\text{O})_{6-n}]^{3-n}$, and $[\text{Rh}(\text{Cl})_n(\text{Br})_{6-n}]^{3-}$. (Data from ref. 49.)

For the two series of complexes $[\text{RhCl}_n(\text{H}_2\text{O})_{6-n}]^{3-n}$ and $[\text{RhCl}_n\text{Br}_{6-n}]^{3-}$ equilibrium constants have been shown to correlate with ^{103}Rh chemical shift. The result is shown in Figure 6.[49] An increase in stability occurs on replacing H_2O by Cl^- and on replacing Cl^- by Br^-. The influence on $\delta(^{103}\text{Rh})$ of these successive changes in the coordination sphere is interpreted in terms of corresponding changes in the d orbital radius, expressed by the nephelauxetic ratio β.[49] Ligand exchange in Rh(III) complexes is very slow, restricting or prohibiting the measurement of some equilibrium constants (e.g., $[\text{Rh}(\text{CN})_6]^{3-}$). For other complexes, such as $\text{K}_3[\text{RhF}_6]^{3-}$, the problem is low stability in solution. In aqueous HF the $[\text{RhF}_6]^{3-}$ ion is rapidly aquated giving mixtures containing $[\text{RhF}_n(\text{H}_2\text{O})_{6-n}]^{3-n}$. An estimate of $\sim$10,990 for $\delta(^{103}\text{Rh})$ of $[\text{RhF}_6]^{3-}$ was obtained by substitution of a calculated value of $\beta/\Delta E$ in Equation (2) (Section 4). From Figure 6 it can be seen that this chemical shift corresponds to log $K < -1$, where K is the equilibrium constant (formation constant). Complexes of high stability, e.g., $[\text{Rh}(\text{CN})_6]^{3-}$ and $[\text{Rh}(\text{SCN})_6]^{3-}$, are of interest in extraction processes by which, for example, rhodium in motor exhaust catalysts can be recovered. Using measured values of $\delta(^{103}\text{Rh})$ for $[\text{Rh}(\text{CN})_6]^{3-}$ (340 ppm) and $[\text{Rh}(\text{SCN})_6]^{3-}$ (2,726 ppm)[42,49] the gradient in Figure 6 can be extrapolated to give values of log K of 47 ± 4 and 35 ± 3 for $[\text{Rh}(\text{CN})_6]^{3-}$ and $[\text{Rh}(\text{SCN})_6]^{3-}$, respectively. This result indicates that SCN^- as well as CN^- may be useful in the hydrometallurgical recovery of rhodium.

The equilibrium constant[85] for the reaction

$$[\text{Rh(acac)}(\text{C}_2\text{H}_4)_2] + \text{alkene} \rightleftarrows [\text{Rh(acac)}(\text{C}_2\text{H}_4)(\text{alkene})] + \text{C}_2\text{H}_4$$

where alkene = propene, *cis*-butene, *trans*-butene, shows a good correlation (Figure 7) with $\delta(^{103}\text{Rh})$, the higher chemical shifts corresponding to a lower stability.[50] With C_2F_4, however, the ^{103}Rh chemical shift is much higher than would be predicted from Figure 7 on the basis of the stability constant. This difference has been interpreted[50,84] as arising from the fact that the bonding in

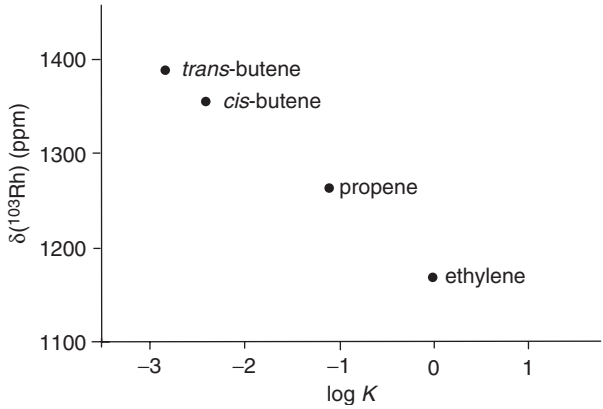

Figure 7 Plot of $\delta(^{103}\text{Rh})$ against log K (K = equilibrium constant) for [Rh(acac)(ethylene)(alkene)]. (Data from ref. 50.)

$Rh(C_2F_4)$ more closely resembles that of a metallocyclopropane than the bonding represented by the Chatt–Duncanson–Dewar model, causing a decrease in $<r_d^{-3}>$ and an increase in $\delta(^{103}\text{Rh})$. The stability–chemical shift relationship for one class of alkenes cannot, therefore, be generalised to other classes.

8.2 Correlation of $\delta(^{103}\text{Rh})$ with Hammett σ

The Hammett σ function is a measure of the ability of a substituent group R on a benzene ring to influence the reactivity of a side chain Y and is defined by the Hammett equation

$$\log(K/K_o) = \sigma\rho \tag{4}$$

where K and K_o are rate or equilibrium constants for reactions of the substituted and unsubstituted (R = H) compounds, respectively, σ is the substituent constant which quantifies the electron-donating and electron-withdrawing properties of R and ρ is the reaction constant which depends upon the reaction, the conditions under which it takes place and the nature of the side chain Y.[86–89] By convention the value of ρ is set to unity for the ionisation of benzoic acids. Two series of values of σ, σ_p and σ_m, are obtained from reactions of *para*- and *meta*-substituted benzene derivatives, respectively. Values of σ reported by McDaniel and Brown[88] based on the difference in pK_a values of benzoic acid and substituted benzoic acids, following Hammett's original definition of σ,[86] are among the most widely accepted.[89]

The ^{103}Rh chemical shift of a rhodium complex is influenced by both steric and electronic factors, the relative contributions of which are usually difficult to distinguish. It is therefore necessary, as far as is possible, to study the two effects in isolation. Electronic effects can be examined by varying ligand substituents that are positioned in such a way as to minimise any steric influence on the orientation of ligands or the metal coordination geometry. The following is a

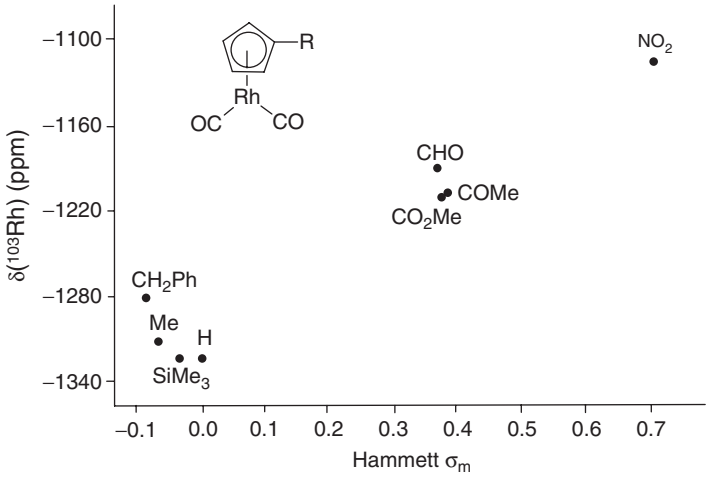

Figure 8 Plot of $\delta(^{103}Rh)$ against Hammett σ_m for complexes $[Rh(\eta^5\text{-}C_5H_4R)(CO)_2]$ (R = $SiMe_3$, H, Me, CH_2Ph, COMe, CO_2Me, CHO, NO_2). (Data from ref. 90.)

brief description of work by von Philipsborn and co-workers,[90] Leitner and co-workers[91] and Elsevier and co-workers.[92]

For a series of complexes $[Rh(\eta^5\text{-}C_5H_4R)(CO)_2]$ (R = $SiMe_3$, H, Me, CH_2Ph, COMe, CO_2Me, CHO, NO_2) the ^{103}Rh chemical shift was plotted against Hammett σ_m, σ_p and the Taft substituent parameters σ_R^0 and σ_I (representing resonance and inductive effects, respectively) for the substituent R.[90] The most significant correlation (0.979) was found with σ_m (Figure 8), the least significant with σ_R^0. The modest correlation with the Taft parameters suggests that the effect of the substituent which, as the substituent becomes increasingly electron withdrawing is to increase $\delta(^{103}Rh)$, is neither a purely resonance nor inductive phenomenon.

Complexes containing bis(phosphine) ligands are extensively used in catalysis, where slight variations in the electronic and/or steric properties of ligands may greatly influence the yield or stereoselectivity. The electronic properties of the ligand $Ph_2P(CH_2)_4PPh_2$ were varied by means of a substituent in the four-position of the phenyl groups in complexes $[Rh(acac^F)\{(4\text{-}XC_6H_4)_2P(CH_2)_4P(4\text{-}XC_6H_4)_2\}]$ ($acac^F$ = hexafluoroacetylacetonate; X = H, Me, OMe, F, Cl, CF_3).[91] A plot of ^{103}Rh chemical shift, which was found to vary over a range of 76 ppm, against Hammett σ_p for the substituent X (Figure 9), shows a linear relationship with a correlation coefficient of 0.986. This study also showed that small variations in coordination geometry induced much larger chemical shift differences (see Section 8.5) than did a change of substituent.

A study[92] of complexes [Rh(H)$(CO)_2$(diphosphine)] (ligands shown in Figure 10), prepared under a syngas (H_2 : CO, 1 : 1) pressure of 20 bar in a sapphire tube, showed a good ($R^2 = 0.960$) correlation between $\delta(^{103}Rh)$, which varied over a range of only 37 ppm, and Hammett σ_p for the substituent Y. A further example,[93] in which a correlation is found between Hammett σ values and $\delta(^{113}Rh)$, is given in Section 8.3.

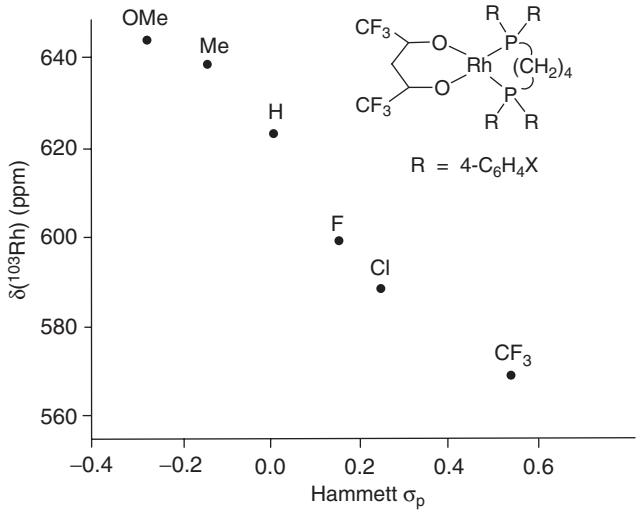

Figure 9 Plot of $\delta(^{103}Rh)$ against Hammett σ_p for complexes $[Rh(acac^F)\{(4\text{-}XC_6H_4)_2P(CH_2)_4P(4\text{-}XC_6H_4)_2\}]$ (X = OMe, Me, H, F, Cl, CF_3). (Data from ref. 91.)

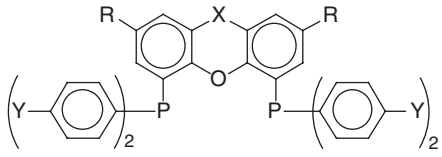

No	X	Y	R	No	X	Y	R
1	H,H	H	H	8	S	CF_3	Me
2	PPh	H	H	9	S	Cl	Me
3	$SiMe_3$	H	H	10	S	F	Me
4	S	H	Me	11	S	Me	Me
5	CMe_2	H	H	12	S	OMe	Me
6	$CCMe_2$	H	H	13	S	NMe_3	Me
7	NH	H	H				

Figure 10 Ligands used to prepare $[Rh(H)(CO)_2(diphosphine)]$ from $[Rh(acac)(CO)_2]$ in benzene under 20 bar H_2/CO (1:1) (ref. 92).

8.3 Correlation of $\delta(^{103}Rh)$ with rate constants and catalytic activity

The following account summarises work by von Philipsborn and co-workers[93,94] who have used ^{103}Rh chemical shifts to predict reaction rates and by Leitner and co-workers[95] who have found a correlation between $\delta(^{103}Rh)$ and catalytic performance.

Complexes $[Rh(\eta^5\text{-}C_5H_4X)(CO)_2]$ (X = H, Me, NMe_2, CF_3, Cl, NO_2) undergo the displacement of a carbonyl by triphenylphospine in decalin at 298 K ((**l**)–(**n**)).

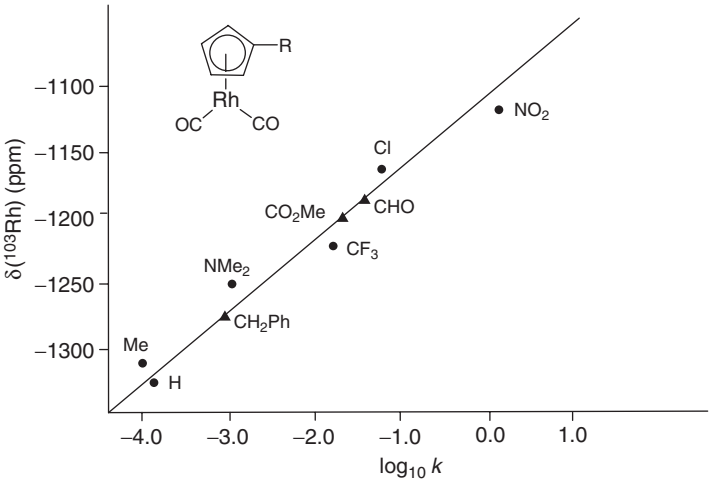

Figure 11 Plot of $\delta(^{103}Rh)$ against log k for CO/PPh_3 displacement in complexes $[Rh(\eta^5\text{-}C_5H_4R)(CO)_2]$. Rates for $R = CH_2Ph$, CO_2Me and CHO predicted from known $\delta(^{103}Rh)$. (Data from ref. 94.)

In this reaction, first reported by Basolo and Cheong[96] who also reported the kinetic data, the intermediacy of a transition state (**m**) having an η^3 coordination mode for the Cp is supported by thermodynamic evidence. A plot of log k, where k is the rate constant for the reaction, against $\delta(^{103}Rh)$ measured for $[Rh(\eta^5\text{-}C_5H_4X)(CO)_2]$ is shown in Figure 11.[94] To a good approximation ($R^2 = 0.973$) the relationship between log k and $\delta(^{103}Rh)$ is linear, permitting the prediction of log k for complexes $[Rh(\eta^5\text{-}C_5H_4X)(CO)_2]$ ($X = CH_2Ph$, CO_2Me, CHO). The ordering of substituents X along the gradient of Figure 11 is not entirely in accord with the sequence of electron-donating and electron-with drawing ability represented by the Hammett σ function. A plot of Hammett σ_p against log k (not shown) for the CO displacement reaction showed that the NMe_2- and Cl-substituted complexes reacted much faster than expected. Since the correlation between log k and $\delta(^{103}Rh)$ holds equally well for all six complexes, some effect must be at work, in the case of $X = NMe_2$ and Cl, which exerts an equal influence on log k and $\delta(^{103}Rh)$ over and above that shared with the other substituents.

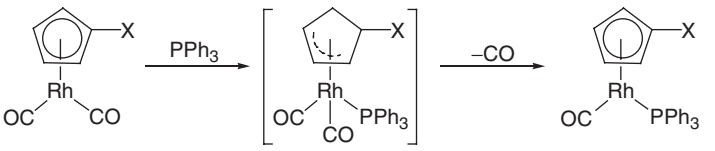

(l) **(m)** **(n)**

Evidence from photoelectron spectroscopic studies[97] indicates a stabilisation of the η^3 intermediate by π donation implying that, in the case of $X = NMe_2$ (NMe_2 is a strong π donor) and X = Cl (Cl is a moderate π donor), the p_π overlap in

the transition state of the rate-determining first step (**m**) should increase the rate of substitution, as observed. It was proposed that there is a similar resonance effect in the ground state or a low-lying electronically excited state of the NMe_2-substituted complex (**o**)–(**q**) which would account for the deshielding of the ^{103}Rh nucleus.[94]

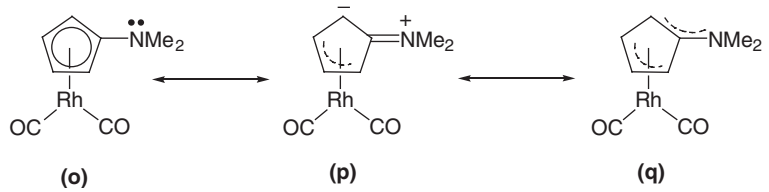

Rate constants for the PPh_3-assisted migration of a coordinated aryl group to a coordinated CO in the complexes [Rh(Cp*)(I)(4-XC_6H_4)(CO)] (X = H, Me, Cl, CHO, CN, NO_2), reported by Maitlis and co-workers,[98] have been correlated with ^{103}Rh chemical shifts.[93] For the complexes [Rh(Cp*)(I)(R)(CO)] (R = 4-substituted phenyl) the range of ^{103}Rh chemical shifts is small and the correlation between $\delta(^{103}\text{Rh})$ and the rate constant is insignificant. For the complexes [Rh(Cp*)(I)(COR)(PPh_3)], where the range of $\delta(^{103}\text{Rh})$ is wider (71 ppm) a plot of $\delta(^{103}\text{Rh})$ against ln*k* (Figure 12) is linear, with a high correlation ($R^2 = 0.991$) as is a plot (not shown) of $\delta(^{103}\text{Rh})$ against Hammett σ ($R^2 = 0.991$). This is the first example of a correlation between a transition metal chemical shift of the product (rather than the reactant) with rate data.

In a catalytic study[95] the relative rate (rate relative to that of the least active catalyst), υ_{rel}, for the catalysed hydrogenation of CO_2 using complexes

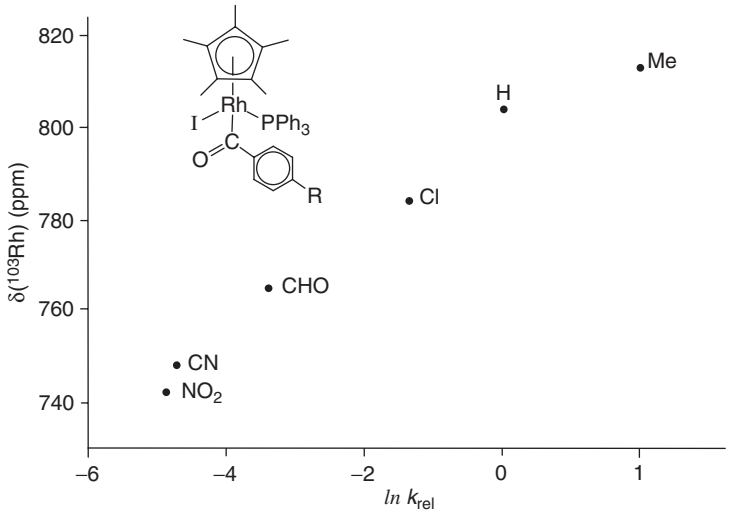

Figure 12 Plot of $\delta(^{103}\text{Rh})$ for [Rh(Cp*)(I)(COC_6H_4-4-R)(PPh_3)] against lnk_{rel} (rate relative to that measured when R = H) for PPh_3-promoted CO insertion in [Rh(Cp*)(I)(C_6H_4-4-R)(CO)]. (Data from ref. 93.)

[Rh(acac^F)(R$_2$P(CH$_2$)$_n$PR$_2$)] ($n = 2$, R = Me, ^{i}Pr, Cy, Ph; $n = 3$, R = Ph; $n = 4$, R = Cy, Ph) was found to be highest for the complex with n=4 and R=Cy. A plot (not shown) of υ_{rel} against $\delta(^{103}Rh)$ was found to be approximately linear with a goodness of fit of $r = 0.953$. In Section 8.5 the influence of steric factors on the ^{103}Rh chemical shifts of these complexes is discussed in greater detail.

8.4 Correlation of $\delta(^{103}Rh)$ with infrared stretching frequencies

The study by von Philipsborn and co-workers[90] described in Section 8.2 also included the following correlation between $\delta(^{103}Rh)$ and the carbonyl stretching frequency of [Rh(η^5-C$_5$H$_4$X)(CO)$_2$] (X = Me$_3$Si, H, Me, CH$_2$Ph, COMe, CO$_2$Me, CHO, NO$_2$). Plots of $\delta(^{103}Rh)$ against both the symmetric (Figure 13) and asymmetric stretching frequencies yielded correlation coefficients of $\sim$0.92. The effect of adding an electron-withdrawing group such as NO$_2$ or CHO to the Cp ring is to increase $\delta(^{103}Rh)$ and to increase the CO stretching frequency, the latter as a result of a reduced availability of electron density for back-donation to the CO antibonding orbitals. The difference in solvent used for the IR (hexane) and NMR (benzene) studies may account for deviations from a simple linear relationship between $\delta(^{103}Rh)$ and υ_{CO}.[90]

8.5 Correlation of $\delta(^{103}Rh)$ with structural and steric parameters

The steric properties of a coordinated phosphine are conveniently represented, for simple monodentate phosphines, by the well-known Tolman cone angle (θ).[99] A correlation between the ^{103}Rh chemical shift of complexes [Rh(Cp*)(X)$_2$(PR$_3$)] (X = Cl, Br, I; PR$_3$ = PMe$_3$, PMe$_2$Ph, P^{n}Bu$_3$, PMePh$_2$, PPh$_3$, P^{i}Pr$_3$) and Tolman θ

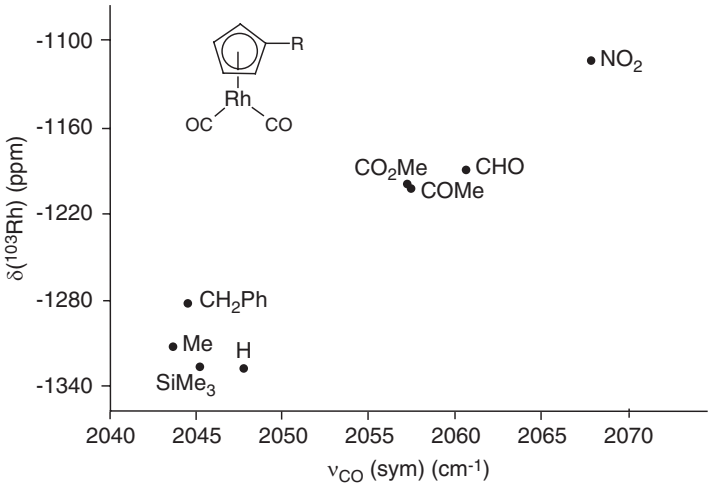

Figure 13 Plot of $\delta(^{103}Rh)$ against symmetric CO stretching frequency for [Rh(η^5-C$_5$H$_4$R)CO)$_2$]. (Data from ref. 90.)

for the phosphine was found by Tedesco and von Philipsborn[100] to decrease in the order Cl ($R^2 = 0.918$) > Br ($R^2 = 0.885$) > I ($R^2 = 0.773$). For complexes [Rh(Cp*)(X)(PR_3)(Ph)] the correlation between $\delta(^{103}Rh)$ and θ was significantly poorer, with R^2 in the range 0.826–0.840. In all cases the trend was found to be an increase in $\delta(^{103}Rh)$ accompanying an increase in θ.

For complexes of bidentate phosphines, which find widespread use in catalysis, the parameter by which the binding of the phosphine has been most frequently characterised is the P–M–P angle (the 'bite angle') which, while of considerable value in defining coordination geometry, is less directly relevant to catalysis. Studies by Leitner and co-workers[95,101] in the area of rhodium-catalysed CO_2 hydrogenation have included the development of the accessible molecular surface (AMS) model as an approach to quantifying the intrinsic steric properties of chelating ligands in catalysis. The AMS model permits analysis not only of the size but also of the shape of the cavity of the active fragment. The AMS parameter for complexes [Rh($acac^F$)($R_2P(CH_2)_nPR_2$)] shows a good match with catalytic activity but is less closely related to $\delta(^{103}Rh)$ than is the P–Rh–P angle.

The influence of bite angle on $\delta(^{103}Rh)$ is shown by the two series of square-planar complexes [Rh($acac^F$)($Ph_2P(CH_2)_nPPh_2$)] and [Rh(acac)($Cy_2P(CH_2)_nPCy_2$)] (**r**). Variations in the chelate ring size are associated with changes in the following geometrical parameters: the P–Rh–P angle, the Rh–P distance, the distortion from planarity as measured by the 'twist' angle and the deviation from an ideal alignment of the phosphorus lone pair with the Rh–P bond axis, as measured by the 'tilt' angle. Although these parameters cannot be varied independently in real molecules their individual contributions have been assessed by density-functional-based calculations for model compounds [Rh($acac^F$)($R_3P(CH_2)_nPR_3$)] (R = H, CH_3), which show a strong dependence of $\delta(^{103}Rh)$ on the Rh–P bond length, which in turn is related to the bite angle. For a five-membered ring (n = 2), $\delta(^{103}Rh)$ is at a minimum, increasing with increasing ring size ($n > 2$) as a result of the parallel increase of the Rh–P distance and the P–Rh–P angle. In a four-membered ring (n = 1) the large deshielding arises from the substantial tilt of the lone pairs of the phosphorus atoms away from the respective Rh–P bond axes.

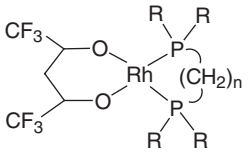

(r)

Effect of ring size on $\delta(^{103}Rh)$ (ref.91).

$\delta(^{103}Rh)$ in parentheses

R = Ph; n = 1 (1130), 2 (438), 3 (567), 4 (623)

R = Cy; n = 1 (1062), 2 (368), 3 (608), 4 (845).

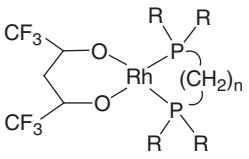

(s)

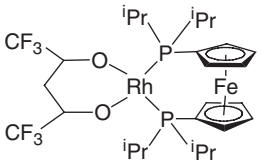

(t)

Ring size effect. X-ray crystallographic data for the following were used in Figs 14 and 15. (refs. 91,101)

(s) n = 1, R = Cy; n = 2, R = Me, ^{i}Pr, Cy, Ph; n = 3, R = Ph; n = 4, R = Cy, Ph.

(t) [Rh(acac^{F})(^{i}Pr$_2$PFcP^{i}Pr$_2$)]

A comparison of $\delta(^{103}\text{Rh})$ and structural parameters (from X-ray crystallography) reported by Leitner and co-workers[101] for the complexes [Rh(acac^{F})(R$_2$P(CH$_2$)$_n$PR$_2$)] (n = 1, R = Cy; n = 2, R = Me, ^{i}Pr, Cy, Ph; n = 3, R = Ph; n = 4, R = Cy, Ph) (**s**) and [Rh(acac^{F})(^{i}Pr$_2$PFcP^{i}Pr$_2$)] (Fc=1,1′-ferrocenyl) (**t**) is shown in Figures 14 and 15, where the formulae are abbreviated to 1Cy, 2Me, 2^{i}Pr, etc. Figure 14 shows $\delta(^{103}\text{Rh})$ decreasing as the P–Rh–P angle is increased from 73.7° to 86°, thereafter increasing as the bond angle expands from 86° to 100°. Figure 15 shows $\delta(^{103}\text{Rh})$ increasing with Rh–P distance in the range 2.176–2.228 Å. A close examination of Figure 14 shows that for complexes represented as 2Me and 2Cy the $\delta(^{103}\text{Rh})$ and P–Rh–P data coincide almost exactly, while in Figure 15 the almost identical values of $\delta(^{103}\text{Rh})$ correspond to Rh–P distances for the two complexes that differ by 0.017 Å. In Figure 15 the Rh–P bond length for 1Cy appears to be quite anomalous if a close correlation between P–Rh–P angle and Rh–P bond length is anticipated, whereas in Figure 14 the data for 1Cy fit a

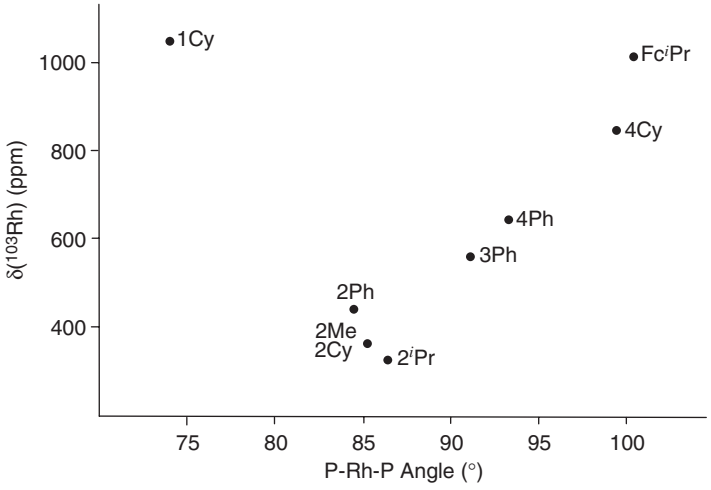

Figure 14 Plot of $\delta(^{103}\text{Rh})$ against P–Rh–P bond angle for complexes [Rh(acac^{F})(R$_2$P(CH$_2$)$_n$PR$_2$)] (see text for details). (Data from refs. 91, 101.)

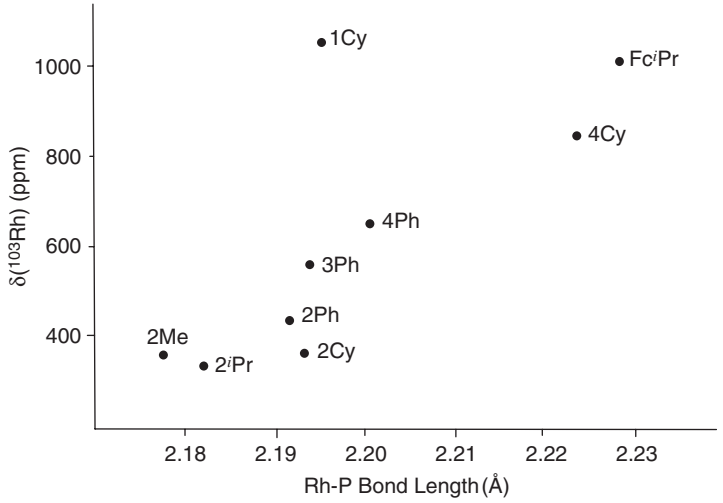

Figure 15 Plot of $\delta(^{103}\text{Rh})$ against Rh–P bond length for complexes $[\text{Rh}(\text{acac}^{\text{F}})(\text{R}_2\text{P}(\text{CH}_2)_n\text{PR}_2)]$ (see text for details). (Data from refs. 91, 101.)

clearly discernable pattern. On the basis of this admittedly limited evidence it would appear that the P–Rh–P angle, rather than the Rh–P bond length, is the structural parameter most closely related to $\delta(^{103}\text{Rh})$. Unfortunately the modelling (see above) of the influence of the P–Rh–P angle did not provide a good match with the experimental data, unlike the modelled influence of Rh–P distance on $\delta(^{103}\text{Rh})$ which agreed fairly closely with observed values.[91]

The influence of ring size upon the rhodium chemical shift of diphosphine complexes has also been examined by Elsevier and co-workers,[62] who observed similar effects with $[\text{Rh}(\text{nbd})(\text{Ph}_2\text{P}(\text{CH}_2)_n\text{PPh}_2)]^+\ \text{ClO}_4^-$ to those observed above for the diphosphine acac^{F} complexes. For $[\text{Rh}(\text{nbd})(\text{Ph}_2\text{P}(\text{CH}_2)_n\text{PPh}_2)]^+$ the largest deshielding was found with $n = 1$ (δ = 193 ppm) and the smallest with $n = 2$ (δ = −390 ppm), increasing thereafter for $n = 3$ ($\delta = -264$ ppm) and $n = 4$ (δ = −210 ppm). The influence of the chelate effect upon $\delta(^{103}\text{Rh})$ is shown by a comparison of $\delta(^{103}\text{Rh})$ for the diphosphine complexes $[\text{Rh}(\text{cod})(\text{R}_2\text{P}(\text{CH}_2)_n\text{PR}_2)]^+\ \text{ClO}_4^-$ (R = Ph, $n = 2$, 4; R = Et, $n = 2$, 5)[62] (**u**) and the monophosphine complexes $[\text{Rh}(\text{cod})(\text{R}_2\text{PR}'_2)]^+\ \text{Y}^-$ (R = Ph, R′ = Me, $\text{Y} = \text{ClO}_4^-$; R, R′ = Et, $\text{Y} = \text{BPh}_4^-$)[102] (**v**) which gives a value $\Delta\delta$, the chemical shift difference between complexes having a chelating ligand and a complex having two nonchelating ligands each equivalent to a fragment of the chelating ligand. Thus, in the case where R = Ph and R′ = Me, $\Delta\delta = 238$ ppm for $n = 2$ and 4 ppm for $n = 4$ and, in the case of R = R′ = Et, $\Delta\delta = 401$ ppm for $n = 2$ and 6 ppm for $n = 5$, the Rh nucleus being more shielded in the diphosphine complexes than in the open-chain complexes. For the seven- (and eight-) membered rings the chelate effect is therefore minimal, whereas for the five-membered rings the effect is large. The difference in $\delta(^{103}\text{Rh})$, $\Delta\delta = 238$ ppm, encountered on going from a five- to a seven-membered ring in $[\text{Rh}(\text{cod})(\text{Ph}_2\text{P}(\text{CH}_2)_n\text{PPh}_2)]^+$ ($n = 2$, 4) is not dissimilar to that observed (185 ppm, see above) on going from a five- to a seven-membered ring in

$[Rh(acac^F)(Ph_2P(CH_2)_nPPh_2)]$[91] ($n = 2$, 4) suggesting that, for complexes having the same coordination geometry (here square planar) the magnitude of the effect may not be greatly influenced by the nonphosphine coligand(s).

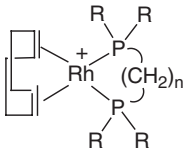

(u)

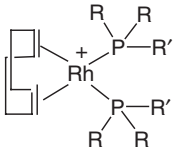

(v)

Chelate effect and ring size (refs. 62, 102).

$\delta(^{103}Rh)$ in parentheses

(u) R = Ph; n = 2 (– 505), 4 (– 271)

R = Et, n = 2 (– 533), 5 (– 138)

(v) R = Ph, R′ = Me (– 267)

R, R′ = Et (– 132)

The chelate effect has also been investigated for complexes of N-donor and O-donor bidentate ligands, where a similar influence on rhodium chemical shifts is found.[103] A chemical shift difference of 193 ppm is found on going from a complex of bipyridyl having a five-membered ring, $[Rh(cod)(bipy)]^+ ClO_4^-$ ($\delta = 816$ ppm) to a complex having nonchelating (pyridine) ligands $[Rh(cod)(py)_2]^+ ClO_4^-$ ($\delta = 1{,}009$ ppm), while for a complex having a six-membered ring, $[Rh(cod)(C_5H_4N–NH–C_5H_4N)]^+ ClO_4^-$ ($\delta = 1{,}035$ ppm) the difference is only 26 ppm. The small difference in $\delta(^{103}Rh)$ between complexes having a six-membered (or larger) ring and open-chain ligands is also found for complexes $[Rh(cod)(Ph_2P(O)–(CH_2)_nP(O)Ph_2)]^+ ClO_4^-$ ($n = 1$, 2) and [Rh(cod)-(bipyO$_2$)] which have $\delta(^{103}Rh)$ in the range 1,362–1,373 ppm, very close to the value (1,350 ppm) found for $[Rh(cod)(Me_2CO)_x]^+ ClO_4^-$.

The chemical shift of rhodium in complexes [Rh(Hdmg)(R)(py)] (Hdmg = monoanion of dimethylglyoxime; R = alkyl) was found by von Philipsborn and co-workers[104] to correlate with the size of the alkyl ligand R, as measured by the Taft parameters *Es* and *Es′*. An increase in $\delta(^{103}Rh)$ accompanying an increase in size of R was interpreted in terms of distortions arising from axial-equatorial ligand repulsion (supported by X-ray crystallographic data) leading to weaker metal–ligand binding interactions and, therefore, smaller ΔE and larger paramagnetic shielding.

9. PARAHYDROGEN-INDUCED POLARISATION (PHIP)

Molecular hydrogen exists in two isomeric forms that arise from differences in nuclear spin configuration (*ortho* and *para*hydrogen). The *ortho* isomer is triply degenerate, corresponding to the direct products of the nuclear wavefunctions

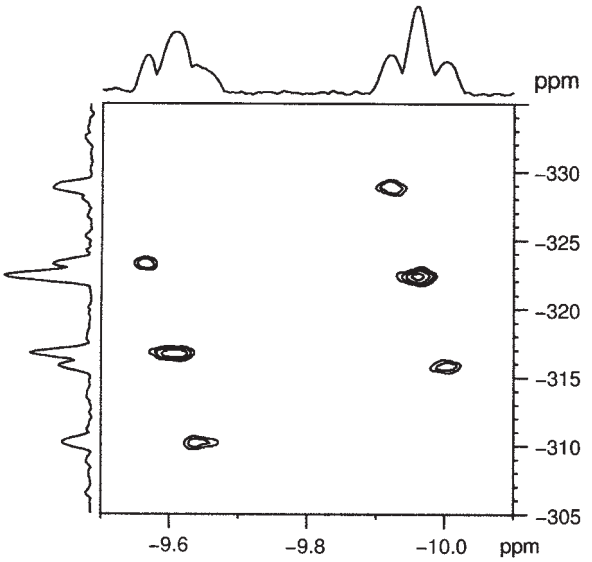

Figure 16 Selected region of the ^{103}Rh-^{1}H HMQC spectrum of [Rh(Cl)(H)$_2$(PMe$_3$)$_3$] obtained using PHIP. (Reproduced from ref. 105, Copyright (2004) Royal Society of Chemistry.)

$\alpha\alpha$ and $\beta\beta$, and the linear combination $\alpha\beta+\beta\alpha$; the *para* isomer exists as the antisymmetric linear combination $\alpha\beta-\beta\alpha$. A sample of molecular hydrogen can be enriched (up to 99.8%) in *para*-hydrogen by cooling it to 18 K in the presence of a paramagnetic catalyst.[105] In the absence of the catalyst reestablishment of the thermodynamic equilibrium between the isomers is slow, allowing *para*-hydrogen-containing samples to be stored for several hours before use. It was shown by Bowers and Weitekamp[106] in 1987 and also by Eisenberg and co-workers[107] that the use of *para*-hydrogen in hydrogenation reactions led to large enhancements in the intensity of ^{1}H NMR signals from the hydrogenated products. In 1995 Duckett and co-workers[108] reported ^{1}H-detected ^{103}Rh NMR data from complexes [Rh(Cl)(H)$_2$(PMe$_3$)$_3$] (Figure 16), [Rh(H)$_2$(PMe$_3$)$_4$]$^+$ Cl$^-$ and [Rh(Cl)$_2$(H)(PMe$_3$)$_3$] using submilligram quantities of material and PHIP enhancement, later applying the PHIP method to the study of a variety of hydrogenation and related reactions of rhodium (with measurement of δ(^{103}Rh))[109–115] and of other metals. The PHIP phenomenon has been reviewed by Eisenberg[116] and by Duckett.[105,117]

It is necessary that the acquisition of data from a *para*-hydrogen-containing material is quite rapid. Duckett and co-workers give details[108] of a modified ^{103}Rh-^{1}H HMQC experiment in which the first $\pi/2(^{1}H)$ pulse is replaced by a $\pi/4(^{1}H)$ pulse (which maximises the initial transverse magnetisation from the *para*hydrogen) and the acquisition time of only 25 ms and recycle time of $\leq$100 ms (optimised independently for each sample) allow spectra of up to 1,024 increments (of one scan each when pulse field gradients are used) to be obtained in less than 3 min. The time constraint is imposed by the rate at which relaxation processes deplete the *para*-hydrogen spin-state population.

10. HIGH-PRESSURE STUDIES

During the last 10 years numerous NMR studies of rhodium-catalysed reactions have been carried out under conditions resembling those of many industrial processes, i.e., under high pressure.[118–133] Details of a sapphire tube and titanium valve assembly and of a high-pressure, high-resolution probe capable of operating with conventional tubes at pressures up to 200 MPa (2 kbar) are given by Helm and Merbach,[134] who used variable pressure ^{17}O NMR to measure rates of H_2O exchange for $[Rh(H_2O)_6]^{3+}$ and aquo ions of other metals. The use of a high-resolution probe containing a pressurisable sample cell has been described by Heaton and co-workers[135,136] in connection with studies (including measurement of $\delta(^{103}Rh)$) of rhodium carbonyl clusters under an atmosphere of ^{13}CO-enriched CO/H_2 at pressures up to 100 MPa.

Another high-pressure study that has made use of ^{103}Rh NMR is described by Elsevier and co-workers,[92] who prepared complexes $[Rh(H)(CO)_2(diphosphine)]$ (Figure 10) that are stable only under a pressure (20 bar) of H_2/CO (synthesis gas). The complexes exist in two isomeric forms, with the bidentate phosphine bound in an equatorial–equatorial (eq–eq) or equatorial–axial (eq–ax) fashion, that interconvert rapidly in solution at all accessible temperatures. A correlation between the ligand Tolman basicity[137] and the ratio of eq–eq/eq–ax isomers (obtained from ^1H NMR and IR data) has been shown to extend to the Hammett σ_p function,[138] which in turn has been shown to correlate with $\delta(^{103}Rh)$,[92] indicating that $\delta(^{103}Rh)$ reflects the eq–eq/eq–ax ratio.

It should be noted that large changes in pressure, in the absence of other, chemical effects, can be expected to influence the metal chemical shift. This has been demonstrated for $[Co(NO_2)_6]^{3-}$ (among other Co complexes)[8,54] in aqueous solution where an increase in ^{59}Co shielding of 46 ppm has been observed to accompany the application of a pressure of 1,000 kg/cm^2. This result is interpreted in terms of a compression of the metal–ligand bond, leading to an increase in ΔE and a decrease in paramagnetic shielding.

11. SOLID-STATE STUDIES

Finely divided rhodium is used in industrial heterogeneous catalysis and in catalytic converters for motor exhausts. In spite of the need for analytical methods to study supported catalysts the low sensitivity and long relaxation time of ^{103}Rh in metallic rhodium have discouraged NMR studies of the metal. In 1997, van der Klink and co-workers[139] obtained ^{103}Rh spectra from particles of rhodium of approximately 3 nm diameter, either supported on TiO_2 or coated with a polymer. The observed Knight shift was found to be dependent on particle size, decreasing as the average particle size became smaller. This result is interpreted in terms of the relative magnitudes of spin and orbital contributions to the Knight shift.[16,139]

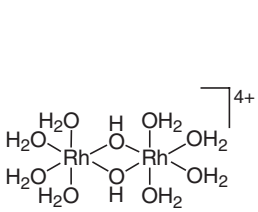

(w)

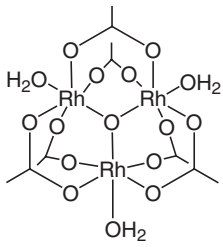

(x)

The first example of a solid-state ^{103}Rh spectrum obtained from a compound of rhodium (rather than from the bulk metal) was reported in 2006 by Phillips and co-workers,[140] who examined crystalline di- and trinuclear clusters containing O-donor ligands ((**w**) and (**x**) and Figure 17). The complex $[(H_2O)_4Rh(\mu\text{-}OH)_2Rh(H_2O)_4]^{4+}$, as the mesitylate salt, was found to give a well-resolved signal at moderate spinning rates, with a chemical shift of 10,131 ppm relative to $[Rh(H_2O)_6]^{3+}$ at 9,916 ppm (equivalent to Ξ (^{103}Rh) = 3.16 MHz), 134 ppm to high frequency of the value observed in solution (9,997 ppm). The trinuclear complex $[Rh_3(\mu\text{-}O)(\mu_2\text{-}O_2CCH_3)_6(H_2O)_3]^+$ ClO_4^- gives a less straightforward spectrum, with three sets of spinning sidebands corresponding to signals at $\delta_{iso} = 9{,}401$, 9,359 and 9,354 ppm. In solution the complex gives a single signal ($\delta = 9{,}390$ ppm)[141] consistent with a structure having D_{3h} symmetry.

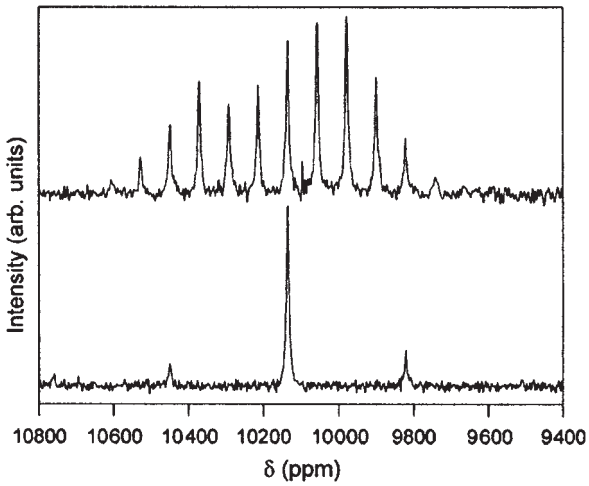

Figure 17 ^{103}Rh{^{1}H} CP-MAS spectra obtained from the mesitylate salt of $[Rh_2(OH)_2(H_2O)_8]^{4+}$ at 298 K with spinning rates of 1.0 kHz (upper) and 4.0 kHz (lower), both spectra acquired with 8 ms contact time, 5 s relaxation delay and 12,000 (upper) and 15,800 (lower) scans. (Reproduced from ref. 140, Copyright (2006) American Chemical Society.)

12. CLUSTERS

Metal cluster compounds offer a dimension of almost endless variety to the chemistry of the transition metals. This borderline between complexes of single metal atoms and of small particles of metal offers a potentially wide range of new chemistry, the study of which will be greatly facilitated by transition metal NMR. Rhodium forms a number of well-defined clusters derived from $Rh_4(CO)_{12}$ and $Rh_6(CO)_{16}$ which have provided the basis of much of the rhodium cluster chemistry to date. By far the largest contribution to the study of small rhodium-containing clusters by ^{103}Rh NMR has been made by Heaton and co-workers,[26,27,136,142–171] who have published more than 30 articles reporting ^{103}Rh data (see Tables A4a and A4b). The following is a brief account of some of their work relating to the acquisition of ^{103}Rh data and to the characterisation of small clusters.

The majority of metal–metal bonded cluster compounds studied to date are stabilised by carbonyl ligands. It is therefore only logical that ^{13}C-^{103}Rh correlated methods, whether ^{13}C-detected ^{103}Rh HMQC or, prior to the advent of indirect detection technology, one-dimensional ^{13}C{^{103}Rh} double resonance, both used extensively by Heaton and co-workers, should be employed (in conjunction with other methods) in the characterisation of derivatives of rhodium carbonyl clusters. It is necessary that the sample be enriched in ^{13}CO. The closely packed structure of a metal cluster together with the presence of edge- or face-bridging carbonyls allows several metal atoms to be spin-coupled to a single carbon. The use of indirect detection in situations where the observed nucleus (^{1}H, ^{13}C, ^{31}P) is spin coupled to more than one metal nucleus requires that the delay time, normally taken to be $1/2J$, be recalculated or, in the case of long-range coupling, estimated.[27] Multiple-metal spin transitions give rise to correlation peaks at positions other than the true chemical shift and may cause the intensity of the peaks arising from the single-metal spin transitions (which occur at the true chemical shift) to fall to zero.[26,27] An example of these effects recorded from $[Rh_6(CO)_{15}\{P(4\text{-}FC_6H_4)_3\}]$ (Figure 18) is

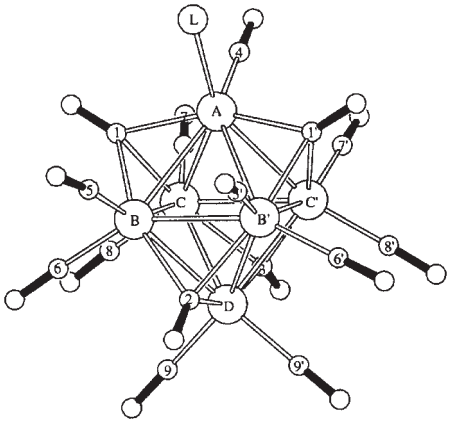

Figure 18 Schematic representation of the structure of $[Rh_6(CO)_{15}(L)]$. (Reproduced from ref. 27, Copyright (2004) Wiley.)

shown in Figure 19a and is compared with a spectrum obtained using the non-conventional delay time of $1/5J$ (Figure 19b).[26]

The stereochemistry of phosphite-substituted derivatives of $[Rh_4(CO)_{12}]$ namely $[Rh_4(CO)_{12-x}\{P(OPh)_3\}_x]$ ($x = 1-4$) (Figure 20 and Table A4a), has been

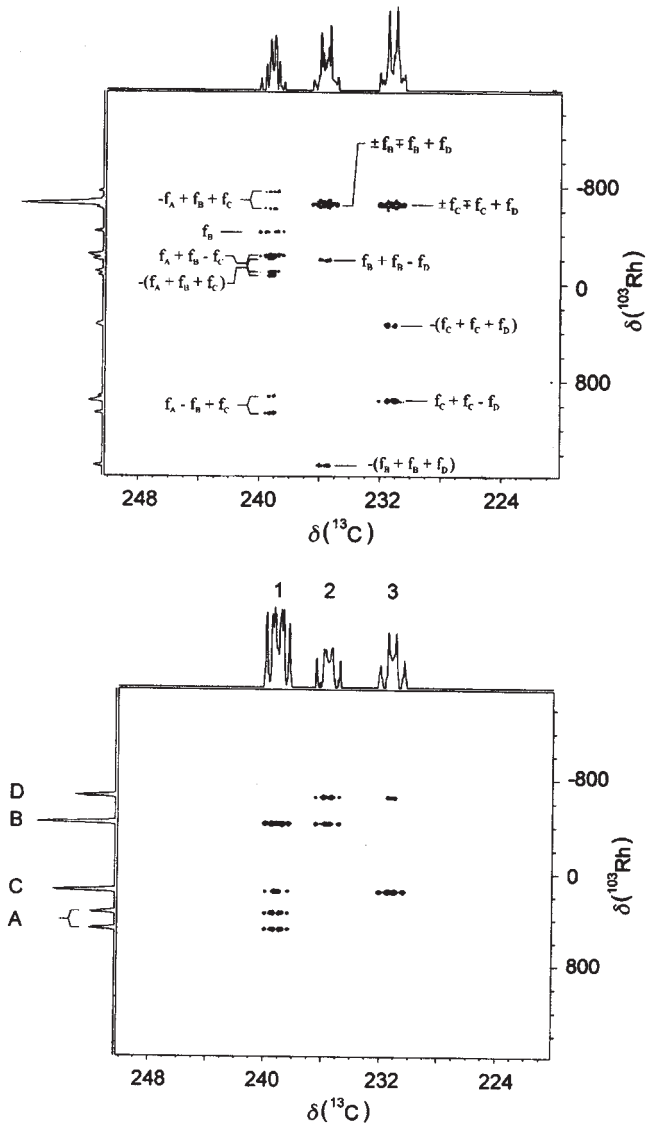

Figure 19 (a) (upper) $^{13}C\{^{103}Rh\}$ HMQC spectrum of $[Rh_6(CO)_{15}\{P(4\text{-}FC_6H_4)_3\}]$ (face-bridging region) obtained with a conventional delay d2 = 1/(2*J*) = 17.9 ms (*J* = 28 Hz). The 'expected' correlations to the face-bridging carbonyls are weak or absent and correlations to the three-rhodium spin coherences are seen. (b) (lower) Spectrum obtained using the delay d2 = 1/(5*J*) = 7.14 ms. Strong correlations are seen at the 'correct' ^{103}Rh chemical shifts. (Reproduced from ref. 26, Copyright (1999) Royal Society of Chemistry.)

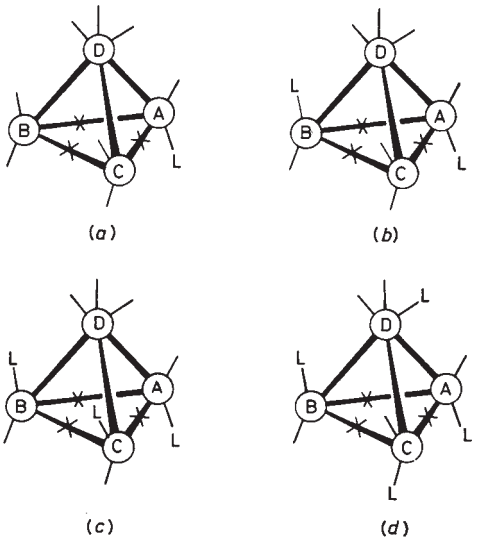

Figure 20 Schematic representation of the stereochemistry of $[Rh_4(CO)_{12-x}L_x]$ {L = $P(OPh)_3$, $x = 1–4$; —X— = μ-CO}. (Reproduced from ref. 152, Copyright (1983) Royal Society of Chemistry.)

established using a combination of directly observed ^{103}Rh NMR[152] (spectra shown in Figure 21) and $^{13}C\{^{103}Rh\}$ NMR, from which the ^{13}C spectra of clusters with 1, 3 and 4 phosphites were fully assigned. The multiplicities of ^{13}C signals showing coupling to either one or two rhodium nuclei and, where relevant a phosphorus, provide the most reliable evidence. No clear rule can be formulated regarding the relative chemical shifts of rhodium in apical and basal positions,[14,159] but it may be more generally true that $^2J(^{103}Rh,^{31}P)$ is only significant between phosphites in radial sites and basal rhodium atoms. This is found to be the case in the spectrum of $[Rh_4(CO)_{10}\{P(OPh)_3\}_2]$ (Figures 20b and 21b) where basal rhodium A and rhodium C couple to the radial phosphite on rhodium B. For $[Rh_4(CO)_9\{P(OPh)_3\}_3]$ each basal rhodium is substituted with a phosphite, one axial and two radial, creating a symmetry which causes rhodium B and rhodium C to become chemically equivalent, forming an AA′XX′ spin system with the directly bonded radial phosphites. Rhodium A shows $^2J(^{103}Rh,^{31}P)$ coupling to the two radial phosphites in addition to ^1J coupling. In $[Rh_4(CO)_8\{P(OPh)_3\}_4]$ each rhodium carries a phosphite substituent. Values of $J(^{103}Rh,^{31}P)$ (Table A4a) are consistent with a larger $^1J(^{103}Rh,^{31}P)$ between a basal rhodium and a radial phosphite than between a basal rhodium and an axial phosphite. A more detailed discussion of NMR studies of clusters is given by Granger.[14]

13. CALCULATED CHEMICAL SHIFTS

Although in a simplified form it is frequently invoked for the purpose of describing influences on nuclear shielding the Ramsey equation[44] is not widely

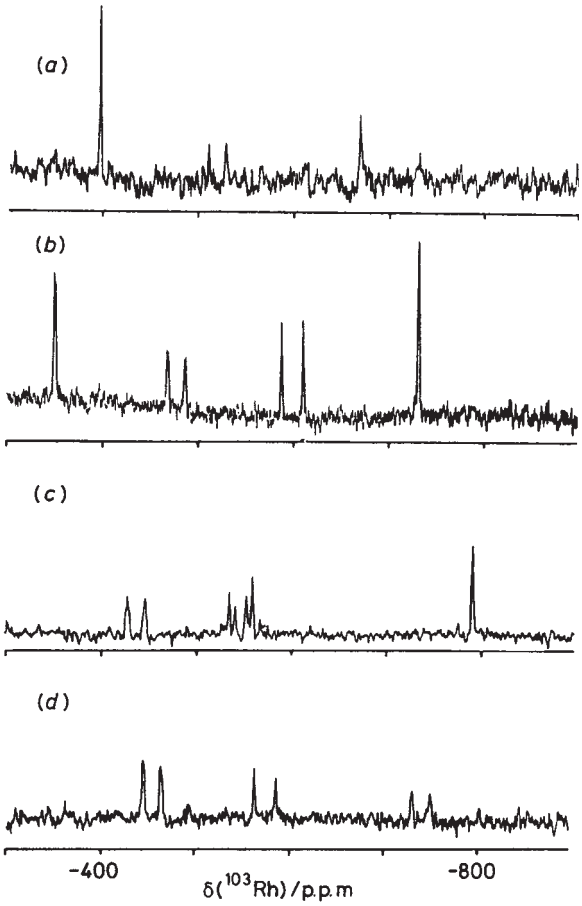

Figure 21 ^{103}Rh spectra (direct observation) of $[Rh_4(CO)_{12-x}L_x]$ {L = P(OPh)$_3$, x = 1–4} in CD_2Cl_2 at −54°C; (a) x = 1, (b) x = 2, (c) x = 3, (d) x = 4. (Reproduced from ref. 152, Copyright (1983) Royal Society of Chemistry.)

used for the calculation of chemical shifts. The limitations of the Ramsey approach and the development of methods designed to overcome the difficulties arising from its use have been described by Webb[33,34] and by Jameson.[35] Methods developed by Pople[172,173] and by Ditchfield[174,175] have been extensively used to calculate chemical shifts of small molecules containing light atoms but have, more recently, given way to the DFT approach, which has the virtue of being simpler and computationally less expensive. The development and application of DFT-based methods to the calculation of transition metal chemical shifts has been reviewed by Bühl et al.[176] For rhodium the use of 'pure DFT' methods has been found to underestimate ligand effects on $\delta(^{103}Rh)$, while pure Hartree–Fock (H–F) methods significantly overestimate ligand effects.[177]

The most successful method of calculating transition metal chemical shifts is that of Bühl,[178] which includes H–F aspects in a DFT method.

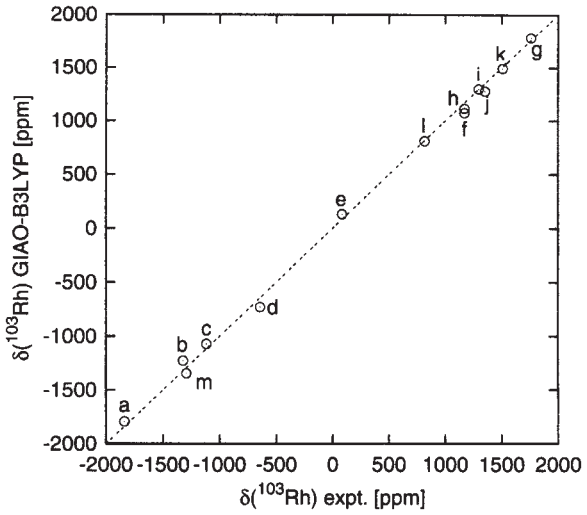

Figure 22 Computed (GIAO-B3LYP) versus experimental ^{103}Rh chemical shifts for $[Rh(Cp)_2]^+$ (a), $[Rh(Cp)(CO)_2]$ (b), $[Rh(\eta^5\text{-}C_5H_4NO_2)(CO)_2]$ (c), $[Rh(CO)_4]^-$ (d), $[Rh(Cl)_2(CO)_2]^-$ (e), $[Rh(acac)(C_2H_4)_2]$ (f), [Rh(acac)(cot)] (g), $[Rh(acac)(C_2H_4)(C_2F_4)]$ (h), [Rh(acac)(cod)] (i), $[Rh(acac)(C_2H_4)$*cis*-$(C_4H_8)]$ (j), $[Rh(acac)($*cis*-$(C_4H_8))_2]$ (k), [Rh(bipy)(cod)]$^+$ (l), $[Rh(Me_2P(CH_2)_2PMe_2)_2]^+$ (m). (Reproduced from ref. 176, Copyright (1999) Wiley.)

Results of calculations using GIAO-B3LYP (gauge-including atomic orbitals – DFT; Beckes's three-parameter exchange DFT/H–F hybrid functional; correlation functional of Lee, Yang and Parr) are shown in Figure 22 which compares calculated and experimental values of $\delta(^{103}Rh)$.[84,176] The correlation between calculated and experimental chemical shifts for a chemically varied series of rhodium (−I), (I) and (III) complexes is high, with a maximum deviation of calculated from experimental $\delta(^{103}Rh)$ of no more than 100 ppm. When viewed in terms of the ^{103}Rh chemical shift range of 12,000 ppm this is a remarkably good result. Beyond the range of $\pm$2,000 ppm, however, agreement with experiment is less good: for $[Rh(acac)_3]$ $\{\delta(^{103}Rh) = 8{,}358$ ppm$\}$ the calculated value is 8,761 ppm.[178]

14. SPIN COUPLING CONSTANTS

Nuclear spin coupling has been formulated in a molecular orbital framework by Pople and Santry.[179] The interactions between magnetic nuclei in a molecule are of two types: the direct dipolar interaction that is averaged to zero by the tumbling motion of a molecule in solution and the indirect interaction arising from polarisation of the electronic environment that is observed in the *J* (scalar) coupling. Three distinct effects induced by the nuclear magnetic moment contribute to *J* coupling: orbital electronic currents, electron spin polarisation and

the Fermi contact interaction, of which the contact interaction exerts the major influence.[179,180] In the contact interaction an antiparallel alignment of a spin 1/2 nucleus (with positive gyromagnetic ratio γ) and an electron (with negative γ) is stabilised relative to the parallel alignment. The magnitude of the interaction is proportional to the probability of finding the electron at the nucleus, and is, therefore, zero unless the electronic wavefunction has some s character. The stabilising effect induces spin polarisation of the molecular orbital (involving mixing of triplet excited states with the ground state) such that the probability of finding the electron in the favoured spin state (antiparallel) at a nucleus is greater than that of the disfavoured state (parallel). For two spin 1/2 nuclei in atoms connected by a σ bond the interaction of an electron in the bond with one of the two nuclei, therefore, has consequences (in terms of the alignment of the second electron of the bond) at the second nucleus. The magnitude of this effect is inversely proportional to the energy separation ΔE between electronic ground and excited states (as found for the chemical shift). The major influences on J are, therefore, the s character of the bond and ΔE, with the electron density in the bond exerting a lesser influence.

The sign of the coupling constant between the nuclei is positive if an antiparallel configuration of the nuclear spins is favoured and negative if a parallel configuration is favoured. The experimentally determined signs of coupling constants involving rhodium are $^{1}J(^{103}\mathrm{Rh},^{1}\mathrm{H})$,[181] $^{1}J(^{103}\mathrm{Rh},^{19}\mathrm{F})$,[182] $^{2}J(^{103}\mathrm{Rh},^{19}\mathrm{F})$[181] and $^{1}J(^{103}\mathrm{Rh},^{31}\mathrm{P})$[181–184] negative; $^{1}J(^{103}\mathrm{Rh},\ ^{15}\mathrm{N})$,[82] $^{1}J(^{119}\mathrm{Sn},^{103}\mathrm{Rh})$,[185] $^{1}J(^{125}\mathrm{Te},^{103}\mathrm{Rh})$[186] and $^{1}J(^{103}\mathrm{Rh},^{103}\mathrm{Rh})$[187] positive. The sign of a coupling constant can be determined relative to a coupling constant of known sign by making use of 'passive' coupling in an appropriate two-dimensional X–Y correlated spectrum.[188,189] In a correlated spectrum involving two nuclei of positive γ (e.g., $^{1}\mathrm{H}$ and $^{31}\mathrm{P}$) with passive coupling to a third nucleus (e.g., $^{103}\mathrm{Rh}$) a positive tilt of the cross peaks indicates that the two passive couplings $^{1}J(^{103}\mathrm{Rh},^{1}\mathrm{H})$ and $^{1}J(^{103}\mathrm{Rh},^{31}\mathrm{P})$, have the same sign; in a correlated spectrum involving two nuclei having opposite signs of γ (e.g., (i) $^{1}\mathrm{H}$ and $^{119}\mathrm{Sn}$ or (ii) $^{31}\mathrm{P}$ and $^{15}\mathrm{N}$) with passive coupling to a third nucleus (e.g., $^{103}\mathrm{Rh}$) a positive tilt of the cross peaks indicates that the two passive couplings of (i) $^{1}J(^{103}\mathrm{Rh},^{1}\mathrm{H})$ and $^{1}J(^{119}\mathrm{Sn},^{103}\mathrm{Rh})$ or (ii) $^{1}J(^{103}\mathrm{Rh},^{31}\mathrm{P})$ and $^{1}J(^{103}\mathrm{Rh},^{15}\mathrm{N})$ have opposite signs. Examples of these are shown in Figure 23,[82] which confirms the signs of couplings for the complex $[\mathrm{Rh}(\mathrm{NCBPh_3})(\mathrm{H})(\mathrm{SnPh_3})(\mathrm{PPh_3})_2]$ to be as follows: $^{2}J(^{15}\mathrm{N},^{1}\mathrm{H})$, $^{2}J(^{31}\mathrm{P},^{1}\mathrm{H})$, $^{1}J(^{103}\mathrm{Rh},^{1}\mathrm{H})$ and $^{1}J(^{103}\mathrm{Rh},^{31}\mathrm{P})$ negative; $^{2}J(^{31}\mathrm{P},^{15}\mathrm{N})$, $^{1}J(^{103}\mathrm{Rh},^{15}\mathrm{N})$, $^{2}J(^{119}\mathrm{Sn},^{1}\mathrm{H})$, $^{2}J(^{119}\mathrm{Sn},^{31}\mathrm{P})$ and $^{1}J(^{119}\mathrm{Sn},^{103}\mathrm{Rh})$ positive. These signs are based on the premise that $^{1}J(^{103}\mathrm{Rh},^{31}\mathrm{P})$ is negative.

The rhodium phosphorus coupling constant has been found to correlate with the donor ability of ligand X in complexes $[\mathrm{Rh}(\mathrm{Hdmg})_2(\mathrm{X})(\mathrm{PPh_3})]$ (Hdmg = monoanion of dimethylglyoxime; X = H_2O, Cl, Me, Et, ^{n}Pr, ^{i}Pr, ^{n}Bu, ^{s}Bu, ^{t}Bu, ^{neo}Pent, adam) decreasing in the sequence H_2O (139 Hz) Cl (123 Hz), Me (66 Hz), ^{i}Pr (56 Hz) adamantyl (48 Hz).[104] The trend of decreasing J(Rh,P) is taken to indicate a weakening of the Rh–P bond as the donor ability of X increases. A correlation has also been found between J(Rh,P) and the Rh–P bond length in

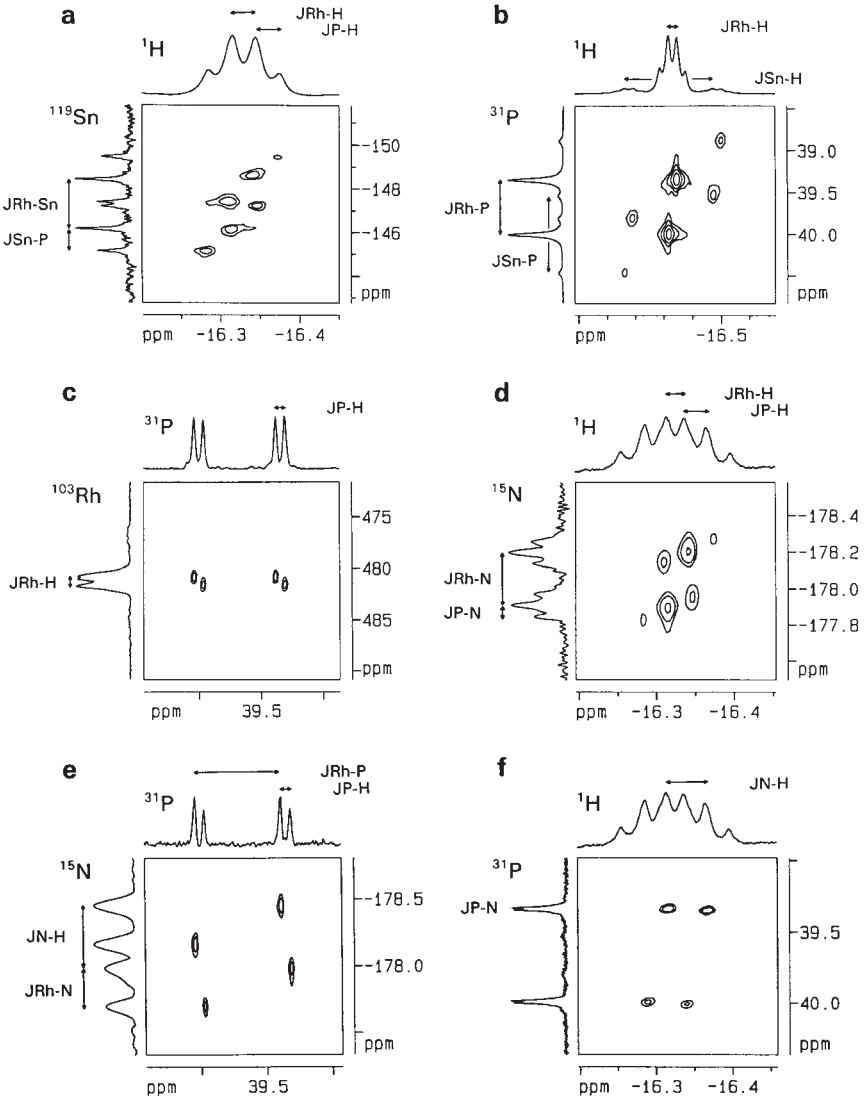

Figure 23 ^{1}H{^{119}Sn} (a); ^{1}H{^{31}P} (b), (f); ^{31}P{^{103}Rh} (c); ^{1}H{^{15}N} (d); and ^{31}P{^{15}N} (e) HMQC spectra recorded from [Rh(NCBPh$_3$)(H)(SnPh$_3$)(PPh$_3$)$_2$] (a–c) and [Rh(^{15}NCBPh$_3$)(H)(SnPh$_3$)(PPh$_3$)$_2$] (d–f) in dichloromethane at 248 K using a Bruker DRX 400 spectrometer with the pulse sequence given in Section 2 (ref. 82).

complexes [Rh(Hdmg)$_2$(X)(PPh$_3$)] (X = Cl, C$_2$Ph, CHCH$_2$, Me, Et, ^{i}Pr, ^{t}Bu),[190] [Rh(L, L′)(CO)(PPh$_3$)] (L,L′ = bidentate anionic ligand),[191] and [Rh(acac^{Fc,R})(CO)(PPh$_3$)] (Fc = ferrocenyl, R = Me, CF$_3$, Ph, Fc).[192]

Rhodium–carbon coupling constants (absolute magnitude, value in Hz) for complexes of various organic ligands are given below, with an indication of

the range in which they are likely to occur. Selected references are given in parentheses.

Acetylene	13–19	(193–196)
Acetylide	36–54 (Cα) 6–14.5 (Cβ)	(193, 197, 198)
Acyl	~18	(199)
Alkene	10–17	(200–202)
Alkyl	18–38	(104, 203)
Allenylidene	51–70 (Cα) 12–18 (Cβ) ~0(Cγ)	(204)
Allyl (η^3)	6–24 (C^1, C^3) 4.5–7.5 (C^2)	(205–208)
Arene	2–3	(209, 210)
Aryl	30–56	(211, 212)
Cp	2–5	(200, 213, 214)
Cp*	6–11	(215)
Cp^R	2–8	(213)
Carbene	17–59 (terminal) 16–39 (bridging)	(216–223)
Carbonyl	47–98 (terminal) 9–52 (bridging)	(224–230)
Carbyne	25–40 (μ_2) 10–40 (μ_3)	(224–226)
Cyanide	~34	(231)
Diene	2–14	(232–234)
Formyl	29–30	(235, 236)
Isocyanide	45–80 (terminal) ~28 (bridging)	(200, 201, 204, 237)
Ketene	19–33 (η^2-CO) 23–24 (η^2-CC)	(238, 239)
Vinyl	24–39	(240)
Vinylidene	46–66(Cα) 12–17 (Cβ)	(193, 240)

Miscellaneous items of interest include the first reported observation of $J(^{103}Rh,^{1}H)$ in 1959 by Griffith and Wilkinson[241] for the complex $K_3[Rh(H)(CN)_5]$ {$J(^{103}Rh,^{1}H) = 13.1$ Hz}, the largest reported value of $J(^{103}Rh,^{1}H)$ of 164 Hz for $[Rh_2(H)_2(CO)_2(\mu\text{-}CO)_2(\mu\text{-}Et_2PCH_2CH_2PPhCH_2PPhCH_2CH_2PEt_2)]$,[2+ 242] $J(^{103}Rh,^{1}H)$ for an agostic hydrogen in $[Rh(2,6\text{-}(^tBu_2PCH_2)_2C_6H_4)(CO)]OTf$ (18.1 Hz),[243] J(Rh,H) for a hydrogen-bonded ligand OH in *trans*-$[Rh(Cl)(CO)(Ph_2PCH_2C^t\text{-}Bu_2OH)_2]$ {$^{1h}J(^{103}Rh,^{1}H) = 2.7$ Hz},[244] $J(^{103}Rh,^{1}H)$ for the HD complex $[R(Cp^*)(Me_2PCH_2PMe_2)(HD)][B(C_6F_5)_4]_2$ (31 Hz),[245] $^{1}J(^{103}Rh,^{31}P)$ for a complex of a cationic phosphenium ligand $[Rh(Cl)\{C_2H_4(N(4\text{-}MeOC_6H_4))_2P\}(PPh_3)_2]OTf$ (311 Hz),[246] $J(^{103}Rh,^{15}N)$ for the interstitial nitride in the cluster $[Rh_6(N)(CO)_{15}][PPh_4]$ (6.1 Hz)[247] and $J(^{205}Tl,^{103}Rh)$ in the range 5,100–5,319 Hz for complexes porphyrinRh–Tlporphyrin.[248] A large difference between the values of $J(^{103}Rh,^{13}C)$ obtained from [Rh(mesityl)$_3$] in solution and in the solid state (128 Hz, more than twice the solution value) has been taken as strong evidence of differences in bonding and geometry on going from solution to the solid state.[249]

15. RELAXATION TIMES

When making measurements of chemical shifts by direct observation knowledge of the relaxation time of the observed nucleus and the principal mechanism by

which relaxation occurs is of obvious value. With the majority of ^{103}Rh measurements now made by indirect detection, for which it is necessary to allow only for the relaxation of ^{1}H or ^{31}P (or ^{13}C, see Section 2) and not ^{103}Rh, the need for ^{103}Rh relaxation data has receded considerably. Nevertheless, for some compounds of rhodium there is at present no alternative to direct observation and for these, in assessing the need for a relaxation agent, it is useful to have some idea of the likely magnitude of the spin-lattice relaxation time (T_1).

Values of ^{103}Rh T_1 have been measured for a number of complexes (Table A12), and vary directly with temperature and inversely with field strength, indicating that chemical shift anisotropy (CSA) makes an important contribution to the relaxation process. From a combined ^{103}Rh and ^{13}C relaxation study of [Rh(Cp)(cod)] Mann and co-workers[250] obtained a ^{103}Rh CSA of 524 ppm and were able to conclude that CSA was by far the predominant relaxation mechanism for this complex. An account of relaxation and related time-dependent processes is given by Howarth.[251]

16. CONCLUSION

^{103}Rh NMR is unlikely to revolutionise the way in which rhodium chemistry is done, but it can provide valuable insights into ligand-binding properties (correlation with stability constants and rate constants) and steric and electronic influences on coordination geometry and reactivity. The high sensitivity of the ^{103}Rh chemical shift to the chemical environment of the rhodium atom makes ^{103}Rh NMR well suited to the study of small changes in the coordination sphere that may be relevant to catalytic and related processes. Areas in which ^{103}Rh NMR is likely to show increased future application are solid-state and high-pressure studies, PHIP-enhanced studies, studies of clusters and the prediction and optimisation of reactivity.

ABBREVIATIONS

acac	acetylacetonate
acac^{F}	fluorinated acac
acet	acetone
acnl	acetonitrile
alkene^{E}	alkene bonded to S, Se
alkyl^{E}	alkyl bonded to N, O, S, etc.
alkyl^{F}	fluorinated alkyl
aq	aqueous solution
benz	benzene
benz^{F}	fluorobenzene
BBN	borabicyclononane
bipy	bipyridyl
bdpp	2,4-$(Ph_2P)_2$pentane

bz	benzyl
bzim	benzimidazole
CHIRAPHOS	(2*S*,3*S*)-bis(Ph_2P)butane
cht	cycloheptatriene
clfm	chloroform
CNR	isocyanide
cod	1,5-cyclooctadiene
cot	cyclooctatetraene
Cp	η^5-cyclopentadienyl
Cp*	pentamethyl Cp
Cp^R	Cp with substituent(s)
Cy	cyclohexyl
CyH	cyclohexane
DCM	dichloromethane
DEPT	distortionless enhancement by polarisation transfer
$diene^P$	phosphadiene
DIOP	2,3-*O*-isopropylidene-2,3-hydroxy-1,4-$(Ph_2P)_2$ butane
DIPAMP	ethane-1,2-bis[(2-methoxyphenyl) phenylphosphine]
DMF	dimethylformamide
DMSO	dimethylsulphoxide
dppb	bis(diphenylphosphino)butane
dppe	1,2-bis(Ph_2P)ethane
DuPHOS	2′,5′,2″,5″-tetraethyl-1,2-bis(phospholanyl) benzene
Fc	ferrocenyl
glup	glucopyranoside
Hdmg	dimethylglyoxime mono-anion
hex	hexane
HMQC	heteronuclear multiple quantum coherence
HSQC	heteronuclear single quantum coherence
ind	η^5-indenyl
INEPT	insensitive nuclei enhanced by polarisation transfer
meth	methanol
nbd	norbornadiene
nitr	nitromethane
ns	not specified
O_2CIsoq	isoquinoline-1-carboxylate
O_2CPy	pyridine-2-carboxylate
O_2CPyraz	pyrazine-2-carboxylate
O_2CQuin	quinoline-2-carboxylate
O_2CQuinox	quinoxaline-2-carboxylate
OTf^-	trifluoromethanesulphonate
OTs^-	*p*-toluenesulphonate
pc	propylene carbonate
py	pyridine
py^R	pyridine with substituent(s)
pz	pyrazole

pz*	3,5-dimethylpyrazole
rt	room temperature
TCNE	tetracyanoethylene
terpy	terpyridyl
THF	tetrahydrofuran
tol	toluene
Tp	tris(pyrazolyl)borate
Tp*	3,5-dimethyl Tp
Tp^R	Tp with substituent(s)
Xantphos	1,8-(Ph_2P)xanthene and derivatives
Z	benzyl oxycarbonyl
ΔE	energy difference between electronic ground and excited state

ACKNOWLEDGEMENTS

I thank Mrs. Shirley Parker for her diligence and endless patience in typing this article, Mrs. Pat Cawthorn for the illustrations and the University of the Witwatersrand.

APPENDIX: LAYOUT OF TABLES

The Tables are intended to be largely self-explanatory, but the following comments may be of some assistance. Rhodium chemical shifts are given in Tables A1–A4, which contain details of complexes of Rh(I) (Table A1), Rh(III) (Table A2), of complexes of other oxidation states (–I, II and V) (Table A3) and of clusters (Tables A4a and A4b). In Tables A1–A3 complexes are listed according to ligand type, which is given in a column headed 'Coordination sphere'. The entries in this column begin with organic ligands shown alphabetically, with the exception of some of the more common ligands (e.g., Cp, diene, CO) which are given towards the end of the list. Abbreviations are given above. Following the organic ligands are H (hydride), P (P-donor), N (N-donor), O (O-donor), F, Cl, Br, I, Si, S, As, Se, Sn and Te. Ligands following the first named ligand are similarly ordered. In this way it is hoped that a ligand type can be quickly identified by scanning the column 'Coordination sphere', avoiding the need to read each formula.

To the right of the 'Compound' column, which gives the formula, are columns showing solvent, temperature and ^{103}Rh chemical shift. Abbreviated solvent names (see Abbreviations) are given, rather than formulae, in order to accelerate access to data. As noted in Sections 5 and 6 rhodium chemical shifts are quite sensitive to changes in solvent and temperature. A report of $\delta(^{103}Rh)$ that is unaccompanied by this information is given an entry 'ns' (not specified) and should be viewed as having associated with it a greater degree of uncertainty than is normal. 'Normal', for this purpose, is generally regarded as being ± 1 ppm. A temperature given as 'rt' (room temperature) probably lies in the range 22 ± 3°C. Allowing for a temperature dependence of 1.5 ppm/K (estimated

upper limit) and taking into account the assumed error limit of ± 1 ppm the likely accuracy of the shift reported at 'room temperature' is $\sim \pm 5$ ppm. Uncertainties in $\delta(^{103}\mathrm{Rh})$ arising from doubts as to the identity of the solvent are likely to be larger than this.

In Table A1 are given two columns of coupling constants '*J*(Rh,P)' and '*J*(Rh,X)' and in Table A2 three columns '*J*(Rh,H)', '*J*(Rh,P)' and '*J*(Rh,X)', where X = ^{13}C, ^{15}N, ^{19}F, etc. The information in columns '*J*(Rh,H)' and '*J*(Rh,P)' is given separately, in order to facilitate access, because of the increasing use of these parameters in deriving delay times for measurements by indirect detection. Other information in the tables is given in footnotes. Tables A5–A11 contain values of coupling constants $J(^{103}\mathrm{Rh},X)$ where X = ^{15}N, ^{19}F, ^{29}Si, ^{77}Se, ^{119}Sn, ^{125}Te and also ^{103}Rh and other metals. In the tables all coupling constants are given as absolute magnitudes, i.e., without regard to sign. Table A12 presents relaxation times for various complexes. Probable signs of several of the coupling constants are given in Section 14.

Table A1 Data for Rh(I) complexes

Coordination Sphere[a]	Compound[b]		Solvent[c]	T (K)[d]	$\delta(^{103}Rh)$[e]	J(Rh,P)[f]	J(Rh,X)[g]	Reference(s)
Acetylide CNR P_2	*trans*-[Rh(C_2Ph)(xylylNC)(PPh_3)$_2$]		tol	300	−687	144		252
acyl $(CO)_2$ P_2	[Rh(COoctyl)$(CO)_2${P(Ph)(N(Et)CO)$_2$N(Et)}$_2$]		tol[h]	223	~ −70	205	J(Rh,C) Rh-CO 70(eq) 42(ax) Rh-acyl 18	124
Alkene η^2-arene Cp	[Rh(Cp)(C_2H_4)(η^2-C_6H_5-CH_3)]	(a)	tol	193	−374			113
	(Rotamers)	(b)			−333			113
Alkene$_2$ Cp	[Rh(Cp)(C_2H_4)$_2$]		acet	300	−945			23
Alkene Cp P	[Rh(Cp)(C_2H_4)(PPh_3)]		THF	310	−1,039	208		253
	[Rh(Cp){P(C_7H_7)$_2$(η^2-C_7H_7)}]		clfm	298	−1,116	241	J(Rh,C) 12.6 (C_7H_7 alkene)	254
Alkene$_2$ Cp^R	[CH_2{(C_5H_4)Rh(C_2H_4)$_2$}$_2$]		benz	296	−929		J(Rh,C) 3.9 (iC_5H_4) 3.9 (αC_5H_4) 4.1 (βC_5H_4) 13.4(C_2H_4)	255
	[CH_2{(C_5H_4)Rh($CH_2CHSiMe_3$)$_2$}$_2$]	(a)	benz	296	−782			255
	(Rotamers)	(b)	benz	296	−780			
		(c)	benz	296	−736 −782			
	[Rh^1(C_2H_4){$C_5H_4CH_2$(C_5H_4)Rh^2(H)($SiEt_3$)(C_2H_4)}] {2 $\delta(^{103}Rh)$ −1,483}		benz	296	(1) −929			255
Alkene Cp^R S	[Rh^1(C_2H_4)(Me_2SO){$C_5H_4CH_2$(C_5H_4)Rh^2(C_2H_4)$_2$}]		DMSO	300	(1) −613 (2) −929		J(Rh^1,C) 30 (C_2H_4)	255
	[CH_2{(C_5H_4)Rh(C_2H_4)(Me_2SO)}$_2$]		DMSO	300	−617			255
Alkene$_2$ indenyl^R	(−)-[Rh(2-menthylindenyl)(C_2H_4)$_2$]		clfm/Et_2O	298	−265[i]		J(Rh,C) 5.9 (C^2) 4.3 (C^1,C^3) 2.7 (C^8,C^9)	256
	syn-[{Rh(C_2H_4)$_2$}$_2$(2,7-Me_2-*as*-indacenediide)]		DCM	300	−652			257
	anti-[{Rh(C_2H_4)$_2$}$_2$(2,7-Me_2-*as*-indacenediide)]		DCM	300	−729			257
Alkene indenyl vinyl Rh	[(η^5-indenyl)Rh^1($CHCH_2$)(MeCH(Me)C)Rh^2(η^5-indeny)]		benz	ns	(1) −560 (2) −574		J(Rh,Rh) 17.0	258
Alkene$_2$ H P N	[Rh(H){NH(dibenzocycloheptenyl)$_2$}(PPh_3)]	(a)	THF	230	−187[j]	144		259
	(Isomers)	(b)	THF	298	−38[j]	138		

Alkene$_2$ P$_2$	*trans*-[Rh{PPh_2(dibenzocycloheptenyl)}$_2$]$^+$ Cl^-		DCM	248	210	131		260
	cis-[Rh{PPh_2(dibenzocycloheptenyl)}$_2$]$^+$ Cl^-		DCM	248	−253	178		260
Alkene$_2$ P$_2$ N	[Rh{PPh_2(dibenzocycloheptenyl)}$_2$(CH_3CN)]$^+$ Cl^-		DCM	213	381	117		260
Alkene$_2$ P N	[Rh{N(dibenzocycloheptenyl)$_2$}(PPh_3)]		THF	200	838[j]	124		259
Alkene P Tp*	[Rh(κ^2-Tp*){P(C_7H_7)$_2$(η^2-C_7H_7)}]		benz	ns	1,175	ns		261
Alkene P$_2$ O	[Rh-{(*Z*)-PhCHC(NHCOMe)CO_2Me}(dppe)]		meth	300	340			68
	[Rh-{(*Z*)-PhCHC(NHCOMe)CO_2^tBu}(dppe)]		meth	300	304			68
	[Rh-{(*Z*)-PhCHC(NHCOMe)CO_2H}(dppe)]		meth	300	315			68
	[Rh-{(*Z*)-PhCHC(NHCOPh)CO_2H}(dppe)]		meth	300	310			68
	[Rh-{(*Z*)-4-HOC_6H_4CHC(NHCOPh)CO_2H}(dppe)]		meth	300	271			68
	[Rh-{(*Z*)-4-$O_2NC_6H_4$CHC(NHCOPh)CO_2H}(dppe)]		meth	300	495			68
	[Rh-{(*Z*)-PhCHC(NHCOMe)CO_2Me}(*SS*-dppb)]	(a)	meth	300	250			68
	(Diasteromers (a) major (b) minor)	(b)			428			
	[Rh-{(*Z*)-PhCHC(NHCOMe)CO_2^tBu}(*SS*-dppb)]	(a)	meth	300	241			68
		(b)			274			
	[Rh-{(*Z*)-PhCHCH(NHCOMe)CO_2H}(*SS*-dppb)]	(a)	meth	300	241			68
		(b)			401			
	[Rh-{(*Z*)-PhCHC(NHCOPh)CO_2H}(*SS*-dppb)]	(a)	meth	300	233			68
		(b)			369			
	[Rh-{(*Z*)-4-HOC_6H_4CHC(NHCOPh)CO_2H}(*SS*-dppb)]	(a)	meth	300	212			68
		(b)			346			
	[Rh-{(*Z*)-4-$O_2NC_6H_4$CHC(NHCOPh)CO_2H}(*SS*-dppb)]	(a)	meth	300	339			68
		(b)			584			
	[Rh{(*Z*)-PhCHC(NHCOMe)CO_2Me}(*S*,*S*-DIPAMP)]	(a)	meth	300	630			68
		(b)			727			
	[Rh{(*Z*)-PhCHC(NHCOMe)CO^{t}Bu}(*S*,*S*-DIPAMP)]	(a)	meth	300	560			68
		(b)			850			
	[Rh{(*Z*)-PhCHC(NHCOMe)CO_2H}(*S*,*S*-DIPAMP)]	(a)	meth	300	590			68
		(b)			675			
	[Rh{(*Z*)-PhCHC(NHCOPh)CO_2H}(*S*,*S*-DIPAMP)]	(a)	meth	300	569			68
		(b)			677			
	[Rh{(*Z*)-4-HOC_6H_4CHC(NHCOPh)CO_2H}(*S*,*S*-DIPAMP)]	(a)	meth	300	491			68
		(b)			538			
	[Rh{(*Z*)-4-$O_2NC_6H_4$CHC(NHCOPh)CO_2H}(*S*,*S*-DIPAMP)]	(a)	meth	300	785			68
		(b)			1,032			
Alkene P$_2$ Cl	[Rh(Cl){PCy_2($CH_2CH_2OCH_3$)}$_2$(C_2H_4)]		benz	295	271	121		262
Alkene$_2$ N$_2$	(*R*, *R*)-[Rh{cycloC_6H_{10}(NHdibenzocycloheptenyl)$_2$}]$^+$ OTf^-		acnl	ns	922		*J*(Rh,C) 11.3, 13.1 (alkene)	263

Table A1 *(Continued)*

Coordination Sphere[a]	Compound[b]		Solvent[c]	*T* (K)[d]	$\delta(^{103}Rh)$[e]	*J*(Rh,P)[f]	*J*(Rh,X)[g]	Reference(s)
	[Rh{cycloC_6H_{10}(Ndibenzocycloheptenyl)(NHdibenzocycloheptenyl)}]		acnl	ns	736		*J*(Rh,C) 9.4, 10.7, 12.0, 16.9 (alkene)	263
	(*S*, *S*)-[Rh{1,2-Ph_2-1,2-(NHdibenzocycloheptenyl)$_2C_2H_2$}]$^+$ OTf^-		acnl	ns	917		*J*(Rh,C) 11.0, 13.1 (alkene)	263
Alkene N_3	[Rh(La{O(2-$SiMe_2$N-4-Mepy)$_2$}$_2$(THF))(C_2H_4)]		benz	297	2,242			264
Alkene$_2$ N Cl	[Rh(Cl)($CH_2^1CH^2CMe_2CH_2NMe_2$)(C_2H_4)]		clfm	298?	652[k]		*J*(Rh,C) 15 ($C^{1/2}$) 11 (C_2H_4)	265
Alkene$_2$ N Cl_2	[Rh_2(μ-Cl)$_2$}NH(dibenzocycloheptenyl)$_2$}$_2$]		DCM	298	2,992[j]			259
Alkene N_2 Cl	[Rh(Cl)($CH_2CHCMe_2CH_2NMe_2$)(CH_3CN)]		acnl	298?	1,696[k]		*J*(Rh,C) 15 ($C^{1/2}$)	265
	[Rh(Cl)($CH_2CHCMe_2CH_2NMe_2$)(4-CNpy)]		DCM	298?	2,029[k]		*J*(Rh,C) 19 ($C^{1/2}$)	265
	[Rh(Cl)($CH_2CHCMe_2CH_2NMe_2$)(py)]		DCM	298?	2,051[k]		*J*(Rh,C) 21 (C^1) 19 (C^2)	265
	[Rh(Cl)($CH_2CHCMe_2CH_2NMe_2$)(4-Me_2Npy)]		DCM	298?	2,095[k]		*J*(Rh,C) 19 (C^1) 20 (C^2)	265
Alkene N_3 La	[Rh(La{O(2-$SiMe_2$N-4-Mepy)$_2$}(C_2H_4)]		benz	297	2,152			264
Alkene$_2$ acac	[Rh(acac)(C_2H_4)$_2$]		DCM	300	1,184			23
			DCM	298	1,180.7			61
			clfm	298	1,180.3			61
			THF	298	1,178.3			61
			acnl	298	1,171.7			61
			meth	298	1,167.2			61
			clfm	270	1,170		*J*(Rh,C) 13.6	50
	[Rh(acac)(C_2H_4)(C_3H_6)]		clfm	270	1,262		*J*(Rh,C) 12.8 (C_2H_4) 13.3, 14.2	50
	[Rh(acac)(C_3H_6)$_2$]	(a)	clfm	270	1,366		*J*(Rh,C) 13.7, 12.5	50
	(Isomers)	(b)	clfm	270	1,315			50

	[Rh(acac)(C_2H_4)(*cis*-2-C_4H_8)]		clfm	270	1,353		*J*(Rh,C) 13.2 (C_2H_4)	50
	[Rh(acac)(*cis*-2-C_4H_8)$_2$]		clfm	270	1,509		*J*(Rh,C) 12.8	50
	[Rh(acac)(C_2H_4)(*trans*-2-C_4H_8)]		clfm	270	1,386		*J*(Rh,C) 16.4, 13.3 (C_2H_4); 12.3	50
	[Rh(acac)(*trans*-2-C_4H_8)$_2$]		clfm	270	1,603		*J*(Rh,C) 14.1, 12.3	50
	[Rh(acac)(*cis*-2-C_4H_8)(*trans*-2-C_4H_8)]		clfm	270	1,561			50
	[Rh(acac)(cyclooctene)$_2$]		clfm	270	1,296		*J*(Rh,C) 13.3	50
Alkene$_2$ acac^F	[Rh(acac^F)(C_2H_4)$_2$]		clfm	270	1,296			50
	[Rh(acac^F)(*cis*-2-C_4H_8)$_2$]		clfm	270	1,644		*J*(Rh,C) 15.0	50
	[Rh(acac^F)(*trans*-2-C_4H_8)$_2$]		clfm	270	1,763		*J*(Rh,C) 14.4, 12.6	50
	[Rh(acac^F)(*cis*-2-C_4H_8)(*trans*-2-C_4H_8)]		clfm	270	1,724			50
alkyl diene P	[Rh(Me)(cod){P(NMe_2)$_3$}]		benz	298	165	245		102
	[Rh(Me)(cod)(P^{n}Bu$_3$)]		benz	298	73	175		102
	[Rh(Me)(cod)(P^{n}Pr$_3$)]		benz	298	73	174		102
	[Rh(Me)(cod)(PEt_3)]		benz	298	57	174		102
	[Rh(Me)(cod)(PMe_3)]		benz	298	23	175		102
	[Rh(Me)(cod){P($OMe)_3$}]		benz	298	−129	307		102
Alkyl diene P$_2$	[Rh(Me)(cod)(PMe_2Ph)$_2$]		DCM	255	−278	125		102
	[Rh(Me)(cod)(PMe_3)$_2$]		tol	253	−332	123		102
Alkyl P$_4$	[Rh(Me)(PMe_3)$_4$]		tol	223	−490			266
			tol	233	−482			266
alkyl^E diene P	[Rh{CH(SO-*p*-tol)PPh_2–*o*-$C_6H_4PPh_2$}(cod)]$^+$ PF_6^-	(a)	clfm	ns	170	153		72
	(Diasteromers)	(b)	clfm	ns	261	152		72
alkyl^E diene N	[Rh(CH_2PPh_2N-*p*-tol)(cod)]		benz	295	787		*J*(Rh,C) 19.3 (CH_2); 9.0, 13.6 (diene)	267
	[Rh{CH(PPh_2N-*p*-tol)$_2$}(cod)]		benz?	rt?	917			268
alkyl^E (CO)$_2$ N	[Rh(CH_2PPh_2N-*p*-tol)(CO)$_2$]		benz	295	−88		*J*(Rh,C) 14.4 (CH_2); 57.9, 65.5 (CO)	267
	[Rh{CH(PPh_2N-*p*-tol)$_2$}(CO)$_2$]		benz?	rt?	11			268
Allyl P$_2$	[Rh(η^3-allyl)(PPh_3)$_2$]		THF	310	−1,021			253
	[Rh(η^3-cyclooctenyl){(–)-bdpp}]		benz	298	−1,002	192		269
	[Rh(η^3-cyclooctenyl){(–)-DIOP}]		benz	298	−1,015	199.6 199.9		269

Table A1 *(Continued)*

Coordination Sphere[a]	Compound[b]	Solvent[c]	T (K)[d]	$\delta(^{103}Rh)$[e]	J(Rh,P)[f]	J(Rh,X)[g]	Reference(s)
Arene cot	$[Rh(\eta^6\text{-}C_6Me_6)(cot)]^+ BF_4^-$	DCM	300	−52			270
	$[Rh^1(\eta^6\text{-}C_6Me_6)\{(cot)Rh^2(Cp)\}]^+ BF_4^-$	DCM	300	(1) 33 (2) −233			270
	$[\{Rh(\eta^6\text{-}C_6Me_6)\}_2(cot)]^{2+} 2BF_4^-$	DCM	300	12			270
Arene P_2	$[Rh(\eta^6\text{-}C_6H_6)Et\text{-}DuPHOS]^+ BF_4^-$	meth	298	−1,116	202		271
	$[Rh(\eta^6\text{-}C_6H_6)(DIPAMP)]^+ BF_4^-$	meth	298	−1,006	207		271
	$[Rh(\eta^6\text{-tol})(Ph\text{-}\beta\text{-glup-OH})]^+ BF_4^-$	meth	298	−762	228		271
	$[Rh(\eta^4\text{-naphth-naphth}PPh_2)(PMePh_2)]^+ BF_4^-$	clfm	298?	−391	200 206		272
Aryl diene P	$[Rh(\eta^1\text{-}C_6H_4\text{-}2\text{-}CH_2PCy_2)(cod)]$	THF	310	22			253
Aryl P_3	$[Rh\{\eta^1\text{-}C_6H_3\text{-}2,6\text{-}(CH_2PPyrrolyl_2)_2\}(PPh_3)]$	THF	295	−734	208 119		273
	$[Rh\{\eta^1\text{-}C_6H_3\text{-}2,6\text{-}(CH_2PPyrrolyl_2)_2\}(PEt_3)]$	benz	295	−781	207 115		273
	$[Rh\{\eta^1\text{-}C_6H_3\text{-}2,6\text{-}(CH_2PPyrrolyl_2)_2\}(PPyrrolyl_3)]$	tol	295	−854	198 178		273
$Carbene_3$ Cl	$[Rh(Cl)\{C_6H_4(NMe)_2C\}_3]$	clfm	rt	2,874		J(Rh,C) 33.1	274
Carbene diene Cl	$[Rh(Cl)\{C_6H_4(NMe)_2C\}(cod)]$	clfm	rt	642		J(Rh,C) 50	274
cht Cp	[Rh(Cp)(cht)]	pent	300	−993			23
cht Cp Rh	$[Rh_2(Cp)_2(\mu\text{-cht})]$	THF	300	−1,142 −676			23
CNR CN P_2	*trans*-$[Rh(CN)(xylylNC)(PPh_3)_2]$	clfm	247	−775	135		60
CNR $CNBPh_3$ P_2	*trans*-$[Rh(CNBPh_3)(xylylNC)(PPh_3)_2]$	clfm	247	−817	129		60
$(CNR)_2$ P_2	$[Rh_2(CNMe)_4\{^tBu_2P(CH_2)_5P^tBu_2\}_2]^{2+} 2BPh_4^-$	DCM	~296	−846	119		275
		acet		−854	119		275
CNR P_2 N	*trans*-$[Rh(N_3)(xylyNC)(PPh_3)_2]$	clfm	300	−251	137		60
			247	−282			
	trans-[Rh(NCO)(xylylNC)$(PPh_3)_2$]	clfm	300	−312	135		60
			247	−346			
	trans-[Rh(NCS)(xylylNC)$(PPh_3)_2$]	clfm	300	−347	133		60
			247	−382			
	trans-$[Rh\{N(CN)_2\}(xylylNC)(PPh_3)_2]$	clfm	300	−363	132		60
			247	−397			
	trans-$[Rh(NCBPh_3)(xylylNC)(PPh_3)_2]$	clfm	300	−388	130		60
			247	−420			

CNR P_2 Cl	$[Rh_2(Cl)_2(CNMe)_2\{^tBu_2P(CH_2)_5P^tBu_2\}_2]$	clfm	~296	−199	130		275
				−205	129		
	trans-$[Rh(Cl)(xylylNC)(PPh_3)_2]$	clfm	300	−250	135		60
			247	−279			
		DCM	300	−261	135		252
CNR P_2 Br	*trans*-$[Rh(Br)(xylylNC)(PPh_3)_2]$	tol	300	−335	134		252
CNR P_2 S	*trans*-$[Rh(SC_6F_5)(xylylNC)(PPh_3)_2]$	tol	300	−366	139		252
cot Cp	[Rh(Cp)(cot)]	acet	300	−348			270
	trans-[Rh(Cp){cot(Rh(Cp))}]	DCM	300	−218			270
	[Rh(Cp){cot(Rh(Ind))}]	DCM	300	−189			270
				87			
	[Rh(Cp){cot(Co(Cp))}]	DCM	300	−256			270
cot Cp Rh	*cis*-[Rh(Cp)(μ-cot){Rh(Cp)}]	clfm	296	−736		*J*(Rh,C) 7.7, 5.4, 2.7(cot); 3.5, 5.0 (Cp)	270
				−1,077			
	$[Rh(Cp)(\mu\text{-cot})\{Rh(Cp)\}]^{2+}\ 2BF_4^-$	nitr	296	−1,607		*J*(Rh,C) 3.2 (cot)	270
	$[Rh(Cp)(\mu\text{-cot})\{Rh(Cp^*)\}]^{2+}\ 2BF_4^-$	nitr	296	−1,240		6.2 (Cp) 7.0 (Cp*)	270
				−1,665			
	$[Rh(Cp)(\mu\text{-cot})\{Rh(cod)\}]^{+}\ BF_4^-$	pc	300	−1,736			23
				−41			
	$[Rh(Cp)(\mu\text{-cot})\{Rh(nbd)\}]^{+}\ BF_4^-$	DCM	300	−1,802			23
				−82			
cot Cp Ru	$[Rh(Cp)(\mu\text{-cot})\{Ru(Cp)\}]^{+}\ PF_6^-$	acet	296	−1,209		*J*(Rh,C) 3.2 (cot) 6.1 (Cp)	270
cot indenyl	[Rh(ind)(cot)]	DCM	300	−18			270
cot indenyl Rh	[Rh(ind)(μ-cot){Rh(ind)}]	DCM	300	115			270
cot diene Fe	$[Rh(cod)(\mu\text{-cot})\{Fe(CO)_3\}]^{+}\ BF_4^-$	pc	300	131			23, 276
	$[Rh(nbd)(\mu\text{-cot})\{Fe(CO)_3\}]^{+}\ BF_4^-$	DCM	300	−67			23, 276
cot acac	[Rh(acac)(cot)]	DCM	300	1,760			23
Tropolone Cp Rh	$[Rh(Cp)(\mu\text{-}C_7H_5O\text{-}2\text{-}OMe)\{Rh(Cp)\}]$	DCM	300	−1,038			23, 276
Tropone Cp Rh	$[Rh(Cp)(\mu\text{-}C_7H_6O)\{Rh(Cp)\}]$	DCM	300	−1,083		*J*(Rh,Rh) 4.8	23, 276
Tropylium Cp Rh	$[Rh(Cp)(\mu\text{-}C_7H_7)\{Rh(Cp)\}]^{+}\ Cl^-$	meth	300	−1,395		*J*(Rh,Rh) 5.2	23, 276

Table A1 *(Continued)*

Coordination Sphere[a]	Compound[b]		Solvent[c]	T (K)[d]	$\delta(^{103}Rh)$[e]	J(Rh,P)[f]	J(Rh,X)[g]	Reference(s)
Tropylium diene Fe	[Rh(cod)(μ-C_7H_7){Fe(CO)$_3$}]		benz	300	−133			23, 276
	[Rh(nbd)(μ-C_7H_7){Fe(CO)$_3$}]		benz	300	−86			23, 276
Tropylium $(CO)_2$ Fe	[Rh(CO)$_2$(μ-C_7H_7){Fe(CO)$_3$}]		acet	300	−739			23
Cp diene	[[Rh(Cp)(butadiene)]		hex	300	−1,256			23
	[Rh(Cp)(cyclobutadiene)]		pent	300	−2,057			23
	[Rh(Cp)(1-Mebutadiene)]		benz	300	−1,004			23
	[Rh(Cp)(1,4-Me_2butadiene)]		hex	300	−1,120			23
	[Rh(Cp)(2,3-Me_2butadiene)]		benz	296	−1,109			277
	[Rh(Cp)(cyclopentadiene)]		benz	300	−958			23
	[Rh(Cp)(1,5-hexadiene)]		hex	300	−780			23
	[Rh(Cp)(1,3-cyclohexadiene)]		THF	300	−1,272			23
	[Rh(Cp)(1,2-$(CH_2)_2$cyclobutane)]		hex	300	−706			23
	[Rh(Cp)(1,3-cycloheptadiene)]		THF	300	−940			23
			acet	300	−938			23
	[Rh(Cp)(nbd)]		THF	300	−786			23
	[Rh(Cp)(cod)]		THF	300	−787			23
			benz	300	−785			23
Cp diene[E]	[Rh(Cp){η^4-(CH_2CMecyclo(CCEtBEtOSiMe_2))}]		tol	ns	−804		J(Rh,Si) 1.1	278
Cp azasilaborole	[Rh(Cp){η^4-(cyclo(CMeCEtBEtNMeSiMe_2))}]		benz	ns	−171		J(Rh,Si) 2.3	279
	[Rh(Cp){η^4-(CH_2CMecyclo(CCEtBEtNMeSiMe_2))}]	(a)	tol	ns	−110		J(Rh,Si) 2.2	279
	(Isomers)	(b)			−737		J(Rh,Si) 1.6	
		(c)			−758		J(Rh,Si) 1.5	
Cp $(CO)_2$	[Rh(Cp)(CO)$_2$]		benz	300	−1,321			23
Cp CO P	[Rh(Cp)(CO){P(cycloheptatrienyl)$_3$}]		benz	298	−1,402		J(Rh,C) 85.6 (CO)	254
Cp P_2	[Rh(Cp){cyclo-(PNMeNCMeCPF_2)}]		clfm	ns	−1,278	306	J(Rh,F) 19	280
Cp* diene	[Rh(Cp*)(2,3-Me_2butadiene)]		benz	296	−1,004			277
Cp^R $(CO)_2$	[Rh(η^5-C_5H_4Me)(CO)$_2$]		benz	298	−1,310			90, 94
	[Rh(η^5-$C_5H_4SiMe_3$)(CO)$_2$]		benz	298	−1,321			90
	[Rh(η^5-$C_5H_4CH_2$Ph)(CO)$_2$]		benz	298	−1,278			90
	[Rh(η^5-C_5H_4CHO)(CO)$_2$]		benz	298	−1,191			90
	[Rh(η^5-C_5H_4COMe)(CO)$_2$]		benz	298	−1,207			90
	[Rh(η^5-$C_5H_4CO_2$Me)(CO)$_2$]		benz	298	−1,205			90

	[Rh(η^5-$C_5H_4CF_3$)$(CO)_2$]	benz	298	−1,220		94
	[Rh(η^5-C_5H_4Cl)$(CO)_2$]	benz	298	−1,166		94
	[Rh(η^5-$C_5H_4NMe_2$)$(CO)_2$]	benz	298	−1,248		94
	[Rh($(\eta^5$-$C_5H_4NO_2)(CO)_2$]	benz	298	−1,117		90, 94
Indenyl diene	[Rh(C_9H_7)(cod)]	benz	303	−487	*J*(Rh,C) 4.6 ($C^{1/3}$) 4.9 (C^2) 2.4 ($C^{8,9}$) 13.4 (diene CH)	281
Indenyl diene^P	[Rh(C_9H_7){cyclo-$P_2(C^tBu)_2$}]	tol?	300	−1,932		282
	[$Rh^1(C_9H_7)$\{μ-cyclo-$P_2(C^tBu)_2$\}$Rh^2(C_9H_7)$\{μ-$P_2(C^tBu)_2$\}$Rh^3(C_9H_7)$]	THF?	193	(1) −564 (2) −1,650 (3) −2,110		282
Indenyl^R diene	[Rh(1-MeC_9H_6)(cod)]	benz	303	−510	*J*(Rh,C) 4.3 (C^1) 5.2 (C^2) 4.6 (C^3) 2.2 (C^8) 2.7 (C^9) 13.4, 14.0 (diene CH)	281
	[Rh(1-PhC_9H_6)(cod)]	benz	303	−437	*J*(Rh,C) 4.0 (C^1) 5.0 (C^2) 4.7 (C^3) 2.0 (C^8) 2.4 (C^9) 13.4, 14.0 (diene CH)	281
	[Rh(5-$NO_2C_9H_6$)(cod)]	benz	303	−413	*J*(Rh,C) 3.8 ($C^{1/3}$) 5.4 (C^2) 2.3 ($C^{8/9}$) 13.0 (diene CH)	281
	[Rh(1,3-$Me_2C_9H_5$)(cod)]	benz	303	−529	*J*(Rh,C) 4.9 ($C^{1/3}$) 5.5 (C^2) 2.5 ($C^{8/9}$) 14.0 (diene CH)	281

Table A1 *(Continued)*

Coordination Sphere[a]	Compound[b]		Solvent[c]	T (K)[d]	$\delta(^{103}Rh)$[e]	$J(Rh,P)$[f]	$J(Rh,X)$[g]	Reference(s)
	[Rh(1,3-$Ph_2C_9H_5$)(cod)]		benz	303	−392		J(Rh,C) 4.3 ($C^{1/3}$) 4.9 (C^2) 1.8 ($C^{8/9}$) 14.0 (diene CH)	281
	[Rh(cod){C_9H_7($Cr(CO)_3$)}]		benz	303	−358			281
	[Rh(cod){1,3-$Me_2C_9H_5$($Cr(CO)_3$)}]		benz	303	−420			281
	[Rh(cod){1,3-$Ph_2C_9H_5$($Cr(CO)_3$)}]		benz	303	−278			281
	(−)-[Rh(2-menthylC_9H_6)(cod)]		clfm/Et_2O	298	−137[i]		J(Rh,C) 3.8 (C^1) 5.9 (C^2) 4.3 (C^3) 2.1, 2.7 ($C^{8/9}$) 13.1, 14.1 (diene CH)	256
	(−)-[Rh(2-menthyl-4,7-$Me_2C_9H_4$)(cod)]		clfm/Et_2O	298	−144[i]		J(Rh,C) 4.0, 4.2 ($C^{1/3}$) 5.4 (C^2) 2.5, 2.6 ($C^{8/9}$) 13.7, 13.8 (diene CH)	256
	[Rh(2-menthyl-4,7-$Me_2C_9H_4$)(cod)]	(a)	clfm/Et_2O	rt	−151[i]		J(Rh,C) 3.7 ($C^{1/8/9}$) 4.3 (C^2) 4.7 (C^3) 13.8, 14.0 (diene CH)	70
	(Diasteromers *pR* (a) *pS* (b))	(b)	clfm/Et_2O	rt	−129[i]		J(Rh,C) 2.6, 3.2, 3.6 ($C^{1/8/9}$) 4.2 (C^1) 4.9 (C^3) 13.6, 14.1 (diene CH)	70

	[Rh(neomenthylC$_9$H$_6$)(cod)]	(a)	clfm/Et$_2$O	rt	−128[i]		*J*(Rh,C) 3.5 (C^1) 4.4 (C^2) 5.2 (C^3) 2.4, 3.0 ($C^{8/9}$) 13.7, 14.0 (diene CH)	70
	(Diasteromers *pR* (a) *pS* (b))	(b)	clfm/Et$_2$O	rt	−137[i]		*J*(Rh,C) 3.7 (C^1) 4.6 (C^2) 5.0 (C^3) 2.2, 2.8 ($C^{8/9}$) 13.7, 13.9 (diene CH)	70
Indacenyl^R diene	[Rh(2,6-Et$_2$-4,8-Me$_2$-*s*-indacenide)(cod)]		benz?	ns	−486			283
	syn-[{Rh(cod)}$_2$(2,6-Et$_2$-4,8-Me$_2$-*s*-indacenediide)]		benz?	ns	−261			283
	anti-[{Rh(cod)}$_2$(2,6-Et$_2$-4,8-Me$_2$-*s*-indacenediide)]		benz?	ns	−334			283
	syn-[{Rh(cod)}$_2$(2,7-Me$_2$–*as*-indacenediide)]		DCM	300	−457			257
	anti-[{Rh(cod)}$_2$(2,7-Me$_2$–*as*-indacenediide)]		DCM	300	−552			257
Indacenyl^R (CO)$_2$	*syn*-[{Rh(CO)$_2$}$_2$(2,7-Me$_2$-*as*-indacenediide)]		DCM	300	−901			257
	anti-[{Rh(CO)$_2$}$_2$(2,7-Me$_2$-*as*-indacenediide)]		DCM	300	−1,008			257
Indenyl (CO)$_2$	[Rh(C$_9$H$_7$)(CO)$_2$]		benz	303	−1,038		*J*(Rh,C) 3.6 ($C^{1/3}$) 6.3 (C^2) 1.9 ($C^{8/9}$)	281
Indenyl^R (CO)$_2$	[Rh(5-NO$_2$C$_9$H$_6$)(CO)$_2$]		benz	303	−987			281
	[Rh(CO)$_2${C$_9$H$_7$(Cr(CO)$_3$)}]		benz	303	−931			281
Diene$_2$	[Rh(cod)$_2$]$^+$		DCM	300	677			257
Diene H P Cl Ru	[Rh(cod)(μ-H)(μ-Cl)(μ-dppm){Ru(H)(dppm)}]		ns	ns	166	134	*J*(Rh,H) 22	284
Diene H P Ru	[Rh(cod)(μ-H)(μ-PhPCH$_2$PPh$_2$){Ru(Ph)(dppm)}]		ns	ns	−238	121	*J*(Rh,H) 19.5	284
Diene P$_2$	[Rh(cod)(PEt$_3$)$_2$]$^+$ BPh$_4^-$		clfm	298	−132	140		102
	[Rh(cod)(P^{n}Bu$_3$)$_2$]$^+$ BPh$_4^-$		clfm	298	−94	140		102
	[Rh(cod)(PMePh$_2$)$_2$]$^+$ ClO$_4^-$		clfm	298	−267	145		102
	[Rh(cod)(PPh$_3$)$_2$]$^+$ BPh$_4^-$		clfm	298	−145	147		102
	[Rh(cod)(PPh$_3$)$_2$]$^+$ PF$_6^-$		DCM	ns	−71	143		285
	[Rh(nbd)(PPh$_3$)$_2$]$^+$ PF$_6^-$		clfm	298	−4	155		102
	[Rh(cod){Ph$_2$P(NCHPh)}$_2$]$^+$ PF$_6^-$		DCM	ns	−274	159		285
	[Rh(cod)(Et$_2$P(CH$_2$)$_2$PEt$_2$)]$^+$ClO$_4^-$		DCM	298	−533	147		62
	[Rh(cod)(Et$_2$P(CH$_2$)$_2$PPh$_2$)]$^+$ClO$_4^-$		DCM	298	−524	152		62
	[Rh(cod)(Ph$_2$P(CH$_2$)$_2$PPh$_2$)]$^+$ ClO$_4^-$		DCM	298	−505	149		62

Table A1 *(Continued)*

Coordination Sphere[a]	Compound[b]	Solvent[c]	T (K)[d]	$\delta(^{103}Rh)$[e]	J(Rh,P)[f]	J(Rh,X)[g]	Reference(s)
	$[Rh(cod)(Ph_2P(CH_2)_4PPh_2)]^+ ClO_4^-$	DCM	298	−271	144		62
	$[Rh(cod)(Et_2P(CH_2)_5PEt_2)]^+ ClO_4^-$	DCM	298	−138	140		62
	$[Rh(nbd)(Ph_2P(CH_2)_2PPh_2)]^+ ClO_4^-$	DCM	298	−390	157		62, 286
	$[Rh(nbd)(Ph_2P(CH_2)_3PPh_2)]^+ ClO_4^-$	DCM	298	−264	149		62, 286
	$[Rh(nbd)(Ph_2P(CH_2)_4PPh_2)]^+ ClO_4^-$	DCM	298	−210	153		62, 286
	$[Rh(cod)\{(Ph_2PCH_2)_2CH(CH_2)_6Si(OMe)_3\}]^+ SbF_6^-$	clfm	296	−350	141		287
	$[Rh(cod)\{1\text{-}Ph_2P\text{-}2\text{-}(CHMePCy_2)Fc\}]^+ BF_4^-$	DCM	298	−229[j]	150 149		288
	$[Rh(cod)\{Ph_2P^a(CH_2)_2PPh_2benzophospholide^bPPh_3\}]^{2+}$ 2OTf$^-$	DCM	298	−76	(a) 134 (b) 162		289
	$[Rh(cod)\{(S)\text{-}Ph_2P(CH_2)_2CH(OMe)CH_2PPh_2\}]^+ BF_4^-$	clfm?	ns	−249	146 144		290
	$[Rh(cod)\{(S)\text{-}Ph_2P(CH_2)_2CH(OH)CH_2PPh_2\}]^+ BF_4^-$	clfm?	ns	−156	143 139		290
	$[Rh(cod)(Ph_2P(CH_2)_4PPh_2)]^+ BF_4^-$	meth	rt	−262			63
	$[Rh(nbd)(Ph_2P(CH_2)_4PPh_2)]^+ BF_4^-$	meth	rt	−210			63
	$[Rh(cod)(DIOP)]^+ BF_4^-$	meth	rt	−233			63
	$[Rh(nbd)(DIOP)]^+ BF_4^-$	meth	rt	−204			63
	$[Rh(cod)\{Ph\text{-}\beta\text{-}glup\text{-}OH\}]^+ BF_4^-$	meth	rt	−305			63
	$[Rh(nbd)\{Ph\text{-}\beta\text{-}glup\text{-}OH\}]^+ BF_4^-$	meth	rt	−296			63
	$[Rh(nbd)\{(R,R)\text{-}Ph_2PCH_2CH(OH)CH(OH)CH_2PPh_2\}]^+ BF_4^-$	meth	297	228			63
	$[Rh(cod)\{(R,R)\text{-}Ph_2PCH_2CH(OH)CH(OH)CH_2PPh_2\}]^+ BF_4^-$	meth	297	−57			63
		meth/DCM	185	−449			
Diene P_2 O	$[Rh(cod)\{(R,R)\text{-}Ph_2PCH_2CH(OH)CH(OH)CH_2PPh_2\}]^+ BF_4^-$	meth/DCM	185	25			63
Diene P N	$[Rh(cod)(PPh_3)(py)]^+ PF_6^-$	clfm	298	415	151		102
	$[Rh(cod)(PPh_3)(4\text{-}Mepy)]^+ PF_6^-$	clfm	298	419	152		102
	$[Rh(cod)(PPh_3)(4\text{-}Me_2Npy)]^+ PF_6^-$	clfm	298	436	152		102
	$[Rh(cod)(NPPh_2CH_2PPh_2)]$	DCM	ns	152	159		285
	$[Rh(cod)(NPPh_2(CH_2)_2PPh_2)]$	DCM	ns	259	157		285
	$[Rh(cod)(NPPh_2\text{-}o\text{-}C_6H_4PPh_2)]$	DCM	ns	208	156		285
	$[Rh(cod)\{Ph_2PCHMePPh_2N(C_6F_4CN)\}]^+ PF_6^-$	DCM	ns	244	153		285
	$[Rh(cod)\{Ph_2PCH_2PPh_2N(C_6F_4CN)\}]^+ PF_6^-$	DCM	ns	234	154		285
	$[Rh(cod)\{Ph_2PCH_2PPh_2N(C_6F_3(CN)_2)\}]^+ PF_6^-$	DCM	ns	264	154		285
	$[Rh(cod)\{Ph_2PCH_2PPh_2N(C_6H_3(NO_2)_2)\}^+ PF_6^-$	DCM	ns	264	153		285
	$[Rh(cod)\{Ph_2PCH_2PPh_2N(C_6H_2F(NO_2)_2)\}]^+ PF_6^-$	DCM	ns	253	154		285
	$[Rh(cod)\{Ph_2P\text{-}o\text{-}C_6H_4PPh_2N(C_6F_4(CN))\}]^+ PF_6^-$	DCM	ns	505	154		285

Diene P N Cl	[Rh(Cl)(cod){((*S*)-2-((1*R*)-1-PPh_2CHMe)$Fc)_2NCHNH$}]		benz	rt	990[j]	137		291
Diene P O	[Rh(cod)(^{Z}AlaSerPPh_2)]$^+$ PF_6^-	(a)	DCM	ns	413	152		73
	(Diastereomers)	(b)	DCM	ns	426	152		
Diene P Cl	[Rh(Cl)(cod)(PEt_3)]		benz	298	385	148		102
	[Rh(Cl)(cod)(P^nPr_3)]		benz	298	401	147		102
	[Rh(Cl)(cod)(P^iPr_3)]		benz	298	519	144		102
	[Rh(Cl(cod)(P^nBu_3)]		benz	298	402	146		102
	[Rh(Cl)(cod)(PCy_3)]		benz	298	527	142		102
	[Rh(Cl)(cod)(PBz_3)]		benz	298	417	151		102
	[Rh(Cl)(cod)(PMe_2Ph)]		benz	298	358	148		102
	[Rh(Cl)(cod)($PMePh_2$)]		benz	298	348	151		102
	[Rh(Cl)(cod)(PPh_3)]		benz	298	393	152		102
	[Rh(Cl)(cod){P(*p*-tol)$_3$}]		benz	298	402	151		102
	[Rh(Cl)(cod){P(NMe_2)$_3$}]		benz	298	557	199		102
	[Rh(Cl)(cod){P(OMe)$_3$}]		benz	298	253	249		102
	[Rh(Cl)(cod){$Ph_2P(CH_2)_2PPh_2$benzophospholidePPh_3}]$^+$ OTf^-		DCM	298	357	153		289
	[Rh(Cl)(cod)(^{z}AlaSerPPh_2)]	(a)	DCM	ns	365	151		73
	(Diastereomers)	(b)	DCM	ns	372	151		
Diene P S	[Rh(cod){Ph_2P-*o*-$C_6H_4CH_2S$(dihydrocamphoryl)}]$^+$ OTf^-		DCM	rt	−60	145	*J*(Rh,C) 9, 11 (diene CH)	292
	[Rh(cod){binaphthyl($O_2POCHPhCH_2SEt$)}]$^+$ BF_4^-		DCM	298	−204	195	*J*(Rh,C) 5.0, 5.7, 9.2, 10.1 (diene CH)	288
Diene Tp	[Rh(Tp)(cod)]		clfm	rt?	1,253			66
Diene Tp*	[Rh(Tp*)(nbd)]		clfm	rt?	1,777			66
	[Rh(Tp*)(cod)]		clfm	rt?	1,107			66
	[Rh(Tp*)(1,3-cod)]		benz	295	1,942			293
Diene Tp^R	[Rh(3-MeTp)(cod)]		clfm	rt?	1,107			66
	[Rh(3-MeTp)(nbd)]		clfm	rt?	1,619			66
	[Rh(3-CF_3-5-MeTp)(cod)]		clfm	rt?	1,129			66
	[Rh(3-CF_3-5-MeTp)(nbd)]		clfm	rt?	1,261			294
	[Rh(3,5-$(CF_3)_2$Tp)(nbd)]		clfm	rt?	1,244			294
	[Rh(3-Ph-5-MeTp)(cod)]		clfm	rt?	1,111			66
	[Rh(3,4,5-Me_3Tp)(cod)]		clfm	rt?	1,110			66
	[Rh(3,5-Me_2-4-ClTp)(cod)]		clfm	rt?	1,101			66
	[Rh(3-^{i}Pr-4-BrTp)(cod)]	(a)	clfm	rt?	1,130			66
	(Isomers)	(b)	clfm	rt?	1,121			
	[Rh(3-^{i}Pr-4-BrTp)(nbd)]	(a)	clfm	rt?	1,274			66
	(Isomers)	(b)	clfm	rt?	1,293			
	[Rh{MeB(3-Mepz)$_3$}(nbd)]		clfm	rt?	1,475			67

Table A1 *(Continued)*

Coordination Sphere[a]	Compound[b]	Solvent[c]	T (K)[d]	$\delta(^{103}Rh)$[e]	J(Rh,P)[f]	J(Rh,X)[g]	Reference(s)
Diene N_2	[Rh{BBN(pz)$_2$}(nbd)]	clfm	rt?	1,097			66
	[Rh{BBN(3-Mepz)$_2$}(cod)]	clfm	rt?	1,205			66
	[Rh{BBN(3-Mepz)$_2$}(nbd)]	clfm	rt?	1,374			66
	[Rh{PhMeB(3-Mepz)$_2$}(cod)]	clfm	rt?	1,136			66
		DCM	298	1,134			288
	[Rh{PhMeB(3-Mepz)$_2$}(nbd)]	clfm	rt?	1,340			66
	[Rh(Bpz$_4$)(cod)]	clfm	298	914			295
	[Rh(Bpz$_4$)(nbd)]	clfm	298	979			295
	[Rh(Bpz$_4$)(duroquinone)]	clfm	298	2,417			295
	[Rh(La{O(2-SiMe$_2$N-4-Mepy)$_2$}$_2$)(cod)]	benz	297	1,087			264
	[Rh(cod){H$_2$C(3,5-Me$_2$pz)$_2$}]$^+$ BF_4^-	acet	298	−142			296
	[Rh(1-NMe-2-NMe$_2$C$_6$H$_4$)(cod)]	THF	310	862			297
		THF	290	848			297
	[Rh(cod)(H$_2$N(CH$_2$)$_2$NH$_2$]$^+$ ClO_4^-	meth	298	751			103
	trans-[Rh(cod){MeNH(CH$_2$)$_2$NHMe}]$^+$ ClO_4^-	meth	298	784			103
	cis-[Rh(cod){MeNH(CH$_2$)$_2$NHMe}]$^+$ ClO_4^-	meth	298	822			103
	[Rh(cod){1,2-(NH$_2$)$_2$C$_6$H$_4$}]$^+$ ClO_4^-	meth	298	801			103
	[Rh(cod){1,8-(NH$_2$)$_2$-naphth}]$^+$ ClO_4^-	meth	298	804			103
	[Rh(cod){H$_2$N(CH$_2$)$_3$NH$_2$}]$^+$ ClO_4^-	meth	298	849			103
	[Rh(cod){Me$_2$N(CH$_2$)$_2$NMe$_2$}]$^+$ ClO_4^-	meth	298	978			103
	[Rh(cod)(^{i}PrNCHCHN^{i}Pr)]$^+$ ClO_4^-	meth	298	914			103
	[Rh(cod){2,6-Me$_2$C$_6$H$_3$N(CH)$_3$NC$_6$H$_3$-2,6-Me$_2$}]$^+$ ClO_4^-	clfm	298	998			103
	[Rh(cod){*bis*(*N*-Phimino)acenaphthene}]$^+$ ClO_4^-	clfm	298	1,025			103
	[Rh(cod){*bis*(*N*-2,6-^{i}Pr$_2$C$_6$H$_3$imino)acenaphthene}]$^+$ ClO_4^-	clfm	298	1,057			103
	[Rh(cod){*bis*(*N*-4-MeOC$_6$H$_4$imino)acenaphthene}]$^+$ ClO_4^-	clfm	298	1,059			103
	[Rh(cod)bipy)]$^+$ ClO_4^-	meth	298	816			103
	[Rh(cod)(4,4′-Me$_2$bipy)]$^+$ ClO_4^-	meth	298	795			103
	[Rh(cod)(py)$_2$]$^+$ ClO_4^-	meth	298	1,009			103
	[Rh(cod)(C$_5$H$_4$N-NH-C$_5$H$_4$N)]$^+$ ClO_4^-	meth	298	1,035			103
	[Rh(5-Phdibenzocyclooctadiene)(CH$_3$CN)$_2$]$^+$ OTf^-	clfm	rt	1,530[j]			298
	[Rh(*R*)-(5-Phdibenzocyclooctadiene){(*R*)-(+)-1,1′-binaphthyl-2,2′-diamine}]$^+$ OTf^-	DCM	rt	1,517[j]			298

Diene acac	[Rh(acac)(cod)]		DCM	300	1,294			23
			clfm	298	1,287			103
	[Rh(acac)(1,3-cycloheptadiene)]		DCM	300	1,195			23
	[Rh(acac){(1,2-CH_2CH)cyclobutane}]		DCM	310	−1,393			297
Diene $(O)_2$	[Rh(cod)(1,2-$(OH)_2$-naphthalene)]$^+$ ClO_4^-		meth	298	1,301			103
	[Rh(cod)$(Me_2CO)_2$]$^+$ ClO_4^-		meth	298	1,350			103
	[Rh(cod)$(bipyO_2)$]$^+$ ClO_4^-		meth	298	1,362			103
	[Rh(cod)$(Ph_2P(O)CH_2P(O)Ph_2)$]$^+$ ClO_4^-		meth	298	1,362			103
	[Rh(cod)$(Ph_2P(O)(CH_2)_2P(O)Ph_2)$]$^+$ ClO_4^-		meth	298	1,373			103
Diene Cl_2	[$Rh_2(\mu$-Cl$)_2$(cod$)_2$]		clfm	298	1,093			103
			benz	310	1,104			297
	[Rh$(Cl)_2$(cod)]$^-$$Et_4N^+$		clfm	298	1,107			103
Azasilaborole acac	[Rh(acac){η^4-cycloCMeCEtBEtNPhSiMe$_2$}]		benz	ns	2,344			279
CN CO P_2	*trans*-[Rh(CN)(CO)$(PPh_3)_2$]		clfm	247	−787	118		60
CN P_3	[Rh(CN)$(PPh_3)_3$]		clfm	300	−449	144		60
						142		
			clfm	247	−427			60
CN P_2 N	*trans*-[Rh(CN)$(PPh_3)_2$(py)]		tol	247	−142	154		60
$CNBR_3$ CO P_2	*trans*-[Rh$(CNBPh_3)(PPh_3)_2$(CO)]		clfm	300	−790	117		60
			clfm	247	−816			
$CNBR_3$ P_3	[Rh$(CNBPh_3)(PPh_3)_3$]		clfm	300	−405	146		60
						137		
			clfm	247	−435			
$CNBR_3$ P_2 N	*trans*-[Rh$(CNBPh_3)(PPh_3)_2$(py)]		tol	247	−233	146		60
$(CO)_2$ H P_2	[Rh(H)$(CO)_2${$Ph_2P(CH_2)_2PPh_2$}]		THF[h]	298	−1,073	118	*J*(Rh,H) 11.0	92
	[Rh(H)$(CO)_2${$Ph_2P(CH_2)_3PPh_2$}]		THF[h]	298	−955	113	*J*(Rh,H) 11.7	92
	[Rh(H)$(CO)_2${1,8-$(Ph_2P)_2$naphthalene}]		benz[h]	298	−954	108	*J*(Rh,H) 13.9	92
	[Rh(H)$(CO)_2${2,2′-$(Ph_2PCH_2)_2$biphenyl}]		benz[h]	298	−898	149	*J*(Rh,H) ~.2	92
	[Rh(H)$(CO)_2${O(*o*-$C_6H_4PPh_2)_2$}]	(1)	benz[h]	298	−829	124	*J*(Rh,H) 11.0	92
	[Rh(H)$(CO)_2$(PhPXantphos)]	(2)	benz[h]	298	−828	126	*J*(Rh,H) 6.6	92
	[Rh(H)$(CO)_2$(Me_2SiXantphos)]	(3)	benz[h]	298	−817	124	*J*(Rh,H) 8.1	92
	[Rh(H)$(CO)_2$(SXantphos)]	(4)	benz[h]	298	−840	128	*J*(Rh,H) 6.6	92
	[Rh(H)$(CO)_2$(Me_2CXantphos)]	(5)	benz[h]	298	−801	127	*J*(Rh,H) 6.6	92
	[Rh(H)$(CO)_2$(Me_2CCXantphos)]	(6)	benz[h]	298	−821	128	*J*(Rh,H) 6.6	92
	[Rh(H)$(CO)_2${phenoxazine$(PPh_2)_2$}]	(7)	benz[h]	298	−785	128	*J*(Rh,H) 5.9	92
	[Rh(H)$(CO)_2${Me_2(SXantphosCF_3)}]	(8)	benz[h]	298	−851	135	*J*(Rh,H) 4.4	92
	[Rh(H)$(CO)_2${Me_2(SXantphosCl)}]	(9)	benz[h]	298	−841	132	*J*(Rh,H) 5.9	92
	[Rh(H)$(CO)_2${Me_2(SXantphosF)}]	(10)	benz[h]	298	−836	131	*J*(Rh,H) 6.6	92
	[Rh(H)$(CO)_2${Me_2(SXantphosMe)}]	(11)	benz[h]	298	−832	126	*J*(Rh,H) 7.3	92
	[Rh(H)$(CO)_2${Me_2(SXantphosOMe)}]	(12)	benz[h]	298	−825	125	*J*(Rh,H) 7.3	92
	[Rh(H)$(CO)_2${Me_2(SXantphosNMe$_2$)}]	(13)	benz[h]	298	−814	122	*J*(Rh,H) 8.8	92

Table A1 *(Continued)*

Coordination Sphere[a]	Compound[b]	Solvent[c]	T (K)[d]	$\delta(^{103}Rh)$[e]	J(Rh,P)[f]	J(Rh,X)[g]	Reference(s)
	$[Rh_2(\mu\text{-}H)(\mu\text{-}CO)(CO)_2(\mu\text{-}Ph_2PCH_2PPh_2)_2]^+$ OTs^-	DCM	243	−482	109	J(Rh,Rh) 0.0	187
CO H P Cl	$[Rh(CO)(PMe_3)(\mu\text{-}H)(\mu\text{-}Cl)Rh(H)(Cl)(PMe_3)_2]$ (Rh(III) δ 347)	benz	348	−688	160		111
CO H P Br	$[Rh(CO)(PMe_3)(\mu\text{-}H)(\mu\text{-}Br)Rh(H)(Br)(PMe_3)_2]$ (Rh(III) δ 182)	benz	348	−69	155		111
CO H P I	$[Rh(CO)(PMe_3)(\mu\text{-}H)(\mu\text{-}I)Rh(H)(I)(PMe_3)_2]$ (Rh(III) δ 210)	benz	348	−733	155		109, 111
CO P_2 N	*trans*-$[Rh(NO_2)(PPh_3)_2(CO)]$	DCM	295	−407	136		182
CO P_2 NCS	*trans*-$[Rh(NCS)(PPh_3)_2(CO)]$	DCM	178	−517	124		182
		clfm	300	−453	125		60
			247	−478			
CO P_2 N	*trans*-$[Rh(N_3)(PPh_3)_2(CO)]$	clfm	300	−377	130		60
			247	−399			
	trans-$[Rh(NCO)(PPh_3)_2(CO)]$	clfm	300	−434	128		60
			247	−457			
	trans-$[Rh\{N(CN)_2\}(PPh_3)_2(CO)]$	clfm	300	−468	124		60
			247	−495			
	trans-$[Rh(NCBPh_3)(PPh_3)_2(CO)]$	clfm	300	−475	123		60
			247	−501			
	$[Rh(k^1\text{-}3,5\text{-}Me_2\text{-}4\text{-}ClTp)(CO)(PMePh_2)_2]$	DCM	233	344	128		299, 300
	$[Rh(k^1\text{-}3,5\text{-}Me_2\text{-}4\text{-}ClTp)(CO)(PMe_3)_2]$	DCM	298	−312	116		300
CO P N_2	$[Rh\{H_2C(3,5\text{-}Me_2pz)_2\}(PPh_3)(CO)]^+$ BF_4^-	acet	298	−91	159	J(Rh,C) 71	296
	$[Rh\{H_2C(3,5\text{-}Me_2pz)_2\}(PMePh_2)(CO)]^+$ BF_4^-	acet	298	−175	153	J(Rh,C) 73	296
CO P_2 O	*trans*-$[Rh(OH)(PPh_3)_2(CO)]$	DCM	253	−300	141		182
	trans-$[Rh(O_2CCH_3)(PPh_3)_2(CO)]$	DCM	243	−261	134		182
	trans-$[Rh(O_2CCF_3)(PPh_3)_2(CO)]$	DCM	243	−276	131		182
CO P_2 O	$[Rh(CO)\{O(CH_2CH_2P^tBu_2)_2\}]^+$ OTf^-	clfm	ns	−526	120		301
$\{(CO)_2$ $Cl_2\}$	$[Rh^1(CO)\{O(CH_2CH_2P^tBu_2)_2\}]^+$ $[Rh^2(Cl)_2(CO)_2]^-$	clfm	ns	(1) −526	121		301
				(2) 84			
CO P_2 F	*trans*-$[Rh(F)(PPh_3)_2(CO)]$	clfm	241	−148	135	J(Rh,F) 52.5	182
$(CO)_2$ P_2 Cl	$[Rh_2(\mu\text{-}Cl)(\mu\text{-}CO)(CO)_2\{\mu\text{-}CH_2C(PPh_2)_2\}_2]+$ Cl^-	DCM?	218	−144			302
	$[Rh_2(\mu\text{-}Cl)(\mu\text{-}CO)(CO)_2(\mu\text{-}Ph_2PCH_2PPh_2)_2]^+$ BPh_4^-	DCM	238	−109	93	J(Rh,Rh) 0.0	187

CO P_2 Cl	*trans*-[Rh(Cl)(PPh_3)$_2$(CO)]	clfm	300	−368	127		20, 25
			247	−387			60, 182
							303
	trans-[Rh(Cl)(PMe_2Ph)$_2$(CO)]	benz	297	−405	118		181
	trans-[Rh(Cl)(PMe_3)$_2$(CO)]	benz	ns	−415	114		184
	[$Rh_2(CO)_2(\mu\text{-Cl})(\mu\text{-}Ph_2PCH_2PPh_2)_2]^+$ BPh_4^-	DCM	rt	−466	114	*J*(Rh,Rh) 2.0	187
	[$Rh_2Cl_2(\mu\text{-CO})(\mu\text{-}Ph_2PCH_2PPh_2)_2$]	DCM	rt	229	120	*J*(Rh,Rh) 10.6	187
CO P Cl_2	[Rh(CO)(μ-Cl)$_2${μ-PPh_2FcP(OMenthyl)$_2$}Rh(CO)]	benz?	ns	−6	178		304
				−47	234		
CO P_2 Cl Rh	[$Rh_2Cl_2(\mu\text{-CO})\{\mu\text{-}CH_2C(PPh_2)_2\}_2$]	DCM?	298	217			302
CO P_2 Cl Ru	[Rh(Cl)(μ-CO)(μ-$Ph_2PCH_2PPh_2$)$_2${$Ru(CO)_2$}]	ns	ns	190	129		284
CO P_2 Br	*trans*-[Rh(Br)(PPh_3)$_2$(CO)]	clfm	295	−421	125		182
	trans-[Rh(Br)(PMe_3)$_2$(CO)]	benz	ns	−448	113		184
	trans-[Rh(Br)(PMe_2Ph)$_2$(CO)]	benz	297	−442	116		181
	[$Rh_2Br_2(\mu\text{-CO})(\mu\text{-}Ph_2PCH_2PPh_2)_2$]	DCM	rt	157	119	*J*(Rh,Rh) 10.5	187
CO P_2 I	*trans*-[Rh(I)(PPh_3)$_2$(CO)]	tol	295	−532	123		182
	trans-[Rh(I)(PMe_2Ph)$_2$(CO)]	benz	297	−524	114		181
	[$Rh_2I_2(\mu\text{-CO})(\mu\text{-}Ph_2PCH_2PPh_2)_2$]	DCM	rt	0	118	*J*(Rh,Rh) 9.6	187
CO P_2 S	[$Rh_2(CO)_2(\mu\text{-S})(\mu\text{-}Ph_2PCH_2PPh_2)_2$]	DCM	rt	−603	131	*J*(Rh,Rh) 2.7	187
	[$Rh_2(CO)_2(\mu\text{-}SCH_2Ph)(\mu\text{-}Ph_2PCH_2PPh_2)_2]^+$ BPh_4^-	DCM	213	−622		*J*(Rh,Rh) 0.4	187
$(CO)_2$ N_2	[$Rh(CO)_2(CH_3CN)_2]^+$ BPh_4^-	acnl	298	−54		*J*(Rh,C) 73 (CO)	305
	cis-[$Rh(CO)_2(py)_2]^+$ ClO_4^-	DCM?	223	73		*J*(Rh,C) 69 (CO) *J*(Rh,N) 19	306
	[$Rh(CO)_2\{H_2C(3,5\text{-}Me_2pz)_2\}]^+$ BPh_4^-	acet	298	−109		*J*(Rh,C) 69	296
	[1,2-{Rh(CO)$_2$(pyrrolyl-2-CHN)}$_2$cyclohehexane]	DCM	rt	46			24
$(CO)_2$ acac	[Rh(acac)$(CO)_2$]	clfm	333	292		*J*(Rh,C) 73 (CO)	305
		clfm	298	288			295
$(CO)_2$ Cl_2	$[Rh(Cl)_2(CO)_2]^-$ NBu_4^+	DCM	200	73		*J*(Rh,C) 72	307
		clfm	243	−17			305
	[$Rh_2(\mu\text{-Cl})_2(CO)_4$]	clfm	333	151		*J*(Rh,C) 77	305
$(CO)_2$ Cl Br	$[Rh(Cl)(Br)(CO)_2]^-$ NBu_4^+	DCM	200	35		*J*(Rh,C) 71 (CO *trans* to Cl) 74 (CO *trans* to Br)	307

Table A1 *(Continued)*

Coordination Sphere[a]	Compound[b]	Solvent[c]	T (K)[d]	$\delta(^{103}Rh)$[e]	$J(Rh,P)$[f]	$J(Rh,X)$[g]	Reference(s)
$(CO)_2$ Cl I	$[Rh(Cl)(I)(CO)_2]^-$ NBu_4^+	DCM	200	−46		J(Rh,C) 68(CO *trans* to Cl) 76 (CO *trans* to I)	307
$(CO)_2$ Br_2	$[Rh(Br)_2(CO)_2]^-$ NBu_4^+	DCM	200	−4		J(Rh,C) 73	307
		clfm	243	47		J(Rh,C) 72	305
	$[Rh_2(\mu\text{-}Br)_2(CO)_4]$	DCM/ clfm	333	−1		J(Rh,C) 74	305
$(CO)_2$ Br I	$[Rh(Br)(I)(CO)_2]^-$ NBu_4^+	DCM	200	−103		J(Rh,C) 74 (CO *trans* to I) 71 (CO *trans* to Br)	307
$(CO)_2$ I_2	$[Rh(I)_2(CO)_2]^-$ NBu_4^+	DCM	200	−221		J(Rh,C) 72	307
CS P_2 Cl	$[Rh(Cl)\{PCy_2(CH_2CHOMe)\}_2(CS)]$	benz	295	380	116		262
CS_2 P_2 Cl	$[Rh(Cl)\{PCy_2(CH_2CH_2OMe)\}_2(\eta^2\text{-}CS_2)]$	benz	295	2,135	132		262
H P_4	$[Rh(H)(PMe_3)_4]$	benz	293	−735			266
	$[Rh(H)\{P(CH_2CH_2PPh_2)_3\}]$	DCM	293	−58	88 162	J(Rh,H) = 17.0	308
H P_3 N	$[Rh(H)\{N(CH_2CH_2PPh_2)_3\}]$	DCM	293	−266	175	J(Rh,H) = 24.2	308
P_4	$[Rh\{Me_2P(CH_2)_2PMe_2\}_2]^+$ ClO_4^-	DCM	298	−901	98		62
	$[Rh\{Et_2P(CH_2)_2PEt_2\}_2]^+$ ClO_4^-	DCM	298	−1,353	126		62
	$[Rh\{Et_2P(CH_2)_5PEt_2\}_2]^+$ ClO_4^-	DCM	298	−401	137		62
	$[Rh\{Et_2P(CH_2)_2PPh_2\}_2]^+$ ClO_4^-	DCM	298	−1,304	135 124		62
	$[Rh\{Ph_2P(CH_2)PPh_2\}_2]^+$ ClO_4^-	DCM	298	−354	116		62
	$[Rh\{Ph_2P(CH_2)_2PPh_2\}_2]^+$ ClO_4^-	DCM	298	−1,167	133		62, 286
	$[Rh\{Ph_2P(CH_2)_2PPh_2\}_2]^+$ BF_4^-	DCM	298	−1,155	133		62
	$[Rh\{Ph_2P(CH_2)_2PPh_2\}_2]^+$ OTf^-	DCM	298	−1,172	133		62
	$[Rh\{Ph_2P(CHCH)PPh_2\}_2]^+$ ClO_4^-	DCM	298	−641	135		62
	$[Rh\{(4\text{-}CF_3C_6H_4)_2P(CH_2)_2P(4\text{-}C_6H_4CF_3)_2\}_2]^+$ Cl^-	acet	298	−1,179	133		62
	$[Rh\{(4\text{-}CF_3C_6H_4)_2P(CH_2)_2P(4\text{-}C_6H_4CF_3)_2\}_2]^+$ PF_6^-	acet	298	−1,215	132		62

	$[Rh\{(C_6F_5)_2P(CH_2)_2P(C_6F_5)_2\}_2]^+$ Cl^-	DCM	298	163	208	62
	$[Rh\{(C_6F_5)_2P(CH_2)_2P(C_6F_5)_2\}_2]^+$ PF_6^-	DCM	298	−671	148	62
	$[Rh\{Ph_2P(CH_2)_2PPh_2\}_2]^+$ $[HB(3,5\text{-}Me_2\text{-}4\text{-}Clpz)_3]^-$	DCM	298	1,225	85	300
	$[Rh(1,1'\text{-}Ph_2\text{-}3,3',4,4'\text{-}Me_4\text{-}2,2'\text{-bisphosphole})_2]^+$ Cl^-	DCM	ns	−731[l]	113	309
P_3 N	$[Rh(N_3)(PPh_3)_3]$	clfm	300	−70	180	60
					146	
			247	−92		
	$[Rh(NCO)(PPh_3)_3]$	clfm	300	−168	173	60
					142	
			247	−192		
	$[Rh(NCS)(PPh_3)_3]$	clfm	300	−156	175	60
					141	
			247	−186		
	$[Rh\{N(CN)_2\}(PPh_3)_3]$	clfm	300	−214	177	60
					139	
			247	−255		
	$[Rh(NCBPh_3)(PPh_3)_3]$	clfm	300	−98	177	60
					139	
			247	−145		
P_2 N_2	*cis*-$[Rh(N_3)(PPh_3)_2(py)]$	tol	247	170	188	60
					170	
	cis-$[Rh(NCO)(PPh_3)_2(py)]$	tol	247	156	186	60
					164	
	cis-$[Rh(NCS)(PPh_3)_2(py)]$	tol	247	147	185	60
					162	
	cis-$[Rh\{N(CN)_2\}(PPh_3)_2(py)]$	tol	247	139	190	60
					160	
	cis-$[Rh(NCBPh_3)(PPh_3)_2(py)]$	tol	247	111	185	60
					160	
	$[Rh(NHPh)_2(PPh_3)_2]^-$ Li^+	THF	203?	225	175	310
	$[Rh\{N,N'\text{-}((S)\text{-}2\text{-}((1R)\text{-}1\text{-}PPh_2CHMe)Fc)_2NCHN\}]$	THF	rt	−42[j]	201	291
P_2 Tp*	$[Rh(Tp^*)(PPh_3)_2]$	DCM	300	329	176	311
	$[Rh(Tp^*)\{P(C_6H_4\text{-}4\text{-}F)_3\}_2]$	DCM	300	313	176	311
P_2 N Cl	*cis*-$[Rh(Cl)(PPh_3)_2(py)]$	tol	247	162	199	60
					164	
P_2 N Cl B	$[Rh\{PhB(C_6H_4\text{-}2\text{-}P^iPr_2)_2\}(Cl)(4\text{-MeNpy})]$	clfm	ns	−7,552[j]	144	312
					170	
P_2 N S	*cis*-$[Rh(S^iPr)(PPh_3)_2(py)]$	tol	248	−49	174	28
					166	

Table A1 *(Continued)*

Coordination Sphere[a]	Compound[b]	Solvent[c]	T (K)[d]	$\delta(^{103}Rh)$[e]	J(Rh,P)[f]	J(Rh,X)[g]	Reference(s)
	cis-[Rh(SCy)(PPh_3)$_2$(py)]	tol	248	−47	174 166		28
	cis-[Rh(SC_6F_5)(PPh_3)$_2$(py)]	tol	248	7	179 165		28
P_3 O	[Rh(O_2CCH_3)(PPh_3)$_3$]	tol	248	−26	177 151		28
	[Rh(O_2CCH_3)($PMePh_2$)$_3$]	tol	248	−138	172 147		28
	[Rh(O_2CCF_3)(PPh_3)$_3$]	tol	248	−38	183 147		28
	[Rh(O_2CPh)(PPh_3)$_3$]	tol	248	−20	175 152		28
P_2 $acac^F$	[Rh($acac^F$){$Ph_2P(CH_2)_2PPh_2$}]	THF	298	438	196		91, 95, 101
	[Rh($acac^F$){$Cy_2P(CH_2)_2PCy_2$}]	THF	298	368	196		95, 101
	[Rh($acac^F$){$^iPr_2P(CH_2)_2P^iPr_2$}]	THF	298	323	195		95, 101
	[Rh($acac^F$){$Me_2P(CH_2)_2PMe_2$}]	THF	298	370	192		95, 101
	[Rh($acac^F$){$Ph_2P(CH_2)_3PPh_2$}]	THF	298	567	183		91, 95, 101
	[Rh($acac^F$){$Ph_2P(CH_2)_4PPh_2$}]	THF	298	623	191		91
	[Rh($acac^F$){$Cy_2P(CH_2)_4PCy_2$}]	THF	298	845	193		95, 101
	[Rh($acac^F$){$^iPr_2PFcP^iPr_2$}]	THF	298	1,012	205		95, 101
	[Rh($acac^F$){$Ph_2P(CH_2)_6PPh_2$}]	THF	298	841	195		101
	[Rh($acac^F$){$Ph_2P(o\text{-}C_6H_4)PPh_2$}]	THF	298	450	195		101
	[Rh($acac^F$){$Ph_2PCH_2(o\text{-}C_6H_4)CH_2PPh_2$}]	THF	298	696	193		101
	[Rh($acac^F$){$Cy_2P(CH_2)(o\text{-}(C_6H_4)_2)(CH_2)PCy_2$}]	THF	298	932	197		101
	[Rh($acac^F$){$Ph_2PFcPPh_2$}]	THF	298	825	205		101
	[Rh($acac^F$){$4\text{-}MeO(C_6H_4)_2P(CH_2)_4P(4\text{-}MeOC_6H_4)_2$}]	THF	298	646	192		91
	[Rh($acac^F$){$4\text{-}Me(C_6H_4)_2P(CH_2)_4P(4\text{-}MeC_6H_4)_2$}]	THF	298	639	191		91
	[Rh($acac^F$){$4\text{-}F(C_6H_4)_2P(CH_2)_4P(4\text{-}FC_6H_4)_2$}]	THF	298	599	191		91
	[Rh($acac^F$){$4\text{-}Cl(C_6H_4)_2P(CH_2)_4P(4\text{-}ClC_6H_4)_2$}]	THF	298	589	191		91
	[Rh($acac^F$){$4\text{-}CF_3(C_6H_4)_2P(CH_2)_4P(4\text{-}CF_3C_6H_4)_2$}]	THF	298	570	190		91
P_2 O_2	[Rh($Cy_2PCH_2CH_2OMe)_2$]$^+$ BPh_4^-	DCM?	243?	65			313
P_2 O_2 S	[Rh($Cy_2PCH_2CH_2OMe)_2(SO_2)$]$^+$ BPh_4^-	DCM?	243?	1,950	174		313
P_2 O Cl S	[Rh(Cl)($Cy_2PCH_2CH_2OCH_3)_2(SO_2)$]	DCM	295	1,650	176 155		65

P_3 Cl	$[Rh(Cl)(PPh_3)_3]$	DCM	305	−81	189		303
					142		
		clfm	300	−19	192		60
					144		
		clfm	247	−18			60
		DCM	300	−82			60
		DCM	247	−106			60
		tol	300	−49			60
		tol	247	−49			60
		DMSO	300	−70			60
	$[Rh(Cl)(PPh_3)\{Ph_2P^a(CH_2)_2PPh_2benzophospholide^bPPh_3\}]^+ BPh_4^-$	DCM	298	32	(a) 205		289
					(b) 130		
P_2 Cl_2	$[Rh_2(\mu\text{-}Cl)_2\{Ph_2P^a(CH_2)_2PPh_2benzophospholide^bPPh_3\}_2]^{2+}$ $2BPh_4^-$	DCM	298	46	(a) 233		289
					(b) 172		
P_2 Cl_2 B	$[Rh_2(\mu\text{-}Cl)_2\{PhB(C_6H_4\text{-}2\text{-}P^iPr_2)_2\}]$	DCM	213	−7,365[j]	167		312
					163		
P_2 Cl S	$[Rh(Cl)(Cy_2PCH_2CH_2OCH_3)_2(SO_2)]$	DCM	295	955	109		65
	$[Rh_2(Cl)_2(\mu\text{-}SO_2)\{\mu\text{-}Ph_2P(CH_2)PPh_2\}_2]$	DCM	rt	949	119	*J*(Rh,Rh) 9.1	187
P_3 Br	$[Rh(Br)(PPh_3)_3]$	DCM	280	−142	192		303
					141		
P_3 I	$[Rh(I)(PPh_3)_3]$	DCM	260	−267	194		303
					139		
P_3 S	$[Rh(S^nPr)(PPh_3)_3]$	tol	248	−59	162		28
					159		
	$[Rh(S^iPr)(PPh_3)_3]$	tol	248	33	162		28
					159		
	$[Rh(SCy)(PPh_3)_3]$	tol	248	39	162		28
					156		
	$[Rh(SCH_2Ph)(PPh_3)_3]$	tol	248	−25	170		28
					158		
	$[Rh(SPh)(PPh_3)_3]$	tol	248	−164	169		28
					150		
	$[Rh(SCPh_3)(PPh_3)_3]$	tol	248	−338	165		28
					151		
	$[Rh(SC_6F_5)(PPh_3)_3]$	tol	248	17	170		28
					148		
	$[Rh(SC_6F_5)(PMePh_2)_3]$	tol	248	−414	168		28
					142		

Table A1 *(Continued)*

Coordination Sphere[a]	Compound[b]	Solvent[c]	T (K)[d]	$\delta(^{103}Rh)$[e]	$J(Rh,P)$[f]	$J(Rh,X)$[g]	Reference(s)
$P_2 S_2$	$[Rh_2(\mu\text{-}S^nPr)_2(PPh_3)_4]$	tol	248	−72	172		28
	$[Rh_2(\mu\text{-}S^iPr)_2(PPh_3)_4]$	tol	248	−41	167		28
	$[Rh_2(\mu\text{-}SCy)_2(PPh_3)_4]$	tol	248	−38	166		28
	$[Rh_2(\mu\text{-}SCH_2Ph)_2(PPh_3)_4]$	tol	248	−338	175		28
	$[Rh_2(\mu\text{-}SPh)_2(PPh_3)_4]$	tol	248	36	169		28
	$[Rh(PPh_3)_2(\mu\text{-}SC_6F_5)_2Rh(H)(SC_6F_5)(PPh_3)(pz^*)]$	DCM	248	239	177		314
	(Rh(III) δ 2,117)				169		
P_3 Si	$[Rh(SiMe_2Ph)(PMe_3)_3]$	benz	293	−802	146		266
	$[Rh(SiPh_3)(PMe_3)_3]$	benz	293	−735			266
P_3 As	$[Rh(Ph_2P(CH_2)_2PPh_2)(Ph_2P(CH)_2AsPh_2)_2]^+ ClO_4^-$	DCM	298	−1,187	156		62, 286
					130		
					129		
P_2 As_2	*cis*-$[Rh(Ph_2P(CH_2)_2AsPh_2)_2]^+ ClO_4^-$	DCM	298	−1,224	151		62, 286
	trans-$[Rh(Ph_2P(CH_2)_2AsPh_2)_2]^+ ClO_4^-$	DCM	298	−1,199	124		62, 286

[a]Listing of organic ligands alphabetical except for Cp, indenyl, diene, CN, CO and a few uncommon ligands, followed by H,P,N,O, halogen and others in order of increasing atomic weight of donor atom.
[b]Some complexes not included in the table can be found in ref. 315 (diene, Schiff base), 316 (acac), 317, 318 (diene, phosphine).
[c]For details see Abbreviations. A question mark (?) indicates that the solvent was not clearly specified but may be as shown.
[d]Temperature may be given as rt (room temperature) or ns (not specified). A question mark (?) indicates that the temperature was not clearly specified but may be as shown.
[e]$\delta(^{103}Rh)$ is given relative to Ξ (^{103}Rh) = 3.16 MHz unless otherwise indicated, i.e., where insufficient information has been given to permit accurate conversion of the reported shift to this scale.
[f]$^1J(Rh,P)$, absolute magnitude in Hz. Signs all probably negative (see Section 14).
[g]$J(Rh,X)$ (X = ^1H, ^{13}C, ^{19}F, etc.), absolute magnitude in Hz. See Section 14 for probable signs.
[h]Sample under high pressure.
[i]Calibrated relative to $[RhCl_6]_3^-$.
[j]Calibration method not specified or not clear.
[k]Calibrated relative to $[Rh(acac)(CO)_2]$.
[l]Calibrated relative to Rh metal.

Table A2 Data for Rh(III) complexes

Coordination sphere[a]	Compound[b]		Solvent[c]	T (K)[d]	$\delta(^{103}Rh)$[e]	J(Rh,H)[f]	J(Rh,P)[g]	J(Rh,X)[h]	Reference(s)
Acetylene P_2 Cl	$[Rh(Cl)\{PCy_2(CH_2CH_2OMe)\}_2(\eta^2\text{-}C_2Ph)]$		benz	295	1,120		109	J(Rh,C) 16.1	262
Acetylide CNR P_2 O_2	$[Rh(C_2Ph)(O_2)(xylylNC)(PPh_3)_2]$		tol	300	1,010		92	J(Rh,C) 47.4 ^2J(Rh,C) 8.2	252
Acetylide H P Tp*	$[Rh(Tp^*)(H)(C_2Ph)(PPh_3)]$		DCM	300	1,423	16.8	131		311
	$[Rh(Tp^*)(H)(C_2Ph)\{P(C_6H_4\text{-}4\text{-}F)_3\}]$		DCM	300	1,417	16.8	132		311
Acetylide P N_4	$[Rh(Hdmg)_2(C_2Ph)(PPh_3)]$		clfm	298	2,265		80	J(Rh,C) 47.4	190
Acetylide P N_5	$[Rh(Hdmg)_2(C_2Ph)(py)]$		clfm	298	2,823				190
Acetylide N_4 S	$[Rh(Hdmg)_2(C_2Ph)(SMe_2)]$		clfm	298	2,465				190
Acyl Cp* P I	$[Rh(Cp^*)(I)(COMe)(PPh_3)]$		clfm	300	849				93
	$[Rh(Cp^*)(I)(COC_6H_4\text{-}4\text{-}Me)(PPh_3)]$		clfm	300	813				93
	$[Rh(Cp^*)(I)(COC_6H_5)(PPh_3)]$		clfm	300	804				93
	$[Rh(Cp^*)(I)(COC_6H_4\text{-}4\text{-}Cl)(PPh_3)]$		clfm	300	784				93
	$[Rh(Cp^*)(I)(COC_6H_4\text{-}4\text{-}CHO)(PPh_3)]$		clfm	300	765				93
	$[Rh(Cp^*)(I)(COC_6H_4\text{-}4\text{-}CN)(PPh_3)]$		clfm	300	748				93
	$[Rh(Cp^*)(I)(COC_6H_4\text{-}4\text{-}NO_2)(PPh_3)]$		clfm	300	742				93
Acyl H P Tp*	$[Rh(Tp^*)(H)(COC_6H_4\text{-}4\text{-}NO_2)(PPh_3)]$		DCM	300	1,730	18.9	163		311
	$[Rh(Tp^*)(H)(COC_6H_4\text{-}4\text{-}NO_2)\{P(C_6H_4\text{-}4\text{-}F)_3\}]$		DCM	300	1,727	19.3	165		311
Acyl P Tp* I	$[Rh(Tp^*)(I)(COMe)(PMe_3)]$		DCM	233	2,945		131	J(Rh,C) 23.8	319
Alkene Cp $(H)_2$	$[Rh(Cp)(H)_2(CH_2CHSiMe_3)]$		tol	203	−1,401	25.3			113
Alkene Cp H Si	$[Rh(Cp)(H)(SiEt_3)(C_2H_4)]$		benz	rt	−1,492	33		J(Rh,Si) 22.2	320
	$[Rh(Cp)(H)(SiEt_3)(CH_2CHCO_2^tBu)]$	(a)	tol	223	−1,362	32		J(Rh,Si) 22	321
	(Isomers)	(b)	tol	223	−1,363	35		J(Rh,Si) 20	
	$[Rh(Cp)(H)(SiMe_3)(CH_2CHCO_2^tBu)]$	(a)	tol	223	−1,348	32		J(Rh,Si) 21	321
		(b)	tol	223	−1,335	36		J(Rh,Si) 21	
	$[Rh(Cp)(H)(SiEt_2H)(CH_2CHCO_2^tBu)]$	(a)	tol	223	−1,425	31		J(Rh,Si) 18	321
		(b)	tol	223	−1,405	34		J(Rh,Si) 19	
	$[Rh(Cp)(H)\{Si(OMe)_3\}(CH_2CHCO_2^tBu)]$	(a)	tol	223	−1,470	32		J(Rh,Si) 39	321
		(b)	tol	223	−1,466	35		J(Rh,Si) 36	
	$[Rh(Cp)(H)(SiMe_2Cl)(CH_2CHCO_2^tBu)]$	(a)	tol	223	−1,362	30		J(Rh,Si) 30	321
		(b)	tol	223	−1,368	30		J(Rh,Si) 30	
Alkene Cp* H Si	$[Rh(Cp^*)(H)(SiMe_3)(C_2H_4)]$		ns	ns	−1,346	37			322
	$[Rh(Cp^*)(H)(SiEt_3)(C_2H_4)]$		CyH	ns	−1,375	35		J(Rh,Si) 17	322, 323
	$[Rh(Cp^*)(H)(SiPh_3)(C_2H_4)]$		ns	ns	−1,403	32			322
	$[Rh(Cp^*)(H)\{Si(OEt)_3\}(C_2H_4)]$		ns	ns	−1,451	36		J(Rh,Si) 45	322

Table A2 *(Continued)*

Coordination sphere[a]	Compound[b]		Solvent[c]	T (K)[d]	$\delta(^{103}Rh)$[e]	J(Rh,H)[f]	J(Rh,P)[g]	J(Rh,X)[h]	Reference(s)
Alkene Cp^R $(H)_2$	$[Rh^1(\mu\text{-}H)_2(C_2H_4)\{C_5H_4CH_2(C_5H_4)Rh^2(SiMe_3)_2\}]$		tol	213	(1) −1,052	25.7			255
					(2) −1,608	17.4		J(Rh,Si) 23.7	
Alkene Cp^R H Si	$[Rh^1(H)(SiMe_3)(C_2H_4)\{C_5H_4CH_2(C_5H_4)Rh^2(C_2H_4)_2\}]$		benz	296	(1) −1,450	34.1		J(Rh,Si) 23.3	255
	{(2) (Rh(I)) δ-929}								
	$[Rh^1(H)(SiEt_3)(C_2H_4)\{C_5H_4CH_2(C_5H_4)Rh^2(C_2H_4)_2\}]$		benz	296	(1) −1,483	33.5		J(Rh,Si) 23.3	255
	{(2) (Rh(I)) δ-929}								
	$[Rh^1(H)(SiMe_3)(C_2H_4)\{C_5H_4CH_2(C_5H_4)Rh^2(H)_2(SiMe_3)_2\}]$		benz	296	(1) −1,450	34.1		J(Rh,Si) 23.3	255
	{(2) (Rh(V)) δ −1,731}								
	$[Rh^1(H)(SiEt_3)(C_2H_4)\{C_5H_4CH_2(C_5H_4)Rh^2(H)_2(SiEt_3)_2\}]$		benz	296	(1) −1,477	33.5		J(Rh,Si) 23.3	255
	{(2) (Rh(V)) δ −1,872}								
Alkene^E Cp* B S	$[Rh(Cp^*)\{CH_2CHS(C_2B_{10}H_{10}S)\}]$		DCM	297	−233			J(Rh,C) 4.4 (Cp*) 8.6 ($Rh\text{-}CH_2$) 13.5 (Rh-CH)	324
	$[Rh(Cp^*)\{CH_2C(Me)S(C_2B_{10}H_{10}S)\}]$	(a)	DCM	297	−243			J(Rh,C) 3.4 (Cp*) 9.4 ($Rh\text{-}CH_2$) 8.9 (Rh,C)	324
	(Isomers)	(b)	DCM	297	77			J(Rh,C) 8,5 (Cp*)	
	$[Rh(Cp^*)\{CH_2C(CH_2OMe)S(C_2B_{10}H_{10}S)\}]$	(a)	DCM	297	−361			J(Rh,C) 3.3 (Cp*) 9.2 ($Rh\text{-}CH_2$) 9.7 (Rh,C)	324
	(Isomers)	(b)	DCM	297	−176			J(Rh,C) 4.1 (Cp*) 8.6 ($Rh\text{-}CH_2$) 14.7 (Rh,C)	
	$[Rh(Cp^*)\{CH_2C(Ph)S(C_2B_{10}H_{10}S)\}]$		DCM	295?	−174			J(Rh,C) 3.5 (Cp*) 9.1 (Rh-C) 9.7 ($Rh\text{-}CH_2$)	325
Alkene^E Cp* B Se	$[Rh(Cp^*)\{CH_2C(CO_2Me)Se(C_2B_{10}H_{10}Se)\}]$	(a)	clfm	293?	−377			J(Rh,Se) 42	326
	(Isomers)	(b)	clfm	293?	−205			J(Rh,Se) 59	

Alkyl aryl Cp* CO	[Rh(Cp*)(Me)(C_6H_4-4-Me)(CO)]	clfm	300	−584				93
	[Rh(Cp*)(Me)(Ph)(CO)]	clfm	300	−578				93
	[Rh(Cp*)(Me)(C_6H_4-4-Cl)(CO)]	clfm	300	−582				93
	[Rh(Cp*)(Me)(C_6H_4-4-CHO)(CO)]	clfm	300	−566				93
	[Rh(Cp*)(Me)(C_6H_4-4-CN)(CO)]	clfm	300	−567				93
	[Rh(Cp*)(Me)(C_6H_4-4-NO_2)(CO)]	clfm	300	−565				93
Alkyl aryl N_2 Cl	[Rh{C_6H_3-2,6-(CH_2NMe_2)$_2$}(Me)(Cl)]	benz	295	3,165				327
	[Rh{C_6H_3-2,6-(CH_2NMe_2)$_2$}(Et)(Cl)]	benz	295	3,163				327
Alkyl aryl N_2 I	[Rh{C_6H_3-2,6-(CH_2NMe_2)$_2$}(Me)(I)]	benz	295	3,179			*J*(Rh,C) 37 (Me)	327
	[Rh{C_6H_3-2,6-(CH_2NMe_2)$_2$}(Et)(I)]	benz	295	3,201				327
Alkyl$_2$ Cp* CO	[Rh(Cp*)($Me)_2$(CO)]	clfm	300	−829				93
Alkyl Cp* CO I	[Rh(Cp*)(Me)(I)(CO)]	clfm	300	−366				93
Alkyl$_2$ Cp* P	[Rh(Cp*)($Me)_2$(PMe_3)]	clfm	300	1,196		170		100
Alkyl Cp* P Cl	[Rh(Cp*)(Me)(Cl)(PMe_3)]	clfm	300	561		159		100
	[Rh(Cp*)(Me)(Cl)(PPh_3)]	clfm	300	678		167		100
Alkyl Cp* P Br	[Rh(Cp*)(Me)(Br)(PMe_3)]	clfm	300	406		158		100
	[Rh(Cp*)(Me)(Br)(PPh_3)]	clfm	300	510		165		100
Alkyl Cp* P I	[Rh(Cp*)(Me)(I)(PMe_3)]	clfm	300	82		157		100
	[Rh(Cp*)(Me)(I)(PPh_3)]	clfm	300	164		165		100
Alkyl Cp^R Si_2 Rh	[Rh^1(Me)(μ-$SiMe_2$)$_2${$C_5H_4CH_2(C_5H_4)Rh^2$(H)}]	benz	296	(1) −1,424			*J*(Rh,Si) 34.9, 46.0	255
(Cp* H Si_2 Rh)				(2) −2,008	40.8		*J*(Rh,Rh) 15	
	[Rh^1(Et)(μ-$SiMe_2$)$_2${$C_5H_4CH_2(C_5H_4)Rh^2$(H)}]	benz	296	(1) −1,342			*J*(Rh,Si) 29.7, 37.6	255
				(2) −2,019	40		*J*(Rh,Rh) 15	
Alkyl Cp^R Si_2 Rh	[Rh^1(Me)(μ-$SiMe_2$)$_2${$C_5H_4CH_2(C_5H_4)Rh^2$($SiMe_3$)}]	benz	296	(1) −1,350			*J*(Rh,Si) 35.6, 46.2	255
(Cp^R Si_2 Rh)				(2) −1,957			*J*(Rh,Si) 40.5 *J*(Rh,Rh) 15	
Alkyl CO P_2 Cl_2	[Rh(Me)($Cl)_2$(PMe_2Ph)$_2$(CO)]	benz	297	499	2.0	84		181
Alkyl CO P_2 Cl I	[Rh(Me)(Cl)(I)(PMe_2Ph)$_2$(CO)]	benz	297	194	2.0	85		181
Alkyl CO P_2 Br_2	[Rh(Me)($Br)_2$(PMe_2Ph)$_2$(CO)]	benz	297	351	2.0	84		181
Alkyl CO P_2 Br I	[Rh(Me)(Br)(I)(PMe_2Ph)$_2$(CO)]	benz	297	267	2.0	85±5		181

Table A2 *(Continued)*

Coordination sphere[a]	Compound[b]	Solvent[c]	T (K)[d]	$\delta(^{103}Rh)$[e]	J(Rh,H)[f]	J(Rh,P)[g]	J(Rh,X)[h]	Reference(s)
Alkyl CO P_2 I_2	$[Rh(Me)(I)_2(PMe_2Ph)_2(CO)]$	benz	297	53 ± 6	2.0	82		181
Alkyl CO P Tp*	$[Rh(Tp^*)(Me)(CO)(PMe_3)]^+ I^-$	DCM	233	1,111		98	J(Rh,C) 17.4 (Me) 61.3 (CO)	319
	$[Rh(Tp^*)(Me)(CO)(PMe_2Ph)]^+ I^-$	DCM	233	1,169		100	J(Rh,C) 17.3 (Me) 60.9 (CO)	319
Alkyl P N_4	$[Rh(Hdmg)_2(Me)(PPh_3)]$	clfm	298	2,038		66	J(Rh,C) 20	104
	$[Rh(Hdmg)_2(Et)(PPh_3)]$	clfm	298	2,033		62	J(Rh,C) 20	104
	$[Rh(Hdmg)_2(^n Pr)(PPh_3)]$	clfm	298	2,057		61	J(Rh,C) 20.5	104
	$[Rh(Hdmg)_2(^i Pr)(PPh_3)]$	clfm	298	2,110		56	J(Rh,C) 20	104
	$[Rh(Hdmg)_2(^n Bu)(PPh_3)]$	clfm	298	2,048		61	J(Rh,C) 20	104
	$[Rh(Hdmg)_2(^i Bu)(PPh_3)]$	clfm	298	2,086		61	J(Rh,C) 20	104
	$[Rh(Hdmg)_2(^t Bu)(PPh_3)]$	clfm	298	2,196		49	J(Rh,C) 22	104
	$[Rh(Hdmg)_2(^{neo}Pent)(PPh_3)]$	clfm	298	2,199		57	J(Rh,C) 22	104
	$[Rh(Hdmg)_2(Adam)(PPh_3)]$	clfm	298	2,212		48		104
	$[Rh(Hdmg)_2(Cy)(PPh_3)]$	clfm	298	2,132		55	J(Rh,C) 21.0	190
	$[Rh(Hdmg)_2(CH_2Ph)(PPh_3)]$	clfm	298	2,066		70	J(Rh,C) 18.3	190
	$[Rh(Hdmg)_2(Me)(PMe_3)]$	clfm	298	1,927		78	J(Rh,C) 18.3	190
	$[Rh(Hdmg)_2(Me)\{P(OPh)_3\}]$	clfm	298	1,928		117	J(Rh,C) 18.3	190
	$[Rh(Hdmg)_2(Et)(PMe_3)]$	clfm	298	1,920		76	J(Rh,C) 18.2	190
	$[Rh(Hdmg)_2(Et)\{P(OPh)_3\}]$	clfm	298	1,926		110	J(Rh,C) 18.3	190
	$[Rh(Hdmg)_2(^n Pr)(PMe_3)]$	clfm	298	1,933		75	J(Rh,C) 18.3	190
	$[Rh(Hdmg)_2(^i Pr)(PMe_3)]$	clfm	298	1,969		73	J(Rh,C) 18.5	190
	$[Rh(Hdmg)_2(^t Bu)(PMe_3)]$	clfm	298	2,022		68	J(Rh,C) 20.0	190
	$[Rh(Hdmg)_2(^i Bu)\{P(OPh)_3\}]$	clfm	298	1,968		110	J(Rh,C) 18.6	190
Alkyl P_2 N_2 Cl	[Rh(Me)(Cl){*N*,*N*′-((*S*)-2-((1*R*)-1-$PPh_2CHMe)Fc)_2NCHN$}]	benz	rt	1,600[i]		131 134	J(Rh,C) 22.3 (Me)	291
Alkyl N_5	$[Rh(Hdmg)_2(Me)(py)]$	clfm	298	2,509			J(Rh,C) 23	104
	$[Rh(Hdmg)_2(Et)(py)]$	clfm	298	2,500			J(Rh,C) 24	104
	$[Rh(Hdmg)_2(^n Pr)(py)]$	clfm	298	2,516			J(Rh,C) 23	104
	$[Rh(Hdmg)_2(^i Pr)(py)]$	clfm	298	2,564			J(Rh,C) 23	104

	[Rh(Hdmg)$_2$(^{n}Bu)(py)]	clfm	298	2,512				J(Rh,C) 24	104
	[Rh(Hdmg)$_2$(^{i}Bu)(py)]	clfm	298	2,552				J(Rh,C) 24	104
	[Rh(Hdmg)$_2$(^{t}Bu)(py)]	clfm	298	2,669				J(Rh,C) 26	104
	[Rh(Hdmg)$_2$(^{neo}Pent)(py)]	clfm	298	2,653				J(Rh,C) 26	104
	[Rh(Hdmg)$_2$(Adam)(py)]	clfm	298	2,680				J(Rh,C) 26	104
Alkyl N_4 O	[Rh(Hdmg)$_2$(Me)(H_2O)]	D_2O	298	2,672				J(Rh,C) 26	104
	[Rh(Hdmg)$_2$(Et)(H_2O)]	D_2O	298	2,656				J(Rh,C) 26	104
	[Rh(Hdmg)$_2$(^{n}Pr)(H_2O)]	D_2O	298	2,665				J(Rh,C) 24	104
	[Rh(Hdmg)$_2$(^{i}Pr)(H_2O)]	D_2O	298	2,714				J(Rh,C) 26	104
	[Rh(Hdmg)$_2$(^{n}Bu)(H_2O)]	D_2O	298	2,681				J(Rh,C) 24	104
	[Rh(Hdmg)$_2$(^{i}Bu)(H_2O)]	D_2O	298	2,712				J(Rh,C) 26	104
	[Rh(Hdmg)$_2$(^{neo}Pent)(H_2O)]	D_2O	298	2,818				J(Rh,C) 28	104
Alkyl N_3 Cl_2	[Rh(Cl_2)(CH_2Ph){py-2,6-(CHN^{i}Pr)$_2$}]	DCM	rt	3,649					328
Alkyl N_3 Br_2	[Rh(Br_2)(Me){4-(4′-^{t}BuC_6H_4)terpy}]	DCM	rt	3,366				J(Rh,C) 21	328
	[Rh(Br_2)(Et){4-(4′-^{t}BuC_6H_4)terpy}]	DCM	rt	3,365				J(Rh,C) 21	328
	[Rh(Br_2)(^{n}Bu){4-(4′-^{t}BuC_6H_4)terpy}]	DCM	rt	3,380				J(Rh,C) 21	328
	[Rh(Br_2)(decyl){4-(4′-^{t}BuC_6H_4)terpy}]	DCM	rt	3,375				J(Rh,C) 21	328
	[Rh(Br_2)(2-propenyl){4-(4′-^{t}BuC_6H_4)terpy}]	DCM	rt	3,533				J(Rh,C) 19.5	328
	[Rh(Br_2)(2-Me-2-propenyl){4-(4′-^{t}BuC_6H_4)terpy}]	DCM	rt	3,345				J(Rh,C) 20	328
	[Rh(Br_2)(3-butenyl){4-(4′-^{t}BuC_6H_4)terpy}]	DCM	rt	3,396				J(Rh,C) 23	328
Alkyl N_4 S	[Rh(Hdmg)(Me)(SMe_2)]	clfm	298	2,214					190
Alkyl^E Cp* S_2	[Rh(Cp*){C(Ph)$CH_2B_{10}H_{10}C_2S_2$}]	DCM	295?	329				J(Rh,C) 6.2 (Cp*) 21.8 (Rh-C)	325
Alkyl^E Cp* Se_2	[Rh(Cp*){C(CO_2Me)$CH_2B_{10}H_{10}C_2Se_2$}]	clfm	295?	1,505				J(Rh,C) 24.5 J(Rh,Se) 11.4 44.5	326
Alkyl^E P N_4	[Rh(Hdmg)$_2$(CH_2Cl)(PPh_3)]	clfm	298	2,082		68		J(Rh,C) 25.8	190
	[Rh(Hdmg)$_2$(CH_2Cl)(PMe_3)]	clfm	298	1,948		78		J(Rh,C) 24.4	190
	[Rh(Hdmg)$_2$(CH_2Br)(PPh_3)]	clfm	298	2,075		71		J(Rh,C) 27.1	190
	[Rh(Hdmg)$_2$(CH_2OMe)(PPh_3)]	clfm	298	2,067		60		J(Rh,C) 21.2	190
	[Rh(Hdmg)(CH_2SiMe_3)(PPh_3)]	clfm	298	2,169		66		J(Rh,C) 21.2	190
Alkyl^E P_2 N_2	[Rh_4(μ-Cl)$_2${μ-ArNPCH(*o*-C_6H_4)CH(*o*-C_6H_4)CH}$_4$(MeCN)$_6$]$^{2+}$	acnl	ns	2,860	153				329
(Alkyl^E P_2 N_2 Cl_2)	2PF_6^- (Ar = 3,5-(CF_3)$_2$$C_6H_4$)				80				
				3,308	83				
					53				

Table A2 *(Continued)*

Coordination sphere[a]	Compound[b]		Solvent[c]	T (K)[d]	$\delta(^{103}Rh)$[e]	J(Rh,H)[f]	J(Rh,P)[g]	J(Rh,X)[h]	Reference(s)
Alkyl^{E} N_5	[Rh(Hdmg)$_2$(CH_2Cl)(py)]		clfm	298	2,621				104
Alkyl^{E} N_3 Cl_2	[Rh(Cl)$_2$(CH_2Cl){py-2,6-(CHN^{i}Pr)$_2$}]		DCM	rt	3,570				328
	[Rh(Cl)$_2$(CH_2Cl){py-2,6-(CHNCy)$_2$}]		DCM	rt	3,569				328
	[Rh(Cl)$_2$(CH_2Cl){py-2,6-(CHN^{t}Bu)$_2$}]		DCM	rt	4,121				328
	[Rh(Cl)$_2$(CH_2Cl){py-2,6-(CHN-*p*-Anisyl)$_2$}]		DCM	rt	3,654				328
	[Rh(Cl)$_2$(CH_2Cl){py-2,6-(C(CH_3)N-*p*-Anisyl)$_2$}]		DCM	rt	3,561				328
Alkyl^{F} CO P_2 Cl I	[Rh(CF_3)(Cl)(I)(PMe_2Ph)$_2$(CO)]		benz	297	706		83	J(Rh,F) 14	181
Alkyl^{F} CO P_2 Br I	[Rh(CF_3)(Br)(I)(PMe_2Ph)$_2$(CO)]		benz	297	625		85	J(Rh,F) 14	181
Alkyl^{F} CO P_2 I_2	[Rh(CF_3)(I)$_2$(PMe_2Ph)$_2$(CO)]		benz	297	453		85	J(Rh,F) 14	181
Alkyl^{F} N_5	[Rh(Hdmg)$_2$(CH_2CF_3)(py)]		clfm	298	2,741				104
$Allyl_3$	[Rh(η^3-allyl)$_3$]		tol	250	−363				297
				270	−355				
Allyl Cp	[Rh(Cp)(η^3-$CH_2CMeCMe_2$)]$^+$ BF_4^-		DCM	196	−597				277
Allyl Cp CO	[Rh(Cp)(η^3-$CH_2CMeCMe_2$)(CO)]$^+$ BF_4^-		nitr	296	−943				277
Allyl Cp Cl	[Rh(Cp)(η^3-$CH_2CMeCMe_2$)(Cl)]		clfm	296	687				277
Allyl Cp*	[Rh(Cp*)(η^3-$CH_2CMeCMe_2$)]$^+$ BF_4^-		DCM	203	−427				277
				296	−344				
Allyl Cp* CO	[Rh(Cp*)(η^3-$CH_2CMeCMe_2$)(CO)]$^+$ BF_4^-		DCM	296	−837				277
$Allyl_2$ acac	[Rh(acac)(η^3-allyl)$_2$]		DCM	250	1,432				297
				270	1,441				
Aryl Cp* CO I	[Rh(Cp*)(I)(C_6H_4-4-Me)(CO)]		clfm	300	−106				93
	[Rh(Cp*)(I)(Ph)(CO)]		clfm	300	−102				93
	[Rh(Cp*)(I)(C_6H_4-*p*-Cl)(CO)]		clfm	300	−122				93
	[Rh(Cp*)(I)(C_6H_4-*p*-CHO)(CO)]		clfm	300	−121				93
	[Rh(Cp*)(I)(C_6H_4-*p*-CN)(CO)]		clfm	300	−127				93
	[Rh(Cp*)(I)(C_6H_4-*p*-NO_2)(CO)]		clfm	300	−134				93
Aryl Cp* P Cl	[Rh(Cp*)(Ph)(Cl)(PMe_3)]		clfm	300	778		154		100
	[Rh(Cp*)(Ph)(Cl)(PMe_2Ph)]		clfm	300	835		155		100
	[Rh(Cp*)(Ph)(Cl)($PMePh_2$)]		clfm	300	852		157		100
	[Rh(Cp*)(Ph)(Cl)(PPh_3)]		clfm	300	984		160		100
Aryl Cp* P Br	[Rh(Cp*)(Ph)(Br)(PMe_3)]		clfm	300	644		154		100
	[Rh(Cp*)(2-MeC_6H_4)(Br)(PMe_3)]	(a)	clfm	300	824		155		100
	(Rotamers)	(b)	clfm	300	827		157		

	[Rh(Cp*)(3-MeC$_6$H$_4$)(Br)(PMe$_3$)]		clfm	300	650		155		100
	[Rh(Cp*)(4-MeC$_6$H$_4$)(Br)(PMe$_3$)]		clfm	300	643		156		100
	[Rh(Cp*)(3,4-Me$_2$C$_6$H$_3$)(Br)(PMe$_3$)]		clfm	300	646		156		100
	[Rh(Cp*)(2,5-Me$_2$C$_6$H$_3$)(Br)(PMe$_3$)]	(a)	clfm	300	822		155		100
	(Rotamers)	(b)	clfm	300	827		158		
	[Rh(Cp*)(4-CF$_3$C$_6$H$_4$)(Br)(PMe$_3$)]		clfm	300	618		152		100
	[Rh(Cp*)(4-FC$_6$H$_4$)(Br)(PMe$_3$)]		clfm	300	638		152		100
	[Rh(Cp*)(4-MeOC$_6$H$_4$)(Br)(PMe$_3$)]		clfm	300	642		154		100
	[Rh(Cp*)(Ph)(Br)(PMe$_2$Ph)]		clfm	300	707		154		100
	[Rh(Cp*)(Ph)(Br)(PMePh$_2$)]		clfm	300	719		156		100
	[Rh(Cp*)(Ph)(Br)(PPh$_3$)]		clfm	300	831		159		100
	[Rh(Cp*)(3-MeC$_6$H$_4$)(Br)(PPh$_3$)]		clfm	300	837		160		100
	[Rh(Cp*)(4-MeC$_6$H$_4$)(Br)(PPh$_3$)]		clfm	300	834		162		100
	[Rh(Cp*)(3,4-MeC$_6$H$_3$)(Br)(PPh$_3$)]		clfm	300	838		163		100
	[Rh(Cp*)(4-FC$_6$H$_4$)(Br)(PPh$_3$)]		clfm	300	848		159		100
	[Rh(Cp*)(4-MeOC$_6$H$_3$)(Br)(PPh$_3$)]		clfm	300	830		159		100
Aryl Cp* P I	[Rh(Cp*)(Ph)(I)(PMe$_3$)]		clfm	300	376		155		100
	[Rh(Cp*)(Ph)(I)(PMe$_2$Ph)]		clfm	300	427		153		100
	[Rh(Cp*)(Ph)(I)(PMePh$_2$)]		clfm	300	437		155		100
	[Rh(Cp*)(Ph)(I)(PPh$_3$)]		clfm	300	547		161		100
Aryl H P Tp*	[Rh(Tp*)(Ph)(H){P(OMe)$_3$}]		benz	295	1,270	23.2	235		293
Aryl P N_4	[Rh(Hdmg)$_2$(Ph)(PPh$_3$)]		clfm	298	2,264		61	*J*(Rh,C) 28	190
	[Rh(Hdmg)$_2$(Ph)(PMe$_3$)]		clfm	298	2,109		74	*J*(Rh,C) 26	190
Aryl N_2 Cl_2	[Rh{C$_6$H$_3$-2,6-(CHNMe)$_2$}(Cl)$_2$]		meth	298	3,888				330
	[Rh{C$_6$H$_3$-2,6-(CHN^{i}Pr)$_2$}(Cl)$_2$]		meth	298	4,185				330
	[Rh{C$_6$H$_3$-2,6-(CHN^{t}Bu)$_2$}(Cl)$_2$]		meth	298	4,587				330
Aryl N_2 Cl Br	[Rh{C$_6$H$_3$-2,6-(CHNMe)$_2$}(Cl)(Br)]		meth	298	3,733				330
	[Rh{C$_6$H$_3$-2,6-(CHN^{i}Pr)$_2$}(Cl)(Br)]		meth	298	4,027				330
	[Rh{C$_6$H$_3$-2,6-(CHN^{t}Bu)$_2$}(Cl)(Br)]		meth	298	4,374				330
Aryl N_2 Cl I	[Rh{C$_6$H$_3$-2,6-(CHN^{i}Pr)$_2$}(Cl)(I)]		meth	298	3,674				330
Aryl N_2 Br_2	[Rh{C$_6$H$_3$-2,6-(CHNMe)$_2$}(Br)$_2$]		meth	298	3,569				330
	[Rh{C$_6$H$_3$-2,6-(CHN^{i}Pr)$_2$}(Br)$_2$]		meth	298	3,862				330
	[Rh{C$_6$H$_3$-2,6-(CHN^{t}Bu)$_2$}(Br)$_2$]		meth	298	4,107				330
Aryl N_2 I_2	[Rh{C$_6$H$_3$-2,6-(CHN^{i}Pr)$_2$}(I)$_2$]		meth	298	3,176				330
Aryl N_4 Br	[Rh(Br)(C$_6$H$_4$-2-CHN^{i}Pr){4-(4′-^{t}BuC$_6$H$_4$)terpy}]		DCM	rt	3,221				328
Aryl N_3 Br_2	[Rh(Br)$_2$(Ph){4-(4′-^{t}BuC$_6$H$_4$)terpy}]		DCM	rt	3,548				328
Carbene$_2$ Cp* S Rh	[Rh$_2$(Cp*)$_2$(μ-CH$_2$)$_2$S$_2$]$^{2+}$ Cl^-, OH^-		DCM	296	1,345[j]			*J*(Rh,C) 26	331
CNR iminyl H P_2 N	[Rh(H){C(4-C$_6$H$_4$NO$_2$)*N*-2-py-3-Me}(CNCy)(PPh$_3$)$_2$]$^+$ BF_4^-		clfm	ns	199	14.7	103		332
CNR P_2 O_2 S	[Rh(SC$_6$F$_5$)(O$_2$)(xylylNC)(PPh$_3$)$_2$]		tol	300	1,601		94		252

Table A2 *(Continued)*

Coordination sphere[a]	Compound[b]	Solvent[c]	T (K)[d]	$\delta(^{103}Rh)$[e]	J(Rh,H)[f]	J(Rh,P)[g]	J(Rh,X)[h]	Reference(s)
Iminyl H P_3 N	[Rh(H){C(3-$C_6H_4NO_2$)*N*-2-py-3-Me}{P(OMe)$_3$}(PPh$_3$)$_2$]$^+$ BF_4^-	clfm	ns	125	14.6	134 104		332
	[Rh(H){C(2-C_6H_4OH)*N*-2-py-3-Me}{P(OMe)$_3$}(PPh$_3$)$_2$]$^+$ BF_4^-	clfm	ns	106	11.0	120 109		332
Iminyl H P_2 CN N	[Rh(CN)(H){C(2-C_6H_4OH)N-2-py-3-Me}(PPh$_3$)$_2$]	clfm	ns	238	11.6	105		332
Iminyl H P_2 N Cl	[Rh(Cl)(H){C(3-$C_6H_4NO_2$)Nbzim}(PPh$_3$)$_2$]	clfm?	rt?	984	16.0	111		333
	[Rh(Cl)(H){C(3-$C_6H_4NO_2$)Nbzim}{P(C_6H_4-4-F)$_3$}]	clfm?	rt?	997				333
	[Rh(Cl)(H){C(3-$C_6H_4NO_2$)N-2-py-3-Me}(PPh$_3$)$_2$]	clfm	ns	830	13.8	114		332
	[Rh(Cl)(H){C(4-$C_6H_4NO_2$)N-2-py-3-Me}(PPh$_3$)$_2$]	clfm	ns	830	14.8	114		332
	[Rh(Cl)(H){C(2-OH-3-$C_6H_3OCH_3$)N-2-py-3-Me}(PPh$_3$)$_2$]	clfm	ns	822	14.0	112		332
Iminyl H P_2 N Br	[Rh(Br)(H){C(3-$C_6H_4NO_2$)N-2-py-3-Me}(PPh$_3$)$_2$]	clfm	ns	739	13.1	114		332
Iminyl H N Cl As_2	[Rh(Cl)(H){C(3-$C_6H_4NO_2$)N-2-py-3-Me}(AsPh$_3$)$_2$]	clfm	ns	981	9.2			332
	[Rh(Cl)(H){C(2-OH-3-$C_6H_3OCH_3$)N-2-py-3-Me}(AsPh$_3$)$_2$]	clfm	ns	968	8.8			332
Iminyl H N_2 As_2	[Rh(NCS)(H){C(3-$C_6H_4NO_2$)N-2-py-3-Me}(AsPh$_3$)$_2$]	clfm	ns	947	9.2			332
Iminyl H N Cl Sb_2	[Rh(Cl)(H){C(2-C_6H_4OH)N-2-py-3-Me}(SbPh$_3$)$_2$]	clfm	ns	800	4.8			332
Vinyl P N_4	[Rh(Hdmg)$_2$(CHCH$_2$)(PPh$_3$)]	clfm	298	2,145		63	J(Rh,C) 25.8	190
	[Rh(Hdmg)$_2$(CHCH$_2$)(PMe$_3$)]	clfm	298	2,017		75	J(Rh,C) 24.8	190
	[Rh(Hdmg)$_2$(CHCH$_2$){P(OPh)$_3$}]	clfm	298	2,034		112	J(Rh,C) 24.7	190
	[Rh(Hdmg)$_2$(*cis*-CHCHPh)(PPh$_3$)]	clfm	298	2,230		62	J(Rh,C) 28.7	190
	[Rh(Hdmg)$_2$(*cis*-CHCHPr)(PPh$_3$)]	clfm	298	2,233		61	J(Rh,C) 27.1	190
	[Rh(Hdmg)$_2$(CPrCH$_2$)(PPh$_3$)]	clfm	298	2,290		57	J(Rh,C) 26.5	190
Vinyl N_3 Br_2	[Rh(Br)$_2$(CHCH$_2$){4-(4′-^{t}BuC_6H_4)terpy}]	DCM	rt	3,415			J(Rh,C) 26.9	328
Vinyl N_4 S	[Rh(Hdmg)$_2$(*cis*-CHCHPh)(SMe$_2$)]	clfm	298	2,397				190
Vinyl Cp* S_2	[Rh(Cp*){C^a(CO$_2$Me)C^b(CO$_2$Me)S($C_2B_{10}H_{10}$)S}]	DCM	293	1,049			J(Rh,C) 5.8 (Cp*) 28.4 (a) 5.9 (b)	334
	[Rh(Cp*){C^a(CO$_2$Me)CHC^c(CO$_2$Me)CHS($C_2B_{10}H_{10}$)S}]	clfm	~295	439			J(Rh,C) 5.1 (Cp*) 36.0 (a) 2.7 (c)	335

Vinyl Cp* Se_2	[Rh(Cp*){C^aHC(CO_2Me)CHC(CO_2Me)Se($C_2B_{10}H_{10}$)Se}]	clfm	295?	120			*J*(Rh,C) 4.7 (Cp*) 33.0 (a) *J*(Rh,Se) 33, 38	326
	[Rh(Cp*){C^a(CO_2Me)CHCHC(CO_2Me)Se($C_2B_{10}H_{10}$)Se}]	clfm	295?	264			*J*(Rh,C) 5.0 (Cp*) 36.0 (a) *J*(Rh,Se) 30, 35	326
$(Cp)_2$	$[Rh(Cp)_2]^+$ Cl^-	pc	300	−1,839				23
Cp P S_2	$[Rh(Cp)(SPh)_2(PMe_3)]$	clfm	rt	388		142		336
	$[Rh(Cp)(S_2C_6H_4)PMe_3]$	clfm	rt	52		142		336
Cp P Se_2	$[Rh(Cp)(SePh)_2(PMe_3)]$	clfm	rt	106		143	*J*(Rh,Se) 56	336
Cp P Te_2	$[Rh(Cp)(TePh)_2(PMe_3)]$	clfm	rt	−553		146	*J*(Rh,Te) 110	336
Cp* $(H)_2$ Si	$[Rh(Cp^*)(H)_2(SiEt_3)]^-$ Li^+	THF	298?	−1,321	41			77
Cp* H Si_2	$[Rh(Cp^*)(H)(SiEt_3)_2]^-$ Li^+	THF	298?	−1,533	35			77
	$[Rh(Cp^*)(H)(SiMe_2Ph)_2]^-$ Li^+	THF	298?	−1,515	35			77
Cp* CO H Si	$[Rh(Cp^*)(H)(SiMe_3)(CO)]$	CyH	298?	−1,453	36			77, 322
	$[Rh(Cp^*)(H)(SiEt_3)(CO)]$	benz	298?	−1,519	36			322
	$[Rh(Cp^*)(H)(SiPh_3)(CO)]$	benz	298?	−1,471	33			322
	$[Rh(Cp^*)(H)(Si(OEt)_3)(CO)]$	benz	298?	−1,543	36			322
Cp* CO H Sn	$[Rh(Cp^*)(H)(SnMe_3)(CO)]$	benz	298	−1,532	29.6		*J*(Rh,Sn) 221	337
	$[Rh(Cp^*)(H)(Sn^nBu_3)(CO)]$	benz	298	−1,553	29.3		*J*(Rh,Sn) 210	337
Cp* H Cl_2	$[Rh_2(Cp^*)_2(Cl)_2(\mu\text{-H})(\mu\text{-Cl})]$	clfm	300	1,427	23			100
Cp* H Br_2	$[Rh_2(Cp^*)_2(Br)_2(\mu\text{-H})(\mu\text{-Br})]$	clfm	300	1,244	22			100
Cp* P_2 Cl	$[Rh(Cp^*)(Cl)(PMe_2Ph)_2]^+$ Cl^-	clfm	ns	425		140		20
	$[Rh(Cp^*)(Cl)(PMe_2Ph)_2]^+$ BPh_4^-	clfm	ns	415		143		20
	$[Rh(Cp^*)(Cl)(PMe_3)_2]^+$ Cl^-	clfm	300	318		131		100
	$[Rh(Cp^*)(Cl)(P^iPr_3)_2]^+$ Cl^-	clfm	300	1,343		137		100
Cp* P_2 Br	$[Rh(Cp^*)(Br)(PMe_3)_2]^+$ Br^-	clfm	300	121		132		100
Cp* P_2 I	$[Rh(Cp^*)(I)(PMe_3)_2]^+$ I^-	clfm	300	−235		133		100
Cp* P Cl_2	$[Rh(Cp^*)(Cl)_2(PMe_3)]$	clfm	300	1,211		137		100
	$[Rh(Cp^*)(Cl)_2(PMe_2Ph)]$	clfm	300	1,240		138		100
	$[Rh(Cp^*)(Cl)_2(P^nBu_3)]$	clfm	300	1,340		139		100
	$[Rh(Cp^*)(Cl)_2(PMePh_2)]$	clfm	300	1,307		140		100
	$[Rh(Cp^*)(Cl)_2(PPh_3)]$	clfm	300	1,434		143		100

Table A2 *(Continued)*

Coordination sphere[a]	Compound[b]	Solvent[c]	T (K)[d]	$\delta(^{103}Rh)$[e]	J(Rh,H)[f]	J(Rh,P)[g]	J(Rh,X)[h]	Reference(s)
	$[Rh(Cp^*)(Cl)_2(P^iPr_3)]$	clfm	300	1,726		137		100
Cp* P Br_2	$[Rh(Cp^*)(Br)_2(PMe_3)]$	clfm	300	920		137		100
	$[Rh(Cp^*)(Br)_2(PMe_2Ph)]$	clfm	300	954		140		100
	$[Rh(Cp^*)(Br)_2(P^nBu_3)]$	clfm	300	1,054		138		100
	$[Rh(Cp^*)(Br)_2(PMePh_2)]$	clfm	300	1,007		142		100
	$[Rh(Cp^*)(Br)_2(PPh_3)]$	clfm	300	1,122		147		100
Cp* P I_2	$[Rh(Cp^*)(I)_2(PMe_3)]$	clfm	300	322		138		100
	$[Rh(Cp^*)(I)_2(PMe_2Ph)]$	clfm	300	359		143		100
	$[Rh(Cp^*)(I)_2(P^nBu_3)]$	clfm	300	448		140		100
	$[Rh(Cp^*)(I)_2(PMePh_2)]$	clfm	300	389		143		100
	$[Rh(Cp^*)(I)_2(PPh_3)]$	clfm	300	467		151		100
Cp* P S_2	$[Rh(Cp^*)(SPh)_2(PMe_3)]$	clfm	rt	461		144		336
	$[Rh(Cp^*)(S_2C_6H_4)(PMe_3)]$	clfm	rt	−11		150		336
	$[Rh(Cp^*)\{S_2C_2(B_{10}H_{10})\}(PMe_3)]$	clfm	rt?	334		150		338
Cp* P Se_2	$[Rh(Cp^*)(SePh)_2(PMe_3)]$	clfm	rt	201		148	J(Rh,Se) 53	336
	$[Rh(Cp^*)\{Se_2C_2(B_{10}H_{10})\}(PMe_3)]$	clfm	rt?	36		148	J(Rh,Se) 26	338
Cp* P Te_2	$[Rh(Cp^*)(TePh)_2(PMe_3)]$	clfm	rt	−384		150	J(Rh,Te) 112	336
	$[Rh(Cp^*)Te_2C_2(B_{10}H_{10})(PMe_3)]$	clfm	rt	−523		146	J(Rh,Te) 45	338
Cp* $(O)_3$	$[Rh(Cp^*)(OAc)_2(H_2O)]$	clfm	ns	2,643				20
	$[Rh(Cp^*)(NO_3)_2]$	D_2O	ns	2,364				20
	$[Rh(Cp^*)\{MoO_4\}]_4$	clfm	ns	4,079			J(Rh,C) 8.8	339
Cp* Cl_3	$[Rh_2(Cp^*)_2(Cl)_2(\mu\text{-}Cl)_2]$	clfm	300	2,303				20, 100
Cp* Br_3	$[Rh(Cp^*)_2(Br)_2(\mu\text{-}Br)_2]$	clfm	300	2,068				100
Cp* I_3	$[Rh_2(Cp^*)_2(I)_2(\mu\text{-}I)_2]$	clfm	300	1,426				100
Cp* S_2	$[Rh(Cp^*)\{S_2C_2(B_{10}H_{10})\}]$	DCM	rt?	1,165				338
	$[Rh(Cp^*)\{S_2C_2(B_{10}H_{10}(CHCHCO_2Me)_2)\}]$	clfm	293	1,210				334
Cp* Se_2	$[Rh(Cp^*)\{Se_2C_2(B_{10}H_{10})\}]$	DCM	rt?	1,150				338
Cp^R H Si_2 Rh	$[Rh^1(H)(\mu\text{-}SiMe_2)_2\{C_5H_4CH_2(C_5H_4)Rh^2(SiMe_3)\}]$	benz	296	(1) −1,952			J(Rh,Si) 29.1, 46.4	255
(Cp^R Si_3 Rh)				(2) −1,965			J(Rh,Si) 34.7 J(Rh,Rh) 14.9	
Cp^R P S_2	$[Rh(C_5H_3^tBu_2)\{S_2C_2(B_{10}H_{10})\}(PMe_3)]$	clfm	rt?	460		144		338
$(CN)_6$	$[Rh(CN)_6]^{3-}$ $3K^+$	$HClO_4$(aq)	298	340				49

CN $(H)_2$ P_3	$[Rh(CN)(H)_2(PPh_3)_3]$	clfm	247	−581	~8.5	110 88		60
CN $(H)_2$ P_2 N	$[Rh(CN)(H)_2(PPh_3)_2(py)]$	tol	300	56	14.2 8.5	113		60
CN P_3 (O_2)	$[Rh(CN)(O_2)(PPh_3)_3]$	clfm	300	1,716		133 95		60
CN P_2 N (O_2)	$[Rh(CN)(O_2)(PPh_3)_2(py)]$	clfm	300	2,003		129 117		60
$CNBR_3$ $(H)_2$ P_3	$[Rh(CNBPh_3)(H)_2(PPh_3)_3]$	clfm	247	−609	~8.0	92 108		60
$CNBR_3$ $(H)_2$ P_2 N	$[Rh(CNBPh_3)(H)_2(PPh_3)_2(py)]$	tol	300	2	14.9 ~9.5	111		60
$CNBR_3$ P_3 (O_2)	$[Rh(CNBPh_3)(O_2)(PPh_3)_3]$	tol	247	1,393		90 130		60
CN P N_4	$[Rh(Hdmg)_2(CN)(PPh_3)]$	clfm	298	2,308				190
$(CN)_2$ Se_4	*trans*-$[Rh(CN)_2(SeCN)_4]^{3-}$ $3^nBu_4N^+$	DCM	243	1,680			*J*(Rh,Se) 35.9 *J*(Rh,C) 36.2	340
CO H P_2 Cl_2	$[Rh(Cl)_2(H)(PMe_2Ph)_2(CO)]$	benz	297	239	17.3	81		181
CO P_2 Cl_3	$[Rh(Cl)_3(PMe_2Ph)_2(CO)]$	benz	297	1,588		70±8		181
	trans-$[Rh(Cl)_3(PMe_3)_2(CO)]$	benz	ns	1,477		72		184
CO P_2 Br_3	$[Rh(Br)_3(PMe_2Ph)_2(CO)]$	benz	297	1,075		73		181
	trans-$[Rh(Br)_3(PMe_3)_2(CO)]$	benz	ns	983		73		184
$(H)_2$ P_4	$[Rh(H)_2(PMe_3)_4]^+Cl^-$	DCM	312	−1,007	14.5	96 86		108, 110
$(H)_2$ P_3 N	$[Rh(N_3)(H)_2(PPh_3)_3]$	clfm	247	119	16.6 9.1	114 91		60
	$[Rh(NCO)(H)_2(PPh_3)_3]$	clfm	247	46	~12 ~9	113 90		60
	$[Rh(NCS)(H)_2(PPh_3)_3]$	clfm	247	21	12.2 9.2	112 88		60
	$[Rh\{N(CN)_2\}(H)_2(PPh_3)_3]$	clfm	247	3	12.9 ~9	112 90		60
	$[Rh(NCBPh_3)(H)_2(PPh_3)_3]$	clfm	247	−40	10.4 9.5	112 93		60
$(H)_2$ P_2 N_2	$[Rh(N_3)(H)_2(PPh_3)_2(py)]$	tol	300	566	23.4 ~14	118		60
	$[Rh(NCO)(H)_2(PPh_3)_2(py)]$	tol	300	537		117		60

Table A2 *(Continued)*

Coordination sphere[a]	Compound[b]	Solvent[c]	T (K)[d]	$\delta(^{103}Rh)$[e]	J(Rh,H)[f]	J(Rh,P)[g]	J(Rh,X)[h]	Reference(s)
	$[Rh(NCS)(H)_2(PPh_3)_2(py)]$	tol	300	511	15.9 14.4	116		60
	$[Rh\{N(CN)_2\}(H)_2(PPh_3)_2(py)]$	tol	300	497	17.5 15	116		60
	$[Rh(NCBPh_3)(H)_2(PPh_3)_2(py)]$	tol	300	441	15.7 15.1	116		60
	$[Rh(H)_2(PPh_3)_2(bipy)]^+ Cl^-$	DCM	rt	1,794	14.4	115		341
$(H)_2 P_2 N O$	$[Rh(O_2CMe)(H)_2(PPh_3)_2(py)]$	tol	248	630	19.6 13	121		28
	$[Rh(O_2CPh)(H)_2(PPh_3)_2(py)]$	tol	248	688		121		28
	$[Rh(O_2CPy)(H)_2(PPh_3)_2]$	clfm	300	523	20.7 14.4	118		28
	$[Rh(O_2CPyraz)(H)_2(PPh_3)_2]$	clfm	300	506	21.1 14.5	118		28
	$[Rh(O_2CQuin)(H)_2(PPh_3)_2]$	clfm	300	453	19.1 16.2	119		28
	$[Rh(O_2CIsoq)(H)_2(PPh_3)_2]$	clfm	300	490	20.3 14.4	119		28
	$[Rh(O_2CQuinox)(H)_2(PPh_3)_2]$	clfm	300	436	19.9 16.4	118		28
$(H)_2 P_2 N Cl$	$[Rh(Cl)(H)_2(PPh_3)_2(py)]$	tol	300 247	485 460		119		60
	$[Rh(Cl)(H)_2(PPh_3)_2(pz^*)]$	DCM	300	387	23.0 14.7	118		314
	$[Rh(Cl)(H)_2(PBz_3)_2(py)]$	tol	275	119	25 14	120		115
	$[Rh(Cl)(H)_2(PCy_3)_2(py)]$	tol	235	337	30	114		115
$(H)_2 P N_2 Cl$	$[Rh(Cl)(H)_2(PBz_3)(py)_2]$	py	255	856	25 14	155		115
	$[Rh(Cl)(H)_2(PCy_3)(py)_2]$	py	235	408	24.7	142		115
$(H)_2 P_2 N S$	$[Rh(S^nPr)(H)_2(PPh_3)_2(py)]$	tol	248	223		118		28
	$[Rh(S^iPr)(H)_2(PPh_3)_2(py)]$	tol	248	215		118		28
	$[Rh(SCy)(H)_2(PPh_3)_2(py)]$	tol	248	206		119		28
	$[Rh(SCH_2Ph)(H)_2(PPh_3)_2(py)]$	tol	248	219		118		28
	$[Rh(SPh)(H)_2(PPh_3)_2(py)]$	tol	248	222		117		28

	$[Rh(SCPh_3)(H)_2(PPh_3)_2(py)]$		tol	248	155		118	28
	$[Rh(S_6F_5)(H)_2(PPh_3)_2(py)]$		tol	248	273		118	28
$(H)_2\ P_3\ O$	$[Rh(O_2CMe)(H)_2(PPh_3)_3]$		tol	248	207		117	28
							89	
	$[Rh(O_2CPh)(H)_2(PPh_3)_3]$		tol	248	183		118	28
							88	
	$[Rh(ONO_2)(H)_2(PPh_3)_3]$		DCM	213	270	8.1	117	342
						6.3	89	
$(H)_2\ P_2\ (O)_2$	$[Rh(O_2NO)(H)_2(PPh_3)_2]$		THF	213	529	24.8	118	342
$(H)_2\ P_2\ O\ Cl$	$[Rh(Cl)(H)_2\{2\text{-}(Cy_2PCH_2)THF\}_2]$		acet	295	780		112	343
$(H)_2\ P_3\ Cl$	$[Rh(Cl)(H)_2(PPh_3)_3]$		clfm	247	57	19.2	89	60
						~8	114	
			tol	247	15			
	$[Rh(Cl)(H)_2(PMe_3)_3]$		DCM	312	−319	27	88	108, 110
						15	103	
	$[Rh(Cl)(H)_2(PBz_3)_3]$		tol	295	−393		113	115
$(H)_2\ P_2\ Cl_2$	$[Rh^1(H)_2(PPh_3)_2(\mu\text{-}Cl)_2Rh(PPh_3)_2]$		Benz	295	(1) 957	21.6	119	114
			DCM	213	(1) 909			
	$[Rh(H)_2(PPh_3)_2(\mu\text{-}Cl)_2Rh(H)_2(PPh_3)]$		DCM	213	661	25.2	119	114
	$[Rh(H)_2(PCy_3)_2(\mu\text{-}Cl)_2Rh(H)_2(PPh_3)_2]$		tol	295	194	26.8	114	115
	$[Rh^1(H)_2(PPh_3)_2(\mu\text{-}Cl)_2Rh(PPh_3)(styrene)]$		benz	300	950	22.7	127	112, 114
						22.1		
	$[Rh(H)_2(PPh_3)_2(\mu\text{-}Cl)_2Rh(PPh_3)(CO)]$		benz	318	925	24.7	118	111
	$[Rh(H)(Cl)(PMe_3)_2(\mu\text{-}H)(\mu\text{-}Cl)Rh(PMe_3)(CO)]$		benz	318	347	29	120	111
	(Rh(I) δ –688)					19		
	$[Rh(H)(Cl)(PPh_3)_2(\mu\text{-}H)(\mu\text{-}Cl)Rh(H)(Cl)(PPh_3)_2]$		DCM	263	814	21.3	140	114
						18.1	120	
$(H)_2\ P_2\ Cl\ Br$	$[Rh(H)_2(PPh_3)_2(\mu\text{-}Cl)(\mu\text{-}Br)Rh(PPh_3)(CO)]$	(a)	benz	323	420	24.5	115	111
						22.6		
	(Isomers)	(b)	benz	323	423	25.5	117	
						21.6		
$(H)_2\ P_2\ Cl\ I$	$[Rh(H)_2(PPh_3)_2(\mu\text{-}Cl)(\mu\text{-}I)Rh(PPh_3)(CO)]$		benz	318	281	25.5	120	111
						23.5		
	$[Rh(H)_2(PPh_3)_2(\mu\text{-}Cl)(\mu\text{-}I)Rh(PPh_3)_2]$		benz	295	710	20.9	111	114
						22.5		
$(H)_2\ P_2\ Br_2$	$[Rh(H)_2(PPh_3)_2(\mu\text{-}Br)_2Rh(PPh_3)(CO)]$		benz	323	345	21.0	115	111
						21.4		
$(H)_2\ P_2\ Br\ I$	$[Rh(H)_2(PPh_3)_2(\mu\text{-}Br)(\mu\text{-}I)Rh(PPh_3)(CO)]$		benz	323	198	24.8	120	111

Table A2 *(Continued)*

Coordination sphere[a]	Compound[b]	Solvent[c]	T (K)[d]	$\delta(^{103}Rh)$[e]	J(Rh,H)[f]	J(Rh,P)[g]	J(Rh,X)[h]	Reference(s)
$(H)_2$ P_2 I_2	$[Rh(H)_2(PPh_3)_2(\mu\text{-}I)_2Rh(PPh_3)(CO)]$	benz	313	32	24.2 23.5	117		111
	$[Rh(H)_2(PPh_3)_2(\mu\text{-}I)_2Rh(PPh_3)_2]$	tol	295	387	22.3	115		114
	$[Rh(H)_2(PPh_3)_2(\mu\text{-}I)_2Rh(H)_2(PPh_3)_2]$	tol	295	246				114
	$[Rh(H)_2(PMe_3)_2(\mu\text{-}I)_2Rh(PMe_3)(CO)]$	benz	318	74	32 30.7	104		111
	$[Rh(H)(I)(PMe_3)_2(\mu\text{-}H)(\mu\text{-}I)Rh(PMe_3)(CO)]$ Rh(I) δ –733)	benz	343	−210	30 19	155 96		111
$(H)_2$ P_3 I	$[Rh(I)(H)_2(PPh_3)_3]$	tol	268	−80	19.3 19.7	114 91		114
	$[Rh(I)(H)_2(PMe_3)_3]$	benz	313	−644	14.4 28.1	102 94		109
$(H)_2$ P_3 S	$[Rh(S^n Pr)(H)_2(PPh_3)_3]$	tol	248	−376		113 91		28
	$[Rh(S^i Pr)(H)_2(PPh_3)_3]$	tol	248	−328		113 89		28
	$[Rh(SCy)(H)_2(PPh_3)_3]$	tol	248	−340		114 90		28
	$[Rh(SCH_2Ph)(H)_2(PPh_3)_3]$	tol	248	−358		113 91		28
	$[Rh(SPh)(H)_2(PPh_3)_3]$	tol	248	−323		112 89		28
	$[Rh(SCPh_3)(H)_2(PPh_3)_3]$	tol	248	−422		113 94		28
	$[Rh(SC_6F_5)(H)_2(PPh_3)_3]$	tol	248	−221		113 86		28
	$[Rh(SC_6F_5)(H)_2(PMePh_2)_3]$	tol	248	−417		110 90		28
$(H)_2$ P_2 Si	$[Rh(H)_2(SiPh_3)(PMe_3)_3]$	benz	293	−1,091		102 89		266
	$[Rh(H)_2(SiMe_2Ph)(PMe_3)_3]$	benz	293	−1,108		100 85		266
	$[Rh(H)_2\{Si(OEt)_3\}(PMe_3)_3]$	benz	293	−1,222		99 85		266
H P N O Sn	$[Rh(O_2CCF_3)(\mu\text{-}H)(SnPh_3)(PPh_3)(4\text{-}MeO_2Cpy)]$	DCM	248	1,405	20.4	141	J(Rh,Sn) 370	185
	$[Rh(O_2CCF_3)(\mu\text{-}H)(SnPh_3)(PPh_3)(py)]$	DCM	248	1,411	20.7	140	J(Rh,Sn) 378	185

H P_2 N O Sn	*cis*-[Rh(O_2CIsoq)(H)($SnPh_3$)(PPh_3)$_2$]		DCM	248	798	16.5	128 93	*J*(Rh,Sn) 313	344
	[Rh(O_2CIsoq)(μ-H)($SnPh_3$)(PPh_3)(4-MeO_2Cpy)]	(a)	DCM	248	1,182	20.2	133	*J*(Rh,Sn) 391	344
	(Isomers)	(b)	DCM	248	1,128	19.5	139	*J*(Rh,Sn) 341	
	[Rh(O_2CIsoq)(μ-H)($SnPh_3$)(PPh_3)(4-MeCOpy)]	(a)	DCM	248	1,181	20.3	133	*J*(Rh,Sn) 389	344
		(b)	DCM	248	1,130	19.7	139	*J*(Rh,Sn) 343	
	[Rh(O_2CIsoq)(μ-H)($SnPh_3$)(PPh_3)(4-Brpy)]	(a)	DCM	248	1,179	20.3	133	*J*(Rh,Sn) 390	344
		(b)	DCM	248	1,123	19.5	140	*J*(Rh,Sn) 344	
	[Rh(O_2CIsoq)(μ-H)($SnPh_3$)(PPh_3)(4-HCOpy)]	(a)	DCM	248	1,181	20.3	133	*J*(Rh,Sn) 392	344
		(b)	DCM	248	1,133	19.5	139	*J*(Rh,Sn) 343	
	[Rh(O_2CIsoq)(μ-H)($SnPh_3$)(PPh_3)(py)]	(a)	DCM	248	1,192	20.4	133	*J*(Rh,Sn) 390	344
		(b)	DCM	248	1,125	19.5	138	*J*(Rh,Sn) 349	
	[Rh(O_2CIsoq)(μ-H)($SnPh_3$)(PPh_3)(4-MeOpy)]	(a)	DCM	248	1,194	20.4	133	*J*(Rh,Sn) 389	344
		(b)	DCM	248	1,125	19.6	139	*J*(Rh,Sn) 353	
	[Rh(O_2CIsoq)(μ-H)($SnPh_3$)(PPh_3)(4-Me_2Npy)]	(a)	DCM	248	1,210	20.5	133	*J*(Rh,Sn) 383	344
		(b)	DCM	248	1,128	19.9	137	*J*(Rh,Sn) 364	
	[Rh(O_2CIsoq)(μ-H)($SnPh_3$)(PPh_3)(py-^{15}N)]	(a)	DCM	248	1,159	20.3	133		344
		(b)	DCM	248	1,119	19.2	141		
$(H)_2$ P_2 N Cl_2	[Rh($Cl)_2$(H)(PPh_3)$_2$(pz*)]		DCM	300	2091	12.9	101		314
H P_2 N Cl Sn	*trans*-[Rh(Cl)(μ-H)($SnPh_3$)(PPh_3)$_2$(4-MeO_2Cpy)]		DCM	213	573	17.6	107	*J*(Rh,Sn) 342	185
	trans-[Rh(Cl)(μ-H)($SnPh_3$)(PPh_3)$_2$(py)]		DCM	213	578	17.7	107	*J*(Rh,Sn) 351	185
	trans-[Rh(Cl)(μ-H)($SnPh_3$){P(C_6H_4-4-F)$_3$}$_2$(4-MeO_2Cpy)]		DCM	213	576	18.3	108	*J*(Rh,Sn) 347	185
	trans-[Rh(Cl)(μ-H)($SnPh_3$){P(C_6H_4-4-F)$_3$}$_2$(py)]		DCM	213	579	18.1	108	*J*(Rh,Sn) 342	185
	trans-[Rh(Cl)(μ-H)($SnPh_3$){P(C_6H_4-4-Me)$_3$}$_2$(4-MeO_2-Cpy)]		DCM	213	607	17.9	106	*J*(Rh,Sn) 350	185
	trans-[Rh(Cl)(μ-H)($SnPh_3$){P(C_6H_4-4-Me)$_3$}$_2$(py)]		DCM	213	606	18.0	106	*J*(Rh,Sn) 358	185
	cis-[Rh(Cl)(μ-H)($SnPh_3$)(PPh_3)$_2$(4-$MeCOC_6H_4CN$)]		DCM	248	171	14.0	109 92	*J*(Rh,Sn) 435	185
	cis-[Rh(Cl)(μ-H)($SnPh_3$)(PPh_3)$_2$(C_6H_5CN)]		DCM	248	182	14.1	110 92	*J*(Rh,Sn) 444	185
	cis-[Rh(Cl)(μ-H)($SnPh_3$)(PPh_3)$_2$(4-$Me_2NC_6H_4CN$)]		DCM	248	212	13.9	110 92	*J*(Rh,Sn) 443	185
H P N Cl Sn	[Rh(Cl)(μ-H)($SnPh_3$)(PPh_3)(4-MeO_2Cpy)]		DCM	213	1,234	21.5	137	*J*(Rh,Sn) 370	185
	[Rh(Cl)(μ-H)($SnPh_3$)(PPh_3)(py)]		DCM	213	1,250	21.8	137	*J*(Rh,Sn) 375	185
	[Rh(Cl)(μ-H)($SnPh_3$)(PPh_3)(4-Me_2Npy)]		DCM	213	1,292	22.3	136	*J*(Rh,Sn) 384	185
	[Rh(Cl)(μ-H)($SnPh_3$){P(C_6H_4-4-F)$_3$}(4-MeO_2Cpy)]		DCM	213	1,220	22.1	139	*J*(Rh,Sn) 361	185
	[Rh(Cl)(μ-H)($SnPh_3$){P(C_6H_4-4-F)$_3$}(py)]		DCM	213	1,234	22.0	138	*J*(Rh,Sn) 367	185
	[Rh(Cl)(μ-H)($SnPh_3$){P(C_6H_4-4-F)$_3$}(4-Me_2Npy)]		DCM	213	1,267	22.5	137	*J*(Rh,Sn) 375	185
	[Rh(Cl)(μ-H)($SnPh_3$){P(C_6H_4-4-Me)$_3$}(4-MeO_2Cpy)]		DCM	213	1,249	21.6	136	*J*(Rh,Sn) 376	185
	[Rh(Cl)(μ-H)($SnPh_3$){P(C_6H_4-4-Me)$_3$}(py)]		DCM	213	1,263	22.0	136	*J*(Rh,Sn) 382	185
	[Rh(Cl)(μ-H)($SnPh_3$){P(C_6H_4-4-Me)$_3$}(4-Me_2Npy)]		DCM	213	1,300	21.7	135	*J*(Rh,Sn) 390	185

Table A2 *(Continued)*

Coordination sphere[a]	Compound[b]	Solvent[c]	T (K)[d]	$\delta(^{103}Rh)$[e]	J(Rh,H)[f]	J(Rh,P)[g]	J(Rh,X)[h]	Reference(s)
H P_2 N S_2	[Rh(H)(S^nPr)$_2$(PPh_3)$_2$(py)]	tol	248	840		110		28
	[Rh(H)(SCy)$_2$(PPh_3)$_2$(py)]	tol	248	782		112		28
	[Rh(H)(SCH_2Ph)$_2$(PPh_3)$_2$(py)]	tol	248	812		110		28
	[Rh(H)(SPh)$_2$(PPh_3)$_2$(py)]	tol	248	817		106		28
H P N S_3	[Rh[1](H)(SC_6F_5)(PPh_3)(3,5-Me_2pz)(μ-SC_6F_5)$_2$Rh(PPh_3)$_2$]	DCM	248	(1) 2,117	10.8	122		314
H P_2 N_2 Sn	*trans*-[Rh($NCBPh_3$)(μ-H)($SnPh_3$)(PPh_3)$_2$(4-MeO_2Cpy)]	DCM	213	481	10.7	106	J(Rh,Sn) 337	185
	trans-[Rh($NCBPh_3$)(μ-H)($SnPh_3$)(PPh_3)$_2$(py)]	DCM	213	481	10.4	106	J(Rh,Sn) 336	185
	trans-[Rh($NCBPh_3$)(μ-H)($SnPh_3$)(PPh_3)$_2$(4-Me_2Npy)]	DCM	213	488	10.4	106	J(Rh,Sn) 336	185
	trans-[Rh(NCO)(μ-H)($SnPh_3$)(PPh_3)$_2$(4-MeO_2Cpy)]	DCM	213	561	10.7	107	J(Rh,Sn) 355	185
	trans-[Rh(NCO)(μ-H)($SnPh_3$)(PPh_3)$_2$(py)]	DCM	213	563	11.0	107	J(Rh,Sn) 352	185
	trans-[Rh(NCO)(μ-H)($SnPh_3$)(PPh_3)$_2$(4-Me_2Npy)]	DCM	213	570	9.8	107	J(Rh,Sn) 354	185
H P N_2 Sn	[Rh($NCBPh_3$)(μ-H)($SnPh_3$)(PPh_3)(1-MeIm)]	DCM	213	1,041	14.4	135	J(Rh,Sn) 356	185
	[Rh($NCBPh_3$)(μ-H)($SnPh_3$)(PPh_3)(4-MeO_2Cpy)]	DCM	213	1,146	15.0	135	J(Rh,Sn) 355	185
	[Rh($NCBPh_3$)(μ-H)($SnPh_3$)(PPh_3)(py)]	DCM	213	1,160	15.1	135	J(Rh,Sn) 361	185
	[Rh($NCBPh_3$)(μ-H)($SnPh_3$)(PPh_3)(4-Me_2Npy)]	DCM	213	1,176	15.5	133	J(Rh,Sn) 367	185
	[Rh(N_3)(μ-H)($SnPh_3$)(PPh_3)(4-MeO_2Cpy)]	DCM	248	1,267	16.9	138	J(Rh,Sn) 367	185
	[Rh(N_3)(μ-H)($SnPh_3$)(PPh_3)(py)]	DCM	248	1,281	18.8	138	J(Rh,Sn) 370	185
	[Rh(N_3)(μ-H)($SnPh_3$)(PPh_3)(4-Me_2Npy)]	DCM	248	1,311	19.4	136	J(Rh,Sn) 381	185
	[Rh(NCO)(μ-H)($SnPh_3$)(PPh_3)(1-MeIm)]	DCM	213	1,130	14.0	137	J(Rh,Sn) 379	185
	[Rh(NCO)(μ-H)($SnPh_3$)(PPh_3)(4-MeO_2Cpy)]	DCM	213	1,226	15.2	137	J(Rh,Sn) 370	185
	[Rh(NCO)(μ-H)($SnPh_3$)(PPh_3)(py)]	DCM	213	1,236	15.2	136	J(Rh,Sn) 371	185
	[Rh(NCO)(μ-H)($SnPh_3$)(PPh_3)(4-Me_2Npy)]	DCM	213	1,253	15.1	135	J(Rh,Sn) 382	185
H P_2 N Sn	[Rh($NCBPh_3$)(H)($SnPh_3$)(PPh_3)$_2$]	DCM	248	120	9.9	111	J(Rh,Sn) 396	345
	[Rh($NCBPh_3$)(H)($SnBu_3$)(PPh_3)$_2$]	DCM	248	−132	11.7	119	J(Rh,Sn) 262	345
H P_2 N_2 Sn	*cis*-[Rh($NCBPh_3$)(μ-H)($SnPh_3$)(PPh_3)$_2$(4-Me_2Npy)]	DCM	248	328	14.4	114 82	J(Rh,Sn) 484	345
H P N_3 Sn	*cis*-[Rh($NCBPh_3$)(μ-H)($SnPh_3$)(PPh_3)(4-Me_2Npy)$_2$]	DCM	248	1,026	16.5	83		345
	trans-[Rh($NCBPh_3$)(μ-H)($SnPh_3$)(PPh_3)(4-Me_2Npy)$_2$]	DCM	248	1,159	16.9	121	J(Rh,Sn) 507	345
H P Tp* Sn	[Rh(Tp*)(H)($SnPh_3$)(PPh_3)]	DCM	300	1,302	10.0	133	J(Rh,Sn) 410	311
	[Rh(Tp*)(H)($SnPh_3$){P(C_6H_4-4-F)$_3$}]	DCM	300	1,283	10.1	134	J(Rh,Sn) 403	311
H P_3 N Au	[Rh(H){Au(PPh_3)}{N($CH_2CH_2PPh_2$)$_3$}]$^+$ PF_6^-	acet	303	−487	14.1	120	^2J(Rh,P) 12	308
H P_4 Au	[Rh(μ-H){Au(PPh_3)}{P($CH_2CH_2PPh_2$)$_3$}]$^+$ PF_6^-	DCM	303	−1,159	17.8	136 105	^2J(Rh,P) 9	308
H P_2 O Cl_2	[Rh(H)(Cl)$_2${PCy$_2$(CH_2CH_2OMe)}$_2$]	DCM	295	1,287	19.7	146 127		262

H P_3 Cl_2	$[Rh(H)(Cl)_2(PMe_3)_3]$	DCM	300	892	21.7	131		108
$^1H_4$ Tp*	$[Rh(Tp^*)(H)_2(H_2)]$	clfm/DCM	253	809	18.6			81, 346
$^1H_3$ ^2H Tp*	$[Rh(Tp^*)(H)_2(H_2)]$ ($^1H:{}^2H$ 3:1)	clfm/DCM	253	796	18.8		*J*(Rh,D) 3	81
$^1H_2$ $^2H_2$ Tp*	$[Rh(Tp^*)(H)_2(H_2)]$ ($^1H:{}^2H$ 1:1)	clfm/DCM	253	785	18.9		*J*(Rh,D) 3	81
^1H $^2H_3$ Tp*	$[Rh(Tp^*)(H)_2(H_2)]$ ($^1H:{}^2H$ 1:3)	clfm/DCM	253	775	18.9		*J*(Rh,D) 3	81
P Tp* (O_2)	$[Rh(Tp^*)(O_2)\{P(C_7H_7)_3\}]$	benz?	ns	4,540				261
P_3 N (O_2)	$[Rh(N_3)(O_2)(PPh_3)_3]$	clfm	300	3,273		148		60
						100		
	$[Rh(NCO)(O_2)(PPh_3)_3]$	clfm	300	3,106		148		60
						96		
	$[Rh(NCS)(O_2)(PPh_3)_3]$	clfm	300	2,994		146		60
						94		
	$[Rh\{N(CN)_2\}(O_2)(PPh_3)_3]$	clfm	300	2,988		147		60
						94		
P_2 N_2 (O_2)	$[Rh(N_3)(O_2)(PPh_3)_2(py)]$	clfm	300	3,363		146		60
						125		
	$[Rh(NCO)(O_2)(PPh_3)_2(py)]$	clfm	300	3,342		145		60
						118		
	$[Rh(NCS)(O_2)(PPh_3)_2(py)]$	clfm	300	3,237		143		60
						116		
	$[Rh\{N(CN)_2\}(O_2)(PPh_3)_2(py)]$	clfm	300	3,261		144		60
						116		
	$[Rh(NCBPh_3)(O_2)(PPh_3)_2(py)]$	clfm	300	3,127		142		60
						115		
P N_4 Cl	$[Rh(Hdmg)_2(Cl)(PPh_3)]$	clfm	298	2,628				190
P N_4 Br	$[Rh(Hdmg)_2(Br)(PPh_3)]$	clfm	298	2,531				190
P N_4 I	$[Rh(Hdmg)_2(I)(PPh_3)]$	clfm	298	2,363				190
P_2 N Cl (O_2)	$[Rh(Cl)(O_2)(PPh_3)_2(py)]$	clfm	300	3,374		151		60
						120		
P_2 $(O)_2$ (O_2)	$[Rh(O_2)(Cy_2PCH_2CH_2OMe)_2]^+BPh_4^-$	DCM?	243?	3,770				313
P_2 $(O)_4$	$[Rh(SO_4)(Cy_2PCH_2CH_2OMe)_2]^+BPh_4^-$	DCM?	243?	4,063		146		313
						140		
P_3 (O_2) Cl	$[Rh(Cl)(O_2)(PPh_3)_3]$	clfm	300	3,130		152		60
						99		
P_4 Cl_2	*cis*-$[Rh(Cl)_2\{o\text{-}C_6H_4(PMe_2)_2\}_2]^+$ Cl^-	DMF	300	99		105		347
						84		
	trans-$[Rh(Cl)_2\{o\text{-}C_6H_4(PMe_2)_2\}_2]^+$ Cl^-	DMF	300	628		83		347

Table A2 *(Continued)*

Coordination sphere[a]	Compound[b]	Solvent[c]	T (K)[d]	$\delta(^{103}Rh)$[e]	J(Rh,H)[f]	J(Rh,P)[g]	J(Rh,X)[h]	Reference(s)
P_3 Cl_3	$[Rh(Cl)_3(PPh_3)_3]$	DCM	305	2,770		113 84		303
P_2 Cl_2 S_2	*cis*-$[Rh(Cl)_2(Ph_2P(CH_2)_2S(CH_2)_2S(CH_2)_2PPh_2)]^+$ PF_6^-	acnl	300	1,405		85		348
P_2 Cl_4	$[Rh_2(Cl)_4(\mu\text{-}Cl)_2(PPh_3)_4]$	DCM	305	2,978		115		303
P_4 Br_2	*cis*-$[Rh(Br)_2\{o\text{-}C_6H_4(PMe_2)_2\}_2]^+$ Br^-	DMF	300	0		106 83		347
	trans-$[Rh(Br)_2\{o\text{-}C_6H_4(PMe_2)_2\}_2]^+$ Br^-	DMF	300	387		82		347
P_3 Br_3	$[Rh(Br)_3(PPh_3)_3]$	DCM	305	2,334		108 84		303
P_4 I_2	*cis*-$[Rh(I)_2\{o\text{-}C_6H_4(PMe_2)_2\}_2]^+$ I^-	DMF	300	−709		104 83		347
	trans-$[Rh(I)_2\{o\text{-}C_6H_4(PMe_2)_2\}_2]^+$ I^-	DMF	300	−364		78		347
N_6	$[Rh(NH_3)_6]^{3+}$ $3Cl^-$	NH_3 (aq)	276	4,766				42
	$[Rh(NO_2)_6]^{3-}$ $3Na^+$	aq	rt	5,580				349
N_3 $(O)_3$	$[Rh(NO_2)_3(H_2O)_3]$	aq	rt	6,570				349
N_3 Cl_3	*mer*-$[RhCl_3(CH_3CN)_3]$	nitr	293	5,712			^4J(Rh,H) 0.55 0.45	350
	fac-$[RhCl_3(CH_3CN)_3]$	nitr	293	5,930				350
N_2 Cl_4	$[Rh(NO_2)_2Cl_4]^{3-}$	aq	rt	6,740				349
N_3 Br_3	$[Rh(Br)_3\{4\text{-}(4'\text{-}^t BuC_6H_4)terpy\}]$	DCM	rt	4,540				328
N_4 S_2	*cis*-$[Rh(NCS)_4(SCN)_2]^{3-}$ $3K^+$	DCM	243	5,038				351
	trans-$[Rh(NCS)_4(SCN)_2]^{3-}$ $3K^+$	DCM	243	5,042				351
N_3 S_3	*mer*-$[Rh(NCS)_3(SCN)_3]^{3-}$ $3K^+$	DCM	243	4,526				351
	fac-$[Rh(NCS)_3(SCN)_3]^{3-}$ $3K^+$	DCM	243	4,496			^1J(Rh,N) 22.9	351
N_2 S_4	*cis*-$[Rh(NCS)_2(SCN)_4]^{3-}$ $3K^+$	DCM	243	3,933			^1J(Rh,N) 21.7	351
	trans-$[Rh(NCS)_2(SCN)_4]^{3-}$ $3K^+$	DCM	243	3,954			^1J(Rh,N) 25.1	351
N S_5	$[Rh(NCS)(SCN)_5]^{3-}$ $3K^+$	DCM	243	3,374			^1J(Rh,N) 22.9	351
$(O)_6$	$[Rh(H_2O)_6]^{3+}$ $3ClO_4^-$	$HClO_4$ (aq)	ns	9,992				352
		$HClO_4$ (aq)	276	9,866				353

			$HClO_4$ (aq)	308	9,931		353
			$HClO_4$ (aq)	276	9,880		42
			$HClO_4$ (aq)	298	9,916		354
	$[Rh_2(\mu\text{-}OH)_2(H_2O)_8]^{4+}$ $4ClO_4^-$		$HClO_4$ (aq)	298	9,997		354, 355
	$[Rh_2(\mu\text{-}OH)_2(H_2O)_8]^{4+}$ $4(mesityleneSO_3^-)$		Solid	298	10,131		140
	$[Rh_3(\mu\text{-}OH)_4(H_2O)_{10}]^{5+}$ $5ClO_4^-$	(a)	$HClO_4$ (aq)	298	10,003	^2J(Rh,Rh) 1.5	354, 355
					9,966		
	(Isomers)	(b)	$HClO_4$ (aq)	298	9,841		355
					9,671		
		(c)	$HClO_4$ (aq)	298	10,049		355
	$[Rh_3(\mu\text{-}O_2CMe)_6(\mu_3\text{-}O)(H_2O)_3]^+$ ClO_4^-		H_2O	298	9,390		141
			Solid	298	9,401		140
					9,359		
					9,354		
$Acac_3$	$[Rh(acac)_3]$		clfm	300	8,358		356
$(O)_5$ F	$[Rh(H_2O)_5F]^{2+}$ $2F^-$		HF (aq)	298	10,524		42
Cl_6	$[RhCl_6]^{3-}$ $3H^+$		HCl (aq)	313	7,985		41
			$HClO_4$ (aq)	276	8,001		353
			HCl (aq)	308	8,075		353
			HCl (aq)	243	7,836		83
	$[Rh_2(\mu\text{-}Cl)_3Cl_6]^{3-}$ $3Bu_4N^+$		pc/DCM	297	8,208		357
Cl_5 S	$[RhCl_5(SMe_2)]^{2-}$ $2^nBu_4N^+$		DCM	ns	6,521		358
Cl_4 S_2	*cis*-$[RhCl_4(SMe_2)_2]^-$ $^nBu_4N^+$		DCM	ns	4,882		358
	trans-$[RhCl_4(SMe_2)_2]^-$ $^nBu_4N^+$		DCM	ns	5,226		358
Cl_3 S_3	*mer*-$[RhCl_3(SMe_2)_3]$		DCM	ns	3,897		358
	fac-$[RhCl_3(SMe_2)_3]$		DCM	ns	3,661		358
Cl_2 S_4	*trans*-$[RhCl_2(SMe_2)_4]^+$ NO_3^-		nitr	ns	3,081		358
Cl_3 As_3	$[Rh(Cl)_3\{MeC(CH_2AsMe_2)_3\}]$		DCM	300	2,428		359
Cl_3 Te_3	*mer*-$[Rh(Cl)_3(TeMe_2)_3]$		DCM	ns	3,179	J(Rh,Te) 71 (Te *trans* to Te) 94 (Te *trans* to Cl)	186
Cl_2 As_4	*cis*-$[Rh(Cl)_2(Me_2As\text{-}o\text{-}C_6H_4AsMe_2)_2]^+$ Cl^-		DMF	300	700		347
	trans-$[Rh(Cl)_2(Me_2As\text{-}o\text{-}C_6H_4AsMe_2)_2]^+$ BF_4^-		DMF	300	1,130		347
	$[Rh(Cl)_2\{As(o\text{-}C_6H_4AsMe_2)_3\}]^+BF_4^-$		DCM	300	1,750		359

Table A2 *(Continued)*

Coordination sphere[a]	Compound[b]	Solvent[c]	T (K)[d]	$\delta(^{103}Rh)$[e]	J(Rh,H)[f]	J(Rh,P)[g]	J(Rh,X)[h]	Reference(s)
Cl_2 Sb_4	*trans*-$[Rh(Cl)_2\{Ph_2Sb(CH_2)_3SbPh_2\}_2]^+$ Cl^-	DCM	300	2,104				360
	trans-$[Rh(Cl)_2\{Me_2Sb\text{-}o\text{-}C_6H_4SbMe_2\}_2]^+$ BF_4^-	DMF	300	2,165				360
Br_6	$[Rh(Br)_6]^{3-}$	HBr (aq)	313	7,077				41
		HBr (aq)	276	7,007				42
		HBr (aq)	243	6,924				83
	$[Rh_2(\mu\text{-}Br)_3(Br)_6]^{3-}$ $3Bu_4N^+$	pc/DCM	297	7,237				357
Br_4 S_2	*cis*-$[Rh(Br)_4(SMe_2)_4]^-$ $^nBu_4N^+$	DCM	ns	4,339				358
	trans-$[Rh(Br)_4(SMe_2)_4]^-$ $^nBu_4N^+$	DCM	ns	4,532				358
Br_3 S_3	*mer*-$[Rh(Br)_3(SMe_2)_3]$	DCM	ns	3,437				358
Br_2 S_4	*trans*-$[Rh(Br)_2(SMe_2)_4]^+$ NO_3^-	nitr	ns	2,756				358
Br_3 As_3	$[Rh(Br)_3\{MeC(CH_2AsMe_2)_3\}]$	DMF	300	1,792				359
Br_2 As_4	*cis*-$[Rh(Br)_2(Me_2As\text{-}o\text{-}C_6H_4AsMe_2)_2]^+$ Br^-	DMF	300	410				347
	trans-$[Rh(Br)_2(Me_2As\text{-}o\text{-}C_6H_4AsMe_2)_2]^+$ Br^-	DMF	300	670				347
	$[Rh(Br)_2\{As(o\text{-}C_6H_4AsMe_2)_2\}]^+$ Br^-	DMF	300	750				359
Br_2 Sb_4	*trans*-$[Rh(Br)_2\{Ph_2Sb(CH_2)_3SbPh_2\}_2]^+$ Br^-	DCM	300	1,535				360
	trans-$[Rh(Br)_2\{Me_2Sb\text{-}o\text{-}C_6H_4SbMe_2\}_2]^+$ BF_4^-	DCM	300	1,757				360
Br_3 Te_3	*mer*-$[Rh(Br)_3(TeMe_2)_3]$	DCM	ns	2,567			J(Rh,Te) 70 (Te *trans* to Te) 93 (Te *trans* to Br)	186
I_4 S_2	*cis*-$[Rh(I)_4(SMe_2)_2]^-$ $^nBu_4N^+$	DCM	ns	3,070				358
	trans-$[Rh(I)_4(SMe_2)_2]^-$ $^nBu_4N^+$	DCM	ns	2,958				358
I_3 S_3	*mer*-$[Rh(I)_3(SMe_2)_3]$	DCM	ns	2,448				358
I_3 As_3	$[Rh(I)_3\{MeC(CH_2AsMe_2)_3\}]$	DMF	300	1,178				359
I_2 As_4	*cis*-$[Rh(I)_2(Me_2As\text{-}o\text{-}C_6H_4AsMe_2)_2]^+$ I^-	DMF	300	−300				347
	trans-$[Rh)(I)_2(Me_2As\text{-}o\text{-}C_6H_4AsMe_2)_2]^+$ BF_4^-	DMF	300	−160				347
	$[Rh(I)_2As(o\text{-}C_6H_4AsMe)_3]^+$ BF_4^-	DMF	300	650				359
I_2 Sb_4	*trans*-$[Rh(I)_2\{Ph_2Sb(CH_2)_3SbPh_2\}_2]^+$ I^-	DCM	300	1,265				360
	trans-$[Rh(I)_2\{Me_2Sb\text{-}o\text{-}C_6H_4SbMe_2\}_2]^+$ BF_4^-	DCM	300	1,131				360

I_3 Te_3	*mer*-$[Rh(I)_3(TeMe_2)_3]$	DCM	ns	1,352	*J*(Rh,Te) 66 (Te *trans* to Te) 69 (Te *trans* to I)	186
S_6	$[Rh(SCN)_6]^{3-}$	DCM	243	2,791		351
		aq	298	2,726		49
	$[Rh\{S_2P(OEt)_2\}_3]$	clfm	298	3,665	^2J(Rh,P) 13	49
Se_6	$[Rh(SeCN)_6]^{3-}$ $3\,^nBu_4N^+$	DCM	243	2,287	*J*(Rh,Se) 44	340

[a]Listing of organic ligands alphabetical except for Cp, indenyl, diene, CN, CO and a few uncommon ligands, followed by H, P, N, O, halogen and others in order of increasing atomic weight of donor atom.
[b]Some complexes not included in the table can be found in refs. 41, 42, 49, 185, 352, 353, 357, 361–365.
[c]For details see Abbreviations. A question mark (?) indicates that the solvent was not clearly specified but may be as shown.
[d]Temperature may be given as rt (room temperature) or ns (not specified). A question mark (?) indicates that the temperature was not clearly specified but may be as shown.
[e]$\delta(^{103}Rh)$ is given relative to $\Xi(^{103}Rh) = 3.16$ MHz unless otherwise indicated, i.e., where insufficient information has been given to permit accurate conversion of the reported shift to this scale.
[f]^1J(Rh,H), absolute magnitude in Hz. Signs all probably negative (see Section 14).
[g]^1J(Rh,P), absolute magnitude in Hz. Signs all probably negative (see Section 14).
[h]*J*(Rh,X) (X = ^{13}C, ^{15}N, etc.), absolute magnitude in Hz. See Section 14 for probable signs.
[i]Calibration method not clear.
[j]Calibrated relative to rhodium metal.

Table A3 Data for Rh(-I), Rh(II) and Rh(V) complexes

Coordination Sphere[a]	Compound		Solvent[b]	T(K)[c]	$\delta(^{103}Rh)$[d]	J(Rh,H)[e]	J(Rh,P)[f]	J(Rh,X)[g]	Reference(s)
Rh(-I)									
$(CO)_4$ Rh(II)	$[Rh(CO)_4]^-$ $[N(PPh_3)_2]^+$		acnl	298	−644			J(Rh,C) 75.2	305
Alkene Cp^R $(H)_2$	$[CH_2\{(C_5H_4)Rh(\mu\text{-}H)(C_2H_4)\}_2]$		tol	203	−1101	22.4			113
Alkene Cp^R Si	$[Rh^1(SiEt_3)\{C_5H_4CH_2(C_5H_4)Rh^2(H)(SiEt_3)(CHCH_2)\}]$	(a)	tol	213	(1) −779	^2J 3.0		J(Rh,Si) 27 J(Rh,Rh) 13.8	255
	(Isomers)	(b)			(1) −666	^2J 10.7		J(Rh,Si) 37 J(Rh,Rh) 14	
(vinyl Cp^R H Si)	((2) Rh(IV))	(a)	tol	213	(2) −1407	35.4		J(Rh,Si) 35	
		(b)			(2) −1399	33.3		J(Rh,Si) 33	
CO_2Me CO P $(O)_2$ Rh	$[Rh_2(CO_2Me)_2(\mu\text{-}MeCO_2)_2(CO)_2\{P(OPh)_3\}_2]$		clfm	ns	1372			J(Rh,C) 73.9 (CO) 36.9 (CO_2Me)	366
	$[Rh_2(CO_2Me)_2(\mu\text{-}MeCO_2)_2(CO)_2(PPh_3)_2]$		clfm	ns	1427			J(Rh,C) 73.2 (CO) 39.7 (CO_2Me)	366
	$[Rh_2(CO_2Me)_2(\mu\text{-}MeCO_2)_2(CO)_2(PCy_3)_2]$		clfm	ns	1404			J(Rh,C) 74.4 (CO) 39.4 (CO_2Me)	366
	$[Rh_2(CO_2Me)_2(\mu\text{-}^iPrCO_2)_2(CO)_2(PPh_3)_2]$		clfm	ns	1407			J(Rh,C) 74.7 (CO) 40.0 (CO_2Me)	366
	$[Rh_2(CO_2Me)_2(\mu\text{-}^iPrCO_2)_2(CO)_2(PCy_3)_2]$		clfm	ns	1371			J(Rh,C) 72.7 (CO) 40.4 (CO_2Me)	366
CO_2Me CO N $(O)_2$ Rh	$[Rh_2(CO_2Me)_2(\mu\text{-}MeCO_2)_2(CO)_2(p\text{-}TolNH_2)_2]$		clfm	ns	1713			J(Rh,C) 79.0 (CO) 38.6 (CO_2Me)	366
CO_2Me CO $(O)_3$ Rh	$[Rh_2(CO_2Me)_2(\mu\text{-}MeCO_2)_2(CO)_2(MeOH)_2]$		meth	ns	1995			J(Rh,C) 74.6 (CO)37.7 (CO_2Me)	366
P $(O)_4$ Rh	$[Rh_2(\mu\text{-}MeCO_2)_4\{P(OMe)_3\}_2]$		DCM	243	6694		134	J(Rh,Rh) 7.9	367,368
	$[Rh^1(\mu\text{-}C_7H_{15}CO_2)_4Rh^2(PPh_3)]$		clfm	297	(1) 6930 (2) 6535				27
	$[Rh^1\{PhC(OMe)(CF_3)CO_2\}_4Rh^2(PPh_3)]$		clfm	~298	(1) 7455 (2) 6963		96	^2J(Rh,P) 23	71
	$[Rh^1\{PhC(OMe)(CF_3)CO_2\}_4Rh^2\{PMePh(NEt_2)\}]$	(a,b)			(1) 7153			^2J(Rh,P) 21	71
	(Diasteromers)	(a)			(2) 6949		106		
		(b)			(2) 6963		106		

N_5 Rh	$[Rh_2\{\mu\text{-}HC(N\text{-}p\text{-}tol)_2\}_2(CH_3CN)_6]^{2+}$ $2BF_4^-$		acnl	298?	4648			^3J(Rh,H) 4	369
N_3 $(O)_2$ Rh	$[Rh_2\{\mu\text{-}HC(NPh)_2\}_2(\mu\text{-}CF_3CO_2)_2$(9-Etguanine)$_2]$		acnl	298?	5552				369
N_2 $(O)_2$ Rh	$[Rh_2\{\mu$-(6-Me-2-O-py)$\}_4]$		DCM	300	5745				370
N $(O)_3$ Rh	$[Rh_2\{\mu$-(6-Me-2-O-py)$\}_4]_2$		DCM	300	7644			J(Rh,Rh) 35	370
(N_3 O Rh)					4322				
Rh(V)									
Cp $(H)_2$ Si_2	$[Rh(Cp)(H)_2(SiEt_3)_2]$		benz	rt	−1931	38.5		J(Rh,Si) 16.6	320
Cp* $(H)_2$ Si_2	$[Rh(Cp^*)(H)_2(SiMe_3)_2]$		benz	rt?	−1573	38.6			77
	$[Rh(Cp^*)(H)_2(SiMe_2Ph)_2]$		benz	rt?	−1619	38			77
	$[Rh(Cp^*)(H)_2(SiEt_3)_2]$		benz	rt?	−1623	30.0			77
Cp^R $(H)_2$ Si_2	$[Rh(C_5H_4SiEt_3)(H)_2(SiEt_3)_2]$		tol	ns	−1908	37.2		J(Rh,Si) 16.8	371
	$[Rh^1(H)_2(SiMe_3)_2\{C_5H_4CH_2(C_5H_4)Rh^2(H)(SiMe_3)(C_2H_4)\}]$ {(2)Rh(III)δ-1450}		benz	296	(1) −1731	39.9		J(Rh,Si) 23.4	255
	$[Rh^1(H)_2(SiEt_3)_2\{C_5H_4CH_2(C_5H_4)Rh^2(H)(SiEt_3)(C_2H_4)\}]$ {(2)Rh(III)δ-1477}		benz	296	(1) −1872	38.5		J(Rh,Si) 16.3	255
	$[Rh^1(H)_2(SiEt_3)_2\{C_5H_4CH_2(C_5H_3SiEt_3)Rh^2(H_2)(SiEt_3)_2\}]$		benz	296	(1) −1850	38		J(Rh,Si) 16.5	255
					(2) −1836	37		J(Rh,Si) 17	
	$[CH_2\{(C_5H_3SiEt_3)Rh(H)_2(SiEt_3)_2\}_2]$	(a)	benz	296	−1837	37		J(Rh,Si) 17	255
	(Isomers)	(b)			−1832				
Cp* $(H)_2$ Sn_2	$[Rh(Cp^*)(H)_2(SnMe_3)_2]$		benz	298?	−1757	28.3		J(Rh,Sn) 151	337
	$[Rh(Cp^*)(H)_2(Sn^nBu_3)_2]$		benz	298?	−1837	27.3		J(Rh,Sn) 146	337
$(H)_3$ P_2 Sn_2	$[Rh(H)(\mu\text{-}H)_2(Sn^nBu_3)_2(PPh_3)_2]$		DCM	248	−1440	14.1	103	J(Rh,Sn) 103	345

[a]Listing of organic ligands as for Tables A1 and A2.
[b]For details see Abbreviations.
[c]Temperature may be given as rt (room temperature) or ns (not specified).
[d]$\delta(^{103}Rh)$ is given relative to $\Xi(^{103}Rh)$ = 3.16 MHz.
[e]^1J(Rh,H), absolute magnitude in Hz. Signs are probably negative (see section 16).
[f]^1J(Rh,P), absolute magnitude in Hz. Signs are probably negative (see section 16).
[g]J(Rh,X) (X = ^{13}C, ^{31}P etc), absolute magnitude in Hz. See section 16 for probable signs.

Table A4a Data for clusters

Geometry[a]	Compound[b]	Solvent[c]	T (K)[d]	$\delta(^{103}Rh)$[e]	^{n}J(Rh,X)[f]	Reference(s)
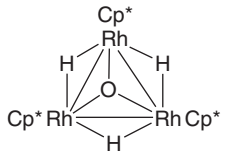	$[(RhCp^*)_3(H)_3(O)]^+PF_6^-$	acet	ns	−136		372
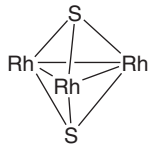	$[Rh_3(S)_2(CO)_6]^+ N(PPh_3)_2^+$	THF	177	−413	^1J(Rh,C) 70.5	373
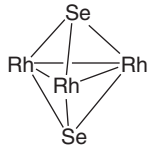	$[Rh_3(Se)_2(CO)_6]^- N(PPh_3)_2^+$	THF	177 298	−428 −394	^1J(Rh,C) 72	373
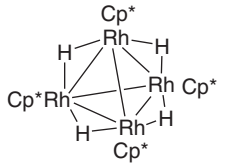	$[Rh_4(Cp^*)_4(H)_4]^{2+}2PF_6^-$	acet	ns	585		374

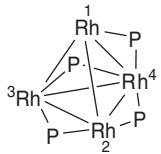	$[Rh_4(CO)_4(\mu\text{-}CO)_2(\mu\text{-}PPh_2)_4]$	DCM	203	(1) 3,785[g] (2) 3,556[g] (3) 3,526[g] (4) 2,673[g]		375
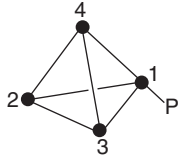	$[Rh_4(CO)_{11}\{P(OPh)_3\}]$	DCM	219	(1) −520 (2) −397 (3) −397 (4) −668	J(Rh,P) 203	152
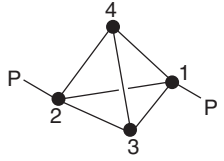	$[Rh_4(CO)_{10}\{P(OPh)_3\}_2]$	DCM	219	(1) −478 (2) −598 (3) −351 (4) −731	^1J(Rh,P) 209 ^2J 15 ^1J(Rh,P) 259 ^2J(Rh,P) 16	152
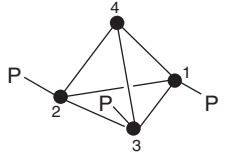	$[Rh_4(CO)_9\{P(OPh)_3\}_3]$	DCM	219	(1) −437 (2) −547 (3) −547 (4) −791	^1J(Rh,P) 214 ^2J 16 ^1J(Rh,P) 263 ^2J 16 ^1J(Rh,P) 263 ^2J 16	152
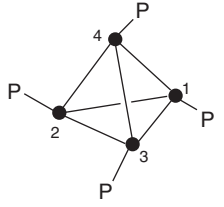	$[Rh_4(CO)_8\{P(OPh)_3\}_4]$	DCM	219	(1) −455 (2) −575 (3) −455 (4) −741	^1J(Rh,P) 214 ^1J(Rh,P) 259 ^1J(Rh,P) 214 ^1J(Rh,P) 215	152

Table A4a *(Continued)*

Geometry[a]	Compound[b]	Solvent[c]	T (K)[d]	$\delta(^{103}Rh)$[e]	$^{n}J(Rh,X)$[f]	Reference(s)
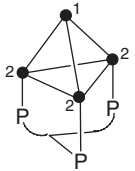	$[Rh_4(CO)_9\{MeC(CH_2PPh_2)_3\}]$	DCM	298	(1) −290 (2) −390		159
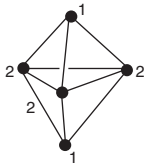	$[Rh_5(CO)_{15}]^{-}$ $N(PPh_3)_2^{+}$	acet	201	(1) −925 (2) −153	$^{1}J(Rh,C)$ 32.7	136, 144
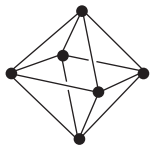	$[Rh_6(CO)_{16}]$	clfm	333	−426	$J(Rh,C)$ 60	153
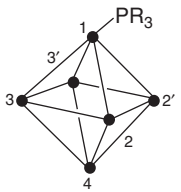	$[Rh_6(CO)_{15}(P^{n}Bu_3)]$	clfm	253	(1) −352 (2) −427 (3) −334 (4) −448	$^{1}J(Rh,P)$ 127	168
	$[Rh_6(CO)_{15}\{P(4\text{-}MeOC_6H_4)_3\}]$	clfm	223	(1) −266 (2) −416 (3) −324 (4) −462	$^{1}J(Rh,P)$ 133	168

	$[Rh_6(CO)_{15}(PPh_3)]$	clfm	250	(1) −303 (2) −445 (3) −347 (4) −484	^1J(Rh,P) 135	168
	$[Rh_6(CO)_{15}\{P(4\text{-}FC_6H_4)_3\}]$	clfm	213	(1) −297 (2) −426 (3) −333 (4) −461	^1J(Rh,P) 138	168
	$[Rh_6(CO)_{15}\{P(4\text{-}ClC_6H_4)_3\}]$	clfm	250	(1) −295 (2) −417 (3) −326 (4) −450	^1J(Rh,P) 139	168
	$[Rh_6(CO)_{15}\{P(4\text{-}CF_3C_6H_4)_3\}]$	clfm	213	(1) −329	^1J(Rh,P) 139	168
	$[Rh_6(CO)_{15}\{P(OPh)_3\}]$	clfm	297	(1) −410 (2) −405 (3) −352 (4) −430	^1J(Rh,P) 240 ^2J(Rh,P) 8.6	168
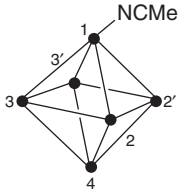	$[Rh_6(CO)_{15}(CH_3CN)]$	tol/clfm/acnl	297	(1) 470 (2) −400 (3) −400 (4) −460		168
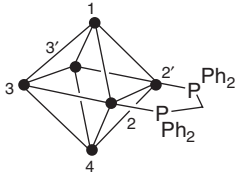	$[Rh_6(CO)_{14}(Ph_2PCH_2PPh_2)]$	clfm	297	(1) −432 (2) −306 (3) −332 (4) −276		165, 170

Table A4a *(Continued)*

Geometry[a]	Compound[b]	Solvent[c]	T (K)[d]	$\delta(^{103}Rh)$[e]	$^{n}J(Rh,X)$[f]	Reference(s)
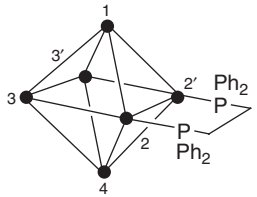	$[Rh_6(CO)_{14}(Ph_2PCH_2CH_2PPh_2)]$	clfm	298	(1) −445 (2) −390 (3) −350 (4) −325		170
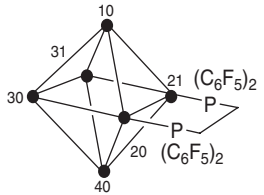	$[Rh_6(CO)_{14}\{(C_6F_5)_2PCH_2CH_2P(C_6F_5)_2\}]$	DCM	220	(10) −410 (20) −380 (21) −292 (30) −363 (31) −385 (40) −343		170
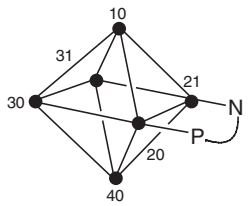	$[Rh_6(CO)_{14}\{Ph_2P(2\text{-}py)\}]$	clfm	298	(10) −450 (20) −410 (21) 650 (30) −370 (31) −415 (40) −315		169
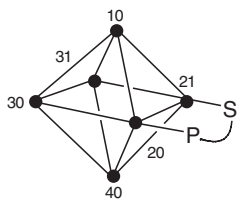	$[Rh_6(CO)_{14}\{Ph_2P(2\text{-thienyl})\}]$	clfm	298	(10) −400 (20) −350 (21) 15 (30) −385 (31) −330 (40) −355		169

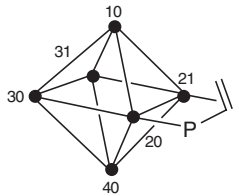	$[Rh_6(CO)_{14}\{Ph_2Pvinyl\}]$	DCM	180	(10) −335 (20) −430 (21) −265 (30) −265 (31) −325 (40) −495		169
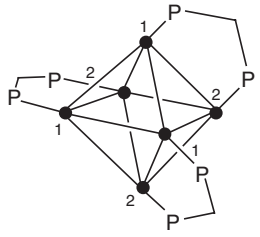	$[Rh_6(CO)_{10}(Ph_2PCH_2PPh_2)_3]$	clfm	213	(1) −371 (2) −152		162
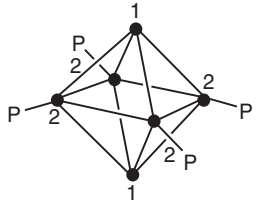	$[Rh_6(CO)_{12}\{P(OPh)_3\}_4]$	clfm	298	(1) −296 (2) −418	*J*(Rh,P) 248	162
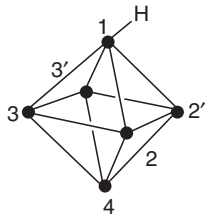	$[Rh_6(CO)_{15}(H)]^-\ NBu_4^+$	acet	203	(1) −538 (2) −374 (3) −475 (4) −478		149

Table A4a *(Continued)*

Geometry[a]	Compound[b]	Solvent[c]	T (K)[d]	$\delta(^{103}Rh)$[e]	$^{n}J(Rh,X)$[f]	Reference(s)
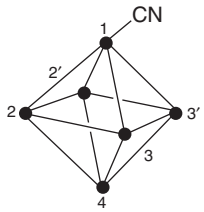	$[Rh_6(CO)_{15}(CN)]^-$ $NMe_3(CH_2Ph)^+$	acet	193	(1) −102 (2) −430 (3) −462 (4) −481		162
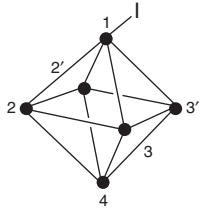	$[Rh_6(CO)_{15}(I)]^-$ NBu_4^+	acet	203	(1) −104 (2) −405 (3) −417 (4) −498		162, 168
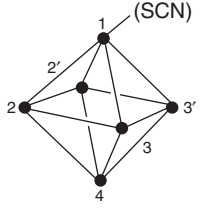	$[Rh_6(CO)_{15}(SCN)]^-$ NBu_4^+	acet	193	(1) 148 (2) −358 (3) −403 (4) −460		162

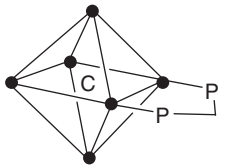	$[Rh_6(C)(CO)_{11}(Ph_2PCH_2PPh_2)]^{2-}$ $2NEt_4^+$	EtCN	rt	−917 −715 −369	^1J(Rh,P) 178 ^2J(Rh,P) 12	161
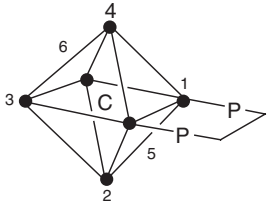	$[Rh_6(C)(CO)_{11}(Ph_2PCH_2CH_2PPh_2)]^{2-}$ $2NEt_4^+$	acnl	rt	(2,4) −921 (1,5) −853 (3,6) −362	^1J(Rh,P) 181 ^2J(Rh,P) 11	161, 164
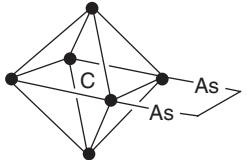	$[Rh_6(C)(CO)_{11}\{(Ph_2AsCH_2CH_2AsPh_2)\}]^{2-}$ $2NEt_4^+$	EtCN	rt	−909 −636 −358		161
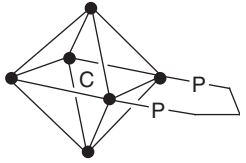	$[Rh_6(C)(CO)_{11}\{Ph_2P(CH_2)_3PPh_2\}]^{2-}$ $2NEt_4^+$	EtCN	rt	−914 −710 −369	^1J(Rh,P) 192 ^2J(Rh,P) 10	161
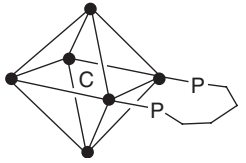	$[Rh_6(C)(CO)_{11}\{Ph_2P(CH_2)_4PPh_2\}]^{2-}$ $2NEt_4^+$	acet	rt	−888 −716 −323	^1J(Rh,P) 173	161

Table A4a *(Continued)*

Geometry[a]	Compound[b]	Solvent[c]	T (K)[d]	$\delta(^{103}Rh)$[e]	^{n}J(Rh,X)[f]	Reference(s)
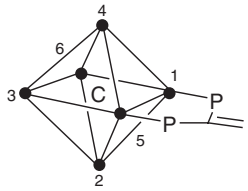	$[Rh_6(C)(CO)_{11}(Ph_2P(CCH_2)PPh_2)]^{2-}$ $2NEt_4^+$	acnl	rt	(2,4) −906 (1,5) −792 (3,6) −363	^{1}J(Rh,P) 181	164
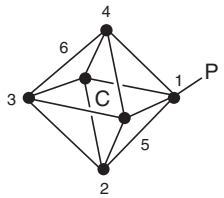	$[Rh_6(C)(CO)_{12}(PPh_3)]^{2-}$ $2NBu_4^+$	acnl/EtCN	203	(1) −770 (2) −935 (3) −341 (4) −989 (5,6) −609	^{1}J(Rh,P) 172	164
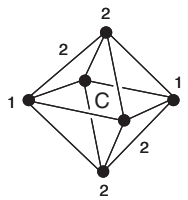	$[Rh_6(C)(CO)_{13}]^{2-}$	THF	177	−1,003 −615		146
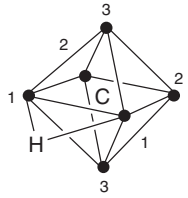	$[Rh_6(C)(CO)_{13}(H)]^{-}$ NEt_4^+	DCM	183	(1) −749 (2) −288 (3) −996	^{1}J(Rh,H) 20 ^{1}J(Rh,C) 17 (carbide)	161

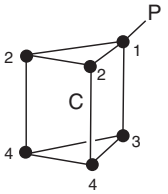	$[Rh_6(C)(CO)_{14}(PPh_3)]^{2-}$ $2NBu_4^+$	acnl	298	(1) −289 (2) −217 (3) −273 (4) −255	*J*(Rh,P) 170	164, 167
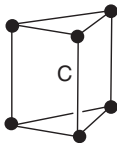	$[Rh_6(C)(CO)_{15}]^{2-}$ $2NBu_4^+$	acet acet acet	248 ns 194	−285 −277 −313		149 376 146
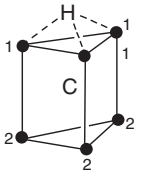	$[Rh_6(C)(CO)_{15}(H)]^-$ NBu_4^+	acet acet	248 248	(1) −416 (2) −153 (1) −412 (2) −144		149 155
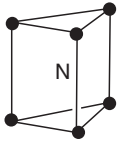	$[Rh(N)(CO)_{15}]^-$	acet	191	−242	*J*(Rh,N) 6.1	146
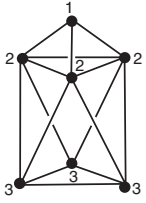	$[Rh_7(CO)_{16}]^{3-}$ $3NEt_4^+$	acnl	243	(1) 483 (2) −376 (3) 690		151

Table A4a *(Continued)*

Geometry[a]	Compound[b]	Solvent[c]	T (K)[d]	$\delta(^{103}Rh)$[e]	$^{n}J(Rh,X)$[f]	Reference(s)
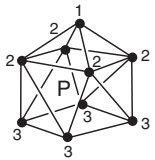	$[Rh_9(P)(CO)_{21}]^{2-}$ $2[CsMe(OCH_2CH_2)_4OMe]^+$	THF	174	(1) −1,413 (2) −1,243 (3) −1,049	J(Rh,P) 34 J(Rh,P) 46	154
	$[Rh_9(P)(CO)_{21}]^{2-}$ $2Et_3NCH_2Ph^+$	acet	ns	(1) −1,423 (2) −1,222 (3) −1,052		376
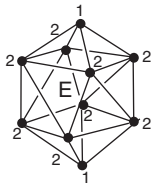	$[Rh_{10}(P)(CO)_{22}]^{3-}$ $3[Cs\{Me(OCH_2CH_2)_4OMe\}]^+$	acet	182	(1) −607 (2) −1,281	J(Rh,P) 56 J(Rh,P) 21	154
	$[Rh_{10}(As)(CO)_{22}]^{3-}$ $3[Cs\{Me(OCH_2CH_2)_4OMe\}]^+$	acet	178	(1) −495 (2) −1,220		154
	$[Rh_{10}(S)(CO)_{22}]^{2-}$ $2[Cs\{Me(OCH_2CH_2)_4OMe\}]^+$	THF	203	(1) −755 (2) −1,169		150, 154
	$[Rh_{11}(CO)_{23}]^{3-}$ $3NMe_4^+$	acet	293	637 153 −205		160
	$[Rh_{12}(Sb)(CO)_{27}]^{3-}$ $3Cs\{Me(OCH_2CH_2)_4OMe\}]^+$	ns	rt	−742		154
	$[Rh_{13}(CO)_{24}(H)]^{4-}$ $4NEt_4^+$	acet	rt	6,370 −340		147, 158
	$[Rh_{13}(CO)_{24}(H)_2]^{3-}$ $3N(PPh_3)_2^+$	acet	rt	4,954 −522 −403		158
		acet	298	4,554		142, 147

			−522	
			−408	
$[Rh_{13}(CO)_{24}(H)_3]^{2-}$ $2Na^+$	acet	298	3,547	142, 147, 158
			−600	
			−532	
$[Rh_{13}(CO)_{24}(H)_4]^-$ $N(PPh_3)_2^+$	acet	rt	2,917	147, 158
			−527	
			−536	
$[Rh_{14}(CO)_{25}]^{4-}$ $4NEt_4^+$	EtCN	213	200	145, 158
			−939	
			320	
			−1,001	
$[Rh_{14}(CO)_{25}(H)]^{3-}$ $3NEt_4^+$	acet	193	136	145, 158
			−840	
			231	
			−973	
			5,936	
$[Rh_{17}(S)_2(CO)_{32}]^{3-}$ $3NMe_3(CH_2Ph)^+$	acet	ns	879	376
			−84	
			−1,458	

[a]Structures shown with spots representing rhodium atoms. Carbonyl ligands omitted.
[b]Compounds shown in order of increasing nuclearity of cluster.
[c]For details see Abbreviations.
[d]Temperatures may be given as rt (room temperature) or ns (not specified).
[e]$\delta(^{103}Rh)$ is given relative to $\Xi(^{103}Rh) = 3.16$ MHz unless otherwise indicated, i.e., where insufficient information has been given to permit accurate conversion of the reported shift to this scale.
[f]J(Rh,X) (X = ^1H, ^{13}C, ^{19}F, etc.), absolute magnitude in Hz.
[g]Calibration method not clear.

Table A4b Data for mixed metal clusters

Geometry[a]	Compound[b]	Solvent[c]	T (K)[d]	$\delta(^{103}Rh)$[e]	$^{n}J(Rh,X)$[f]	Reference(s)
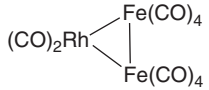	$[Fe_2\ Rh(CO)_x]^-$ (x=10 or 11)	ns	188	0		148, 153
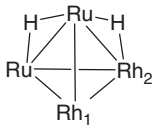	$[Ru_2Rh_2(H)_2(\mu\text{-}CO)_3(CO)_9]$	DCM	277	(1) −637 (2) −270	$1J(Rh^2,H)$ 17.0	157
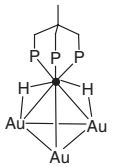	$[Rh(\mu\text{-}H)_2\{MeC(CH_2PMePh)_3\}\{Au(PPh_3)\}_3]^+\ PF_6^-$	DCM	310	−1,090	^1J(Rh,H) 12.8 ^1J(Rh,P) 95	377
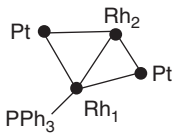	$[Rh_2Pt_2(CO)_9(PPh_3)_3]$	ns	ns	(1) −227 (2) −206		166
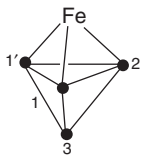	$[FeRh_4(CO)_{15}]^{2-}2N(PPh_3)_2^+$	ns	203	(1) 59 (2) −242 (3) −1,171		148, 153

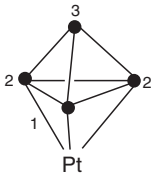	$[Rh_4Pt(CO)_{12}]^{2-}$ $2N^nBu_4^+$	THF	183	(1) 233 (2) −475 (3) −432	^1J(Pt,Rh) 44	156
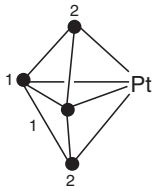	$[Rh_4Pt(CO)_{14}]^{2-}$ $2N^nBu_4^+$	ns	168	(1) −297 (2) −1,072		156
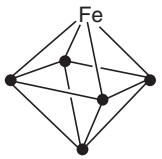	$[FeRh_5(CO)_{16}]^-$ $NMe_3(CH_2Ph)^+$	THF	203	(1) −401 (2) −502		148, 153
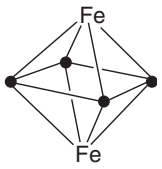	*trans*-$[Fe_2Rh_4(CO)_{16}]^{2-}$ $2NMe_3(CH_2Ph)^+$	acet	203	−409		148, 153
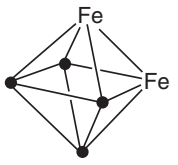	*cis*-$[Fe_2Rh_4(CO)_{16}]^{2-}$ $2NMe_3(CH_2Ph)^+$	acet	203	−409 −453		148, 153

Table A4b *(Continued)*

Geometry[a]	Compound[b]	Solvent[c]	T (K)[d]	$\delta(^{103}Rh)$[e]	$^{n}J(Rh,X)$[f]	Reference(s)
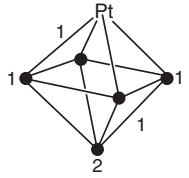	$[Rh_5Pt(CO)_{15}]^-$ NEt_4^+	acet	298	(1) −243 (2) −495	^{1}J(Pt,Rh) 24 ^{2}J(Pt,Rh) 73	156
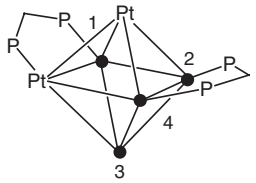	$[Rh_4Pt_2(CO)_{11}(Ph_2PCH_2PPh_2)_2]$	DCM	298	(1) −151 (2) −295 (3) ? (4) −444		171
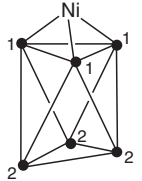	$[NiRh_6(CO)_{16}]^{2-}$ $2N(PPh_3)_2^+$	THF	196	(1) −376 (2) 692		151
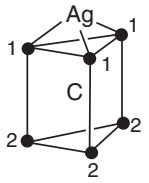	$[Rh_6(C)(CO)_{15}\{Ag(PEt_3)\}]^{2-}$ $2NMe_3(CH_2Ph)^+$	acet	193	(1) −473 (2) −283		155

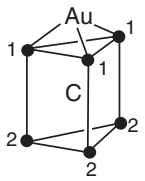	$[Rh_6(C)(CO)_{15}\{Au(PEt_3)\}]^{2-}$ $2NMe_3(CH_2Ph)^+$	acet	193	(1) −433 (2) −272	155, 163
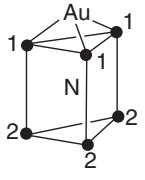	$[Rh_6(N)(CO)_{15}\{Au(PPh_3)\}]$	THF	rt	(1) −447 (2) −296	163

[a]Structures shown with spots representing rhodium atoms.
[b]Compounds shown in order of increasing nuclearity of cluster.
[c]For details see Abbreviations.
[d]Temperatures may be given as rt (room temperature) or ns (not specified).
[e]$\delta(^{103}Rh)$ is given relative to $\Xi(^{103}Rh) = 3.16$ MHz unless otherwise indicated, i.e., where insufficient information has been given to permit accurate conversion of the reported shift to this scale.
[f]$J(Rh,X)$ ($X = {}^1H$, ^{13}C, ^{19}F, etc.), absolute magnitude in Hz.

Table A5a $J(^{103}Rh,^{15}N)$ and other data for Rh(I) complexes

Coordination sphere	Compound	Solvent[a]	$^{1}J(Rh,N)$[b]	$J(Rh,P)$[c]	Reference
Alkene Cp N	[Rh(Cp){$CH_2CHC(OH)(2\text{-}C_5H_4N)_2$}]	benz	22.8		378
Alkene P_2 $NCBPh_3$	*trans*-[Rh($^{15}NCBPh_3$)$(PPh_3)_2(C_2H_4)$]	tol	21.9	124	379
Alkene P py^R Cl	[Rh(Cl)$(PPh_3)(C_2H_4)${3,5-$(MeO_2C)_2$-4-$PhC_5H_2^{15}N$}]	tol	12.2	166	380
η^2–arene CO P N	[Rh(CO){$Ph_2POCH(Ph)CH(Me)N(Me)CHPh_2$}]$^+$ ClO_4^-	DCM	10.5		381
Cp N O	[Rh(Cp){$CO(2\text{-}C_5H_4N)_2$}]	benz	33.6		378
Diene N_2	[Rh(cod){3,6-$(2\text{-}C_5H_4N)_2$pyridazine}]$^+$ BF_4^-	nitr	26.0 (py) 20.5 (pdz)		382
	[Rh(nbd){3,6-$(2\text{-}C_5H_4N)_2$pyridazine}]$^+BF_4^-$	nitr	19.7 (py) 24.1 (pdz)		382
CNR P_2 $CNBPh_3$	*trans*-[Rh($C^{15}NBPh_3$)$(PPh_3)_2$(xylylNC)]	clfm	4.2 (^2J)	128	379
CNR P_2 $NCBPh_3$	*trans*-[Rh($^{15}NCBPh_3$)$(PPh_3)_2$(xylylNC)]	clfm	17.8	131	379
$CNBPh_3$ CO P_2	*trans*-[Rh[$C^{15}NBPh_3$)$(PPh_3)_2$(CO)]	clfm	4.1 (^2J)	121	379
$CNBPh_3$ P_3	[Rh($C^{15}NBPh_3$)$(PPh_3)_3$]	clfm	3.9 (^2J)	146 137	379
$CNBPh_3$ P_2 py	*trans*-[Rh($C^{15}NBPh_3$)$(PPh_3)_2$(py)]	tol	5.0 (^2J)	146	379
CO P_2 $NCBPh_3$	*trans*-[Rh$(NCBPh_3)(PPh_3)_2$(CO)]	clfm	18.3	123	379
CO P_2 py	*trans*-[Rh$(PPh_3)_2$(CO)(py)]$^+$ ClO_4^-	DCM	16	129	383
CO P_2 N	[Rh$(PPh_3)_2$(CO){1,8-diazabicyclo[5,4,0]undec-7-ene}]$^+$ ClO_4^-	DCM	17	134	384
	trans-[Rh$(H_2NC_6H_4\text{-}o\text{-}NHPh)(PPh_3)_2$(CO)]	DCM	12.1	133	385
CO P py^R Cl	[Rh(Cl)(PPh_3)(CO){3,5-$(MeO_2C)_2$-4-$PhC_5H_2^{15}N$}]	tol	13.2	159	380
CO P N Cl	[Rh(Cl)(CO){$Ph_2POCH(Ph)CH(Me)NMe_2$}]	benz	11.5	184	381
$(CO)_2$ py_2 Cl	[Rh(Cl)$(CO)_2(py)_2$]	DCM	17.6 16.8		306
$(CO)_2$ py Cl	*cis*-[Rh(Cl)$(CO)_2$(py)]	DCM	15.9		306
$(CO)_2$ N Cl	[$Rh_2(\mu\text{-}NH_2NH_2)(CO)_4(Cl)_2$]	meth	11.8		386
	[$Rh_2(\mu\text{-}N^aH_2N^bHMe)(CO)_4(Cl)_2$]	DCM	(a) 11.0 (b) 11.1		386
	[$Rh_2(\mu\text{-}N^aH_2N^bHPh)(CO)_4(Cl)_2$]	THF	(a) 10.7 (b) 11.1		386

$(CO)_2$ N Cl	$[Rh(CO)_2(MeNHNHMe)(Cl)]$	THF	12.1		386
	$[Rh(CO)_2(Me_2NNMe_2)(Cl)]$	clfm	14.9		386
CO py_2 Cl	*trans*-$[Rh(Cl)(CO)(py)_2]$	DCM	18.6		306
CO py Cl_2	*trans*-$[Rh_2(\mu\text{-}Cl)_2(CO)_2(py)_2]$	DCM	13.5		306
P_3 $NCBPh_3$	$[Rh(^{15}NCBPh_3)(PPh_3)_3]$	clfm	18.1	177	379
				139	
P_3 $NCB(CF_3)_3$	$[Rh\{NCB(CF_3)_3\}(PPh_3)_3]$	DCM	17.9		387
P_3 py	$[Rh(PPh_3)_3(py)]^+$ Cl^-	DCM	14	161	383
P_2 $NCBPh_3$ py	*cis*-$[Rh(^{15}NCBPh_3)(PPh_3)_2(py)]$	tol	17.8	186	379
				160	
P_2 $NCBPh_3$ py^R	*cis*-$[Rh(^{15}NCBPh_3)(PPh_3)_2(4\text{-}Me_2Npy)]$	tol	17.2	187	379
				158	
	cis-$[Rh(^{15}NCBPh_3)(PPh_3)_2(4\text{-}CNpy)]$	tol	18.4	184	379
				162	
P_2 N_2	$[Rh(PPh_3)_2(N^aH_2NHCH_2N^bHNH_2)]^+$ NO_3^-	DCM	(a) 12	177	388
			(b) 13	173	
	$[Rh_2(PPh_3)_4(\mu\text{-}H_2NNHCH_2NHNH_2)_2]^{2+}$ $2NO_3^-$	DCM	12 (NH_2)	176	388
			13 (NH)	175	
	$[Rh\{1\text{-}NH_2\text{-}2\text{-}(NHPh)C_6H_4\}(PPh_3)_2]$	DCM	10	183	385
			10.4	182	
	cis-$[Rh(PPh_3)_2(py)_2]^+$ Cl^-	DCM	28	168	383
P_2 py Cl	*cis*-$[Rh(Cl)(PPh_3)_2(py)]$	DCM	15	202	383
P_2 N Cl	*trans*-$[Rh(Cl)(P^iPr_3)_2(^{15}N_2)]$	tol	28	122	389
			4 (^2J)		
	trans-$[Rh(Cl)(PCy_3)_2(^{15}N_2)]$	DCM	30		390
	cis-$[Rh(Cl)(PPh_3)_2\{3,5\text{-}(MeO_2C)_2\text{-}4\text{-}PhC_5H_2^{15}N\}]$	tol	13.8	195	380
				166	
P_2 py^R S	*cis*-$[Rh(SC_6F_5)(PPh_3)_2\{3,5\text{-}(MeO_2C)_2\text{-}4\text{-}PhC_5H_2^{15}N\}]$	tol	14.5	176	380
				168	
P_2 NS Cl	*trans*-$[Rh(Cl)(\eta^2\text{-}C_6H_5^{15}NSO)(P^iPr_3)_2]$	tol	15.5	109	391

[a] For details see Abbreviations.
[b] ^1J(Rh,N), absolute magnitude in Hz. The sign of $^1J(^{103}Rh,^{15}N)$ is probably positive (see Section 14).
[c] ^1J(Rh,P), absolute magnitude in Hz. Signs all probably negative (see Section 14).

Table A5b $J(^{103}Rh,^{15}N)$ and other data for Rh(III) complexes

Coordination sphere	Compound[a]	Solvent[b]	$^1J(Rh,N)$[c]	$^1J(Rh,H)$[d]	$^1J(Rh,P)$[e]	Reference
Acetylide H P_2 N py^R	$[Rh(N_3)(C_2Ph)(H)(PPh_3)_2\{3,5\text{-}(MeO_2C)_2\text{-}4\text{-}PhC_5H_2^{15}N\}]$	tol	7.8	16.4	104	380
Acetylide H P_2 *N*CO py^R	$[Rh(NCO)(C_2Ph)(H)(PPh_3)_2\{3,5\text{-}(MeO_2C)_2\text{-}4\text{-}PhC_5H_2^{15}N\}]$	tol	7.5	16.1	103	380
Acetylide H P_2 py^R Cl	$[Rh(Cl)(C_2Ph)(H)(PPh_3)_2\{3,5\text{-}(MeO_2C)_2\text{-}4\text{-}PhC_5H_2^{15}N\}]$	tol	6.9	15.1	104	380
Alkyl aryl N_2 O_2	$[Rh^1(\text{norbornyl})(CH_3CN^a)(CH_3OH)_2\kappa^2\text{–}(N,C)\text{-}\{3\text{-}(2\text{-}C_5H_4N^b)\text{pyridazine}^c\text{-}6\text{-}(2\text{-}C_5H_4N^d)\}Rh^2(nbd)]$ {(1) Rh(III), (2) Rh(I)}	meth	45.9 (1,a), 42.4 (2,b), 40.2 (2,c), 24.7 (1,d)			382
Alkyl Cp N O	$[Rh(Cp)(CH_2CH_2C(O)(2\text{-}C_5H_4N)_2)]$	benz	19.8			378
Alkyl P N_4	$[Rh(Hdmg)_2(Me)(PPh_3)]$	clfm	19.9			392
	$[Rh(Hdmg)_2(Et)(PPh_3)]$	clfm	20.4			392
	$[Rh(Hdmg)_2(^iPr)(PPh_3)]$	clfm	20.3			392
	$[Rh(Hdmg)_2(^tBu)(PPh_3)]$	clfm	20.7			392
$alkyl^E$ P N_4	$[Rh(Hdmg)_2(CH_2Cl)(PPh_3)]$	clfm	19.7			392
$alkyl^F$ P N_4	$[Rh(Hdmg)_2(CH_2CF_3)(PPh_3)]$	clfm	19.0			392
Alkyl N_4 O	$[Rh(Hdmg)_2(Me)(D_2O)]$	D_2O	21.2			392
Alkyl N_4 py	$[Rh(Hdmg)_2(Me)(py)]$	clfm	20.4 (dmg) 7.2 (py)			392
	$[Rh(Hdmg)_2(^nPr)(py)]$	clfm	21.1 (dmg) 6.8 (py)			392
	$[Rh(Hdmg)_2(^nBu)(py)]$	clfm	21.1 (dmg) 6.4 (py)			392
	$[Rh(Hdmg)_2(^sBu)(py)]$	clfm	21.4 (dmg) 21.3 (dmg) 5.5 (py)			392
	$[Rh(Hdmg)_2(^iBu)(py)]$	clfm	20.8 (dmg) 6.2 (py)			392
	$[Rh(Hdmg)_2(\text{neopentyl})(py)]$	clfm	20.8 (dmg) 5.8 (py)			392
$alkyl^E$ N_4 py	$[Rh(Hdmg)(CH_2Cl)(py)]$	clfm	20.2 (dmg) 8.1 (py)			392
$alkyl^F$ N_4 py	$[Rh(Hdmg)(CH_2CF_3)(py)]$	clfm	19.3 (dmg) 8.7			392
$CNBPh_3$ $(H)_2$ P_3	$[Rh(C^{15}NBPh_3)(H)_2(PPh_3)_3]$	clfm	1.5 (^2J)	8	108 91	379

$CNBPh_3$ H P_2 Sn	[Rh($C^{15}NBPh_3$)(H)($SnPh_3$)(PPh_3)$_2$]	clfm	3.2 (^2J)	7.0	107	379
CO P_2 NO Cl	[Rh(Cl)(^{15}NO)(CO)(P^iPr_3)$_2$]$^+$ ClO_4^-	DCM	4.5			393
$(H)_2$ P_3 $NCBPh_3$	[Rh($^{15}NCBPh_3$)(H)$_2$(PPh_3)$_3$]	tol	11.9	10.4	112	379
				9.5	93	
$(H)_2$ P_2 $NCBPh_3$ py	[Rh($^{15}NCBPh_3$)(H)$_2$(PPh_3)$_2$(py)]	tol	11.5	15.7	116	379
				15.1		
$(H)_2$ P_2 $NCBPh_3$ py^R	[Rh($^{15}NCNPh_3$)(H)$_2$(PPh_3)$_2$(4-Me_2Npy)]	tol	11.3	15.6	116	379
				14.3		
	[Rh($^{15}NCNPh_3$)(H)$_2$(PPh_3)$_2$(4-CNpy)]	tol	11.7	15.8	115	379
				15.8		
$(H)_2$ P_2 N O	[Rh(H)$_2$(pyridine-2-carboxylate)(PPh_3)$_2$]	DCM	9.7		118	394
	[Rh(H)$_2$(6-methylpyridine-2-carboxylate)(PPh_3)$_2$]	DCM	9.7		120	394
	[Rh(H)$_2$(pyrazine-2-carboxylate)(PPh_3)$_2$]	DCM	9.6		118	394
	[Rh(H)$_2$(quinoline-2-carboxylate)(PPh_3)$_2$]	DCM	9.2		119	394
	[Rh(H)$_2$(isoquinoline-1-carboxylate)(PPh_3)$_2$]	DCM	10.1		119	394
	[Rh(H)$_2$(quinoxaline-2-carboxylate)(PPh_3)$_2$]	DCM	9.1		118	394
H P_2 $NCBPh_3$ py Sn	*trans*-[Rh($^{15}NCBPh_3$)(H)($SnPh_3$)(PPh_3)$_2$(py)]	DCM	11.8	10.5	106	345
H P_2 $NCBPh_3$ py^R Sn	*trans*-[Rh($^{15}NCBPh_3$)(H)($SnPh_3$)(PPh_3)$_2$(4-Me_2Npy)]	DCM	11.4	10.6	106	345
	cis-[Rh($^{15}NCBPh_3$)(H)($SnPh_3$)(PPh_3)$_2$(4-Me_2Npy)]	DCM	11.3	14.4	114	345
					82	
	trans-[Rh($^{15}NCBPh_3$)(H)($SnPh_3$)(PPh_3)$_2$(4-MeO_2Cpy)]	DCM	12.4	10.3	106	345
H P_2 $NCBPh_3$ Si	[Rh($^{15}NCBPh_3$)(H)($SiPh_3$)(PPh_3)$_2$]	clfm	14.7	15.5	122	379
H P_2 $NCBPh_3$ Sn	[Rh($^{15}NCBPh_3$)(H)($SnPh_3$)(PPh_3)$_2$]	DCM	15.3	9.9	111	345
	[Rh($^{15}NCBPh_3$)(H)($SnBu_3$)(PPh_3)$_2$]	DCM	15.2	11.7	119	345
H P $NCBPh_3$ py_2^R Sn	*trans*-[Rh($^{15}NCBPh_3$)(H)($SnPh_3$)(PPh_3)(4-Me_2Npy)$_2$]	DCM	11.5	16.9	121	345
H P $NCBPh_3$ py^R Sn	[Rh($^{15}NCBPh_3$)(H)($SnPh_3$)(PPh_3)(py)]	DCM	12.3	15.1	135	345
	[Rh($^{15}NCBPh_3$)(H)($SnPh_3$)(PPh_3)(4-Me_2Npy)]	DCM	11.1	15.5	133	345
	[Rh($^{15}NCBPh_3$)(H)($SnPh_3$)(PPh_3)(4-MeO_2Cpy)]	DCM	11.8	15.5	135	345
P_3 N Cl	[Rh(Cl)($^{15}N_2$Ph)($PMePh_2$)$_3$]$^+$ PF_6^-	DCM	~15 (Nα)			395
			29 (Nβ)			
P_2 $NCBPh_3$ py (O_2)	*cis*-[Rh($^{15}NCBPh_3$)(O_2)(PPh_3)$_2$(py)]	tol	20.2		143	379
					116	
	cis-[Rh($^{15}NCBPh_3$)(O_2)(PPh_3)$_2$(4-Me_2Npy)]	tol	20.0		144	379
					114	
	cis-[Rh($^{15}NCBPh_3$)(O_2)(PPh_3)$_2$(4-CNpy)]	tol	19.9		141	379
					118	
P N_4 Cl	[Rh(Hdmg)$_2$(Cl)(PPh_3)]	clfm	18.1			392
N_4 py Cl	[Rh(Hdmg)$_2$(Cl)(py)]	clfm	17.9 (dmg)			392
			17.8 (py)			
N_4 py I	[Rh(Hdmg)$_2$(I)(py)]	clfm	18.3 (dmg)			392
			15.6 (py)			

Table A5b *(Continued)*

Coordination sphere	Compound[a]	Solvent[b]	^1J(Rh,N)[c]	^1J(Rh,H)[d]	^1J(Rh,P)[e]	Reference
N_5 S	$[Rh(^{15}NH_3)_5\{SC(NMe_2)_2\}]^{3+}$ 3OTf$^-$	H_2O	13.4 12.5			396
N_5 X	$[Rh(^{15}NH_3)_5X]^{n+}$ NH_3 *cis* (c) or *trans* (t) to X	H_2O				397
X=H_2O			13.9(c) 17.3 (t)			397
OH^-			14.2 (c) 13.9(t)			397
Cl^-			13.4 (c) 15.4 (t)			397
Br^-			13.4 (c) 14.9 (t)			397
I^-			13.4 (c) 13.4 (t)			397
NH_3			14.2 (c) 14.2 (t)			397
$-ONO^-$			14.2 (c) 15.1 (t)			397
$-NO_2^-$			14.4 (c) 12.2 (t)			397
$-NCS^-$			13.7 (c) 16.1 (t)			397
$-SCN^-$			13.7 (c) 13.7 (t)			397
$-NCO^-$			13.2 (c) 15.1 (t)			397
$-CN^-$			13.2 (c) 10.3 (t)			397

[a]Some complexes not included in the table can be found in refs. 398 and 399.
[b]For details see Abbreviations.
[c]J(Rh,N), absolute magnitude in Hz. The sign of $^1J(^{103}Rh,^{15}N)$ is probably positive (see Section 14).
[d] ^1J(Rh,H), absolute magnitude in Hz. Signs all probably negative (see Section 14).
[e] ^1J(Rh,P), absolute magnitude in Hz. Signs all probably negative.

Table A6a $^{1}J(^{103}Rh,^{19}F)$ and other data for Rh(I) and Rh(III) complexes

Coordination sphere	Compound	Solvent[a]	^{1}J(Rh,F)[b]	^{1}J(Rh,P)[c]	^{n}J(Rh,X)[d]	Reference
Acetylene P_2 F	*trans*-[Rh(F)(PhC_2Ph)(P^iPr_3)$_2$]	benz	80.1	125	^{1}J(Rh,C) 16.2	400
Alkene P_2 F	*trans*-[Rh(F)(C_2H_4)(P^iPr_3)$_2$]	benz	76.3	130	^{1}J(Rh,C) 15.3	400
Alkene$_2$ F_2	[Rh$_2$(μ-F)$_2$(cyclooctene)$_4$]	benz	55.5			401
Allenylidene P_2 F	*trans*-[Rh(F)($CCCPh_2$)(P^iPr_3)$_2$]	benz	23.0	141	^{2}J(Rh,C) 14.2	402
	trans-[Rh(F)(CCC(Ph)^{t}Bu)(P^iPr_3)$_2$]	benz	20.3	142		402
Vinylidene P_2 F	*trans*-[Rh(F)(CCH_2)(P^iPr_3)$_2$]	benz	14.5	145		403
	trans-[Rh(F)(CCHPh)(P^iPr_3)$_2$]	benz	13.4	144	^{1}J(Rh,C) 52.3 ^{2}J(Rh,C) 15.1	400
Diene P F	[Rh(F)(cod)(PPh_3)]	DCM	72.3	156	^{1}J(Rh,C) 13.7, 8.9	401
	[Rh(F)(cod){P(4-$MeOC_6H_4$)$_3$}]	tol	71.6	161	^{1}J(Rh,C) 14.5, 6.8	401
	[Rh(F)(cod)(P^iPr_3)]	benz	78.7	154	^{1}J(Rh,C) 14.4, 7.8	401
	[Rh(F)(cod)(PCy_3)]	benz	77.2	153	^{1}J(Rh,C) 14.7	401
CO P_2 F	*trans*-[Rh(F)(CO)(P^iPr_3)$_2$]	benz	49.6	131	^{1}J(Rh,C) 68.1	400
P_3 F	[Rh(F)(PPh_3)$_3$]	benz	77.6	181 154		404
	trans-[Rh(F)(PPh_3)$_2$($PFPh_2$)]	benz	58.5	207 150	^{2}J(Rh,F) 15	404
F_6	$[Rh(F)_6]^{3-}$ $3K^+$	HF (aq)	244			405

[a] For details see Abbreviations.
[b] ^{1}J(Rh,F), absolute magnitude in Hz. Signs probably negative (see Section 14).
[c] ^{1}J(Rh,P), absolute magnitude in Hz. Signs probably negative (see Section 14).
[d] ^{1}J(Rh,X) (X = ^{13}C), absolute magnitude in Hz.

Table A6b $^{2}J(^{103}Rh, ^{19}F)$ and other data for Rh(−I), Rh(I) and Rh(III) complexes

Coordination sphere	Compound[a]	Solvent[b]	^{2}J(Rh,F)[c]	^{1}J(Rh,P)[d]	J(Rh,X)[e]	Reference
Alkene CF_3 $(CNR)_3$	[Rh(CF_3)(xylylNC)$_3$(maleicanhydride)]	clfm	9.3			406
	[Rh(CF_3)(xylylNC)$_3$(TCNE)]	clfm	14.2			406
Alkene CF_3 $(CNR)_2$ P	[Rh(CF_3)(xylylNC)$_2$(PPh_3)(maleicanhydride)]	benz	10.2	127		406
	[Rh(CF_3)(xylylNC)$_2$(PPh_3)(TCNE)]	clfm	14.4	100		406
Alkene PF_3 Cl_2	[Rh$_2$(μ-Cl)$_2$(PF_3)$_2$(C_2H_4)$_2$]	Et_2O	27.0			407
Alkyl CF_3 $(CNR)_3$ I	[Rh(I)(Me)(CF_3)(xylylNC)$_3$]	clfm	15.8			406
CF_3 C_4F_9 $(CNR)_3$ I	[Rh(I)(CF_3)($^{n}C_4F_9$)(xylylNC)$_3$]	clfm	13.6			406
CF_3 aryl P_2 Cl	[Rh(Cl)(CF_3){2,6-($^{t}Bu_2PCH_2$)$_2$$C_6H_3$}]	benz	21.3	117		408
CF_3 $(CNR)_3$	[Rh(CF_3)(xylylNC)$_3$]	benz	24.3			406
CF_3 $(CNR)_3$ P	[Rh(CF_3)(xylylNC)$_3$(PPh_3)]	tol	8.1	76		409
	[Rh(CF_3)(xylylNC)$_3${P(4-$MeOC_6H_4$)$_3$}]	tol	7.5	76		409
CF_3 $(CNR)_2$ P	*trans*-[Rh(CF_3)(xylylNC)$_2$(PPh_3)]	tol	26.0	102	^{1}J(Rh,C) 59.7 (CN)	409
	trans-[Rh(CF_3)(xylylNC)$_2${P(4-$MeOC_6H_4$)$_3$}]	tol	25.2	102		409
	trans-[Rh(CF_3)(^{t}BuNC)$_2$(PPh_3)]	benz	27.4	146	^{1}J(Rh,C) 49.2 (CN)	409
CF_3 $(CNR)_2$ P (O_2)	[Rh(CF_3)(O_2)(xylylNC)$_2$(PPh_3)]	clfm	10.4	68	^{1}J(Rh,C) 60.6 (CN)	409
	[Rh(CF_3)(O_2)(xylylNC)$_2${P(4-$MeOC_6H_4$)$_3$}]	clfm	10.7	71	^{1}J(Rh,C) 54.4 (CN)	409
CF_3 $(CNR)_2$ P S	[Rh(CF_3)(xylylNC)$_2$(PPh_3)(SO_2)]	benz	19.8	92		406
CF_3 diene P	[Rh(CF_3)(cod)(PPh_3)]	benz	19	178		409
	[Rh(CF_3)(cod){P(4-$MeOC_6H_4$)$_3$}]	benz	20	176		409
	[Rh(CF_3)(cod)($P^{i}Pr_3$)]	benz?	17.9	159		409
	[Rh(CF_3)(cod)(PCy_3)]	benz?	19.2	161		409
	[Rh(CF_3)(nbd)(PPh_3)]	tol	22.0	183		409

CF_3 $(CO)_3$ P	$[Rh(CF_3)(CO)_3(PPh_3)]$	tol	8.0	70	^1J(Rh,C) 71.1 (CO)	409
CF_2R Cp* P O	$[Rh(Cp^*)(CF_2C_6F_4\text{-}2\text{-}O)(PMe_3)]$	acet	12	160		410
			8			
Allyl $(PF_3)_3$	$[Rh(allyl)(PF_3)_3]$*	benz[F]	18			411
Cp $(PF_3)_2$	$[Rh(Cp)(PF_3)_2]$	benz	32			412
$(PF_3)_2$ Cl_2	$[Rh_2(\mu\text{-}Cl)_2(PF_3)_4]$	benz	31.5			407
$(PF_3)_2$ Br_2	$[Rh_2(\mu\text{-}Br)_2(PF_3)_4]$	benz	31.5			413
$(PF_3)_2$ I_2	$[Rh_2(\mu\text{-}I)_2(PF_3)_4]$	benz	31			413
PF_3 P_2 Cl	*trans*-$[Rh(Cl)(PF_3)(PPh_3)_2]$	benz	32			407
$(PF_2R)_4$	$[Rh(PF_2NMe_2)_4]^-$ K^+ {Rh(–1)}	benz	~31			414
$(PF_2R)_2$ Cl_2	$[Rh_2(\mu\text{-}Cl)_2(PF_2NMe_2)_4]$	clfm	28			414
$(PF_2R)_2$ acac	$[Rh(acac)\{OC(NMePF_2)_2\}]$	clfm	17.7	278		415
$(PF_2R)_2$ Cl_2	$[Rh_2(\mu\text{-}Cl)_2\{OC(NMePF_2)_2\}_2]$	clfm	16.6	284		415
$(PFR_2)_2$ Cl_2	$[Rh(Cl)_2\{PF(O_2C_6H_4)\}_2]^-$ NMe_4^+	clfm	33.3	312		415
	$[Rh_2(\mu\text{-}Cl)_2\{PF(O_2C_6H_4)\}_4]$	clfm	31.7	320		415
$(PF_2R)_2$ Cl_2	$[Rh_2(\mu\text{-}Cl)_2\{PF_2CCl_3\}_4]$	clfm	21.0			407

[a]Some compounds exhibiting ^3J(Rh,F) and ^4J(Rh,F) in the range 1–7 Hz can be found in refs. 416 and 417.
[b]For details see Abbreviations.
[c] ^2J(Rh,F), absolute magnitude in Hz.
[d] ^1J(Rh,P), absolute magnitude in Hz. Signs probably negative (see Section 14).
[e] ^1J(Rh,X) (X = ^{13}C), absolute magnitude in Hz.

Table A7 $J(^{103}Rh,^{29}Si)$ and other data for Rh(I), Rh(III) and Rh(V) complexes

Coordination sphere	Compound[a]	Solvent[b]	^1J(Rh,Si)[c]	^1J(Rh,H)[d]	^1J(Rh,P)[e]	Reference
Alkene Cp H Si	[Rh(Cp)(H)($SiEt_3$)(C_2H_4)]	benz	22.2	33.2		320
Alkyl P N_2 Cl Si	[Rh(Cl)(CH_2Ph){MeSi(8-quinolyl)$_2$}(PPh_3)]	benz	74		167	418
Alkyl$_2$ N_2 Si	[Rh(CH_2Ph)$_2${MeSi(8-quinolyl)$_2$}]	DCM	60.3	3 (^2J)		418
Alkyl N_3 Si	[Rh(CH_2Ph){MeSi(8-quinolyl)$_2$}(CH_3CN)]$^+$ PF_6^-	DCM	40	2.5 (^2J)		418
Alkyl N_2 Si_2	[Rh(η^1-C_8H_{13})($SiPh_3$){MeSi(8-quinolyl)$_2$}]	benz	65 (SiMe) 45 ($SiPh_3$)			418
	[Rh(η^1-C_8H_{13})(Si($OSiMe_3$)$_3$){MeSi(8-quinolyl)$_2$}]	benz	69 (SiMe) 86 ($Si(O)_3$)			418
Allyl P N_2 Si	[Rh(η^3-CH_2Ph){MeSi(8-quinolyl)$_2$}(PPh_3)]$^+$ OTf^-	THF	70	~ 5.0 (^2J)	167	418
Cp (H)$_2$ Si_2	[Rh(Cp)(H)$_2$($SiEt_3$)$_2$] (Rh(V))	benz	16.6	38.3		320
Cp H P Si	[Rh(Cp)(H)($SiEt_3$)(PPh_3)]	benz	12.7	29.1	188	419
	[Rh(Cp)(H)(Si^iPr_3)(PPh_3)]	tol	9.8	28.2	185	419
Cp H Si_3	[Rh(Cp)(H)($SiEt_3$)$_3$] (Rh(V))	tol	22.9	35.3		371
	[Rh(Cp)(H)($SiMe_3$)$_3$] (Rh(V))	tol	22.5	36.6		371
	[Rh(Cp)(H)($SiEt_3$)$_2$($SiMe_3$)] (Rh(V))	tol	33.3 ($SiMe_3$) 19.2 ($SiEt_3$)	35.9		371
	[Rh(Cp)(H)($SiEt_3$)($SiMe_3$)$_2$] (Rh(V))	tol	26.6 ($SiMe_3$) 17.9 ($SiEt_3$)	35.4		371
Cp* (H)$_2$ Si_2	[Rh(Cp*)(H)$_2$($SiEt_3$){Si(OMe)$_3$}] (Rh(V))	ns	34.2 (SiO_3) 14.8 ($SiEt_3$)	38.6		420
Cp* P N Si	[Rh(Cp*)($SiPh_3$)(PMe_3)(4-$MeOC_6H_4CN$)]$^+$ B((CF_3)$_2$$C_6H_3$)$_4^-$	DCM	20		146	421
Diene N_2 Si	[Rh(cod){MeSi(8-quinolyl)$_2$}] (Rh(I))	benz	33			418
H_2 P_3 Si	[Rh(H)$_2$($SiHPh_2$){PhB($CH_2P^iPr_2$)$_2$}(PMe_3)]	benz	239			422
	fac-[Rh(H)$_2$($SiPh_2Cl$)(PMe_3)$_3$]	benz	41		100 90	423
H P_3 Cl Si	*mer*-[Rh(H)(Cl)($SiHPh_2$)(PMe_3)$_3$]	benz	43	15	100 90	423
	mer-[Rh(H)(Cl)($SiPh_2Cl$)(PMe_3)$_3$]	benz	48	15	94 93	423
	[Rh(H)(Cl)($Me_2Si(CH_2)_2PPh_2$)(PMe_3)$_2$]	benz	26.1	15	110 (PPh_2) 108 (PMe_3 *trans* to PPh_2)	424
H P_2 O Si	[Rh(H)($SiHPh_2$)(OTf)(P^iPr_3)$_2$]	tol	62	29.6	112	425

H P N_2 Si	$[Rh(H)\{MeSi(8\text{-quinolyl})_2\}(PPh_3)]^+ B(C_6F_5)_4^-$	DCM	40	22	144	418
H P_2 Cl Si	$[1,2\text{-}C_2\{SiMe_2Rh(H)(Cl)(P^iPr_3)_2\}_2]$	DCM	36.4		116	193
	$[Rh(H)(Cl)\{Si(OH)^iPr_2\}(PEt_3)_2]$	benz	31.4	27.2	119	426
	$[Rh(H)(Cl)\{Si(OSiMe_3)Me_2\}(PPh_3)_2]$	DCM	29.4	24	129	427
	$[Rh(H)(Cl)\{Si(OEt)_3\}(PPh_3)_2]$	DCM	49.6	24	122	427
	$[Rh(H)(Cl)\{Si(OEt)_2Me\}(PPh_3)_2]$	DCM	36.8	24	126	427
	$[Rh(H)(Cl)\{Si(OEt)Me_2\}(PPh_3)_2]$	DCM	29.4	24	128	427
H P_2 I Si	$[Rh(H)(I)\{Si(OSiMe_3)Me_2\}(PPh_3)_2]$	DCM	29.4	25	127	427
	$[Rh(H)(I)\{Si(OEt)_3\}(PPh_3)_2]$	DCM	49.2	26	120	427
	$[Rh(H)(I)\{Si(OEt)_2Me\}(PPh_3)_2]$	DCM	36.8	26	126	427
	$[Rh(H)(I)\{Si(OEt)Me_2\}(PPh_3)_2]$	DCM	29.4	26	125	427
H P Cl Si_2 Rh	$[Rh_2(H)_2(\mu\text{-}Cl)(\mu\text{-}SiPh_2)(\mu\text{-}SiPh_3)(P^iPr_3)_2]$	benz	50			428
	$[Rh_2(H)_2(\mu\text{-}Cl)\{\mu\text{-}Si(4\text{-}FC_6H_4)_2\}\{\mu\text{-}Si(4\text{-}FC_6H_4)_3\}(P^iPr_3)_2]$	benz	50			428
H N_2 Si_2	$[Rh(H)(SiPh_3)\{MeSi(8\text{-quinolyl})_2\}]$	benz	55 ($SiMe_3$) 55 ($SiPh_3$)	28		418
P_2 N_2 Cl Si	$[Rh(Cl)\{MeSi(8\text{-quinolyl})_2\}(PMe_3)_2]^+ Cl^-$	DCM	28		117	418
P_2 N_2 Si	$[Rh\{MeSi(8\text{-quinolyl})_2\}(Ph_2P(CH_2)_2PPh_2)]$ (Rh(I))	benz	145		190	418
P_2 O Si	$[Rh(SiPh_2OTf)(P^iPr_3)_2]$	tol	106		150	425
P N_2 Cl_2 Si	$[Rh(Cl)_2\{MeSi(8\text{-quinolyl})_2\}(PPh_3)]$	DCM	24.2		128	418
P N_2 Cl Si	$[Rh(Cl)\{MeSi(8\text{-quinolyl})_2\}(PPh_3)]^+ B(C_6F_5)_4^-$	DCM	29.5		126	418
N_5 Si	$[Rh\{MeSi(8\text{-quinolyl})_2\}(CH_3CN)_3]^{2+}$ $2OTf^-$	DCM	20.3			418
N_2 Cl_2 Si	$[Rh_2(Cl)_4\{MeSi(8\text{-quinolyl})_2\}_2]$	DMSO	22.0			418
Si_4	$[Rh\{cyclo\text{-}Si(1,2\text{-}(N^tBu)_2CHCH)\}_4]^+$	THF	82.5			429
	$[Rh\{cyclo\text{-}Si(1,2\text{-}(N^tBu)_2CH_2CH_2)\}_4]^+$	THF	76.6			429

[a]Some compounds exhibiting ^2J(Rh,Si) in the range 1.6–2.1 Hz can be found in ref. 430.
[b]For details see Abbreviations.
[c] ^1J(Rh,Si), absolute magnitude in Hz.
[d] ^1J(Rh,H), absolute magnitude in Hz. Signs probably negative (see Section 14).
[e] ^1J(Rh,P), absolute magnitude in Hz. Signs probably negative (see Section 14).

Table A8 $J(^{103}Rh,^{119}Sn)$ and other data for Rh(I) and Rh(III) compounds (see also Table A2)

Coordination sphere	Compound	Solvent[a]	^1J(Rh,Sn)[b]	^1J(Rh,H)[c]	^1J(Rh,P)[d]	Reference
Rh(I)						
Diene P_2 Sn	$[Rh(SnCl_3)(nbd)(PPh_3)_2]$	DCM/benz	580		132	431
	$[Rh(SnCl_2Br)(nbd)(PPh_3)_2]$	DCM/benz	543		132	431
	$[Rh(SnClBr_2)(nbd)(PPh_3)_2]$	DCM/benz	513		133	431
	$[Rh(SnBr_3)(nbd)(PPh_3)_2]$	DCM/benz	482		133	431
	$[Rh(SnCl_3)(nbd)(PEtPh_2)_2]$	DCM/benz	543		131	431
	$[Rh(SnCl_2Br)(nbd)(PEtPh_2)_2]$	DCM/benz	525		132	431
	$[Rh(SnClBr_2)(nbd)(PEtPh_2)_2]$	DCM/benz	482		132	431
	$[Rh(SnBr_3)(nbd)(PEtPh_2)_2]$	DCM/benz	452		131	431
Diene N_2 Sn	$[Rh(SnCl_3)(nbd)(PhNC(Me)C(Me)NPh)]$	acet	615			432
	$[Rh(SnCl_3)(nbd)(H_2NNC(Me)C(Me)NOH)]$	acet	535			432
	$[Rh(SnCl_3)(nbd)(H_2NNC(Me)C(Me)NNH_2)]$	acet	535			432
Diene Cl Sn	$[Rh(Sn(HC\{SiMe_2N(2\text{-}MeOC_6H_4)\}_3(cod)(LiCl)]$	benz	872			433
Sn_5	$[Rh(SnCl_3)_5]^{4-}$	HCl (aq)	806			434
Rh(III)						
Cp* CO H Sn	$[Rh(Cp^*)(H)(SnMe_3)(CO)]$	benz	221	29.6		337
	$[Rh(Cp^*)(H)(Sn^nBu_3)(CO)]$	benz	210	29.3		337
Cp* N_2 Sn	$[Rh(Cp^*)(4,4\text{-}^tBu_2\text{-}2,2'\text{-bipy})(SnB_{11}H_{11})]$	DMSO	~700			435
Cl_5 Sn	$[Rh(SnCl_3)Cl_5]^{3-}$	HCl (aq)	864			434
Cl_4 Sn_2	$[Rh(SnCl_3)_2Cl_4]^{3-}$	HCl (aq)	796			434
Cl_3 Sn_3	$[Rh(SnCl_3)_3Cl_3]^{3-}$	HCl (aq)	718			434
Cl_2 Sn_4	$[Rh(SnCl_3)_4Cl_2]^{3-}$	HCl (aq)	590			434
Cl Sn_5	$[Rh(SnCl_3)_5Cl]^{3-}$	HCl (aq)	547			434
Rh(V)						
Cp* $(H)_2$ Sn_2	$[Rh(Cp^*)(H)_2(SnMe_3)_2]$	benz	151	28.3		337
	$[Rh(Cp^*)(H)_2(Sn^nBu_3)_2]$	benz	146	27.3		337
$(H)_3$ P_2 Sn_2	$[Rh(H)(\mu\text{-}H)_2(Sn^nBu_3)_2(PPh_3)_2]$	tol	103	14.1	103	436
	$[Rh(H)(\mu\text{-}H)_2(SnPh_3)_2(PPh_3)_2]$	tol	148	11.9	100	436

[a]For details see Abbreviations.
[b]^1J(Rh,Sn), absolute magnitude in Hz. Signs probably positive, (see Section 14).
[c]^1J(Rh,H), absolute magnitude in Hz. Signs probably negative, (see Section 14).
[d]^1J(Rh,H), absolute magnitude in Hz. Signs probably negative, (see Section 14).

Table A9 $J(^{103}Rh,^{77}Se)$ and other data for Rh(I) and Rh(III) complexes

Coordination sphere	Compound		Solvent[a]	^1J(Rh,Se)[b]	^1J(Rh,P)[c]	Reference(s)
Vinyl Cp* P Se	[Rh(Cp*)(k^2-SeCHCHCHCH)(PMe_3)]		benz	56.3	159	437
Cp P Se_2	[Rh(Cp)($SePh)_2$(PMe_3)]		clfm	56	143	336
Cp Se_3	[Rh_2(Cp)$_2$($Se^1Ph)_2$(μ-$Se^2Ph)_2$]		clfm	(1) 59.0		438
				(2) 47.5		
	[Rh_2(Cp)$_2$(μ-SePh)$_3$]$^+$ Cl^-		clfm	43.5		438
Cp* P Se_2	[Rh(Cp*)($SePh)_2$(PMe_3)]		clfm	53	148	336, 338
Cp* P Se_2	[Rh(Cp*){$Se_2C_2(B_{10}H_{10})$}(PMe_3)]		clfm	26 ± 4	148	338
Cp* Se_3	[Rh(Cp*){$MeC(CH_2SeMe)_3$}]$^{2+}$ 2PF_6^-		acnl/ clfm	34		439
	[Rh_2(Cp*)$_2$(μ-$Se^1Ph)_3$]$^+$[Rh(Cp*)($Se^2Ph)_3$]$^-$		THF	(1) 41.0		438
				(2) 56.0		
Cp* Se_2	[Rh(Cp*)($SePh)_2$]		clfm	50.5		438
	[Rh(Cp*){$Se_2C_2(B_{10}H_{10})$}]		DCM	138 ± 5		338
Cl_2 Se_4	*cis*-[$Rh(Cl)_2$(1,5-diselenacyclooctane)$_2$]$^+$ BF_4^-		DMF	43		440
				36		
	trans-[$Rh(Cl)_2$(1,5-diselenacyclooctane)$_2$]$^+$ BF_4^-		DMF	42		440
	cis-[$Rh(Cl)_2$(1,5,9,13-tetraselenacyclohexadecane)]$^+$ PF_6^-		DMF	37		440
				36		
	trans-[$Rh(Cl)_2$(1,5,9,13-tetraselenacyclohexadecane)]$^+$ PF_6^-		nitr	30		440, 441
Cl_3 Se_3	[$Rh(Cl)_3${$MeC(CH_2SeMe)_3$}]	(a)	DMSO	41		442
	Conformers	(b)		39		
				38		
	[$Rh(Cl)_3${$(MeSeCH_2CH_2CH_2)_2Se$}]	(a)	DCM	43.5		442
	Conformers			39		
		(b)		52		
				50		
		(c)		42		
				38		
				37		
Br_2 Se_4	*cis*-[$Rh(Br)_2$(1,5,9,13-tetraselenacyclohexadecane)]$^+$ PF_6^-		DMF	37		440
				36		
	trans-[$Rh(Br)_2$(1,5,9,13-tetraselenacyclohexadecane)]$^+$ PF_6^-		nitr	32		440
Se_6	[Rh{$MeC(CH_2SeMe)_3$}$_2$]$^{3+}$ 3PF_6^-		nitr/ clfm	43		443
				42		

[a]For details see Abbreviations.
[b]^1J(Rh,Se), absolute magnitude in Hz.
[c]^1J(Rh,P), absolute magnitude in Hz.

Table A10 $J(^{103}Rh,^{125}Te)$ and other data for Rh(I) and Rh(III) complexes

Coordination sphere	Compound		Solvent[a]	^1J(Rh,Te)[b]	^1J(Rh,P)[c]	^1J(Rh,X)[d]	Reference(s)
Vinyl Cp Te Rh	$[(TeEt_2)Rh(Cp)\{\mu\text{-}C_2(CF_3)_2\}Rh(Cp)(CO)]$		clfm	110		^3J(Rh,F) 3.4, 2.8	444
	$[Te(CMe_2)_4Rh(Cp)\{\mu\text{-}C_2(CF_3)_2\}Rh(Cp)(CO)]$		benz	86		^3J(Rh,F) 3.2, 2.7	444
Cp* diene-Te	$[Rh(Cp^*)(\text{tellurophene})]^{2+}$ $2OTf^-$		acet	20		J(Rh,C) 7.6, 4.4 (C_4H_4Te) 7.6 (Cp*)	445
Cp* P Te_2	$[Rh(Cp^*)\{Te_2C_2(B_{10}H_{10})\}(PMe_3)]$		clfm	45 ± 5	146		338
Cp* S_2 Te	$[Rh(Cp^*)\{MeS(CH_2)_3Te(CH_2)_3SMe\}]^+$ PF_6^-		acet	94			446
Cp* Te_3	$[Rh(Cp^*)\{MeC(CH_2TeMe)_3\}]^{2+}$ $2PF_6^-$		acnl/clfm	91			439
	$[Rh(Cp^*)\{MeC(CH_2TePh)_3\}]^{2+}$ $2PF_6^-$		acnl/clfm	91			439
Cp* Te_3	$[Rh(Cp^*)\{Te(CH_2CH_2CH_2TeMe)_2\}]^{2+}$ $2PF_6^-$	(a)	acet	95			447
	Conformers	(b)		89			
		(c)		80			
	$[Rh(Cp^*)\{Te(CH_2CH_2CH_2TePh)_2\}]^{2+}$ $2PF_6^-$	(a)	acet	98			447
	Conformers	(b)		93			
		(c)		80			
Cp* Te	$[Rh(Cp^*)(\text{dibenzotellurophene})]^{2+}$ $2OTf^-$		acet	88			445
Cp* Cl_2 Te	$[Rh(Cp^*)(Cl)_2(\text{dibenzotellurophene})]$		acet	142		^1J(Rh,C) 7.6	445
	$[Rh(Cp^*)(Cl)_2(2\text{-telluraindane})]$		clfm	108			445, 448
Cp* Te	$[Rh(Cp^*)(2\text{-telluraindane})]^{2+}$ $2OTf^-$		clfm	66			448
Diene Te_3	$[Rh(cod)\{MeC(CH_2TeMe)_3\}]^+$ PF_6^-		clfm/DCM	79			439
Cl_2 Te_4	$[RhCl)_2\{MeTe(CH_2)_3TeMe\}_2]^+$ PF_6^-		clfm/DCM	60			449
	$[RhCl)_2\{PhTe(CH_2)_3TePh\}_2]^+$ PF_6^-		clfm/DCM	75			449
	$[RhCl)_2\{o\text{-}C_6H_4(TeMe)_2\}_2]^+$ PF_6^-		clfm/DCM	90			449
Cl_3 Te_3	$[RhCl)_3(1,3\text{-dihydrobenzo[c]tellurophene})_3]$	(a)	clfm	90			450
	{*fac* (a) and *mer* (b) isomers}	(b)		70			
	$[RhCl)_3\{Te(CH_2)_4\}_3]$	(a)	DCM	92			451
	{*fac* (a) and *mer* (b) isomers}	(b)		95			
				72			

[a]For details see Abbreviations.
[b]^1J(Rh,Te), absolute magnitude in Hz. Signs probably positive (see Section 14).
[c]^1J(Rh,P), absolute magnitude in Hz. Signs (all) probably negative (see Section 14).
[d]J(Rh,X) (X = ^{13}C, ^{19}F), absolute magnitude in Hz. Sign of $^1J(^{103}Rh,^{19}F)$ probably negative.

Table A11 $J(^{103}Rh,^{103}Rh)$ and $J(^{103}Rh,M)$ (M = ^{183}W, ^{195}Pt, ^{199}Hg, ^{207}Tl)

Coordination sphere	Compound		Solvent[a]	J(Rh,Rh)[b]	J(Rh,M)[c]	Reference
Alkene vinyl indenyl Rh	$[Rh_2(C_9H_7)_2(\mu\text{-}CHCH_2)_2]$		benz	17.0		258
Alkyl carbene$_2$ Cp* Rh	$[Rh_2(Cp^*)_2(\mu\text{-}CH_2)_2\{(\mu\text{–}(CH_2)_2CHCH_2CHCH_2\}]$		acet	13.5		452
	$[Rh_2(Cp^*)_2\{(\mu\text{-}CH_2)_2(\mu\text{–}CH_2)_2CMeCH_2CMeCH_2\}]$		acet	13.2		452
Carbene$_2$ Cp* P Rh	$[Rh_2(Cp^*)_2(\mu\text{-}CH_2)_2(\mu\text{-}Ph_2PCH_2PPh_2)]^{2+}$ $2PF_6^-$		clfm	12.4		452
	$[Rh_2(Cp^*)_2(\mu\text{-}CH_2)_2(\mu\text{-}Ph_2PCH_2CH_2PPh_2)]^{2+}$ $2PF_6^-$		clfm	11.9		452
Carbene Cp CO Rh	$[Rh_2(Cp)_2(\mu\text{-}CH_2)(CO)_2]$		benz	4.4		453
Cp $(CO)_2$ Rh	$[Rh_2(Cp)_2(\mu\text{-}CO)(CO)_2]$		clfm	4.2		453
Cp H_3 P Rh	$[Rh_2(Cp)_2(\mu\text{-}H)_3(P^iPr_3)_2]$		nitr	11.4		454
Cp $(NO)_2$ Rh	$[Rh_2(Cp)_2(\mu\text{-}NO)_2]$		clfm	4.4		453
CO H P_2 Si Rh	$[Rh_2(H)_2(CO)_2(\mu\text{-}SiHPh)(\mu\text{-}Ph_2PCH_2PPh_2)_2]$		DCM	5		455
CO P_2 O Rh	$[Rh_2(CO)_2(\mu\text{-}OAc)(\mu\text{-}Ph_2PCH_2PPh_2)_2]^+$ BPh_4^-		DCM	0.7		456
$(CO)_2$ P_2 Cl Rh	$[Rh_2(\mu\text{-}Cl)(CO)_2(\mu\text{-}CO)(\mu\text{-}Ph_2PCH_2PPh_2)_2]^+$ BPh_4^-		DCM	128 ± 25		457
CO P_2 Cl Rh	$[Rh_2(CO)_2(\mu\text{-}Cl)(\mu\text{-}Ph_2PCH_2PPh_2)_2]^+$ BPh_4^-		DCM	25		457
CO P S_2 Rh	$[Rh_2(CO)_2\{P(OPh)_3\}_2(\mu_3\text{-}S)_2\{Zr(\eta^5\text{-}1,3^tBu_2C_5H_3)_2\}]$	(a)	benz	21		458
	(Rotamers)	(b)		24		
H_2 P Cl Si Rh	$[Rh_2(H)_2(\mu\text{-}H)(\mu\text{-}Cl)(SiPh_3)_2(P^iPr_3)_2]$		benz	49		459
	$[Rh_2(H)_2(\mu\text{-}H)(\mu\text{-}Cl)\{Si(4\text{-}CF_3OC_6H_4)_3\}_2(P^iPr_3)_2]$		benz	44		459
	$[Rh_2(H)_2(\mu\text{-}H)(\mu\text{-}Cl)\{\mu\text{-}^iPr_2SiOSi^iPr_2\}(P^iPr_3)_2]$		benz	45		459
P_2 Cl S Rh	$[Rh_2Cl_2(\mu\text{-}SO_2)(\mu\text{-}Ph_2PCH_2PPh_2)_2]$		DCM	167 ± 15		457
S_6	$[Rh\{(\mu\text{-}S)_2W(S)_2\}_3]^{3-}$ $3NEt_4^+$		DMF		$^1J(^{183}W,^{103}Rh)$ 4.8	460
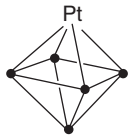	$[Rh_5Pt(CO)_{15}]^-$ NEt_4^+		THF		$^1J(^{195}Pt,^{103}Rh)$ 24.4 $^2J(^{195}Pt,^{103}Rh)$ 73.2	461
CO P_2 Cl_2 Hg	$[Rh(Cl)_2(HgCl)(CO)(PEtPh_2)_2]$		DCM?		$^1J(^{199}Hg,^{103}Rh)$ 426	462
N_4 Tl	$[Rh(Ph_4\ porphyrin)Tl(Ph_4\ porphyrin)]$		clfm		$^1J(^{205}Tl,^{103}Rh)$ 5,319	248
	$[Rh(Ph_4\ porphyrin)Tl(Et_8\ porphyrin)]$		clfm		$^1J(^{205}Tl,^{103}Rh)$ 5,100	248
	$[Rh(Et_8\ porphyrin)Tl(Ph_4\ porphyrin)]$		clfm		$^1J(^{205}Tl,^{103}Rh)$ 5,255	248
	$[Rh(Et_8\ porphyrin)Tl(Et_8\ porphyrin)]$		clfm		$^1J(^{205}Tl,^{103}Rh)$ 5,249	248

[a] For details see Abbreviations.
[b] ^1J(Rh,Rh), absolute magnitude in Hz. Sign likely to be positive (see Section 14).
[c] ^1J(Rh,M), signs have not been measured.

Table A12 Relaxation times

Coordination sphere	Compound	Solvent[a]	T (K)	Field (T)	T_1 (s)	T_2/s	Reference
Alkene$_2$ acac	[Rh(acac)(C_2H_4)$_2$]	DCM	270	9.4	1.7		297
		DCM	250	9.4	0.9		
Allyl$_3$	[Rh(η^3-allyl)$_3$]	tol	270	9.4	18.2		297
			250	9.4	13.1		
Allyl$_2$ acac	Rh(η^3-allyl)$_2$(acac)]	DCM	270	9.4	5.9		297
		DCM	250	9.4	3.0		
Allyl Cp*	[Rh(Cp*)(η^3-$CH_2CMeCMe_2$)]$^+BF_4^-$	DCM	296	9.4	5.6		277
		DCM	203	9.4	0.8		
Cp diene	[Rh(Cp)(cod)]	benz	300	2.1	60±4	27±1	23
		tol	339	9.4	12.7		250
		tol	309	9.4	8.6		250
		tol	271	9.4	5.2		250
		tol	240	9.4	2.4		250
Cp*diene	[Rh(Cp*)(2,3-Me_2butadiene)]	benz	296	9.4	6.5		277
		benz	203	9.4	0.7		
Cp* P Cl_2	[Rh(Cp*)$(Cl)_2(PPh_3)$]	DCM	300	9.4	1.5		463
				14.1	0.7		
Diene N_2	[Rh(1-NMe-2-$NMe_2C_6H_4$)(cod)]	THF	310	9.4	1.5		297
		THF	310	5.9	3.6		297
		THF	290	9.4	1.1		297
Diene acac	[Rh(acac)(1,2-(CH_2CH)cyclobutane)]	DCM	310	9.4	1.5		297
Diene Cl_2	[$Rh_2(Cl)_2(cod)_2$]	benz	310	9.4	1.7		297
		benz	310	5.9	3.5		297
Diene N_2	[Rh(BPz_4)(cod)]	clfm	298	9.4	0.51(±0.05)		295
		clfm	213	9.4	0.060 (±0.002)		
	[Rh(BPz_4)(nbd)]	clfm	298	9.4	0.53 (±0.07)		295
	[Rh(BPz_4)(duroquinone)]	clfm	298	9.4	0.62 (±0.05)		295
$acac_3$	[Rh$(acac)_3$]	clfm	300	2.1	62.8 (±4.4)	51.0 (±3.6)	356
		clfm	325	9.4	32		297
			310	9.4	39		
		clfm	300	2.1	82±3	67±2	23

[a]For details see Abbreviations.

REFERENCES

1. W. von Philipsborn, *Pure Appl. Chem.*, 1986, **58**, 513.
2. W. von Philipsborn, *Chem. Soc. Rev.*, 1999, **28**, 95.
3. R. G. Kidd and R. J. Goodfellow, in: *NMR and the Periodic Table*, R. K. Harris and B. E. Mann, eds., Academic Press, London, 1978.
4. R. G. Kidd, *Ann. Rep. NMR Spectrosc.*, 1980, **10a**, 1.
5. J. J. Dechter, *Prog. Inorg. Chem.*, 1985, **33**, 393.
6. R. Benn and A. Rufińska, *Angew. Chem. Int. Ed. Engl.*, 1986, **25**, 861.
7. J. Mason, *Chem. Rev.*, 1987, **87**, 1299.
8. R. J. Goodfellow, in: *Multinuclear NMR*, J. Mason, ed., Plenum, New York, 1987.
9. D. Rehder, *Coord. Chem. Rev.*, 1991, **110**, 161.
10. B. E. Mann, *Ann. Rep. NMR Spectrosc.*, 1991, **23**, 141.
11. G. A. Kirakosyan, *Koord. Khim.*, 1993, **19**, 507.
12. B. Wrackmeyer, *Chem. Unserer Zeit*, 1994, **28**, 309.
13. L. Öhrström, *Comments Inorg. Chem.*, 1996, **18**, 305.
14. P. Granger, in: *Advanced Applications of NMR to Organometallic Chemistry*, M. Gielen, R. Willem and B. Wrackmeyer, eds., Wiley, Chichester, 1996.
15. F. López-Ortiz and R. J. Carbajo, *Curr. Org. Chem.*, 1998, **2**, 97.
16. J. Fraissard, *Catal. Today*, 1999, **51**, 481.
17. B. E. Mann, in: *NMR of Newly Accessible Nuclei*, P. Laszlo, ed., Academic Press, New York, 1983.
18. B. E. Mann, in: *Transition Metal NMR*, P. S. Pregosin, ed., Elsevier, Amsterdam, 1991.
19. J. M. Ernsting, S. Gaemers and C. J. Elsevier, *Magn. Reson. Chem.*, 2004, **42**, 721.
20. D. S. Gill, O. A. Gansow, F. J. Bennis and K. C. Ott, *J. Magn. Reson.*, 1979, **35**, 459.
21. G. A. Morris and R. Freeman, *J. Am. Chem. Soc.*, 1979, **101**, 760.
22. D. M. Doddrell, D. T. Pegg and M. R. Bendall, *J. Magn. Reson.*, 1982, **48**, 323.
23. E. Maurer, S. Rieker, M. Schollbach, A. Schwenk, T. Egolf and W. von Philipsborn, *Helv. Chim. Acta*, 1982, **65**, 26.
24. C. Brevard, G. C. van Stein and G. van Koten, *J. Am. Chem. Soc.*, 1981, **103**, 6746.
25. C. Brevard and R. Schimpf, *J. Magn. Reson.*, 1982, **47**, 528.
26. B. T. Heaton, J. A. Iggo, I. S. Podkorytov, D. J. Smawfield, S. P. Tunk and R. Whyman, *J. Chem. Soc. Dalton Trans.*, 1999, 1917.
27. B. T. Heaton, J. A. Iggo, I. S. Podkorytov and S. P. Tunik, *Magn. Reson. Chem.*, 2004, **42**, 769.
28. L. Carlton, *Magn. Reson. Chem.*, 1997, **35**, 153.
29. A. Bax, R. H. Griffey and B. L. Hawkins, *J. Magn. Reson.*, 1983, **55**, 301.
30. R. Benn and A. Rufińska, *Magn. Reson. Chem.*, 1988, **26**, 895.
31. D. Nanz and W. von Philipsborn, *J. Magn. Reson.*, 1991, **92**, 560.
32. S. Berger, T. Fäcke and R. Wagner, *Magn. Reson. Chem.*, 1996, **34**, 4.
33. G. A. Webb, in: *NMR and the Periodic Table*, R. K. Harris and B. E. Mann, eds., Academic Press, London, 1978.
34. G. A. Webb, in: *NMR of Newly Accessible Nuclei*, P. Laszlo, ed., Academic Press, New York, 1983.
35. C. J. Jameson and J. Mason, in: *Multinuclear NMR*, J. Mason, ed., Plenum Press, New York, 1987, Chapter 3.
36. N. Juranić, *Coord. Chem. Rev.*, 1989, **96**, 253.
37. C. K. Jørgensen, *Progr. Inorg. Chem.*, 1962, **4**, 73.
38. C. K. Jørgensen, *Struct. Bond.*, 1966, **1**, 3.
39. F. A. Cotton and G. Wilkinson, *Advanced Inorganic Chemistry*, Third Edition, Wiley, New York, 1972, 604–605.
40. R. F. Fenske, K. G. Caulton, D. D. Radtke and C. C. Sweeney, *Inorg. Chem.*, 1966, **5**, 960.
41. B. E. Mann and C. M. Spencer, *Inorg. Chim. Acta*, 1983, **76**, L65.
42. M. C. Read, J. Glaser and M. Sandström, *J. Chem. Soc. Dalton Trans.*, 1992, 233.
43. F. A. Cotton and G. Wilkinson, *Advanced Inorganic Chemistry*, Third Edition, Wiley, New York, 1972, 577–578.
44. N. F. Ramsey, *Phys. Rev.*, 1950, **78**, 699.
45. W. Bramley, M. Brorson, A. M. Sargeson and C. E. Schäffer, *J. Am. Chem. Soc.*, 1985, **107**, 2780.

46. N. Juranić, *Inorg. Chem.*, 1985, **24**, 1599.
47. N. Juranić, *J. Am. Chem. Soc.*, 1988, **110**, 8341.
48. N. Juranić, *J. Magn. Reson.*, 1987, **71**, 144.
49. M. C. Read, J. Glaser, I. Persson and M. Sandström, *J. Chem. Soc. Dalton Trans.*, 1994, 3243.
50. B. Åkermark, M. R. A. Blomberg, J. Glaser, L. Öhrström, S. Wahlberg, K. Wärnmark and K. Zetterberg, *J. Am. Chem. Soc.*, 1994, **116**, 3405.
51. R. Weiss and J. G. Verkade, *Inorg. Chem.*, 1979, **18**, 529.
52. J. G. Verkade, *Pure Appl. Chem.*, 1980, **52**, 1131.
53. R. Freeman, G. R. Murray and R. E. Richards, *Proc. Roy. Soc. Lond. Ser. A*, 1957, **242**, 455.
54. G. B. Benedek, R. Englman and J. A. Armstrong, *J. Chem. Phys.*, 1963, **39**, 3349.
55. T. H. Brown and S. M. Cohen, *J. Chem. Phys.*, 1973, **58**, 395.
56. C. J. Jameson, *J. Am. Chem. Soc.*, 1987, **109**, 2586.
57. C. J. Jameson, D. Rehder and M. Hoch, *J. Am. Chem. Soc.*, 1987, **109**, 2589.
58. A. D. Buckingham, T. Schaefer and W. G. Schneider, *J. Chem. Phys.*, 1960, **32**, 1227.
59. I. Ando and G. A. Webb, *Org. Magn. Reson.*, 1981, **15**, 111.
60. L. Carlton, *Magn. Reson. Chem.*, 2004, **42**, 760.
61. B. Åkermark, J. Glaser, L. Öhrström and K. Zetterberg, *Organometallics*, 1991, **10**, 733.
62. J. M. Ernsting, C. J. Elsevier, W. G. J. de Lange and K. Timmer, *Magn. Reson. Chem.*, 1991, **29**, S118.
63. M. Bühl, W. Baumann, R. Kadyrov and A. Börner, *Helv. Chim. Acta*, 1999, **82**, 811.
64. S. Borns, R. Kadyrov, D. Heller, W. Baumann, A. Spannenberg, R. Kempe, J. Holz and A. Börner, *Eur. J. Inorg. Chem.*, 1998, 1291.
65. E. Lindner, B. Keppeler, R. Fawzi and M. Steimann, *Chem. Ber.*, 1996, **129**, 1103.
66. U. E. Bucher, A. Currao, R. Nesper, H. Rüegger, L. M. Venanzi and E. Younger, *Inorg. Chem.*, 1995, **34**, 66.
67. U. E. Bucher, T. F. Fässler, M. Hunziker, R. Nesper, H. Rüegger and L. M. Venanzi, *Gaz. Chim. Ital.*, 1995, **125**, 181.
68. B. R. Bender, M. Koller, D. Nanz and W. Von Philipsborn, *J. Am. Chem. Soc.*, 1993, **115**, 5889.
69. T. Ohkuma and R. Noyori, *Chemtracts Org. Chem.*, 1993, **6**, 325.
70. H. Schumann, O. Stenzel, S. Dechert, F. Girgsdies and R. L. Halterman, *Organometallics*, 2001, **20**, 2215.
71. D. Magiera, W. Baumann, I. S. Podkorytov, J. Omelanczuk and H. Duddeck, *Eur. J. Inorg. Chem.*, 2002, 3253.
72. R. Zurawinski, B. Donnadieu, M. Mikolajczyk and R. Chauvin, *Organometallics*, 2003, **22**, 4810.
73. C. Meyer, M. Scherer, H. Schönberg, H. Rüegger, S. Loss, V. Gramlich and H. Grützmacher, *J. Chem. Soc. Dalton Trans.*, 2006, 137.
74. F. Näumann, D. Rehder and V. Pank, *J. Organomet. Chem.*, 1982, **240**, 363.
75. H. C. E. McFarlane, W. McFarlane and D. S. Rycroft, *J. Chem. Soc. Dalton Trans.*, 1976, 1616.
76. C. Brown, B. T. Heaton and J. Sabounchei, *J. Organomet. Chem.*, 1977, **142**, 413.
77. J. Ruiz, B. E. Mann, C. M. Spencer, B. F. Taylor and P. M. Maitlis, *J. Chem. Soc. Dalton Trans.*, 1987, 1963.
78. C. J. Jameson, *J. Chem. Phys.*, 1977, **66**, 4983.
79. C. J. Jameson and H. J. Osten, *Ann. Rep. NMR Spectrosc.*, 1986, **17**, 1.
80. M. R. Bendall and D. M. Doddrell, *Aust. J. Chem.*, 1978, **31**, 1141.
81. D. Nanz, W. von Philipsborn, U. E. Bucher and L. M. Venanzi, *Magn. Reson. Chem.*, 1991, **29**, S38.
82. L. Carlton, unpublished results.
83. W. Kuhr, G. Peters and W. Preetz, *Z. Naturforsch.*, 1989, **44b**, 1402.
84. M. Bühl, M. Håkansson, A. H. Mahmoudkhani and L. Öhrström, *Organometallics*, 2000, **19**, 5589.
85. R. Cramer, *J. Am. Chem. Soc.*, 1967, **89**, 4621.
86. L. P. Hammett, *J. Am. Chem. Soc.*, 1937, **59**, 96.
87. H. H. Jaffé, *Chem. Rev.*, 1953, **53**, 191.
88. D. H. McDaniel and H. C. Brown, *J. Org. Chem.*, 1958, **23**, 420.
89. C. Hansch, A. Leo and R. W. Taft, *Chem. Rev.*, 1991, **91**, 165.
90. P. B. Graham, M. D. Rausch, K. Täschler and W. von Philipsborn, *Organometallics*, 1991, **10**, 3049.
91. W. Leitner, M. Bühl, R. Fornika, C. Six, W. Baumann, E. Dinjus, M. Kessler, C. Krüger and A. Rufińska, *Organometallics*, 1999, **18**, 1196.

92. F. R. Bregman, J. M. Ernsting, F. Müller, M. D. K. Boele, L. A. van der Veen and C. J. Elsevier, *J. Organomet. Chem.*, 1999, **592**, 306.
93. V. Tedesco and W. von Philipsborn, *Organometallics*, 1995, **14**, 3600.
94. M. Koller and W. von Philipsborn, *Organometallics*, 1992, **11**, 467.
95. R. Fornika, H. Görls, B. Seemann and W. Leitner, *J. Chem. Soc. Chem. Commun.*, 1995, 1479.
96. M. Cheong and F. Basolo, *Organometallics*, 1988, **7**, 2041.
97. D. L. Lichtenberger, S. K. Renshaw, F. Basolo and M. Cheong, *Organometallics*, 1991, **10**, 148.
98. M. Bassetti, G. J. Sunley, F. P. Fanizzi and P. M. Maitlis, *J. Chem. Soc. Dalton Trans.*, 1990, 1799.
99. C. A. Tolman, *Chem. Rev.*, 1977, **77**, 313.
100. V. Tedesco and W. von Philipsborn, *Magn. Reson. Chem.*, 1996, **34**, 373.
101. K. Angermund, W. Baumann, E. Dinjus, R. Fornika, H. Görls, M. Kessler, C. Krüger, W. Leitner and F. Lutz, *Chem. Eur. J.*, 1997, **3**, 755.
102. C. J. Elsevier, B. Kowall and H. Kragten, *Inorg. Chem.*, 1995, **34**, 4836.
103. J. G. Donkervoort, M. Bühl, J. M. Ernsting and C. J. Elsevier, *Eur. J. Inorg. Chem.*, 1999, 27.
104. F. Asaro, G. Costa, R. Dreos, G. Pellizer and W. von Philipsborn, *J. Organomet. Chem.*, 1996, **513**, 193.
105. D. Blazina, S. B. Duckett, J. P. Dunne and C. Godard, *J. Chem. Soc. Dalton Trans.*, 2004, 2601.
106. C. R. Bowers and D. P. Weitekamp, *J. Am. Chem. Soc.*, 1987, **109**, 5541.
107. T. Eisenschmid, R. U. Kirss, P. P. Deutsch, S. I. Hommeltoft, R. Eisenberg, J. Bargon, R. G. Lawler and A. L. Balch, *J. Am. Chem. Soc.*, 1987, **109**, 8089.
108. S. B. Duckett, G. K. Barlow, M. G. Partridge and B. A. Messerle, *J. Chem. Soc. Dalton Trans.*, 1995, 3427.
109. P. D. Morran, S. A. Colebrooke, S. B. Duckett, J. A. B. Lohman and R. Eisenberg, *J. Chem. Soc. Dalton Trans.*, 1998, 3363.
110. B. A. Messerle, C. J. Sleigh, M. G. Partridge and S. B. Duckett, *J. Chem. Soc. Dalton Trans.*, 1999, 1429.
111. P. D. Morran, S. B. Duckett, P. R. Howe, J. E. McGrady, S. A. Colebrooke, R. Eisenberg, M. G. Partridge and J. A. B. Lohman, *J. Chem. Soc. Dalton Trans.*, 1999, 3949.
112. S. A. Colebrooke, S. B. Duckett and J. A. B. Lohman, *J. Chem. Soc. Chem. Commun.*, 2000, 685.
113. C. Godard, P. Callaghan, J. L. Cunningham, S. B. Duckett, J. A. B. Lohman and R. N. Perutz, *J. Chem. Soc. Chem. Commun.*, 2002, 2836.
114. S. A. Colebrooke, S. B. Duckett, J. A. B. Lohman and R. Eisenberg, *Chem. Eur. J.*, 2004, **10**, 2459.
115. R. Zhou, J. A. Aguilar, A. Charlton, S. B. Duckett, P. I. P. Elliott and R. Kandiah, *J. Chem. Soc. Dalton Trans.*, 2005, 3773.
116. R. Eisenberg, *Acc. Chem. Res.*, 1991, **24**, 110.
117. S. B. Duckett and D. Blazina, *Eur. J. Inorg. Chem.*, 2003, 2901.
118. M. C. Payne and D. J. Cole-Hamilton, *J. Chem. Soc. Dalton Trans.*, 1997, 3167.
119. C. Bianchini, M. V. Jiménez, A. Meli, S. Moneti, V. Patinec and F. Vizza, *Organometallics*, 1997, **16**, 5696.
120. I. T. Horváth, G. Kiss, R. A. Cook, J. E. Bond, P. A. Stevens, J. Rábai and E. Mozeleski, *J. Am. Chem. Soc.*, 1998, **120**, 3133.
121. C. Bianchini, H. M. Lee, A. Meli and F. Vizza, *Organometallics*, 2000, **19**, 849.
122. R. Churlaud, U. Frey, F. Metz and A. E. Merbach, *Inorg. Chem.*, 2000, **39**, 304, 4137.
123. U. Nettekoven, P. C. J. Kamer, M. Widhalm and P. W. N. M van Leeuwen, *Organometallics*, 2000, **19**, 4596.
124. S. C. van der Slot, P. C. J. Kamer, P. W. N. M van Leeuwen, J. A. Iggo and B. T. Heaton, *Organometallics*, 2001, **20**, 430.
125. I. del Rio, W. G. J. de Lange, P. W. N. M. van Leeuwen and C. Claver, *J. Chem. Soc. Dalton Trans.*, 2001, 1293.
126. C. R. Yonker and J. C. Linehan, *J. Organomet. Chem.*, 2002, **650**, 249.
127. L. Ropartz, K. J. Haxton, D. F. Foster, R. E. Morris, A. M. Z. Slawin and D. J. Cole-Hamilton, *J. Chem. Soc. Dalton Trans.*, 2002, 4323.
128. R. P. J. Bronger, P. C. J. Kamer and P. W. N. M. van Leeuwen, *Organometallics*, 2003, **22**, 5358.
129. V. E. Slagt, P. W. N. M. van Leeuwen and J. N. H. Reek, *Angew. Chem. Int. Ed.*, 2003, **42**, 5619.

130. J. I. van der Vlugt, R. Sablong, P. C. M. M. Magusin, A. M. Mills, A. L. Spek and D. Vogt, *Organometallics*, 2004, **23**, 3177.
131. Z. Béni, L. Guidoni, G. Laurenczy, U. Roethlisberger and R. Roulet, *J. Chem. Soc. Dalton Trans*., 2005, 310.
132. L. Leclercq, F. Hapiot, S. Tilloy, K. Ramkisoensing, J. N. H. Reek, P. W. N. M. van Leeuwen and E. Monflier, *Organometallics*, 2005, **24**, 2070.
133. C. Bianchini, W. Oberhauser, A. Orlandini, C. Giannelli and P. Frediani, *Organometallics*, 2005, **24**, 3692.
134. L. Helm and A. E. Merbach, *J. Chem. Soc. Dalton Trans*., 2002, 633.
135. B. T. Heaton, J. Jonas, T. Eguchi and G. A. Hoffman, *J. Chem. Soc. Chem. Commun*., 1981, 331.
136. B. T. Heaton, L. Strona, J. Jonas, T. Eguchi and G. A. Hoffman, *J. Chem. Soc. Dalton Trans*., 1982, 1159.
137. P. B. Dias, M. E. Minas de Piedade and J. A. Martinho Simões, *Coord. Chem. Rev*., 1994, **135/136**, 737.
138. L. A. van der Veen, M. D. K. Boele, F. R. Bregman, P. C. J. Kamer, P. W. N. M. van Leeuwen, K. Goubitz, J. Fraanje, H. Schenk and C. Bo, *J. Am. Chem. Soc*., 1998, **120**, 11616.
139. P.-A. Vuissoz, T. Yonezawa, D. Yang, J. Kiwi and J. J. van der Klink, *Chem. Phys. Lett*., 1997, **264**, 366.
140. B. L. Phillips, J. R. Houston, J. Feng and W. H. Casey, *J. Am. Chem. Soc*., 2006, **128**, 3912.
141. J. R. Houston, P. Yu and W. H. Casey, *Inorg. Chem*., 2005, **44**, 5176.
142. S. Martinengo, B. T. Heaton, R. J. Goodfellow and P. Chini, *J. Chem. Soc. Chem. Commun*., 1977, 39.
143. B. T. Heaton, L. Strona, S. Martinengo and P. Chini, *J. Organomet. Chem*., 1980, **194**, C29.
144. A. Fumagalli, T. F. Koetzle, F. Takusagawa, P. Chini, S. Martinengo and B. T. Heaton, *J. Am. Chem. Soc*., 1980, **102**, 1740.
145. B. T. Heaton, C. Brown, D. O. Smith, L. Strona, R. J. Goodfellow, P. Chini and S. Martinengo, *J. Am. Chem. Soc*., 1980, **102**, 6175.
146. B. T. Heaton, L. Strona and S. Martinengo, *J. Organomet. Chem*., 1981, **215**, 415.
147. B. T. Heaton, *Phil. Trans. Roy. Soc. Lond. A*, 1982, **308**, 95.
148. A. Cerioti, G. Longoni, M. Manassero, M. Sansoni, R. Della Pergola, B. T. Heaton and D. O. Smith, *J. Chem. Soc. Chem. Commun*., 1982, 886.
149. B. T. Heaton, L. Strona, S. Martinengo, D. Strumolo, R. J. Goodfellow and I. H. Sadler, *J. Chem. Soc. Dalton Trans*., 1982, 1499.
150. L. Garlaschelli, A. Fumagalli, S. Martinengo, B. T. Heaton, D. O. Smith and L. Strona, *J. Chem. Soc. Dalton Trans*., 1982, 2265.
151. B. T. Heaton, R. Della Pergola, L. Strona, D. O. Smith and A. Fumagalli, *J. Chem. Soc. Dalton Trans*., 1982, 2553.
152. B. T. Heaton, L. Strona, R. Della Pergola, L. Garlaschelli, U. Sartorelli and I. H. Sadler, *J. Chem. Soc. Dalton Trans*., 1983, 173.
153. A. Ceriotti, G. Longoni, R. Della Pergola, B. T. Heaton and D. O. Smith, *J. Chem. Soc. Dalton Trans*., 1983, 1433.
154. B. T. Heaton, L. Strona, R. Della Pergola, J. L. Vidal and R. C. Schoening, *J. Chem. Soc. Dalton Trans*., 1983, 1941.
155. B. T. Heaton, L. Strona, S. Martinengo, D. Strumolo, V. G. Albano and D. Braga, *J. Chem. Soc. Dalton Trans*., 1983, 2175.
156. A. Fumagalli, S. Martinengo, P. Chini, D. Galli, B. T. Heaton and R. Della Pergola, *Inorg. Chem*., 1984, **23**, 2947.
157. J. Pursiainen, T. A. Pakkanen, B. T. Heaton, C. Seregni and R. J. Goodfellow, *J. Chem. Soc. Dalton Trans*., 1986, 681.
158. C. Allevi, B. T. Heaton, C. Seregni, L. Strona, R. J. Goodfellow, P. Chini and S. Martinengo, *J. Chem. Soc. Dalton Trans*., 1986, 1375.
159. C. Allevi, M. Golding, B. T. Heaton, C. A. Ghilardi, S. Midollini and A. Orlandini, *J. Organomet. Chem*., 1987, **326**, C19.
160. A. Fumagalli, S. Martinengo, G. Ciani, A. Sironi and B. T. Heaton, *J. Chem. Soc. Dalton Trans*., 1988, 163.

161. S. Bordoni, B. T. Heaton, C. Seregni, L. Strona, R. J. Goodfellow, M. B. Hursthouse, M. Thornton-Pett and S. Martinengo, *J. Chem. Soc. Dalton Trans.*, 1988, 2103.
162. C. Allevi, S. Bordoni, C. P. Clavering, B. T. Heaton, J. A. Iggo, C. Seregni and L. Garlaschelli, *Organometallics*, 1989, **8**, 385.
163. T. Blum, B. T. Heaton, J. A. Iggo, J. Sabounchei and A. K. Smith, *J. Chem. Soc. Dalton Trans.*, 1994, 333.
164. T. Blum, M. P. Brown, B. T. Heaton, A. S. Hor, J. A. Iggo, J. S. Z. Sabounchei and A. K. Smith, *J. Chem. Soc. Dalton Trans.*, 1994, 513.
165. S. P. Tunik, I. S. Podkorytov, B. T. Heaton, J. A. Iggo and J. Sampanthar, *J. Organomet. Chem.*, 1998, **550**, 221.
166. F. M. Dolgushin, E. V. Grachova, B. T. Heaton, J. A. Iggo, I. O. Koshevoy, I. S. Podkorytov, D. J. Smawfield, S. P. Tunik, R. Whyman and A. I. Yanovskii, *J. Chem. Soc. Dalton Trans.*, 1999, 1609.
167. J. S. Z. Sabounchei, B. T. Heaton, J. A. Iggo, C. Jakob and I. S. Podkorytov, *J. Cluster Sci.*, 2001, **12**, 339.
168. E. V. Grachova, B. T. Heaton, J. A. Iggo, I. S. Podkorytov, D. J. Smawfield, S. P. Tunik and R. Whyman, *J. Chem. Soc. Dalton Trans.*, 2001, 3303.
169. E. V. Grachova, M. Haukka, B. T. Heaton, E. Nordlander, T. A. Pakkanen, I. S. Podkorytov and S. P. Tunik, *J. Chem. Soc. Dalton Trans.*, 2003, 2468.
170. D. H. Farrar, E. V. Grachova, M. Haukka, B. T. Heaton, J. A. Iggo, T. A. Pakkanen, I. S. Podkorytov and S. P. Tunik, *Inorg. Chim. Acta*, 2003, **354**, 11.
171. I. O. Koshevoy, E. V. Grachova, S. P. Tunik, M. Haukka, T. A. Pakkanen, B. T. Heaton, J. A. Iggo and I. S. Podkorytov, *J. Chem. Soc. Dalton Trans.*, 2004, 3893.
172. J. A. Pople, *J. Chem. Phys.*, 1962, **37**, 53, 60.
173. J. A. Pople, *Mol. Phys.*, 1964, **7**, 301.
174. R. Ditchfield, *J. Chem. Phys.*, 1972, **56**, 5688.
175. R. Ditchfield, *Mol. Phys.*, 1974, **27**, 789.
176. M. Bühl, M. Kaupp, O. L. Malkina and V. G. Malkin, *J. Comput. Chem.*, 1999, **20**, 91.
177. M. Bühl, *Organometallics*, 1997, **16**, 261.
178. M. Bühl, *Chem. Phys. Lett.*, 1997, **267**, 251.
179. J. A. Pople and D. P. Santry, *Mol. Phys.*, 1964, **8**, 1.
180. C. J. Jameson and J. Mason, in: *Multinuclear NMR*, J. Mason, ed., Plenum, New York, 1987, Chapters 2 and 4.
181. E. M. Hyde, J. D. Kennedy, B. L. Shaw and W. McFarlane, *J. Chem. Soc. Dalton Trans.*, 1977, 1571.
182. I. J. Colquhoun and W. McFarlane, *J. Magn. Reson.*, 1982, **46**, 525.
183. P. L. Goggin, R. J. Goodfellow, J. R. Knight, M. G. Norton and B. F. Taylor, *J. Chem. Soc. Dalton Trans.*, 1973, 2220.
184. J. Browning, P. L. Goggin, R. J. Goodfellow, M. G. Norton, A. J. M. Rattray, B. F. Taylor and J. Mink, *J. Chem. Soc. Dalton Trans.*, 1977, 2061.
185. L. Carlton, *Inorg. Chem.*, 2000, **39**, 4510.
186. S. J. Anderson, J. R. Barnes, P. L. Goggin and R. J. Goodfellow, *J. Chem. Res. (S)*, 1978, 286.
187. A. L. Davis and R. J. Goodfellow, *J. Chem. Soc. Dalton Trans.*, 1993, 2273.
188. M. G. Partridge, B. A. Messerle and L. D. Field, *Organometallics*, 1995, **14**, 3527.
189. G. Otting, L. P. Soler and B. A. Messerle, *J. Magn. Reson*, 1999, **137**, 413.
190. M. Ludwig, L. Öhrström and D. Steinborn, *Magn. Reson. Chem.*, 1995, **33**, 984.
191. G. J. J. Steyn, A. Roodt, I. Poletaeva and Y. S. Varshavsky, *J. Organomet. Chem.*, 1997, **536–537**, 197.
192. J. Conradie, G. J. Lamprecht, S. Otto and J. C. Swarts, *Inorg. Chim. Acta*, 2002, **328**, 191.
193. H. Werner, M. Baum, D. Schneider and B. Windmüller, *Organometallics*, 1994, **13**, 1089.
194. H. Werner, O. Gevert and P. Haquette, *Organometallics*, 1997, **16**, 803.
195. M. A. Esteruelas, F. J. Lahoz, M. Martín, E. Oñate and L. A. Oro, *Organometallics*, 1997, **16**, 4572.
196. C. J. Adams, N. G. Connelly, D. J. H. Emslie, O. D. Hayward, T. Manson, A. G. Orpen and P. H. Rieger, *J. Chem. Soc. Dalton Trans.*, 2003, 2835.
197. I. Ara, J. R. Berenguer, E. Eguizábal, J. Forniés, E. Lalinde, A. Martín and F. Martínez, *Organometallics*, 1998, **17**, 4578.
198. M. Schäfer, J. Wolf and H. Werner, *Organometallics*, 2004, **23**, 5713.
199. A. G. Kent, B. E. Mann and C. P. Manuel, *J. Chem. Soc. Chem. Commun.*, 1985, 728.

200. S. T. Belt, S. B. Duckett, D. M. Haddleton and R. N. Perutz, *Organometallics*, 1989, **8**, 748.
201. M. C. Nicasio, M. Paneque, P. J. Pérez, A. Pizzano, M. L. Poveda, L. Rey, S. Sirol, S. Taboada, M. Trujillo, A. Monge, C. Ruiz and E. Carmona, *Inorg. Chem.*, 2000, **39**, 180.
202. H. Werner, G. Canepa, K. Ilg and J. Wolf, *Organometallics*, 2000, **19**, 4756.
203. R. Zhou, C. Wang, Y. Hu and T. C. Flood, *Organometallics*, 1997, **16**, 434.
204. H. Werner, R. Wiedemann, M. Laubender, B. Windmüller and J. Wolf, *Chem. Eur. J.*, 2001, **7**, 1959.
205. J.-C. Choi, K. Osakada and T. Yamamoto, *Organometallics*, 1998, **17**, 3044.
206. M. Manger, J. Wolf, M. Teichert, D. Stalke and H. Werner, *Organometallics*, 1998, **17**, 3210.
207. S. Ikeda, Y. Maruyama and F. Ozawa, *Organometallics*, 1998, **17**, 3770.
208. I. I. R. Salas, M. A. Paz-Sandoval and H. Nőth, *Organometallics*, 2002, **21**, 4696.
209. A. Kempter, C. Gemel, N. J. Hardman and R. A. Fischer, *Inorg. Chem.*, 2006, **45**, 3133.
210. H. Bönnemann, R. Goddard, J. Grub, R. Mynott, E. Raabe and S. Wendel, *Organometalllics*, 1989, **8**, 1941.
211. R. S. Hay-Motherwell, B. Hussain-Bates, M. B. Hursthouse and G. Wilkinson, *J. Chem. Soc. Chem. Commun.*, 1990, 1242.
212. R. Cohen, B. Rybtchinski, M. Gandelman, H. Rozenberg, J. M. L. Martin and D. Milstein, *J. Am. Chem. Soc.*, 2003, **125**, 6532.
213. M. Arthurs, S. M. Nelson and M. G. B. Drew, *J. Chem. Soc. Dalton Trans.*, 1977, 779.
214. E. Bleuel, P. Schwab, M. Laubender and H. Werner, *J. Chem. Soc. Dalton Trans.*, 2001, 266.
215. C. Pettinari, R. Pettinari, M. Fianchini, F. Marchetti, B. W. Skelton and A. H. White, *Inorg. Chem.*, 2005, **44**, 7933.
216. H. Werner, P. Schwab, E. Bleuel, N. Mahr, P. Steinert and J. Wolf, *Chem. Eur. J.*, 1997, **3**, 1375.
217. Z.-Q. Wang, J. Martínez and P. M. Maitlis, *Inorg. Chim. Acta*, 1998, **280**, 62.
218. T. Pechmann, C. D. Brandt and H. Werner, *J. Chem. Soc. Dalton Trans.*, 2003, 1495.
219. T. Pechmann, C. D. Brandt and H. Werner, *Chem. Eur. J.*, 2004, **10**, 728.
220. J. A. Mata, A. R. Chianese, J. R. Miecznikowski, M. Poyatos, E. Peris, J. W. Faller and R. H. Crabtree, *Organometallics*, 2004, **23**, 1253.
221. N. M. Scott, R. Dorta, E. D. Stevens, A. Correa, L. Cavallo and S. P. Nolan, *J. Am. Chem. Soc.*, 2005, **127**, 3516.
222. J. R. Wigginton, S. J. Trepanier, R. McDonald, M. J. Ferguson and M. Cowie, *Organometallics*, 2005, **24**, 6194.
223. X.-Y. Yu, B. O. Patrick and B. R. James, *Organometallics*, 2006, **25**, 2359.
224. J. C. Jefferey, C. Marsden and F. G. A. Stone, *J. Chem. Soc. Dalton Trans.*, 1985, 1315.
225. J. A. Abad, E. Delgado, M. E. Garcia, M. J. Grosse-Ophoff, I. J. Hart, J. C. Jefferey, M. S. Simmons and F. G. A. Stone, *J. Chem. Soc. Dalton Trans.*, 1987, 41.
226. S. J. Davies, J. A. K. Howard, M. U. Pilotti and F. G. A. Stone, *J. Chem. Soc. Dalton Trans.*, 1989, 1855.
227. B. T. Sterenberg, R. McDonald and M. Cowie, *Organometallics*, 1997, **16**, 2297.
228. D. S. A. George, R. McDonald and M. Cowie, *Organometallics*, 1998, **17**, 2553.
229. A. Vigalok, B. Rybtchinski, L. J. W. Shimon, Y. Ben-David and D. Milstein, *Organometallics*, 1999, **18**, 895.
230. D. S. A. George, R. W. Hilts, R. McDonald and M. Cowie, *Organometallics*, 1999, **18**, 5330.
231. W. P. Griffith, M. J. Mockford and A. C. Skapski, *J. Chem. Soc. Chem. Commun.*, 1984, 407.
232. H. Werner, M. Manger, U. Schmidt, M. Laubender and B. Weberndörfer, *Organometallics*, 1998, **17**, 2619.
233. M. Bosch, M. Laubender, B. Weberndörfer and H. Werner, *Chem. Eur. J.*, 1999, **5**, 2203.
234. G. Fries, J. Wolf, K. Ilg, B. Walfort, D. Stalke and H. Werner, *J. Chem. Soc. Dalton Trans.*, 2004, 1873.
235. B. B. Wayland, A. Duttaahmed and B. A. Woods, *J. Chem. Soc. Chem. Commun.*, 1983, 142.
236. X.-X. Zhang, G. F. Parks and B. B. Wayland, *J. Am. Chem. Soc.*, 1997, **119**, 7938.
237. C. Tejel, M. A. Ciriano, J. A. López, F. J. Lahoz and L. A. Oro, *Organometallics*, 1997, **16**, 4718.
238. E. Bleuel, M. Laubender, B. Weberndörfer and H. Werner, *Angew. Chem. Int. Ed.*, 1999, **38**, 156.
239. D. B. Grotjahn, G. A. Bikzhanova and J. L. Hubbard, *Organometallics*, 1999, **18**, 5614.
240. H. Werner, R. Wiedemann, P. Steinert and J. Wolf, *Chem. Eur. J.*, 1997, **3**, 127.

241. W. P. Griffith and G. Wilkinson, *J. Chem. Soc.*, 1959, 2757.
242. R. C. Matthews, D. K. Howell, W.-J. Peng, S. G. Train, W. D. Treleaven and G. G. Stanley, *Angew. Chem. Int. Ed.*, 1996, **35**, 2253.
243. A. Vigalok, O. Uzan, L. J. W. Shimon, Y. Ben-David, J. M. L. Martin and D. Milstein, *J. Am. Chem. Soc.*, 1998, **120**, 12539.
244. P. B. Hitchcock, M. F. Lappert and I. A. MacKinnon, *J. Chem. Soc. Chem. Commun.*, 1993, 1015.
245. R. Gelabert, M. Moreno, J. M. Lluch, A. Lledós, V. Pons and D. M. Heinekey, *J. Am. Chem. Soc.*, 2004, **126**, 8813.
246. M. B. Abrams, B. L. Scott and R. T. Baker, *Organometallics*, 2000, **19**, 4944.
247. S. Martinengo, G. Ciani, A. Sironi, B. T. Heaton and J. Mason, *J. Am. Chem. Soc.*, 1979, **101**, 7095.
248. D. Daphnomili, W. R. Scheidt, J. Zajicek and A. G. Coutsolelos, *Inorg. Chem.*, 1998, **37**, 3675.
249. R. S. Hay-Motherwell, S. U. Koschmieder, G. Wilkinson, B. Hussain-Bates and M. B. Hursthouse, *J. Chem. Soc. Dalton Trans.*, 1991, 2821.
250. H. Adams, N. A. Bailey, B. E. Mann, B. F. Taylor, C. White and P. Yavari, *J. Chem. Soc. Dalton Trans.*, 1987, 1947.
251. O. Howarth, in: *Multinuclear NMR*, J. Mason, ed., Plenum, New York, 1987, Chapter 5.
252. L. Carlton, L. V. Mokoena and M. A. Fernandes, *Inorg. Chem.*, 2007 (submitted).
253. R. Benn, H. Brenneke and A. Rufińska, *J. Organomet. Chem.*, 1987, **320**, 115.
254. M. Herberhold, W. Milius and S. Eibl, *Z. Anorg. Allg. Chem.*, 1999, **625**, 341.
255. J. L. Cunningham and S. B. Duckett, *J. Chem. Soc. Dalton Trans.*, 2005, 744.
256. H. Schumann, O. Stenzel, S. Dechert, F. Girgsdies and R. L. Halterman, *Organometallics*, 2001, **20**, 5360.
257. L. Orian, A. Bisello, S. Santi, A. Ceccon and G. Saielli, *Chem. Eur. J.*, 2004, **10**, 4029.
258. P. Caddy, M. Green, L. E. Smart and N. White, *J. Chem. Soc. Chem. Commun.*, 1978, 839.
259. P. Maire, T. Büttner, F. Breher, P. Le Floch and H. Grützmacher, *Angew. Chem. Int. Ed.*, 2005, **44**, 6318.
260. F. Breher, H. Rüegger, M. Mlakar, M. Rudolph, S. Deblon, H. Schönberg, S. Boulmaâz, J. Thomaier and H. Grützmacher, *Chem. Eur. J.*, 2004, **10**, 641.
261. M. Herberhold, S. Eibl, W. Milius and B. Wrackmeyer, *Z. Anorg. Allg. Chem.*, 2000, **626**, 552.
262. E. Lindner, B. Keppeler, H. A. Mayer, K. Gierling, R. Fawzi and M. Steimann, *J Organomet. Chem.*, 1996, **526**, 175.
263. P. Maire, F. Breher, H. Schönberg and H. Grützmacher, *Organometallics*, 2005, **24**, 3207.
264. H. Noss, W. Baumann, R. Kempe, T. Irrgang and A. Schulz, *Inorg. Chim. Acta*, 2003, **345**, 130.
265. M. Cocivera, A. J. McAlees, R. McCrindle and P. Szczecinski, *J. Organomet. Chem.*, 1982, **235**, 97.
266. M. Aizenberg, J. Ott, C. J. Elsevier and D. Milstein, *J. Organomet. Chem.*, 1998, **551**, 81.
267. P. Imhoff, S. C. A. Nefkens, C. J. Elsevier, K. Goubitz and C. H. Stam, *Organometallics*, 1991, **10**, 1421.
268. P. Imhoff, R. van Asselt, J. M. Ernsting, K. Vrieze, C. J. Elsevier, W. J. J. Smeets, A. L. Spek and A. P. M. Kentgens, *Organometallics*, 1993, **12**, 1523.
269. S. Lange, K. Wittmann, B. Gabor, R. Mynott and W. Leitner, *Tetrahedron Asymmetry*, 1998, **9**, 475.
270. J. H. Bieri, T. Egolf, W. Von Philipsborn, U. Piantini, R. Prewo, U. Ruppli and A. Salzer, *Organometallics*, 1986, **5**, 2413.
271. D. Heller, H.-J. Drexler, A. Spannenberg, B. Heller, J. You and W. Baumann, *Angew. Chem. Int. Ed.*, 2002, **41**, 777.
272. M. Soleilhavoup, L. Viau, G. Commenges, C. Lepetit and R. Chauvin, *Eur. J. Inorg. Chem.*, 2003, 207.
273. E. Kossoy, M. A. Iron, B. Rybtchinski, Y. Ben-David, L. J. W. Shimon, L. Konstantinovski, J. M. L. Martin and D. Milstein, *Chem. Eur. J.*, 2005, **11**, 2319.
274. E. Çetinkaya, P. B. Hitchcock, H. Küçükbay, M. F. Lappert and S. Al-Juaid, *J. Organomet. Chem.*, 1994, **481**, 89.
275. C. Crocker, R. J. Errington, R. Markham, C. J. Moulton and B. L. Shaw, *J. Chem. Soc. Dalton Trans.*, 1982, 387.
276. A. Salzer, T. Egolf and W. von Philipsborn, *Helv. Chim. Acta*, 1982, **65**, 1145.
277. B. Buchmann, U. Piantini, W. von Philipsborn and A. Salzer, *Helv. Chim. Acta*, 1987, **70**, 1487.

278. R. Köster, G. Seidel, R. Boese and B. Wrackmeyer, *Chem. Ber.*, 1988, **121**, 597.
279. R. Köster, G. Seidel, B. Wrackmeyer and D. Schlosser, *Chem. Ber.*, 1989, **122**, 2055.
280. M. D. Mikoluk, R. McDonald and R. G. Cavell, *Organometallics*, 1999, **18**, 3306.
281. A. Ceccon, C. J. Elsevier, J. M. Ernsting, A. Gambaro, S. Santi and A. Venzo, *Inorg. Chim. Acta*, 1993, **204**, 15.
282. P. Binger, B. Biedenbach, R. Mynott, R. Benn, A. Rufińska, P. Betz and C. Krüger, *J. Chem. Soc. Dalton Trans*., 1990, 1771.
283. E. Esponda, C. Adams, F. Burgos, I. Chavez, J. M. Manriquez, F. Delpech, A. Castel, H. Gornitzka, M. Rivière-Baudet and P. Rivière, *J. Organomet. Chem*., 2006, **691**, 3011.
284. B. Delavaux, B. Chaudret, J. Devilliers, F. Dahan, G. Commenges and R. Poilblanc, *J. Am. Chem. Soc*., 1986, **108**, 3703.
285. D. J. Law, G. Bigam and R. G. Cavell, *Can. J. Chem*., 1995, **73**, 635.
286. C. J. Elsevier, J. M. Ernsting and W. G. J. De Lange, *J. Chem. Soc. Chem. Commun*., 1989, 585.
287. E. Lindner, S. Brugger, S. Steinbrecher, E. Plies, M. Seiler, H. Bertagnolli, P. Wegner and H. A. Mayer, *Inorg. Chim. Acta*, 2002, **327**, 54.
288. M. Valentini, K. Selvakumar, M. Wörle and P. S. Pregosin, *J. Organomet. Chem*., 1999, **587**, 244.
289. S. Häp, M. Nieger, D. Gudat, M. Betke-Hornfeck and D. Schramm, *Organometallics*, 2001, **20**, 2679.
290. A. Börner, A. Kless, R. Kempe, D. Heller, J. Holz and W. Baumann, *Chem. Ber.*, 1995, **128**, 767.
291. A. Bertogg and A. Togni, *Organometallics*, 2006, **25**, 622.
292. A. Albinati, J. Eckert, P. Pregosin, H. Rüegger, R. Salzmann and C. Stössel, *Organometallics*, 1997, **16**, 579.
293. A. Ferrari, M. Merlin, S. Sostero, H. Rüegger and L. M. Venanzi, *Helv. Chim. Acta*, 1999, **82**, 1454.
294. E. Del Ministro, O. Renn, H. Rüegger, L. M. Venanzi, U. Burckhardt and V. Gramlich, *Inorg. Chim. Acta*, 1995, **240**, 631.
295. M. Cocivera, G. Ferguson, R. E. Lenkinski, P. Szczecinski, F. J. Lalor and D. J. O'Sullivan, *J. Magn. Reson*., 1982, **46**, 168.
296. E. Teuma, M. Loy, C. Le Berre, M. Etienne, J.-C. Daran and P. Kalck, *Organometallics*, 2003, **22**, 5261.
297. R. Benn, H. Brenneke and R.-D. Reinhardt, *Z. Naturforsch*., 1985, **40b**, 1763.
298. F. Läng, F. Breher, D. Stein and H. Grützmacher, *Organometallics*, 2005, **24**, 2997.
299. F. Malbosc, P. Kalck, J.-C. Daran and M. Etienne, *J. Chem. Soc. Dalton Trans*., 1999, 271.
300. M. Paneque, S. Sirol, M. Trujillo, E. Carmona, E. Gutiérrez-Puebla, M. A. Monge, C. Ruiz, F. Malbosc, C. Serra-Le Berre, P. Kalck, M. Etienne and J. C. Daran, *Chem. Eur. J*., 2001, **7**, 3869.
301. K. Timmer, D. H. M. W. Thewissen and J. M. Marsman, *Recl. Trav. Chim. Pays-Bas*, 1988, **107**, 248.
302. R. H. Dawson, M. M. Harding, S. Maginn and A. K. Smith, *Inorg. Chim. Acta*, 1988, **149**, 281.
303. T. H. Brown and P. J. Green, *J. Am. Chem. Soc*., 1970, **92**, 2359.
304. J.-C. Hierso, F. Lacassin, R. Broussier, R. Amardeil and P. Meunier, *J. Organomet. Chem*., 2004, **689**, 766.
305. C. Brown, B. T. Heaton, L. Longhetti, W. T. Povey and D. O. Smith, *J. Organomet. Chem*., 1980, **192**, 93.
306. B. T. Heaton, C. Jacob and J. T. Sampanthar, *J. Chem. Soc. Dalton Trans*., 1998, 1403.
307. B. T. Heaton, C. Jacob and S. Moffet, *J. Organomet. Chem*., 1993, **462**, 347.
308. C. Bianchini, C. J. Elsevier, J. M. Ernsting, M. Peruzzini and F. Zanobini, *Inorg. Chem*., 1995, **34**, 84.
309. M. Gouygou, O. Tissot, J.-C. Daran and G. G. A. Balavoine, *Organometallics*, 1997, **16**, 1008.
310. J.-J. Brunet, G. Commenges, D. Neibecker, K. Philippot and L. Rosenberg, *Inorg.Chem*., 1994, **33**, 6373.
311. V. Cîrcu, M. A. Fernandes and L. Carlton, *Inorg. Chem*., 2002, **41**, 3859.
312. S. Bontemps, H. Gornitzka, G. Bouhadir, K. Miqueu and D. Bourissou, *Angew. Chem. Int. Ed*., 2006, **45**, 1611.
313. E. Lindner, B. Keppeler, H. A. Mayer and K. Gierling, *J. Organomet. Chem*., 1996, **515**, 139.
314. V. Cîrcu, M. A. Fernandes and L. Carlton, *Polyhedron*, 2003, **22**, 3293.
315. R. Bonnaire, D. Davoust and N. Platzer, *Org. Magn. Reson*., 1984, **22**, 80.
316. L. Öhrström, S. Strömberg, J. Glaser and K. Zetterberg, *J. Organomet. Chem*., 1998, **558**, 123.
317. N. M. Agh-Atabay, C. Bayat and U. Yazgic, *Rev. Inorg. Chem*., 1998, **18**, 223.

318. N. Feiken, P. Pregosin and G. Trabesinger, *Organometallics*, 1998, **17**, 4510.
319. V. Chauby, J.-C. Daran, C. Serra-Le Berre, F. Malbosc, P. Kalck, O. D. Gonzalez, C. E. Haslam and A. Haynes, *Inorg. Chem.*, 2002, **41**, 3280.
320. S. B. Duckett, D. M. Haddleton, S. A. Jackson, R. N. Perutz, M. Poliakoff and R. K. Upmacis, *Organometallics*, 1988, **7**, 1526.
321. K. A. M. Ampt, S. B. Duckett and R. N. Perutz, *J. Chem. Soc. Dalton Trans.*, 2004, 3331.
322. J. Ruiz, P. O. Bentz, B. E. Mann, C. M. Spencer, B. F. Taylor and P. M. Maitlis, *J. Chem. Soc. Dalton Trans.*, 1987, 2709.
323. P. O. Bentz, J. Ruiz, B. E. Mann, C. M. Spencer and P. M. Maitlis, *J. Chem. Soc. Chem. Commun.*, 1985, 1374.
324. M. Herberhold, H. Yan, W. Milius and B. Wrackmeyer, *Chem. Eur. J.*, 2002, **8**, 388.
325. M. Herberhold, H. Yan, W. Milius and B. Wrackmeyer, *J. Organomet. Chem.*, 2000, **604**, 170.
326. M. Herberhold, H. Yan, W. Milius and B. Wrackmeyer, *Z. Anorg. Allg. Chem.*, 2000, **626**, 1627.
327. A. A. H. van der Zeijden, G. van Koten, J. M. Ernsting, C. J. Elsevier, B. Krijnen and C. H. Stam, *J. Chem. Soc. Dalton Trans.*, 1989, 317.
328. B. C. de Pater, E. J. Zijp, H.-W. Frühauf, J. M. Ernsting, C. J. Elsevier, K. Vrieze, P. H. M. Budzelaar and A. W. Gal, *Organometallics*, 2004, **23**, 269.
329. J. Liedtke, H. Rüegger, S. Loss and H. Grützmacher, *Angew. Chem. Int. Ed.*, 2000, **39**, 2478.
330. W. J. Hoogervorst, K. Goubitz, J. Fraanje, M. Lutz, A. L. Spek, J. M. Ernsting and C. J. Elsevier, *Organometallics*, 2004, **23**, 4550.
331. K. Isobe, Y. Ozawa, A. Vázquez de Miguel, T.-W. Zhu, K.-M. Zhao, T. Nishioka, T. Ogura and T. Kitagawa, *Angew. Chem. Int. Ed.*, 1994, **33**, 1882.
332. C. Arz, P. S. Pregosin and C. Anklin, *Magn. Reson. Chem.*, 1987, **25**, 158.
333. A. Albinati, C. Arz and P. S. Pregosin, *J. Organomet. Chem.*, 1988, **356**, 367.
334. M. Herberhold, H. Yan, W. Milius and B. Wrackmeyer, *Angew. Chem. Int. Ed.*, 1999, **38**, 3689.
335. M. Herberhold, H. Yan, W. Milius and B. Wrackmeyer, *Chem. Eur. J.*, 2000, **6**, 3026.
336. M. Herberhold, T. Daniel, D. Daschner, W. Milius and B. Wrackmeyer, *J. Organomet. Chem.*, 1999, **585**, 234.
337. J. Ruiz, C. M. Spencer, B. E. Mann, B. F. Taylor and P. M. Maitlis, *J. Organomet. Chem.*, 1987, **325**, 253.
338. M. Herberhold, G.-X. Jin, H. Yan, W. Milius and B. Wrackmeyer, *J. Organomet. Chem.*, 1999, **587**, 252.
339. Y. Hayashi, K. Toriumi and K. Isobe, *J. Am. Chem. Soc.*, 1988, **110**, 3666.
340. J.-U. Rohde and W. Preetz, *Z. Anorg. Allg. Chem.*, 2000, **626**, 1550.
341. B. T. Heaton, C. Jacob, W. Heggie, P. R. Page and I. Villax, *Magn. Reson. Chem.*, 1991, **29**, S21.
342. B. T. Heaton, J. A. Iggo, C. Jacob, H. Blanchard, M. B. Hursthouse, I. Ghatak, M. E. Harman, R. G. Somerville, W. Heggie, P. R. Page and I. Villax, *J. Chem. Soc. Dalton Trans.*, 1992, 2533.
343. E. Lindner, K. Gierling, B. Keppeler and H. A. Mayer, *Organometallics*, 1997, **16**, 3531.
344. L. Carlton, M. A. Fernandes and E. Sitabule, *Proc. Nat. Acad. Sci. USA*, 2007, **104**, 6969.
345. L. Carlton, R. Weber and D. C. Levendis, *Inorg. Chem.*, 1998, **37**, 1264.
346. U. E. Bucher, T. Lengweiler, D. Nanz, W. von Philipsborn and L. M. Venanzi, *Angew. Chem. Int. Ed.*, 1990, **29**, 548.
347. A. M. Hill, W. Levason, S. R. Preece and M. Webster, *Polyhedron*, 1997, **16**, 1307.
348. N. R. Champness, R. J. Forder, C. S. Frampton and G. Reid, *J. Chem. Soc. Dalton Trans.*, 1996, 1261.
349. A. V. Belyaev, A. B. Venediktov, M. A. Fedotov and S. P. Khranenko, *Koord. Khim*, 1986, **12**, 690.
350. O. Renn, H. Rüegger, L. M. Venanzi, J. Gallus, V. Gramlich and A. Martelletti, *Inorg. Chim. Acta*, 1995, **240**, 575.
351. W. Preetz, G. Peters and J.-U. Vogt, *Z. Naturforsch.*, 1993, **48b**, 348.
352. B. E. Mann and C. Spencer, *Inorg. Chim. Acta*, 1982, **65**, L57.
353. C. Carr, J. Glaser and M. Sandström, *Inorg. Chim. Acta*, 1987, **131**, 153.
354. M. C. Read, J. Glaser, M. Sandström and I. Toth, *Inorg. Chem.*, 1992, **31**, 4155.
355. L. Spiccia, J. M. Aramini, S. J. Crimp, A. Drljaca, E. T. Lawrenz, V. Tedesco and H. J. Vogel, *J. Chem. Soc. Dalton Trans.*, 1997, 4603.
356. K.-D. Grüninger, A. Schwenk and B. E. Mann, *J. Magn. Reson.*, 1980, **41**, 354.

357. J.-U. Vogt, G. Peters and W. Preetz, *Z. Anorg. Allg. Chem.*, 1995, **621**, 186.
358. S. J. Anderson, J. R. Barnes, P. L. Goggin and R. J. Goodfellow, *J. Chem. Res. (M)*, 1978, 3601.
359. A. M. Hill, W. Levason, S. R. Preece and C. S. Frampton, *Inorg. Chim. Acta*, 1997, **254**, 99.
360. A. M. Hill, W. Levason and M. Webster, *Inorg. Chim. Acta*, 1998, **271**, 203.
361. H. C. E. McFarlane, W. McFarlane and R. J. Wood, *Bull. Soc. Chim. Belg.*, 1976, **85**, 864.
362. J. R. Barnes, P. L. Goggin and R. J. Goodfellow, *J. Chem. Res (S)*, 1979, 118.
363. M. A. Fedotov, V. A. Shipachev and L. M. Levchenko, *Russ. J. Coord. Chem.*, 1999, **25**, 31.
364. A. V. Belyaev, M. A. Fedotov, S. P. Khranenko and V. A. Emel'yanov, *Russ. J. Coord. Chem.*, 2001, **27**, 855.
365. M. A. Fedotov, *Russ. J. Coord. Chem.*, 2002, **28**, 573.
366. Y. S. Varshavsky, T. G. Cherkasova, I. S. Podkorytov, K. A. Lyssenko and A. B. Nikol'skii, *J. Organomet. Chem.*, 2003, **665**, 156.
367. E. B. Boyar and S. D. Robinson, *Inorg. Chim. Acta*, 1982, **64**, L193.
368. E. B. Boyar and S. D. Robinson, *J. Chem. Soc. Dalton Trans.*, 1985, 629.
369. K. V. Catalan, J. S. Hess, M. M. Maloney, D. J. Mindiola, D. L. Ward and K. R. Dunbar, *Inorg. Chem.*, 1999, **38**, 3904.
370. C. D. Garner, M. Berry and B. E. Mann, *Inorg. Chem.*, 1984, **23**, 1500.
371. S. B. Duckett and R. N. Perutz, *J. Chem. Soc. Chem. Commun.*, 1991, 28.
372. A. Nutton, P. M. Bailey and P. M. Maitlis, *J. Organomet. Chem.*, 1981, **213**, 313.
373. D. Galli, L. Garlaschelli, G. Ciani, A. Fumagalli, S. Martinengo and A. Sironi, *J. Chem. Soc. Dalton Trans.*, 1984, 55.
374. P. Espinet, P. M. Bailey, P. Piraino and P. M. Maitlis, *Inorg. Chem.*, 1979, **18**, 2706.
375. E. Gullo, S. Detti, G. Laurenczy and R. Roulet, *J. Chem. Soc. Dalton Trans.*, 2002, 4577.
376. O. A. Gansow, D. S. Gill, F. J. Bennis, J. R. Hutchison, J. L. Vidal and R. C. Schoening, *J. Am. Chem. Soc.*, 1980, **102**, 2449.
377. D. Imhof, H. Rüegger, L. M. Venanzi and T. R. Ward, *Magn. Reson. Chem.*, 1991, **29**, S73.
378. C. Godard, S. B. Duckett, S. Parsons and R. N. Perutz, *J. Chem. Soc. Chem. Commun.*, 2003, 2332.
379. L. Carlton and R. Weber, *Inorg. Chem.*, 1996, **35**, 5843.
380. L. Carlton and G. de Sousa, *Polyhedron*, 1993, **12**, 1377.
381. V. F. Kuznetsov, G. A. Facey, G. P. A. Yap and H. Alper, *Organometallics*, 1999, **18**, 4706.
382. R. Dorta, L. Konstantinovski, L. J. W. Shimon, Y. Ben-David and D. Milstein, *Eur. J. Inorg. Chem.*, 2003, 70.
383. B. T. Heaton, J. A. Iggo, C. Jacob, J. Nadarajah, M. A. Fontaine, R. Messere and A. F. Noels, *J. Chem. Soc. Dalton Trans.*, 1994, 2875.
384. J. V. Barkely, C. J. Davies, B. T. Heaton and C. Jacob, *J. Chem. Soc. Dalton Trans.*, 1995, 2861.
385. C. J. Davies, B. T. Heaton and C. Jacob, *J. Chem. Soc. Chem. Commun.*, 1995, 1177.
386. J. V. Barkely, B. T. Heaton, C. Jacob, R. Mageswaran and J. T. Sampanthar, *J. Chem. Soc. Dalton Trans.*, 1998, 697.
387. M. Finze, E. Bernhardt, H. Willner and C. Lehmann, *Organometallics*, 2006, **25**, 3070.
388. B. T. Heaton, C. Jacob, G. L. Monks, M. B. Hursthouse, I. Ghatak, R. G. Somerville, W. Heggie, P. R. Page and I. Villax, *J. Chem. Soc. Dalton Trans.*, 1996, 61.
389. D. L. Thorn, T. H. Tulip and J. A. Ibers, *J. Chem. Soc. Dalton Trans.*, 1979, 2022.
390. J. R. Dilworth, S. Donovan-Mtunzi, C. T. Kan, R. L. Richards and J. Mason, *Inorg. Chim. Acta*, 1981, **53**, L161.
391. R. Meij, D. J. Stufkens, K. Vrieze, W. van Gerresheim and C. H. Stam, *J. Organomet. Chem.*, 1979, **164**, 353.
392. G. H. Rentsch, W. Kozminski, W. von Philipsborn, F. Asaro and G. Pellizer, *Magn. Reson. Chem.*, 1997, **35**, 904.
393. L. K. Bell, D. M. P. Mingos, D. G. Tew, L. F. Larkworthy, B. Sandell, D. C. Povey and J. Mason, *J. Chem. Soc. Chem. Commun.*, 1983, 125.
394. L. Carlton and M.-P. Belciug, *J. Organomet. Chem.*, 1989, **378**, 469.
395. B. L. Haymore, M. Hughes, J. Mason and R. L. Richards, *J. Chem. Soc. Dalton Trans.*, 1988, 2935.

396. C. G. Barry, E. C. Turney, C. S. Day, G. Saluta, G. L. Kucera and U. Bierbach, *Inorg. Chem.*, 2002, **41**, 7159.
397. T. G. Appleton, J. R. Hall and S. F. Ralph, *Inorg. Chem.*, 1988, **27**, 4435.
398. K. S. Bose and E. H. Abbott, *Inorg. Chem.*, 1977, **16**, 3190.
399. K. J. Bradd, B. T. Heaton, C. Jacob, J. T. Sampanthar and A. Steiner, *J. Chem. Soc. Dalton Trans.*, 1999, 1109.
400. J. Gil-Rubio, B. Weberndörfer and H. Werner, *J. Chem. Soc. Dalton Trans.*, 1999, 1437.
401. J. Vicente, J. Gil-Rubio, D. Bautista, A. Sironi and N. Masciocchi, *Inorg. Chem.*, 2004, **43**, 5665.
402. J. Gil-Rubio, B. Weberndörfer and H. Werner, *Angew. Chem. Int. Ed.*, 2000, **39**, 786.
403. J. Gil-Rubio, M. Laubender and H. Werner, *Organometallics*, 2000, **19**, 1365.
404. S. A. Macgregor, D. C. Roe, W. J. Marshall, K. M. Bloch, V. I. Bakhmutov and V. V. Grushin, *J. Am. Chem. Soc.*, 2005, **127**, 15304.
405. V. A. Shipachev, S. V. Zemskov and S. V. Tkachev, *Koord. Khim.*, 1980, **6**, 1237.
406. J. Vicente, J. Gil-Rubio, J. Guerrero-Leal and D. Bautista, *Organometallics*, 2005, **24**, 5634.
407. D. A. Clement and J. F. Nixon, *J. Chem. Soc. Dalton Trans.*, 1972, 2553.
408. M. E. van der Boom, Y. Ben-David and D. Milstein, *J. Am. Chem. Soc.*, 1999, **121**, 6652.
409. J. Vicente, J. Gil-Rubio, J. Guerrero-Leal and D. Bautista, *Organometallics*, 2004, **23**, 4871.
410. R. P. Hughes, D. C. Lindner, L. M. Liable-Sands and A. L. Rheingold, *Organometallics*, 2001, **20**, 363.
411. J. F. Nixon, B. Wilkins and D. A. Clement, *J. Chem. Soc. Dalton Trans.*, 1974, 1993.
412. M. A. Bennett and D. J. Patmore, *Inorg. Chem.*, 1971, **10**, 2387.
413. J. F. Nixon and J. R. Swain, *J. Chem. Soc. Dalton Trans.*, 1972, 1044.
414. D. A. Clement and J. F. Nixon, *J. Chem. Soc. Dalton Trans.*, 1973, 195.
415. P. B. Hitchcock, S. Morton and J. F. Nixon, *J. Chem. Soc. Dalton Trans.*, 1985, 1295.
416. M. E. Howden, R. D. W. Kemmitt and M. D. Schilling, *J. Chem. Soc. Dalton Trans.*, 1983, 2459.
417. R. P. Hughes, R. B. Laritchev, A. Williamson, C. D. Incarvito, L. N. Zakharov and A. L. Rheingold, *Organometallics*, 2002, **21**, 4873.
418. P. Sangtrirutnugul, M. Stradiotto and T. D. Tilley, *Organometallics*, 2006, **25**, 1607.
419. S. N. Heaton, M. G. Partridge, R. N. Perutz, S. J. Parsons and F. Zimmermann, *J. Chem. Soc. Dalton Trans.*, 1998, 2515.
420. J. Ruiz and P. M. Maitlis, *J. Chem. Soc. Chem. Commun.*, 1986, 862.
421. F. L. Taw, A. H. Mueller, R. G. Bergman and M. Brookhart, *J. Am. Chem. Soc.*, 2003, **125**, 9808.
422. L. Turculet, J. D. Feldman and T. D. Tilley, *Organometallics*, 2004, **23**, 2488.
423. K. Osakada, S. Sarai, T. Koizumi and T. Yamamoto, *Organometallics*, 1997, **16**, 3973.
424. M. Okazaki, S. Ohshitanai, H. Tobita and H. Ogino, *J. Chem. Soc. Dalton Trans.*, 2002, 2061.
425. R. Goikhman and D. Milstein, *Chem. Eur. J.*, 2005, **11**, 2983.
426. R. Goikhman, M. Aizenberg, L. J. W. Shimon and D. Milstein, *Organometallics*, 2003, **22**, 4020.
427. Y. Nishihara, M. Takemura and K. Osakada, *Organometallics*, 2002, **21**, 825.
428. T. Koizumi, K. Osakada and T. Yamamoto, *Organometallics*, 1998, **17**, 5721.
429. E. Neumann and A. Pfaltz, *Organometallics*, 2005, **24**, 2008.
430. S. S. D. Brown, S. N. Heaton, M. H. Moore, R. N. Perutz and G. Wilson, *Organometallics*, 1996, **15**, 1392.
431. M. Garralda, V. Garcia, M. Kretschmer, P. S. Pregosin and H. Rüegger, *Helv. Chim. Acta*, 1981, **64**, 1150.
432. L. Fidalgo, M. A. Garralda, R. Hernández and L. Ibarlucea, *Inorg. Chim. Acta*, 1993, **207**, 121.
433. M. Lutz, C. Galka, M. Haukka, T. Pakkanen and L. H. Gade, *Eur. J. Inorg. Chem.*, 2002, 1968.
434. H. Moriyama, T. Aoki, S. Shinoda and Y. Saito, *J. Chem. Soc. Dalton Trans.*, 1981, 639.
435. T. Marx, L. Wesemann and S. Dehnen, *Z. Anorg. Allg. Chem.*, 2001, **627**, 1146.
436. L. Carlton and R. Weber, *Inorg. Chem.*, 1993, **32**, 4169.
437. D. A. Vicic, A. W. Myers and W. D. Jones, *Organometallics*, 1997, **16**, 2751.
438. M. Herberhold, M. Keller, W. Kremnitz, T. Daniel, W. Milius and B. Wrackmeyer, *Z. Anorg. Allg. Chem.*, 1998, **624**, 1324.
439. W. Levason, S. D. Orchard, G. Reid and J. M. Street, *J. Chem. Soc. Dalton Trans.*, 2000, 2537.
440. W. Levason, J. J. Quirk and G. Reid, *J. Chem. Soc. Dalton Trans.*, 1996, 3713.

441. P. F. Kelly, W. Levason, G. Reid and D. J. Williams, *J. Chem. Soc. Chem. Commun*., 1993, 1716.
442. E. G. Hope, W. Levason, S. G. Murray and G. L. Marshall, *J. Chem. Soc. Dalton Trans*., 1985, 2185.
443. W. Levason, S. D. Orchard and G. Reid, *Inorg. Chem*., 2000, **39**, 3853.
444. M. P. Devery, R. S. Dickson, B. W. Skelton and A. H. White, *Organometallics*, 1999, **18**, 5292.
445. K. Badyal, W. R. McWhinnie, H. L. Chen and T. A. Hamor, *J. Chem. Soc. Dalton Trans*., 1997, 1579.
446. M. Hesford, W. Levason, S. D. Orchard and G. Reid, *J. Organomet. Chem*., 2002, **649**, 214.
447. A. J. Barton, W. Levason, G. Reid and A. J. Ward, *Organometallics*, 2001, **20**, 3644.
448. K. Badyal, W. R. McWhinnie, J. Homer and M. C. Perry, *J. Organomet. Chem*., 1998, **555**, 279.
449. W. Levason, S. D. Orchard, G. Reid and V.-A. Tolhurst, *J. Chem. Soc. Dalton Trans*., 1999, 2071.
450. W. Levason, G. Reid and V.-A. Tolhurst, *J. Chem. Soc. Dalton Trans*., 1998, 3411.
451. T. Kemmitt, W. Levason, R. D. Oldroyd and M. Webster, *Polyhedron*, 1992, **11**, 2165.
452. B. E. Mann, N. J. Meanwell, C. M. Spencer, B. F. Taylor and P. M. Maitlis, *J. Chem. Soc. Dalton Trans*., 1985, 1555.
453. R. J. Lawson and J. R. Shapley, *Inorg. Chem*., 1978, **17**, 2963.
454. H. Werner, J. Wolf and A. Höhn, *J. Organomet. Chem*., 1985, **287**, 395.
455. W.-D. Wang, S. I. Hommeltoft and R. Eisenberg, *Organometallics*, 1988, **7**, 2417.
456. J. T. Mague and S. H. De Vries, *Inorg. Chem*, 1982, **21**, 1632.
457. J. T. Mague and A. R. Sanger, *Inorg. Chem*., 1979, **18**, 2060.
458. M. A. F. Hernandez-Gruel, J. J. Pérez-Torrente, M. A. Ciriano, A. B. Rivas, F. J. Lahoz, I. T. Dobrinovitch and L. A. Oro, *Organometallics*, 2003, **22**, 1237.
459. K. Osakada, T. Koizumi and T. Yamamoto, *Organometallics*, 1997, **16**, 2063.
460. K. E. Howard, T. B. Rauchfuss and S. R. Wilson, *Inorg. Chem*., 1988, **27**, 3561.
461. A. Fumagalli, S. Martinengo, P. Chini, A. Albinati, S. Bruckner and B. T. Heaton, *J. Chem. Soc. Chem. Commun*., 1978, 195.
462. A. R. Sanger, *Can. J. Chem*., 1984, **62**, 822.
463. W. Koźmiński and W. von Philipsborn, *J. Magn. Reson*., 1995, **116**, 262.

CHAPTER 4

The Indirect Detection of Metal Nuclei by Correlation Spectroscopy (HSQC and HMQC)

Jonathan A. Iggo, Jianke Liu and **Gillian Overend**

Contents

Abstract

This review discusses 2D HXQC methods for the indirect detection of the NMR spectrum of metal nuclei. The workings of several pulse sequences and of coherence selection are briefly outlined. The spin systems likely to be

Department of Chemistry, University of Liverpool, Donnan and Robert Robinson Laboratories, Oxford Street, Liverpool L69 7ZD, UK

Annual Reports on NMR Spectroscopy, Volume 63
ISSN 0066-4103, DOI 10.1016/S0066-4103(07)63004-X

encountered in HXQC NMR studies of metal coordination and cluster compounds are analysed and appropriate modifications to the standard experiments discussed. In the second part, the literature describing the application of HXQC methods to the detection of the resonances of metal nuclei, since 1999 are reviewed and tables of data presented.

1. INTRODUCTION

The detection of the NMR resonances of the metal nucleus in an inorganic or organometallic complex is a powerful tool in inorganic chemistry. The chemical shift of a metal nucleus can be very sensitive to small electronic, steric or geometrical changes in the coordination sphere, and the multiplicity of the resonance(s) can provide valuable information about the number and types of ligands present. Observation of the metal nucleus has the advantage that information is obtained directly from the centre of interest rather than second hand, inferred from the NMR spectrum of a ligand such as hydride or phosphine, and that the range of metal chemical shifts can be very large and thus informative of the environment of the metal nucleus. The disadvantage is that relaxation of the metal nucleus can be very slow, and many metal nuclei are of low sensitivity requiring very long total acquisition times to achieve useable signal to noise ratios (or even observe the resonance at all). Although this situation can be partially ameliorated by using polarization transfer, principally via the INEPT pulse sequence and its variants, this lack of sensitivity has limited the observation of the NMR spectra of most metal nuclei to a few, specialist groups.[1–9]

1.1 Advantages of indirect detection

2D correlation spectroscopy became routine in "organic" NMR spectroscopy in the 1980s; its application, in particular the introduction of indirect detection methods, principally HMQC[10–12] and HSQC,[13] to "inorganic" systems has revolutionized the NMR spectroscopy of metal nuclei as a result of the sensitivity gain, and hence much shorter experiment times necessary.[3,14] The sensitivity of any heteronuclear NMR experiment is related to the gyromagnetic ratios of the starting and the detected spins and a relaxation term, Equation (1).

$$\frac{S}{N} \propto \gamma_{start}\gamma_{detect}^{3/2}[1 - \exp\{-1/T_{1,start} \times RD\}] \quad (1)$$

where γ_{start} and γ_{detect} are the gyromagnetic ratios of the initially excited and detector spins, respectively, $T_{1,start}$ is the spin–lattice relaxation time constant of the excited spin and RD the experiment recycle time.

For HMQC and HSQC-type experiments, $\gamma_{start} = \gamma_I$, $\gamma_{detect} = \gamma_I$, hence the sensitivity $\sim\gamma_I^{5/2}$ (*cf.* a direct, polarization transfer experiment such as INEPT, $\gamma_{start} = \gamma_I$, $\gamma_{detect} = \gamma_S$, sensitivity $\sim\gamma_I\gamma_S^{3/2}$). Clearly, if detection of the metal

resonance is the aim of the experiment, HMQC and HSQC will be most effective when the detector nucleus has a high γ. Note, however, that indirect detection cannot compensate for a low natural abundance of the spin of interest since only the satellites from coupling to the metal are observed. Nonetheless, the sensitivity enhancement that can be achieved can be very large, Table 1.

Additionally, the HSQC and HMQC experiments provide a correlation map linking coupled sensitive and insensitive spins. The principle disadvantage of these techniques is that the number of sensitive spins (i.e., ligands) cannot be determined directly from the multiplicity of the (indirectly detected) metal nucleus since this information is intentionally ''refocused'' by the pulse sequence.

1.2 The metal chemical shift

The shielding of a nucleus can be described by Equation (2), in which σ_d refers to the diamagnetic term and arises from the influence of core electrons, and σ_p is the paramagnetic term.

$$\sigma = \sigma_d + \sigma_p \tag{2}$$

The diamagnetic term is essentially constant for any given metal, unless the valence shell is s, in which case $\sigma_p \sim 0$, and σ_d only determines the shielding. The chemical shift range of such a nuclide is small being of the order of a few tens of ppm. In contrast, the paramagnetic term, σ_p, gives a large shielding effect and dominates for transition and p-block metals, hence the chemical shift ranges of

Table 1 Theoretical enhancement factors for spin-1/2 metal nuclides

Metal nuclide	γ (10^7 rad s^{-1} T^{-1})	Enhancement factor *via* detection by			
		^{1}H	^{13}C[a]	^{19}F	^{31}P
^{57}Fe	0.8680624	5273	167	4532	551
^{77}Se	5.1253857	62	2	54	7
^{89}Y	1.3162791	1862	59	1601	195
^{103}Rh	0.8468	5610	178	4822	586
^{109}Ag	1.2518634	2111	67	1815	221
^{113}Cd	5.9609155	43	1	37	4
^{119}Sn	10.0317	12	0	10	1
^{125}Te	8.5108404	18	1	15	2
^{171}Yb	4.7288	76	2	65	8
^{183}W	1.1282403	2738	87	2353	286
^{187}Os	0.6192895	12265	389	10543	1282
^{195}Pt	5.8385	45	1	39	5
^{199}Hg	4.8457916	72	2	62	7
^{205}Ti	15.6921808	4	0	3	0
^{207}Pb	5.58046	50	2	43	5

[a]Assuming enrichment to 100%.

these nuclides are large, of the order of 10^3 to 10^4 ppm. There are two principal contributions to σ_p – the nephelauxetic effect of the ligands and contributions from mixing in of excited states, Equation (3),

$$-\sigma_p \propto (k^2 < r^{-3} >)(\Delta E^{-1}) \quad (3)$$

where the first term reflects the nephelauxetic effects, which are related to the inverse cube of the valence shell radius and k is the orbital reduction factor – a large k reflects little ligand contribution to the MO –, and the second term reflects mixing in of excited states, which shows an inverse dependence on the electronic excitation energy. For transition metal complexes, nephelauxetic effects dominate for hard, weak field ligands such as fluoride, oxygen-donors etc. Inspection of Equation (3) reveals that $|\sigma_p|$ will then increase as the covalent character of the M–L bond decreases and/or r decreases. Since σ_p acts in opposition to σ_d shielding decreases, the chemical shift becomes more positive. For strong field ligands, mixing in of excited states will be the dominant contribution to σ_p; $|\sigma_p|$ decreases as ΔE, the (average) energy of the d $\leftrightarrow$ d transition(s), increases. Once again shielding decreases, the chemical shift becomes more positive.[2,4,14] Recent advances in DFT are enabling the precise calculation of metal chemical shifts.[15–19] It should, however, be recognized that (some) metal nuclei show large temperature and solvent effects, thus, for example, Carlton[20] has recently determined the solvent and temperature effects on δ_{Rh} for a large number of square planar Rh(I) complexes, $[Rh(X)(PPh_3)_3]$ [X = Cl, N_3, NCO, NCS, $N(CN)_2$, $NCBPh_3$, $CNBPh_3$, CN] and derivatives containing CO, isocyanide, pyridine, H_2 and O_2. δ_{Rh} was obtained indirectly using the standard HMQC pulse sequence.

1.3 Referencing of spectra

Referencing of the NMR spectra of metal nuclei has often been problematic, since this nearly always involves an external reference. Furthermore, for some nuclei, e.g., ^{103}Rh and ^{195}Pt, several references are in use. The chemical shift may also show large concentration and/or temperature variations. In an effort to establish universal NMR standards, and hence chemical shift scales, IUPAC have recently adopted a procedure in which all NMR spectra are, effectively, referenced to the ^{1}H signal of TMS.[21]

The procedure can be summarized thus:

1. Record a ^{1}H NMR spectrum of TMS in the same solvent as that used for the real sample. If TMS is compatible with the sample under study, then simply add TMS to the sample and record the ^{1}H NMR spectrum in addition to the spectrum of interest.
2. Note the *absolute* frequency of TMS = Θ_{TMS}.
3. Look up the reference frequency, Ξ_X, (against TMS = 100 MHz exactly) for the nuclide of interest (X) in Table 2 or 3.
4. Record the NMR spectrum of the sample of interest.
5. The zero of the ppm scale for the nuclide X is then $\Xi_X \times \Theta_{TMS}/100$ MHz, exactly.

Table 2 The spin properties of selected spin-1/2 metal nuclei[a]

Isotope	Natural abundance (χ/%)	Magnetic moment (μ/μ_N)	Magnetogyric ratio ($\gamma/10^7$ rad s^{-1} T^{-1})	Frequency ratio[b] (Ξ %)	Reference compound	Sample conditions[c]	Relative receptivity[d] (D^C)
^{1}H	99.9885	4.837353570	26.7522128	100.000000[e]	Me_4Si	$CDCl_3$, φ=1%	5.87×10^3
^{57}Fe	2.119	0.1569636	0.8680624	3.237778	$Fe(CO)_5$	80% in C_6D_6	4.25×10^{-3}
^{77}Se	7.63	0.92677577	5.1253857	19.071513	Me_2Se	Neat/C_6D_6	3.15
^{89}Y	100	−0.23801049	−1.3162791	4.900198	$Y(NO_3)_3$	H_2O/D_2O	0.700
^{103}Rh	100	−0.1531	−0.8468	3.186447[f,g]	$Rh(acac)_3$	$CDCl_3$, sat.	0.186
^{109}Ag	48.161	−0.22636279	−1.2518634	4.653533	$AgNO_3$	D_2O, sat.	0.290
^{113}Cd[h]	12.22	−1.0778568	−5.9609155	22.193175	Me_2Cd	Neat	7.94
^{119}Sn	8.59	−1.81394	−10.0317	37.290632	Me_4Sn	Neat/C_6D_6	26.6
^{125}Te	7.07	−1.5389360	−8.5108404	31.549769	Me_2Te	Neat/C_6D_6	13.4
^{171}Yb	14.28	0.85506	4.7288	17.499306	$Yb(C_5Me_5) \cdot THF_2$	THF, 0.171 M	4.63
^{183}W	14.31	0.20400919	1.1282403	4.166387	Na_2WO_4	D_2O, 1 M	6.31×10^{-2}
^{187}Os	1.96	0.1119804	0.6192895	2.282331	OsO_4	CCl_4, 0.98 M	1.43×10^{-3}
^{195}Pt	33.832	1.0557	5.8385	21.496784[f]	Na_2PtCl_6	D_2O, 1.2 M	20.7
^{199}Hg	16.87	0.87621937	4.8457916	17.910822	Me_2Hg[i]	Neat	5.89
^{205}Ti	70.476	2.83747094	15.6921808	57.683838	$Ti(NO_3)_3$	H_2O, inf. dilution	8.36×10^2
^{207}Pb	22.1	1.00906	5.58046	20.920599	Me_4Pb	Neat/C_6D_6	11.8

[a] Adapted from ref. 21. © IUPAC.
[b] Ratio, expressed as a percentage, of the resonance frequency of the reference to that of the protons of TMS at infinite dilution (in practice at $\varphi = 1\%$) in $CDCl_3$.
[c] M, molarity in mol dm^{-3} (solution); m, molality in mol kg^{-1} (solvent). See [a] for further details.
[d] D^C is the receptivity relative to that of ^{13}C, see *NMR and the Periodic Table*, R. K. Harris and B. E. Mann (eds.), Academic Press (1978).
[e] By definition.
[f] The precise values 3.160000 MHz and 21.400000 have also been suggested as the references for ^{103}Rh and ^{195}Pt, respectively.[22,23]
[g] Subject to considerable variation with temperature.
[h] Long-lived radioactive isotope.
[i] The high toxicity of this compound means its use should be discouraged.

Table 3 The spin properties of selected quadrupolar metal nuclei[a]

Isotope	Spin	Natural abundance (χ/%)	Magnetic moment (μ/μ_N)	Magnetogyric ratio ($\gamma/10^7$ rad s^{-1} T^{-1})	Quadrupole moment (Q/fm^2)	Frequency ratio[b] (Ξ %)	Reference sample	Sample conditions[c]	Line width factor[d] (λ/fm^4)	Relative receptivity[e] (D^C)
^{6}Li	1	7.59	1.1625637	3.9371709	−0.0808	14.716086	LiCl	D_2O, 9.7 m	0.033	3.79
^{7}Li	3/2	92.41	4.20407505	10.3977013	−4.01	38.863797	LiCl	D_2O, 9.7 m	21	1.59×10^3
^{9}Be	3/2	100	−1.520136	−3.759666	5.288	14.051813	$BeSO_4$	D_2O, 0.43 m	37	81.5
^{23}Na	3/2	100	2.8629811	7.0808493	10.4	26.451900	NaCl	D_2O, 0.1 M	140	5.45×10^2
^{25}Mg	5/2	10.00	−1.01220	−1.63887	19.94	6.121635	$MgCl_2$	D_2O, 11 M	130	1.58
^{27}Al	5/2	100	4.3086865	6.9762715	14.66	26.056859	$Al(NO_3)_3$	D_2O, 1.1 m	69	1.22×10^3
^{39}K	3/2	93.2581	0.50543376	1.2500608	5.85	4.666373	KCl	D_2O, 0.1 M	46	2.79
^{43}Ca	7/2	0.135	−1.494067	−1.803069	−4.08	6.730029	$CaCl_2$	D_2O, 0.1 M	2.3	5.10×10^{-2}
^{45}Sc	7/2	100	5.3933489	6.5087973	−22.0	24.291747	$Sc(NO_3)_3$	D_2O, 0.06 M	66	1.78×10^3
^{47}Ti	5/2	7.44	−0.93294	−1.5105	30.2	5.637534	$TiCl_4$	Neat	290	0.918
^{49}Ti	7/2	5.41	−1.25201	−1.51095	24.7	5.639037	$TiCl_4$	Neat	83	1.20
^{51}V	7/2	99.750	5.8380835	7.0455117	−5.2	26.302948	$VOCl_3$	Neat/C_6D_6	3.7	2.25×10^3
^{53}Cr	3/2	9.501	−0.61263	−1.5152	−15.0	5.652496	K_2CrO_4	D_2O, sat.	300	0.507
^{55}Mn	5/2	100	4.1042437	6.6452546	33.0	24.789218	$KMnO_4$	D_2O, 0.82 m	350	1.05×10^3
^{59}Co	7/2	100	5.247	6.332	42.0	23.727074	$K_3[Co(CN)_6]$	D_2O, 0.56 m	240	1.64×10^3
^{61}Ni	3/2	1.1399	−0.96827	−2.3948	16.2	8.936051	$Ni(CO)_4$	Neat/C_6D_6	350	0.240
^{63}Cu	3/2	69.17	2.8754908	7.1117890	−22.0	26.515473	$[Cu(CH_3CN)_4][ClO_4]$	CH_3CN, sat.	650	3.82×10^2
^{65}Cu	3/2	30.83	3.07465	7.60435	−20.4	28.403693	$[Cu(CH_3CN)_4][ClO_4]$	CH_3CN, sat.	550	2.08×10^2

^{67}Zn	5/2	4.10	1.035556	1.676688	15.0	6.256803	$Zn(NO_3)_2$	D_2O, sat.	72	0.692
^{71}Ga	3/2	39.892	3.307871	8.181171	10.7	30.496704	$Ga(NO_3)_3$	D_2O, 1.1 m	150	3.35×10^2
^{73}Ge	9/2	7.73	−0.9722881	−0.9360303	−19.6	3.488315	$(CH_3)_4Ge$	Neat	28	0.642
^{87}Rb[f]	3/2	27.83	3.552582	8.786400	13.35	32.720454	RbCl	D_2O, 0.01 M	240	2.90×10^2
^{87}Sr	9/2	7.00	−1.2090236	−1.1639376	33.5	4.333822	$SrCl_2$	D_2O, 0.5 M	83	1.12
^{91}Zr	5/2	11.22	−1.54246	−2.49743	−17.6	9.296298	$Zr(C_5H_5)_2Cl_2$	CH_2Cl_2, sat.	99	6.26
^{93}Nb	9/2	100	6.8217	6.5674	−32.0	24.476170	$K[NbCl_6]$	CH_3CN, sat.	76	2.87×10^3
^{95}Mo	5/2	15.92	−1.082	−1.751	−2.2	6.516926	Na_2MoO_4	D_2O, 2 M	1.5	3.06
^{99}Tc[f]	9/2	–	6.281	6.046	−12.9	22.508326	NH_4TcO_4	D_2O	12	–
^{99}Ru	5/2	12.76	−0.7588	−1.229	7.9	4.605151	$K_4[Ru(CN)_6]$	D_2O, 0.3 M	20	0.848
^{101}Ru	5/2	17.06	−0.8505	−1.371	45.7	5.161369	$K_4[Ru(CN)_6]$	D_2O, 0.3 M	670	1.59
^{115}In[f]	9/2	95.71	6.1256	5.8972	81.0	21.912629	$In(NO_3)_3$	D_2O, 0.1 M	490	1.98×10^3
^{121}Sb	5/2	57.21	3.9796	6.4435	−36.0	23.930577	$KSbCl_6$	CH_3CN, sat	410	5.48×10^2
^{133}Cs	7/2	100	2.9277407	3.5332539	−0.343	13.116142	$CsNO_3$	D_2O, 0.1 M	0.016	2.84×10^2
^{137}Ba	3/2	11.232	1.21013	2.99295	24.5	11.112928	$BaCl_2$	D_2O, 0.5 M	800	4.62
^{139}La	7/2	99.910	3.1556770	3.8083318	20.0	14.125641	$LaCl_3$	D_2O, 0.01 M	54	3.56×10^2
^{181}Ta	7/2	99.988	2.6879	3.2438	317.0	11.989600	$KTaCl_6$	CH_3CN, sat.	1.4×10^4	2.20×10^2
^{187}Re[f]	5/2	62.60	3.8096	6.1682	207.0	22.751600	$KReO_4$	D_2O, 0.1 M	1.4×10^4	5.26×10^2
^{209}Bi	9/2	100	4.5444	4.3750	−51.6	16.069288	$Bi(NO_3)_2$	$HNO_3/D_2O/H_2O$	200	8.48×10^2

[a] Adapted from ref. 21. © IUPAC.
[b] Ratio of the resonance frequency of the reference to that of the protons of TMS at infinite dilution (in practice at $\varphi = 1\%$) in $CDCl_3$.
[c] M, molarity in mol dm^{-3} (solution); m, molality in mol kg^{-1} (solvent). See [a] for further details.
[d] $l = (2I+3)Q^2/I^2(2I-1)$. The values are quoted, arbitrarily, to 2 significant figures.
[e] D^C is the receptivity relative to that of ^{13}C.
[f] Radioactive, with a long half-life.

6. Enter this value into the appropriate parameter on the spectrometer, e.g., SF on a Bruker Avance spectrometer.

Tables 2 and 3 also give the reference compound on which each chemical shift is based. It should be noted that:

1. Under the IUPAC scheme, these compounds act as *secondary* references.
2. Some of the reference compounds chosen by IUPAC differ from common practice, e.g., many workers reference ^{103}Rh to $\Xi_{Rh} = 3.16\,MHz$ when $\Theta_{TMS} = 100\,MHz$.
3. Some reference compounds are extremely hazardous, e.g., $Fe(CO)_5$, $HgMe_2$, OsO_4, $PbMe_4$ etc. In these cases the IUPAC scheme should be followed.
4. The chemical shifts of many nuclides of interest to the inorganic chemist, e.g., ^{31}P, ^{103}Rh and ^{195}Pt, show large temperature, concentration and/or solvent shifts; referencing to an absolute frequency, rather than a compound makes good sense.
5. Given the above, the temperature and concentration, as well as the solvent, need to be given when reporting data.

In the first part of this article, the HMQC, and HSQC experiments, and some of their relevant variants are described, and the relative merits of the experiments discussed. 1D experiments designed to determine metal–ligand nucleus scalar coupling constants are intentionally excluded since these do not result in the observation of the metal resonance. The area was last reviewed by Gudat[24] in 1999. The second part of this review provides a compendium of NMR data for metal complexes studied by HMQC and HSQC methods over the last *ca*. 10 years.

2. 2D NMR SPECTROSCOPY

There are usually four parts to a 2D NMR experiment: preparation, evolution, mixing and acquisition, Figure 1. Each sequence is, of course, preceded by a recovery period for the excited spins to relax back to Boltzmann equilibrium. During the preparation period, one or more pulses, interspersed with delays are used to create, and exchange coherence between spins or to destroy coherences that would otherwise give undesired signals in the final spectrum. During the evolution period, the spin system evolves under the influence of the interaction(s) selected during the preparation period, for example the chemical shift of a second nucleus, scalar coupling between spins, diffusion, etc. During the subsequent mixing period, coherence transfer between those nuclear spins encoded in the evolution period and those detected during the acquisition period occurs. Thus, the acquired FID is modulated by the information exchanged between spins during the evolution period. A series of FIDs is recorded, in which the length of the evolution period is systematically increased, creating a second time dimension, characterized by the variable evolution time t_1, Figure 1 (top left). Fourier transformation of these FIDs gives a series of spectra, in which the

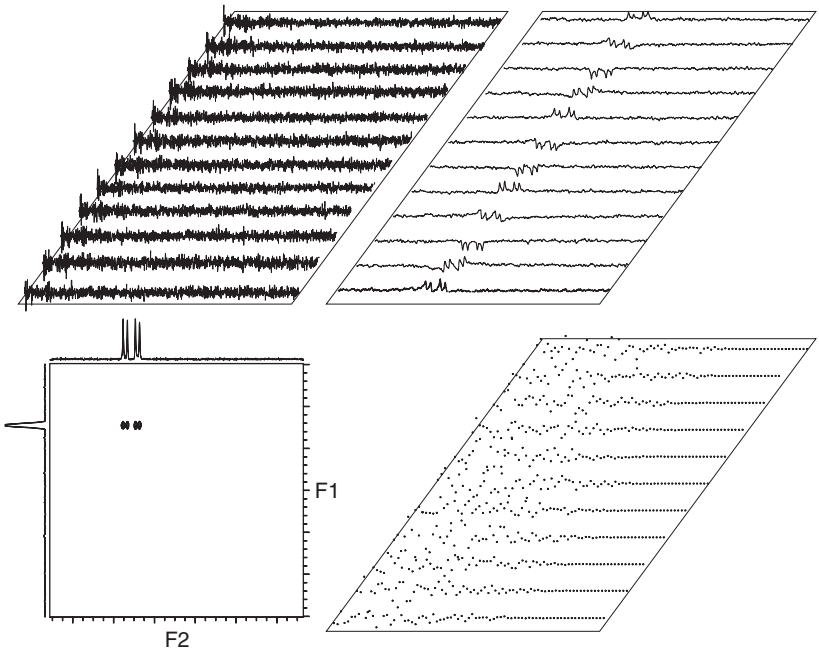

Figure 1 Schematic outline of a generalized 2D NMR. A series of 1D FIDs, modulated by the interaction of interest and an incremented time delay is recorded (top left), and Fourier transformed to give a series of 1D spectra (top right) which will be modulated by the interaction of interest and separated by the incremented time delay. A second series of FIDs is created by "reading" up the stack of spectra (bottom right). Fourier transformation of this set of FIDs gives a 2D spectrum in which peaks appear that correlate the directly observed chemical shift with the interaction(s) of interest (bottom left).

intensities of the peaks are modulated as a function of t_1 and the interactions between spins that were active during the evolution time, Figure 1 (top right). A second set of FIDs can thus be created ''perpendicular'' to these spectra by plotting the intensity, at each frequency in the spectrum, as a function of t_1, Figure 1 (bottom right). Fourier transformation with respect to t_1 produces a map, in which peaks (correlations) occur that link resonances by the NMR interaction(s) that was active during the evolution period. By convention, the directly detected dimension is labelled F2, and the dimension created by the incremented delays, t_1, is labelled F1. For example, if scalar coupling between ^{103}Rh and ^{31}P is used to place NMR coherence on ^{103}Rh during the preparation period, and the ^{103}Rh chemical shift is active during the evolution period, then δ(Rh) will appear in the F1 dimension. Assuming we are directly observing the ^{31}P NMR spectra then δ(P) will appear in the F2 dimension and correlations will appear in the 2D spectrum that link coupled ^{103}Rh and ^{31}P spins, i.e., the ^{31}P, ^{103}Rh heteronuclear correlation spectrum, Figure 1 (bottom left).

2.1 HMQC and HSQC pulse sequences

There is a bewildering array of variants of the basic HMQC and HSQC pulse sequences. The distinction between these two families of experiments is that in the first, magnetization is stored as multiple quantum coherence during the evolution period, while in the second it is stored as single-quantum coherence. This impacts on the interactions that are active during the pulse sequence, on relaxation processes, and hence on the line-widths in the final spectrum. In order to decide which experiment is the most appropriate to a particular sample, it is necessary first to look at the workings, and their consequences, of the pulse sequences. http://www-keeler.ch.cam.ac.uk/lectures/index.html and http://www.pitt.edu/~pkm9/pravat.pdf are highly recommended to the reader for detailed information on the workings of pulse sequences, phase cycling, gradient selection, etc.

2.1.1 HMQC

The basic HMQC sequence uses multiple quantum coherences to correlate the chemical shifts of a detector spin I and a scalar coupled spin S. The pulse sequence is shown in Figure 2. The centrally placed 180° I pulse p2 refocuses the evolution of the I spin chemical shift over the entire pulse sequence, therefore we only need to consider evolution of the I spin under the influence of scalar coupling. (S spin chemical shifts are, of course not refocused by p2, so must be considered.)

The sequence begins with a 90° X pulse on I followed by a delay, normally set to $1/\{2J(\mathrm{IS})\}$, which together create anti-phase magnetization. Since $d_2 = 1/\{2J(\mathrm{IS})\}$, the cosine term vanishes and the sine term is unity, Equation (4) (in the equations that follow, only the "active" element is given above the arrow).

$$\mathrm{I}_Z \xrightarrow{90^\circ(\mathrm{I})_X} -\mathrm{I}_Y \xrightarrow{J(\mathrm{IS}),\ t_1=1/2J} 2\mathrm{I}_X\mathrm{S}_Z \tag{4}$$

p3 converts this anti-phase magnetization into zero- and double-quantum coherences, Equation (5).

$$2\mathrm{I}_X\mathrm{S}_Z \xrightarrow{90^\circ(\mathrm{S})_X} -2\mathrm{I}_X\mathrm{S}_Y \tag{5}$$

This magnetization evolves under the influence of the S spin chemical shift

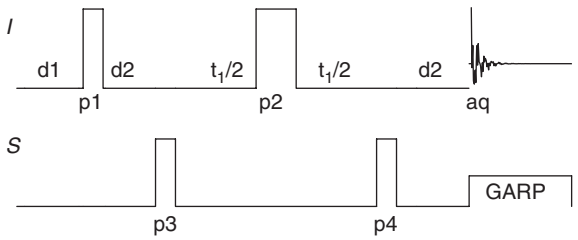

Figure 2 The basic HMQC pulse sequence. To eliminate signals from I spins not coupled to S, the phases of p3, and of the receiver alternate $X,-X$. Additional phase cycling may be used, e.g., to eliminate the effects of pulse imperfections.

during the incremented delay t_1 and is converted back into observable I spin magnetization by p4, Equation (6).

$$-2I_XS_Y \xrightarrow{\Omega S_Z.t} -2I_XS_Y\cos(\Omega_S \cdot t_1) + 2I_XS_X\sin(\Omega_S \cdot t_1)$$
$$\xrightarrow{(90^\circ)S_X} -2I_XS_Z\cos(\Omega_S \cdot t_1) + 2I_XS_Z\sin(\Omega_S \cdot t_1) \quad (6)$$

The delay $d_2 = 1/\{2J(\mathrm{IS})\}$ after p4 allows IS coupling to refocus, converting the anti-phase magnetization into in-phase magnetization, Equation (7). This delay is only strictly necessary in the basic sequence if decoupling of the S spin is used during acquisition.

$$-2I_XS_Z\cos(\Omega_S \cdot t_1) + 2I_XS_Z\sin(\Omega_S \cdot t_1) \xrightarrow{J(\mathrm{IS})\cdot t} -I_Y\cos(\Omega_S.t_1) + 2I_XS_Z\sin(\Omega_S \cdot t_1) \quad (7)$$

Only the single-quantum coherence is observed; the unobservable multiple quantum coherence can, however, be converted into observable single-quantum magnetization, to give a sensitivity enhanced version of the experiment. Note, however, that sensitivity enhanced pulse sequences usually recover this magnetization only from a spin pair and should therefore be used with care.

Successful implementation of the experiment requires accurate setting of the delay d_2, which can be measured directly from the 1D spectrum of the detector, or via the 1D HMQC sequence if the satellites due to coupling to the metal are not clearly visible. Where several, isolated, metal sites are present, each showing different coupling to the detector use of an accordion-type experiment, in which the delays d_2 are replaced by an incremented delay t_{acc}, has been proposed.[25]

2.1.2 HSQC

The HSQC pulse sequence employs an INEPT transfer followed by a reverse INEPT sequence to correlate I and S spins via single-quantum coherence. The basic sequence is shown in Figure 3. The central 180° I pulse, p4, refocuses J(IS) in F1 and the I spin chemical shift and is omitted from the analysis below for simplicity.

The sequence begins with a 90° X pulse on I followed by a delay d_2, set to $1/\{4J(\mathrm{IS})\}$, during which I–S scalar coupling and I chemical shift develops. The latter is refocused by p2 and the subsequent delay d_2. However, due to the simultaneous 180° pulse on S, the magnetization after the second d_2 delay is modulated by J(IS). Since $d_2 = 1/\{4J(\mathrm{IS})\}$, the cosine term vanishes and the sine term is unity, Equation (8), thus pure anti-phase I spin magnetization is

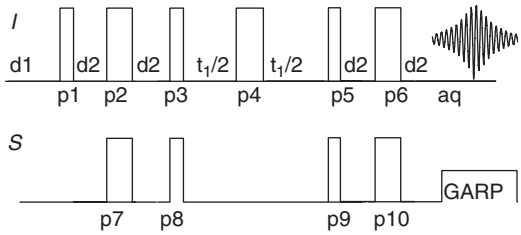

Figure 3 The basic HSQC pulse sequence. The phase of p3 and p5 is Y, p4 alternates X, $-X$; p9 $(X)_2$, $(-X)_2$; and p7 and p10 $(X)_4$, $(-X)_4$. The receiver alternates X,$-X$.

produced. The simultaneous 90° pulses, p3 and p8, transfer this coherence to S.

$$\begin{aligned} I_Z &\xrightarrow{90^\circ(I)_X} -I_Y \xrightarrow{J(IS)\cdot t} -I_Y\cos(\pi Jt) + 2I_XS_Z\sin(\pi Jt) \\ &\xrightarrow{2d_2=1/2J} 2I_XS_Z \\ &\xrightarrow{90^\circ(I)_{-Y},90^\circ(S)_X} -2I_ZS_Y \end{aligned} \tag{8}$$

S spin chemical shifts develop during the incremented delay t_1, Equation (9) – remember p4 refocuses J(IS).

$$-2I_ZS_Y \xrightarrow{\Omega S_Z\cdot t} -2I_ZS_Y\cos(\Omega_S\cdot t_1) + 2I_ZS_X\sin(\Omega_S\cdot t_1) \tag{9}$$

This magnetization is transferred back to I by the simultaneous 90° pulses p5 and p9. As before, a spin-echo period follows during which I–S scalar coupling and I chemical shift develop. The latter is refocused by p6 and the subsequent delay d_2, while the simultaneous 180° pulse on S, p10, means the magnetization after the second d_2 delay is again modulated by J(IS). Since $d_2 = 1/\{4J(IS)\}$, the cosine term vanishes and the sine term is unity, Equation (10), thus in phase I spin magnetization is produced.

$$\begin{aligned} &-2I_ZS_Y\cos(\Omega_S\cdot t_1) + 2I_ZS_X\sin(\Omega_S\cdot t_1) \\ &\xrightarrow{90^\circ(I)_Y,(S)_X} -2I_XS_Z\cos(\Omega_S\cdot t_1) + 2I_XS_X\sin(\Omega_S\cdot t_1) \\ &\xrightarrow{J(IS)\cdot t,2d_2=1/2J} I_Y\cos(\Omega_S\cdot t_1) - 2I_XS_X\sin(\Omega_S\cdot t_1) \end{aligned} \tag{10}$$

Phase cycling is used to remove magnetization from I spins not coupled to S, e.g., in a ^{1}H, ^{195}Pt experiment, from molecules containing NMR silent platinum, and from double quantum terms.

2.1.3 Comments on the HMQC and HSQC sequences

The HMQC sequence uses a small number of pulses, i.e., it is short, while the HSQC sequence uses 10 pulses. The HMQC sequence is therefore relatively less affected by pulse imperfections/mis-setting, which result in a reduction in intensity of the desired coherences. Furthermore, storing the magnetization as multiple quantum coherence, which has a relatively longer characteristic spin–spin relaxation time, should afford higher resolution. HMQC has therefore been favoured by most workers in the field, since, in principle, it should give better signal to noise. In practice there is often little to choose between the various pulse sequences, see Figure 4 which presents slices through the spectra of the PPh_3 adduct of $[Rh_2(\mu\text{-octanoate})_4]$ recorded using a variety of HMQC and HSQC sequences. The same number of scans were used in each experiment; pulse lengths were not optimized since, for most metal nuclei, it is impractical to measure the 90° pulse lengths for every sample; Figure 4 therefore presents a realistic picture of what result *might*, in real life, be obtained. For this sample, the sensitivity enhanced HSQC experiment has a slight advantage in signal to noise while the HMQC variants give a slightly sharper peak.

Other factors to bear in mind include passive coupling and exchange. Passive coupling between I spins modulates the multiple quantum coherence, resulting

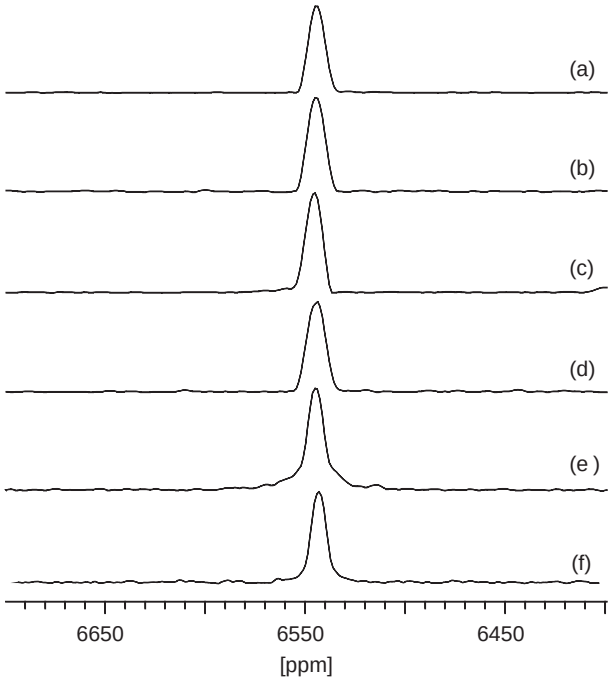

Figure 4 Slices through the spectra of the PPh_3 adduct of $[Rh_2(\mu\text{-octanoate})_4]$ (0.06 M) recorded using: (a) sensitivity improved, echo–anti-echo HSQC; (b) echo–anti-echo gradient selected HSQC; (c) phase cycle selected, phase sensitive HSQC; (d) echo–anti-echo gradient selected HMQC; (e) gradient selected HMQC; and (f) phase cycle selected, HMQC. (e) and (f) are most commonly used in the indirect detection of metal resonances.

in splitting of the signals in the F1 (S spin) dimension of an HMQC spectrum, but is absent from the HSQC spectrum, Figure 5. The HMQC experiment is also more affected by exchange broadening, since both the I and S spins are in the *xy* plane; exchange is, of course, commonplace in transition metal chemistry. Which experiment gives the better signal to noise ratio will therefore depend both on the peculiarities of the system under study and on the accuracy with which pulse lengths and delays are set.

2.2 Coherence selection

In both HMQC and HSQC it is necessary to eliminate unwanted signals, e.g., signals that are not modulated by the coherence of interest, and/or that arise from molecules that do not contain the spin pair of interest (which will always be present if the metal nuclide is less than 100% abundant). There are several ways of doing this; phase cycling, phase cycling in conjunction with a BIRD sequence, spin-locking or gradient selection. The two most commonly employed methods are phase cycling and gradient selection.

2.2.1 Phase cycle selection

Phase cycle selection is easily understood in the terms of the vector picture of nuclear spin magnetization. In the rotating frame, a pulse rotates the magnetization vector. The strength of the pulse determines the amount of rotation, and the phase of the pulse is defined by the axis about which the magnetization is rotated. The pulse strength, and phases of the excitation pulse and receiver are set by the pulse programme. The appearance of the resulting spectrum, i.e., whether it shows positive or negative peaks, absorption or dispersion lineshapes, will depend on the relative phases of the magnetization vector and the receiver. This is shown in Figure 6 for a 90° pulse. Inspection of Figure 6 reveals that it is possible to choose the receiver phase, with respect to the magnetization vector, so that the magnetization from successive FIDs adds or cancels – this is the basis of phase cycle selection. Phase cycle selection is a subtractive process; the phases of the pulses and of the receiver are arranged so that the desired coherences sum while undesired signals cancel. Subtractive

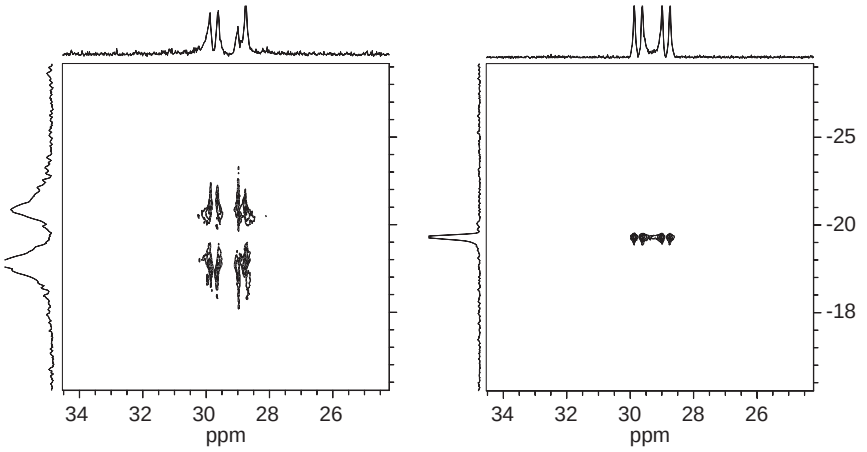

Figure 5 Phase sensitive $^{31}P,^{103}Rh\{^{1}H\}$ HMQC (left) and HSQC (right) spectra of Wilkinson's catalyst, $[Rh(PPh_3)_3Cl]$, (30 mg in 0.8 mL $CDCl_3$, 295 K) illustrating the splitting of the resonances in F1 (^{103}Rh) by passive couplings between the *cis* and *trans* phosphine ligands. Only the *trans*-PPh_3 region is shown.

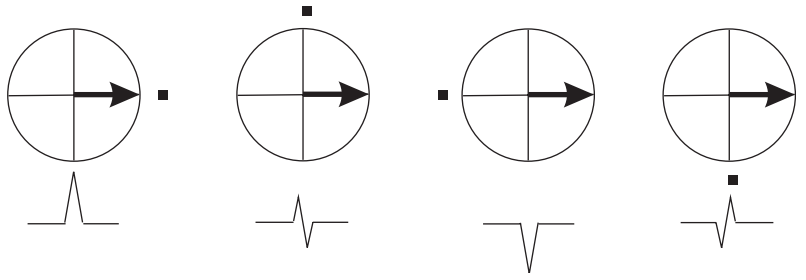

Figure 6 The expected lineshape in the spectrum for different relative phases of the magnetization (→) and the receiver (■).

processes are never perfect resulting in breakthrough of the undesired signals and in t_1 noise which can severely degrade the final 2D spectrum.

2.2.2 Coherence transfer pathway approach

The vector model provides a simple explanation of phase cycling, however, in complex pulse sequences a more rigorous approach is needed to design the optimum phase cycling scheme to discriminate between wanted and unwanted signals, always assuming that a pulse sequence that generates the desired coherences has been designed. The CTP approach is an aid to determining the effect of the phase cycling/gradient selection on the coherences present. Coherences are given a label, p, the coherence order, according to the way in which they respond to rotation about the z-axis. Single-quantum coherence has $p = \pm 1$, double $p = \pm 2$ and so on; z-magnetization, "zz" terms and zero-quantum coherence have $p = 0$. The pulses of the pulse sequence transfer coherences from one order to one or more different orders, the coherence experiencing a phase shift of $-\Delta p\phi$ as a result, where ϕ is the phase shift of the pulse causing the change in coherence order Δp, i.e., the change in coherence order produced by a pulse is labelled by the phase of the pulse and the size of this label depends on the change in coherence order. These changes in coherence order are shown below the pulse sequence, e.g., Figure 7, which shows the coherence transfer pathways in the HMQC experiment.

In an HMQC experiment, the aim of the phase cycle is to eliminate signals from I spins not coupled to S by cycling the phase of a pulse which affects the desired coherence but not that of isolated I spins. This pulse could be either p3 or p4, each of which give a change in coherence order of $\Delta p_S = \pm 1$, while $\Delta p_I = 0$. Table 4 gives the phase shift, $-\Delta p\phi$, experienced by the $\Delta p_S = +1$ transferred coherence and the phase shift of the receiver needed to sum the signals from this coherence. Clearly, a 0, −180 alternation of the receiver phase will cause signals from isolated I spins

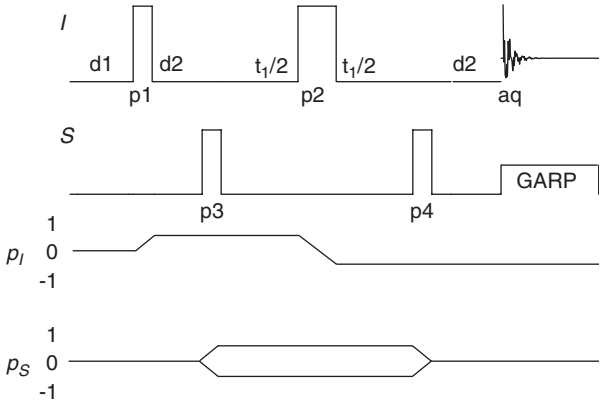

Figure 7 The coherence transfer pathways in the HMQC experiment. The coherence orders required at each point in the pulse sequence, and the changes in coherence order produced by each pulse are indicated by the solid lines beneath the sequence; the desired change in coherence order is selected by the appropriate phase cycle.

to cancel while preserving the signal from the $\Delta p_S = +1$ transferred coherence. Similarly, a 0, +180 alternation of the receiver phase will preserve signals from the $\Delta p_S = -1$ transferred coherence. These two receiver phase cycles are equivalent, thus both $\Delta p_S = \pm 1$ transferred coherences are selected. This is the origin of the greater signal intensity available in phase cycle selected, as opposed to gradient selected, HMQC; the latter can select only one coherence transfer pathway.

2.2.3 Gradient selection

Field gradient pulses offer an alternative method to select particular coherence pathways. The application of a field gradient to the sample causes transverse magnetization and other coherences to dephase. However, if an equal and opposite gradient pulse is applied, then an equal but opposite ''de-dephasing'' of the magnetization occurs and a gradient echo is produced. In fact, the refocusing gradient can be adjusted so that only some coherences are refocused, while unwanted signals continue to dephase and hence are ''lost''. However, gradients can only refocus one of the coherence transfer pathways, *N*- or *P*-type, Figure 8,

Table 4 Phase shift, $-\Delta p\phi$, experienced by the transferred coherence in the HMQC experiment on altering the phase of p3

Step	Pulse phase	Phase shift experienced by transfer with $\Delta p = +1$	Required receiver phase
1	0	0	0
2	180	−180	−180

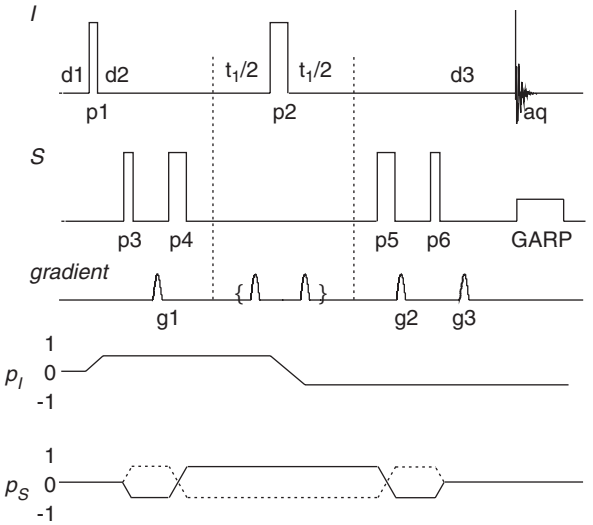

Figure 8 An echo–anti-echo version of the HMQC pulse sequence that affords absorption lineshapes. The gradient pulses in parentheses are optional and remove magnetization resulting from mis-setting of p2.

in the HMQC sequence in a single experiment resulting in a lower intrinsic sensitivity compared with phase cycle selection. The CTP approach is routinely used to describe coherence transfer in gradient selected experiments.

2.3 Gradient HMQC and HSQC

2.3.1 Gradient enhanced HMQC

There are several variants of HMQC using gradient selection, Figure 8 shows an echo–anti-echo version that affords absorption lineshapes. As mentioned above, gradients can only refocus one of the two coherence transfer pathways in a single experiment; the two possible pathways are shown as solid and dashed lines, respectively. Recording alternate spectra, in which the sign of gradient g3 is reversed, allows the pathway of the solid line (*N*-type or echo spectrum) or the dashed pathway (*P*-type or anti-echo spectrum) to be recorded. Combining the results affords a spectrum with pure absorption lineshapes.

As in the non-gradient version, chemical shift evolution of the I spins across the whole sequence is refocused by the 180° I pulse, p2. Since this pulse is positioned midway between gradients g1 and g2, which have equal strengths, the dephasing of the I spin coherence caused by g1 is refocused by g2, i.e., there is no net dephasing of the I spin part of the heteronuclear multiple quantum coherence by the two gradients. The S spin coherence, however, does experience net dephasing as a result of g1 and g2 that is not refocused until g3. Refocusing will occur when the gradient strengths satisfy Equation (11), where the + and – signs refer to the *P*- and *N*-type spectra, respectively.

$$\mp 2(g1)(\gamma_S) - (g3)(\gamma_I) = 0 \tag{11}$$

The S spin pulses, p4 and p5, and their associated delays are needed to refocus chemical shift evolution during the two g1 gradient pulses. Magnetization from I spins not coupled to S, and therefore not involved in heteronuclear multiple quantum coherence, is dephased by the final gradient g3. Better suppression of these unwanted signals is usually achieved by this dephasing than can be achieved by subtractive phase cycling, hence t_1 noise is much reduced.

Figure 9 shows the ''non-phase sensitive'' version of the gradient HMQC sequence that is commonly used, although it gives skew lineshapes from which coupling constants cannot be measured accurately.

Note, in this sequence the three gradients have different strengths; refocusing occurs when Equation (12) is satisfied.

$$(g1)(\gamma_I + \gamma_S) + (g2)(-\gamma_I + \gamma_S) + (g3)(-\gamma_I) = 0 \tag{12}$$

2.3.2 Gradient enhanced HSQC

Figure 10 illustrates a simple implementation of gradient selection in the HSQC experiment.

Suppression of unwanted magnetization, which is especially important if the natural abundance of S is $< 100\%$, is achieved by applying a gradient immediately

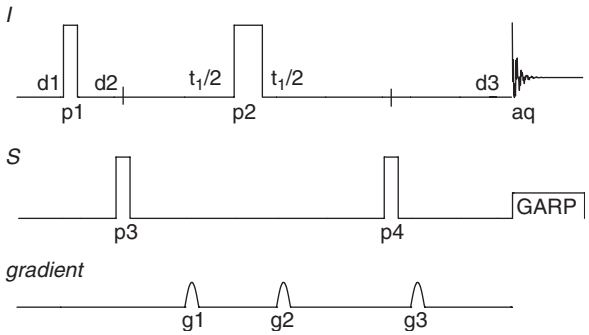

Figure 9 The "non-phase sensitive" version of the HMQC sequence.

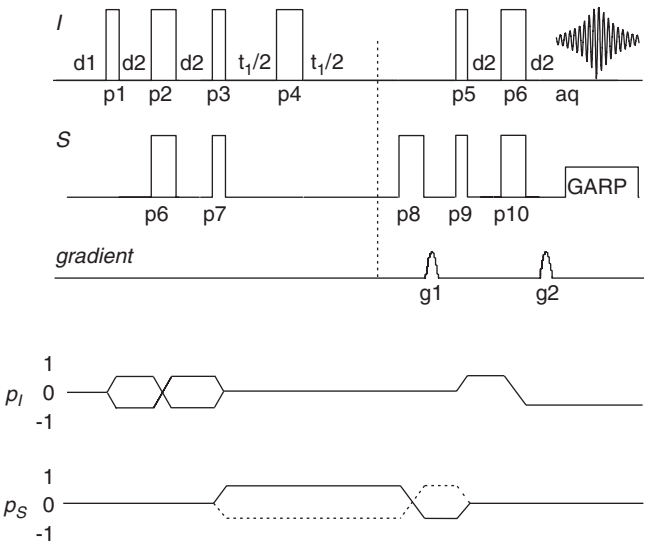

Figure 10 A gradient selected HSQC experiment. The coherence transfer pathway for an *N*-type spectrum is shown by the solid line, that for the *P*-type spectrum by the dashed line.

before p9, when there is transverse S spin magnetization, Equation (9), (neglecting p8, which in combination with the delay τ, refocuses phase errors which accumulate during g1, $\tau = g1$). The first gradient pulse, g1, dephases the S spin magnetization which, after transfer to the I spins, is refocused by g2. Alternating the sign of g2 and combining the echo and anti-echo spectra that result, gives a spectrum with absorption mode lineshapes. The gradients required to bring about refocusing again depend on γ_I and γ_S, Equation (13); as before the – and + signs refer to the *N*- and *P*-type spectra, respectively.

$$\mp (g1)(\gamma_S) - (g2)(\gamma_I) = 0 \tag{13}$$

2.3.3 Comments on gradient vs. phase cycle selection

In contrast to the phase cycling method of coherence selection/rejection, gradient selection is not subtractive, thus subtraction errors are absent from the spectra giving much reduced t_1 noise. In practice, the advantage gradient acceleration offers in HMQC/HSQC spectroscopy will be different for different S spins[26] because only one coherence pathway is selected in gradient accelerated HMQC, i.e., *half* the signal intensity is *discarded* resulting in a loss of sensitivity. Paradoxically, where the S nuclide is less than 100% abundant, gradient selection may be the better choice since breakthrough of signals from molecules containing NMR silent "S" nuclei is much better suppressed. Furthermore, sensitivity improved gradient experiments are available, however, the increased length of the pulse sequences allows for additional dephasing of the desired magnetization with some loss of signal. Note, however, that the sensitivity improvement is often restricted to a particular spin system (usually one I spin and one S). A further advantage of gradient selection is that there is no need to complete a number of steps determined by the phase cycle, it is possible to acquire HMQC and HSQC spectra using only two or one scan(s) per F1 increment on strong samples, resulting in considerable saving of spectrometer time.

Phase cycle, rather than gradient, selection retains both coherence pathways, in principle increasing the signal intensity. Furthermore, many S nuclides have high natural abundance (^{89}Yb, ^{103}Rh, ^{109}Ag, etc.); suppression of signals from molecules containing NMR silent "S" nuclei is, therefore, not such an issue. If the *intensity* of the desired signal is the limiting factor, then phase cycle selection may be preferred. If phase cycling must be used and S is appreciably $<100\%$ abundant, then a BIRD sequence[27] and/or a spinlock[28] to purge signals from molecules containing NMR silent "S" nuclei should be considered. The latter allows acquisition of an HMQC spectrum of a strong sample using 1 or 2 scans per increment, i.e., with the same time saving as gradient selection, the former may result in excessively long recovery delays with degassed samples.

Overall S/N may be better in the gradient accelerated experiment, because of the better rejection of unwanted signals, even though the desired signal is weaker. Paradoxically, therefore, it may be useful to use gradient acceleration to suppress the noise in the spectra if the indirectly observed spin has low natural abundance.

2.4 Relayed HXQC spectroscopy

The HMQC and HSQC sequences described above can be applied either as proton or heteronuclide detected experiments. Although proton detection is always more sensitive, in practice a suitable coupling between ^{1}H and the metal may not exist. Gudat[29] has recently suggested relay experiments, in order to take advantage of the sensitivity gain offered by ^{1}H detection. The experiment requires the presence of coupling between a donor ligand X (e.g., a phosphine) and the metal, and between the donor nucleus and the protons in the backbone of the ligand, allowing relayed ^{1}H,X/X,M coherence transfers to be used to afford a ^{1}H-detected, ^{1}H,M spectra. Although such experiments would normally be

three-dimensional, a 2D version, with a fixed mixing time, is usually all that is required for coordination and organometallic compounds since there will be only one or two metal chemical shifts present in the spectrum, allowing only the relevant slices of the 3D cube to be recorded. Two schemes were proposed.

The first scheme can be regarded loosely as a 3D HSQC experiment, Figure 11.[30,31] HzXzM*y* double anti-phase magnetization is created at point "a" by a double INEPT transfer ^{1}H to X to M, (applying Equation (8), first to the ^{1}H,X spin pair gives –HzX*y* coherence, then to X,M gives HzXzM*y*). This is phase-encoded by gradient g1 during the subsequent M spin-echo before being returned to the *z*-axis by the 90° M pulse that follows the spin-echo period, to yield longitudinal three-spin magnetization HzXzMz. (The spoil gradient pulse, gs, removes residual transverse magnetization.) This is returned to the transverse plane as double anti-phase M-magnetization by the final 90° pulse of the preparation period, and allowed to evolve during t_1; double reverse INEPT transfer from M to X to ^{1}H converts this back to observable proton magnetization. Gradient g2 selects the desired magnetization prior to acquisition, the refocusing condition is

$$(g2)(\gamma_H) - (g1)(\gamma_M) = 0 \tag{14}$$

For most coordination and organometallic complexes, selective excitation of individual ligand donor groups is not necessary. If required, Gudat reports that this can be achieved by using either low-power rectangular pulses or Gaussian shaped pulses on X.

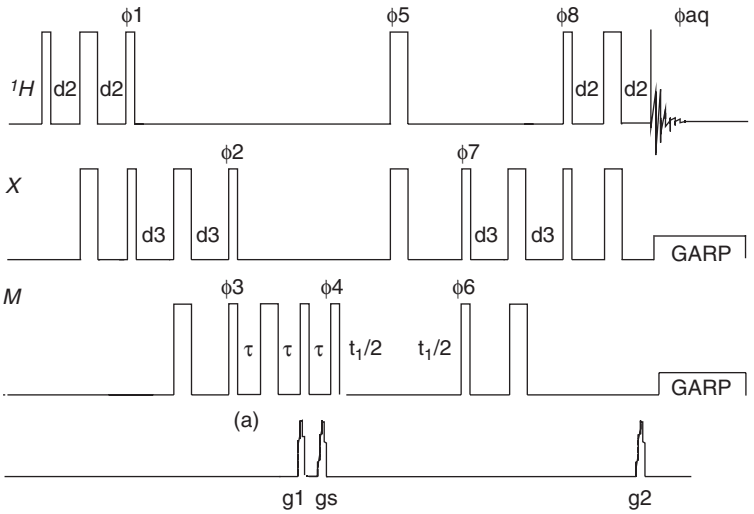

Figure 11 A double INEPT sequence for transfer from ^{1}H to X to M (X = NMR active donor, e.g., ^{31}P) to allow use of the sensitivity advantage of ^{1}H detection in the indirect detection of a metal nucleus. d_2 and d_3 are set to $1/\{4J(HX)\}$ and $1/\{4J(XM)\}$, respectively. $\phi 1,2,7,8 = Y$; $\phi 4 = -Y$; $\phi 3 = Y_2, -Y_2$; $\phi 5 = X_4, -X_4$; $\phi 6$ alternates X, $-X$ and $\phi aq = X, -X, -X, X$. τ should be as short as possible consistent with gradient recovery.

Unwanted metal–H and metal–X couplings in F1 are refocused by the 180° pulses to ^{1}H and X in the middle of t_1. Note, however, that if selective pulses are used here, only couplings to the *excited* X nucleus are refocused which may be advantageous since couplings to passive X nuclei may provide additional structural information. The large spectral range and high Larmor frequencies of some transition metals may require the use of composite 180° pulses on M or splitting the required spectral range over several experiments. (As is also the case for 2D experiments.)

The second sequence, Figure 12, again uses INEPT for the ^{1}H,X transfer but an HMQC scheme is used for the X,M coherence transfer step; *cf.* 3D 'out-and-back' correlation experiments[30,32] based on the HNCA experiment.[33] This has the advantage of not requiring a 180° pulse on the metal channel. As before, the INEPT sequence generates $-H_zX_y$ coherence and a spoil gradient gs is used to improve suppression of unwanted magnetization. The desired magnetization evolves under the influence of J(XM), Equation (4), to give $H_zX_xM_z$ coherence which is converted to $H_xX_yM_x$ three-spin-coherence by the simultaneous 90° pulses on H and M, Equation (4). This evolves during t_1 (*cf.* Equation (6)) under the influence of the M chemical shift (heteronuclear interactions are refocused by the 180° pulses on H and X midway through the evolution period). The remaining pulses convert this magnetization back to observable ^{1}H magnetization, the desired coherences being selected via the gradients g1 and g2. Refocusing occurs when

$$(g2)(\gamma_H) - 2(g1)(\gamma_M) = 0 \tag{15}$$

Figure 13 shows the ^{31}P-relayed ^{1}H,^{183}W shift correlations of the diazaphosphole complex **1** recorded using the pulse sequence of Figure 12.[29] The d_2 delays can be tuned to select a particular correlation. Thus, using $d_2 \sim 1/(2^1J(WP))$ affords

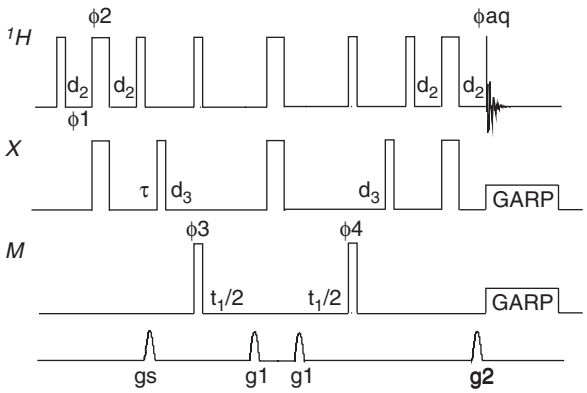

Figure 12 An alternative scheme to use the sensitivity advantage of ^{1}H detection in the indirect detection of a metal nucleus. INEPT is used for the ^{1}H,X transfer and HMQC for the X, M coherence transfer step. d_2 and d_3 are set to $1/\{4J(HX)\}$ and $1/\{2J(XM)\}$, respectively. $\phi1 = X_4, -X_4$; $\phi2 = Y$; $\phi3$ alternates $X, -X$; $\phi4 = X_2, -X_2$; and $\phi aq = X, -X, -X, X$. τ is as short as possible consistent with gradient recovery.

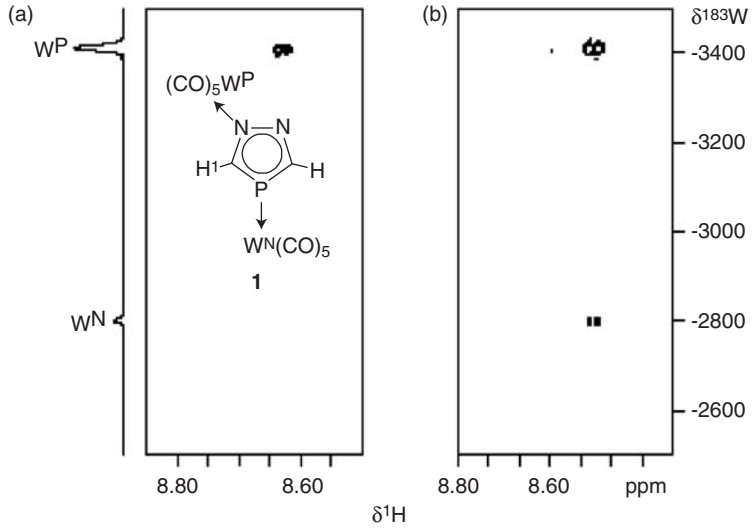

Figure 13 The ^{31}P-relayed ^{1}H,^{183}W shift correlation spectrum of **1**. Two ^{31}P-relayed ^{1}H,^{183}W correlation spectra were measured using the pulse sequence of Figure 12: (a) $d_3 = 1.66$ ms, $J(WP) = 300$ Hz and (b) $d_3 = 50$ ms, $J(WP) = 10$ Hz; $^{1}J(W^{P}P) = 259$ Hz and $^{3}J(W^{N}P) = 3.2$ Hz, respectively. A non-selective ^{31}P excitation pulse, and decoupling of ^{31}P during acquisition was used. d_2 was set to 5.7 ms corresponding to $J(PH) = 44$ Hz. The doublet splitting in F2 is due to $^{3}J(H,H)$. Adapted with permission from ref. 29. Copyright 2003 Wiley-VCH Verlag GmbH & Co.

exclusively the correlation to W^P $\delta_W = -3426$, Figure 13(a), while tuning d_2 to the long-range $^{3}J(WP)$ coupling gives an additional correlation to W^N $\delta_W = -2205$.

2.5 HMBC spectroscopy

There have been a few recent reports that use HMBC sequences to determine Rh chemical shifts, (see Table 10).[34–36] The HMBC sequence is, in effect, an HMQC sequence preceded by a low pass filter and was originally designed to eliminate magnetization arising from one bond couplings in ^{1}H,^{13}C HMQC spectroscopy. In principle, there should be no advantage over HMQC when applied to the indirect detection of metal nuclei since there is unlikely to be a need to distinguish between one bond and long-range couplings.

3. SPIN SYSTEMS

The descriptions of the pulse sequences above relate to ''simple'' spin systems, in which there is only one S spin in the coupled system, and all nuclei are spin-1/2. Unlike ^{13}C or ^{15}N, the natural abundance of many metal nuclides is high and can be 100%. High natural abundance of the metal spin is, therefore, a challenge in polymetallic systems since degenerate *insensitive* nuclei will be present.[37]

Examples include transition metal cluster compounds, e.g., of rhodium or platinum, and that contain edge- and/or face-bridging carbonyl ligands,[38] and bimetallic and cluster compounds containing phosphorus containing hetero-ligands. Many metal nuclei of interest are quadrupolar. It is important to appreciate that such spin systems may (will) not behave as ''normal'' $^{1}H–^{13}C$, or $^{1}H–^{15}N$ systems and can give spurious, or no correlations if experimental methodology is simply transferred from ''organic'' systems.

3.1 I_nS_m systems

3.1.1 Multiple S spin transitions in HMQC spectra

In polymetallic compounds multiple metal spin transitions and inequivalent couplings of metal spins to the ligands will affect the HMQC spectrum. This contrasts with the situation in organic compounds in which the natural abundance of ^{13}C or ^{15}N is so low as to make the occurrence of even two such centres in a molecule negligible. Account must, therefore, be taken of the effect of multi-metal spin flips on the spectra since these will not be removed by the ''usual'' phase cycling and will distort the coherence spectra both with regard to the position and intensity of the resonances. Indeed, for many systems the intensity of the desired signal vanishes using conventional phase cycling and preparation delay, d_2. One solution to this problem is to modify the phase cycling such that all coherences will appear; Ruegger and Moskau[39] have developed a set of rules to identify those correlations corresponding to single-metal spin flips in such spectra of some dimeric platinum–phosphine systems. The disadvantage of such an approach is the plethora of coherences detected. An alternative approach is to modify the preparation delay, d_2, such that only coherences arising from single-metal spin flips are detected.[40–42] There are two distinct, problematic situations when applying HMQC to metal complexes/cluster compounds: (1) the detector nucleus couples to more than one metal centre in approximately equal fashion, for example edge-bridging, face-bridging or interstitial ligands. This system we designate IS_n; an exact analytical solution exists for the optimal preparation delay, d_2, which will maximize the intensities of correlations resulting from metal single-spin transitions while minimizing the intensity of metal multiple spin coherences; and (2) the detector spin couples very differently to several metal spins through one, two or more bond couplings, designated $IS^1S^2\ldots$, and we wish to optimize the preparation delay, d_2, for the detection of either or both the directly bonded or/and the remote metal nuclei. In this case there is no direct analytical solution for d_2, which must be determined by inspection of the calculated behaviour of the spectral intensities as a function of d_2.

3.1.1.1 A face-bridging ligand as detector. The face-bridging carbonyl ligand is a common structural motive in metal carbonyl cluster chemistry and provides an example of an IS_3 spin system in which the detector nucleus (^{13}C) can couple to three, essentially equivalent, in terms of J(Rh–C), metals. An example of such a

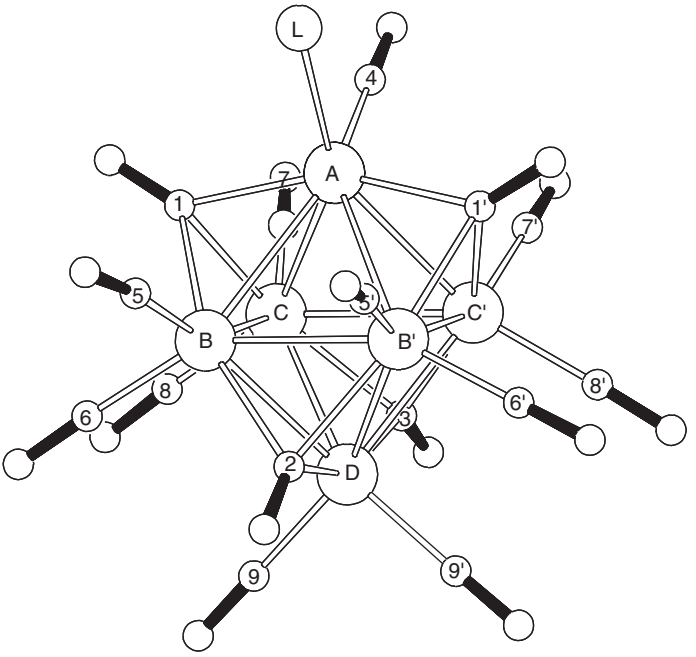

Figure 14 Schematic representation of the structure of $[Rh_6(CO)_{15}L]$.

system is the face-bridging carbonyl group in $[Rh_6(CO)_{15}L]$, (L = PR_3 (R = alkyl, aryl), $P(OPh)_3$, NCMe, I, etc.),[43] Figure 14.

The effect of the HMQC pulse sequence, Figure 2, on a face-bridging carbonyl coupled to three rhodium atoms can be described using the product operator formalism.[37] At the beginning of the evolution period t_1, just after the first 90°-^{103}Rh pulse, the state of the four-spin face-bridging ^{13}C–$^{103}Rh_3$ system is given by Equation (16).

$$\sigma = (0\mathrm{Rh}) + (1\mathrm{Rh}) + (2\mathrm{Rh}) + (3\mathrm{Rh}) \tag{16}$$

where

$$(0\mathrm{Rh}) = \mathrm{C}(\pi/2 - \Omega_\mathrm{C} d_2)\cos^3(\pi J d_2)$$

$$(1\mathrm{Rh}) = 2\mathrm{C}(\pi - \Omega_\mathrm{C} d_2) \times \{\mathrm{Rh}_\mathrm{A}(\pi/2) + \mathrm{Rh}_\mathrm{B}(\pi/2) + \mathrm{Rh}_\mathrm{C}(\pi/2)\}\cos^2(\pi J d_2)\sin(\pi J d_2)$$

$$(2\mathrm{Rh}) = 4\mathrm{C}(3\pi/2 - \Omega_\mathrm{C} d_2) \times \{\mathrm{Rh}_\mathrm{A}(\pi/2)\mathrm{Rh}_\mathrm{B}(\pi/2) + \mathrm{Rh}_\mathrm{A}(\pi/2)\mathrm{Rh}_\mathrm{C}(\pi/2) + \mathrm{Rh}_\mathrm{B}(\pi/2)\mathrm{Rh}_\mathrm{C}(\pi/2)\} \times \cos(\pi J d_2)\sin^2(\pi J d_2)$$

$$(3\mathrm{Rh}) = 8\mathrm{C}(2\pi - \Omega_\mathrm{C} d_2) \times \mathrm{Rh}_\mathrm{A}(\pi/2)\mathrm{Rh}_\mathrm{B}(\pi/2)\mathrm{Rh}_\mathrm{C}(\pi/2)\sin^3(\pi J d_2)$$

and $\mathrm{C}(\varphi)$ and $\mathrm{Rh}_i(\varphi)$ denote the carbon and rhodium spin operators, respectively where, for arbitrary phase φ, $\mathrm{S}(\varphi) = \mathrm{S}_x \cos\varphi + \mathrm{S}_y \sin\varphi$ and S is either C or Rh_i. The chemical shift of carbon is Ω_C, J is the coupling constant and d_2 is the delay used in the pulse sequence for polarization transfer, Figure 2. Spin operators belonging to the three different rhodium atoms are numbered by the subscripts A, B and C. It is convenient to refer to the operators (0Rh), (1Rh), (2Rh) and (3Rh) as zero-,

single-, two- and three-rhodium spin coherences, respectively, since we are interested principally in the order of the coherence with respect to rhodium. The zero-rhodium spin coherence (0Rh) contains no rhodium spin operators so cannot be used to correlate the carbon and rhodium chemical shifts. Magnetization arising from this term is eliminated by the phase cycling used in the standard HMQC experiment (see Section 2.2.2). The terms (1Rh), (2Rh) and (3Rh) evolve under the action of the rhodium chemical shifts, $\Omega_{Rh(A)}$, $\Omega_{Rh(B)}$ and $\Omega_{Rh(C)}$ and can be used to correlate carbon and rhodium shifts. Cross peaks resulting from (2Rh), through zero- and double-rhodium quantum coherences, are suppressed by the standard phase cycling while (1Rh) gives cross peaks at the expected rhodium chemical shifts through single-rhodium quantum transitions. These cross peaks appear as 1 : 1 : 1 : 1 quartets in the carbon dimension, F2. The magnitude of each component of the quartets is given by

$$\left|(1/16)\cos^2(\pi J d_2)\sin(\pi J d_2)\right| \tag{17}$$

which reaches a maximum at

$$d_2 = (1/\pi J)arctg(\sqrt{2}/2) \approx 1/(5J) \tag{18}$$

The maximal magnitude of Equation (17) is $(\sqrt{3})/72$, thus these single-rhodium spin cross peaks are approximately an order of magnitude weaker than those arising from a terminal Rh(CO) moiety (which can be shown to equal 1/4). Importantly, the maximum does not occur at the conventional preparation delay, $d_2 = 1/(2J)$, when the intensity of these cross peaks is zero, but at $1/(5J)$. Evolution of the three-rhodium spin coherence (3Rh) under the action of the rhodium chemical shifts gives three (net) single-quantum peaks and one triple-quantum cross peak in the 2D spectrum, all of which appear as 1 : 3 : 3 : 1 quartets centred at Ω_C in the carbon dimension, however, in the rhodium dimension the three single-quantum peaks occur at $-\Omega_{Rh(A)}+\Omega_{Rh(B)}+\Omega_{Rh(C)}$, $\Omega_{Rh(A)}-\Omega_{Rh(B)}+\Omega_{Rh(C)}$ and $\Omega_{Rh(A)}+\Omega_{Rh(B)}-\Omega_{Rh(C)}$ while the triple-quantum peak occurs at $-\Omega_{Rh(A)}-\Omega_{Rh(B)}-\Omega_{Rh(C)}$. The magnitude of the single- and three-quantum peaks (the height of the inner quartet lines) reaches a maximum of 3/64 at the conventional value of $d_2 = 1/(2J)$. Figure 15 shows the inverse detected HMQC ^{13}C–{^{103}Rh} spectra of this cluster recorded using preparation delays, $d_2 = 1/(2J)$ and $1/(5J)$, $J = 28$ Hz, a value typical of ^{103}Rh coupling to a face-bridging ^{13}CO. The only single-spin–single-quantum rhodium correlation seen in the correlation map on the left of Figure 15 is the correlation C(1)–Rh(B). All other cross peaks seen are due to three-rhodium spin operators (triple-quantum and single-quantum with respect to rhodium). Two of the three-spin–single-quantum correlations are fortuitously located at the expected coordinates of the ''correct'' correlations C(2)–Rh(D) and C(3)–Rh(D) because the cluster contains two equivalent atoms Rh(B) and Rh(C). By contrast, in the correlation map on the right of Figure 15, in which the unconventional preparation delay $d_2 = 1/(5J)$ has been used, cross peaks are observed at the ''correct'' places even though the preparation delay, d_2, is sufficiently far removed from the conventional value that no correlations might have been expected to be observed. These single-quantum (with respect to rhodium) transitions are produced by single-rhodium spin operators and are

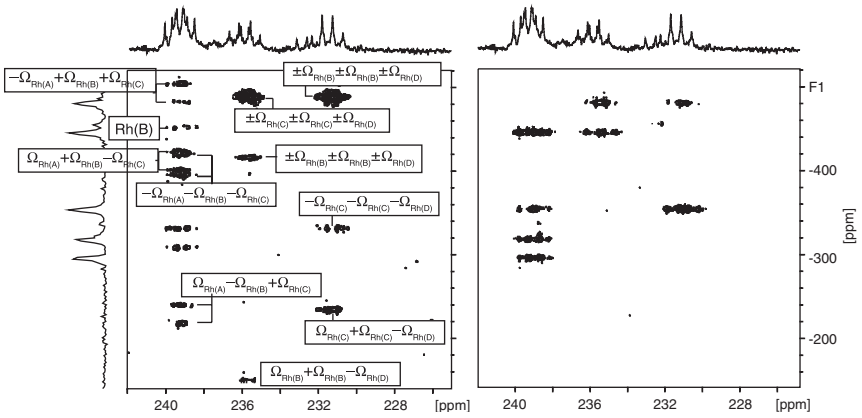

Figure 15 The inverse detected HMQC ^{13}C–{^{103}Rh} spectra of $[Rh_6(CO)_{15}\{P(4\text{-}F\text{–}C_6H_4)_3\}]$ recorded using preparation delays, d_2, of; (left)$1/(2J)$, and (right) $1/(5J)$, $J = 28$ Hz.

observed due to their intensities reaching a maximum at $1/(5J)$ while the intensity of correlations due to multiple rhodium spin transitions is close to zero for this delay. Fortuitously, for rhodium carbonyl clusters, couplings to the terminal carbonyls (70 Hz) are approximately 2.5 times greater than those to face-bridging carbonyls (28 Hz) allowing the single-rhodium spin correlations to both face-bridging and terminal carbonyls to be observed in a single experiment.

3.1.1.2 An edge-bridging or interstitial I spin as the detector. The effects described above are expected whenever the detector nucleus is coupled to several metal spins that can act as a unit. Edge-bridging carbonyls, hydrides or diorganophosphides, and interstitial carbides and phosphides are also frequently encountered in transition metal carbonyl clusters and other polymetallic compounds.[38] The above analysis is readily generalized and it is found that the ''correct'' signals for a IS_n group are maximal at

$$d_2 = \frac{1}{\pi J} arctg \frac{1}{\sqrt{n-1}} \tag{19}$$

3.1.1.3 The three-spin system ^{31}P–$^{103}Rh(A)$–$^{103}Rh(B)$ in which the detector nucleus couples differently to the metal nuclei. In the systems described above, the coupling between the metal spins and the detector nucleus are sufficiently similar that they may be regarded as equivalent, however, when couplings over one, two, etc., bonds are present this will clearly not be the case, for example in $[Rh_2(carboxylate)_4(L)]$ the one and two bond couplings are of the order of 100 and 20 $\sim$ 35 Hz, respectively. The behaviour of the three-spin system ^{31}P–$^{103}Rh(A)$–$^{103}Rh(B)$, $^1J(P\text{–}Rh(A)) = J_1$ and $^2J(P\text{–}Rh(B)) = J_2$, in the HMQC experiment can be described as follows. At the beginning of the evolution

period t_1, just after the first 90° ^{103}Rh pulse, the state of the three-spin system is given by Equation (20).

$$\sigma = (0\mathrm{Rh}) + (1\mathrm{Rh_A}) + (1\mathrm{Rh_B}) + (2\mathrm{Rh_{AB}}) \tag{20}$$

where

$$(0\mathrm{Rh}) = \mathrm{P}(\pi/2)\cos(\pi J_1 \mathrm{d}_2)\cos(\pi J_2 \mathrm{d}_2),$$
$$(1\mathrm{Rh_A}) = -2\mathrm{P}(0)\mathrm{Rh_A}(\pi/2)\sin(\pi J_1 \mathrm{d}_2)\cos(\pi J_2 \mathrm{d}_2)$$
$$(1\mathrm{Rh_B}) = -2\mathrm{P}(0)\mathrm{Rh_B}(\pi/2)\cos(\pi J_1 \mathrm{d}_2)\sin(\pi J_2 \mathrm{d}_2),$$
and
$$(2\mathrm{Rh_{AB}}) = -4\mathrm{P}(\pi/2)\mathrm{Rh_A}(\pi/2)\mathrm{Rh_B}(\pi/2)\sin(\pi J_1 \mathrm{d}_2)\sin(\pi J_2 \mathrm{d}_2)$$

The ^{31}P chemical shift frequency is set to zero in these equations. The zero- and two-rhodium spin coherences (0Rh) and ($2\mathrm{Rh_{AB}}$) are suppressed by normal phase cycling. The single-rhodium terms ($1\mathrm{Rh_A}$) and ($1\mathrm{Rh_B}$) produce cross peaks at the true rhodium chemical shifts, $\Omega_{\mathrm{Rh(A)}}$ and $\Omega_{\mathrm{Rh(B)}}$, the magnitude of the cross peaks being determined by the geometric factors. The preparation delays, d_2, which give maximum intensities of the cross peaks, do not coincide with extrema of $\sin(\pi J_1 t)$ and $\sin(\pi J_2 t)$ so must be evaluated numerically. Consider now the cases of $[\mathrm{Rh_2}\{\mu_2\text{-PhC(OMe)(CF}_3\mathrm{)CO}_2\}_4(\mathrm{PPh_3})]$, (PhC(OMe)(CF$_3$)CO$_2$ = MTPA)[41] and $[\mathrm{Rh_2}(\mu_2\text{-C}_7\mathrm{H}_{15}\mathrm{CO}_2)_4(\mathrm{PPh_3})]$ for which ^1J(Rh–P) = 95.5 and ^2J(Rh–P) = 21.6 Hz and 96.6 and 33.6 Hz, respectively. In the case of $[\mathrm{Rh_2}\{\mu_2\text{-MPTA}\}_4(\mathrm{PPh_3})]$, multiple metal spin flips are an inconvenience, Rh(A) and Rh(B) can be observed, albeit in separate experiments and with reduced intensity for Rh(B), using the appropriate conventional preparation delay, $\mathrm{d}_2 = 1/(2J)$. However, inspection of Figure 16, which shows the behaviour of the geometric factors for $[\mathrm{Rh_2}(\mu_2\text{-C}_7\mathrm{H}_{15}\mathrm{CO}_2)_4(\mathrm{PPh_3})]$, reveals that, for $[\mathrm{Rh_2}(\mu_2\text{-C}_7\mathrm{H}_{15}\mathrm{CO}_2)_4(\mathrm{PPh_3})]$, in which J_1 is nearly an odd integral multiple of J_2, $J_1/J_2 = 2.9$, the intensity of the correlation due to Rh(B) is *close to zero* if $\mathrm{d}_2 = 1/(2J_2)$ is used. This can be seen in Figure 17; using a "conventional" preparation delay, $\mathrm{d}_2 = 1/(2J_1) = 5.2$ ms, gives the

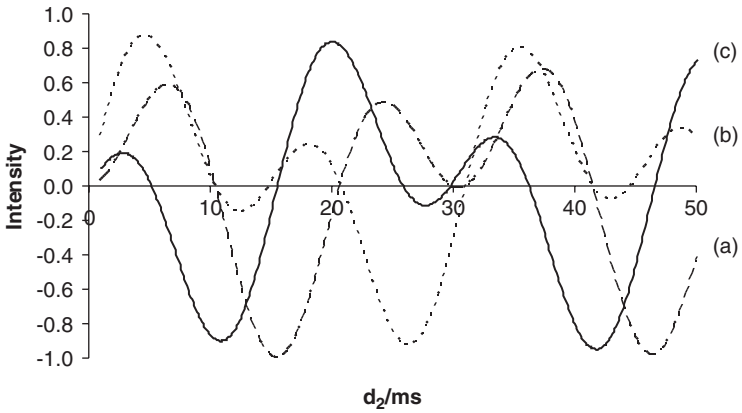

Figure 16 The behaviour of the geometric factors of $1\mathrm{Rh_A}$ and $1\mathrm{Rh_B}$ as a function of preparation delay d_2. (a) ($1\mathrm{Rh_{AB}}$); (b) ($1\mathrm{Rh_A}$); (c) ($1\mathrm{Rh_B}$) for ^1J(Rh–P) = 95.5 and ^2J(Rh–P) = 33.6 Hz.

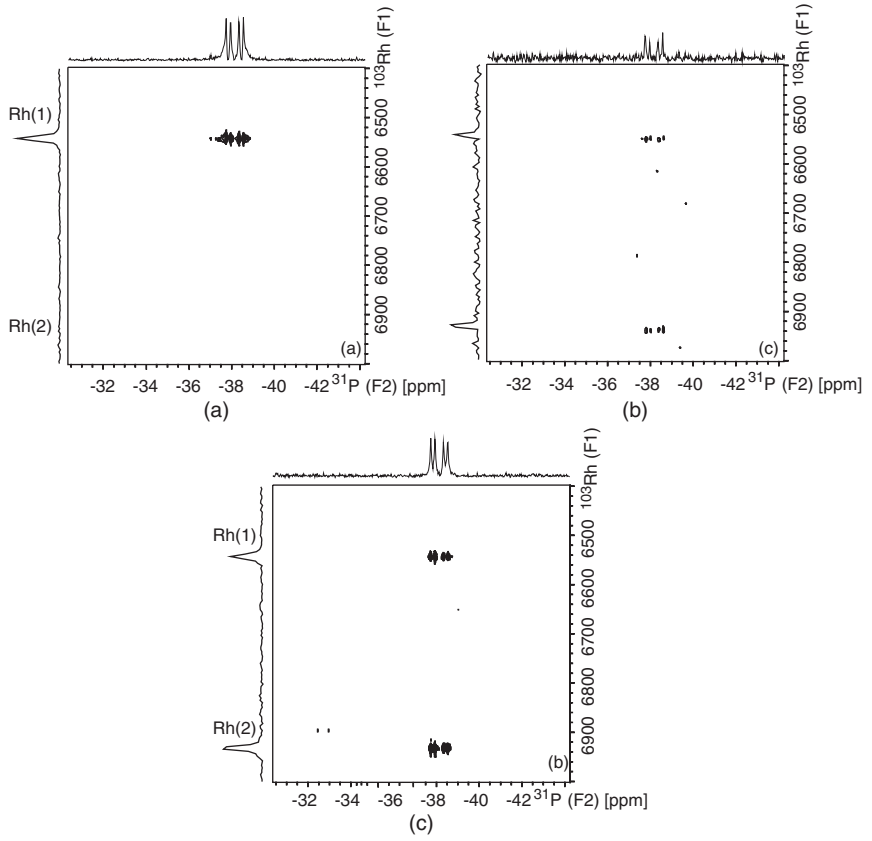

Figure 17 The ^{31}P–^{103}Rh-HMQC NMR spectrum of $[Rh_2(\mu_2\text{-}C_7H_{15}CO_2)_4(PPh_3)]$. (a) Using a "conventional" preparation delay, $d_2 = 1/(2J_1) = 5.2$ ms, gives the correlation due to Rh(A); (b) a delay of $1/(2J_2) = 14.9$ ms gives very weak correlations to Rh(A) and Rh(B); (c) a delay of 7.7 ms allows cross peaks from both Rh(A) and Rh(B), to be observed simultaneously with good sensitivity.

correlation due to Rh(A) with good sensitivity, Figure 17(a) while a delay of $1/(2J_2) = 14.9$ ms does not allow detection of Rh(B), Figure 17(b). A delay of 7.7 ms allows cross peaks from both Rh(A) and Rh(B), to be observed simultaneously with reasonable sensitivity Figure 17(c) – cross peaks due to ($2Rh_{AB}$) are removed by standard phase cycling.

In summary, the magnitude of the signals in the 2D HMQC spectra of polynuclear metal complexes is strongly affected by multi-metal spin transitions. In unfavourable cases, the cross peaks due to single-metal spin coherences (which occur at the true chemical shift of the metal centre) can be zero while signals due to multiple metal spin transitions (which occur at the sum or difference, with respect to the centre of the F1 dimension, of the true chemical shifts) dominate the spectrum. HMQC experiments on complex multiple spin systems require a detailed preliminary theoretical analysis of the spin system if erroneous results are to be avoided.

3.2 *para*-Hydrogen enhanced HMQC

The inherent low sensitivity of NMR spectroscopy makes the detection and characterization of reaction intermediates, which might be present in low concentration, difficult. One technique that can circumvent this problem is the use of *para*-enriched hydrogen.[44] Any molecule of high symmetry that contains coupled, equivalent, magnetically active nuclei can exist in isomeric forms that differ only in their nuclear spin arrangements. Thus, dihydrogen has two isomers, *ortho*-hydrogen, in which the nuclear spin wavefuntions correspond to the combinations $\alpha\alpha$, $\beta\beta$, and the linear combination $\alpha\beta+\beta\alpha$, and *para*-hydrogen (*p*-H_2), which exists as the anti-symmetric linear combination ($\alpha\beta-\beta\alpha$). Enhanced ^{1}H NMR signals are observed on addition of H_2 in the *para*-spin state to a molecule. In the absence of an applied magnetic field this is the PASADENA (*para*-hydrogen *a*nd *s*ynthesis *a*llow *d*ramatically *e*nhanced *n*uclear *a*lignment) or PHIP (*para-h*ydrogen *i*nduced *p*olarization) effect. For example, oxidative addition of *p*-H_2 to Vaska's complex, [IrCl(CO)(PPh_3)$_2$], occurs in a concerted, pairwise manner, and places the hydrides in a mutually *cis* orientation giving the metal dihydride complex [IrCl(CO)(H)$_2$(PPh_3)$_2$], in which the hydride ligands are magnetically distinct, and only the $\alpha\beta$ and $\beta\alpha$ spin states of the product are populated. Large population differences will exist across transitions that involve these hydride ligands, and hence signal intensities will be large. The resonances of the hydride ligands will also appear in anti-phase with respect to *J*(HH). If the reaction involving *p*-H_2 occurs in a weak magnetic field, a different effect, dubbed ALTADENA (*a*diabatic *l*ongitudinal *t*ransport *a*fter *d*issociation *e*ngenders *n*et *a*lignment), is observed. This arises because under these conditions the coupling between the nuclei is large compared to their frequency difference and hence the lower energy $\alpha\beta$ or $\beta\alpha$ level is populated. In the corresponding ^{1}H NMR spectrum, only two enhanced transitions are observed. When a reaction does not go to completion before the sample is placed in the NMR spectrometer both ALTADENA[45] and PASADENA[46,47] effects are observed simultaneously.

PHIP enhanced magnetization can be applied in many 2D experiments. In the example above, the time averaged spin state of the hydride magnetization in the *para*-hydrogen derived dihydride is longitudinal two spin order, and can be represented using the product operator formalism as $I_Z^A I_Z^B$ where A and B represent the two protons that originated from *para*-hydrogen. On application of a hard pulse of flip angle ϕ about the *x*-axis, the magnetization becomes: $1/2\{I_Z^A I_Z^B \cos 2\phi - I_Z^A I_Y^B \sin 2\phi - I_Y^A I_Z^B \sin 2\phi + I_Y^A I_Y^B \sin 2\phi\}$ and the observable signal arises from the anti-phase $I_Z I_Y$ terms. When A and B represent inequivalent hydride ligands the resonances for A and B appear anti-phase with respect to *J*(AB), the coupling constant between the two hydrogen nuclei, and yield optimal signal intensity when ϕ is $\pi/4$. The anti-phase magnetization generated by application of a 45° pulse will follow the usual evolution pathways. Thus, in the case of HMQC the initial pulse length must be changed to 45°. The proton spins must then be allowed to evolve with respect to both *J*(HH) and *J*(H*S*) during d_2. In organometallic complexes, *J*(HH) is typically small, corresponding to a slow evolution time, and consequently it is only necessary to modify the HMQC

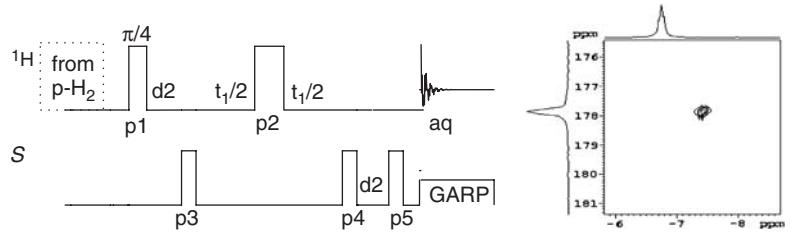

Figure 18 A modified HMQC sequence for use with *para*-hydrogen enhancement (left). At right is the *para*-hydrogen enhanced ^{1}H–^{13}C HMQC spectrum of [IrH$_2$Cl(CO)(PPh$_3$)$_2$].

experiment by replacing the initial 90° pulse to protons with a 45° pulse, p1. The fixed delays (d_2) must be optimized for heteronuclear magnetization transfer. The HMQC sequence is completed with a purge pulse, p5, Figure 18.

para-H_2 enhancement has been used to study a series of binuclear Rh^{III}–Rh^{I} dihydrides [(PR$_3$)(H)$_2$Rh(μ-X)$_2$Rh(CO)(PR$_3$)] (X = Cl, Br or I). When R = Ph, the chemical shift of the Rh^{III} centre moves sequentially upfield, from δ_{Rh} = 925 to 32 ppm, in the order (μ-Cl)$_2$, (μ-Cl)(μ-Br), (μ-Cl)(μ-I), (μ-Br)$_2$, (μ-Br)(μ-I), (μ-I)$_2$, exemplifying the hard/soft nature of bridging ligands on the effective radius of the Rh atoms, Section 1.2 and Section 4.2.2.2.1. When the binuclear complex is of the form [(PMe$_3$)$_2$(X)(H)Rh(μ-H)(μ-X)Rh(CO)(PMe$_3$)], (X = Cl, Br or I), both the Rh^{I} and Rh^{III} centres can be detected by Rh–H HMQC via the bridging hydride. The chemical shift of the Rh^{III} centre ranges from δ_{Rh} 347 to −210 ppm and the Rh^{I} centre in the chloro and iodo compounds is reported to be δ_{Rh} −688 and −733 ppm, respectively, the shift reported for the bromo compound, δ_{Rh} = −69 ppm, appears anomalous.[48,49] Messerle et al.[50] studied the addition of *p*-H_2 to [Rh(PMe$_3$)$_4$Cl] and [Rh(PMe$_3$)$_3$Cl] which affords [Rh(H)$_2$(PMe$_3$)$_4$]Cl and [Rh(H)$_2$Cl(PMe)$_3$]. Rh chemical shifts of δ_{Rh} −1007 and −319 ppm, and J(Rh,H) = 14.5 and 27 Hz, respectively, were reported. Similarly, Zhou et al.[51] used *para*-hydrogen enhanced ^{1}H–^{103}Rh-HMQC to determine the Rh chemical shifts for a series of compounds [RhCl(H)$_2$(PR$_3$)$_2$(py)] (PR$_3$ = PBz$_3$, PPh$_3$ and PCy$_3$; py = C$_5$H$_5$N, or 4-Me- C$_5$H$_4$N). Chemical shifts were in the range δ = −393 to 408 ppm.

3.3 Quadrupolar nuclei

The indirect observation of the NMR spectrum of a quadrupolar nucleus poses certain problems: (1) efficient quadrupolar relaxation will result in dephasing of the desired resonances, and (2) the behaviour of the nuclear spins will be influenced by the presence of the manifold of quadrupolar energy levels, hence the design of the pulse sequence must be reassessed.

3.3.1 Half-integer spin nuclei

The behaviour of half-integer spin nuclei in the HMQC experiment has been described using the product operator formalism by Amoureux[52] with particular reference to solid-state measurements, but solution samples are also discussed. NB: In their paper, the detector spin is referred to as S, the indirectly observed

spin as I, contrary to the normal convention in describing the HMQC experiment. In solution, or when the quadrupolar interaction is weak, the appearance of spectra recorded using a spin-1/2 detector coupled to a quadrupolar half-integer nucleus is essentially similar to that of a pair of spin-1/2 nuclei. The observed correlations are centred at the respective chemical shifts and are split by J_{SS} in F2 and J_{II} in F1. The application of 2D inverse detection to half-integer spin nuclei has also been discussed by Gudat[53] who reported the successful observation of X,Y correlations between spin-1/2 and quadrupolar nuclei, Figure 19, but noted that modification of the pulse sequences and empirical adjustment of the delays is required. In the imidovanadium complexes studied $^{1}J(^{51}V–^{31}P) \sim 210$ Hz, and $^{2}J(^{51}V–^{31}P) \sim 30$ Hz. Using $d_2 = 1/\{4\ ^{2}J(^{51}V–^{31}P)\} \sim 4.1$ ms for a 2D-INEPT transfer resulted in near total loss of signal due to rapid relaxation induced by the ^{51}V quadrupole. Empirically, the greatest cross peak intensities were obtained using d_2=0.1 ms. Additionally, experiments were carried out without ^{51}V decoupling during acquisition allowing omission of the refocusing delay immediately prior to acquisition that would otherwise be required. Nevertheless, rapid quadrupole induced relaxation of the ^{51}V nuclei reduced the signal to noise ratio substantially in the spectra – the S/N ratio in 1D ^{31}P, ^{51}V HMQC experiments was reported to be <1% that obtained in a normal ^{31}P NMR experiment – and severely restricted the acquisition time and thus the achievable resolution in F1. The use of the quadrupolar nucleus ^{6}Li as detector has also been analysed and optimized experiments described.[54]

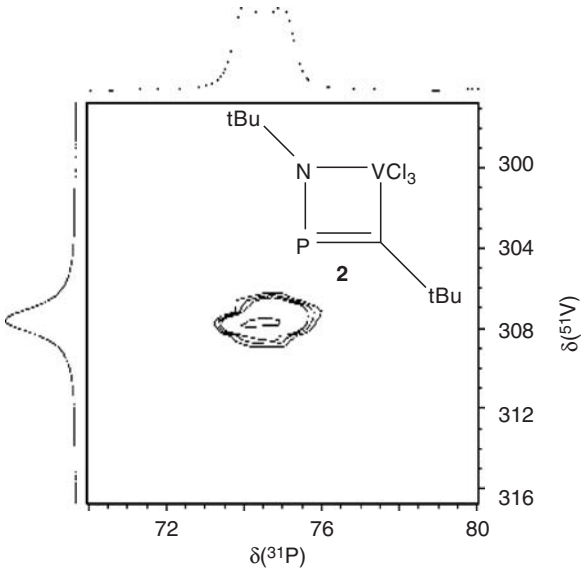

Figure 19 ^{31}P detected 2D-^{31}P,^{51}V{H} INEPT spectrum of **2**. Experimental conditions: spectral width in F2 2,450 Hz, and 2,500 Hz in F1; dephasing delay (INEPT) 0.9 ms, relaxation delay 2 ms, acquisition time 52 ms. 64 experiments of 120 scans and 256 data points were recorded, total acquisition time 7 min. The spectrum is displayed in magnitude mode. Reproduced with permission from ref. 53. Copyright 2002 Wiley-VCH Verlag GmbH & Co.

3.3.2 Spin-1 nuclei

The behaviour of spin-1 nuclei has been analysed by Nanz and von Philipsborn.[55] Two pulse sequences, designed to select single, Figure 20, or double, Figure 21, quantum (with respect to the quadrupolar nucleus) coherences, respectively, were devised – in the latter case, the observed correlation does not, of course, occur at the chemical shift of the quadrupolar nucleus. Although the examples given focused on ^{2}H and ^{14}N, in principle, the same considerations apply to metal nuclei of spin-1.

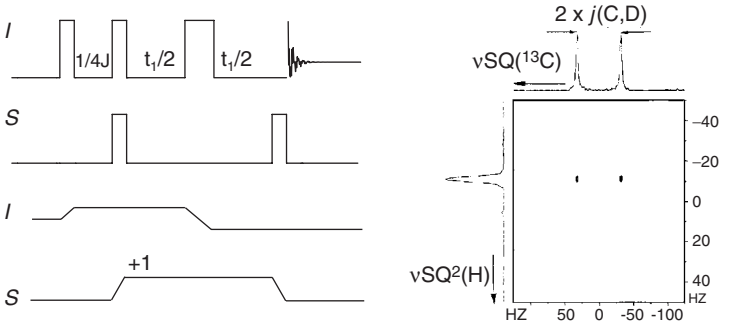

Figure 20 Left: Pulse sequence for indirect detection of single-quantum coherence to a spin-1 nucleus. The indicated coherence pathway is selected by phase cycling the first S pulse and the receiver phase $\{X, -X, Y, -Y\}$. The 180° pulse on I was cycled $\{X\}_4$, $\{-X\}_4$. Right: ^{13}C, ^{2}H HMQC spectrum of $CDCl_3$. The signal in F2 is a (1, 0, −1) triplet which appears as a "doublet" in the magnitude spectrum. Reprinted from ref. 55. Copyright (1992), with permission from Elsevier.

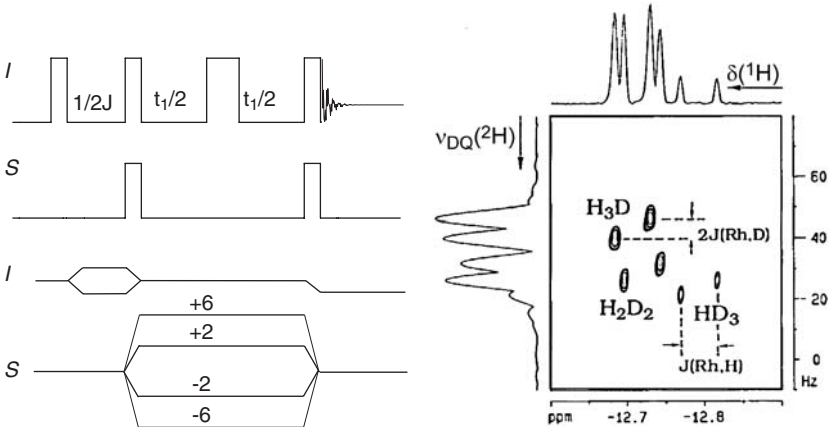

Figure 21 Left: Pulse sequence for indirect detection of double quantum coherence to a spin-1 nucleus. The indicated coherence pathways are selected by phase cycling the first S pulse $\{X, Y, -X, -Y\}$, and the receiver phase $\{X, -X\}_2$ in order to suppress $p_S = \pm 1, 0$ coherences. Both *N*- and *P*-type coherences $p_S = \pm 2$ are selected. Right: ^{1}H, ^{2}H double S quantum HMQC spectrum of $[RhH_{4-x}D_x(pybox)]$. Phase sensitive detection was used, see reference for further details. Only isotopomers containing both ^{1}H and ^{2}H are seen. Reprinted from ref. 55. Copyright (1992), with permission from Elsevier.

3.4 *J* correlation in solid-state NMR

In the solid state, strong dipolar, chemical shift and quadrupolar contributions to the line-width can make *J* couplings difficult to observe. Nonetheless, it is possible to use *J* couplings, even if they are not directly resolved in the spectra, to obtain 2D correlation spectra that describe through bond linkages of the metal sites to e.g., ^{31}P centres in a solid. Such experiments, which were originally developed for spin-1/2 nuclei, provide alternative information to that obtained from heteronuclear correlation NMR of solids in which coherence transfer is achieved through space via dipolar cross polarization.[56–58] An advantage of INEPT and HMQC schemes is that they do not require spin-locking. For half-integer quadrupolar nuclei such as ^{27}Al, spin-locking and optimization of CP can be difficult to implement under MAS since the best Hartmann–Hahn matching condition will vary from site to site in the solid, and will depend on several experimental parameters.[59,60] Furthermore, MAS is not capable of totally removing quadrupolar interactions (only first order effects for the central transition are averaged out provided that the MAS rate is significantly larger than the anisotropy), hence there is a significant additional broadening compared to spin-1/2 nuclei. Very fast relaxation of quadrupolar spins is another significant problem in *J*-HETCOR schemes since the mixing delays in the pulse sequences are inversely proportional to the *J* coupling constant between the spins I and S. Rapid transverse relaxation may result in significant loss of the desired magnetization, forcing the use of much shorter, non-optimal delays which itself will result in a much reduced signal.[52]

J spectroscopy in solids most often involves half-integer quadrupolar nuclei; a theoretical treatment of such systems has been provided by Kao and Grey for an INEPT experiment on the isolated spin pairs spin-1/2 S and half-integer (3/2 or 5/2) spin I,[61] and by Amoureux[52] more generally for HMQC and refocused-INEPT experiments involving half-integer spins. In their paper, Amoureux et al., also compared the results of several *J* and dipolar correlation experiments applied to the ^{27}Al–^{31}P spin pairs in $AlPO_4$-14. The sensitivities of the various approaches were found to be comparable in this case. However, the signal intensities obtained by the two techniques will depend on the particular spin pair reflecting, e.g., the gyromagnetic ratios of the nuclides, quadrupolar interactions and relaxation effects.[52]

4. REVIEW OF RECENT REPORTS OF THE INDIRECT DETECTION OF METAL NUCLEI

4.1 Alkali and alkaline earth metals

Of the metals of Groups 1 and 2, only lithium appears to have been studied in solution using HXQC methods. Both ^{6}Li and ^{7}Li have been studied using either ^{1}H,[62,63] or ^{31}P[3,64] as detector. ^{6}Li would seem to be the preferred isotope due to its significantly slower relaxation resulting from its smaller quadrupolar moment. However, ^{6}Li has low natural abundance (7.4%), frequently necessitating

^{6}Li-enriched samples to achieve reasonable experiment times. ^{7}Li on the other hand, has high natural abundance (92.6%) and a larger γ, $\gamma^{7}\text{Li}/\gamma^{6}\text{Li} \sim 2.6$. ^{7}Li NMR spectra therefore have greater dispersion and larger coupling constants than those of ^{6}Li isotope: chemical shift dispersion is determined by σ_d in ^{7}Li and is therefore small; in organolithium compounds, the spin–spin coupling is also usually small (>2 Hz) for ^{13}C, ^{15}N and ^{31}P and (<1 Hz) for ^{1}H.[65] The faster relaxation of ^{7}Li does, however, pose problems since the line-width of the ^{7}Li resonance may exceed the small differences in chemical shift. Furthermore, transverse magnetization arising from broad signals may be completely lost during the preparation delays of the HXQC pulse sequence due to relaxation via T_2, so that no correlations are observed.

Lithium-6 and 7 have also been used as the detector spin, especially in the characterization of lithium aggregates, via correlations to ^{13}C,[54,66–70] ^{15}N[71] and ^{29}Si.[72] Ortiz et al., for example has reported success using ^{7}Li in ^{7}Li detected ^{7}Li–^{31}P HMQC experiments on lithiated phosphazenes where the use of ^{7}Li detection resulted in shorter overall experiment times due to its rapid relaxation compared to ^{31}P.[64,73,74]

4.2 d-Block metals

The NMR spectroscopy of transition metals has been reviewed regularly.[1,4,5,9]

4.2.1 Early-transition metals

^{51}V, ^{53}Cr,[75] ^{55}Mn[76] and ^{91}Zr[77] all have useful spins and reasonable receptivity, but are quadrupolar. Rapid relaxation, therefore, means these systems are best studied by direct methods,[4,78,79] although there has been one report of indirect observation of ^{51}V via ^{31}P.[53]

4.2.1.1 Group 6: ^{183}W NMR. Among the early transition metals, tungsten has been most studied by NMR spectroscopy. Considering its low receptivity, the indirect detection of ^{183}W via ^{1}H, ^{183}W and ^{31}P, ^{183}W-HMQC has been widely used for structural determination of tungsten complexes; gains of *ca.* 2,800- and 290-fold in sensitivity are expected using ^{1}H and ^{31}P detection, respectively. ^{183}W chemical shifts span several thousand ppm, therefore HMQC, rather than HSQC, has been used to determine the ^{183}W chemical shifts of tungsten complexes. Carbajo et al. has studied a series of alkenylcarbyne tungsten complexes using inverse 2D HMQC NMR spectroscopy.[80,81] For the cationic complex $[(\text{dppe})(\text{CO})_2\text{LW}{\equiv}\text{C–CH=CR}_2]^{+}\text{BF}_4^{-}$ (dppe = 1,2-bis(diphenylphosphino) ethane; L = MeCN, PMe_3, CO), ^{183}W shielding increases with increasing π-acceptor ability of the ligands, Table 5. A normal halogen dependence was found in the neutral complexes $[(\text{dppe})(\text{CO})_2\text{XW}{\equiv}\text{C–CH=CR}_2]$, ^{183}W shielding decreasing with increasing electronegativity I < Br < Cl < F, Table 5. The decreasing ^{183}W shielding with increasing size of the ring substituent on the alkenylcarbyne ligand of chloride complexes $[(\text{dppe})(\text{CO})_2\text{ClW}{\equiv}\text{C–CH=CR}_2]$ was attributed to a combination of electronic and steric effects. A higher signal to noise ratio was

Table 5 Collection of X–^{183}W HMQC spectroscopic data

Compound	^{183}W/ppm	X	^{n}J(X–^{183}W)/Hz	NMR	T/K	Solvent	Ref.
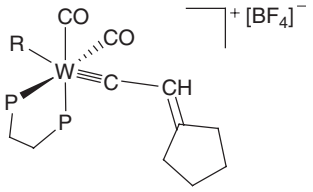	R= MeCN –1786 PMe_3 –2018 CO –2218	^{1}H ^{31}P	10–20 ^{1}J = 235	HMQC	303	$CDCl_3$	80,81
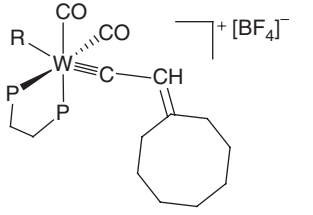	R= MeCN –1775 PMe_3 –2003 CO –2197	^{1}H ^{31}P	10–20 ^{1}J = 235	HMQC	303	$CDCl_3$	80,81
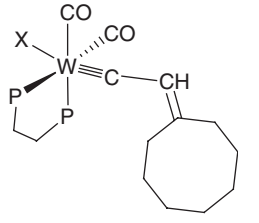	X= F –1567 Cl –1723 Br –1770 Cl –1873	^{1}H ^{31}P	10–20 ^{1}J = 235	HMQC	303	$CDCl_3$	80

Table 5 *(Continued)*

Compound	^{183}W/ppm	X	^{n}J(X–^{183}W)/Hz	NMR	T/K	Solvent	Ref.
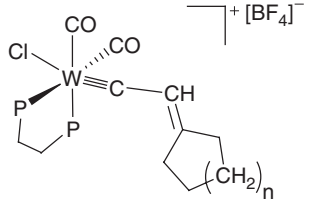	N= 1 –1739 2 –1733 3 –1725 4 –1720	^{1}H ^{31}P	10–20 ^{1}J = 235	HMQC	303	$CDCl_3$	80
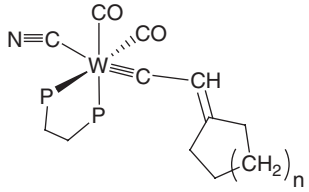	N= 1 –2116 4 –2100	^{1}H ^{31}P	10–20 ^{1}J = 235	HMQC	303	$CDCl_3$	80
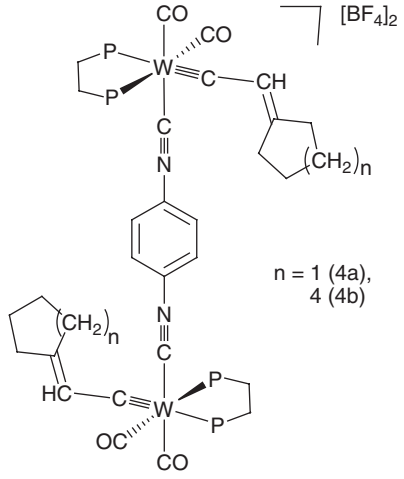	4a –2127 4b –2108	^{1}H ^{31}P	10–20 ^{1}J = 235	HMQC	303	$CDCl_3$	81

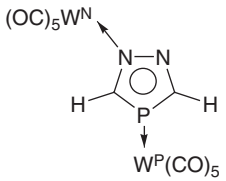	W^P –3426 W^N –2205	^{31}P	$J_{PH} = 44$ $^1J_{WP} = 300$ $^3J_{WP} = 10$	^1H–(^{31}P)–^{183}W Relayed-HMQC	29
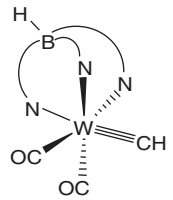	−1407	^1H	$^2J = 83$	HMQC	85

Aqueous $[WO_4]^{2-}$ ($\Xi = 4.166388$ MHz, ^{183}W)

obtained by proton detection of ^{183}W through long-range coupling ($^{n}J(^{183}W,^{1}H)$ = 10–20 Hz) than phosphorus detection of the metal via one bond coupling ($^{1}J(^{183}W,^{31}P)$ = 235 Hz) despite the longer mixing delays required by the smaller J. The ^{183}W chemical shifts in a series of $[W(CO)_5L]$ complexes of cyclotriphosphazenes $[N_3P_3(2,2'\text{-dioxybiphenyl})_2(OC_5H_4N\text{-}4)_2]$ and $[N_3P_3(2,2'\text{-dioxybiphenyl})(OC_5H_4N\text{-}4)_4]$, were found to be highly sensitive towards slight electronic modifications on the ligands far from the coordination site.[82] The ^{183}W NMR spectroscopy of polyoxo anions has been reviewed several times recently.[78,83,84]

4.2.2 Platinum group metals

4.2.2.1 Group 8: ^{187}Os NMR. Due to its low NMR receptivity, ^{57}Fe NMR spectra have rarely been reported. Given its low γ and the possibility of suitable detector nuclides in the ligands (^{1}H, ^{13}C and ^{31}P) ^{57}Fe would seem to be a prime candidate for indirect detection. Nevertheless, there appear to be no such reports although Wrackmeyer[15,86–88] has made several studies of ferrocene derivatives using high levels of isotopic enrichment. Similarly, there have been occasional reports of the direct detection of ^{99}Ru NMR spectra of coordination complexes and there is a rather larger number of reports of the ^{99}Ru and ^{101}Ru NMR spectroscopy of magnetic materials, however, there appear to be no reports of the indirect detection of the NMR spectra of either nuclide.

^{187}Os is the most insensitive nucleus in the periodic table, and is extremely difficult to observe by conventional NMR techniques. Significant increases in sensitivity (1,300-fold and 12,000-fold, respectively) can be achieved using ^{31}P or ^{1}H-detected 2D HMQC spectroscopy. However, the larger values of J(Os,P) relative to J(Os,H) reduces relaxation losses that might occur when ^{187}Os T_2 relaxation time is short, thus, in practice, it is possible to obtain better sensitivity for metal detection through ^{187}Os–^{31}P rather than ^{187}Os–^{1}H HMQC.

^{187}Os–^{1}H HMQC/HMBC and ^{187}Os–^{31}P HMQC have been used to determine the ^{187}Os chemical shifts of a series of triosmium carbonyl complexes.[89,90] The trend in ^{187}Os chemical shifts of hydride bridged triosmium clusters with diphosphine ligands $[Os_3(\mu\text{-}H)_2(CO)_8(L)]$ (L = dppm, dppe, dppp) is approximately in accordance with the lengths of alkyl bridge in the diphosphine ligands, Table 6.[91]

4.2.2.2 Group 9: ^{103}Rh NMR. Although of very high receptivity, like ^{55}Mn, ^{59}Co[93–95] gives very broad lines as a result of rapid quadrupolar relaxation, its NMR spectrum has therefore only been detected directly. The NMR spectrum of ^{193}Ir has never been observed. In contrast, ^{103}Rh is the most studied transition metal nucleus by NMR and significant sensitivity gains can be achieved using indirect detection.[14] HMQC has, therefore, been widely used in NMR studies of ^{103}Rh.[4,7,14] This review discusses ^{103}Rh NMR HMQC data published over the last 10 years specifically focusing on updating the literature since Elsevier's review in 2004.[14] An overview of the general properties of the metal complexes is presented such as formal oxidation state, ligand type and complex geometry. Tables giving Rh-HMQC data including chemical shift and coupling constants from the

Table 6 Collection of $^{1}H–^{187}Os$ HMQC spectroscopic data

Compound	^{187}Os/ppm	X nuclei	$^{n}J(X–^{187}Os)$/Hz	NMR	T/K	Solvent	Ref.
Os(*p*-cymene)Cl_2PMe_3	−2226	^{31}P	$^{1}J_{OsP} = 272$	HMQC	300	CD_2Cl_2	92
Os(*p*-cymene)H_2PMe_3	−5265	^{31}P	$^{1}J_{OsP} = 264$	HMQC	300	CD_2Cl_2	92
		^{1}H	$^{1}J_{OsH} = 79$				
$[Os_3(\mu\text{-}H)_2(CO)_{10}]$	−11302	^{1}H	$^{1}J_{OsH} = 44$	HMQC	298	$CDCl_3$	91
$[Os_3(\mu\text{-}H)_2(CO)_8(\mu\text{-tolBINAP})]$	−11345	^{1}H	$^{1}J_{OsH} = 44$	2D-HMQC	298	$CDCl_3$	91
$[Os_3(\mu\text{-}H)_2(CO)_8$ (dppm)]	−11525	^{1}H	$^{1}J_{OsH} = 42$	2D-HMQC	298	$CDCl_3$	91
$[Os_3(\mu\text{-}H)_2(CO)_8$ (dppe)]	−11417	^{1}H	$^{1}J_{OsH} = 43$	2D-HMQC	298	$CDCl_3$	91
$[Os_3(\mu\text{-}H)_2(CO)_8$ (dppp)]	−11238	^{31}P	$^{1}J_{OsP} = 209$	2D-HMQC	298	$CDCl_3$	91
$[Os_3(\mu\text{-}H)_2(CO)_8(\mu\text{-tolBINAP})]$	−11345	^{1}H	$^{1}J_{OsH} = 38$	2D-HSQC	298	$CDCl_3$	91
$[Os_3(\mu\text{-}H)(CO)_8(\mu\text{-tolBINAP-H})]$	−11150	^{1}H	$^{1}J_{OsH} = 30.7$	2D-HMQC	298	$CDCl_3$	91
	−12720		$^{1}J_{OsH} = 33.7$				
Os(*p*-cymene)Cl_2PMe_3	−2226	^{31}P	$^{1}J_{OsP} = 272$	HMQC	300	CD_2Cl_2	92
Os(*p*-cymene)H_2PMe_3	−5265	^{31}P	$^{1}J_{OsP} = 264$	HMQC	300	CD_2Cl_2	92
		^{1}H	$^{1}J_{OsH} = 79$				
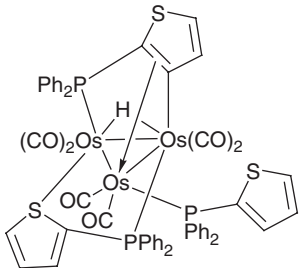	−13965	^{31}P	$^{1}J_{OsP} = 147$	2D-HMQC	173		90
	−13230		$^{1}J_{OsP} = 211$				

literature over the past decade are also included. ^{103}Rh chemical shifts are quoted relative to $\Xi = 3.16$ MHz unless otherwise stated; some authors do not state which reference has been used.

4.2.2.2.1 ^{103}Rh chemical shifts

4.2.2.2.1.1 SOLVENT AND TEMPERATURE EFFECTS. Carlton has recently determined the solvent and temperature effects on δ_{Rh} for a large number of square planar Rh(I) complexes, $[Rh(X)(PPh_3)_3]$, (X=Cl^-, N_3^-, NCO^-, NCS^-, $N(CN)_2^-$, $NCBPh_3^-$, $CNBPh_3^-$, CN^-) and derivatives containing CO, isocyanide, pyridine, H_2 and O_2 and reports that solvent effects are more pronounced in chloroform, and toluene than in dichloromethane, are deshielding, and ligand dependent – more polarizable ligands having a larger effect. The solvent effects become more evident at low temperatures, and are attributed to hydrogen-bonding interactions between the metal or X and the solvent. Carlton[20] also found that the ligands X could be ordered according to their influence on δ_{Rh}, giving a sequence that is essentially invariate over a wide range of complexes, Table 7.

The temperature effect on δ_{Rh} is well known and arises as a result of the vibration of metal–ligand bonds. ΔE, and hence the paramagnetic contribution to the shielding, σ_p, is sensitive to the population of the vibrational states, which itself is temperature dependent, resulting in a temperature dependence of the metal chemical shift – vibrational shielding – shielding increases as temperature decreases, i.e., δ_{Rh} becomes more negative, Figure 22. Deviations from the expected linear trend seen in Figure 21 were attributed to specific interactions between the solvent and X, or the metal.

4.2.2.2.1.2 FORMAL OXIDATION STATE. It is now believed that the type of ligand, complex geometry, bond distances and deviations from ideal bond angles are more important influences on the Rh chemical shift than the formal oxidation state of the complex.[14] This is exemplified by Cunningham et al.'s[96] recent report in which the photochemical reactions of a dinuclear complex $[CH_2(\eta^5\text{-}C_5H_4)_2\{Rh(C_2H_4)\}_2]$ with dmso, or various silanes gave novel reaction products with a wide range of Rh oxidation states. Even in complexes in which both Rh centres have the same oxidation state, δ_{Rh} differs significantly due to the type of ligands present. See Table 8.

4.2.2.2.1.3 LIGAND TYPE. The type and strength of the ligand donor atoms present in the first coordination sphere of Rh affect the chemical shift, Table 9.[14]

Table 7 Solvent and ligand X effects on δ_{Rh} in $[Rh(X)(PPh_3)_3]$ at 300 K[a]

Solvent	$CNBPh_3^-$	CN^-	$N(CN)_2^-$	NCO^-	NCS^-	$NCBPh_3^-$	N_3^-	Cl^-
$CHCl_3$	−405	−449	−214	−168	−156	−98	−70	−19
C_7H_8	−387	−445	−192	−144	−123	−96	−61	−49
CH_2Cl_2	−437	−522	−226	−190	−178	−107	−96	−82
DMSO		−503	−210	−168	−142		−81	−70

[a]Relative to $\Xi = 3.16$ MHz. Concentrations in the range 0.01–0.02 M. δ_{Rh} was obtained indirectly using the standard HMQC pulse sequence, Figure 2.

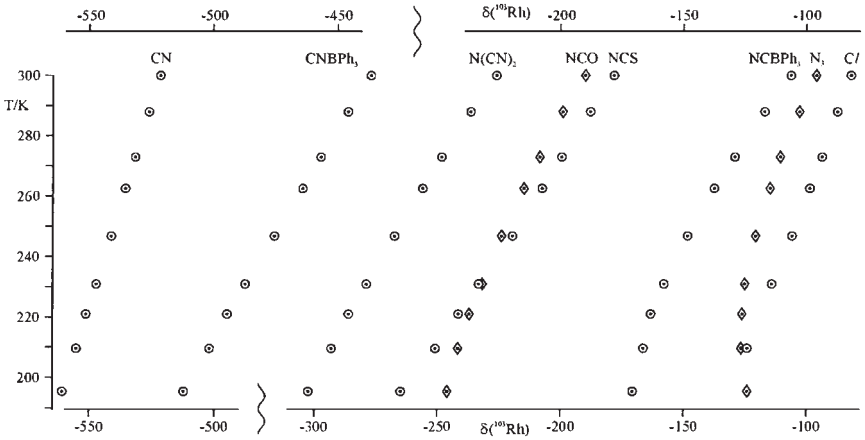

Figure 22 δ_{Rh} vs. temperature for the complexes [Rh(X)$(PPh_3)_3$], (X = Cl^-, N_3^-, NCO^-, NCS^-, $N(CN)_2^-$, $NCBPh_3^-$, $CNBPh_3^-$, CN] dissolved in dichloromethane ([Rh] ~ 0.01 M). Reproduced with permission from ref. 20. Copyright 2004 Wiley-VCH Verlag GmbH & Co.

Generally, more electron withdrawing and/or bulky substituents bonded to a transition metal centre, result in a more positive metal chemical shift. The lower electron density on the metal leads to a smaller ΔE which in turn leads to an increase in σ_p (see Section 1.2),[97] i.e., deshielding follows the trend O > Cl ≈ N > Br > I > S ≈ Se > Te > P ≈ As ≈ Sb ≈ H ≈ C* ≈ C (C* = sp^2 carbon).[97,98] This trend is aptly demonstrated by the series of aryl-rhodium dihalide and aryl-rhodium methyl halide complexes of bis(imino)aryl type tridentate ligands of the type [RhX_2(NCN)] and [RhX(CH_3)(NCN)] (where X = Cl^-, Br^- or I^-; NCN = bis(imino) aryl ligand),[99] the general trend being a decrease in the chemical shift of the Rh^{III} centre as the halide group is descended. de Pater et al.[97] observed a similar trend in δ_{Rh} for the products of oxidative addition of a variety of alkyl bromides to [Rh^I(Br)(4′-(4-*tert*-butylphenyl)-2,2′ : 6′,2″-terpyridine)], Table 9. Vinyl, allyl and phenyl ligands induce a lower ligand field hence a more positive chemical shift than do alkyl ligands.

The Rh chemical shifts of mono and binuclear Rh(I) complexes of *s*- and *as*-hydroindacenide and indacenediide bridging ligands with COD, ethylene and carbonyl ancillary ligands have been determined using HMBC, Table 9. The indacenyl complexes bearing carbonyl ligands exhibiting the largest shielding followed by the ethylene then COD derivatives as expected (Section 1.2). However, in the *anti*/*syn*-complexes the *anti* isomer is always the more shielded by approximately 100 ppm. Density functional theory was also used to determine the Rh NMR shielding constants to rationalize electronic and structural differences on chemical shift.[34]

The Rh chemical shift of [RhL_2-{η^5-(2-ferrocenyl)indenyl}] complexes (where L_2 = COD, nbd, 2 × CO) have been determined and compared to those of [RhL_2-{η^5-(1-ferrocenyl)indenyl}] compounds and some reference compounds. The downfield shift of $\delta(^{103}Rh)$ of the former complexes does not fit with the electron donating properties of ferrocenyl. It was proposed that the substituent on the

Table 8 Variation of Rh chemical shift with oxidation state in some derivatives of $[CH_2(\eta^5\text{-}C_5H_4)_2][Rh(C_2H_4)_2]_2$ and related compounds

Complex	δ Rh$^{(I)}$	δ Rh$^{(II)}$	δ Rh$^{(III)}$	δ Rh$^{(IV)}$	δ Rh$^{(V)}$	J(Rh, Rh)/Hz	T/K	Solvent	Ref.
$[CH_2(\eta^5\text{-}C_5H_4)_2\{Rh(C_2H_4)_2\}_2]$	−929						296	C_6D_6	96
$[CH_2(\eta^5\text{-}C_5H_4)_2\{Rh(C_2H_4)_2 \cdot Rh(C_2H_4)(dmso)\}]$	−613						296	DMSO-d_6	96
	−929								
$[CH_2(\eta^5\text{-}C_5H_4)_2\{Rh(dmso)_2\}_2]$	−617						296	C_6D_6	96
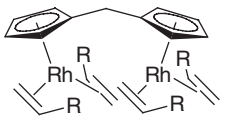	−782						296	C_6D_6	96
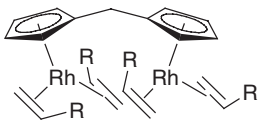	−780						296	C_6D_6	96
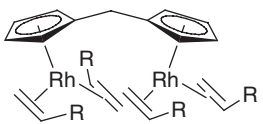	−736								96
	−782								
$[CH_2(\eta^5\text{-}C_5H_4)_2\{Rh(C_2H_4)_2 \cdot Rh(C_2H_4)(SiEt_3)H\}]$	−929		−1483				296	C_6D_6	96
$[CH_2(\eta^5\text{-}C_5H_4)_2\{Rh(C_2H_4)(SiEt_3)H\}_2]$			−1480				296	C_6D_6	96
$[CH_2(\eta^5\text{-}C_5H_4)_2\{Rh(C_2H_4)(SiEt_3)H \cdot Rh(SiEt_3)_2(H)\}]$			−1477		−1872		296	C_6D_6	96
$[CH_2(\eta^5\text{-}C_5H_4)_2\{Rh(SiEt_3)_2(H)_2\}_2]$					−1873		296	C_6D_6	96
$[CH_2(\eta^5\text{-}C_5H_4)_2\{RhH(\mu\text{-}SiEt_2)\}_2]$				−2033		16.5	296	C_6D_6	96
$[CH_2(\eta^5\text{-}C_5H_4)_2\{(RhEt)(\mu\text{-}SiEt_2)_2\ (RhH)\}]$				−2019		15	296	C_6D_6	96

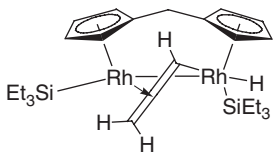		−779	−1342 −1407		13.8	296	Toluene-d_8	96
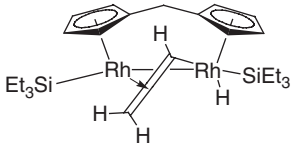		−666	−1399		14	296	Toluene-d_8	96
$[(\eta^5\text{-}C_5H_4)CH_2(C_5H_3SiEt_3)\{Rh(SiEt_3)_2(H)_2\}_2]$				−1836 −1850		296	C_6D_6	96
$[CH_2(\eta^5\text{-}C_5H_3SiEt_3)_2\{Rh(SiEt_3)_2(H)_2\}_2]$				−1837		296	C_6D_6	96
$[CH_2(\eta^5\text{-}C_5H_3SiEt_3)_2\{Rh(SiEt_3)_2(H)_2\}_2]$				−1832		296	C_6D_6	96
$[CH_2(\eta^5\text{-}C_5H_4)_2\{Rh(C_2H_4)_2\{Rh(C_2H_4)(SiMe_3)H\}]$	−929	−1450				296	C_6D_6	96
$[CH_2(\eta^5\text{-}C_5H_4)_2\{Rh(C_2H_4)(SiMe_3)H\}_2]$		−1449				296	C_6D_6	96
$[CH_2(\eta^5\text{-}C_5H_4)_2\{Rh(C_2H_4)(SiMe_3)H\ Rh(SiMe_3)_2(H)_2\}]$		−1450		−1731		296	C_6D_6	96
$[CH_2(\eta^5\text{-}C_5H_4)_2\{Rh(SiMe_3)_2(H)_2\}_2]$				−1732		296	C_6D_6	96
$[CH_2(\eta^5\text{-}C_5H_4)_2\{Rh(Me(\mu\text{-}SiMe_2)_2(RhH)\}]$			−2008 −1424		15	296	C_6D_6	96
$[CH_2(\eta^5\text{-}C_5H_4)_2\{Rh(SiMe_3(\mu\text{-}SiMe_2)_2(RhMe)\}]$			−1350 −1957		14.7	296	C_6D_6	96
$[CH_2(\eta^5\text{-}C_5H_4)_2\{Rh(SiMe_3(\mu\text{-}SiMe_2)_2(RhH)\}]$			−1952 −1965		14.8	296	C_6D_6	96
$[CH_2(\eta^5\text{-}C_5H_4)_2\{Rh(C_2H_4)(\mu\text{-}H)_2Rh(SiMe_3)_2\}]$		−1052		−1608		296	Toluene-d_8	96

Table 9 Variation in Rh chemical shifts with ligand type

Complex	δ_{Rh}/ppm	*J*(Rh,X)/Hz	T/K	Solvent	Ref.
[Rh(κ-*C*,κ-*N*,κ-*N*′-bis(*N*-methyl)isophthalaldimin-2-yl)$(Cl)_2$]	3888		298	CD_3OD	99
[Rh(κ-*C*,κ-*N*,κ-*N*′-bis(*N*-methyl)isophthalaldimin-2-yl)(Cl)(Br)]	3733		298	CD_3OD	99
[Rh(κ-*C*,κ-*N*,κ-*N*′-bis(*N*-methyl)isophthalaldimin-2-yl)$(Br)_2$]	3569		298	CD_3OD	99
[Rh(κ-*C*,κ-*N*,κ-*N*′-bis(*N*-isopropyl)isophthalaldimin-2-yl)$(Cl)_2$]	4185		298	CD_3OD	99
[Rh(κ-*C*,κ-*N*,κ-*N*′-bis(*N*-isopropyl)isophthalaldimin-2-yl)(Cl)(Br)]	4027		298	CD_3OD	99
[Rh(κ-*C*,κ-*N*,κ-*N*′-bis(*N*-isopropyl)isophthalaldimin-2-yl)$(Br)_2$]	3862		298	CD_3OD	99
[Rh(κ-*C*,κ-*N*,κ-*N*′-bis(*N*-isopropyl)isophthalaldimin-2-yl)(Cl)(I)]	3674		298	CD_3OD	99
[Rh(κ-*C*,κ-*N*,κ-*N*′-bis(*N*-isopropyl)isophthalaldimin-2-yl)$(I)_2$]	3176		298	CD_3OD	99
[Rh(κ-*C*,κ-*N*,κ-*N*′-bis(*N*-*tert*-butyl)isophthalaldimin-2-yl)$(Cl)_2$]	4587		298	CD_3OD	99
[Rh(κ-*C*,κ-*N*,κ-*N*′-bis(*N*-*tert*-butyl)isophthalaldimin-2-yl)(Cl)(Br)]	4374		298	CD_3OD	99
[Rh(κ-*C*,κ-*N*,κ-*N*′-bis(*N*-*tert*-butyl)isophthalaldimin-2-yl)$(Br)_2$]	4107		298	CD_3OD	99
[Rh(κ-*C*,κ-*N*,κ-*N*′-bis(*N*-isopropyl)isophthalaldimin-2-yl)$(Cl)_2$(pyridine-d_5)]	4133		298	CD_2Cl_2/ pyridine-d_5	99
[Rh(κ-*C*,κ-*N*,κ-*N*′-bis(*N*-isopropyl)isophthalaldimin-2-yl)(Cl)(Br)(pyridine-d_5)]	4002		298	CD_2Cl_2/ pyridine-d_5	99
[Rh(κ-*C*,κ-*N*,κ-*N*′-bis(*N*-isopropyl)isophthalaldimin-2-yl)$(Br)_2$(pyridine-d_5)]	3847		298	CD_2Cl_2/ pyridine-d_5	99
[Rh(κ-*C*,κ-*N*,κ-*N*′-bis(*N*-isopropyl)isophthalaldimin-2-yl)$(I)_2$(pyridine-d_5)]	3204		298	$CDCl_3$	99
[Rh(κ-*C*,κ-*N*,κ-*N*′-bis(*N*-*tert*-butyl)isophthalaldimin-2-yl)$(Cl)_2$(pyridine-d_5)]	4783		298	$CDCl_3$/ pyridine-d_5	99
[Rh(κ-*C*,κ-*N*,κ-*N*′-bis(*N*-*tert*-butyl)isophthalaldimin-2-yl)(Cl)(Br)(pyridine-d_5)]	4637		298	$CDCl_3$/ pyridine-d_5	99
[Rh(κ-*C*,κ-*N*,κ-*N*′-bis(*N*-*tert*-butyl)isophthalaldimin-2-yl)$(Br)_2$(pyridine-d_5)]	4477		298	$CDCl_3$/ pyridine-d_5	99
[Rh(κ-*C*,κ-*N*,κ-*N*′-bis(*N*-isopropyl)isophthalaldimin-2-yl)$(Br)_2(PPh_3)$]	2595	^1J(Rh,P) 128	298	CD_2Cl_2	99
[Rh(κ-*C*,κ-*N*,κ-*N*′-bis(*N*-isopropyl)isophthalaldimin-2-yl)(CH_3)(Br)]	2450		298	$CDCl_3$	99

[Rh(κ-*C*,κ-*N*,κ-*N*′-bis(*N*-isopropyl)isophthalaldimin-2-yl)(CH_3)(I)]	2388		298	CD_2Cl_2	99
[Rh(κ-*C*,κ-*N*,κ-*N*′-bis(*N*-*tert*-butyl)isophthalaldimin-2-yl)(CH_3)(Br)]	2369		298	$CDCl_3$	99
[Rh(κ-*C*,κ-*N*,κ-*N*′-bis(*N*-*tert*-butyl)isophthalaldimin-2-yl)(CH_3)(Cl)]	2418		298	$CDCl_3$	99
[((2-Isopropylimino)phenyl)Rh(Br)(Me)(4′-(4-*tert*-butylphenyl)-2,2′ : 6′,2″-terpyridine)]Br	3221		298	CD_3OD	97
[Rh(Br)$_3$(4′-(4-*tert*-butylphenyl)-2,2′ : 6′,2″-terpyridine)]	4540		298	CD_2Cl_2	97
[Rh(Br)$_2$(Me)(4′′-(4-*tert*-butylphenyl)-2,2′ : 6′,2″-terpyridine)]	3366		298	CD_2Cl_2	97
[Rh(Br)$_2$(Et)(4′-(4-*tert*-butylphenyl)-2,2′ : 6′,2″-terpyridine)]	3365		298	CD_2Cl_2	97
[Rh(Br)$_2$(Bu)(4′-(4-*tert*-butylphenyl)-2,2′ : 6′,2″-terpyridine)]	3380		298	CD_2Cl_2	97
[Rh(Br)$_2$(decyl)(4′-(4-*tert*-butylphenyl)-2,2′ : 6′,2″-terpyridine)]	3375		298	CD_2Cl_2	97
[Rh(Br)$_2$(ethenyl)(4′-(4-*tert*-butylphenyl)-2,2′ : 6′,2″-terpyridine)]	3415		298	CD_2Cl_2	97
[Rh(Br)$_2$(2-propenyl)(4′-(4-*tert*-butylphenyl)-2,2′ : 6′,2″-terpyridine)]	3533		298	CD_2Cl_2	97
[Rh(Br)$_2$(2-methyl-2-propenyl)(4′-(4-*tert*-butylphenyl)-2,2′ : 6′,2″-terpyridine)]	3545		298	CD_2Cl_2	97
[Rh(Br)$_2$(3-butenyl)(4′-(4-*tert*-butylphenyl)-2,2′ : 6′,2″-terpyridine)]	3396		298	CD_2Cl_2	97
[Rh(Br)$_2$(Ph)(4′-(4-*tert*-butylphenyl)-2,2′ : 6′,2″-terpyridine)]	3548		298	CD_2Cl_2	97
[(2,6-diethyl-4,8-dimethyl-*s*-indacenide){Rh(COD)}]	−486	^2J(Rh,H) 2		C_6D_6	35
syn-[(2,6-diethyl-4,8-dimethyl-*s*-indacenediide){Rh(COD)$_2$}]	−261	^3J(Rh,H) 1.5		C_6D_6	35
anti-[(2,6-diethyl-4,8-dimethyl-*s*-indacenediide){Rh(COD)$_2$}]	−334	^3J(Rh,H) 1.4		C_6D_6	35
anti-[(2,7-dimethyl-*as*-indacenediide){Rh(CO)$_2$}$_2$]	−1008		300	CD_2Cl_2	34
[(2,6-dimethyl-5-hydro-*s*-indacenide)Rh(CO)$_2$]	−987		300	CD_2Cl_2	34
[(2,7-dimethyl-8-hydro-*as*-indacenide)Rh(CO)$_2$]	−972		300	CD_2Cl_2	34
syn-[(2,7-dimethyl-*as*-indacenediide){Rh(CO)$_2$}$_2$]	−901		300	CD_2Cl_2	34
anti-[(2,7-dimethyl-*as*-indacenediide){Rh(C_2H_4)$_2$}$_2$]	−729		300	CD_2Cl_2	34
syn-[(2,7-dimethyl-*as*-indacenediide){Rh(C_2H_4)$_2$}$_2$]	−652		300	CD_2Cl_2	34
anti-[(2,7-dimethyl-*as*-indacenediide){Rh(COD)$_2$}]	−552		300	CD_2Cl_2	34
syn-[(2,7-dimethyl-*as*-indacenediide){Rh(COD)$_2$}]	−457		300	CD_2Cl_2	34
[(2,6-dimethyl-5-hydro-*s*-indacenide)Rh(COD)]	−421		300	CD_2Cl_2	34
[(2,7-dimethyl-8-hydro-*as*-indacenide)Rh(COD)]	−399		300	CD_2Cl_2	34
$[Rh(COD)]_2^+$	677		300	CD_2Cl_2	34
[Rh(COD){η^5-(1-ferrocenyl)indenyl}]	−381		300	CD_2Cl_2	36

Table 9 *(Continued)*

Complex	δ_{Rh}/ppm	J(Rh,X)/Hz	T/K	Solvent	Ref.
[Rh(COD){η^5-(2-ferrocenyl)indenyl}]	−345		300	CD_2Cl_2	36
[Rh(nbd){η^5-(1-ferrocenyl)indenyl}]	−398		300	CD_2Cl_2	36
[Rh(nbd){η^5-(2-ferrocenyl)indenyl}]	−377		300	CD_2Cl_2	36
[Rh$(CO)_2${η^5-(1-ferrocenyl)indenyl}]	−870		300	CD_2Cl_2	36
[Rh(COD)(Biphemp)]BF_4	−109			CD_2Cl_2	100
[Rh(COD)(Biphemp)]PF_6	−109.9			CD_2Cl_2	100
[Rh(COD)(Biphemp)]CF_3SO_3	−109.4			CD_2Cl_2	100

ferrocenyl ring, especially when in the 2 position, increases the allyl nature of the Rh-indenyl bonding mode, this change in coordination affecting the chemical shift more than the electronic effect, Table 9.[36]

The counterion used to form a salt, has little effect on chemical shift as it does not influence the electron density on the Rh centre. This can be seen in the Rh chemical shifts in CD_2Cl_2 of [Rh(1,5-COD)(Biphemp)]X salts (Biphemp = 6,6′-(dimethylbiphenyl-2,2′-diyl)bis(diphenylphosphine) and $X = BF_4^-$, PF_6^- and $CF_3SO_3^-$) in which there is very little change in chemical shift (δ −109 to −109.9 ppm) on changing the counterion.[100]

4.2.2.2.1.4 Complex geometry. The geometry of the complex has a major influence on Rh chemical shifts. For example, the upfield shift found for $[Rh(L^a)(COD)]BF_4$, $\delta_{Rh} = -29$ vs. $[Rh(L^b)(COD)]BF_4$, $\delta_{Rh} = -157$ ppm (L, see Table 10) is attributed to a change in the Rh coordination sphere.[101]

In general, δ_{Rh} increases with increasing coordination number; four coordinate complexes < five coordinate complexes < six coordinate complexes.[14] For example, the complex $[Rh_4(BABAR\text{-}Phos)_4(Cl)_2(MeCN)_6](PF_6)_2$, (see Table 10) contains a planar centrosymmetric $Rh_4(\mu\text{-}P)_4$ ring which intersects with a perpendicular $Rh_2(\mu_2\_Cl)_2$ ring.[102] The chemical shift of the distorted octahedral Rh at the intersection of the rings, is $\delta_{Rh} = 3{,}308$ ppm while that of the distorted square pyramidal Rh of the eight-membered ring is $\delta_{Rh} = 2{,}860$ ppm.

A comprehensive library of chiral bisphospholane ligands has been prepared for enantioselective Rh-catalysed hydrogenation. The ligands differ from one another in the nature of the bridge between the two phospholane moieties which are formed by three-, four-, five- or six-membered heterocyclic or alicyclic rings. Increasing ring strain as a function of both P–Rh–P angle and Rh–P bond length affects the Rh chemical shift with the most stable complexes/least strained ligands giving the most negative chemical shift, Table 10.[103]

The Rh chemical shift was used to identify the bonding mode in [(2,6-diethyl-4,8-dimethyl-*s*-indacenide){Rh(COD)}] and *syn* and *anti*-[(2,6-diethyl-4,8-dimethyl-*s*-inda-cenediide){$Rh(COD\}_2$]. The *s*-indacene was found to show intermediate coordination between three and five on a scale of [(η^3-cyclooctenyl) Rh(COD)] = −9 and [(η^5-Cp)Rh(COD)] = −777. Also Rh centre slippage could be seen in the *syn*-complex compared to the *anti*-complex using Rh chemical shifts, reflecting more η^3 character and increased steric repulsion in the *syn*-complex, Table 9.[35]

However, it is often difficult to separate the electronic and steric influences on chemical shift.[97]

For example, Kossoy et al.[104] prepared a number of Rh complexes containing a novel π-accepting, pincer ligand, dipyrrolylphosphinoxylene. The ^{103}Rh chemical shift of the hydride complex [Rh^{III}(dipyrrolylphosphinoxylene)(Cl)(H)(PPh_3)] occurs at $\delta_{Rh} = -89.5$ ppm, and [Rh^{I}(dipyrrolylphosphinoxylene)(PR_3)] (R = PPh_3, PEt_3 and $PPyr_3$) for which $\delta_{Rh} = -734$, −781 and −854 ppm, respectively.

4.2.2.2.2 Rhodium cluster compounds. Both mono- and di-substituted derivatives of $[Rh_6(CO)_{16}]$ containing a range of monophosphine, heterobidentate

Table 10 Influence of geometry on Rh chemical shift

Complex	δ_{Rh}/ppm	J(Rh,H)/Hz	J(Rh,X)/Hz	T/K	Solvent	Ref.
$[Rh_4(BABAR\text{-}Phos)_4(Cl)_2(MeCN)_6]PF_6$	3308		55, 153		CH_3CN with 10% CD_3CN	102
BABAR-PHOS=	2860					
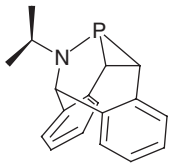						
$[Rh(COD)(camphordiphosphane\ L^a)]BF_4$	−29					101
$[Rh(COD)(camphordiphosphane\ L^b)]BF_4$	−157				CD_3OD	101
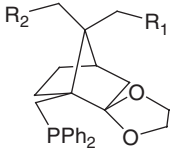 La: $R_1 = PPh_2$, $R_2 = H$ Lb: $R_1 = H$, $R_2 = PPh_2$						
$[Rh(dipyrrolylphosphinoxylene)(Cl)(H)(PPh_3)]$	−89.5	22.3	138.52	295	Toluene-d_8	104
$[Rh(dipyrrolylphosphinoxylene)(PPh_3)]$	−734		208.3	295	THF-d_8	104
$[Rh(dipyrrolylphosphinoxylene)(PEt_3))]$	−781		207.3	295	C_6D_6	104
$[Rh(dipyrrolylphosphinoxylene)(PPyr_3)]$	−853.7		198.5	295	Toluene-d_8	104
$[Rh(COD)(bisphospholane\text{-}1b)]BF_4$	−246			298	Acetone-d_6	103

bisphospholane-1b=

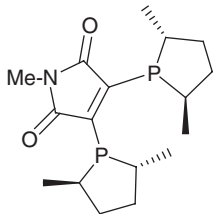

[Rh(COD)(bisphospholane-1c)]BF_4	−355	298	Acetone-d_6	103

bisphospholane-1c=

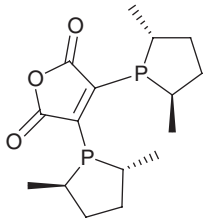

[Rh(COD)(bisphospholane-1d)]BF_4	−376	298	Acetone-d_6	103

bisphospholane-1d=

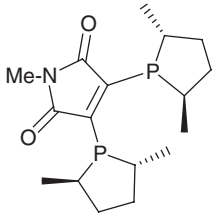

Table 10 *(Continued)*

Complex	δ_{Rh}/ppm	*J*(Rh,H)/Hz	*J*(Rh,X)/Hz	T/K	Solvent	Ref.
[Rh(COD)(bisphospholane-1e)]BF_4 bisphospholane-1e= 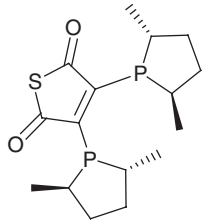	−386			298	Acetone-d_6	103
[Rh(COD)(bisphospholane-1f)]BF_4 bisphospholane-1f= 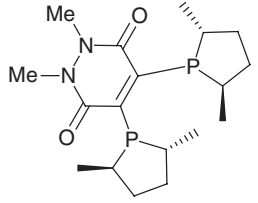	−467			298	Acetone-d_6	103

bridging phosphine and bridging diphosphine ligands have been studied using ^{13}C–{^{103}Rh} and ^{31}P–{^{103}Rh} HMQC.[105–107] This series has further been extended to include a mono-substituted Rh carbide $[Rh_6C(CO)_{15}(PPh_3)]^{2-}$.[108] The heterometallic clusters $[Rh_2Pt_2(\mu\text{-}CO)_3(CO)_4(PPh_3)_3]$[109] and $[Rh_4Pt_2(CO)_{11}(dppm)_2]$[110] have also been studied. δ_{Rh} for the unsubstituted Rh centres in Rh_6 clusters falls in the range −300 to −500 ppm. δ_{Rh} of the substituted centre is less negative by *ca.* 100 ppm for PR_3, with greater downfield shifts seen for sulphur or nitrogen donor atoms the chemical shift increases to *ca.* 15 and 650 ppm, respectively, Table 11. This reflects the known trend that the nature of adjacent ligands plays an important part in Rh chemical shift.[107] (Table 12–18)

4.2.2.3 Group 10: ^{195}Pt NMR. There are few reports of the NMR spectroscopy of ^{61}Ni,[123,124] or ^{105}Pd.[125] Spin-1/2 ^{195}Pt has high natural abundance and good receptivity, thus is normally directly observed. However, *ca.* 40-fold increases in sensitivity are available through indirect detection via ^{1}H or ^{19}F and *ca.* fivefold via ^{31}P. The connectivity information available via HXQC can also be a useful aid in assignment of the NMR spectra. Gradient selected HMQC has thus proven to be a powerful tool to determine δ ^{195}Pt rapidly, Table 19,[126–128] although some variants of the pulse sequence cannot be applied due to the large values of J(PtP) resulting in ''negative'' time delays. ^{1}H-, ^{31}P-, ^{19}F-detected 2D HMQC ^{195}Pt NMR spectroscopy has been used to characterize organoplatinum complexes; recent reports of HMQC NMR of square planar platinum(II) and octahedral platinum(IV) complexes are collected in Table 19. Besides stable organoplatinum complexes, Pt–H–P agostic interactions and structural fluxionality of platinum bis-ethylene adducts have also been studied using ^{1}H–^{195}Pt HMQC at low temperature.[129] The *cis* and *trans* configurational stability of organometallic square planar (phosphane)diarylplatinum(II) complexes[130] and (bis-dmso)diarylplatinum(II) complexes[131] have been systematically investigated by ^{31}P–^{195}Pt HMQC and ^{1}H–^{195}Pt HMQC, respectively. Correlations to ^{13}C, where there is no sensitivity enhancement, $^{105}_{\gamma}Pt \sim {}^{13}_{\gamma}C$ and there is a low natural adundance of ^{13}C, can be observed via a relayed experiment similar to that reported by Gudat,[29] Figure 11. In this way, the configurational isomers of some platinum complexes of *N*,*N*-dialkyl-*N*′-acyl(aroyl) thioureas were differentiated unambiguously, Figure 23.[132]

Although HMQC NMR is suitable for compounds with known coupling constants, there is some exceptions, 2D HMQC with BIRD sequence in the preparation period has been used to determine the heteronuclear spin–spin coupling constants J(^{195}Pt–^{13}C) of (formamide)platinum(IV) complex.[133]

4.2.3 Post-transition metals

4.2.3.1 Group 11: $^{107/109}Ag$ NMR. Only $^{107/109}Ag$ are useful for high-resolution NMR studies. Although both isotopes are spin-1/2, and of high natural abundance (^{107}Ag 51.8% and ^{109}Ag 48.2%), the low receptivity (*ca.* 0.2 vs. ^{13}C) and extremely long spin–lattice relaxation times mean that silver NMR experiments benefit from indirect detection via 2D HSQC or HMQC due to

Table 11 Representative Rh chemical shifts in cluster complexes

Cluster	δ_{Rh}/ppm						^1J(Rh,P)/Hz	T/K	Solvent	Ref.
	RhA	RhB	RhC	RhD	RhE	RhF				
$[Rh_6(CO)_{15}(PBu^n_3)]$[a]	−352	−427	−334	−448			127	253	$CDCl_3$	105
$[Rh_6(CO)_{15}(P(4\text{-}MeO\text{-}C_6H_4)_3)]$	−266	−416	−324	−462			133	223	$CDCl_3$	105
$[Rh_6(CO)_{15}(PPh_3)]$	−303	−445	−347	−484			134.6	250	$CDCl_3$	105
$[Rh_6(CO)_{15}(P(4\text{-}F\text{-}C_6H_4)_3)]$	−297	−426	−333	−461			138	213	$CDCl_3$	105
$[Rh_6(CO)_{15}(P(4\text{-}Cl\text{-}C_6H_4)_3)]$	−295	−417	−326	−450			139	250	$CDCl_3$	105
$[Rh_6(CO)_{15}(P(OPh_3)]$	−410	−405	−352	−430			240	297	$CDCl_3$	105
$[Rh_6(CO)_{15}I]$	−104	−405	−417	−498				203	$CDC(O)CD_3$	105
$[Rh_6(CO)_{15}(NCMe)]$	470	−400	−400	−460				297	$PhCD_3/CDCl_3/CH_3CN$	105
$[Rh_6C(CO)_{14}(PPh_3)]^{2-}$	−289	−217	−273	−255			13.3[b]	298	CD_3CN	108
$[Rh_6C(CO)_{14}(PPh_3)]^{2-}$	−326	−232	−291	−270				203	CD_3CN	108
$[Rh_6(CO)_{14}(dppm)]$	−432	−306	−306	−332	−332	−276	142	298	$CDCl_3$	106
$[Rh_6(CO)_{14}(dppe)]$	−445	−390	−390	−350	−350	−325	141, 139	298	$CDCl_3$	106
$[Rh_6(CO)_{14}(dppe)]$	−410	−380	−292	−363	−385	−343	157, 159	220	CD_2Cl_2	106
$[Rh_6(CO)_{14}(dppe)]$	−379	−349	−261	−332	−354	−312		298[c]	CD_2Cl_2	106
$[Rh_6(CO)_{14}$(diphenyl(2-pyridyl)phosphine)]	−400	−350	15	−385	−330	−355	140	298	$CDCl_3$	107
$[Rh_6(CO)_{14}$(diphenyl(2-thieyl)phosphine)]	−450	−410	650	−370	−415	−315	143	298	$CDCl_3$	107
$[Rh_6(CO)_{14}$(diphenylvinylphosphine)]	−335	−430	−265	−265	−325	−495	125	180	CD_2Cl_2	107
$[Rh_6(CO)_{14}$(diphenylvinylphosphine)]	−288	−383	−218	−218	−278	−448		298[c]	CD_2Cl_2	107
$[Rh_2Pt_2(\mu\text{-}CO)_3(CO)_4(PPh_3)_3]$	−227	−206								109
$[Rh_4Pt_2(CO)_{11}(dppm)_2]$	−151	−295	−444				158	298	CD_2Cl_2	110

[a]See Figure 14 for atom numbering scheme.
[b]^1J(Rh,C).
[c]Adjusted to 298 K.

Table 12 Rh chemical shifts for complexes prepared using *para*-H_2

Complex	δ_{Rh}	^1J(Rh,H)/Hz	T/K	Solvent	Ref.
$[(PPh_3)_2H_2Rh(\mu\text{-}Cl)_2Rh(CO)(PPh_3)]$	925	24.7, 24.6		C_6D_6	49
$[(PPh_3)_2H_2Rh(\mu\text{-}Br)_2Rh(CO)(PPh_3)]$	345	21.0, 21.4		C_6D_6	49
$[(PPh_3)_2H_2Rh(\mu\text{-}I)_2Rh(CO)(PPh_3)]$	32	24.2, 23.5		C_6D_6	49
$[(PPh_3)_2H_2Rh(\mu\text{-}Cl)(\mu\text{-}I)Rh(CO)(PPh_3)]$	281	25.5, 23.5		C_6D_6	49
$[(PPh_3)_2H_2Rh(\mu\text{-}Br)(\mu\text{-}I)Rh(CO)(PPh_3)]$	198	24.8, 24.8		C_6D_6	49
$[(PPh_3)_2H_2Rh(\mu\text{-}Cl)(\mu\text{-}Br)Rh(CO)(PPh_3)]$	423	25.5, 21.6		C_6D_6	49
$[(PPh_3)_2H_2Rh(\mu\text{-}Cl)(\mu\text{-}Br)Rh(CO)(PPh_3)]$	420	24.5, 22.6		C_6D_6	49
$[(PMe_3)_2H_2Rh(\mu\text{-}I)_2Rh(CO)(PMe_3)]$	74	32, 30.7		C_6D_6	49
$[(PMe_3)_2ClHRh(\mu\text{-}Cl)(\mu\text{-}H)_2Rh(CO)(PMe_3)]$	347 −688	19, 29, 24.8		C_6D_6	49
$[(PMe_3)_2BrHRh(\mu\text{-}Br)(\mu\text{-}H)_2Rh(CO)(PMe_3)]$	182 −69	19.1, 30.2, 24		C_6D_6	49
$[(PMe_3)_2IHRh(\mu\text{-}I)(\mu\text{-}H)_2Rh(CO)(PMe_3)]$	−210 −733	19, 30, 23		C_6D_6	49
$[Rh(H)_2I(PMe_3)_3]$	−644		313	C_6D_6	48
$[RhH_2(PMe_3)_4]Cl$	−1007	14.5	312	Methylenechloride-d_2	50
$[RhH_2Cl(PMe)_3]$	−319	27	312	Methylenechloride-d_2	50
$[RhCl(H)_2(PBz_3)_3]$	−393	12, 20	295	Toluene-d_7 or benzene-d_5	51
$[RhCl(H)_2(PBz_3)_2(py)]$	119	14, 25	275	Toluene-d_7 or benzene-d_5	51
$[RhCl(H)_2(PBz_3)(py)_2]$	856	14, 25	255	Toluene-d_7 or benzene-d_5	51
$[RhCl(H)_2(PPh_3)_3]$	98.5	18	275	Toluene-d_7 or benzene-d_5	51
$[RhCl(H)_2(PPh_3)_2(py)]$	304	17, 21	275	Toluene-d_7 or benzene-d_5	51
$[\{RhCl(H)_2(PCy_3)_2\}_2]$	194	26.8	295	Toluene-d_7 or benzene-d_5	51
$[RhCl(H)_2(PCy_3)(py)_2]$	337	30, 30	235	Toluene-d_7 or benzene-d_5	51
$[RhCl(H)_2(PCy)_3(Py)_2]$	408	24.7, 24.6	235	Toluene-d_7 or benzene-d_5	51

Table 13 ^{103}Rh chemical shifts for diene complexes detected via ^{1}H,^{103}Rh and ^{31}P,^{103}Rh HXQC spectroscopy

Complex	δ_{Rh}/ppm	T/K	Solvent	Ref.
[Rh(1,3-COD)Tp^{Me2}]	1942	295	C_6D_6	111
[RhH(Ph)(P(O)Me)$_3$)Tp^{Me2}]	1270	295	C_6D_6	111
[Rh(COD)(1,2-en)]ClO_4	751	298	CD_3OD	98
trans-[Rh(COD)(dmeda)]ClO_4	784	298	CD_3OD	98
cis-[Rh(COD)(dmeda)]ClO_4	822	298	CD_3OD	98
[Rh(COD)(1,2-(NH$_2$)C$_6$H$_4$)]ClO_4	801	298	CD_3OD	98
[Rh(COD)(1,8-(NH$_2$)$_2$-naphthalene]ClO_4	804	298	CD_3OD	98
[Rh(COD)(1,3-pn)]ClO_4	849	298	CD_3OD	98
[Rh(COD)(tmeda)]ClO_4	978	298	CD_3OD	98
[Rh(COD)(tmeda)][Rh(COD)Cl_2]	949	230	CD_3OD	98
	1065			
[Rh(COD)(^{i}Pr-DAB)]ClO_4	914	298	CD_3OD	98
[Rh(COD)(ABK)]	998	298	$CDCl_3$	98
[Rh(COD)(BIAN-R)]ClO_4 (R=C$_6$H$_5$)	1025	298	$CDCl_3$	98
[Rh(COD)(BIAN-R)]ClO_4 (R=2,6-(^{i}Pr)$_2$C$_6$H$_3$)	1057	298	$CDCl_3$	98
[Rh(COD)(BIAN-R)]ClO_4 (R=4-OMeC$_6$H$_4$)	1059	298	$CDCl_3$	98
[Rh(COD)(4,4′-Me$_2$-bipy)]ClO_4	795	298	CD_3OD	98
[Rh(COD)(bipy)]ClO_4	816	298	CD_3OD	98
[Rh(COD)(py)$_2$]ClO_4	1009	298	CD_3OD	98
[Rh(COD)(C$_5$H$_4$N-NH-C$_5$H$_4$N)]ClO_4	1035	298	CD_3OD	98
[Rh(COD)Cl]$_2$	1093	298	$CDCl_3$	98
[Rh(COD)Cl_2]Et$_4$N	1107	298	$CDCl_3$	98
[Rh(COD)(acac)]	1287	298	$CDCl_3$	98
Rh(COD)(1,2-(HO)$_2$-napthalene)]ClO_4	1301	298	CD_3OD	98
[Rh(COD)(Me$_2$CO)$_x$]ClO_4	1350	298	CD_3OD	98
[Rh(COD)(dppmO$_2$)]ClO_4	1362	298	CD_3OD	98
[Rh(COD)(bipyO$_2$)]ClO_4	1362	298	CD_3OD	98
[Rh(COD)(dppeO$_2$)]ClO_4	1373	298	CD_3OD	98
[Rh(COD)(dppb{OH}$_2$)]BF_4	−57		CD_3OD	112
[Rh(COD)(diop)]BF_4	−233		CD_3OD	112
[Rh(COD)(dppb)]BF_4	−262		CD_3OD	112
[Rh(COD)(Ph-b-glup-OH)]BF_4	−305		CD_3OD	112
[Rh(COD)Cp]	−785	300	CD_2Cl_2	36
[Rh(COD)Ind]	−487	300	CD_2Cl_2	36
[Rh(COD)(η^3-cyclooctenyl)]	−9	300	CD_2Cl_2	36
[Rh(nbd)Cp]	−786	300	CD_2Cl_2	36
[Rh(nbd)Ind]	−520	300	CD_2Cl_2	36
[Rh(nbd)(diop)]BF_4	−204		CD_3OD	112
[Rh(nbd)(dppb)]BF_4	−210		CD_3OD	112
[Rh(nbd)(Ph-b-glup-OH)]BF_4	−296		CD_3OD	112

Table 14 ^{103}Rh chemical shifts for carboxylate complexes detected via ^{31}P,^{103}Rh HXQC spectroscopy

Complex	δ_{Rh}/ppm	^{1}J(Rh,P)/Hz	T/K	Solvent	Ref.
$[Rh(O_2CCH_3)(PPh_3)_3]$	−26	176.8, 150	248	Toluene	113
$[Rh(O_2CCF_3)(PPh_3)_3]$	−38	183.3, 147.3	248	Toluene	113
$[Rh_2$(R)-MTPA$_4(PPh_3)]$	6963	^{1}J(Rh,P) = 96.1	298	$CDCl_3$/acetone-d_6	41
	7455	^{2}J(Rh,P) = 23.3			
$[Rh_2$(R)-MTPA$_4$(P(Ph)(CH$_3$)(NEt$_2$))]	6949, 7153[a]	^{1}J(Rh,P) = 106.2	298	$CDCl_3$/acetone-d_6	41
	6963, 7153[a]	^{2}J(Rh,P) = 21.5			
		^{1}J(Rh,P) = 106.2			
		^{2}J(Rh,P) = 23			
$[Rh(O_2CPh)(PPh_3)_3]$	−20	175.0, 152.2	248	Toluene	113
$[Rh(O_2CCH_3)(PmePh_2)_3]$	−138	172.5, 147.1	248	Toluene	113
cis-$[Rh(O_2CCH_3)(PPh_3)_2(py)]$	342	191.4, 175.0	248	10% pyridine–toluene	113
cis-$[Rh(O_2CPh)(PPh_3)_2(py)]$	328	193.1, 172.3	248	10% pyridine–toluene	113
trans-$[Rh(O_2CCH_3)(PPh_3)_2(py)]$	225	170.5	248	Chloroform	113
trans-$[Rh(O_2CCF_3)(PPh_3)_2(py)]$	208	171.4	248	10% pyridine–toluene	113

[a]Two diastereoisomers present.

Table 15 ^{103}Rh chemical shifts for thiolate complexes detected via HXQC spectroscopy

Complex	δ_{Rh}/ppm	^{1}J(Rh,P)/Hz	T/K	Solvent	Ref.
$[Rh(SC_6F_5)(PPh_3)_3]$	17	169.6, 148.3	248	Toluene	113
$[Rh(SCPh_3)(PPh_3)_3]$	−338	164.6, 150.6	248	Toluene	113
$[Rh(SPh)(PPh_3)_3]$	−164	168.7, 149.6	248	Toluene	113
$[Rh(SCH_2Ph)(PPh_3)_3]$	−25	169.6, 157.7	248	Toluene	113
$[Rh(S^iPr)(PPh_3)_3]$	33	158.6, 161.7	248	Toluene	113
$[Rh(S^nPr)(PPh_3)_3]$	−59	162.2, 158.8	248	Toluene	113
$[Rh(SCy)(PPh_3)_3]$	39	156.3, 162.5	248	Toluene	113
$[Rh(SC_6F_5)(PMePh_2)_3]$	−414	167.6, 142.1	248	Toluene	113
$[Rh_2(SC_6F_5)_2(PPh_3)_4]$	311	176.4	248	Toluene	113
	363		248	Toluene	113
$[Rh_2(SCPh_3)_2(PPh_3)_4]$	−338	174.6	248	Toluene	113
$[Rh_2(SPh)_2(PPh_3)_4]$	36	169	248	Toluene	113
$[Rh_2(S^iPr)_2(PPh_3)_4]$	−41	166.6	248	Toluene	113
$[Rh_2(S^nPr)_2(PPh_3)_4]$	−72	172.5	248	Toluene	113
$[Rh_2(SCy)_2(PPh_3)_4]$	−38	166.5	248	Toluene	113
cis-$[Rh(SC_6F_5)(PPh_3)_2(py)]$	7	165.2, 178.9	248	10% pyridine–toluene	113
cis-$[Rh(S^iPr)(PPh_3)_2(py)]$	−49	173.7, 165.6	248	10% pyridine–toluene	113
cis-$[Rh(SCy)(PPh_3)_2(py)]$	−47	174.5, 166.0	248	10% pyridine–toluene	113

the high signal enhancement factors of 2,143 for ^{1}H{^{109}Ag} and 223 for ^{31}P{^{109}Ag}, which, in combination with the shorter recovery delay required for ^{1}H, as opposed to ^{107,109}Ag relaxation, allow much shorter experiment times. (Table 20)

Table 16 ^{103}Rh chemical shifts for dienyl complexes detected via HXQC spectroscopy

Complex	δ_{Rh}/ppm	T/K	Solvent	Ref.
$[CpRh(CO)_2]$	−1321	300	CD_2Cl_2	36
$[(Ind)Rh(CO)_2]$	−1038	300	CD_2Cl_2	36
$[CpRh(PMe_3)(SPh)_2]$	388.2	298	$CDCl_3$	114
$[CpRh(PMe_3)(SePh)_2]$	106.5	298	$CDCl_3$	114
$[CpRh(PMe_3)(TePh)_2]$	−553.0	298	$CDCl_3$	114
$[Cp^*Rh(PMe_3)(SPh)_2]$	461.3	298	$CDCl_3$	114
$[Cp^*Rh(PMe_3)(SePh)_2]$	201.5	298	$CDCl_3$	114
$[Cp^*Rh(PMe_3)(TePh)_2]$	−384.0	298	$CDCl_3$	114
$[CpRh(PMe_3)(S_2C_6H_4)]$	52.0	298	$CDCl_3$	114
$[Cp^*Rh(PMe_3)(S_2C_6H_4)]$	−11.0	298	$CDCl_3$	114
$[Cp^*Rh[S_2C_2(B_{10}H_{10})]$	1165		CD_2Cl_2	115
$[Cp^*Rh[Se_2C_2(B_{10}H_{10})]$	1150		CD_2Cl_2	115
$[Cp^*Rh(PMe_3)\{S_2C_2(B_{10}H_{10})\}]$	334		$CDCl_3$	115
$[Cp^*Rh(PMe_3)\{Se_2C_2(B_{10}H_{10})\}]$	36		$CDCl_3$	115
$[Cp^*Rh(PMe_3)\{Te_2C_2(B_{10}H_{10})\}]$	−523		$CDCl_3$	115
$[(C_5H_3^tBu_2)Rh(PMe_3)\{S_2C_2(B_{10}H_{10})\}]$	460		$CDCl_3$	115

4.2.3.2 Group 12: ^{113}Cd, ^{199}Hg NMR. ^{113}Cd and ^{199}Hg are both useful for high-resolution NMR studies, both are spin-1/2, and have reasonable sensitivities 7.94 and 5.89 vs. ^{13}C. Furthermore, the gyromagnetic ratios, about one fifth that of ^{1}H would suggest that useful sensitivity enhancement could be obtained, however, a suitable detector nucleus is rarely present. ^{1}H–^{113}Cd HMQC NMR of cadmium model complexes such as Cd–EDTA has been used to study biological systems. Scalar coupling between the cadmium atom and the surrounding protons of the protein in which it is bound can be used to establish metal–ligand connectivities, providing a valuable tool for the structural elucidation of enzymes, proteins, etc. Accordion-HMQC[25] experiments, which allow simultaneous detection of correlations between protons and a heteronucleus when widely varying coupling constants, have been suggested to overcome the wide range of $J(^{113}Cd,^{1}H)$ encountered, Figure 24. A few examples are given in Table 21, where the chemical shifts of ^{113}Cd cannot be precisely assigned for the complex biological systems.

4.3 p-Block metals

4.3.1 Group 13

All but indium of the group 13 metals have NMR active isotopes. ^{205}Tl has sufficiently high receptivity (*ca.* $2 \times {}^{31}$P) that indirect detection is unnecessary. The other metals have largely been studied in the solid state in recent years, where attention has focused on network connectivity in alumino-[52,148–150] and gallo-[151] phosphates and other phosphorus containing zeolitic materials.[152] Massiot[153] has also reported HMQC HETCOR spectra between ^{31}P and ^{27}Al in

Table 17 ^{103}Rh chemical shifts for rhodium-hydride complexes detected via ^{1}H,^{103}Rh and ^{31}P,^{103}Rh HXQC spectroscopy

Complex	δ_{Rh}		J(Rh,H)/Hz	J(Rh, X)/Hz	T/K	Solvent	Ref.
	via ^{1}H	via ^{31}P					
[Rh(H)(CO)$_2$(DPEphos)]	−828.9	−828.6	11	124	298	C_6D_6	116
[Rh(H)(CO)$_2$(phenyl-*P*-xantphos)]	−828.2	−827.9	6.6	126	298	C_6D_6	116
[Rh(H)(CO)$_2$(sixantphos)]	−817.4	−817.1	8.1	124	298	C_6D_6	116
[Rh(H)(CO)$_2$(thixantphos)]	−840	−840.1	6.6	128	298	C_6D_6	116
[Rh(H)(CO)$_2$(xantphos)]	−800.8	−800.9	6.6	127	298	C_6D_6	116
[Rh(H)(CO)$_2$(Isopropenyl-xantphos)]	−821.1	−821	6.6	128	298	C_6D_6	116
[Rh(H)(CO)$_2$(*N*-xantphos)]	−785.3	−785.2	5.9	128	298	C_6D_6	116
[Rh(H)(CO)$_2$(*p*-trifluoromethyl-thixantphos)]	−850.9	−851	4.4	135	298	C_6D_6	116
[Rh(H)(CO)$_2$(*p*-chloro-thixantphos)]	−840.7	−840.7	5.9	132	298	C_6D_6	116
[Rh(H)(CO)$_2$(*p*-fluoro-thixantphos)]	−835.6	−835.7	6.6	131	298	C_6D_6	116
[Rh(H)(CO)$_2$(methyl-thixantphos)]	−831.5	−831.6	7.3	126	298	C_6D_6	116
[Rh(H)(CO)$_2$(methoxy-thixantphos)]	−825.3	−825.4	7.3	125	298	C_6D_6	116
[Rh(H)(CO)$_2$(dimethlyamino-thixantphos)]	−814.3	−814.2	8.8	122	298	C_6D_6	116
[Rh(H)(CO)$_2$(BISBI)]	−897.6	−897.6	2	149	298	C_6D_6	116
[Rh(H)(CO)$_2$(dppe)]	−1073		11	118	298	THF-d_8	116
[Rh(H)(CO)$_2$(dppp)]	−954.9		11.7	113	298	THF-d_8	116
[Rh(H)(CO)$_2$(1,8dppn)]	−953.6		13.9	108	298	C_6D_6	116
[Rh(H)(CO)$_2$(BINAPHOS)]	−969.6		9.5	118.8	298	C_6D_6	116
[Rh(NCBPh$_3$)(H)(SnPh$_3$)(PPh$_3$)$_2$]	120			111.1	248	CD_2Cl_2	117
[Rh(NCBPh$_3$)(H)(SnBu$_3$)(PPh$_3$)$_2$]	−132			119.2	248	CD_2Cl_2	117
trans-[Rh(NCBPh$_3$)(H)(SnPh$_3$)(PPh$_3$)$_2$(py)]	512			106.2	248	CD_2Cl_2	117
trans-[Rh(NCBPh$_3$)(H)(SnPh$_3$)(PPh$_3$)$_2$(4-Me$_2$Npy)]	519			105.9	248	CD_2Cl_2	117
trans-[Rh(NCBPh$_3$)(H)(SnPh$_3$)(PPh$_3$)$_2$(4-MeO$_2$Cpy)]	510			106.3	248	CD_2Cl_2	117
cis-[Rh(NCBPh$_3$)(H)(SnPh$_3$)(PPh$_3$)$_2$(4-Me$_2$Npy)]	328			114.4	248	CD_2Cl_2	117
cis-[Rh(NCBPh$_3$)(H)(SnPh$_3$)(PPh$_3$)(4-Me$_2$Npy)]$_2$	1026			82.2, 82.9	248	CD_2Cl_2	117
trans-[Rh(NCBPh$_3$)(H)(SnPh$_3$)(PPh$_3$)(4-Me$_2$Npy)]$_2$	1159			121.3	248	CD_2Cl_2	117

Table 17 *(Continued)*

Complex	δ_{Rh} via ^{1}H	δ_{Rh} via ^{31}P	J(Rh,H)/Hz	J(Rh, X)/Hz	T/K	Solvent	Ref.
$[Rh(NCBPh_3)(H)(SnPh_3)(PPh_3)(py)]$	1184			134.6	248	CD_2Cl_2	117
$[Rh(NCBPh_3)(H)(SnPh_3)(PPh_3)(4\text{-}Me_2Npy)]$	1204			132.6	248	CD_2Cl_2	117
$[Rh(NCBPh_3)(H)(SnPh_3)(PPh_3)(4\text{-}MeO_2Cpy)]$	1171			135.3	248	CD_2Cl_2	117
$[Rh(H)\{(\mu\text{-}H)SnPh_3\}_2(PPh_3)_2]$	−1440			103.2	300	CD_2Cl_2	117
$[Rh(O_2CCH_3)(H)_2(PPh_3)_2]$	646			120.5	248	Toluene	113
$[Rh(O_2CCH_3)(H)_2(PPh_3)_3]$	207			117.4, 89.4,	248	Toluene	113
$[Rh(O_2CCH_3)(H)_2(PPh_3)_3]$	183			118.5, 88.3	248	Toluene	113
$[Rh(O_2CCH_3)(H)_2(PPh_3)_2(py)]$	630			121.1	248	10% pyridine–toluene	113
$[Rh(O_2CCH_3)(H)_2(PPh_3)_2(py)]$	688			121.2	248	10% pyridine–toluene	113
$[Rh(O_2CPy)(H)_2(PPh_3)_2]$	490			118.5	248	Chloroform	113
	593				300		
$[Rh(O_2CPyraz)(H_2)(PPh_3)_2]$	476			117.7	248	Chloroform	113
	506				300		
$[Rh(O_2CQuin)(H_2)(PPh_3)_2]$	419			118.7	248	Chloroform	113
	453				300		
$[Rh(O_2Clsoq)(H_2)(PPh_3)_2]$	457			118.9	248	Chloroform	113
	490				300		
$[Rh(O_2CQuinox)(H_2)(PPh_3)_2]$	405			118	248	Chloroform	113
	436				300		
$[Rh(SC_6F_5)(H)_2(PMePh_2)_3]$	−417			110, 89.7	248	Toluene	113
$[Rh(SC_6F_5)(H_2)(PPh_3)_3]$	−221			112.7, 86.4	248	Toluene	113
$[Rh(SCPh_3)(H)_2(PPh_3)_3]$	−422			113.4, 93.7	248	Toluene	113
$[Rh(SPh)(H)_2(PPh_3)_3]$	−323			111.9, 88.9	248	Toluene	113
$[Rh(SCH_2Ph)(H)_2(PPh_3)_3]$	−358			112.7, 90.8	248	Toluene	113
$[Rh(S^{i}Pr)(H)_2(PPh_3)_3]$	−328			113.3, 89.5	248	Toluene	113
$[Rh(S^{n}Pr)(H)_2(PPh_3)_3]$	−376			113.3, 90.9	248	Toluene	113

$[Rh(SCy)(H)_2(PPh_3)_3]$	−340	113.6, 89.8	248	Toluene	113
$[Rh(SC_6F_5)(H)_2(PPh_3)_2(py)]$	273	118.2	248	10% pyridine–toluene	113
$[Rh(SCPh_3)(H)_2(PPh_3)_2(py)]$	155	118.1	248	10% pyridine–toluene	113
$[Rh(SPh)(H)_2(PPh_3)_2(py)]$	222	116.6	248	10% pyridine–toluene	113
$[Rh(SCH_2Ph)(H)_2(PPh_3)_2(py)]$	219	117.6	248	10% pyridine–toluene	113
$[Rh(S^iPr)(H)_2(PPh_3)_2(py)]$	215	118.5	248	10% pyridine–toluene	113
$[Rh(S^nPr)(H)_2(PPh_3)_2(py)]$	223	118.3	248	10% pyridine–toluene	113
$[Rh(SCy)(H)_2(PPh_3)_2(py)]$	206	118.8	248	10% pyridine–toluene	113
$[Rh(SPh)_2(H)(PPh_3)_2(py)]$	817	106	248	10% pyridine-toluene	113
$[Rh(SCH_2Ph)_2(H)(PPh_3)_2(py)]$	812	109.7	248	10% pyridine–toluene	113
$[Rh(S^nPr)_2(H)(PPh_3)_2(py)]$	840	110.1	248	10% pyridine–toluene	113
$[Rh(SCy)_2(H)(PPh_3)_2(py)]$	782	111.9	248	10% pyridine–toluene	113
$[Rh(H)_2(k^1\text{-TFPO})(k^2\text{-TFPO})Cl]$	780	112.3	295	Acetone-d_6	118

Table 18 ^{103}Rh chemical shifts for miscellaneous complexes detected via HXQC spectroscopy

Complex	δ_{Rh}/ppm	^{1}J(Rh,P)/Hz	T/K	Solvent	Ref.
$[Rh(H\text{-}MOP)(MePh_2P)]BF_4$ 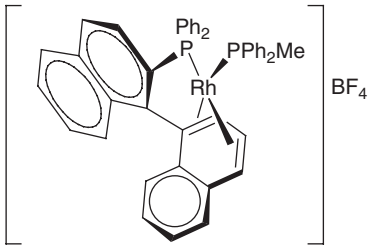	−391	206, 199.6		$CDCl_3$	119
$[Rh(CO)_2(C(O)C_8H_{17}(L^c)_2]$ L^c= 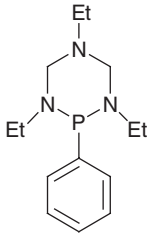	−70	^{1}J(Rh,P) = 205 ^{1}J(Rh,C) = 70, 18, 42	183	Toluene-d_8	120

$[(LP^4)\{RhCl(CO)\}_2]$ LP^4= 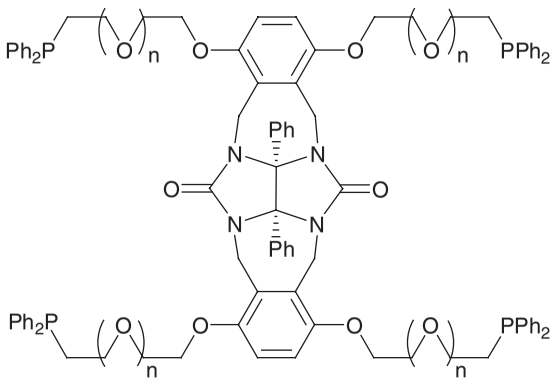	−419	$^1J_{Rh-P}$ 123		$CDCl_3$	121
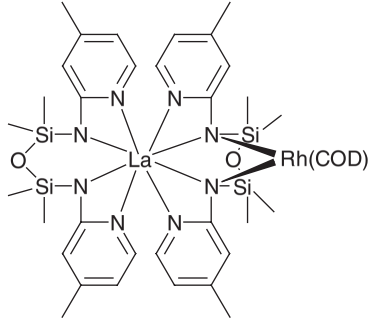	1087		298	Benzene	122

Table 18 *(Continued)*

Complex	δ_{Rh}/ppm	^{1}J(Rh,P)/Hz	T/K	Solvent	Ref.
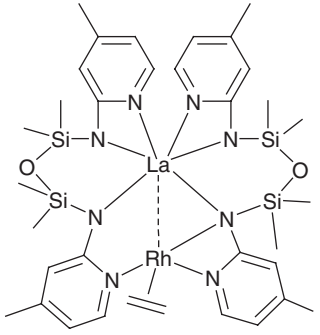	2151		298	Benzene	122
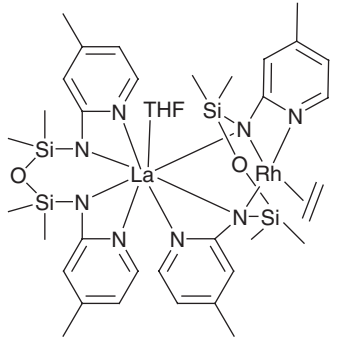	2242		298	Benzene	122

Table 19 Collection of ^{1}H–^{195}Pt HMQC spectroscopic data

Compound	^{195}Pt/ppm	X	$^{n}J(X–^{195}Pt)$/Hz	NMR	T/K	Solvent	Ref.
Platinum(II) complexes							
$[Pt(Ph)_2(PEt_3)_2]$	−4568	^{31}P	$^{1}J = 1790$	gsHMQC		$CDCl_3$	130
syn-$[Pt(2\text{-}Tol)_2(PEt_3)_2]$	−4471	^{31}P	$^{1}J = 1751$	gsHMQC		Acetone-d_6	130
anti-$[Pt(2\text{-}Tol)_2(PEt_3)_2]$	−4466	^{31}P	$^{1}J = 1739$	gsHMQC		Acetone-d_6	130
$[Pt(3\text{-}Tol)_2(PEt_3)_2]$	−4570	^{31}P	$^{1}J = 1764$	gsHMQC	303	Acetone-d_6	130
$[Pt(4\text{-}Tol)_2(PEt_3)_2]$	−4566	^{31}P	$^{1}J = 1780$	gsHMQC		Acetone-d_6	130
$[Pt(Xyl)_2(PEt_3)_2]$	−4311	^{31}P	$^{1}J = 2848$	gsHMQC		Acetone-d_6	130
$[Pt(Mes)_2(PEt_3)_2]$	−4306	^{31}P	$^{1}J = 2841$	gsHMQC		Acetone-d_6	130
cis-$[Pt(dmso)_2(Ph)_2]$	−4217	^{1}H	$^{3}J = 69.7$	gsHMQC	303	CD_2Cl_2	131
anti-$[Pt(dmso)_2(2\text{-}Tol)_2]$	−4157	^{1}H	$^{3}J = 77.8$	gsHMQC	303	CD_2Cl_2	131
syn-$[Pt(dmso)_2(Ph)_2]$	−4165	^{1}H	$^{3}J = 73$	gsHMQC	303	CD_2Cl_2	131
cis-$[Pt(dmso)_2(3\text{-}Tol)_2]$	−4220	^{1}H	$^{3}J = 70.9$	gsHMQC	303	CD_2Cl_2	131
cis-$[Pt(dmso)_2(4\text{-}Tol)_2]$	−4212	^{1}H	$^{3}J = 69.3$	gsHMQC	303	CD_2Cl_2	131
cis-$[Pt(SCF_3)Cl(PPh_3)_2]$	−4511	^{31}P	$^{1}J(Pt,P) = 3033, 3725$	HMQC	294	CD_2Cl_2	127
		^{19}F	$^{3}J(Pt,F) = 63$				
trans-$[Pt(SCF_3)Cl(PPh_3)_2]$	−4480	^{31}P	$^{1}J(Pt,P) = 2625$	HMQC	294	CD_2Cl_2	127
		^{19}F	$^{3}J(Pt,F) = 118$				
cis-$[Pt(SCF_3)_2(PPh_3)_2]$	−4621	^{31}P	$^{1}J(Pt,P) = 3147$	HMQC	294	CD_2Cl_2	127
		^{19}F	$^{3}J(Pt,F) = 70$				
trans-$[Pt(SCF_3)_2(PPh_3)_2]$	−4673	^{31}P	$^{1}J(Pt,P) = 2634$	HMQC	294	CD_2Cl_2	127
		^{19}F	$^{3}J(Pt,F) = 83$				
$[Pt(\eta^3\text{-}1,3\text{-}Ph_2C_3H_3)\text{-}(PPFPz\{3\text{-}^{t}Bu\})]PF_6$	−4453	^{1}H	77, 49, 11	HMQC	213	THF-d_8	134
cis-$[Pt(L^1\text{-}S,O)_2]$	ZZ −2731	^{1}H	$^{1}J = 140$	^{1}H–(^{13}C)–^{195}Pt HMQC[a]	298	$CDCl_3$	132
	ZE −2735	^{13}C	$^{4}J = 30$				
	EE −2739						
cis-$[Pt(L^2\text{-}S,O)_2]$	ZZ −2707	^{1}H	$^{1}J = 140$	^{1}H–(^{13}C)–^{195}Pt HMQC	298	$CDCl_3$	132

Table 19 *(Continued)*

Compound	^{195}Pt/ppm	X	^{n}J(X–^{195}Pt)/Hz	NMR	T/K	Solvent	Ref.
	ZE −2709 EE −2711	^{13}C	$^{4}J = 30$				
cis-[Pt(L^1-S,O)$_2$]	−2733	^{1}H ^{13}C	$^{1}J = 140$ $^{4}J = 30$	^{1}H–(^{13}C)–^{195}Pt HMQC	298	$CDCl_3$	132
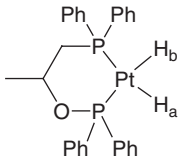	−820	^{1}H	^{1}J(Pt,H$_b$) = 1076 ^{1}J(Pt,H$_a$) = 1204	HMQC		Tol-d_8	135
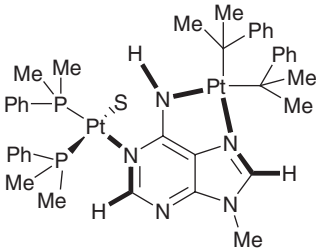	−4378 −4272	^{1}H	$^{2}J = 89$	HMBC		DMSO-d_8	136
[(trpy)Pt$_2$(mcyt-N^3,N^4)]$^{3+}$	−2630 −2540	^{1}H	$^{2}J = 15$,$^{5}J = 7$ $^{4}J = 20$				137
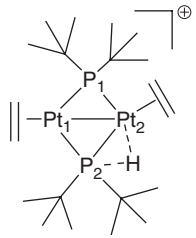	Pt$_2$ −6495 Pt$_1$ −5962	^{1}H	363	HMQC	213	CD_2Cl_2	129

cis-[{Pt(NH_3)$_2$(Hetgua-N^7)(mcyt-N^3-N^4)}$_2$][ClO_4]$_4$ · 5H_2O	−816	^{1}H	^4J = 9.2;^5J = 8.3; ^3J = 5.2	HMQC		D_2O	138
cis-[(PMe_3)$_2$Pt{1-MeTy(-H)$_3$}{C(NH)NH_2}]ClO_4	−4633	^{31}P	3100	HMQC		DMSO-d_6	139
			3119				
Platinum(IV) complexes							
[PtClMe_3(abpy)]	−2529	^{1}H	^2J = 75	gsHMQC		DMSO-d_8	126
[PtBrMe_3(abpy)]	−2666	^{1}H	^2J = 75	gsHMQC		DMSO-d_8	126
[PtIMe_3(abpy)]	−2899	^{1}H	^2J = 75	gsHMQC		DMSO-d_8	126
[PtClMe_3(bpym)]	−2539	^{1}H	^2J = 75	gsHMQC		DMSO-d_8	126
[PtBrMe_3(bpym)]	−2658	^{1}H	^2J = 75	gsHMQC		DMSO-d_8	126
[PtIMe_3(bpym)]	−2872	^{1}H	^2J = 75	gsHMQC		DMSO-d_8	126
cis-[$PtCl_4$(O=)$CHNHMe$}$_2$]	−381	^{13}C	^2J = 2	BIRD-HMQC		DMSO-d_6	133
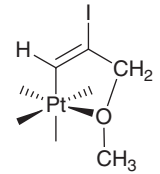	−2228.5	^{1}H	^2J = 410 ^3J = 4.8	HMQC		$CDCl_3$	140
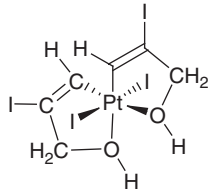	−2380	^{1}H	31	HMQC	273	NaI/CD_3OD	140
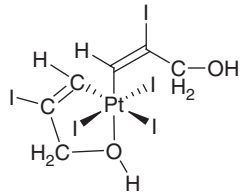	−2960	^{1}H	95 33	HMQC	273	NaI/CD_3OD	140

Table 19 *(Continued)*

Compound	^{195}Pt/ppm	X	^{n}J(X–^{195}Pt)/Hz	NMR	T/K	Solvent	Ref.
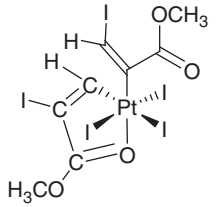	−2350	^{1}H	50	gsHMQC		CD_3OD	141
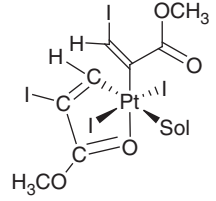	−3018	^{1}H	50	gsHMQC		CD_3OD	141

$J_{Pt,H}$ = 77 Hz, allyl H, *anti*, *trans* N; $J_{Pt,H}$ = 56 Hz, allyl H, *central*; $J_{Pt,H} \approx 11$ Hz, Pz H.
[a]H dected ^{13}C–^{195}Pt correlation spectrum by means of a double magnetization transfer experiment in which magnetization be relayed from ^{1}H to ^{13}C to ^{195}Pt and back to ^{13}C and ^{1}H.

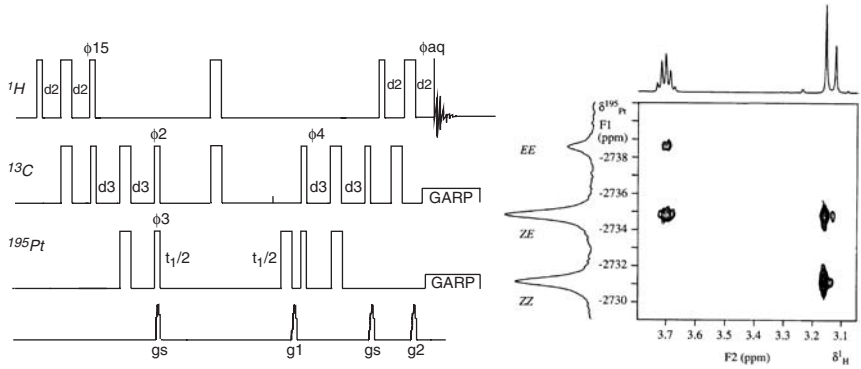

Figure 23 Left: Pulse sequence for acquiring ^{1}H–(^{13}C)–^{195}Pt-relayed correlation spectra for *cis*-[Pt(L^{1}–S,O)$_2$]. d_2 = 1.785 ms ($1/\{4\ ^{1}J(C,H)\}$ and d_3 = 6.25 ms. See reference for phase cycling. g1 : g2 = $\gamma_H : \gamma_{Pt}$ = 4.66 : 1.0. g1 was inverted for every other FID to achieve *N/P* type selection. Right: The ^{1}H detected ^{1}H–(^{13}C)–^{195}Pt correlation spectrum of *cis*-[Pt(L^{1}–S,O)$_2$]. The correlations between the overlapping ^{1}H resonances of the *N*-CH$_2$– moieties at *ca.* 3.7 ppm and the ^{195}Pt peaks at −2,739 and −2,735 ppm confirm the assignments to the *cis*-[Pt(*ZE*-L^{1}–S,O)$_2$] and *cis*-[Pt(*EE*-L^{1}–S,O)$_2$] isomers, respectively. The ^{195}Pt peak at −2,735 ppm shows correlations to both the *N*-CH$_3$ and *N*-CH$_2$– resonances, which can only occur for the *cis*-[Pt(*ZE*-L^{1}–S,O)$_2$] isomer, while the correlation between the −2,731 ppm peak and the *N*-CH$_3$ resonance at 3.17 ppm, confirms the *cis*-[Pt(*ZZ*-L^{1}–S,O)$_2$] assignment. Adapted with permission from ref. 132. Copyright 2003 Wiley-VCH Verlag GmbH & Co.

Table 20 Collection of X–^{109}Ag HMQC spectroscopic data

Compound	^{109}Ag/ppm	X nuclei	^{n}J(X–^{109}Ag)/Hz	NMR	T/K	Solvent	Ref.
[Ag(d2pype)$_2$]NO$_3$	1411	^{31}P	^{1}J(Ag,P) = 266	HMQC	243	CD_3OD	142
{[Ag(d2pype)$_2$]NO$_3$}$_2$	1417	^{31}P	^{1}J(Ag,P) = 218, 326	HMQC	243	CD_3OD	142
{[Ag(d2pype)$_2$]NO$_3$}$_3$	1397 1386	^{31}P	^{1}J(Ag,P) = 203, 330, 257	HMQC	243	CD_3OD	142
[Ag(d3pype)$_2$]NO$_3$	1418	^{31}P	^{1}J(Ag,P) = 266	HMQC	295	D_2O	142
[Ag(d4pype)$_2$]NO$_3$	1378	^{31}P	^{1}J(Ag,P) = 263	HMQC	295	CD_3OD	142
[(TROPP^{Ph})$_2$Ag^{I}]O$_3$SCF$_3$	905.4	^{1}H	^{3}J(Ag,H) = 7	HMQC		$CDCl_3$	143
[PNP][Ag(CF$_3$)$_2$]	556	^{19}F	^{2}J(Ag,F) = 100	HMQC		THF-d_8	144
	945	^{1}H		HMQC			145

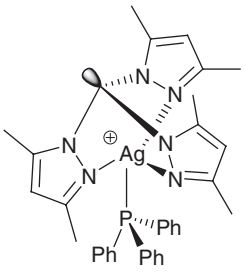

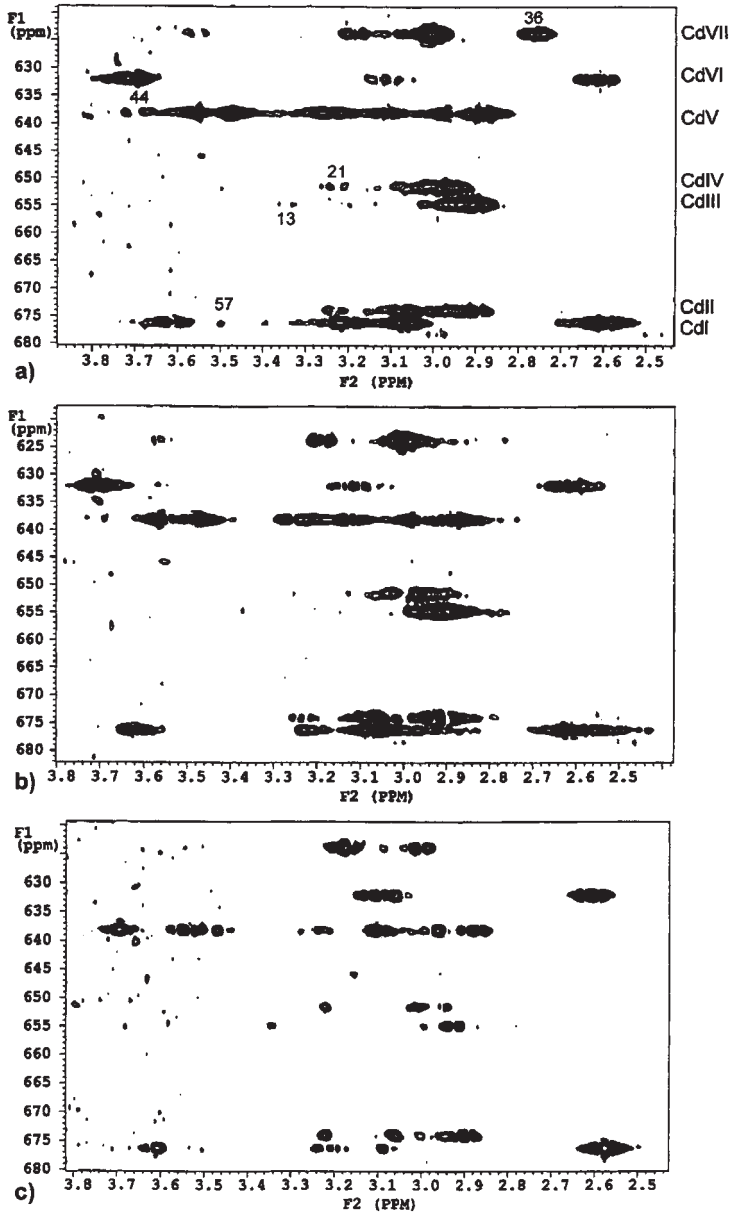

Figure 24 Top: accordion $^{1}H–^{113}Cd$-HMQC, *J*min = 10 Hz, *J*max = 40 Hz; (bottom) standard $^{1}H–^{113}Cd$-HMQC optimized for (left) *J* = 40, and (right) 20 Hz on mouse metallothionein-1 at 25°C, pH 6.5, see reference for further details. Cross peaks, indicating correlations between cadmium ions and cysteine β-protons peaks, that are clearly visible in the accordion spectrum are either weak (e.g., Cys44–CdV, Cys57–CdI) or missing (e.g., Cys36–CdVII, Cys21–CdIV) in the standard HMQC spectra. Reproduced with permission from ref. 25. Copyright 2000 Wiley-VCH Verlag GmbH & Co.

Table 21 Collection of X–^{113}Cd HMQC spectroscopic data

Compound	^{113}Cd/ppm	^{n}J(X–^{113}Cd)/Hz	NMR	T/K	Solvent	Ref.
^{113}Cd(IZ-AC)$_3$	572		HMQC	300	D_2O	146
Dicadmium BcII in	343.6	15	HMQC		D_2O	147
the presence of one	372.4	31				
equivalent of						
R-thiomandelate						
Mouse		10–40	Accordion–	298	D_2O	25
metallothionein-1			HMQC			

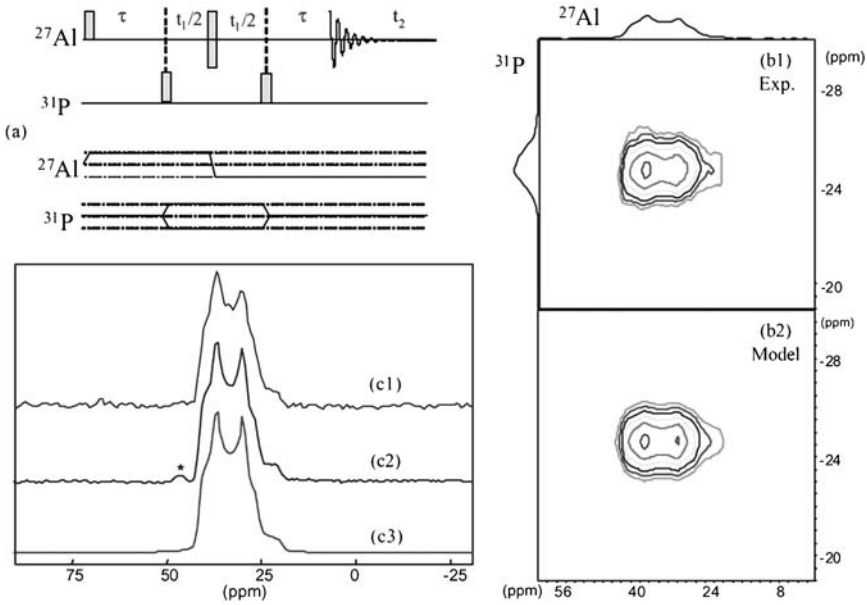

Figure 25 MAS *J*-HMQC {^{31}P}^{27}Al spectrum of $AlPO_4$ berlinite $\nu_R = 13$ kHz. (a) *J*-HMQC pulse sequence; (b, top) experimental ($d_2 = 5.5$ ms) and (b, bottom) modelled 2D *J*-HMQC spectra showing second order ^{27}Al lineshape in F2 ($\delta_{iso} = 42.9$ ppm, $C_Q = 4.07$ MHz, $\eta_Q = 0.34$); (c, top) the ^{27}Al projection of the *J*-HMQC, (c, middle) the ^{27}Al 1D MAS spectrum (* is the $n = 0$ spinning sideband of the satellite transitions), and (c, bottom) the model ideal lineshape. Reprinted from ref. 153. Copyright (2003), with permission from Elsevier.

aluminophosphates and between ^{17}O and ^{27}Al in a glass.[154] These experiments are usually run using ^{27}Al detection, reflecting the higher receptivity and faster relaxation of ^{27}Al vs. ^{31}P. (Figure 25)

4.3.2 Group 14: ^{117,119}Sn, ^{207}Pb

Of the group 14 metals tin has been intensively studied using indirect methods to detect both ^{117}Sn and ^{119}Sn, Table 22. The relative ease with which the NMR spectra of ^{117}Sn and ^{119}Sn can be measured directly means that the advantages of

Table 22 Collection of $^{1}H–^{119}Sn$ HMQC spectroscopic data[a]

Compound	^{119}Sn/ppm	X	$^{n}J(X–^{119/117}Sn)$/Hz	NMR technique	T/K	Solvent	Ref.
$HO(CH_2)_3SnCl_3$	−137[b]	^{1}H	$^{2}J = 94$, $^{3}J = 262$	1D-HMQC[c]		CD_2Cl_2	156
$HO(CH_2)_3SnCl_3$	−235[b,d]	^{1}H	$^{2}J = 107$, $^{3}J = 274$	1D-HMQC[c]		Acetone-d_6	156
$HO(CH_2)_4SnCl_3$	−172[b]	^{1}H	$^{2}J = 96$, $^{3}J = 323$	1D-HMQC[c]		CD_2Cl_2	156
$HO(CH_2)_4SnCl_3$	−252[b,d]	^{1}H	$^{2}J = 108$, $^{3}J = 341$	1D-HMQC[c]		Acetone-d_6	156
$HO(CH_2)_5SnCl_3$	−179[b,d]	^{1}H	$^{2}J = 108$, $^{3}J = 246$	1D-HMQC[c]		Acetone-d_6	156
$CH_3O(CH_2)_2O(CH_2)_3SnCl_3$	−157.4[b]	^{1}H	$^{2}J = 97$, $^{3}J = 269$	1D-gHMQC[c]		$CDCl_3$	157
$[(CH_3)_2N(CH_2)_2]_2SnF_2$	−295.5	^{1}H	$^{2}J = 105$; $^{3}J = 154$	HMQC	333	CCl_4/C_6D_6	158
$[CH_3O(CH_2)_3]_4Sn$	−4.3	^{1}H	$^{2}J = 51.2$, $^{3}J = 47.8$	1D-HMQC[c]		$CDCl_3$	155
$[CH_3O(CH_2)_3]_3SnCl$	49.0	^{1}H	$^{2}J = 60.8$, $^{3}J = 86.2$	1D-HMQC[c]		$CDCl_3$	155
$[CH_3O(CH_2)_3]_2SnCl_2$	−108.6	^{1}H	$^{2}J = 95.9$, $^{3}J = 195.8$	1D-HMQC[c]		$CDCl_3$	155
$[CH_3O(CH_2)_3]SnCl_3$	−138.5	^{1}H	$^{2}J = 104.9$, $^{3}J = 254.2$	1D-HMQC[c]		$CDCl_3$	155
$[CH_3O(CH_2)_3]SnPh_3$	−99.6	^{1}H	$^{2}J = 56.8$, $^{3}J = 65.6$	1D-HMQC[c]		$CDCl_3$	159
$[CH_3O(CH_2)_3]SnPh_2Cl$	−79.5	^{1}H	$^{2}J = 76.8$, $^{3}J = 134.5$	1D-HMQC[c]		$CDCl_3$	159
$[CH_3O(CH_2)_3]SnPhCl_2$	−83.0	^{1}H	$^{2}J = 86.6$, $^{3}J = 169.3$	1D-HMQC[c]		$CDCl_3$	159
$[CH_3O(CH_2)_3]Sn(SCNEt_2)_3$	−774.2	^{1}H	$^{2}J = 107.3$, $^{3}J = 151.8$	1D-HMQC[c]		$CDCl_3$	159
$[CH_3O(CH_2)_3]Sn(SCNEt_2)_2Cl$	−582.1	^{1}H	$^{2}J = 102.0$, $^{3}J = 153.9$	1D-HMQC[c]		$CDCl_3$	159
$[CH_3O(CH_2)_3]Sn(SCNEt_2)Cl_2$	−392.4	^{1}H	$^{2}J = 105.2$, $^{3}J = 283.1$	1D-HMQC[c]		$CDCl_3$	159
$[(CH_3)_3N(CH_2)_3]_2SnCH_3$	−10	^{1}H	$^{4}J = 1.50$, $^{6}J = 0.33$	J-HMQC		CD_2Cl_2	160
$[(CH_3)_3N(CH_2)_3]_2SnPh$	−83.5	^{1}H	$^{4}J = 1.03$, $^{6}J = 0.37$	J-HMQC		CD_2Cl_2	160
$[(CH_3)_3N(CH_2)_3]_2Sn^{t}Bu$	−20.5	^{1}H	$^{4}J < 1$, $^{6}J = 0.57$	J-HMQC		CD_2Cl_2	160
$[(CH_3)_3C(CH_2)_3]_2SnCH_3$	−2.7	^{1}H	$^{4}J = 1.87$, $^{6}J = 0.59$	J-HMQC		CD_2Cl_2	160
$[(CH_3)_3C(CH_2)_3]_2SnPh$	−72.7	^{1}H	$^{4}J = 1.36$, $^{6}J = 0.62$	J-HMQC		CD_2Cl_2	160
$(Bu_3Sn)_2CH\text{-}CH(CH_2Ph)CO_2CH_3$	4.6	^{1}H	$^{3}J = 66$; $^{3}J = 97$	HMQC		$CDCl_3$	161
	0.6						
$[(CH_3)_2N(CH_2)_2]_2SnF_2$	−295.5	^{1}H	$^{2}J = 105$; $^{3}J = 154$	HMQC	333	CCl_4/C_6D_6	158
$Sn_5(O)_2(ONep)_6$	−251	^{1}H	$^{3}J = 2 \sim 50$	HMQC		THF-d_8	162
	−257		$^{4}J = 2 \sim 50$				
$\{(BuSn)_{12}O_{14}(OH)_6\}(4\text{-}CH_3C_6H_4SO_3)_2$	−282.8 (Sn_p)[e]		101, 126	HMQC		CD_2Cl_2	163

	−461.8 (Sn_h)[e]		160, 125				
Ph_3SnH		^1H	$^1J = 1935$	1D-gHMQC[c]	298	C_6D_6	164
trans-$[Pd(H)(SnCl_3)(PCy_3)_2]$	154	^1H	$^2J = 1760$	HMQC		THF-d_8	165

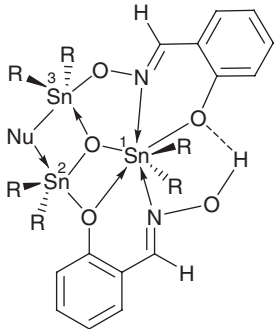

Nu=EtCH(Me)CH_2O-		^1H		HMQC	303	C_6D_6	166
R=Me	Sn(1)		$^2J = 114$				
	−460.0						
	Sn(2)		$^2J = 75$				
	−141.8		$^3J = 11, 12$				
	Sn(3)		$^2J = 75$				
	−130.6		$^3J = 13, 14$				
Nu=OH,				HMQC	270	$CDCl_3$	
R=Me	Sn(1)		$^2J = 111$				
	−458.5						
	Sn(2)		$^2J = 76$				
	−142.6		$^4J < 2$				
	Sn(3)		$^2J = 76$				
	−130.9		$^2J, ^4J < 2$				
$[(CH_3)_2N(CH_2)_2]_2SnF_2$	−292	^{19}F	$^1J = 2782$	geHMQC	303	CCl_4/C_6D_6	158
$[(^tBu_2FSn)_2O]_2$	−121.2	^{19}F	$^1J = 2340$;	geHMQC		$CDCl_3$	167

Table 22 *(Continued)*

Compound	^{119}Sn/ppm	X	^{n}J(X–$^{119/117}$Sn)/Hz	NMR technique	T/K	Solvent	Ref.
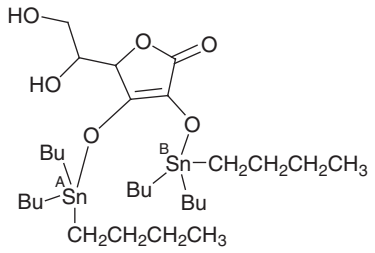	Sn(A) 152.5 Sn(B) 123.6	^{13}C	^{1}J = 840, 704 ^{1}J = 349, ^{2}J = 20 ^{3}J = 66 ^{1}J = 364, ^{2}J = 18 ^{3}J = 64	HMQC	303	$CDCl_3$	168
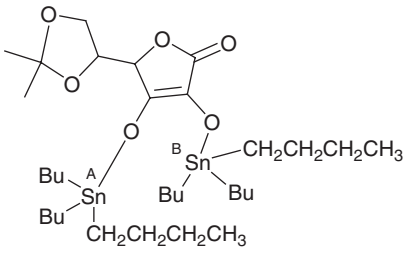	Sn(A) 152.5 Sn(B) 123.6	^{13}C	^{1}J = 350, ^{2}J = 21 ^{3}J = 68 ^{1}J = 365, ^{2}J = 18 ^{3}J = 64	HMQC		$CDCl_3$	168
Erythromycin A	−234 −294	^{1}H	107 105	HMQC			169

[a] ^{119}Sn resonances were referenced to the absolute frequency of Me_4Sn [Ξ(^{119}Sn) = 37.290665 MHz], concentration = 20 mg/mL.
[b] J(Sn,H) measured by 1D-HMQC, δ(Sn) by INEPT.
[c] Concentrated solution of 100 mg/0.5 mL.
[d] For fresh solutions in sealed tubes.
[e] Sn_P = five-coordinated tin; Sn_h = six-coordinated tin.

^{1}H–^{119}Sn HMQC in organotin chemistry are similar to those ^{1}H–^{13}C HMQC affords organic chemistry, i.e., it provides information about connectivities, rather than simply allowing determination of δ(Sn). However, in contrast to the well-documented and fairly narrow ranges of ^{13}C chemical shifts and $^{1}J(^{1}H–^{13}C)$ coupling constants, δ(Sn) spans the range = 400 to −400 ppm while $^{1}J(^{1}H–^{119}Sn)$ varies from 1,500–1,950 Hz, and $^{n}J(^{1}H–^{119}Sn)$ (n = 2–6) from 0 to 300 Hz. Furthermore, prediction of the magnitude of $^{n}J(^{1}H–^{119}Sn)$ is not straightforward with the ranges of both ^{2}J and ^{3}J varying widely and overlapping. ^{119}Sn chemical shifts show significant solvent dependence, e.g., those of trichlorostannyl alcohols, $HO(CH_2)_nSnCl_3$ (n = 3–5), differ by *ca.* 100 ppm in CD_2Cl_2 vs. d_6-acetone. This is ascribed to a $(CD_3)_2C{=}O \rightarrow Sn$ interaction in acetone, whilst in CD_2Cl_2, intramolecular coordination of the hydroxyl group to tin means that $HO(CH_2)_nSnCl_3$ (n = 3, 4) exist as 5- or 6-membered rings, which are in fast equilibrium with the open chain form in the solution.[155]

There are several reports of the direct observation of ^{73}Ge,[170] but indirect observation does not appear to have been used despite its low γ, presumably reflecting the difficulties associated with rapid quadrupolar relaxation. Similarly, there are many reports of the direct detection of ^{207}Pb, however, there has been only one report of the indirect detection of ^{207}Pb. The ^{207}Pb chemical shift is quite sensitive to the coordination environment and can be used to probe the coordination environment of Pb(II) in complex biological or environmental samples. The ^{1}H–^{207}Pb HMQC spectra of $[Pb(EDTA)]^{2-}$ and $[Pb(EDTA\text{-}N_4)]^{2+}$ (EDTA-N_4 = ethylenediamine tetraacetamide) show correlations at $\delta(^{207}Pb)$ were

Table 23 Collection of X–^{207}Pb HMQC spectroscopic data

Compound	^{207}Pb/ppm	^{n}J(X–^{207}Pb)/Hz	NMR	T/K	Solvent	Ref.
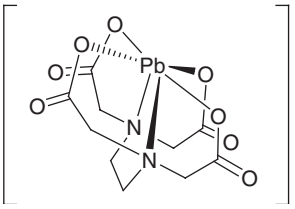	2441	$^{3}J_{PbH}$ = 17.6 ~20	HMQC	298	D_2O	171
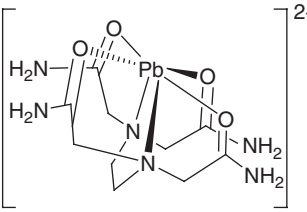	1764.3	$^{3}J_{PbH}$ = 14.3 17.0	HMQC	298	D_2O	171

Table 24 Collection of $^{1}H–^{77}Se$ HMQC spectroscopic data

Compound	^{77}Se/ppm	$^{n}J(^{1}H–^{77}Se)$/Hz	NMR	T/K	Solvent	Ref.
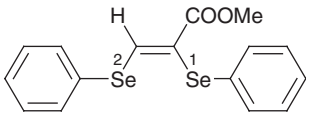	Se1 356.7 Se2 462.9	$J = 9.7$	HMQC	293	$CDCl_3$	182
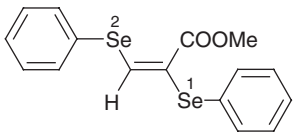	Se1 435.1 Se2 535.5	$J = 5$	HMQC	293	$CDCl_3$	182
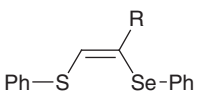		$J = 5$	HMQC		$CDCl_3$	185
R= -CH_2OH	400.3, 343.8					
-CH_2CH_2OH	403.6, 382.3[184]					
-(cyclo-$C_6H_{10}OH$)	416.9, 320.0					
-$CH_2N(CH_3)_2$	403.9, 379.7					

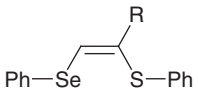		$J = 5$	2D-HMQC	$CDCl_3$	185
R= -CH_2OH	392.5				184
-CH_2CH_2OH	397.0				
-(cyclo-$C_6H_{10}OH$)	406.5				
-$CH_2N(CH_3)_2$	397.3				
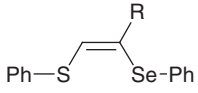		$J = 5$	2D-HMQC	$CDCl_3$	185
R= -CH_2OH	329.5				184
-CH_2CH_2OH	369.4				
-(cyclo-$C_6H_{10}OH$)	296.4				
-$CH_2N(CH_3)_2$	365.3				
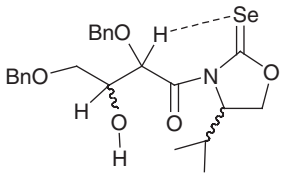	431	$^1J = 7$	2D-gsHMQC	$CDCl_3$	177
	436	$^1J = 7$	2D-gsHMQC	$CDCl_3$	177

Table 24 *(Continued)*

Compound	^{77}Se/ppm	$^{n}J(^{1}H–^{77}Se)$/Hz	NMR	T/K	Solvent	Ref.
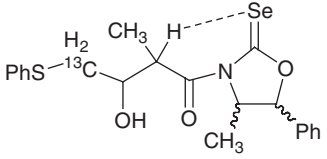						
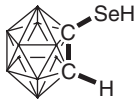	733	$^{3}J = 50$	2D-HMQC		$CDCl_3$	186
Selenized yeast (from Celecoxib/ selenium study)	64.9	$^{2}J = 20$	2D-HMQC		D_2O	176
Selenized yeast (from Clark trial)	137.8	$^{2}J = 20$	2D-HMQC		D_2O	176
l,l-selenocystine	294.3	$^{2}J = 13.7, 23.6$	1D ^{77}Se-filtered HMQC		D_2O–1 M DCl	183

2,441 and 1,764, respectively, to the methylene protons of the ligands. The observed trend in chemical shifts and the presence of correlations in the ^{207}Pb–^{1}H HMQC spectrum to the methylene protons of $[Pb(EDTA)]^{2-}$ and to both (NCH_2CH_2N) and (NCH_2CONH_2) in $[Pb(EDTA\text{-}N_4)]^{2+}$, ($^{3}J$(Pb,H) ~ 20 Hz), confirmed that ^{207}Pb is coupled through three bonds to both sets of methylene protons in $[Pb(EDTA\text{-}N_4)]^{2+}$, i.e., in aqueous solution at physiological pH, $Pb(EDTA\text{-}N_2)$ is O-bound and neutral, and $[Pb(EDTA\text{-}N)_4]^{2+}$ is O-bound and carries a +2 charge.[171] (Table 23)

4.3.3 Group 15: ^{77}Se

The relative receptivities of ^{77}Se and ^{125}Te (3.15 and 13.4 vs. ^{13}C) are moderate and there is a good body of NMR data for both nuclei that has been obtained by direct NMR methods.[172] Although indirect detection greatly enhances the sensitivity of both ^{77}Se and ^{125}Te,[173] there has been only a small number of studies reporting NMR data obtained by HMQC or HSQC methods for organoselenium and tellurium compounds, Table 24.[174–181] ^{1}H–^{77}Se HMQC NMR spectroscopy allows reliable measurement of the chemical shifts of bis-selenium-substituted alkenes allowing *Z*- and *E*-isomers to be readily distinguished due to the large chemical shift difference for ^{77}Se.[182] Although the $J(^{1}H,^{77}Se)$ coupling constants are generally measured from 1D NMR, they can also be determined using a 1D ^{77}Se-filtered HMQC experiment with optimized re- and defocusing delays and selective ^{1}H-decoupling.[183] Gradient-selected ^{1}H–^{77}Se HMQC NMR spectroscopy has also been used to reveal an unusual hydrogen bond through C–H · · · Se in aldols of chiral *N*-acyl selones, for which a coupling constant of $^{1}J_{HSe} = 7$ Hz was determined.[177]

5. CONCLUSIONS

A wide range of 2D HXQC methods for the indirect detection of the NMR spectrum of metal nuclei has been developed. The spin systems likely to be encountered in HXQC NMR studies of metal coordination and cluster compounds have been analysed and appropriate modification of the standard experiments discussed. HXQC spectroscopy has begun to be implemented in the solid state, and to quadrupolar nuclei despite the additional challenges imposed by fast transverse relaxation. Suitable hardware, including inverse, low range broadband, triple resonance probes, is now available from some equipment manufacturers as standard items. To date, attention has focussed on detection of ^{103}Rh and ^{195}Pt but there seems good reason to expect the number of studies of other nuclei to increase rapidly.

ABBREVIATIONS

σ_d	Diamagnetic contribution to shielding
σ_p	Paramagnetic contribution to shielding

ΔE	Average ligand field splitting
CP	Cross polarization
F1	Indirectly observed dimension
F2	Directly observed dimension
ge	Gradient enhanced
gs	Gradient selected
HETCOR	Heteronuclear correlation spectroscopy
HMBC	Heteronuclear multiple bond correlation spectroscopy
HMQC	Heteronuclear multiple quantum correlation spectroscopy
HSQC	Heteronuclear single-quantum correlation spectroscopy
HXQC	Any of the above
INEPT	Insensitive nucleus enhancement by polarization transfer
MAS	Magic angle spinning
T_1	Spin–lattice relaxation time constant
T_2	Spin–spin relaxation time constant

Ligands

1,2-en	1,2 ethylenediamine
1,3-pn	1,3-propylenediamine
1-MeTy	1-methylthymine
ABK	acetylacetonato-bis(2,6-dimethylphenyl)ketimine anion
abpy	2,2′-azobispyridine
abpy	2,2′-azobispyridine
acac	acetylacetonate
BIAN	bis(imino)acenaphthene
Biphemp	(6,6′-dimethylbiphenyl-2,2′-diyl)bis(diphenylphosphine)
bipy	2,2′-bipyridyl
bipyO_2	*N*,*N*′,2,2′-dipyridine dioxide
Bpym	2,2′-bipyrimidine
COD	cyclooctadiene
Cp	cyclopentadienyl
Cp*	pentamethylcyclopentadienyl
d2pype	1,2-bis(di-2-pyridylphosphino)ethane
d3pype	1,2-bis(di-3-pyridylphosphino)ethane
d3pype	1,2-bis(di-3-pyridylphosphino)ethane
d4pype	1,2-bis(di-4-pyridylphosphino)ethane
DAB	glyoxalbis(isopropylimine)
dmeda	1,2,*N*,*N*′-dimethylethylenediamine
dppe	1,2-bis(diphenylphosphino) ethane
dppef	1,2-bis(diperfluorophenylphosphino)ethane
dppeO_2	1,2-bis(diphenylphosphane oxide)ethane
dppm	1,2-bis(diphenylphosphino) methane
dppmO_2	1,1-bis(diphenylphosphane oxide)methane
dppp	1,2-bis(diphenylphosphino) propane
Hetgua	9-ethylguanine

Ind	indenyl
L^1-S,O	*N*-methyl-*N*-ethyl-*N*′-(2,2-dimethylpropanoyl)thiourea
L^2-S,O	*N*-methyl-*N*-(*n*-butyl)-*N*′-benzoylthiourea
L^2-S,O	*N*-methyl-*N*-(*n*-butyl)-*N*′-benzoylthiourea
mcyt	1-methylcytosine
Mes	mesityl
MTPA	$[(PhC(OMe)(CF_3)CO_2]^-$
nbd	norbornadiene
ONep	OCH_2CMe_3
PBz_3	tricyclobenzylphosphine
PCy_3	tricyclohexylphosphine
PNP	bis(triphenylphosphoranyliden)ammonium
PPFPz{3-^{t}Bu}	3-*tert*-butyl-1-{1-{R}-[2-(S_p)-diphenylphosphanylferrocenyl]ethyl}-1*H*-pyrazole
py	pyridine
TFPO	chloro[dicyclohexyl(tetrahydrofurfuryl)phosphine-P][dicyclohexyl-(tetrahydrofurfuryl)phosphine-P,O]-*cis*-dihydridorhodium(III)
tmeda	*N*,*N*,*N*′,*N*′-tetramethylethylenediamine
tolBINAP	(R)-2,2′-bis(di-4-tolylphosphino)-1,10-binaphthyl
Tp^{Me2}	hydrotris(3,5-dimethylpyrazolyl)borato
$TROPP^{Ph}$	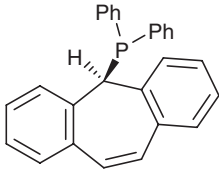
trpy	2,2′::6′,2″-terpyridine

ACKNOWLEDGEMENTS

The authors wish to thank many colleagues for their contributions to the work, particularly Dr Ivan Podkorytov for his invaluable help with the analysis of multiple metal spin systems, and the groups of Prof Brian Heaton and Prof Sergey Tunik for the provision of many samples. Prof Simon Duckett is thanked for the information on *para*-hydrogen enhanced HMQC and Dr Yaroslav Khimyak for helpful suggestions during the preparation of the manuscript. The financial support of the EPSRC and INTAS is gratefully acknowledged.

REFERENCES

1. P. S. Pregosin, *Transition Metal Nuclear Magnetic Resonance*, Elsevier, Amsterdam, 1991.
2. J. Mason, *Chem. Rev.*, 1987, **87**, 1299–1312.
3. F. Lopez-Ortiz and R. J. Carbajo, *Curr. Org. Chem.*, 1998, **2**, 97–130.
4. W. von Philipsborn, *Chem. Soc. Rev.*, 1999, **28**, 95–105.
5. W. Vonphilipsborn, *Pure Appl. Chem.*, 1986, **58**, 513–528.

6. B. E. Mann, in: *NMR of Newly Accessible Nuclei*, P. Laszlo, ed., Academic Press, New York, 1983, p. 302.
7. R. Benn and A. Rufinska, *Angew. Chem. Int. Ed. Engl.*, 1986, **25**, 861–881.
8. G. A. Kirakosyan, *Koord. Khim.*, 1993, **19**, 507–525.
9. B. Wrackmeyer, *Chem. Unser. Zeit*, 1994, **28**, 309–320.
10. L. Muller, *J. Am. Chem. Soc.*, 1979, **101**, 4481–4484.
11. A. Bax and S. Subramanian, *J. Magn. Reson.*, 1986, **67**, 565–569.
12. A. Bax, R. H. Griffey and B. L. Hawkins, *J. Magn. Reson.*, 1983, **55**, 301–315.
13. G. Bodenhausen and D. J. Ruben, *Chem. Phys. Lett.*, 1980, **69**, 185–189.
14. J. M. Ernsting, S. Gaemers and C. J. Elsevier, *Magn. Reson. Chem.*, 2004, **42**, 721–736.
15. B. Wrackmeyer and M. Herberhold, *Struct. Chem.*, 2006, **17**, 79–83.
16. M. Buhl, S. Grigoleit, H. Kabrede and F. T. Mauschick, *Chem. Eur. J.*, 2005, **12**, 477–488.
17. J. Autschbach and S. H. Zheng, *Magn. Reson. Chem.*, 2006, **44**, 989–1007.
18. A. Bagno, G. Casella and G. Saielli, *J. Chem. Theory Comp.*, 2006, **2**, 37–46.
19. H. P. Hratchian and M. C. Milletti, *J. Mol. Struct. : THEOCHEM*, 2005, **724**, 45–52.
20. L. Carlton, *Magn. Reson. Chem.*, 2004, **42**, 760–768.
21. R. K. Harris, E. D. Becker, S. M. C. De Menezes, R. Goodfellow and P. Granger, *Pure Appl. Chem.*, 2001, **73**, 1795–1818.
22. S. J. Anderson, J. R. Barnes, P. L. Goggin and R. J. Goodfellow, *J. Chem. Res., M*, 1978, 3601.
23. P. L. Goggin, Goodfell. Rj and F. J. S. Reed, *J. Chem. Soc., Dalton Trans.*, 1974, 576–585.
24. D. Gudat, *Annu. Rep. NMR Spectrosc.*, Vol 38, 1999, **38**, 139–202.
25. K. Zangger and I. M. Armitage, *Magn. Reson. Chem.*, 2000, **38**, 452–458.
26. W. F. Reynolds and R. G. Enriquez, *Magn. Reson. Chem.*, 2001, **39**, 531–538.
27. J. R. Garbow, D. P. Weitekamp and A. Pines, *Chem. Phys. Lett.*, 1982, **93**, 504–509.
28. J. M. Nuzillard, G. Gasmi and J. M. Bernassau, *J. Magn. Reson., Ser. A*, 1993, **104**, 83–87.
29. D. Gudat, *Magn. Reson. Chem.*, 2003, **41**, 253–259.
30. T. Saito, R. E. Medsker, H. J. Harwood and P. L. Rinaldi, *J. Magn. Reson., Ser. A*, 1996, **120**, 125–128.
31. J. P. Marino, H. Schwalbe, C. Anklin, W. Bermel, D. M. Crothers and C. Griesinger, *J. Am. Chem. Soc.*, 1994, **116**, 6472–6473.
32. S. Berger and P. Bast, *Magn. Reson. Chem.*, 1993, **31**, 1021–1023.
33. L. E. Kay, M. Ikura, R. Tschudin and A. Bax, *J. Magn. Reson.*, 1990, **89**, 496–514.
34. L. Orian, A. Bisello, S. Santi, A. Ceccon and G. Saielli, *Chem. Eur. J.*, 2004, **10**, 4029–4040.
35. E. Esponda, C. Adams, F. Burgos, I. Chavez, J. M. Manriquez, F. Delpech, A. Castel, H. Gornitzka, M. Riviere-Baudet and P. Riviere, *J. Organomet. Chem.*, 2006, **691**, 3011–3017.
36. S. Santi, L. Orian, C. Durante, A. Bisello, F. Benetollo, L. Crociani, P. Ganis and A. Ceccon, *Chem. Eur. J.*, 2007, **13**, 1955–1968.
37. D. Nanz and W. Vonphilipsborn, *J. Magn. Reson.*, 1991, **92**, 560–571.
38. B. T. Heaton, J. A. Iggo, I. S. Podkorytov, D. J. Smawfield and S. P. Tunik, in: *Metal Clusters in Chemistry,* P. Braunstein, L. Oro and P. Raithby, eds., Wiley-VCH, Weinheim, 1999, pp. 960–1000.
39. H. Ruegger and D. Moskau, *Magn. Reson. Chem.*, 1991, **29**, S11–S15.
40. B. T. Heaton, J. A. Iggo, I. S. Podkorytov, D. J. Smawfield, S. P. Tunik and R. Whyman, *J. Chem. Soc., Dalton Trans.*, 1999, 1917–1919.
41. D. Magiera, W. Baumann, I. S. Podkorytov, J. Omelanczuk and H. Duddeck, *Eur. J. Inorg. Chem.*, 2002, 253–3257.
42. B. T. Heaton, J. A. Iggo, I. S. Podkorytov and S. P. Tunik, *Magn. Reson. Chem.*, 2004, **42**, 769–775.
43. D. H. Farrar, E. V. Grachova, A. Lough, C. Patirana, A. J. Poe and S. P. Tunik, *J. Chem. Soc., Dalton Trans.*, 2001, 2015–2019.
44. D. Blazina, S. B. Duckett, J. P. Dunne and C. Godard, *Dalton Trans.*, 2004, 2601–2609.
45. M. G. Pravica and D. P. Weitekamp, *Chem. Phys. Lett.*, 1988, **145**, 255–258.
46. C. R. Bowers and D. P. Weitekamp, *J. Am. Chem. Soc.*, 1987, **109**, 5541–5542.
47. T. C. Eisenschmid, R. U. Kirss, P. P. Deutsch, S. I. Hommeltoft, R. Eisenberg, J. Bargon, R. G. Lawler and A. L. Balch, *J. Am. Chem. Soc.*, 1987, **109**, 8089–8091.
48. P. D. Morran, S. A. Colebrooke, S. B. Duckett, J. A. B. Lohman and R. Eisenberg, *J. Chem. Soc., Dalton Trans.*, 1998, 3363–3365.

49. P. D. Morran, S. B. Duckett, P. R. Howe, J. E. McGrady, S. A. Colebrooke, R. Eisenberg, M. G. Partridge and J. A. B. Lohman, *J. Chem. Soc., Dalton Trans*., 1999, 3949–3960.
50. B. A. Messerle, C. J. Sleigh, M. G. Partridge and S. B. Duckett, *J. Chem. Soc., Dalton Trans*., 1999, 1429–1435.
51. R. R. Zhou, J. A. Aguilar, A. Charlton, S. B. Duckett, P. I. P. Elliott and R. Kandiah, *Dalton Trans*., 2005, 3773–3779.
52. J. P. Amoureux, J. Trebosc, J. Wiench and M. Pruski, *J. Magn. Reson*., 2007, **184**, 1–14.
53. D. Gudat, U. Fischbeck, F. Tabellion, M. Billen and F. Preuss, *Magn. Reson. Chem*., 2002, **40**, 139–146.
54. B. S. Xiang, M. D. Winemiller, T. F. Briggs, D. J. Fuller and D. B. Collum, *Magn. Reson. Chem*., 2001, **39**, 137–140.
55. D. Nanz and W. Vonphilipsborn, *J. Magn. Reson*., 1992, **100**, 243–255.
56. D. P. Burum and A. Bielecki, *J. Magn. Reson*., 1991, **94**, 645–652.
57. P. Caravatti, G. Bodenhausen and R. R. Ernst, *Chem. Phys. Lett*., 1982, **89**, 363–367.
58. B. J. vanRossum, H. Forster and H. J. M. deGroot, *J. Magn. Reson*., 1997, **124**, 516–519.
59. A. J. Vega, *J. Magn. Reson*., 1992, **96**, 50–68.
60. L. Frydman and J. S. Harwood, *J. Am. Chem. Soc*., 1995, **117**, 5367–5368.
61. H. M. Kao and G. P. Grey, *J. Magn. Reson*., 1998, **133**, 313–323.
62. H. E. Mons, H. Gunther and A. Maercker, *Chem. Ber*., 1993, **126**, 2747–2751.
63. M. A. Jacobson, I. Keresztes and P. G. Williard, *J. Am. Chem. Soc*., 2005, **127**, 4965–4975.
64. I. Fernandez and F. L. Ortiz, *Chem. Commun*., 2004, 1142–1143.
65. H. Gunther, *J. Braz. Chem. Soc*., 1999, **10**, 241–262.
66. W. Bauer, *J. Am. Chem. Soc*., 1996, **118**, 5450–5455.
67. X. F. Sun, M. D. Winemiller, B. S. Xiang and D. B. Collum, *J. Am. Chem. Soc*., 2001, **123**, 8039–8046.
68. T. F. Briggs, M. D. Winemiller, D. B. Collum, R. L. Parsons, A. H. Davulcu, G. D. Harris, J. M. Fortunak and P. N. Confalone, *J. Am. Chem. Soc*., 2004, **126**, 5427–5435.
69. R. L. Parsons, J. M. Fortunak, R. L. Dorow, G. D. Harris, G. S. Kauffman, W. A. Nugent, M. D. Winemiller, T. F. Briggs, B. S. Xiang and D. B. Collum, *J. Am. Chem. Soc*., 2001, **123**, 9135–9143.
70. A. Thompson, E. G. Corley, M. F. Huntington, E. J. J. Grabowski, J. F. Remenar and D. B. Collum, *J. Am. Chem. Soc*., 1998, **120**, 2028–2038.
71. J. H. Gilchrist, A. T. Harrison, D. J. Fuller and D. B. Collum, *Magn. Reson. Chem*., 1992, **30**, 855–859.
72. B. Bohler and H. Gunther, *Tetrahedron Lett*., 1996, **37**, 8723–8724.
73. G. R. Gomez, I. Fernandez, F. L. Ortiz, R. D. Price, M. G. Davidson, M. F. Mahon and J. A. K. Howard, *Organometallics*, 2007, **26**, 514–518.
74. R. D. Price, I. Fernandez, G. R. Gomez, F. L. Ortiz, M. G. Davidson, J. A. Cowan and J. A. K. Howard, *Organometallics*, 2004, **23**, 5934–5938.
75. D. L. Bryce and R. E. Wasylishen, *Phys. Chem. Chem. Phys*., 2001, **3**, 5154–5157.
76. K. J. Ooms, K. W. Feindel, V. V. Terskikh and R. E. Wasylishen, *Inorg. Chem*., 2006, **45**, 8492–8499.
77. M. Buhl, G. Hopp, W. von Philipsborn, S. Beck, M. H. Prosenc, U. Rief and H. H. Brintzinger, *Organometallics*, 1996, **15**, 778–785.
78. M. A. Fedotov and R. I. Maksimovskaya, *J. Struct. Chem*., 2006, **47**, 952–978.
79. S. Gaemers, J. Groenevelt and C. J. Elsevier, *Eur. J. Inorg. Chem*., 2001, 829–835.
80. R. J. Carbajo, L. Zhang and F. Lopez-Ortiz, *Magn. Reson. Chem*., 1998, **36**, 807–814.
81. L. Zhang, M. P. Gamasa, J. Gimeno, M. F. C. G. da Silva, A. J. L. Pombeiro, C. Graiff, M. Lanfranchi and A. Tiripicchio, *Eur. J. Inorg. Chem*., 2000, 1707–1715.
82. G. A. Carriedo, F. J. G. Alonso, J. L. Garcia, R. J. Carbajo and F. L. Ortiz, *Eur. J. Inorg. Chem*, 1999, 1015–1020.
83. Y. G. Chen, J. Gong and L. Y. Qu, *Coord. Chem. Rev*., 2004, **248**, 245–260.
84. J. Buddrus and J. Lambert, *Magn. Reson. Chem*., 2002, **40**, 3–23.
85. A. E. Enriquez, P. S. White and J. L. Templeton, *J. Am. Chem. Soc*., 2001, **123**, 4992–5002.
86. B. Wrackmeyer, E. V. Klimkina, W. Milius, M. Siebenbürger, O. L. Tok and M. Herberhold, *Eur. J. Inorg. Chem*., 2007, **2007**, 103–109.
87. B. Wrackmeyer, O. L. Tok, A. Ayazi, H. E. Maisel and M. Herberhold, *Magn. Reson. Chem*., 2004, **42**, 827–830.
88. B. Wrackmeyer, O. L. Tok and A. A. Koridze, *Magn. Reson. Chem*., 2004, **42**, 750–755.

89. M. J. Stchedroff, S. Aime, R. Gobetto, L. Salassa and E. Nordlander, *Magn. Reson. Chem.*, 2002, **40**, 107–113.
90. N. K. K. Kazemifar, M. J. Stchedroff, M. A. Mottalib, S. Selva, M. Monari and E. Nordlander, *Eur. J. Inorg. Chem.*, 2006, 2058–2068.
91. M. J. Stchedroff, V. Moberg, E. Rodriguez, A. E. Aliev, J. Bottcher, J. W. Steed, E. Nordlander, M. Monari and A. J. Deeming, *Inorg. Chim. Acta*, 2006, **359**, 926–937.
92. A. G. Bell, W. Kozminski, A. Linden and W. von Philipsborn, *Organometallics*, 1996, **15**, 3124–3135.
93. P. Granger, J. Hirschinger, K. Elbayed, C. Sizun, P. Kempgens, J. Raya, J. Rose and P. Braunstein, *J. Chim. Phys. Phys.-Chim. Biol.*, 1999, **96**, 1479–1485.
94. P. Kempgens, K. Elbayed, J. Raya, P. Granger, J. Rose and P. Braunstein, *Inorg. Chem.*, 2006, **45**, 3378–3383.
95. M. J. Chen, R. J. Klingler, J. W. Rathke and K. W. Kramarz, *Organometallics*, 2004, **23**, 2701–2707.
96. J. L. Cunningham and S. B. Duckett, *Dalton Trans*, 2005, 744–759.
97. B. C. de Pater, E. J. Zijp, H. W. Fruhauf, J. M. Ernsting, C. J. Elsevier and K. Vrieze, *Organometallics*, 2004, **23**, 269–279.
98. J. G. Donkervoort, M. Buhl, J. M. Ernsting and C. J. Elsevier, *Eur. J. Inorg. Chem*, 1999, 27–33.
99. W. J. Hoogervorst, K. Goubitz, J. Fraanje, M. Lutz, A. L. Spek, J. M. Ernsting and C. J. Elsevier, *Organometallics*, 2004, **23**, 4550–4563.
100. P. G. A. Kumar, P. S. Pregosin, T. M. Schmid and G. Consiglio, *Magn. Reson. Chem.*, 2004, **42**, 795–800.
101. I. V. Komarov, A. Monsees, A. Spannenberg, W. Baumann, U. Schmidt, C. Fischer and A. Borner, *Eur. J. Org. Chem*, 2003, 138–150.
102. J. Liedtke, H. Ruegger, S. Loss and H. Grutzmacher, *Angew. Chem., Int. Ed.*, 2000, **39**, 2478–2481.
103. J. Holz, O. Zayas, H. J. Jiao, W. Baumann, A. Spannenberg, A. Monsees, T. H. Riermeier, J. Almena, R. Kadyrov and A. Borner, *Chem. Eur. J.*, 2006, **12**, 5001–5013.
104. E. Kossoy, M. A. Iron, B. Rybtchinski, Y. Ben-David, L. J. W. Shimon, L. Konstantinovski, J. M. L. Martin and D. Milstein, *Chem. Eur. J.*, 2005, **11**, 2319–2326.
105. E. V. Grachova, B. T. Heaton, J. A. Iggo, I. S. Podkorytov, D. J. Smawfield, S. P. Tunik and R. Whyman, *J. Chem. Soc., Dalton Trans.*, 2001, 3303–3311.
106. D. H. Farrar, E. V. Grachova, M. Haukka, B. T. Heaton, J. A. Iggo, T. A. Pakkanen, I. S. Podkorytov and S. P. Tunik, *Inorg. Chim. Acta*, 2003, **354**, 11–20.
107. E. V. Grachova, M. Haukka, B. T. Heaton, E. Nordlander, T. A. Pakkanen, I. S. Podkorytov and S. P. Tunik, *Dalton Trans*, 2003, 2468–2473.
108. J. S. Z. Sabounchei, B. T. Heaton, J. A. Iggo, C. Jacob and I. S. Podkorytov, *J. Cluster Sci.*, 2001, **12**, 339–348.
109. F. M. Dolgushin, E. V. Grachova, B. T. Heaton, J. A. Iggo, I. O. Koshevoy, I. S. Podkorytov, D. J. Smawfield, S. P. Tunik, R. Whyman and A. I. Yanovskii, *J. Chem. Soc., Dalton Trans.*, 1999, 1609–1614.
110. I. O. Koshevoy, E. V. Grachova, S. P. Tunik, M. Haukka, T. A. Pakkanen, B. T. Heaton, J. A. Iggo and I. S. Podkorytov, *Dalton Trans*, 2004, 3893–3899.
111. A. Ferrari, M. Merlin, S. Sostero, H. Ruegger and L. M. Venanzi, *Helv. Chim. Acta*, 1999, **82**, 1454–1457.
112. M. Buhl, W. Baumann, R. Kadyrov and A. Borner, *Helv. Chim. Acta*, 1999, **82**, 811–820.
113. L. Carlton, *Magn. Reson. Chem.*, 1997, **35**, 153–158.
114. M. Herberhold, T. Daniel, D. Daschner, W. Milius and B. Wrackmeyer, *J. Organomet. Chem.*, 1999, **585**, 234–240.
115. M. Herberhold, G. X. Jin, H. Yan, W. Milius and B. Wrackmeyer, *J. Organomet. Chem.*, 1999, **587**, 252–257.
116. F. R. Bregman, J. M. Ernsting, F. Muller, M. D. K. Boele, L. A. van der Veen and C. J. Elsevier, *J. Organomet. Chem.*, 1999, **592**, 306–311.
117. L. Carlton, R. Weber and D. C. Levendis, *Inorg. Chem.*, 1998, **37**, 1264–1271.
118. E. Lindner, K. Gierling, B. Keppeler and H. A. Mayer, *Organometallics*, 1997, **16**, 3531–3535.
119. M. Soleilhavoup, L. Viau, G. Commenges, C. Lepetit and R. Chauvin, *Eur. J. Inorg. Chem*, 2003, 207–212.

120. S. C. van der Slot, P. C. J. Kamer, P. van Leeuwen, J. A. Iggo and B. T. Heaton, *Organometallics*, 2001, **20**, 430–441.
121. G. C. Dol, S. Gaemers, M. Hietikko, P. C. J. Kamer, P. van Leeuwen and R. J. M. Nolte, *Eur. J. Inorg. Chem*, 1998, 1975–1985.
122. H. Noss, W. Baumann, R. Kempe, T. Irrgang and A. Schulz, *Inorg. Chim. Acta*, 2003, **345**, 130–136.
123. T. J. Bastow and G. W. West, *J. Phys.: Condens. Matter*, 2003, **15**, 8389–8406.
124. K. D. Behringer and J. Blumel, *Magn. Reson. Chem*., 1995, **33**, 729–733.
125. M. A. Fedotov and V. A. Likholobov, *Bull. Acad. Sci. USSR Div. Chem. Sci*., 1984, **33** 1751–1751
126. D. Gudat, A. Dogan, W. Kaim and A. Klein, *Magn. Reson. Chem*., 2004, **42**, 781–787.
127. N. V. Kirij, W. Tyrra, D. Naumann, I. Pantenburg and Y. L. Yagupolskii, *Z. Naturforsch*., 2006, **632**, 284–288.
128. W. J. Hoogervorst, A. L. Koster, M. Lutz, A. L. Spek and C. J. Elsevier, *Organometallics*, 2004, **23**, 1161–1164.
129. P. Leoni, F. Marchetti, L. Marchetti and V. Passarelli, *Chem. Commun*, 2004, 2346–2347.
130. D. Gudat, V. K. Jain, A. Klein, T. Schurr and S. Zalis, *Eur. J. Inorg. Chem*, 2005, 4056–4063.
131. A. Klein, T. Schurr, A. X. Knodler, D. Gudat, K. W. Klinkhammer, V. K. Jain, S. Zalis and W. Kaim, *Organometallics*, 2005, **24**, 4125–4131.
132. D. Argyropoulos, E. Hoffmann, S. Mtongana and K. R. Koch, *Magn. Reson. Chem*., 2003, **41**, 102–106.
133. N. A. Bokach, S. I. Selivanov, V. Y. Kukushkin, M. Haukka, M. F. C. G. da Silva and A. J. L. Pombeiro, *Eur. J. Inorg. Chem*, 2001, 2805–2809.
134. L. Hintermann, F. Lang, P. Maire and A. Togni, *Eur. J. Inorg. Chem*, 2006, 1397–1412.
135. M. Jang, S. B. Duckett and R. Eisenberg, *Organometallics*, 1996, **15**, 2863–2865.
136. B. Longato, L. Pasquato, A. Mucci and L. Schenetti, *Eur. J. Inorg. Chem*, 2003, 128–137.
137. S. Cosar, M. B. L. Janik, M. Flock, E. Freisinger, E. Farkas and B. Lippert, *J. Chem. Soc., Dalton Trans*., 1999, 2329–2336.
138. G. Kampf, M. Willermann, E. Zangrando, L. Randaccio and B. Lippert, *Chem. Commun*, 2001, 747–748.
139. B. Longato, G. Bandoli, A. Mucci and L. Schenetti, *Eur. J. Inorg. Chem*, 2001, 3021–3029.
140. V. P. Ananikov, S. A. Mitchenko and I. P. Beletskaya, *J. Organomet. Chem*., 2000, **604**, 290–295.
141. V. P. Ananikov, S. A. Mitchenko and I. P. Beletskaya, *J. Organomet. Chem*., 2001, **636**, 175–181.
142. S. J. Berners-Price, R. J. Bowen, P. J. Harvey, P. C. Healy and G. A. Koutsantonis, *J. Chem. Soc., Dalton Trans*., 1998, 1743–1750.
143. J. Thomaier, S. Boulmaaz, H. Schonberg, H. Ruegger, A. Currao, H. Grutzmacher, H. Hillebrecht and H. Pritzkow, *New J. Chem*., 1998, **22**, 947–958.
144. W. Tyrra, *Heteroat. Chem*., 2002, **13**, 561–566.
145. I. Krummenacher, H. Ruegger and F. Breher, *Dalton Trans*, 2006, 1073–1081.
146. X. Q. Li, K. Suzuki, K. Kanaori, K. Tajima, A. Kashiwada, H. Hiroaki, D. Kohda and T. Tanaka, *Protein Sci*., 2000, **9**, 1327–1333.
147. C. Damblon, M. Jensen, A. Ababou, I. Barsukov, C. Papamicael, C. J. Schofield, L. Olsen, R. Bauer and G. C. K. Roberts, *J. Biol. Chem*., 2003, **278**, 29240–29251.
148. M. Deschamps and D. Massiot, *J. Magn. Reson*., 2007, **184**, 15–19.
149. C. A. Fyfe, J. L. Bretherton, J. Skibsted, M. H. Zahedi-Niaki and S. Kalliaguine, *Recent Advances in the Science and Technology of Zeolites and Related Materials, Pts A-C*, 2004, **154**, 1238–1245.
150. C. A. Fyfe, H. M. Z. Altenschildesche, K. C. Wong-Moon, H. Grondey and J. M. Chezeau, *Solid State Nucl. Magn. Reson*., 1997, **9**, 97–106.
151. V. Montouillout, C. M. Morais, A. Douy, F. Fayon and D. Massiot, *Magn. Reson. Chem*., 2006, **44**, 770–775.
152. K. Damodaran, J. W. Wiench, S. M. C. de Menezes, Y. L. Lam, J. Trebosc, J. P. Amoureux and M. Pruski, *Microporous Mesoporous Mater.*, 2006, **95**, 296–305.
153. D. Massiot, F. Fayon, B. Alonso, J. Trebosc and J. P. Amoureux, *J. Magn. Reson*., 2003, **164**, 160–164.
154. D. Iuga, C. Morais, Z. H. Gan, D. R. Neuville, L. Cormier and D. Massiot, *J. Am. Chem. Soc*., 2005, **127**, 11540–11541.
155. T. Lebl, A. Smicka, J. Brus and C. Bruhn, *Eur. J. Inorg. Chem*, 2003, 143–148.

156. M. Biesemans, R. Willem, S. Damoun, P. Geerlings, E. R. T. Tiekink, P. Jaumier, M. Lahcini and B. Jousseaume, *Organometallics*, 1998, **17**, 90–97.
157. J. Susperregui, M. Bayle, J. M. Leger, G. Deleris, M. Biesemans, R. Willem, M. Kemmer and M. Gielen, *J. Organomet. Chem.*, 1997, **546**, 559–565.
158. N. Pieper, C. KlausMrestani, M. Schurmann, K. Jurkschat, M. Biesemans, I. Verbruggen, J. C. Martins and R. Willem, *Organometallics*, 1997, **16**, 1043–1052.
159. T. Lebl, P. Zoufala and C. Bruhn, *Eur. J. Inorg. Chem*, 2005, 2536–2544.
160. M. Biesemans, J. C. Martins, K. Jurkschat, N. Pieper, S. Seemeyer and R. Willem, *Magn. Reson. Chem.*, 2004, **42**, 776–780.
161. J. C. Meurice, J. G. Duboudin, M. Ratier, M. Petraud, R. Willem and M. Biesemans, *Organometallics*, 1999, **18**, 1699–1705.
162. T. J. Boyle, T. M. Alam, M. A. Rodriguez and C. A. Zechmann, *Inorg. Chem.*, 2002, **41**, 2574–2582.
163. C. Eychenne-Baron, F. Ribot, N. Steunou, C. Sanchez, F. Fayon, M. Biesemans, J. C. Martins and R. Willem, *Organometallics*, 2000, **19**, 1940–1949.
164. J. C. Martins, F. Kayser, P. Verheyden, M. Gielen, R. Willem and M. Biesemans, *J. Magn. Reson.*, 1997, **124**, 218–222.
165. D. H. Nguyen, Y. Coppel, M. Urrutigoity and P. Kalck, *J. Organomet. Chem.*, 2005, **690**, 2947–2951.
166. A. Meddour, A. Bouhdid, M. Gielen, M. Biesemans, F. Mercier, E. R. T. Tiekink and R. Willem, *Eur. J. Inorg. Chem.*, 1998, 1467–1472.
167. J. Beckmann, M. Biesemans, K. Hassler, K. Jurkschat, J. C. Martins, M. Schurmann and R. Willem, *Inorg. Chem.*, 1998, **37**, 4891–4897.
168. A. Lycka, D. Micak, J. Holecek, M. Biesemans, J. C. Martins and R. Willem, *Organometallics*, 2000, **19**, 703–706.
169. J. C. Martins, R. Willem, F. A. G. Mercier, M. Gielen and M. Biesemans, *J. Am. Chem. Soc.*, 1999, **121**, 3284–3291.
170. Y. Takeuchi and T. Takayama, *Annu. Rep. NMR Spectrosc., Vol 54*, 2005, **54**, 155–200.
171. E. S. Claudio, M. A. ter Horst, C. E. Forde, C. L. Stern, M. K. Zart and H. A. Godwin, *Inorg. Chem.*, 2000, **39**, 1391–1397.
172. H. Duddeck, *Adv. Solid State NMR Studies Mater. Polym.: A Special Volume Dedicated to Isao Ando*, 2004, **52**, 105–166.
173. R. S. Glass, *Phosphorus, Sulfur, Silicon Relat. Elem.*, 1998, **136**, 159–174.
174. H. Poleschner and K. Seppelt, *Magn. Reson. Chem.*, 2002, **40**, 777–780.
175. M. Koketsu, K. Mizutani, T. Ogawa, A. Takahashi and H. Ishihara, *J. Org. Chem.*, 2004, **69**, 8938–8941.
176. E. Block, R. S. Glass, N. E. Jacobsen, S. Johnson, C. Kahakachchi, R. KaminskI, A. Skowronska, H. T. Boakye, J. F. Tyson and P. C. Uden, *J. Agric. Food Chem.*, 2004, **52**, 3761–3771.
177. R. Michalczyk, J. G. Schmidt, E. Moody, Z. Z. Li, R. L. Wu, R. B. Dunlap, J. D. Odom and L. A. Silks, *Angew. Chem. Int. Ed.*, 2000, **39**, 3067–3070.
178. R. Marek, L. Kralik and V. Sklenar, *Tetrahedron Lett.*, 1997, **38**, 665–668.
179. R. L. Wu, G. Hernandez, J. D. Odom, R. B. Dunlap and L. A. Silks, *Chem. Commun.*, 1996, 1125–1126.
180. B. Wrackmeyer, R. Koster and G. Seidel, *Magn. Reson. Chem.*, 1995, **33**, 493–496.
181. T. B. Schroeder, C. Job, M. F. Brown and R. S. Glass, *Magn. Reson. Chem.*, 1995, **33**, 191–195.
182. V. P. Ananikov and I. P. Beletskaya, *Russ. Bull. Chem.*, 2003, **52**, 811–816.
183. M. Salzmann, E. M. Stocking, L. A. Silks and H. Senn, *Magn. Reson. Chem.*, 1999, **37**, 672–675.
184. V. P. Ananikov, M. A. Kabeshov, I. P. Beletskaya, G. G. Aleksandrov and I. L. Eremenko, *J. Organomet. Chem.*, 2003, **687**, 451–461.
185. V. P. Ananikov and I. P. Beletskaya, *Dokl. Chem.*, 2003, **389**, 81–86.
186. S. Canales, O. Crespo, M. C. Gimeno, P. G. Jones and A. Laguna, *Inorg. Chem.*, 2004, **43**, 7234–7238.

SUBJECT INDEX

This page intentionally left blank